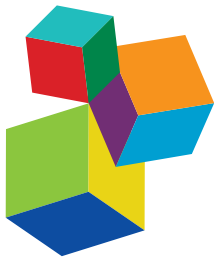


ELECTROCHEMICALLY ACTIVE MICROORGANISMS

EDITED BY: Yong Xiao, Feng Zhao and Haoyi Cheng
PUBLISHED IN: Frontiers in Microbiology



Frontiers Copyright Statement

© Copyright 2007-2018 Frontiers Media SA. All rights reserved.

All content included on this site, such as text, graphics, logos, button icons, images, video/audio clips, downloads, data compilations and software, is the property of or is licensed to Frontiers Media SA ("Frontiers") or its licensees and/or subcontractors. The copyright in the text of individual articles is the property of their respective authors, subject to a license granted to Frontiers.

The compilation of articles constituting this e-book, wherever published, as well as the compilation of all other content on this site, is the exclusive property of Frontiers. For the conditions for downloading and copying of e-books from Frontiers' website, please see the Terms for Website Use. If purchasing Frontiers e-books from other websites or sources, the conditions of the website concerned apply.

Images and graphics not forming part of user-contributed materials may not be downloaded or copied without permission.

Individual articles may be downloaded and reproduced in accordance with the principles of the CC-BY licence subject to any copyright or other notices. They may not be re-sold as an e-book.

As author or other contributor you grant a CC-BY licence to others to reproduce your articles, including any graphics and third-party materials supplied by you, in accordance with the Conditions for Website Use and subject to any copyright notices which you include in connection with your articles and materials.

All copyright, and all rights therein, are protected by national and international copyright laws.

The above represents a summary only. For the full conditions see the Conditions for Authors and the Conditions for Website Use.

ISSN 1664-8714
ISBN 978-2-88945-651-2
DOI 10.3389/978-2-88945-651-2

About Frontiers

Frontiers is more than just an open-access publisher of scholarly articles: it is a pioneering approach to the world of academia, radically improving the way scholarly research is managed. The grand vision of Frontiers is a world where all people have an equal opportunity to seek, share and generate knowledge. Frontiers provides immediate and permanent online open access to all its publications, but this alone is not enough to realize our grand goals.

Frontiers Journal Series

The Frontiers Journal Series is a multi-tier and interdisciplinary set of open-access, online journals, promising a paradigm shift from the current review, selection and dissemination processes in academic publishing. All Frontiers journals are driven by researchers for researchers; therefore, they constitute a service to the scholarly community. At the same time, the Frontiers Journal Series operates on a revolutionary invention, the tiered publishing system, initially addressing specific communities of scholars, and gradually climbing up to broader public understanding, thus serving the interests of the lay society, too.

Dedication to Quality

Each Frontiers article is a landmark of the highest quality, thanks to genuinely collaborative interactions between authors and review editors, who include some of the world's best academicians. Research must be certified by peers before entering a stream of knowledge that may eventually reach the public - and shape society; therefore, Frontiers only applies the most rigorous and unbiased reviews.

Frontiers revolutionizes research publishing by freely delivering the most outstanding research, evaluated with no bias from both the academic and social point of view. By applying the most advanced information technologies, Frontiers is catapulting scholarly publishing into a new generation.

What are Frontiers Research Topics?

Frontiers Research Topics are very popular trademarks of the Frontiers Journals Series: they are collections of at least ten articles, all centered on a particular subject. With their unique mix of varied contributions from Original Research to Review Articles, Frontiers Research Topics unify the most influential researchers, the latest key findings and historical advances in a hot research area! Find out more on how to host your own Frontiers Research Topic or contribute to one as an author by contacting the Frontiers Editorial Office: researchtopics@frontiersin.org

ELECTROCHEMICALLY ACTIVE MICROORGANISMS

Topic Editors:

Yong Xiao, Institute of Urban Environment (CAS), China

Feng Zhao, Institute of Urban Environment (CAS), China

Haoyi Cheng, Research Center for Eco-Environmental Sciences (CAS), China

Citation: Xiao, Y., Zhao, F., Cheng, H., eds (2018). Electrochemically Active Microorganisms. Lausanne: Frontiers Media. doi: 10.3389/978-2-88945-651-2

Table of Contents

- 05** *Petrophilic, Fe(III) Reducing Exoelectrogen Citrobacter sp. KVM11, Isolated From Hydrocarbon Fed Microbial Electrochemical Remediation Systems*
Krishnaveni Venkidusamy, Ananda Rao Hari and Mallavarapu Megharaj
- 19** *Temporal Microbial Community Dynamics in Microbial Electrolysis Cells – Influence of Acetate and Propionate Concentration*
Ananda Rao Hari, Krishnaveni Venkidusamy, Krishna P. Katuri, Samik Bagchi and Pascal E. Saikaly
- 33** *Electricity Generation by Shewanella Decolorationis S12 Without Cytochrome c*
Yonggang Yang, Guannan Kong, Xingjuan Chen, Yingli Lian, Wenzong Liu and Meiying Xu
- 41** *Impact of Ferrous Iron on Microbial Community of the Biofilm in Microbial Fuel Cells*
Qian Liu, Bingfeng Liu, Wei Li, Xin Zhao, Wenjing Zuo and Defeng Xing
- 50** *Electrochemical Potential Influences Phenazine Production, Electron Transfer and Consequently Electric Current Generation by Pseudomonas aeruginosa*
Erick M. Bosire and Miriam A. Rosenbaum
- 61** *Energy Efficiency and Productivity Enhancement of Microbial Electrosynthesis of Acetate*
Edward V. LaBelle and Harold D. May
- 70** *An Overview of Electron Acceptors in Microbial Fuel Cells*
Deniz Ucar, Yifeng Zhang and Irini Angelidaki
- 84** *The Denitrification Characteristics and Microbial Community in the Cathode of an MFC With Aerobic Denitrification at High Temperatures*
Jianqiang Zhao, Jinna Wu, Xiaoling Li, Sha Wang, Bo Hu and Xiaoqian Ding
- 95** *Identification of Electrode Respiring, Hydrocarbonoclastic Bacterial Strain Stenotrophomonas maltophilia MK2 Highlights the Untapped Potential for Environmental Bioremediation*
Krishnaveni Venkidusamy and Mallavarapu Megharaj
- 107** *What is the Essence of Microbial Electroactivity?*
Christin Koch and Falk Harnisch
- 112** *Characterization of Electricity Generated by Soil in Microbial Fuel Cells and the Isolation of Soil Source Exoelectrogenic Bacteria*
Yun-Bin Jiang, Wen-Hui Zhong, Cheng Han and Huan Deng
- 122** *Single-Genotype Syntropy by Rhodopseudomonas palustris is not a Strategy to Aid Redox Balance During Anaerobic Degradation of Lignin Monomers*
Devin F. R. Doud and Largus T. Angenent
- 132** *A Novel Electrophototrophic Bacterium Rhodopseudomonas palustris Strain RP2, Exhibits Hydrocarbonoclastic Potential in Anaerobic Environments*
Krishnaveni Venkidusamy and Mallavarapu Megharaj

- 144 The Low Conductivity of *Geobacter uraniireducens* Pili Suggests a Diversity of Extracellular Electron Transfer Mechanisms in the Genus *Geobacter***
Yang Tan, Ramesh Y. Adhikari, Nikhil S. Malvankar, Joy E. Ward, Kelly P. Nevin, Trevor L. Woodard, Jessica A. Smith, Oona L. Snoeyenbos-West, Ashley E. Franks, Mark T. Tuominen and Derek R. Lovley
- 154 Effects of Incubation Conditions on Cr(VI) Reduction by c-type Cytochromes in Intact *Shewanella oneidensis* MR-1 Cells**
Rui Han, Fangbai Li, Tongxu Liu, Xiaomin Li, Yundang Wu, Ying Wang and Dandan Chen
- 166 Segregation of the Anodic Microbial Communities in a Microbial Fuel Cell Cascade**
Douglas M. Hodgson, Ann Smith, Sonal Dahale, James P. Stratford, Jia V. Li, André Grünning, Michael E. Bushell, Julian R. Marchesi and C. Avignone Rossa
- 177 K-shell Analysis Reveals Distinct Functional Parts in an Electron Transfer Network and its Implications for Extracellular Electron Transfer**
Dewu Ding, Ling Li, Chuanjun Shu and Xiao Sun
- 189 Performance of Denitrifying Microbial Fuel Cell With Biocathode Over Nitrite**
Huimin Zhao, Jianqiang Zhao, Fenghai Li and Xiaoling Li
- 196 Carbon Material Optimized Biocathode for Improving Microbial Fuel Cell Performance**
Hairti Tursun, Rui Liu, Jing Li, Rashid Abro, Xiaohui Wang, Yanmei Gao and Yuan Li
- 205 Pyrosequencing Reveals a Core Community of Anodic Bacterial Biofilms in Bioelectrochemical Systems From China**
Yong Xiao, Yue Zheng, Song Wu, En-Hua Zhang, Zheng Chen, Peng Liang, Xia Huang, Zhao-Hui Yang, I-Son Ng, Bor-Yann Chen and Feng Zhao



Petrophilic, Fe(III) Reducing Exoelectrogen *Citrobacter* sp. KVM11, Isolated From Hydrocarbon Fed Microbial Electrochemical Remediation Systems

Krishnaveni Venkidusamy^{1,2*}, Ananda Rao Hari³ and Mallavarapu Megharaj^{1,2,4}

¹ Centre for Environmental Risk Assessment and Remediation (CERAR), University of South Australia, Mawson Lakes, SA, Australia, ² CRC for Contamination Assessment and Remediation of the Environment (CRCCARE), Mawson Lakes, SA, Australia, ³ Division of Sustainable Development, Hamad Bin Khalifa University, Education City, Doha, Qatar, ⁴ Global Centre for Environmental Remediation (GCER), Faculty of Science, The University of Newcastle, Callaghan, NSW, Australia

OPEN ACCESS

Edited by:

Yong Xiao,
Institute of Urban Environment (CAS),
China

Reviewed by:

Baogang Zhang,
China University of Geosciences,
China
Gefu Zhu,
Institute of Urban Environment (CAS),
China

*Correspondence:

Krishnaveni Venkidusamy
krishnaveni.venkidusamy@
mymail.unisa.edu.au

Specialty section:

This article was submitted to
Microbiotechnology, Ecotoxicology
and Bioremediation,
a section of the journal
Frontiers in Microbiology

Received: 21 February 2017

Accepted: 14 February 2018

Published: 12 March 2018

Citation:

Venkidusamy K, Hari AR and
Megharaj M (2018) Petrophilic, Fe(III)
Reducing Exoelectrogen *Citrobacter*
sp. KVM11, Isolated From
Hydrocarbon Fed Microbial
Electrochemical Remediation
Systems *Front. Microbiol.* 9:349.
doi: 10.3389/fmicb.2018.00349

Exoelectrogenic biofilms capable of extracellular electron transfer are important in advanced technologies such as those used in microbial electrochemical remediation systems (MERS). Few bacterial strains have been, nevertheless, obtained from MERS exoelectrogenic biofilms and characterized for bioremediation potential. Here we report the identification of one such bacterial strain, *Citrobacter* sp. KVM11, a petrophilic, iron reducing bacterial strain isolated from hydrocarbon fed MERS, producing anodic currents in microbial electrochemical systems. Fe(III) reduction of $90.01 \pm 0.43\%$ was observed during 5 weeks of incubation with Fe(III) supplemented liquid cultures. Biodegradation screening assays showed that the hydrocarbon degradation had been carried out by metabolically active cells accompanied by growth. The characteristic feature of diazo dye decolorization was used as a simple criterion for evaluating the electrochemical activity in the candidate microbe. The electrochemical activities of the strain KVM11 were characterized in a single chamber fuel cell and three electrode electrochemical cells. The inoculation of strain KVM11 amended with acetate and citrate as the sole carbon and energy sources has resulted in an increase in anodic currents (maximum current density) of 212 ± 3 and 359 ± 1 mA/m² with respective coulombic efficiencies of 19.5 and 34.9% in a single chamber fuel cells. Cyclic voltammetry studies showed that anaerobically grown cells of strain KVM11 are electrochemically active whereas aerobically grown cells lacked the electrochemical activity. Electrobioremediation potential of the strain KVM11 was investigated in hydrocarbonoclastic and dye detoxification conditions using MERS. About 89.60% of 400 mg l⁻¹ azo dye was removed during the first 24 h of operation and it reached below detection limits by the end of the batch operation (60 h). Current generation and biodegradation capabilities of strain KVM11 were examined using an initial concentration of 800 mg l⁻¹ of diesel range hydrocarbons (C9-C36) in MERS (maximum current

density 50.64 ± 7 mA/m²; power density 4.08 ± 2 mW/m², $1000\ \Omega$, hydrocarbon removal $60.14 \pm 0.7\%$). Such observations reveal the potential of electroactive biofilms in the simultaneous remediation of hydrocarbon contaminated environments with generation of energy.

Keywords: petrophilic, electroactive biofilms, *Citrobacter* sp. KVM11, iron reducing, extracellular electron flow, microbial electrochemical remediation systems, hydrocarbonoclastic potential

INTRODUCTION

Electrochemical oxidation by electroactive biofilms is vital to the performance of microbial electrochemical remediation systems (MERS) and enhanced removal of contaminants. Such remediation systems transform the chemical energy available in organic pollutants into electrical energy by capitalizing on the biocatalytic potential of electroactive communities (Morris and Jin, 2012; Venkidusamy et al., 2016). These systems offer a unique platform to study the electro-microbial process involved in bioremediation of oil pollutants (Venkidusamy et al., 2016) and heavy metals (Qiu et al., 2017; Wang et al., 2017), etc., The electroactive biofilms are those that have the capabilities of extracellular electron flow (EET) to degrade substrates that range from easily degradable natural organic compounds to xenobiotic compounds such as petroleum hydrocarbon (PH) contaminants (Venkidusamy et al., 2016; Zhou et al., 2016). Such biofilms can be formed by a single bacterial species (pure strain) (Venkidusamy and Megharaj, 2016a,b) or by multiple bacterial species (mixed culture) (Morris et al., 2009). The dominant view, until recently is that multiple bacterial species are better suited for its commercial applications (Chae et al., 2009), while the single bacterial species are selected to study their physiology and electrochemical performance (Xing et al., 2008; Zhi et al., 2014; Venkidusamy and Megharaj, 2016a,b; Qiu et al., 2017).

Petrochemical products are widespread contaminants that have long been of serious concern for environmental public health. Of these, diesel range hydrocarbons (DRH) became the most encountered environmental pollutants due to its increasing anthropogenic activities. Microbial removal of these DRH compounds is claimed to be an efficient, economical and versatile alternative to the established physicochemical treatments that are prone to cause recontamination by secondary contaminants (Hong et al., 2005; Megharaj et al., 2011). The biodegradation of these compounds at the soil surface has been well documented for a century (Atlas, 1991; Chaillan et al., 2004) whereas sub-surface biodegradation awaits further research on deeper insights into the metabolic activities involved and the extent and rate of hydrocarbon degradation (Röling et al., 2003). Such anaerobic, hydrocarbon contaminated reservoirs are dominated by obligate and facultative “petrophilic” (microorganisms capable of degrading hydrocarbons (Mandri and Lin, 2007) microbial communities (Singh et al., 2014). These microbial communities can adjust their metabolism based on the availability of terminal electron acceptors and can have more complex enzymatic systems involved in the degradation of contaminants. However, the rate of microbial utilization of these PH compounds is very slow especially under anaerobic environments where the availability of

relevant electron acceptors is limited (Widdel et al., 2006; Focht, 2008; Morris et al., 2009). Emerging technologies on the removal of such recalcitrant contaminants using electrodes and biofilms are gaining new interest in their applications due to its enhanced remediation (Venkidusamy et al., 2016) and continuous sink for electron acceptors such as electrodes in an economical way (Wang and Ren, 2013; Li et al., 2014).

To date, however, the mechanisms of EET are well characterized in iron reducing microbial strains from a couple of dominant model taxa such as *Geobacter* (Bond and Lovley, 2003; Reguera et al., 2005) and *Shewanella* (Kim et al., 2002; El-Naggar et al., 2010), the delta-gamma subgroups of Proteobacteria. Beyond these model taxa, however, electrochemical enrichments and 16S rRNA gene sequencing-based studies from diverse environments have shown the presence of physiologically and phylogenetically diverse, electroactive microbial communities on fuel cell electrodes. These microbial communities include the members of Alphaproteobacteria (Zuo et al., 2008), Betaproteobacteria (Chaudhuri and Lovley, 2003), Gammaproteobacteria (Kim et al., 2002), Deltaproteobacteria (Holmes et al., 2006), and Firmicutes (Wrighton et al., 2008). Of these, *Gammaproteobacteria* was the dominant class, and several bacterial strains from this class have been isolated either from electrochemical systems fed with wastewater or defined carbon sources and their physiological roles have been studied (Choo et al., 2006; Logan and Regan, 2006). Many of these exoelectrogens are dissimilatory Fe(III) reducers that possess the ability to reduce the insoluble Fe(III) in different environments such as sediments and groundwater aquifers (Caccavo et al., 1994; Coates et al., 1999; Kunapuli et al., 2010; Venkidusamy et al., 2015). For instance, *Geobacter sulfurreducens*, a dissimilatory Fe(III) reducer isolated from PH contaminated aquifers showed maximum current density of 65 mA/m² using acetate as a carbon source (Bond and Lovley, 2003). Recent studies have shown the diversity of different genetic groups of Fe(III) reducers such as, *Thermoanaerobacter pseudoethanolicus* (Lusk et al., 2015), *Thermuncola ferriacetica* (Parameswaran et al., 2013), *Geoalkalibacter* sp. (Badalamenti et al., 2013) *Clostridium butyricum* (Park et al., 2001) etc., which can transfer electrons to solid phase electron acceptors with co-degradation of recalcitrant contaminants (Kunapuli et al., 2010). For instance, *Rhodopseudomonas palustris* strain RP2, a dissimilatory Fe(III) reducer isolated from PH fed MERS has been shown to produce a maximum current density of 21 ± 3 mA/m²; with simultaneous removal of $47 \pm 2.7\%$ in MERS within 30 days (Venkidusamy and Megharaj, 2016b). It is important to note that the microbial community composition is divergent in

MERS (Morris et al., 2009; Venkidusamy et al., 2016) fed with contaminants such as petrochemicals and the physiology of such microbial populations remains to be explored. Recent research on removal of such recalcitrant contaminants using MERS is gaining interest in its practical applications by employing selected bacterial species for sub-surface PH bioremediation (Morris et al., 2009; Venkidusamy et al., 2016). This makes the identification of such bacterial population with functions of electrode respiration and PH degradation, fundamental to investigating the contaminant removal processes in MERS systems.

Our study was motivated by both apparent nature of Fe(III) reducing electroactive biofilms and contaminant degradation that represents the possibilities of microbe-electrode-contaminant interactions in MERS systems. In our laboratory, hydrocarbon fed MERS have been successfully demonstrated for the enhanced removal of PH contaminants (Venkidusamy et al., 2016). The subsequent isolation and characterization of single bacterial species from the exoelectrogenic biofilms of PH fed MERS suggests that isolated bacterial strains gained an advantage of extracellular electrode respiration (Venkidusamy et al., 2015; Venkidusamy and Megharaj, 2016a) and Fe(III) reduction (Venkidusamy and Megharaj, 2016b) as reported earlier. In this study, we report one such Fe(III) reducing bacterial strain phylogenetically related to *Citrobacter* genus and designated as *Citrobacter* sp. KVM11. The strain was found to be a facultative anaerobe. The electrochemical activity was determined by using fuel cell experiments (in different conditions) and voltammetry studies. Here, we show the existence of current generation and biodegradation capabilities by the strain KVM11 in PH fed, and azo dye fed MERS for the first time. Our findings contribute to the emerging view that MERS has great potential to offer a new route to the sustainable bioremedial process of contamination with simultaneous energy recovery by its electroactive biofilms.

MATERIALS AND METHODS

Bacterial Strain

The bacterial strain used in the study was isolated from the electrode attached biofilm of a hydrocarbon-fed electrochemical reactors through serial dilution techniques. The initial source of inoculum for the PH fed MERS was a mix of PH contaminated groundwater and activated sludge. These MERS were operated in a fed-batch mode (30 days) over a period of 12 months with a PH concentration of 800 mg l^{-1} as described earlier (Venkidusamy et al., 2016). Bacterial cells from the electrode biofilm were extracted into a sterile phosphate buffer and shaken vigorously to separate the cells from the electrode. The extracted cell suspensions were serially diluted and plated onto modified Hungate's mineral medium (Hungate, 1950) containing acetate (20 mM) as an electron donor and ferric(III) citrate as the electron acceptor (10 mM) and incubated anaerobically in a glove box (Don Whitley Scientific, MG500, Australia) for a period of 3 weeks. Single colonies were selected and transferred to Luria-Bertani (LB) agar plates. Media used throughout the study were Luria-Bertani medium (Sambrook et al., 1989) and Bushnell Hass

medium (Hanson et al., 1993). A chemically defined medium supplemented with Wolfe's trace elements and vitamins was used in the microbial electrochemical studies as previously described (Oh et al., 2004). One liter of growth medium contains (g l^{-1}) KCl 0.13, Na_2HPO_4 4.09, NaH_2PO_4 2.544, NH_4Cl 0.31. The pH of the medium was adjusted to 7.0 ± 0.2 and further fortified with Wolfe's trace elements and vitamins. The purified strain was stored in glycerol: Bushnell Hass broth and glycerol: Luria-Bertani broth (1:20) at -80°C . Biolog-GN2 (Biolog Inc., United States) plates were used to determine the utilization of various carbon sources under anaerobic conditions according to the manufacturer's instructions.

Iron (III) Reduction Experiments

Fe(III) citrate (10 mM) served as the terminal electron acceptor in anaerobic iron reduction experiments. The cells were grown in Wolfe's medium using acetate (20 mM) supplemented with trace elements and vitamins (Lovley and Phillips, 1988a). All procedures for Fe(III) reduction experiments, from medium preparation to manipulating the strain were performed using standard anaerobic conditions. All solution transfers and samplings of the cell cultures were transferred under anaerobic (10% hydrogen, 10% carbon dioxide, and 80% nitrogen) (Don Whitley Scientific, MG500, Australia) conditions using syringes and needles that had been sterilized. Fe(III) reduction was determined using the ferrozine assay (Lovley and Phillips, 1988b). The bacterial suspension was added to a pre-weighed vial containing 0.5 M HCl. HCl extracted samples were added to 5 ml of ferrozine (1 g l^{-1}) in 50 mM HEPES buffer. The filtered samples were then analyzed in a UV-Vis spectrophotometer (maxima@ $\lambda 562 \text{ nm}$) to quantify the Fe(II) formation as previously described (Lovley and Phillips, 1988b).

Microscopy

Bacterial samples for transmission electron microscopy were fixed in an electron microscopy fixative (4% paraformaldehyde/1.25% glutaraldehyde in PBS, + 4% sucrose, pH-7.2) and washed with buffer. Samples were postfixed in 2% aqueous osmium tetroxide. They were dehydrated in a graded series of ethanol and then infiltrated with Procure/Araldite epoxy resin. Blocks were polymerized overnight at 70°C . Sections were cut on a Leica UC6 Ultramicrotome using a diamond knife, stained with uranyl acetate and lead citrate and examined in an FEI Tecnai G2 Spirit Transmission Electron Microscope. The samples were also prepared using a heavy metal negative staining method involving phosphotungstic acid. The electrode samples were also fixed and prepared as described earlier (Venkidusamy et al., 2016). The dried brush samples were examined with a scanning electron microscope (Quanta FEG 450, FEI) at an accelerating voltage of 20 kV.

Phylogenetic Analysis

The genomic DNA of the bacterial strain was extracted using the UltraClean microbial DNA isolation kit (MO BIO, CA) following the manufacturer's instructions. The universal primers E8F (5'-AGAGTTGATCCTGGCTCAG3') and 1541R (5'AAGGAGGTGATCCANCCRCA 3') were used to amplify

16S rRNA gene according to the procedure by Weisburg et al. (1991). The polymerase chain reaction (PCR) mix of 50 μ l contained the following: 10 μ l of Gotaq 5X buffer, 2.0 μ l of MgCl₂ (25 mM), 1 μ l of dNTP mix (1 mM), 2 μ l of each primer (100 mM), 10–15 ng of purified DNA, and 2.5 U Taq DNA polymerase (Promega, Australia). PCR amplification was performed with an initial denaturation for 5 min, followed by 35 cycles of the 60 s at 94°C, 30 s of annealing at 40–60°C, 60 s of extension at 72°C, and a final extension at 72°C for 10 min, using a Bio-Rad thermal cycler. The PCR products were purified via the UltraClean PCR clean-up kit (Mo Bio, CA) following the manufacturer's instructions, and sequenced by the Southern Pathology Sequencing Facility at Flinders Medical Centre (Adelaide, South Australia). *In silico* analysis of 16S rRNA gene sequences was done by using the blast programs to search the GenBank and NCBI databases¹. The highest hit for the isolate KVM11 was used for ClustalW alignment and phylogenetic relationship generation. The neighbor-joining tree was constructed using the molecular evolutionary genetic analysis package version 5.0 (MEGA 5.0) based on 1000 bootstrap values (Tamura et al., 2011).

Assessment of Electrochemical Activity and Biodegradation Potential

Experiments were also performed to evaluate the possible candidate electroactive bacterial strain by *in vivo* decolorization assay using diazo dyes as described earlier (Hou et al., 2009). Experiments were carried out both aerobically and anaerobically using 20 ml of nutrient broth (Peptone-15g; D(+)-glucose-1g; Yeast extract-3g; NaCl-6g) with a concentration of 400 mg l⁻¹ of an azo dye, Reactive Black5 (RB5). The dye degradation was monitored by observing the decrease in absorbance of suspension at 595 nm under a UV-visible spectroscopy system (Agilent model 8458) and visible color change. All decolorization studies were maintained in triplicate for each experiment, and the activity was expressed as percentage degradation. The hydrocarbon degradation potential of strain KVM11 was evaluated by measuring the reduction of metabolic indicators such as dichlorophenol indophenol (DCPIP) and tetrazolium salts (Piröllo et al., 2008).

Fuel Cell Experiments

MFC Construction and Operation

Single chamber bottle MFCs were made from laboratory bottles with a capacity of 320 ml as previously described by Logan (2008) (Supplementary Figure S1). The liquid volume of the chamber was 280 ml. Anodes were carbon paper or graphite fiber brushes of 5 cm in diameter and 7 cm in length. The graphite brushes were treated as previously described (Feng et al., 2010). The cathode was made using flexible carbon cloth coated with a hydrophobic PTFE layer with added diffusional layers on the air breathing side whereas the hydrophilic side was coated using a mixture of Nafion perfluorinated ion exchange ionomer binder solution, carbon and platinum catalyst (0.5 g of 10% loading (Cheng et al.,

2006). The surface area of the anodic electrode was calculated using a porous analyser, and the cathode's total projected area was 15.6 cm². All the electrodes were thoroughly rinsed in deionized water and stored in distilled water prior to use. The electrodes were attached using copper wire, and all exposed surface areas were covered by non-conductive epoxy resin (Jay Car, Australia). All the reactors were steam sterilized in an autoclave before use. The bacterial cell suspension was prepared by pipetting bacterial cells (cell density, 1% 1OD culture) into a sterile centrifuge tube by centrifugation at 4500 rpm for 20 min. The supernatant was decanted, and the pellet containing cells were washed and resuspended in PBS before inoculation into MERS. The anode compartment was fed with 50 mM PBS (neutral pH) and salts as stated earlier (Oh et al., 2004). Acetate and citrate were used as carbon sources (1 g/L) in fuel cell experiments. The anode chamber was purged with nitrogen gas to maintain anaerobic conditions. The anolyte was agitated using a magnetic stirrer operating at 100 rpm. Open circuit (OC) MFC studies were also carried out and then switched to the closed circuit with a selected external load (R-1000 Ω unless stated otherwise). Solutions were replaced under anaerobic chamber when the voltage dropped to a low level (\leq 10 mV). All the reactors were maintained at room temperature in triplicates.

Electrochemical Analysis

Bacterial cells grown in Fe(III) citrate liquid cultures were harvested and used for electrochemical studies. The direct electrode reaction of the cells was examined using cyclic voltammetry (CV) using a conventional three electrode electrochemical cell with a 25 ml capacity. Cyclic voltammograms of the bacterial suspension were obtained using a potentiostat (Electrochemical analyser, BAS 100B, United States) connected to a personal computer. Cells were examined under nitrogen atmosphere at 25°C. A glassy carbon working electrode (3 mm, diameter, MF-2012, BAS) and silver/silver chloride reference electrode (MW-4130, BAS) and platinum counter electrode (MW-4130, BAS) were used in a conventional three-electrode system. The working electrodes were polished with alumina slurry on cotton wool followed by ultra-sonic treatments for about 10 min. The electrochemical cells were purged with nitrogen gas for 15 min before each measurement. The scan rate was 5 mV s⁻¹ with a potential range from -800 to 800 mV.

Electrobioremeditaion Experiments

Hydrocarbon biodegradation potential was monitored under MERS conditions using 1% (1 OD) inoculum and 800 mg l⁻¹ of DRH as a sole source of carbon. All cell cultures were maintained in triplicate for each experiment. Reactive Black 5 was used as sole source of energy in dye degradation experiments using the strain at a concentration of 50 mg l⁻¹ in MFC studies. LB medium was used in decolorization studies with an external load of 1000 Ω . MFCs were operated in a fed-batch mode until the voltage fell to a low level (\leq 10 mV) and then the anolyte solution was replaced under anaerobic (10% hydrogen, 10% carbon dioxide, and 80% nitrogen) (Don Whitley Scientific, MG500, Australia) conditions. All procedures for degradation experiments, from medium

¹<http://www.ncbi.nlm.nih.gov>

preparation to manipulating the strain were performed using standard anaerobic conditions. OC and abiotic controls (AC) were prepared for each set of biodegradation experiments. All the reactors were maintained at room temperature in triplicates.

Analytical Methods and Calculations

Fe(III) reduction was monitored by measuring Fe(II) production using the ferrozine method (Lovley and Phillips, 1988b). The fuel cells were continuously monitored for voltage generation across the resistor using a digital multimeter (Keithley Instruments, Inc., Cleveland, OH, United States) linked to a multi-channel scanner (Module 7700, Keithly Instruments, United States). Unless otherwise stated, all the MFC cycles were loaded with an external resistance of $1000\ \Omega$. Current (I) and power (P) were calculated as previously described (Logan, 2008) and normalized to the cathode surface area (mW/m^2). Graphite fiber surface area was also measured using a Brunauer-Emmett-Teller (BET) isotherm (Mi micrometrics, Gemini V, Particle and Surface Science Pty Ltd). DRH concentrations were measured by GC-FID using a HP-5 capillary column (15 m length, 0.32 mm thickness, 0.1 mm internal diameter) following the USEPA protocol (USEPA, 1996). The resulting chromatograms were analyzed using Agilent software (GC-FID Agilent model 6890) to identify the hydrocarbon degradation products. Chemical oxygen demand was measured by COD analyzer using effluent samples from the reactors reactors fed with acetate and citrate (Chemetrics, K-7365). Polarization curves were plotted by using various external loads with a range of $10\ \Omega$ to open circuit. Coulombic efficiency (CE) was calculated at the end of the cycle from COD removal as previously described by Logan (2008).

Nucleotides Accession Number

The 16S rRNA gene sequence obtained from this study has been deposited in the European nucleotide achieve database collections under the accession number KY693675.

RESULTS AND DISCUSSION

Strain Isolation, Phenotype, Phylogenetic Analysis and Taxonomy

A bacterial strain designated KVM11 was isolated from PH fed MERS operated free of external mediators by serial dilution and plating techniques. Cultures with a single morphotype were obtained and found to be composed of double membrane bilayers (Gram-negative), short bacilli shaped ($2\text{--}4\ \mu\text{m}$ in length), facultatively anaerobic, motile using flagella in tufts or individual for its locomotion (Figure 1). Cell growth on LB medium produces creamy, translucent colonies with a shiny surface. Cell reproduction occurred via binary fission with two identical daughter cells. A 1418 bp (almost entire length) target fragment of 16S rRNA was amplified by PCR using a genomic DNA of strain KVM11 and 16S rRNA primers. Using this multiple alignment, the neighborhood phylogenetic

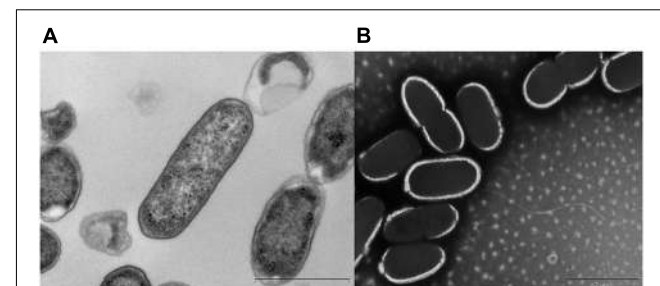


FIGURE 1 | Transmission electron micrographs of *Citrobacter* sp. KVM11. Bacterial cells were fixed in electron microscopy fixative (4% paraformaldehyde/1.25% glutaraldehyde in PBS, + 4% sucrose, pH-7.2) and washed with buffer. **(A)** Transverse section of the polymerized cells of KVM11, bar scale 100 nm **(B)** Negatively stained cells of KVM11 with filaments, bar scale 200 nm. The samples were prepared using a heavy metal staining method involving phosphotungstic acid. Samples were examined in an FEI Tecnai G2 Spirit Transmission Electron Microscope.

tree was constructed as shown in Figure 2. The taxonomic position of strain KVM11 showed a close affiliation with the genus *Citrobacter* in the class of Gammaproteobacteria. The closest recognized relatives of this strain were *Citrobacter freundii* ATCC 8090, *C. freundii* strain NBRC 12681, *C. freundii* strain LMG 3246, *C. braakii* strain 167, *C. murliniae* strain CDC 2970-59 which shared 99% similarity in their 16S rRNA gene sequence. These *Citrobacter* sp. constitute one of the most diverse, known commensal inhabitants that colonizes a variety of aquatic environments, soil, sewage sludges and gastrointestinal tracts of both humans and animals (Wang et al., 2000; Narde et al., 2004).

Physiological and Metabolic Properties

The bacterial strain is a mesophile that typically grows at temperatures ranging from 25 to 37°C . The strain was negative for oxidase and positive for catalase. The bacterial strain KVM11 can grow based on environmental signals of aerobic and anaerobic heterotrophic mechanisms as reported earlier in other strains of this genus (Oh et al., 2003). The strain was shown to be capable of dissimilatory nitrate reduction through biochemical analysis as seen in a number of exoelectrogenic bacterial strains (Xing et al., 2010; Venkidusamy and Megharaj, 2016a). The cells were grown under anoxic, chemoheterotrophic conditions with Fe(III) citrate as a terminal electron acceptor to investigate the dissimilatory Fe(III) reduction trait. Fe(III) reduction was monitored by color change and hydroxylamine Fe(II) extraction assay. The color change of medium from pale yellow to dark greenish precipitate was observed in inoculated liquid cultures under anaerobic conditions. Their colonies were coated with Fe(II) precipitate as reported for other groups of exoelectrogens such as *Geobacter*, *Aeromonas* sp. and Fe(III) enriched samples (Pham et al., 2003; Chung and Okabe, 2009; Liu et al., 2016). Fe(III) reduction of $75.33 \pm 0.70\%$ was observed during 4 weeks of incubation with Fe(III) supplemented liquid cultures (Figure 3) whereas heat killed controls showed no reduction. Moreover, by the

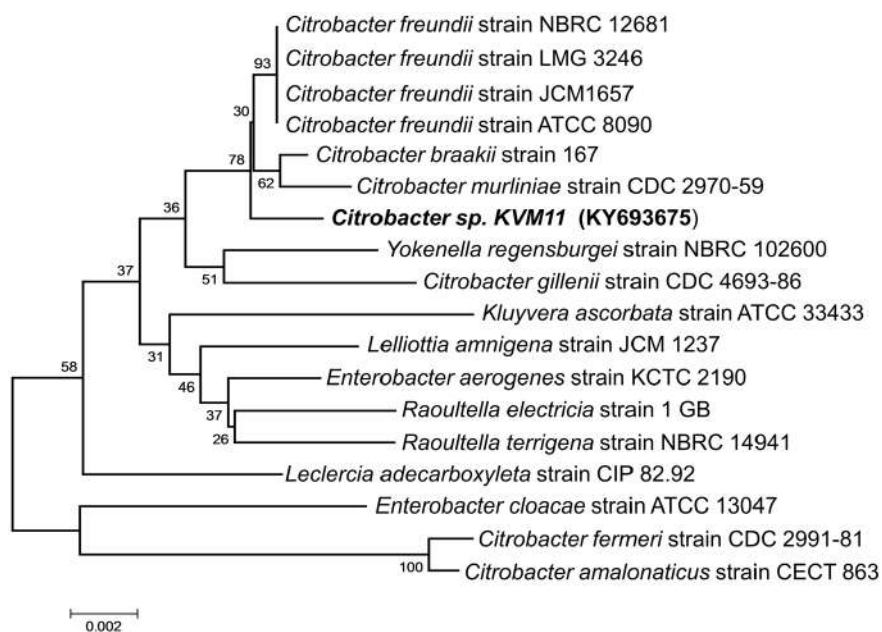


FIGURE 2 | Phylogenetic tree based on 16S rRNA gene sequences showing the positions of the isolated *Citrobacter* sp. KVM11 and closest representatives of other *Citrobacter* sp. The sequences of *Citrobacter fermeri* and *C. amalonaticus* formed an outgroup sequence. The tree was constructed from 1,418 aligned bases using the neighbor-joining method. The number at nodes show the percentages of occurrence of the branching order in thousand bootstrapped trees. Scale bar represents 0.005 substitution per nucleotide position.

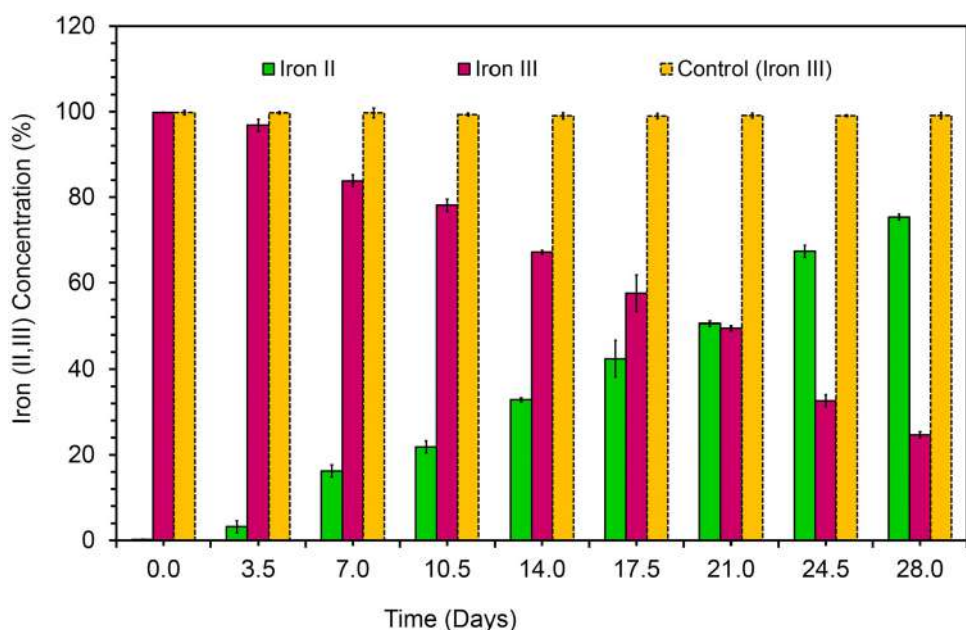


FIGURE 3 | Dissimilatory Fe(III) oxide reduction in anaerobically incubated cells of strain KVM11 at designated intervals (Ferrozine assay). Yellow bar represents the percent of Fe(III) reduction in chemotropically grown control cells; Pink bar represents Fe(III) reduction in anaerobically incubated samples of KVM11; Green bar shows Fe(II) formation in incubated samples of KVM11. Cells were inoculated into an anaerobic vials containing growth medium, electron donor: 20 mM acetate and electron acceptor: 10 mM Fe(III).

end of 36-day incubation there was a $90.01 \pm 0.43\%$ reduction of Fe(III). Abiotic loss of Fe(III) measured under each stage was less than 2%. Recent investigations have revealed the

potential of using Fe(III) reducers in microbial electrochemical systems which include *Thermoanaerobacter pseudoethanolicus* (Lusk et al., 2015), *Thermimicrobium ferriacetica* (Parameswaran

et al., 2013), *Geoalkalibacter* sp., (Badalamenti et al., 2013) and *Clostridium butyricum* (Park et al., 2001). With regards to the *Citrobacter* strains, for example, *Citrobacter* sp. LAR-1 (Liu et al., 2016) and *C. freundii* Z7 (Huang et al., 2015) have also shown to be Fe(III) reducing exoelectrogens, although the rate of Fe(III) reduction is unknown. The strain KVM11 displayed a wide nutritional spectrum as highlighted by its utilization of various carbon sources under anaerobic conditions from its counterparts, *Citrobacter* sp. LAR-1 (Liu et al., 2016) *C. freundii* Z7 (Huang et al., 2015) (Table 1). However, the strain showed a different carbon source profile than the previously reported strains of *Citrobacter* with regards to its ability to assimilate a range of substrates including alanine, phenylalanine, adonitol, aminobutyric acid, lactose, etc., (Brenner et al., 1993, 1999). The increased cell content seen in cell cultures supplemented with glucose and pyruvate under anoxic conditions in the absence of electron acceptors depicts that the strain is also capable of fermentation as previously reported (Xu and Liu, 2011). Thus, this strain shares general characteristics with the *Citrobacter*, a genus of Enterobacteriaceae (Garrity et al., 2005).

TABLE 1 | Phenotype and metabolic properties of *Citrobacter* sp. KVM11.

Particulars	<i>Citrobacter</i> sp. KVM11	<i>Citrobacter</i> sp. LAR-1 (Liu et al., 2016)	<i>Citrobacter</i> freundii Z7 (Huang et al., 2015)
Cell length (μm)	2–4	2–4	1–5
Cell shape	short bacilli	short bacilli	short bacilli
Motility	+	+	+
Optimum pH	6.5–7.2	6.5–7.0	6.5–7.0
Exoelectrogenic behavior	+	+	+
Nitrate reduction	+	NA	NA
Denitrification	+	NA	NA
Petroleum hydrocarbons	+	NA	NA
Catalase	+	NA	NA
Indophenol oxidase	–	NA	NA
Glucose fermentation	+	+	+
Lactose fermentation	+	+	+
Tween hydrolysis	–	NA	NA
Urea hydrolysis	+	+	NA
Acetate	+	+	+
Arabinose	+	NA	NA
Adonitol	+	NA	NA
Celllobiose	+	+	NA
Fructose	+	NA	NA
Maltose	+	NA	NA
Mannitol	–	+	NA
Xylose	–	+	NA
Citrate	+	+	+
Rhamnose	+	+	+
Gluconate	+	+	NA
N-Acetylglucosamine	–	+	NA
Sulfide production	+	NA	NA

(+): Positive reaction; (–): Negative reaction; Not available: (NA).

Hydrocarbon Degradation Assays

The petrochemical degradation potential of strain KVM11 was assessed through a preliminary investigation of hydrocarbon consumption, a concomitant increase in biomass and reduction of redox electron acceptors such as DCPIP and tetrazolium indicators. The strain KVM11 discolored the redox indicator from the blue to violet during the first 24 h and complete discoloration was observed by the end of 120 h when DRH was the sole carbon and energy source. The respiratory reduction of tetrazolium salts is another criterion employed by many researchers (Olga et al., 2008; Piröllo et al., 2008) to determine the dehydrogenase activity of hydrocarbon degrading bacterial strains. The formation of a red precipitate from the tetrazolium was observed while the AC remained unchanged. Upon reduction of this salt, the color changed to red due to the formation of insoluble formazan by the production of superoxide radicals and electron transport in the bacterial respiratory chain (Haines et al., 1996). It is evident from the screening assays that the strain KVM11 possess the hydrocarbon biodegradation potential by involving redox reactions in which electrons are donated to terminal electron acceptors during the cell respiration as previously described in other hydrocarbonoclastic strains (Olga et al., 2008; Venkidusamy and Megharaj, 2016a,b). The reduction of a lipophilic mediator such as DCPIP (blue to colorless) coupled with the formation of oxidized products showed that the biodegradation had been carried out by metabolically active cells involving growth, and not by adsorption to cells associated with the water-carbon interface (Kubota et al., 2008). It is of interest that, the aerobic mineralization of PH as its sole carbon source highlights the cosmopolitan presence of *Citrobacter* sp. in petrochemical contaminated sites (Singh and Lin, 2008; Morris et al., 2009).

Assessment of Electrochemical Activity

The characteristic feature of diazo dye decolorization was used as a simple criterion for evaluating the possible electrochemical activity in microbial candidate in the present study as stated earlier (Hou et al., 2009). To assess the electrochemical activity of the isolate, aerobic and anaerobic cultures were grown in nutrient broth supplemented with 400 mg l⁻¹ of Reactive Black5. The complete disappearance of the characteristic absorption peak at the region of λ_{max} (597) and simultaneous decolorization of dye were observed after 48 h in aerobically grown samples. The highest rate of decolorization of azoic dye was observed at the end of 60 h under aerobic incubations (95.03%, Figure 4), whereas this tended to be faster under anaerobic conditions. RB5 azoic dye was almost completely decolorized (99.73%) in 48 h by *Citrobacter* sp. strain KVM11 under anaerobic conditions (Figure 4) as reported in another exoelectrogenic strain of *Shewanella* sp. (Pearce et al., 2006). This is in agreement with the previous studies on the assessment of electrochemically active microbial strains using azo dye fed MFC arrays (Hou et al., 2009). The blue pigmented dead cell pellet from the heat-killed cells in control showed a passive adsorption of dye, whereas colorless cell pellets obtained from the living cultures demonstrated the reduction of the RB5 indicator.

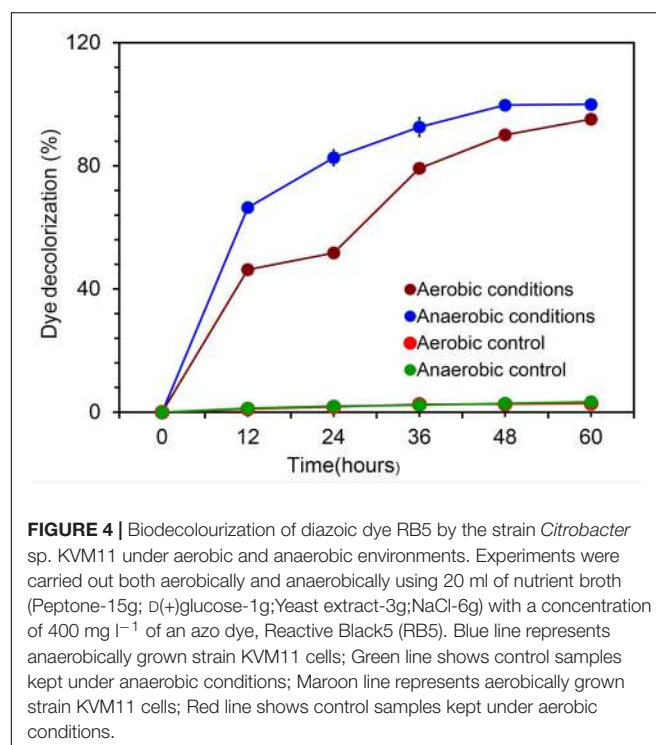


FIGURE 4 | Biodecolourization of diazoic dye RB5 by the strain *Citrobacter* sp. KVM11 under aerobic and anaerobic environments. Experiments were carried out both aerobically and anaerobically using 20 ml of nutrient broth (Peptone-15g; D(+)-glucose-1g; Yeast extract-3g; NaCl-6g) with a concentration of 400 mg l⁻¹ of an azo dye, Reactive Black5 (RB5). Blue line represents anaerobically grown strain KVM11 cells; Green line shows control samples kept under anaerobic conditions; Maroon line represents aerobically grown strain KVM11 cells; Red line shows control samples kept under aerobic conditions.

Dye decolorization occurs because of a reductive electrophilic cleavage of the chromophore, a functional group of azo linkage, by biocatalysts as reported earlier (Sun et al., 2009; Satapanajaru et al., 2011).

Exoelectrogenic Behaviors of Strain KVM11

Current Generation in Microbial Electrochemical Cells Fed With Acetate and Citrate

To confirm the extracellular access to the insoluble electron acceptors, the exoelectrogenic properties of the strain KVM11 were investigated in three different conditions (i) acetotrophic (ii) dye decolorization, and (iii) hydrocarbonoclastic, using microbial electrochemical systems. To initiate bacterial growth on a brush electrode, cells of exponential phase cultures grown in Fe(III) citrate (10 mM) were inoculated in an anodic chamber of a single chamber MFC. Upon inoculation with strain KVM11, the anodic current was generated within a few hours using sodium acetate (20 mM) as a sole carbon source. During the first cycle, the voltage was steadily increased, and a maximum open circuit voltage between the electrodes was 0.720 ± 25 mV. Once the voltage stabilized, the electrodes were connected through a fixed resistance (1000 Ω). The present study exhibited a maximum power density of 212 mW/m² (Figure 5) with a recovery of 13.3% (Figure 6) as an electrical current using the strain KVM11 in acetotrophic conditions. Such findings suggest that the strain KVM11 is also capable of utilizing insoluble electron acceptors with the additional distinctive features making this strain unique from its counterparts (Xu and Liu, 2011; Huang et al., 2015; Liu et al., 2016), which include, (i) ability

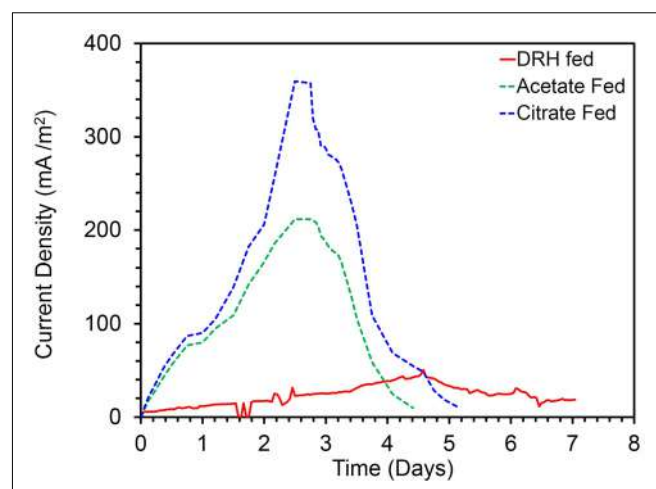


FIGURE 5 | Current production by *Citrobacter* sp. KVM11 in single chamber MFCs containing brush anodes. Green dotted line shows a representative cycle of current production in acetate (1g/L) fed MFCs; Blue dotted line shows a representative cycle of current production in citrate (1g/L) fed MFCs; Red dotted line shows a representative cycle of current production in diesel range hydrocarbons (DRH) (800mg/L).

to degrade PH, (ii) dye detoxification in MERS, and (iii) anoxic Fe(III) reduction. The typical polarization curve of *Citrobacter* strain KVM11 (Figure 7) in an acetate-fed MFC indicated a large potential drop due to activational losses as shown in other exoelectrogenic strains (Park et al., 2001; Pham et al., 2003; Venkidusamy and Megharaj, 2016a,b). Scanning electron micrographs (SEM) from the final cycle electrode revealed its colonization by bacteria, forming multilayers of a thick biofilm around the electrode surface (Figure 8). Current generation by strain KVM11 also examined using sodium citrate as their sole carbon source at the same external resistance. When the repeatable and stable performance of current output was achieved, citrate fed MFC generated the maximum power density of 195.82 mW/m² at a current density of 359.64 mA/m². The overall calculated CE was 28.9% (Figure 6). Regardless of the types of substrates tested, *Citrobacter* sp. KVM11 produced anodic currents (acetate 212 ± 3 mA/m²; citrate 359 ± 4 mA/m²) in MFCs. These experimental results supported the fact that Fe(III) reducing *Citrobacter* sp. strain KVM11 can be used as an exoelectrogen in microbial electrochemical systems as previously described in *Citrobacter* sp. LAR-1 (Liu et al., 2016).

Electron Transfer Mechanism of Strain KVM11

To further investigate the exoelectrogenic nature of the strain KVM11, the interaction between electrodes and cell suspensions on glassy carbon electrodes was observed. Cell suspensions of the strain were prepared from Fe(III) (10 mM) supplemented cultures and their electrochemical activities examined in respective aerobic and anaerobic conditions as stated earlier (Park et al., 2001; Pham et al., 2003). According to the voltammograms, the anaerobically grown cells of strain KVM11 showed electrochemical activity through the presence

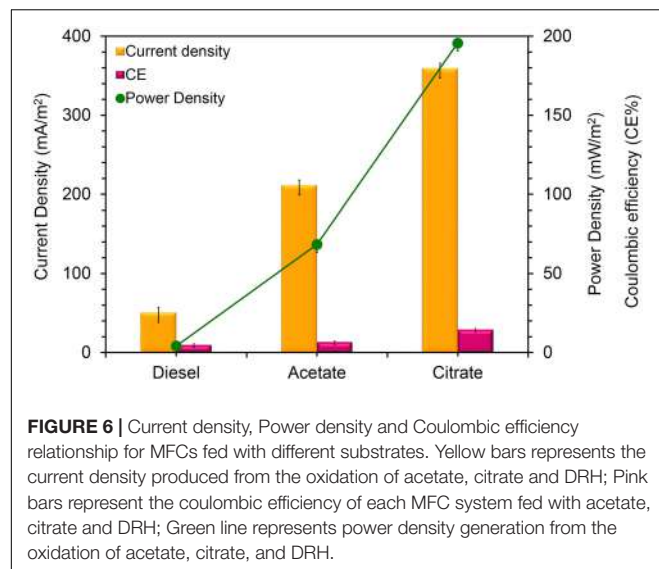


FIGURE 6 | Current density, Power density and Coulombic efficiency relationship for MFCs fed with different substrates. Yellow bars represents the current density produced from the oxidation of acetate, citrate and DRH; Pink bars represent the coulombic efficiency of each MFC system fed with acetate, citrate and DRH; Green line represents power density generation from the oxidation of acetate, citrate, and DRH.

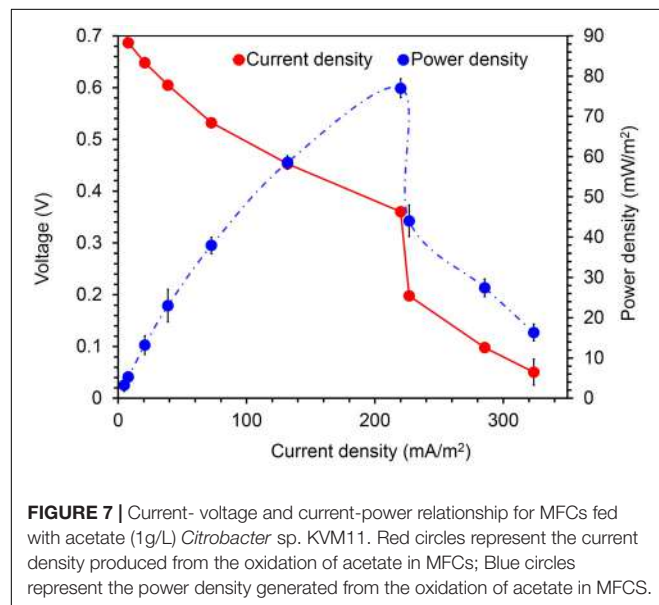


FIGURE 7 | Current-voltage and current-power relationship for MFCs fed with acetate (1g/L) *Citrobacter* sp. KVM11. Red circles represent the current density produced from the oxidation of acetate in MFCs; Blue circles represent the power density generated from the oxidation of acetate in MFCs.

of a reduction peak ranging from -100 to -310 mV and oxidation peaks at the range of $+100$ mV to $+300$ mV observed against the Ag/AgCl reference electrode (Figure 9). The asymmetry of CV peaks at different potentials (-800 to 800 mV) indicates that the reaction is a quasi-reversible reaction. One redox couple was observed from the CV peak, and a number of electrons ($e = 1$) transferred was calculated from the Nernst equation (Logan, 2008). The mid-potential of the CV peaks showed -205 mV, which is characteristic of the c-type cytochromes as reported earlier (Myers and Myers, 1992; Kim et al., 1999). For example, the midpoint potentials of OmcA (c-type cytochromes) reported in *Shewanella* MR-1 biofilm were -201 and -208 mV (Kim et al., 1999). No obvious redox pair peak was observed from the suspension of aerobically grown cells or autoclaved controls. The results

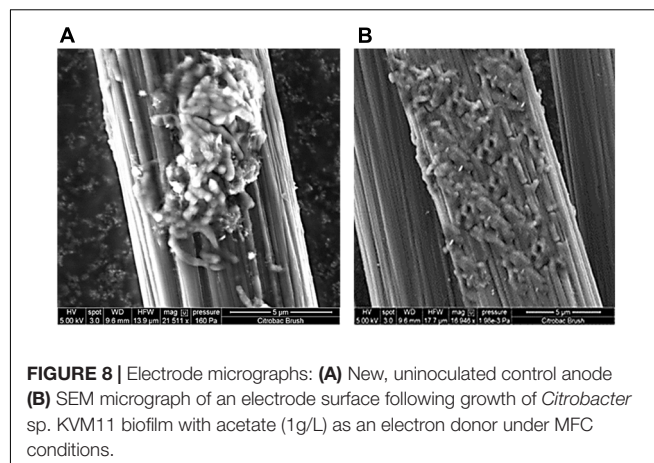


FIGURE 8 | Electrode micrographs: **(A)** New, uninoculated control anode **(B)** SEM micrograph of an electrode surface following growth of *Citrobacter* sp. KVM11 biofilm with acetate (1g/L) as an electron donor under MFC conditions.

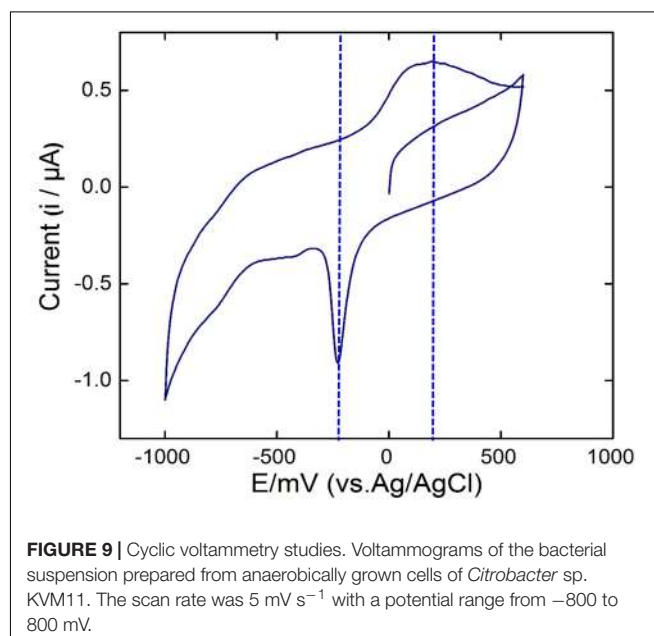


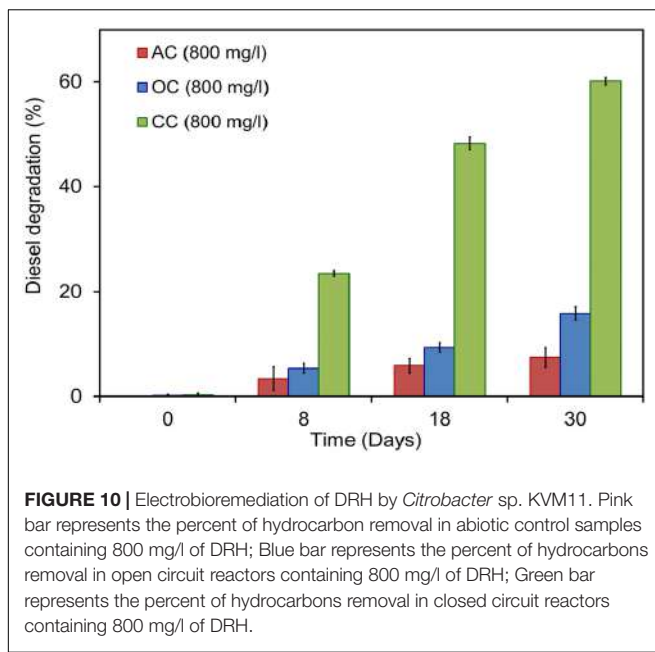
FIGURE 9 | Cyclic voltammetry studies. Voltammograms of the bacterial suspension prepared from anaerobically grown cells of *Citrobacter* sp. KVM11. The scan rate was 5 mV s^{-1} with a potential range from -800 to 800 mV.

also perhaps indicated that oxygenated liquid cultures prevent the synthesis of the outer membrane cytochromes which plays a major role in electron transfer mechanisms (Kim et al., 2002).

Electrobioremediation Potential of Strain KVM11

Energy Generation in Hydrocarbon Fed MERS

Citrobacter sp. have been widely examined for its bioremediation potential because of its wide spectrum use of various xenobiotic pollutants (Macaskie et al., 1995; Narde et al., 2004; Qiu et al., 2009, 2017; Wang et al., 2017). Members of this genus have been found along with other predominant genera of hydrocarbon degraders including *Acinetobacter*, *Pseudomonas*, *Alcaligenes*, and *Sphingomonas* in oil-contaminated environments as stated earlier (Chikere et al., 2012). Recent studies on the electrochemically mediated

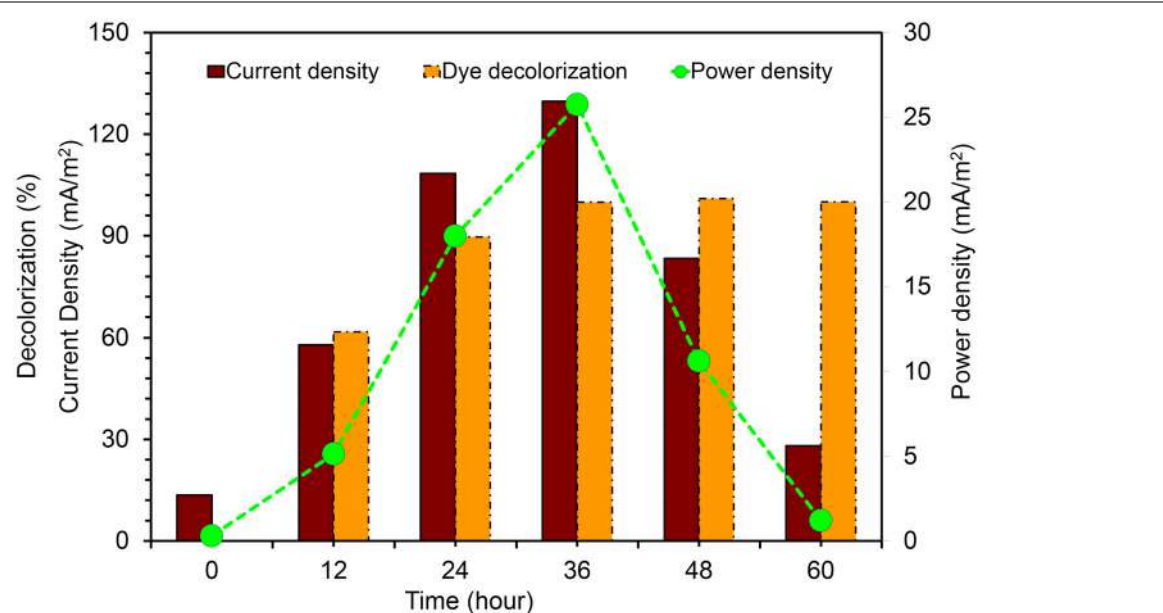


degradation of hydrocarbons demonstrated the presence of *Citrobacter* sp. in the anodic microbial communities (Morris et al., 2009; Venkidusamy et al., 2015). The capability of hydrocarbon mineralization by *Citrobacter* sp. has been demonstrated earlier only under aerobic conditions (Singh and Lin, 2008; AlDisi et al., 2016). However, the bioremediation of these compounds in anaerobic environments or MERS by the genus *Citrobacter* is previously unknown. In the present study,

experiments were conducted to examine the exoelectrogenic property of the strain KVM11 using DRH (concentration of 800 mg l^{-1}) as a sole carbon source in hydrocarbon fed MERS systems for five consecutive runs. A maximum current and power density obtained at this concentration were $50.64 \pm 7 \text{ mA/m}^2$, $4.08 \pm 2 \text{ mW/m}^2$ (Figure 6). An average of $60.14 \pm 0.67\%$ DRH removal with the simultaneous electrical current recovery of 9.6% (Figure 6) was observed in closed circuit MERS (Figure 10) at the end of the batch studies (30 days). In the case of the abiotic (AC) and open circuit (OC) controls, DRH removal rates were low ($7.45 \pm 1.99\%$, $15.84 \pm 1.23\%$, respectively) by the end of the batch study. An increase in current (70.57 mA/m^2) and power densities (15.04 mW/m^2) were observed in a similar device through earlier investigations (Venkidusamy et al., 2015) on mixed culture hydrocarbonoclastic enrichments suggesting that the higher rate of substrate assimilation ($83 \pm 2.6\%$) in hydrocarbons fed MERS. Similar effects have been shown by other authors using different substrates including recalcitrant contaminants (Luo et al., 2009; Shen et al., 2012; Hassan et al., 2016). This perhaps indicates the presence of a complex ecology in the mixed culture hydrocarbonoclastic enrichments and its synergistic effects between hydrocarbonoclastic and exoelectrogenic bacterial groups in hydrocarbon fed MERS systems. Therefore, enrichment of selective bacterial population is needed during the bioaugmentation process of MERS systems to enhance the contaminant degradation with simultaneous energy gain.

Energy Generation in Dye Fed MERS

The current was rapidly generated in all dye fed MFCs inoculated with KVM11 cells within few hours of using azoic dye as an



energy source at a fixed resistance of $1000\ \Omega$. The maximum output range of voltage, current density, and power density were $200 \pm 2\text{ mV}$, $125.9 \pm 4\text{ mA/m}^2$, and $25 \pm 0.75\text{ mW/m}^2$, respectively. Constant and repeatable power cycles were obtained during four changes of the anolytes of the anode chamber. Using RB5 concentration of 400 mg l^{-1} in MFC, 61.74% was removed during the first 12 h of operation. After 24 h, almost 89.60% of RB5 was decolorized, and it was below detection limits at the end of the batch operation (60 h) as shown in **Figure 11**. Recent investigations have revealed the potential of using such pure cultures of heterotrophic biofilms in MERS for dye detoxification (Chen et al., 2010a,b). For example, Chen et al. (2010a), reported the possibility of using pure cultures of *Proteus hauseri* in MFC, however, decolorization efficiency and power densities generated were much lower. The performance of these microbial electrochemical cells using pure cultures of exoelectrogens for dye detoxification were considerably affected by a number of reactor parameters, operating conditions and efficacy of bacterial strains used as reported earlier (Min et al., 2005; Logan, 2008).

In summary, the findings presented in our study suggest that the strain KVM11 is capable of utilizing solid electron acceptors through extracellular transfer mechanisms without the addition of external mediators. The biodegradation experiments showed the evidence for the existence of electrochemical mediated degradation capability in *Citrobacter* sp. KVM11 in MERS conditions. An increasing number of studies demonstrate the potential use of facultative anaerobes in MERS for enhanced degradation of recalcitrant contaminants (Morris et al., 2009; Huang et al., 2011; Yan et al., 2012; Venkidusamy et al., 2015; Venkidusamy and Megharaj, 2016a,b). However, the optimization of such contaminant degrading mechanism will require a deeper understanding at molecular level through proteomics or transcriptomics of those microbial candidates.

CONCLUSION

Based on molecular and metabolic characterization, we identified that the strain KVM11 obtained from MERS represents a novel strain that is phylogenetically related to *Citrobacter* sp. A dissimilatory reduction of Fe(III) by strain KVM 11 confirmed the possibilities of using iron

REFERENCES

- AlDisi, Z., Jaoua, S., Al-Thani, D., AlMeer, S., and Zouari, N. (2016). "Isolation, screening and activity of hydrocarbon-degrading bacteria from harsh soils," in *Proceedings of the World Congress on Civil, Structural, and Environmental Engineering*, (Prague). doi: 10.11159/icesdp16.104
- Atlas, R. M. (1991). Microbial hydrocarbon degradation—bioremediation of oil spills. *J. Chem. Technol. Biotechnol.* 52, 149–156. doi: 10.1002/jctb.280520202
- Badalamenti, J. P., Krajmalnik-Brown, R., and Torres, C. I. (2013). Generation of high current densities by pure cultures of anode-respiring *Geoalkalibacter* spp. under alkaline and saline conditions in microbial electrochemical cells. *mBio* 4:e00144-13. doi: 10.1128/mBio.00144-13

reducers in microbial electrochemical systems as previously described (Liu et al., 2016). While the exoelectrogenic metabolism of this species is previously known (Xu and Liu, 2011; Liu et al., 2016), our present findings demonstrated for the first time the bioelectrochemical degradation of hydrocarbons and its associated electrochemical properties. Identification of such organisms from MERS expands the known diversity of exoelectrogens and provides the novel strain to explore the three-way interaction between microbe-electrode-contaminant through EET mechanism. Also, bioelectrochemically mediated detoxification of diazoic dye by strain KVM11 reveals its potential for application in the treatment of waste from textile industries using MERS. Altogether, our findings reflect the metabolic versatility of *Citrobacter* sp. KVM11 which holds promise in the bioelectrochemical remediation of recalcitrant xenobiotics with simultaneous energy generation, in the form of electricity. Further, electromicrobiological studies show the potential of unfolding molecular mechanism of complex interactions of *Citrobacter* sp. KVM11 between solid phase electron acceptors and contaminants. The availability of complete genome and its analysis will provide more details about the functions of this bacterium.

AUTHOR CONTRIBUTIONS

KV and MM proposed the study. KV conducted the experiments under the supervision of MM. KV and ARH analyzed the data and prepared the draft with contributions from MM.

ACKNOWLEDGMENTS

KV thanks Australian Federal Government, University of South Australia for International Postgraduate Scholarship award (IPRS) and CRCCARE for the research top-up award.

SUPPLEMENTARY MATERIAL

The Supplementary Material for this article can be found online at: <https://www.frontiersin.org/articles/10.3389/fmicb.2018.00349/full#supplementary-material>

- Bond, D. R., and Lovley, D. R. (2003). Electricity production by *Geobacter sulfurreducens* attached to electrodes. *Appl. Environ. Microbiol.* 69, 1548–1555. doi: 10.1128/AEM.69.3.1548-1555.2003
- Brenner, D. J., Grimont, P. A., Steigerwalt, A. G., Fanning, G., Ageron, E., and Riddle, C. F. (1993). Classification of citrobacteria by DNA hybridization: designation of *Citrobacter farmeri* sp. nov., *Citrobacter youngae* sp. nov., *Citrobacter braakii* sp. nov., *Citrobacter werkmanii* sp. nov., *Citrobacter sedlakii* sp. nov., and three unnamed *Citrobacter* genospecies. *Int. J. Syst. Bacteriol.* 43, 645–658. doi: 10.1099/00207713-43-4-645
- Brenner, D. J., O'Hara, C. M., Grimont, P. A., Janda, J. M., Falsen, E., Aldova, E., et al. (1999). Biochemical Identification of *Citrobacter* Species Defined by DNA Hybridization and Description of *Citrobacter gillenii* sp. nov. (Formerly *Citrobacter* genospecies 10) and *Citrobacter murliniae*

- sp. nov. (Formerly *Citrobacter genomospecies* 11). *J. Clin. Microbiol.* 37, 2619–2624.
- Caccavo, F., Lonergan, D. J., Lovley, D. R., Davis, M., Stolz, J. F., and McInerney, M. J. (1994). *Geobacter sulfurreducens* sp. nov., a hydrogen-and acetate-oxidizing dissimilatory metal-reducing microorganism. *Appl. Environ. Microbiol.* 60, 3752–3759.
- Chae, K.-J., Choi, M.-J., Lee, J.-W., Kim, K.-Y., and Kim, I. S. (2009). Effect of different substrates on the performance, bacterial diversity, and bacterial viability in microbial fuel cells. *Biores. Technol.* 100, 3518–3525. doi: 10.1016/j.biortech.2009.02.065
- Chaillan, F., Le Flèche, A., Bury, E., Phantavong, Y.-H., Grimont, P., Saliot, A., et al. (2004). Identification and biodegradation potential of tropical aerobic hydrocarbon-degrading microorganisms. *Res. Microbiol.* 155, 587–595. doi: 10.1016/j.resmic.2004.04.006
- Chaudhuri, S. K., and Lovley, D. R. (2003). Electricity generation by direct oxidation of glucose in mediatorless microbial fuel cells. *Nat. Biotechnol.* 21, 1229–1232. doi: 10.1038/nbt867
- Chen, B.-Y., Zhang, M.-M., Chang, C.-T., Ding, Y., Lin, K.-L., Chiou, C.-S., et al. (2010a). Assessment upon azo dye decolorization and bioelectricity generation by *Proteus hauseri*. *Bioresour. Technol.* 101, 4737–4741. doi: 10.1016/j.biortech.2010.01.133
- Chen, B.-Y., Zhang, M.-M., Ding, Y., and Chang, C.-T. (2010b). Feasibility study of simultaneous bioelectricity generation and dye decolorization using naturally occurring decolorizers. *J. Taiwan Inst. Chem. Eng.* 41, 682–688. doi: 10.1016/j.jtice.2010.02.005
- Cheng, S., Liu, H., and Logan, B. E. (2006). Increased performance of single-chamber microbial fuel cells using an improved cathode structure. *Electrochim. Commun.* 8, 489–494. doi: 10.1016/j.elecom.2006.01.010
- Chikere, C. B., Chikere, B. O., and Okpokwasili, G. C. (2012). Bioreactor-based bioremediation of hydrocarbon-polluted Niger Delta marine sediment, Nigeria. *3 Biotech* 2, 53–66. doi: 10.1007/s13205-011-0030-8
- Choo, Y. F., Lee, J., Chang, I. S., and Kim, B. H. (2006). Bacteria communities in microbial fuel cells enriched with high concentrations of glucose and glutamate. *J. Microbiol. Biotechnol.* 16, 1481–1484.
- Chung, K., and Okabe, S. (2009). Characterization of electrochemical activity of a strain ISO2-3 phylogenetically related to *Aeromonas* sp. isolated from a glucose-fed microbial fuel cell. *Biotechnol. Bioeng.* 104, 901–910. doi: 10.1002/bit.22453
- Coates, J. D., Ellis, D. J., Gaw, C. V., and Lovley, D. R. (1999). *Geothrix fermentans* gen. nov., sp. nov., a novel Fe (III)-reducing bacterium from a hydrocarbon-contaminated aquifer. *Int. J. Syst. Evol. Microbiol.* 49, 1615–1622. doi: 10.1099/00207713-49-4-1615
- El-Naggar, M. Y., Wanger, G., Leung, K. M., Yuzvinsky, T. D., Southam, G., Yang, J., et al. (2010). Electrical transport along bacterial nanowires from *Shewanella oneidensis* MR-1. *Proc. Natl. Acad. Sci. U.S.A.* 107, 18127–18131. doi: 10.1073/pnas.1004880107
- Feng, Y., Yang, Q., Wang, X., and Logan, B. E. (2010). Treatment of carbon fiber brush anodes for improving power generation in air-cathode microbial fuel cells. *J. Power Sources* 195, 1841–1844. doi: 10.1016/j.jpowsour.2009.10.030
- Foght, J. (2008). Anaerobic biodegradation of aromatic hydrocarbons: pathways and prospects. *J. Mol. Microbio. Biotechnol.* 15, 93–120. doi: 10.1159/0001234
- Garrity, G. M., Bell, J. A., and Lilburn, T. (2005). “Class I. Alphaproteobacteria class. nov.” in *Bergey’s Manual® of Systematic Bacteriology*, eds D. J. Brenner, N. R. Krieg, and J. T. Staley (Springer: Boston), 1–574.
- Haines, J. R., Wrenn, B. A., Holder, E. L., Strohmeier, K. L., Herrington, R. T., and Venosa, A. D. (1996). Measurement of hydrocarbon-degrading microbial populations by a 96-well plate most-probable-number procedure. *J. Ind. Microbiol.* 16, 36–41. doi: 10.1007/BF01569919
- Hanson, K., Desai, J. D., and Desai, A. J. (1993). A rapid and simple screening technique for potential crude oil degrading microorganisms. *Biotechnol. Tech.* 7, 745–748. doi: 10.1007/BF00152624
- Hassan, H., Jin, B., Dai, S., Ma, T., and Saint, C. (2016). Chemical impact of catholytes on *Bacillus subtilis*-catalysed microbial fuel cell performance for degrading 2, 4-dichlorophenol. *Chem. Eng. J.* 301, 103–114. doi: 10.1016/j.cej.2016.04.077
- Holmes, D. E., Chaudhuri, S. K., Nevin, K. P., Mehta, T., Methé, B. A., Liu, A., et al. (2006). Microarray and genetic analysis of electron transfer to electrodes in *Geobacter sulfurreducens*. *Environ. Microbiol.* 8, 1805–1815. doi: 10.1111/j.1462-2920.2006.01065.x
- Hong, J. H., Kim, J., Choi, O. K., Cho, K.-S., and Ryu, H. W. (2005). Characterization of a diesel-degrading bacterium, *Pseudomonas aeruginosa* IU5, isolated from oil-contaminated soil in Korea. *World J. Microbiol. Biotechnol.* 21, 381–384. doi: 10.1007/s11274-004-3630-1
- Hou, H., Li, L., Cho, Y., de Figueiredo, P., and Han, A. (2009). Microfabricated microbial fuel cell arrays reveal electrochemically active microbes. *PLoS One* 4:e6570. doi: 10.1371/journal.pone.0006570
- Huang, J., Zhu, N., Cao, Y., Peng, Y., Wu, P., and Dong, W. (2015). Exoelectrogenic bacterium phylogenetically related to *Citrobacter freundii*, isolated from anodic biofilm of a microbial fuel cell. *Appl. Biochem. Biotechnol.* 175, 1879–1891. doi: 10.1007/s12010-014-1418-9
- Huang, L., Cheng, S., and Chen, G. (2011). Bioelectrochemical systems for efficient recalcitrant wastes treatment. *J. Chem. Technol. Biotechnol.* 86, 481–491. doi: 10.1002/jctb.2551
- Hungate, R. E. (1950). The anaerobic mesophilic cellulolytic bacteria. *Bacteriol. Rev.* 14, 1–49.
- Kim, B.-H., Kim, H.-J., Hyun, M.-S., and Park, D.-H. (1999). Direct electrode reaction of Fe (III)-reducing bacterium, *Shewanella putrefaciens*. *J. Microbiol. Biotechnol.* 9, 127–131. doi: 10.1371/journal.pone.0147899
- Kim, H. J., Park, H. S., Hyun, M. S., Chang, I. S., Kim, M., and Kim, B. H. (2002). A mediator-less microbial fuel cell using a metal reducing bacterium, *Shewanella putrefaciens*. *Enzyme Microb. Technol.* 30, 145–152. doi: 10.1016/S0141-0229(01)00478-1
- Kubota, K., Koma, D., Matsumiya, Y., Chung, S. Y., and Kubo, M. (2008). Phylogenetic analysis of long-chain hydrocarbon-degrading bacteria and evaluation of their hydrocarbon-degradation by the 2, 6-DCPIP assay. *Biodegradation* 19, 749–757. doi: 10.1007/s10532-008-9179-1
- Kunapuli, U., Jahn, M. K., Lueders, T., Geyer, R., Heipieper, H. J., and Meckenstock, R. U. (2010). *Desulfotobacterium aromaticivorans* sp. nov. and *Geobacter toluenoxydans* sp. nov., iron-reducing bacteria capable of anaerobic degradation of monoaromatic hydrocarbons. *Int. J. Syst. Evol. Microbiol.* 60, 686–695. doi: 10.1099/ijts.0.003525-0
- Li, W.-W., Yu, H.-Q., and He, Z. (2014). Towards sustainable wastewater treatment by using microbial fuel cells-centered technologies. *Energy Environ. Sci.* 7, 911–924. doi: 10.1039/C3EE43106A
- Liu, L., Lee, D.-J., Wang, A., Ren, N., Su, A., and Lai, J.-Y. (2016). Isolation of Fe (III)-reducing bacterium, *Citrobacter* sp. LAR-1, for startup of microbial fuel cell. *Int. J. Hydrogen Energy* 41, 4498–4503. doi: 10.1016/j.ijhydene.2015.07.072
- Logan, B. E. (2008). *Microbial Fuel Cells*. Hoboken, NY: John Wiley & Sons.
- Logan, B. E., and Regan, J. M. (2006). Electricity-producing bacterial communities in microbial fuel cells. *Trends Microbiol.* 14, 512–518. doi: 10.1016/j.tim.2006.10.003
- Lovley, D. R., and Phillips, E. J. (1988a). Manganese inhibition of microbial iron reduction in anaerobic sediments. *Geomicrobiol. J.* 6, 145–155. doi: 10.1080/01490458809377834
- Lovley, D. R., and Phillips, E. J. (1988b). Novel mode of microbial energy metabolism: organic carbon oxidation coupled to dissimilatory reduction of iron or manganese. *Appl. Environ. Microbiol.* 54, 1472–1480.
- Luo, H., Liu, G., Zhang, R., and Jin, S. (2009). Phenol degradation in microbial fuel cells. *Chem. Eng. J.* 147, 259–264. doi: 10.1016/j.cej.2008.07.011
- Lusk, B. G., Khan, Q. F., Parameswaran, P., Hameed, A., Ali, N., Rittmann, B. E., et al. (2015). Characterization of electrical current-generation capabilities from thermophilic bacterium *Thermoanaerobacter pseudethanolicus* using xylose, glucose, cellobiose, or acetate with fixed anode potentials. *Environ. Sci. Technol.* 49, 14725–14731. doi: 10.1021/acs.est.5b04036
- Macaskie, L. E., Hewitt, C. J., Shearer, J. A., and Kent, C. A. (1995). Biomass production for the removal of heavy metals from aqueous solutions at low pH using growth-decoupled cells of a *Citrobacter* sp. *Int. Biodeterior. Biodegradation* 35, 73–92. doi: 10.1016/0964-8305(95)00050-F
- Mandri, T., and Lin, J. (2007). Isolation and characterization of engine oil degrading indigenous microorganisms in Kwazulu-Natal, South Africa. *Afr. J. Biotechnol.* 6, 23–27.

- Megharaj, M., Ramakrishnan, B., Venkateswarlu, K., Sethunathan, N., and Naidu, R. (2011). Bioremediation approaches for organic pollutants: a critical perspective. *Environ. Int.* 37, 1362–1375. doi: 10.1016/j.envint.2011.06.003
- Min, B., Kim, J., Oh, S., Regan, J. M., and Logan, B. E. (2005). Electricity generation from swine wastewater using microbial fuel cells. *Water Res.* 39, 4961–4968. doi: 10.1016/j.watres.2005.09.039
- Morris, J. M., and Jin, S. (2012). Enhanced biodegradation of hydrocarbon-contaminated sediments using microbial fuel cells. *J. Hazard. Mater.* 213, 474–477. doi: 10.1016/j.jhazmat.2012.02.029
- Morris, J. M., Jin, S., Crimi, B., and Pruden, A. (2009). Microbial fuel cell in enhancing anaerobic biodegradation of diesel. *Chem. Eng. J.* 146, 161–167. doi: 10.1016/j.cej.2008.05.028
- Myers, C. R., and Myers, J. M. (1992). Localization of cytochromes to the outer membrane of anaerobically grown *Shewanella putrefaciens* MR-1. *J. Bacteriol.* 174, 3429–3438. doi: 10.1128/jb.174.11.3429–3438.1992
- Narde, G. K., Kapley, A., and Purohit, H. J. (2004). Isolation and characterization of *Citrobacter* strain HPC255 for broad-range substrate specificity for chlorophenols. *Curr. Microbiol.* 48, 419–423. doi: 10.1007/s00284-003-4230-2
- Oh, S., Min, B., and Logan, B. E. (2004). Cathode performance as a factor in electricity generation in microbial fuel cells. *Environ. Sci. Technol.* 38, 4900–4904. doi: 10.1021/es049422p
- Oh, Y. K., Seol, E. H., Kim, J. R., and Park, S. (2003). Fermentative biohydrogen production by a new chemoheterotrophic bacterium *Citrobacter* sp. Y19. *Int. J. Hydrogen Energy* 28, 1353–1359. doi: 10.1016/S0360-3199(03)00024-7
- Olga, P., Petar, K., Jelena, M., and Srdjan, R. (2008). Screening method for detection of hydrocarbon-oxidizing bacteria in oil-contaminated water and soil specimens. *J. Microbiol. Methods* 74, 110–113. doi: 10.1016/j.mimet.2008.03.012
- Parameswaran, P., Bry, T., Popat, S. C., Lusk, B. G., Rittmann, B. E., and Torres, C. I. (2013). Kinetic, electrochemical, and microscopic characterization of the thermophilic, anode-respiring bacterium *Thermuncola ferriacetica*. *Environ. Sci. Technol.* 47, 4934–4940. doi: 10.1021/es400321c
- Park, H. S., Kim, B. H., Kim, H. S., Kim, H. J., Kim, G. T., Kim, M., et al. (2001). A novel electrochemically active and Fe (III)-reducing bacterium phylogenetically related to *Clostridium butyricum* isolated from a microbial fuel cell. *Anaerobe* 7, 297–306. doi: 10.1006/anae.2001.0399
- Pearce, C. I., Christie, R., Boothman, C., von Canstein, H., Guthrie, J. T., and Lloyd, J. R. (2006). Reactive azo dye reduction by *Shewanella* strain J18 143. *Biotechnol. Bioeng.* 95, 692–703. doi: 10.1002/bit.21021
- Pham, C. A., Jung, S. J., Phung, N. T., Lee, J., Chang, I. S., Kim, B. H., et al. (2003). A novel electrochemically active and Fe (III)-reducing bacterium phylogenetically related to *Aeromonas hydrophila*, isolated from a microbial fuel cell. *FEMS Microbiol. Lett.* 223, 129–134. doi: 10.1016/S0378-1097(03)00354-9
- Piröllo, M., Mariano, A., Lovaglio, R., Costa, S., Walter, V., Hausmann, R., et al. (2008). Biosurfactant synthesis by *Pseudomonas aeruginosa* LBI isolated from a hydrocarbon-contaminated site. *J. Appl. Microbiol.* 105, 1484–1490. doi: 10.1111/j.1365-2672.2008.03893
- Qiu, R., Zhang, B., Li, J., Lv, Q., Wang, S., and Gu, Q. (2017). Enhanced vanadium (V) reduction and bioelectricity generation in microbial fuel cells with biocathode. *J. Power Sources* 359, 379–383. doi: 10.1016/j.jpowsour.2017.05.099
- Qiu, R., Zhao, B., Liu, J., Huang, X., Li, Q., Brewer, E., et al. (2009). Sulfate reduction and copper precipitation by a *Citrobacter* sp. isolated from a mining area. *J. Hazard. Mater.* 164, 1310–1315. doi: 10.1016/j.jhazmat.2008.09.039
- Reguera, G., McCarthy, K. D., Mehta, T., Nicoll, J. S., Tuominen, M. T., and Lovley, D. R. (2005). Extracellular electron transfer via microbial nanowires. *Nature* 435, 1098–1101. doi: 10.1038/nature03661
- Röling, W. F., Head, I. M., and Larter, S. R. (2003). The microbiology of hydrocarbon degradation in subsurface petroleum reservoirs: perspectives and prospects. *Res. Microbiol.* 154, 321–328. doi: 10.1016/S0923-2508(03)00086-X
- Sambrook, J., Fritsch, E. F., and Maniatis, T. (1989). *Molecular Cloning*. New York, NY: Cold spring harbor laboratory press.
- Satapanajaru, T., Chompuchan, C., Suntornchot, P., and Pengthamkeerati, P. (2011). Enhancing decolorization of Reactive Black 5 and Reactive Red 198 during nano zerovalent iron treatment. *Desalination* 266, 218–230. doi: 10.1016/j.desal.2010.08.030
- Shen, J., Feng, C., Zhang, Y., Jia, F., Sun, X., Li, J., et al. (2012). Bioelectrochemical system for recalcitrant p-nitrophenol removal. *J. Hazard. Mater.* 209, 516–519. doi: 10.1016/j.jhazmat.2011.12.065
- Singh, A., Van Hamme, J. D., Kuhad, R. C., Parmar, N., and Ward, O. P. (2014). “Subsurface petroleum microbiology,” in *Geomicrobiol. Biogeochem*, N. Parmar and A. Singh eds (Berlin: Springer), 153–173.
- Singh, C., and Lin, J. (2008). Isolation and characterization of diesel oil degrading indigenous microorganisms in Kwazulu-Natal, South Africa. *Afr. J. Biotechnol.* 7, 1927–1932. doi: 10.5897/AJB07.728
- Sun, J., Hu, Y.-Y., Bi, Z., and Cao, Y.-Q. (2009). Simultaneous decolorization of azo dye and bioelectricity generation using a microfiltration membrane air-cathode single-chamber microbial fuel cell. *Bioresour. Technol.* 100, 3185–3192. doi: 10.1016/j.biortech.2009.02.002
- Tamura, K., Peterson, D., Peterson, N., Stecher, G., Nei, M., and Kumar, S. (2011). MEGA5: molecular evolutionary genetics analysis using maximum likelihood, evolutionary distance, and maximum parsimony methods. *Mol. Biol. Evol.* 28, 2731–2739. doi: 10.1093/molbev/msr121
- USEPA (1996). *Updates, I, II, IIIA and III: Test Methods for Evaluating Solid Wastes, Physical/Chemical Methods*, SW-846 Method 8015B-, 3rd Edn. Washington, DC: U.S. Government Printing Office.
- Venkidusamy, K., and Megharaj, M. (2016a). A novel electrophototrophic bacterium *Rhodopseudomonas palustris* strain RP2, exhibits hydrocarbonoclastic potential in anaerobic environments. *Front. Microbiol.* 7:1071. doi: 10.3389/fmicb.2016.01071
- Venkidusamy, K., and Megharaj, M. (2016b). Identification of electrode respiring, hydrocarbonoclastic bacterial strain *Stenotrophomonas maltophilia* MK2 highlights the untapped potential for environmental bioremediation. *Front. Microbiol.* 7:1965. doi: 10.3389/fmicb.2016.01965
- Venkidusamy, K., Megharaj, M., Marzorati, M., Lockington, R., and Naidu, R. (2016). Enhanced removal of petroleum hydrocarbons using a bioelectrochemical remediation system with pre-cultured anodes. *Sci. Total Environ.* 539, 61–69. doi: 10.1016/j.scitotenv.2015.08.098
- Venkidusamy, K., Megharaj, M., Schröder, U., Karouta, F., Mohan, S. V., and Naidu, R. (2015). Electron transport through electrically conductive nanofilaments in *Rhodopseudomonas palustris* strain RP2. *RSC Adv.* 5, 100790–100798. doi: 10.1039/C5RA08742B
- Wang, G., Zhang, B., Li, S., Yang, M., and Yin, C. (2017). Simultaneous microbial reduction of vanadium (V) and chromium (VI) by *Shewanella loihica* PV-4. *Bioresour. Technol.* 227, 353–358. doi: 10.1016/j.biortech.2016.12.070
- Wang, H., and Ren, Z. J. (2013). A comprehensive review of microbial electrochemical systems as a platform technology. *Biotechnol. Adv.* 31, 1796–1807. doi: 10.1016/j.biotechadv.2013.10.001
- Wang, J.-T., Chang, S.-C., Chen, Y.-C., and Luh, K.-T. (2000). Comparison of antimicrobial susceptibility of *Citrobacter freundii* isolates in two different time periods. *J. Microbiol. Immunol. Infect.* 33, 258–262.
- Weisburg, W. G., Barns, S. M., Pelletier, D. A., and Lane, D. J. (1991). 16S ribosomal DNA amplification for phylogenetic study. *J. Bacteriol.* 173, 697–703. doi: 10.1128/jb.173.2.697–703.1991
- Widdel, F., Boetius, A., and Rabus, R. (2006). “Anaerobic biodegradation of hydrocarbons including methane,” in *The prokaryotes*, eds M. Dworkin, S. Falkow, E. Rosenberg, K. H. Schleifer, and E. Stackebrandt (New York, NY: Springer), 1028–1049.
- Wrighton, K. C., Agbo, P., Warnecke, F., Weber, K. A., Brodie, E. L., DeSantis, T. Z., et al. (2008). A novel ecological role of the Firmicutes identified in thermophilic microbial fuel cells. *ISME J.* 2, 1146–1156. doi: 10.1038/ismej.2008.48
- Xing, D., Cheng, S., Logan, B. E., and Regan, J. M. (2010). Isolation of the exoelectrogenic denitrifying bacterium *Comamonas denitrificans* based on dilution to extinction. *Appl. Microbiol. Biotechnol.* 85, 1575–1587. doi: 10.1007/s00253-009-2240-0

- Xing, D., Zuo, Y., Cheng, S., Regan, J. M., and Logan, B. E. (2008). Electricity generation by *Rhodopseudomonas palustris* DX-1. *Environ. Sci. Technol.* 42, 4146–4151. doi: 10.1021/es800312v
- Xu, S., and Liu, H. (2011). New exoelectrogen *Citrobacter* sp. SX-1 isolated from a microbial fuel cell. *J. Appl. Microbiol.* 111, 1108–1115. doi: 10.1111/j.1365-2672.2011.05129.x
- Yan, Z., Song, N., Cai, H., Tay, J. H., and Jiang, H. (2012). Enhanced degradation of phenanthrene and pyrene in freshwater sediments by combined employment of sediment microbial fuel cell and amorphous ferric hydroxide. *J. Hazard. Mater.* 199, 217–225. doi: 10.1016/j.jhazmat.2011.10.087
- Zhi, W., Ge, Z., He, Z., and Zhang, H. (2014). Methods for understanding microbial community structures and functions in microbial fuel cells: a review. *Bioresour. Technol.* 171, 461–468. doi: 10.1016/j.biortech.2014.08.096
- Zhou, L., Deng, D., Zhang, D., Chen, Q., Kang, J., Fan, N., et al. (2016). Microbial electricity generation and isolation of exoelectrogenic bacteria based on petroleum hydrocarbon-contaminated soil. *Electroanalysis* 28, 1510–1516. doi: 10.1002/elan.201501052
- Zuo, Y., Xing, D., Regan, J. M., and Logan, B. E. (2008). Isolation of the exoelectrogenic bacterium *Ochrobactrum anthropi* YZ-1 by using a U-tube microbial fuel cell. *Appl. Environ. Microbiol.* 74, 3130–3137. doi: 10.1128/AEM.02732-07

Conflict of Interest Statement: The authors declare that the research was conducted in the absence of any commercial or financial relationships that could be construed as a potential conflict of interest.

The reviewer GZ and handling Editor declared their shared affiliation.

Copyright © 2018 Venkidusamy, Hari and Megharaj. This is an open-access article distributed under the terms of the Creative Commons Attribution License (CC BY). The use, distribution or reproduction in other forums is permitted, provided the original author(s) and the copyright owner are credited and that the original publication in this journal is cited, in accordance with accepted academic practice. No use, distribution or reproduction is permitted which does not comply with these terms.



Temporal Microbial Community Dynamics in Microbial Electrolysis Cells – Influence of Acetate and Propionate Concentration

Ananda Rao Hari^{1*}, Krishnaveni Venkidusamy², Krishna P. Katuri¹, Samik Bagchi³ and Pascal E. Saikaly^{1*}

¹ Biological and Environmental Sciences and Engineering Division, Water Desalination and Reuse Research Center, King Abdullah University of Science and Technology, Thuwal, Saudi Arabia, ² Centre for Environmental Risk Assessment and Remediation, University of South Australia, Mawson Lakes, SA, Australia, ³ Department of Civil, Environmental, and Architectural Engineering, University of Kansas, Lawrence, KS, United States

OPEN ACCESS

Edited by:

Yong Xiao,
Institute of Urban Environment (CAS),
China

Reviewed by:

Christin Koch,
Helmholtz-Zentrum für
Umweltforschung (UFZ), Germany
Zheng Chen,
Xi'an Jiaotong-Liverpool University,
China

*Correspondence:

Ananda Rao Hari
hari.anandaraao@kaust.edu.sa
Pascal E. Saikaly
pascal.saikaly@kaust.edu.sa

Specialty section:

This article was submitted to
Microbiotechnology, Ecotoxicology
and Bioremediation,
a section of the journal
Frontiers in Microbiology

Received: 15 February 2017

Accepted: 05 July 2017

Published: 20 July 2017

Citation:

Hari AR, Venkidusamy K, Katuri KP, Bagchi S and Saikaly PE (2017)
Temporal Microbial Community Dynamics in Microbial Electrolysis Cells – Influence of Acetate and Propionate Concentration.
Front. Microbiol. 8:1371.
doi: 10.3389/fmicb.2017.01371

Microbial electrolysis cells (MECs) are widely considered as a next generation wastewater treatment system. However, fundamental insight on the temporal dynamics of microbial communities associated with MEC performance under different organic types with varied loading concentrations is still unknown, nevertheless this knowledge is essential for optimizing this technology for real-scale applications. Here, the temporal dynamics of anodic microbial communities associated with MEC performance was examined at low (0.5 g COD/L) and high (4 g COD/L) concentrations of acetate or propionate, which are important intermediates of fermentation of municipal wastewaters and sludge. The results showed that acetate-fed reactors exhibited higher performance in terms of maximum current density (I : $4.25 \pm 0.23 \text{ A/m}^2$), coulombic efficiency (CE: $95 \pm 8\%$), and substrate degradation rate ($98.8 \pm 1.2\%$) than propionate-fed reactors (I : $2.7 \pm 0.28 \text{ A/m}^2$; CE: $68 \pm 9.5\%$; substrate degradation rate: $84 \pm 13\%$) irrespective of the concentrations tested. Despite of the repeated sampling of the anodic biofilm over time, the high-concentration reactors demonstrated lower and stable performance in terms of current density (I : 1.1 ± 0.14 to $4.2 \pm 0.21 \text{ A/m}^2$), coulombic efficiency (CE: 44 ± 4.1 to $103 \pm 7.2\%$) and substrate degradation rate (64.9 ± 6.3 to $99.7 \pm 0.5\%$), while the low-concentration reactors produced higher and dynamic performance (I : 1.1 ± 0.12 to $4.6 \pm 0.1 \text{ A/m}^2$; CE: 52 ± 2.5 to $105 \pm 2.7\%$; substrate degradation rate: 87.2 ± 0.2 to $99.9 \pm 0.06\%$) with the different substrates tested. Correlating reactor's performance with temporal dynamics of microbial communities showed that relatively similar anodic microbial community composition but with varying relative abundances was observed in all the reactors despite differences in the substrate and concentrations tested. Particularly, *Geobacter* was the predominant bacteria on the anode biofilm of all MECs over time suggesting its possible role in maintaining functional stability of MECs fed with low and high concentrations of acetate and propionate. Taken together, these results provide new insights on the microbial community dynamics and its correlation to performance in MECs fed with different concentrations of acetate and propionate, which are important volatile fatty acids in wastewater.

Keywords: microbial community dynamics, microbial electrolysis cells, acetate, propionate, *Geobacter*

INTRODUCTION

Microbial electrolysis cells (MECs) offer an alternative approach to effectively treat various organic waste streams with recovery of the inherent energy as hydrogen. In MECs, certain microorganisms known as exoelectrogens transport the electrons generated during the oxidation of organics in wastewater to the anode. The electrons and protons that are generated during oxidation at the anode are utilized at the cathode for H₂ evolution reaction through the addition of minimum voltage (0.6 V) to the circuit (Logan et al., 2008). Two new and important applications of MECs are: (1) the addition of electrodes directly into anaerobic digestion (AD), in order to improve performance and increase the methane concentration in the product gas (Guo et al., 2013; Feng et al., 2015a,b; Cai et al., 2016; Liu et al., 2016). Accumulation of volatile fatty acids (VFAs) such as acetate and propionate while treating high strength wastewater, is an important concern that leads to loss in methane production and process failure of methanogenic systems such as AD (Fernandez et al., 2000; Hashsham et al., 2000; Goux et al., 2015). For example, accumulation of propionate (>20 mM) at high organic loading rates is detrimental to methanogenic systems (Pullammanappallil et al., 2001; Gallert and Winter, 2008; Ma et al., 2009; Freguia et al., 2010). Thus, propionate removal is necessary for the stable operation of AD; and (2) integrating MECs to membrane bioreactors (MBRs), in what is referred to as anaerobic electrochemical MBR, for recovering energy and water from low strength wastewaters such as municipal wastewater (Katuri et al., 2014, 2016; Werner et al., 2016). In municipal wastewater, acetate and propionate represent the main VFAs, and their concentrations fluctuate resulting in a diverse and temporally fluctuating microbial communities. For MECs to become a viable anaerobic technology, it should adequately treat different concentrations (i.e., low and high) of acetate and propionate generated from various waste streams having different organic strength.

Anode-associated microorganisms are an important component of MECs. So far, attempts to integrate MECs to AD or MBRs have focused on the engineering aspects, reactor design and material optimization, with limited understanding of the microbial communities in the anode of MECs in response to different concentrations of acetate and propionate. Therefore, a deeper insight into the microbial community dynamics in response to different concentrations of acetate and propionate and linking it to system performance is needed. To date, most microbial studies in MECs were based on a single sampling event (typically at the end of the MEC operation) (Parameswaran et al., 2010; Lu et al., 2012b; Ruiz et al., 2014; Hari et al., 2016a,b), which provides little information on the electrochemical selection and development of microbial communities over time and how this is correlated to system performance. Nevertheless, very few studies examined the dynamics of microbial communities in MECs. For example, Lu et al. (2012a) observed a relatively similar anodic microbial community composition dominated by *Geobacter* and *Bacteroidetes* over a period of 125 days in MECs fed with acetate. Also, Kiely et al. (2011) showed that changing the operational environment

from microbial fuel cell (MFC) to MEC fed with potato wastewater, dairy wastewater or acetate favors a higher relative abundance of *Geobacter* due to lack of oxygen intrusion into the system. In MFCs oxygen intrusion to the anode from the aerobic cathode affects the microbial community structure and metabolic activity of anaerobic microorganisms (Shehab et al., 2013).

To the best of our knowledge, studies understanding the temporal dynamics of microbial communities in connection to reactor performance in MECs fed with low or high concentrations of acetate or propionate have not yet been performed. Therefore, the objective of this study was to examine the temporal dynamics of microbial communities in the anodes of MECs fed with low (0.5 g COD/L) or high concentration (4 g COD/L) of acetate or propionate and relating it with reactor performance. These two different concentrations of VFAs were chosen to mimic the low and high strength wastewater containing acetate and propionate (Pullammanappallil et al., 2001; Gallert and Winter, 2008; Ma et al., 2009; Freguia et al., 2010). To address this objective, well controlled laboratory MECs were operated for a period of 70 days. Microbial communities were sampled periodically during the 70 days of batch operation and characterized by 16S rRNA gene sequencing. In addition, reactor performance in terms of current density, coulombic efficiency (CE), and substrate removal rate was continuously monitored over time.

MATERIALS AND METHODS

Construction of MECs

Two chambered cube-shaped MECs (each chamber with a 20-mL working volume) were constructed as previously described (Hari et al., 2016a). The two chambers were separated by an anion exchange membrane (5 cm²; AMI 7001, Membranes International, Glen Rock, NJ, United States). A glass gas collection tube (15 mL) was attached to the top of both the anode and cathode chambers. Gasbags (0.1 L Cali -5 -Bond. Calibrate, Inc.) were connected to the top of the glass gas collection tubes to collect more volume of gas. The anodes were graphite fiber brushes (2.5 cm diameter × 2 cm long; PANEX 33 fibers, ZOLTEK Inc., St. Louis, MO, United States). The cathodes (projected surface area of 7 cm²) were made using carbon cloth (type B-1B, E-TEK) containing 0.5 mg/cm² of Pt (Santoro et al., 2013) on the side facing the anode, and four polytetrafluoroethylene diffusion layers on another side.

Enrichment and Operation

All MEC anodes were initially enriched in single chambered air-cathode MFCs as previously described (Call and Logan, 2008; Hari et al., 2016a) using anaerobic digester sludge (Manfouha Wastewater Treatment Plant, Riyadh, Saudi Arabia) as inoculum. Enrichment in air-cathode MFCs was done to avoid methanogenesis as oxygen intrusion through the cathode affects their growth (Hari et al., 2016a). The growth

medium (pH 8.9) consisted of bicarbonate buffer (80 mM), nutrients (6.71 g/L NaH₂CO₃, 0.31 g/L NH₄Cl, 0.05 g/L Na₂HPO₄, 0.03 g/L NaH₂PO₄), Wolfe's vitamin (10 mL/L) and trace mineral (10 mL/L) solutions (Ambler and Logan, 2011; Hari et al., 2016a,b). The medium was supplemented with two different concentrations (0.5 g COD/L or 4 g COD/L) of propionate or acetate as the energy and carbon source. The growth medium was boiled and then cooled to room temperature by sparging with N₂:CO₂ (80:20, vol/vol) gas mix for 30 min to remove any dissolved oxygen and was then autoclaved. The MFC anodes were transferred to individual MECs after three cycles of reproducible voltage (500 mV, over a 1 kΩ external resistor). Similar growth medium with different concentrations (0.5 g COD/L or 4 g COD/L) of propionate or acetate was used during MFC and MEC mode of operation. The duration of operation in MFC mode for the low concentration reactors (0.5 g COD/L) was ~8–15 days, and ~20–35 days for high concentration reactors (4 g COD/L).

A fixed voltage of 0.7 V was applied to the MECs using a power source (3645A, Array, Inc.). A total of eight MECs were operated in a parallel. Four MECs were fed only with acetate (referred to as A-reactors), and another four MECs were fed only with propionate (referred to as P-reactors). One set of duplicate MECs were operated with a low concentration of propionate (0.5 g COD/L, referred to as PL-reactors), a second set of duplicate MECs were operated with high propionate concentration (4 g COD/L, referred to as PH-reactors), a third set of duplicate MECs were operated with a low concentration of acetate (0.5 g COD/L, referred to as AL-reactors) and a fourth set of duplicate MECs were operated with high acetate concentration (4 g COD/L, referred to as AH-reactors). All reactor types (i.e., PL, PH, AL, and AH) were operated in a fed-batch mode in a temperature controlled room (30°C). When the current dropped to below 0.3 mA (PL ~36 h/cycle; PH ~4–5 days/cycle; AL ~26 h/cycle; AH ~4–5 days/cycle), the reactor solution was replaced with fresh medium and sparged with nitrogen gas (99.999%). The same growth medium was used in the anodic and cathodic compartments; however, propionate and acetate were only added to the anode medium.

Analyzes and Calculations

The current in the circuit was determined at 20 min intervals by measuring the voltage across a resistor (10 Ω) in the circuit using a data acquisition system (Model 2700; Keithley Instruments Inc.). The current density, I (A/m²) was calculated based on the projected cathode surface area. The concentrations of propionate and acetate were analyzed by high-performance liquid chromatograph (HPLC) (Thermo Scientific, Accela, United States) equipped with a photo-diode array (210 nm) and an ultraviolet detector. An Aminex HPX-87H column (Bio-Rad Laboratories, Hercules, CA, United States) was used to separate the VFAs. Sulfuric acid (5 mM) was used as the mobile phase at a flow rate of 650 μL/min, and the pressure was maintained at 9650 kPa. The total elution time was 30 min, and each sample was measured in triplicate, and

the average concentrations were reported (Lee et al., 2009). The performance of the MECs was evaluated by the current density of the reactor, I (A/m²); CE (%); substrate (propionate and acetate) removal (%) as previously described (Hari et al., 2016a,b).

16S rRNA Gene Sequencing

Over the course of the experiments, samples for microbial community analysis were periodically collected at different time periods (AL/PL: 0, 10, 30, 50, and 70 days; AH/PH: 0, 15/20, 35, and 70 days) from the anode and suspension of each reactor. Both biofilm and suspension samples were collected in an anaerobic glove box (Coy Laboratory Products Inc.), which was maintained under oxygen free environment. Day 0 for the anode samples represents the MFC anode that was transferred to individual MECs after three cycles of reproducible voltage (500 mV, over a 1 kΩ external resistor). The anode samples were collected by cutting about half of one round of the anode fibers using flame sterilized scissors. The graphite fiber brush anodes used in this study contained ten rounds of fiber brush (Supplementary Figure S1). At the end of the experiment, around ~20% (four sampling events for high substrate concentrations) to 25% (five sampling event for low substrate concentrations) of the total brush surface area have been sampled for microbial analysis. The suspension samples (5 mL) were collected by pipetting into a sterile centrifuge tube followed by centrifugation at 10,000 × g for 8 min. The supernatant was decanted and the pellet was stored at -80°C for further analyses. Genomic DNA was extracted using the PowerSoil DNA extraction kit (MO BIO Laboratories, Inc., Carlsbad, CA, United States) following the manufacturer's instructions. The quality (A₂₆₀/A₂₈₀) and quantity (A₂₆₀) of the extracted genomic DNA was determined using a NanoDrop 1000 spectrophotometer (Thermo Fisher Scientific, Waltham, MA, United States).

Triplicate PCR reactions were performed for each sample in a 25 μL reaction volume using the HotStarTaq Plus Master Mix (Qiagen, Valencia, CA, United States) containing Hot Start Taq DNA polymerase (5 units/μL), 400 μM of each dNTP, 10× PCR buffer containing 3 mM MgCl₂, 0.5 μM of each primer, and 100–200 ng of template DNA. The Bacterial (V3–V4 region) and archaeal (V3–V6 region) 16S rRNA genes were amplified using domain specific primer sets (Klindworth et al., 2012): 341F (5'-Lib-L/A-Key-Barcode-CA Linker-CCTACGGGNGGCWGCAG-3') and 785R (5'-Lib-L/A-Key-TC Linker-GACTACHVGGGTATCTAATCC-3') for the domain Bacteria; and 519F (5'-Lib-L/A-Key-Barcode-CA Linker-CAGCMGCCGCGGTAA-3') and 1041R (5'-Lib-L/A-Key-TC Linker-GGCCATGCACCWCCTCTC-3') for the domain Archaea. A unique 8-bp error-correcting barcode was used to tag each PCR product. PCR was performed using a C1000 Thermal Cycler (Bio-Rad, Hercules, CA, United States). For bacteria, the PCR conditions were as follows: initial denaturation at 95°C for 5 min, followed by 27 cycles of denaturation at 94°C for 1 min, annealing at 56°C for 1 min, extension at 72°C for 1 min and a final extension at 72°C for 7 min. For

archaea, the PCR conditions were as follows: denaturation at 95°C for 5 min, followed by 35 cycles of denaturation at 94°C for 1 min, annealing at 55°C for 1 min, extension at 72°C for 1 min and a final extension at 72°C for 10 min (Klindworth et al., 2012).

The triplicate PCR products from each sample were pooled and then loaded on agarose gel and purified using the Qiaquick gel extraction Kit (Qiagen, Valencia, CA, United States) according to the manufacturer's protocol. The concentration of the PCR products was measured with a Qubit® 2.0 Fluorometer using the PicoGreen® dsDNA quantitation assay (Invitrogen, Carlsbad, CA, United States). The purified barcoded amplicons from each sample were pooled in equimolar concentration and sequenced on the Roche 454 FLX Titanium genome sequencer (Roche, Indianapolis, IN, United States) according to manufacturer's instructions.

The bacterial and archaeal 16S rRNA sequences were processed using the Quantitative Insights Into Microbial Ecology (QIIME v 1.9.0) pipeline (Caporaso et al., 2010b). Raw reads were first demultiplexed, trimmed and filtered for quality. The minimum acceptable length was set to 200 bp (Caporaso et al., 2010b). Sequences were clustered into operational taxonomic units (OTUs) at 97% sequence similarity using the uclust algorithm (Edgar, 2010). A representative sequence from each OTU was aligned using PyNAST (Caporaso et al., 2010a), and these were phylogenetically assigned to a taxonomic identity using the RDP Naive Bayesian rRNA classifier at a confidence threshold of 80% (Wang et al., 2007). Chimeric sequences were identified and removed from the aligned sequences using Chimera Slayer as implemented in QIIME. Rarified OTU tables were used to generate alpha and beta diversity metrics by normalizing to the lowest sequence read (4,100 sequences) between the samples. For alpha diversity measurements, both non-phylogenetic based metrics (observed OTUs, Shannon diversity index (H) and Chao 1 richness estimator) and phylogenetic based metric (phylogenetic diversity (PD_whole)) were calculated with QIIME. Temporal variation of bacterial community was analyzed by non-metric multidimensional scale (NMDS) using PRIMER 6 software (version 6.1.13) and PERMANOVA+ add-on (version 1.0.3). NMDS ordination was generated based on Bray–Curtis matrix (beta diversity) in QIIME. Phylogenetic diversity of abundant bacterial taxa was visualized in a heatmap using PRIMER 7 software.

Statistical Analyses

Statistical methods were used to determine the similarity in bacterial community structure among samples. Temporal variation of bacterial community was analyzed by NMDS which was performed with Bray–Curtis matrix using QIIME and statistical software PRIMER 6 (version 6.1.13) and PERMANOVA+ add-on (version 1.0.3). Analysis of similarity (ANOSIM) was used to determine if the differences among samples is statistically significant using Bray–Curtis measure of similarity (QIIME), where the R -value ranges between 0 (complete similarity) to 1 (complete separation). Student's t -test was performed in Microsoft Excel for all the comparisons.

Nucleotide Sequence Accession Numbers

The 16S r RNA gene sequencing reads have been deposited in European Nucleotide Archive under the accession number PRJEB19042.

RESULTS

Performance of MECs at Low and High Concentrations of Acetate and Propionate

A-reactors showed a higher maximum current density ($4.25 \pm 0.23 \text{ A/m}^2$) than P-reactors ($2.7 \pm 0.28 \text{ A/m}^2$) ($P \leq 0.05$, Student's t -test for all comparisons) irrespective of the concentrations tested (Figure 1). Also, A-reactors displayed a short lag time of 5–10 days (Figures 1A,B), whereas, P-reactors exhibited delayed startup of 10–20 days to reach maximum current density (Figures 1A,B). High concentration reactors showed relatively stable current density irrespective of the substrate tested (Figure 1B), while it was dynamic in the low concentration reactors (Figure 1A). For instance, in PL reactors, the maximum current density increased from 1 A/m^2 on day 2 to 2.3 A/m^2 on day 10 followed by a decrease in

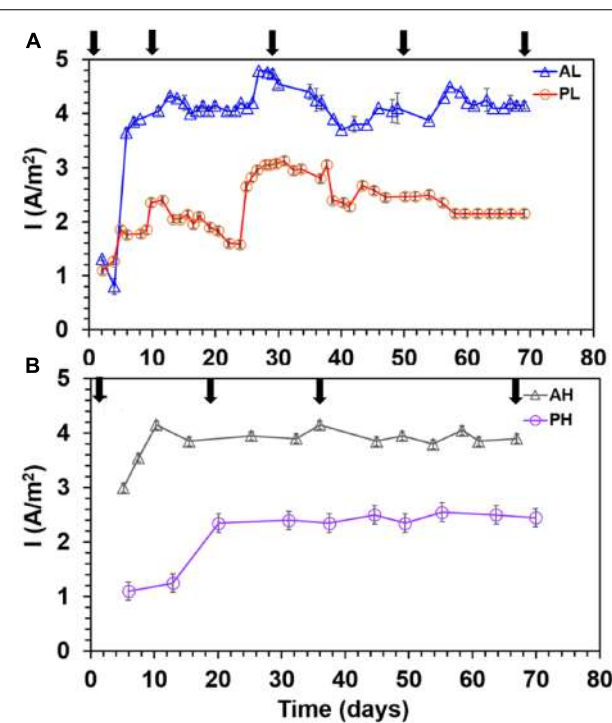


FIGURE 1 | Maximum current density profile in duplicate MECs fed with low and high concentrations of acetate and propionate. **(A)** MECs fed with low substrate concentration; **(B)** MECs fed with high substrate concentration. Arrows indicate anode biofilm sampling for DNA extraction. Each data point represents the average (duplicate reactors) of the maximum current density recorded in each batch test.

the maximum current density of 1.5 A/m^2 on day 22. Then maximum current density of 3.3 A/m^2 was reached on day 23 and remained steady until day 35 of operation (**Figure 1A**). Furthermore, it relatively decreased to 2.2 A/m^2 in the next 4 days and eventually reached a stable electrical current of 2.5 A/m^2 until the termination of the experiment on day 70. Cutting a portion of the anode fibers at each sampling event caused a decline in electrical current production in the low concentration reactors irrespective of the substrate tested (**Figure 1A** and Supplementary Figures S2A,C). However, high concentration reactors showed stable performance despite of the sampling event (**Figure 1B** and Supplementary Figures S2B,D). It should be noted that the MECs were operated at a fixed voltage of 0.7 V and the resulting anode potential was $-0.23 \pm 0.09 \text{ V}$ vs. SHE (P-reactors) and $\sim -0.15 \pm 0.1 \text{ V}$ vs. SHE (A-reactors).

The average CE (%) for the whole period (i.e., 70 days) of operation of the MECs was: AL ($96.7 \pm 9\%$), AH ($93 \pm 5\%$), PL ($73 \pm 9\%$), and PH ($63 \pm 8\%$) (**Figure 2**). The A-reactors yielded higher CE ($95 \pm 8\%$) than the P-reactors ($68 \pm 9.5\%$) ($P \leq 0.05$). Particularly, the CE of few batches of A-reactors were $>100\%$ (**Figure 2**). Furthermore, the CE in the A-reactors was more stable in comparison to the P-reactors (**Figure 2**). Irrespective of the substrate tested, low concentration reactors (AL/PL: $86 \pm 10\%$) produced a relatively higher CE than the high concentration reactors (AH/PH: $78 \pm 7.5\%$) ($P \leq 0.05$) (**Figure 2**).

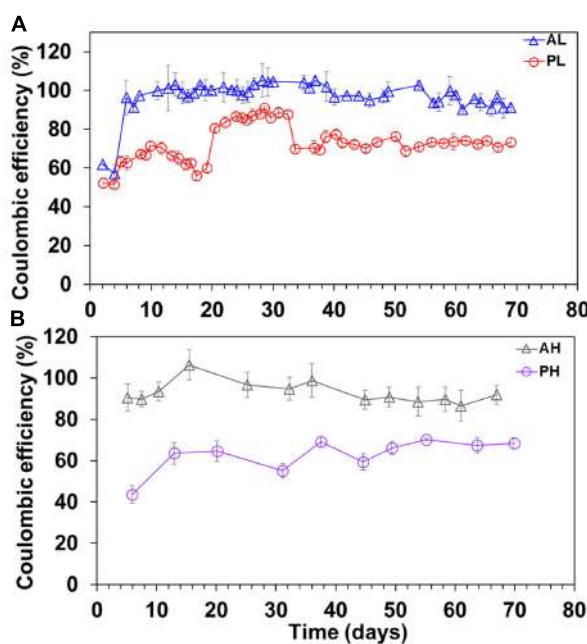


FIGURE 2 | Coulombic efficiency (CE) in duplicate MECs fed with low and high concentrations of acetate or propionate. **(A)** MECs fed with low acetate concentration (AL); **(B)** MECs fed with high acetate concentration (AH); **(A)** MECs fed with low propionate concentration (PL); **(B)** MECs fed with high propionate concentration (PH). The values correspond to the average of the duplicate reactors. Each data point represents the average (duplicate reactors) of the CE recorded in each batch test.

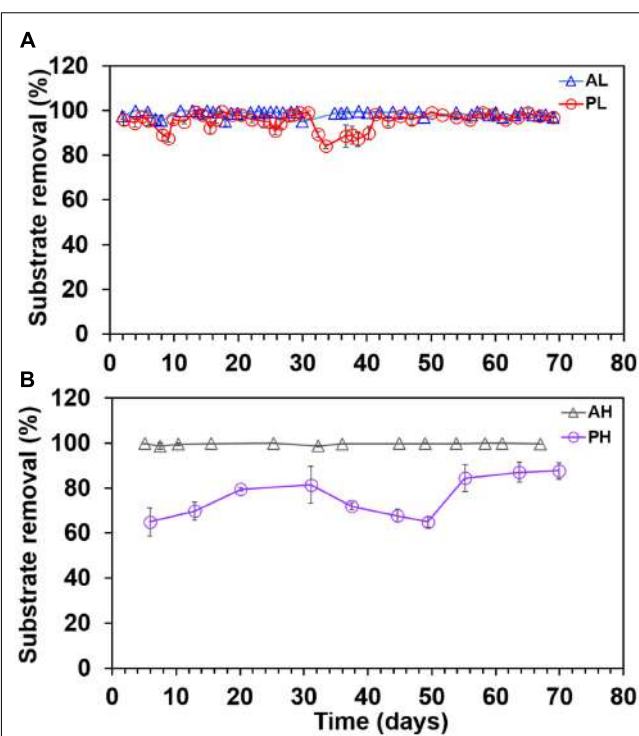


FIGURE 3 | Substrate removal trend in duplicate MECs fed with low and high concentrations of acetate and propionate. **(A)** MECs fed with low acetate concentration (AL); **(B)** MECs fed with high acetate concentration (AH); **(A)** MECs fed with low propionate concentration (PL); **(B)** MECs fed with high propionate high (PH). Each data point represents the average (duplicate reactors) of substrate removal recorded in each batch test.

Substrate removal was nearly complete in A-reactors ($98.8 \pm 1.2\%$) with no significant difference between AL and AH-reactors ($P > 0.2$) (**Figures 3A,B**), whereas, variable percentage of substrate removal was noticed in P-reactors (PL: $93 \pm 8.6\%$; PH: $75 \pm 14\%$) (**Figures 3A,B**). The substrate removal rates (g COD/L/Day) were, for AL (0.33 ± 0.05), AH (0.90 ± 0.14), PL (0.27 ± 0.06), and PH (0.46 ± 0.05) reactors. Also, the pH of the medium was 7.6 ± 0.5 in A- and P-reactors at the end of fed-batch cycle.

The error bars in **Figure 2** were relatively bigger than **Figures 1, 3** because several data points (every 20 min of batch time) from each batch test were used to calculate the CE, whereas one data point was used to determine the maximum current density and substrate removal for each batch cycle.

Microbial Community Analysis

16S rRNA gene sequencing was used to characterize the bacterial and archaeal communities of anode and suspension samples from duplicate MEC reactors (AL, AH, PL, and PH). A total of 1,066,983 (bacteria) and 503,327 (archaea) high quality reads (average length of $\sim 400 \text{ bp}$) were obtained after denoising, quality filtering, and removal of chimeric sequences. For downstream analysis, OTUs with 97% sequence identity threshold were used.

Bacterial Community Diversity

For alpha diversity measures, we subsampled the dataset to an even depth of 4,100 sequences across the samples to remove inherent heterogeneity of sampling depth. This number was chosen, as it corresponds to the lowest number of sequence reads detected. The diversity values across the anode and suspension samples of A- and P-reactors ranged as follows: observed OTUs (74–1225), Chao 1 (216–3465), Shannon diversity index (H; 2.2–6.9), and phylogenetic diversity (PD; 12–79) (**Tables 1, 2**). The bacterial diversity was higher in the anode and suspension

of P-reactors than A-reactors based on observed OTUs, Chao 1, PD and H (**Tables 1, 2**). Also, the high concentration-fed reactors (AH/PH) revealed a higher diversity than low concentration-fed reactors (AL/PL) (**Tables 1, 2**). Time series analysis of A-reactors indicated that bacterial diversity of anode and suspension samples was higher on day 0 (i.e., MFC mode of operation) and considerably reduced at the end of the experiment (i.e., day 70) (**Table 1**). Likewise, the P-reactors, particularly, PH-reactors showed a similar trend on day 0 (anode and suspension), and relatively decreased at the end of the experiment (**Table 2**).

TABLE 1 | Measures of alpha diversity of bacterial phylotypes in acetate reactors.

Sample	Chao1	Observed OTUs	PD index	Shannon diversity index
A_AL_0	808 ± 100	238 ± 12	29 ± 1.7	5.3 ± 0.12
A_AL_10	216 ± 71	74 ± 4	12 ± 0.8	2.18 ± 0.08
A_AL_30	262 ± 73	79 ± 6	12 ± 0.8	2.39 ± 0.08
A_AL_50	223 ± 74	85 ± 8	13 ± 0.8	2.82 ± 0.07
A_AL_70	274 ± 41	119 ± 4	17 ± 0.8	5.05 ± 0.05
S_AL_0	547 ± 72	213 ± 9	26 ± 1.2	5.64 ± 0.09
S_AL_10	274 ± 56	95 ± 4	12 ± 0.8	3.69 ± 0.06
S_AL_30	271 ± 80	102 ± 8	13 ± 1	3.88 ± 0.07
S_AL_50	298 ± 88	107 ± 6	16 ± 1	4.39 ± 0.09
S_AL_70	128 ± 9	85 ± 1	12 ± 0.1	4.33 ± 0.01
A_AH_0	906 ± 169	244 ± 15	30 ± 1.6	5.54 ± 0.11
A_AH_15	745 ± 125	217 ± 10	24 ± 1.6	4.99 ± 0.10
A_AH_35	404 ± 83	159 ± 7	21 ± 0.9	4.9 ± 0.09
A_AH_70	559 ± 81	188 ± 8	21 ± 1.1	4.78 ± 0.07
S_AH_0	628 ± 107	225 ± 9	27 ± 1.4	5.63 ± 0.06
S_AH_15	765 ± 126	235 ± 8	26 ± 1.2	5.54 ± 0.07
S_AH_35	551 ± 109	191 ± 8	22 ± 0.7	5.74 ± 0.05
S_AH_70	435 ± 28	181 ± 5	18 ± 0.5	4.51 ± 0.06

A, anode; S, suspension.

TABLE 2 | Measures of alpha diversity of bacterial phylotypes in propionate reactors.

Sample	Chao1	Observed OTUs	PD index	Shannon diversity index
A_PL_0	1948 ± 125	560 ± 20	46 ± 2	6.03 ± 0.07
A_PL_10	1364 ± 225	385 ± 12	33 ± 2	4.92 ± 0.11
A_PL_30	1062 ± 122	341 ± 11	30 ± 1	4.18 ± 0.07
A_PL_50	1370 ± 82	399 ± 4	34 ± 0.5	5.03 ± 0.02
A_PL_70	1820 ± 121	543 ± 7	44 ± 0.7	6.4 ± 0.02
S_PL_0	2511 ± 347	641 ± 10	51 ± 2	6.8 ± 0.04
S_PL_10	1467 ± 100	446 ± 6	38 ± 0.7	5.9 ± 0.09
S_PL_30	1046 ± 131	365 ± 10	31 ± 1	4.74 ± 0.06
S_PL_50	1664 ± 24	568 ± 1	44 ± 0.05	6.79 ± 0.004
S_PL_70	1969 ± 252	524 ± 15	45 ± 2	6.12 ± 0.14
A_PH_0	3465 ± 265	1225 ± 14	75 ± 2	6.5 ± 0.04
A_PH_20	2858 ± 172	1051 ± 18	65 ± 1	6.2 ± 0.06
A_PH_35	2415 ± 190	887 ± 15	57 ± 0.8	5.5 ± 0.04
A_PH_70	2395 ± 227	899 ± 18	58 ± 1.5	5.6 ± 0.04
S_PH_0	2496 ± 117	1065 ± 15	65 ± 1	6.84 ± 0.07
S_PH_20	2885 ± 14	1032 ± 1	62 ± 0.03	6.26 ± 0.04
S_PH_35	2029 ± 110	899 ± 23	54 ± 2	6.81 ± 0.04
S_PH_70	1607 ± 171	625 ± 15	41 ± 1	4.42 ± 0.02

A, anode; S, suspension.

In contrast, PL-reactors (anode and suspension) revealed that the bacterial diversity was higher on day 0 and significantly reduced with time until day 50 ($P < 0.05$), followed by an increase in diversity on day 70 (Table 1). No clear trend could be observed for propionate-fed MECs when comparing alpha diversity between anode and suspension samples. For example, in PL reactors, the diversity of suspension samples was higher than anode samples, whereas in PH MECs diversity was higher in the anode than suspension samples for all the sampling periods (Table 2). In contrast, a clear trend in diversity was observed in AL and AH reactors, where diversity was higher in suspension than anode samples for all the sampling periods except day 70 (Table 1).

Bacterial Community Structure

Non-metric multidimensional scaling analysis based on Bray-Curtis revealed that all the samples (anode and suspension) had a gradual succession away from the initial conditions and a relatively similar pattern of succession was observed between low and high concentration-fed reactors (Figure 4). However, the development and succession paths of anodic bacterial communities were different between A- and P-reactors (Figure 4). For example, A-reactors showed that all the anodes (AL: 10, 30, 50, and 70 days; AH: 15, 35, and 70 days) were clustered together and distantly away from the initial anode samples (0 days) (Figures 5A,B). In contrast, P-reactors showed that the anode samples (PL: 10, 30, and 50; PH: 20 and 35 days) were clustered together and away from the anode sample at day 70 (Figures 4C,D). Also, NMDS results showed that the temporal

variation in the bacterial community structure was higher for the suspension samples (A- and P- reactors) than the anode samples as can be seen by their wider distribution in the ordination plot (Figure 4). Temporal variation in the microbial community structure within the suspension samples (different sampling points) was significant ($p = 0.0001$, $R = 0.6357$) as confirmed by ANOSIM. Whereas, lower temporal variation was obtained in the microbial community structure within biofilm samples ($p = 0.003$, $R = 0.2243$). Statistically significant difference between the anode and suspension microbial community structure was found using ANOSIM ($p = 0.0001$, $R = 0.7283$).

Bacterial Community Composition and Dynamics

A heatmap was generated to represent the various phylotypes identified from the A- and P-reactors down to the lowest classification level possible (class, order, family, or genus) (Figure 5 and Supplementary Tables S1–S4). Highly abundant phylotypes belonging to the different detected bacterial classes are discussed below:

*Delta*proteobacteria

Four phylotypes belonging to the class *Delta*proteobacteria were relatively abundant in the A- and P-reactors (Figure 5 and Supplementary Tables S1–S4). Among *Delta*proteobacteria, *Geobacter* was highly dominant over time (10 to 70 days) in the anode of A- and P-reactors (Figure 5A,C). *Geobacter* was detected in very low fraction (<1%) in the A-reactors at day 0. However, it became highly dominant (AL: $52 \pm 13\%$; AH: $49 \pm 4\%$) over time (10 to 70 days) (Figure 5A). The relative

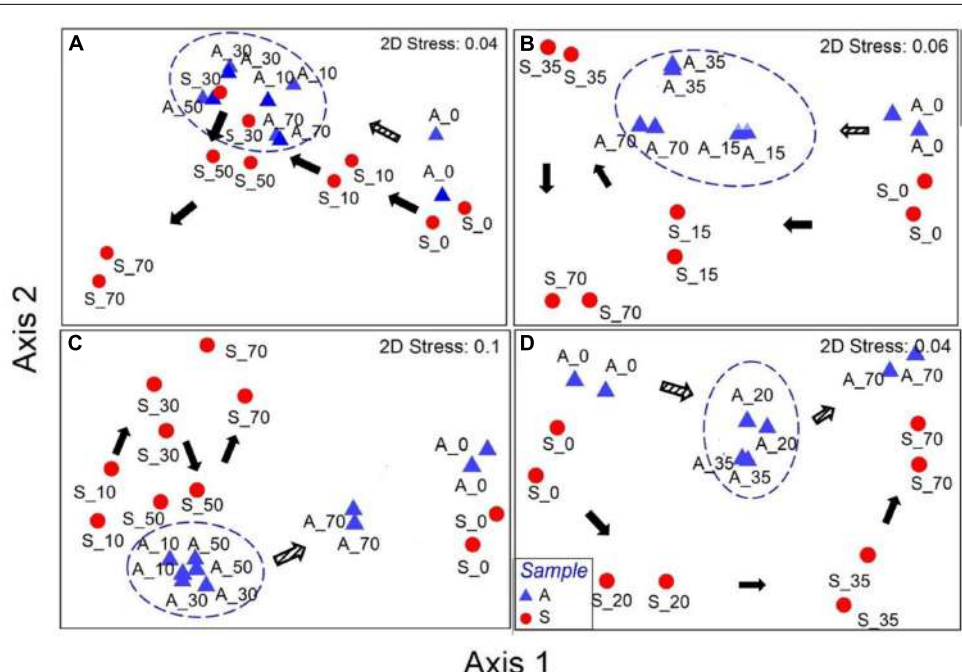


FIGURE 4 | Non-metric multidimensional scaling plots based on Bray-Curtis distance for **(A)** AL, **(B)** AH, **(C)** PL, and **(D)** PH reactors. A, anode and S, suspension. The numbers after the symbols represent the sampling day (AL/PL: days 0, 10, 30, 50, and 70; AH/PH: days 0, 15/20, 35, and 70). Duplicate samples are shown as individual data points in the plots. Circles were manually drawn to represent the clusters of converging anodic bacterial community over time. Arrows indicate the pattern of evolution in the microbial community from day 0. Unfilled and filled arrows represent the anode and suspension samples, respectively.

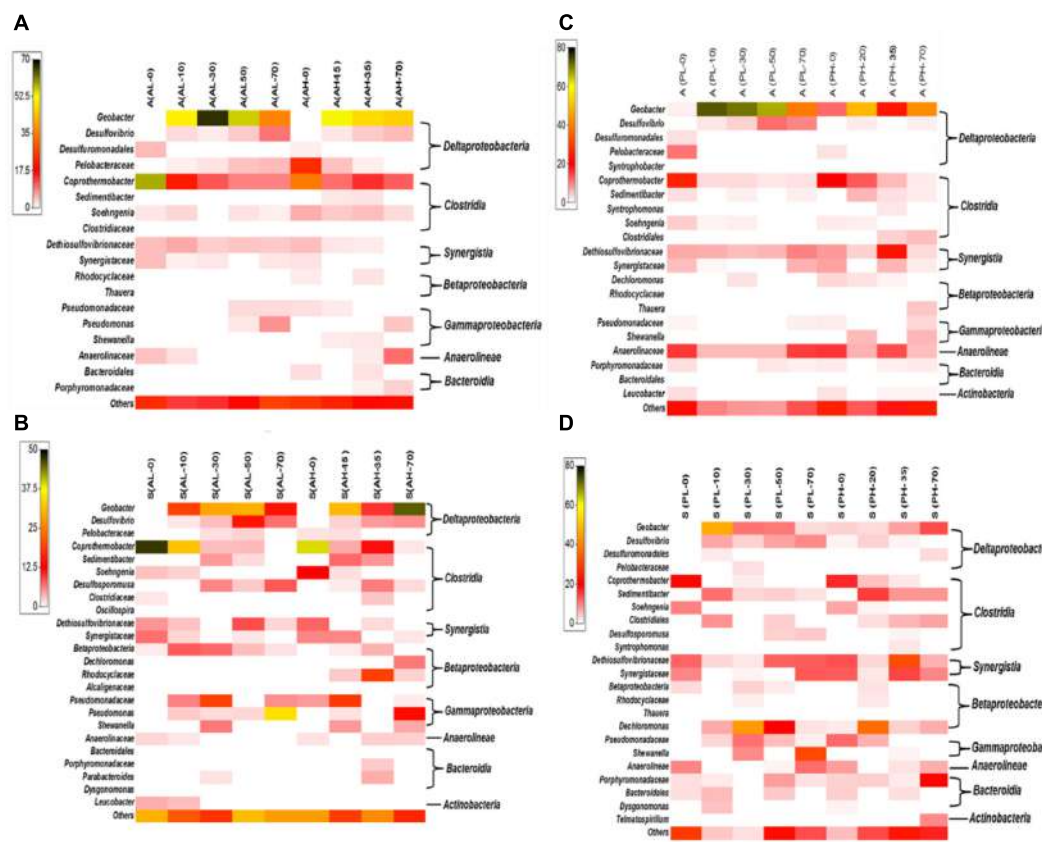


FIGURE 5 | Heat map distribution of bacterial phylotypes classified to the lowest level possible (class, order, family or genus) for A- and P- reactors: anode of A-reactors (**A**), suspension of A-reactors (**B**), anode of P-reactors (**C**) and suspension of P-reactors (**D**). A, anode and S, suspension. Bacterial phyla representing less than 1% of the relative abundance are classified as others. The taxa level shown on the left-hand side of the panel represents the lowest classification level possible (order, family or genus), while the taxa level on the right-hand side represents class. Scale on top left-side of each panel is relative abundance (%). Each cell represents the average of duplicate reactors. Each column represents a specific sampling period (AL/PL: days 0, 10, 30, 50, and 70; AH/PH: days 0, 15/20, 35, and 70). Day 0 represents the MFC anode that was transferred to individual MECs after three cycles of reproducible voltage.

abundance of *Geobacter* in the anode of P-reactors was different between low and high concentration-fed reactors (Figure 5C). For example, its relative abundance was $1.4 \pm 0.5\%$ at day 0 of PL-reactors, and it significantly increased to reach $70 \pm 3.4\%$ between days 10 and 50 days followed by a significant decrease to $39 \pm 2.3\%$ ($P < 0.05$) on day 70 (Figure 5C). In contrast, PH-reactors revealed that the relative abundance of *Geobacter* was dynamic over time (Figure 5C). For instance, the relative abundance of *Geobacter* was $11.5 \pm 1.8\%$ on day 0 and increased to $48.7 \pm 6.1\%$ on day 20 (Figure 5C). Following operation at day 35, the relative abundance of *Geobacter* was drastically reduced to $23.3 \pm 2.7\%$, but it increased again to reach $41.9 \pm 6.2\%$ on day 70. The higher abundance of *Geobacter* at day 0 in the PH reactors was due to the relatively longer period of operation (35 days) compared to AL (8 days), AH (20 days), and PL (15 days) reactors. Collectively, the above results show that electrochemical selection of *Geobacter* significantly enhanced in MEC mode of operation as evidenced by the significant increase in their relative abundance after day 0 (Supplementary Tables S1–S4). The suspensions of A- and P-reactors revealed that the relative abundance of *Geobacter* was dynamic over time (3–45%)

(Figures 5B,D). *Desulfovibrio* was relatively identified in all the samples of A- and P-reactors (1–14%) (Figure 5). *Pelobacteraceae* was relatively more abundant in the anode of A-reactors (1–23%) than P-reactors (2–11%). *Desulfuromonadales* was present during the early stages of A- and P-reactors (1–5%) (Figure 5).

Clostridia

Seven phylotypes belonging to the class *Clostridia* were frequently observed in all the samples of A- and P-reactors (Figure 5). *Copotermobacter* was highly abundant in A-reactors than P-reactors (Figure 5). Specifically, it was abundant during earlier stages of reactor operation (between day 0 and 20) (A-reactors: $45 \pm 11\%$; P-reactors: $22 \pm 3.5\%$) and was significantly reduced during later stages of reactor operation (days 50 and 70) (A-reactors: $7.7 \pm 5\%$; P-reactors: $2.5 \pm 1.7\%$) ($P < 0.05$) (Figures 5A,). *Sedimentibacter* was relatively abundant over time in the P-reactors (1–14%) than A-reactors (2–7%). Particularly, it was more prevalent in the suspension than the anode of A- and P-reactors. *Sohengenia* was present in the anode of A-reactors over time (1–6%), and it was present only during the early stages of operation in the P-reactors (1–9%). *Syntrophomonas* was

present only in the anode of PH-reactors (2%). *Desulfosporomusa* was observed only in the suspension. Specifically, it was more prevalent in the A- reactors (1–8%) than P-reactors (1–4%) (**Figure 5**).

Synergistia

Two different phylotypes (*Dethiosulfovibrionaceae* and *Synergistaceae*) belonging to the class *Synergistia* were consistently observed in the A- and P-reactors over time (**Figure 5**). Specifically, *Dethiosulfovibrionaceae* was dominant throughout the operation of the P-reactors (anode and suspension) than A-reactors (**Figures 5C,D**). In addition, *Synergistaceae* was found to be dominant in the suspension than the anode of A- and P-reactors (**Figures 5B,D**).

Betaproteobacteria

Four different phylotypes belonging to the class *Betaproteobacteria* were observed in the samples of A- and P-reactors (**Figure 5**). *Dechloromonas* was considerably abundant in the suspension of P-reactors over time (2–41%). *Rhodocyclaceae* was relatively abundant (3–19%) in the suspension of AH-reactors over time (**Figure 5B**).

Gammaproteobacteria

Three different phylotypes (*Pseudomonas*, *Pseudomonadaceae*, and *Shewanella*) belonging to the class *Gammaproteobacteria* were observed in the A- and P-reactors (**Figure 5**). Specifically, *Pseudomonas* and *Pseudomonadaceae* were relatively dominant over time in the A-reactors than the P-reactors (**Figure 5**). *Shewanella* was noticed as a minor fraction in the A- and P-reactors (**Figure 5**). However, it was more prevalent (29 ± 2.5%) in the suspension of PL-reactors on day 70 (**Figure 5D**).

Bacteroidia

Four different phylotypes of the class *Bacteroidia* (*Dysgonomonas*, *Bacteroidales*, *Porphyromonadaceae*, and *Parabacteroides*) were noticed in the A- and P-reactors (**Figure 5**). *Porphyromonadaceae* and *Bacteroidales* were relatively more dominant in the P-reactors (7 ± 4%) than the A-reactors (3 ± 0.4%) (**Figure 5**), particularly it was more prevalent in the suspension than the anode of the P-reactors (**Figure 5D**). *Parabacteroides* was present only in the suspension of A-reactors (**Figure 5B**).

Anaerolineae

Only one phylotype of the class *Anaerolineae* namely *Anaerolinaceae* was observed in the A- and P-reactors (**Figure 5**). It was more abundant (3–16%) in the P-reactors than the A-reactors. Specifically, it was more dominant in the anode than the suspension of P-reactors (**Figures 5C,D**).

Archaeal Community Composition and Dynamics

Archaeal 16S rRNA gene sequences revealed the dominance of *Methanobacteriaceae* (74.5 ± 13%) (hydrogenotrophic methanogens) in all the samples (anode and suspension) of A- and P-reactors (Supplementary Figure S3). Particularly, the most abundant genera was *Methanobacterium* in all the samples of A-reactors (65 ± 13%) (Supplementary Figures S3A,B) and the anode of P-reactors (57 ± 15%) (Supplementary

Figure S3C). Whereas, *Methanobrevibacter* was more abundant in the suspension of P-reactors (61 ± 12%) (Supplementary Figure S3D).

Temporal analysis of archaeal 16S rRNA gene sequences of A-reactors revealed the predominance of *Methanobacterium* (65 ± 13%) over time followed by *Methanobrevibacter* (10 ± 6%), *Thermoplasmata* (WCHD3-02) and *Crenarchaeota* (MCG) (excluding days 0 and 10 of AL-reactor samples which failed to amplify) (Supplementary Figures S3A,B). Also, A-reactors contained a minor fraction of unclassified *Methanobacteriaceae*, *Methanospirillum*, *Methanosarcina*, and *Methanosaeta*. In contrast, temporal analysis of the archaeal community of P-reactors displayed that the anodes were dominated by the hydrogenotrophic methanogens, *Methanobacterium* (PL: 51 ± 12%; PH: 64 ± 18%) followed by acetoclastic methanogens, *Methanosaeta* (PL: 10 ± 6%; PH: 14 ± 4%) (Supplementary Figure S3C). In addition, other sub-dominant communities were observed namely unclassified *Methanobacteriaceae*, *Methanobrevibacter*, *Methanospirillum*, *Methanosarcina*, and *Thermoplasmata* (WCHD3-02). *Methanobrevibacter* (PL: 64 ± 15%; PH: 60 ± 14%) was dominant in the suspension samples of P-reactors followed by *Methanobacterium* (PL: 12 ± 8%; PH: 25 ± 15%) (Supplementary Figure S3D).

DISCUSSION

The results gathered in this study demonstrated that A-reactors produced greater performance than the P-reactors in terms of current density, CE, and substrate removal efficiency regardless of the concentrations tested (**Figures 1–3**). Acetate in the A-reactors can be directly consumed by *Geobacter* for electricity generation, whereas, in the P-reactors, electricity generation requires microbial partnership between propionate degraders and intermediate consumers (e.g., *Geobacter*) resulting in more loss of electrons to various other competing electron sinks [biomass synthesis and production of soluble microbial products (SMPs)] as previously described (Lee et al., 2008; Ishii et al., 2014; Vanwonterghem et al., 2014; Hari et al., 2016a,b). In addition, A-reactors produced CEs greater than 100% in some of the batches (**Figures 2A,B**) possibly due to (1) H₂ cycling from the cathode to the anode (Lee et al., 2009; Siegert et al., 2014; Zhu et al., 2014); (2) oxidation of intracellular biopolymers such as polyhydroxyalkanoates (Koch et al., 2014); or (3) utilization of stored energy in the cells (Siegert et al., 2014). In general, high concentration reactors (AH/PH) exhibited lower reactor performance in terms of maximum current density and CE (**Figures 1, 2**) than the low concentration reactors (AL/PL), possibly due to loss of electrons to other competing electron sinks as described previously (Hari et al., 2016a,b). Nevertheless, high concentration reactors (AH/PH) showed stable (reproducible) performance, despite repeated disturbance of the anode biofilm over time for sampling. The effect of disturbance caused by frequent sampling was more pronounced in AL and PL reactors where reduction in current density was observed followed by recovery to maximum current density in a short period (**Figure 1** and Supplementary Figure S2). This suggests the

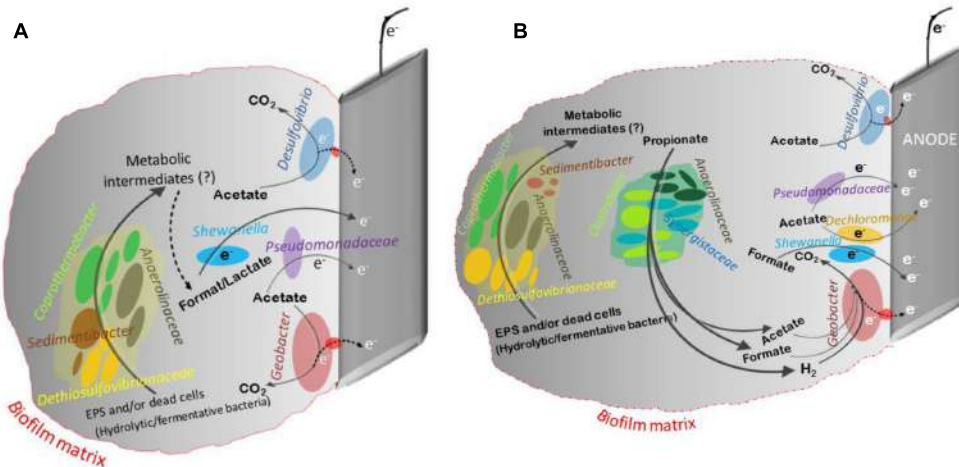


FIGURE 6 | A schematic describing the potential key members in the community and their interaction in the anode of MECs fed with acetate (**A**) or propionate (**B**). This schematic was developed based on the available information from the literature on the microbial communities. Members of *Geobacter*, *Shewanella* (Luo et al., 2017), *Desulfovibrio* and *Pseudomonadaceae* spp. are known to use the anode as their electron acceptor (Koch and Harnisch, 2016). The presence of complex carbohydrates and proteins in the extracellular polymeric substances (EPS) and/or endogenous decay of dead cells in the anodic biofilm matrix can act as a source of substrate for various hydrolytic/fermentative bacterial communities, like *Anaerolineaceae*, *Sedimentibacter*, *Dethiosulfovibrionaceae*, and *Copriothermobacter*. This process might lead to the production of unknown metabolic intermediates (e.g., acetate, propionate, formate, lactate, H₂, etc.), and these intermediates can act as an electron and carbon source for the growth of other microbial communities (fermenters and exoelectrogens). For example, members of *Copriothermobacter* spp. were found to have strong intracellular and extracellular protease activity capable of protein and peptide degradation. Additionally, they were identified in anaerobic systems as important hydrogen producers (Tandishabo et al., 2012). Development of mixed populations of species belonging to *Firmicutes*, *Synergistetes*, *Copriothermobacteria*, and *Anaerolineae* were observed in microbial fuel cell (MFC) fed with acetate (Fu et al., 2013) and of root exudate-driven MFCs (Cabezas et al., 2015). Members of *Clostridia*, *Synergistia*, and *Anaerolineae* were reported to be propionate oxidizers and were abundant in propionate and acetate fed MECs, propionate enriched soils, and anaerobic digester sludge (Chauhan et al., 2004; Kraglund et al., 2007; Yamada et al., 2007; Ito et al., 2011; Lesnik and Liu, 2014; Ruiz et al., 2014; Cabezas et al., 2015).

self-optimization of MECs for attaining stable (reproducible) performance after disturbance.

Regardless of the substrate and concentrations tested, the anodic microbial community structure between duplicate MEC reactors was similar at each sampling event (Figure 4). During MEC mode of operations, a relatively similar anodic bacterial community structure was observed in the A-reactors over time regardless of the concentration tested, whereas in the P-reactors the bacterial communities at day 70 were clustered separately from the remainder of the samples (Figure 4). The succession observed in the anode of A- and P-reactors where dominance of *Copriothermobacter* and *Anaerolineaceae* on day 0 (MFC mode of operation) was replaced by *Geobacter* on day 10, and the eventual dominance of *Geobacter* over time (days 10 to 70) (Figure 5) suggests that operation in MEC mode not only influenced the dominance of *Geobacter* but also decreased the bacterial diversity over time (10–70 days) (Tables 1, 2) (Kiely et al., 2011; Lu et al., 2012a). It should be noted that the dominance of *Geobacter* was also observed on the anode of MECs fed with domestic wastewater (Heidrich et al., 2014). At the end of MEC operation (day 70), AL and PL reactors showed a decrease in the relative abundance of *Geobacter*, but it remained the predominant community, accompanied by an increase in the relative abundance of several phylotypes (e.g., *Desulfovibrio* and *Pseudomonas* in AL reactors and *Dethiosulfovibrionaceae*, *Synergistaceae*, and *Anaerolineaceae* in PL reactors) (Figures 5A,C), however, the current density

remained stable (Figure 1). An earlier study on pilot scale MEC treating domestic wastewater showed in addition to the *Geobacter*, the dominance of the hydrolytic microorganism *Synergistia* (*Dethiosulfovibrionaceae*), which likely resulted in more positive impact on the reactor performance (Heidrich et al., 2014). *Anaerolineae* was found as a predominant group in the electrode of integrated MEC-Anaerobic digestion system (Liu et al., 2016) and was also detected as a dominant organism in the anode of MFCs fed with the root exudates of rice field soil (Cabezas et al., 2015), suggesting that it likely played a role as an exoelectrogen and/or fermenter; however, its role in this study is unclear. In the case of the PH-reactors, a stable trend in the maximum current density with each cycle was observed despite varying microbial community structure over a time (days 20–70) (Figure 5C). These results suggest that functional stability was maintained despite changes in community structure. Previous studies reported that the anodic microbial communities in MFCs are flexible and can self-select and self-optimize to maintain functional stability (Ishii et al., 2012; Koch et al., 2014). In the current study, the predominance of *Geobacter* on the anode over time (Figures 5A,C) was essential for maintaining relatively stable current density pattern (Figure 1) of MECs fed with low or high concentrations of acetate or propionate. This suggests that the presence of members of the genus *Geobacter* on the anode is likely essential for successful implementation of MECs for full-scale anaerobic treatment of low and high strength wastewater.

Although, the current study was not designed to test spatial variation in microbial community structure, we cannot rule out that some of the variations observed in the microbial community structure over time could be due to spatial variation (i.e., different sampling positions). Nevertheless, previous studies reported no spatial variation in the microbial community structure on both planar and volumetric electrodes. For example, Vargas et al. (2013) showed that the anodic microbial community at different locations on planar (carbon cloth) and volumetric anodes (fiber brush anodes) was homogenous based on 16S rRNA gene sequencing. The anode fiber brush used in the current study was similar to the one used by Vargas et al. (2013). Dennis et al. (2013) specifically designed a reactor setup to address if changes in microbial diversity observed over time in a bioelectrochemical system can be related to community development rather than spatial variation within the reactor. Their 16S rRNA genes sequencing results revealed no spatial variation in the diversity of microbial communities associated with different planar electrodes within a single time point. Using fluorescence *in situ* hybridization (FISH), Kiely et al. (2011) showed that *Geobacter sulfurreducens* was homogenously dispersed on the anode fibers of a potato wastewater fed MECs.

In addition, the microbial community composition and structure was compared between the anode biofilm and suspension samples. The bacterial community structure in the suspension of A- and P-reactors was highly dynamic compared to the biofilm samples as revealed by NMDS (**Figure 4**) and ANOSIM. However, similar bacterial composition was observed between the anode and suspension samples, where the dominant members on the anode were also present in suspension (Supplementary Tables S1–S4). This similarity in bacterial composition between the biofilm and suspension samples could be due to biofilm detachment. This was supported by the presence of high abundance of *Geobacter* (3–45%) in the suspension samples (**Figures 5B,D** and Supplementary Tables S2, S4). It is well known that members of the genus *Geobacter* are strongly associated with the anode, and their presence in solution was due to biofilm detachment. It should be noted, that at the end of each batch cycle the anolyte solution was emptied and replaced with fresh autoclaved solution, and current generation was immediately observed for both acetate- and propionate-fed MECs. Taken together, these results suggest that the main microbial functions (exoelectrogenesis and fermentation) were taking place at the anode and the slight turbidity observed in the anolyte solution of the acetate- and propionate-fed reactors was possibly due to biofilm detachment.

Analysis of 16S rRNA gene pyrosequencing data revealed that the classical propionate degraders such as *Syntrophobacter* spp., *Smithella* spp., and *Pelotomaculum* spp. that are typically present in methanogenic systems were not detected on the anode and suspension in the current study. It is possible that the conditions in the anode chamber favored the presence of other propionate degraders. In the current study, P-reactors were dominated by diverse phylotypes belonging to *Clostridia*, *Synergistia*, and *Anaerolineae* (**Figures 5B,D**). Members of these classes were reported to be propionate oxidizers and were abundant in propionate and acetate fed MECs, propionate enriched soils, and

anaerobic digester sludge (Chauhan et al., 2004; Kragelund et al., 2007; Yamada et al., 2007; Ito et al., 2011; Lesnik and Liu, 2014; Ruiz et al., 2014; Cabezas et al., 2015). A schematic diagram based on 16S rRNA gene sequencing data was generated describing the potential key members in the community and their interaction in the anode of MECs fed with acetate or propionate (**Figure 6**). It should be noted that in-depth community analysis using 16S rRNA gene pyrosequencing allows for speculation about possible interactions between different members in the community when utilizing an organic substrate (Aracic et al., 2014). However, it does not provide information on the metabolically active members in the community. Alternatively, stable isotope probing (SIP) with labeled propionate combined with 16S rRNA gene sequencing should be used in future studies to provide a better insight into the carbon flow during propionate oxidation and to allow the identification of metabolically active members in the community (i.e., linking phylogeny to function) that are involved in propionate oxidation (Dumont and Murrell, 2005). Also, additional insights into the physiology of electrode communities can be obtained using metatranscriptomics (Ishii et al., 2013; Aracic et al., 2014).

In terms of substrate removal, AL, AH, and PL showed nearly complete removal of substrate ($97 \pm 2\%$), whereas substrate removal was $75 \pm 14\%$ in the PH-reactors (**Figure 3B**). In methanogenic systems, propionate oxidation is highly endergonic (+72 kJ/mole) and performed by syntrophic consortia of microorganisms (Stams and Plugge, 2009). In such environments, acetogenic bacteria oxidize propionate to acetate and hydrogen (or formate), which are then utilized by acetoclastic (acetate) and hydrogenotrophic methanogens (H_2 or formate) to produce CH_4 or CO_2 (Boone and Xun, 1987). In general, accumulation of high concentrations of propionate (>20 mM) is detrimental to AD processes (Pullammanappallil et al., 2001; Gallert and Winter, 2008; Ma et al., 2009). In MECs, complete removal of propionate at elevated substrate concentration (36 mM) requires microbial partnership between fermenters, hydrogenotrophic methanogens and *Geobacter* (Hari et al., 2016b). Both *Geobacter* and hydrogenotrophic methanogens consumed the intermediates (acetate, H_2 , and formate) generated by fermenters, and kept their concentrations low resulting in more energetically favorable fermentation, and hence complete removal of propionate (Hari et al., 2016b). In the current study, the incomplete degradation of propionate in PH reactors was possibly due to lack of hydrogenotrophic methanogenesis, which was not a major sink (data not shown) of electrons. The lack of methanogenesis in the current study was possibly due to the fact that the MEC anodes were initially enriched in single chamber air-cathode MFCs, where oxygen intrusion through the cathode might have affected the growth of methanogens. In another study, we operated the P-reactors under MEC (oxygen free environment) mode from the start of the experiment, and this provided a suitable environment for the enrichment of hydrogenotrophic methanogens resulting in methane being an important sink (Hari et al., 2016b).

While the use of an applied voltage in the current study was useful for understanding the temporal dynamics of microbial communities in connection to reactor performance in MECs fed

with low or high concentrations of acetate or propionate, the anode potentials in the reactors were not controlled. However, at all tested conditions the variation in the anode potential was low ($\sim -0.15 \pm 0.1$ V to -0.23 ± 0.09 V vs. SHE) resulting in relatively similar anodic microbial community composition but with varying relative abundance. It is known that operating MECs as set anode potential (SAP) can influence the anodic microbial community structure (Torres et al., 2009; Hari et al., 2016b). For example, in propionate-fed MECs higher microbial diversity was observed at more positive SAP (0.25 V vs. SHE) than lower SAPs (0 V and -0.25 V). Also, similar dominant genera (*Geobacter*, *Smithella*, and *Syntrophobacter*) were observed on the anode of all tested SAPs, but their relative abundance varied depending on SAP (Hari et al., 2016b). Similarly, in acetate fed-MECs higher phylogenetic diversity was observed on the anode at positive SAP (0.37 V vs. SHE) than lower SAPs (-0.15 , 0.09, and 0.02 V vs. SHE), which were mainly dominated by *G. sulfurreducens* (Torres et al., 2009). Taken together, these results suggest that the more energy available for growth at higher positive SAPs was likely captured by diverse microorganisms resulting in higher diversity.

In an earlier study, it was shown using a similar MEC setup and operated under the same conditions that multiple paths of carbon and electron flow (via acetate/H₂ or acetate/formate) to electrical current could occur simultaneously during propionate oxidation in the anode of MECs regardless of the concentration tested (Hari et al., 2016a). In methanogenic systems, processing of substrates through multiple routes in parallel is essential for maintaining functional stability in response to organic overloading (Fernandez et al., 2000; Hashsham et al., 2000). In a similar fashion, this multiple paths of electron flow from the substrate in the anode of MECs should result in a higher functional stability of the system. Despite the high concentration (36 mM) of propionate used in the current study, the removal of propionate was still high ($\sim 75\%$) in the PH reactors. Therefore, the anode of MECs could potentially be integrated with existing AD processes to improve propionate degradation and functional stability.

CONCLUSION

Our findings indicated that MECs are functionally stable in performance regardless of the carbon source (acetate and

REFERENCES

- Ambler, J. R., and Logan, B. E. (2011). Evaluation of stainless steel cathodes and a bicarbonate buffer for hydrogen production in microbial electrolysis cells using a new method for measuring gas production. *Int. J. Hydrogen Energy* 36, 160–166. doi: 10.1016/j.ijhydene.2010.09.044
- Aracic, S., Semenec, L., and Franks, A. E. (2014). Investigating microbial activities of electrode-associated microorganisms in real-time. *Front. Microbiol.* 5:663. doi: 10.3389/fmich.2014.00663
- Boone, D. R., and Xun, L. (1987). Effects of pH, temperature, and nutrients on propionate degradation by a methanogenic enrichment culture. *Appl. Environ. Microbiol.* 53, 1589–1592.
- Cabezas, A., Pommerenke, B., Boon, N., and Friedrich, M. W. (2015). *Geobacter*, *Anaeromyxobacter* and *Anaerolineae* populations are enriched on anodes of root exudate-driven microbial fuel cells in rice field soil. *Environ. Microbiol. Rep.* 7, 489–497. doi: 10.1111/1758-2229.12277
- Cai, W., Han, T., Guo, Z., Varrone, C., Wang, A., and Liu, W. (2016). Methane production enhancement by an independent cathode in integrated anaerobic reactor with microbial electrolysis. *Bioresour. Technol.* 208, 13–18. doi: 10.1016/j.biortech.2016.02.028
- Call, D., and Logan, B. E. (2008). Hydrogen production in a single chamber microbial electrolysis cell lacking a membrane. *Environ. Sci. Technol.* 42, 3401–3406. doi: 10.1021/es0801822
- Caporaso, J. G., Bittinger, K., Bushman, F. D., DeSantis, T. Z., Andersen, G. L., and Knight, R. (2010a). PyNAST: a flexible tool for aligning sequences to a template alignment. *Bioinformatics* 26, 266–267. doi: 10.1093/bioinformatics/btp636
- Caporaso, J. G., Kuczynski, J., Stombaugh, J., Bittinger, K., Bushman, F. D., Costello, E. K., et al. (2010b). QIIME allows analysis of high-throughput

propionate) and concentrations (0.5 g COD/L and 4 g COD/L) tested. *Geobacter* was the dominant genus at the anode of all the tested conditions. Their predominance was essential for maintaining relatively stable current density pattern despite frequent sampling of the anodic biofilms over time. The results of this study showed the potential of MECs as a viable alternative technology for anaerobic treatment of low and high strength synthetic solutions, containing acetate or propionate. However, defined solutions of acetate or propionate are not representative of the complexity of real wastewaters, and future studies focusing on the temporal dynamics of microbial communities and its correlation to system performance in MECs fed with real wastewater (containing various VFAs with differing concentrations) are needed to determine the robustness of MECs as an anaerobic treatment technology.

AUTHOR CONTRIBUTIONS

AH and PS conceptualized and designed the experiments. AH performed the experiments, analyzed data and wrote the manuscript. KV, KK, and PS helped in thoughtful discussion and revised the manuscript. SB helped in microbial community analysis.

ACKNOWLEDGMENTS

This work was sponsored by a Ph.D. fellowship, a Global Research Partnership-Collaborative Fellows Award (GRP-CF-2011-15-S) and Center Competitive Funding (FCC/1/1971-05-01) to PS from King Abdullah University of Science and Technology (KAUST). The authors thank Prof. Bruce E. Logan, Pennsylvania State University, United States for comments and suggestions on previous versions of this manuscript.

SUPPLEMENTARY MATERIAL

The Supplementary Material for this article can be found online at: <http://journal.frontiersin.org/article/10.3389/fmich.2017.01371/full#supplementary-material>

- community sequencing data. *Nat. Methods* 7, 335–336. doi: 10.1038/nmeth.f.303
- Chauhan, A., Ogram, A., and Reddy, K. (2004). Syntrophic-methanogenic associations along a nutrient gradient in the Florida Everglades. *Appl. Environ. Microbiol.* 70, 3475–3484. doi: 10.1128/AEM.70.6.3475-3484.2004
- Dennis, P. G., Guo, K., Imelfort, M., Jensen, P., Tyson, G. W., and Rabaey, K. (2013). Spatial uniformity of microbial diversity in a continuous bioelectrochemical system. *Bioresour. Technol.* 129, 599–605. doi: 10.1016/j.biortech.2012.11.098
- Dumont, M. G., and Murrell, J. C. (2005). Stable isotope probing—linking microbial identity to function. *Nat. Rev. Microbiol.* 3, 499–504. doi: 10.1038/nrmicro1162
- Edgar, R. C. (2010). Search and clustering orders of magnitude faster than BLAST. *Bioinformatics* 26, 2460–2461. doi: 10.1093/bioinformatics/btq461
- Feng, Y., Liu, Y., and Zhang, Y. (2015a). Enhancement of sludge decomposition and hydrogen production from waste activated sludge in a microbial electrolysis cell with cheap electrodes. *Environ. Sci. Water Res. Technol.* 1, 761–768. doi: 10.1039/C5EW00112A
- Feng, Y., Zhang, Y., Chen, S., and Quan, X. (2015b). Enhanced production of methane from waste activated sludge by the combination of high-solid anaerobic digestion and microbial electrolysis cell with iron-graphite electrode. *Chem. Eng. J.* 259, 787–794. doi: 10.1016/j.cej.2014.08.048
- Fernandez, A. S., Hashsham, S. A., Dollhopf, S. L., Raskin, L., Glagoleva, O., Dazzo, F. B., et al. (2000). Flexible community structure correlates with stable community function in methanogenic bioreactor communities perturbed by glucose. *Appl. Environ. Microbiol.* 66, 4058–4067. doi: 10.1128/AEM.66.9.4058-4067.2000
- Freguia, S., Teh, E. H., Boon, N., Leung, K. M., Keller, J., and Rabaey, K. (2010). Microbial fuel cells operating on mixed fatty acids. *Bioresour. Technol.* 101, 1233–1238. doi: 10.1016/j.biortech.2009.09.054
- Fu, Q., Kobayashi, H., Kawaguchi, H., Vilcaez, J., Wakayama, T., Maeda, H., et al. (2013). Electrochemical and phylogenetic analyses of current-generating microorganisms in a thermophilic microbial fuel cell. *J. Biosci. Bioeng.* 115, 268–271. doi: 10.1016/j.jbiosc.2012.10.007
- Gallert, C., and Winter, J. (2008). Propionic acid accumulation and degradation during restart of a full-scale anaerobic biowaste digester. *Bioresour. Technol.* 99, 170–178. doi: 10.1016/j.biortech.2006.11.014
- Goux, X., Calusinska, M., Lemaigre, S., Marynowska, M., Klocke, M., Udelhoven, T., et al. (2015). Microbial community dynamics in replicate anaerobic digesters exposed sequentially to increasing organic loading rate, acidosis, and process recovery. *Biotechnol. Biofuels* 8, 122. doi: 10.1186/s13068-015-0309-9
- Guo, X., Liu, J., and Xiao, B. (2013). Bioelectrochemical enhancement of hydrogen and methane production from the anaerobic digestion of sewage sludge in single-chamber membrane-free microbial electrolysis cells. *Int. J. Hydrogen Energy* 38, 1342–1347. doi: 10.1016/j.ijhydene.2012.11.087
- Hari, A. R., Katuri, K. P., Gorron, E., Logan, B. E., and Saikaly, P. E. (2016a). Multiple paths of electron flow to current in microbial electrolysis cells fed with low and high concentrations of propionate. *Appl. Microbiol. Biotechnol.* 100, 5999–6011. doi: 10.1007/s00253-016-7402-2
- Hari, A. R., Katuri, K. P., Logan, B. E., and Saikaly, P. E. (2016b). Set anode potentials affect the electron fluxes and microbial community structure in propionate-fed microbial electrolysis cells. *Sci. Rep.* 6:38690. doi: 10.1038/srep38690
- Hashsham, S. A., Fernandez, A. S., Dollhopf, S. L., Dazzo, F. B., Hickey, R. F., Tiedje, J. M., et al. (2000). Parallel processing of substrate correlates with greater functional stability in methanogenic bioreactor communities perturbed by glucose. *Appl. Environ. Microbiol.* 66, 4050–4057. doi: 10.1128/AEM.66.9.4050-4057.2000
- Heidrich, E. S., Edwards, S. R., Dolfing, J., Cotterill, S. E., and Curtis, T. P. (2014). Performance of a pilot scale microbial electrolysis cell fed on domestic wastewater at ambient temperatures for a 12month period. *Bioresour. Technol.* 173, 87–95. doi: 10.1016/j.biortech.2014.09.083
- Ishii, S., Suzuki, S., Norden-Krichmar, T. M., Nealson, K. H., Sekiguchi, Y., Gorby, Y. A., et al. (2012). Functionally stable and phylogenetically diverse microbial enrichments from microbial fuel cells during wastewater treatment. *PLoS ONE* 7:e30495. doi: 10.1371/journal.pone.0030495
- Ishii, S. I., Suzuki, S., Norden-Krichmar, T. M., Phan, T., Wanger, G., Nealson, K. H., et al. (2014). Microbial population and functional dynamics associated with surface potential and carbon metabolism. *ISME J.* 8, 963–978. doi: 10.1038/ismej.2013.217
- Ishii, S. I., Suzuki, S., Norden-Krichmar, T. M., Tenney, A., Chain, P. S., Scholz, M. B., et al. (2013). A novel metatranscriptomic approach to identify gene expression dynamics during extracellular electron transfer. *Nat. Commun.* 4:1601. doi: 10.1038/ncomms2615
- Ito, T., Yoshiguchi, K., Ariesyadi, H. D., and Okabe, S. (2011). Identification of a novel acetate-utilizing bacterium belonging to *Synergistes* group 4 in anaerobic digester sludge. *ISME J.* 5, 1844–1856. doi: 10.1038/ismej.2011.59
- Katuri, K., Bettahalli, N. M. S., Wang, X., Matar, G., Chisca, S., Nunes, P. S., et al. (2016). A microfiltration polymer-based hollow fiber cathode as a promising advanced material for simultaneous recovery of energy and water. *Adv. Mater.* 28, 9504–9511. doi: 10.1002/adma.201603074
- Katuri, K., Werner, C. M., Sandoval, R. J., Chen, W., Logan, B., Lai, Z., et al. (2014). A novel anaerobic electrochemical membrane bioreactor (AnEMBR) with conductive hollow-fiber membrane for treatment of low-organic strength solutions. *Environ. Sci. Technol.* 48, 12833–12841. doi: 10.1021/es504392n
- Kiely, P. D., Cusick, R., Call, D. F., Selembro, P. A., Regan, J. M., and Logan, B. E. (2011). Anode microbial communities produced by changing from microbial fuel cell to microbial electrolysis cell operation using two different wastewaters. *Bioresour. Technol.* 102, 388–394. doi: 10.1016/j.biortech.2010.05.019
- Klindworth, A., Pruesse, E., Schweer, T., Peplies, J., Quast, C., Horn, M., et al. (2012). Evaluation of general 16S ribosomal RNA gene PCR primers for classical and next-generation sequencing-based diversity studies. *Nucleic Acids Res.* 41, e1. doi: 10.1093/nar/gks808
- Koch, C., and Harnisch, F. (2016). Is there a specific ecological niche for electroactive microorganisms? *ChemElectroChem* 3, 1282–1295. doi: 10.1002/celc.201600079
- Koch, C., Popiel, D., and Harnisch, F. (2014). Functional redundancy of microbial anodes fed by domestic wastewater. *ChemElectroChem* 1, 1923–1931. doi: 10.1002/celc.201402216
- Kraglund, C., Caterina, L., Borger, A., Thelen, K., Eikelboom, D., Tandoi, V., et al. (2007). Identity, abundance and ecophysiology of filamentous *Chloroflexi* species present in activated sludge treatment plants. *FEMS Microbiol. Ecol.* 59, 671–682. doi: 10.1111/j.1574-6941.2006.00251.x
- Lee, H.-S., Parameswaran, P., Kato-Marcus, A., Torres, C. I., and Rittmann, B. E. (2008). Evaluation of energy-conversion efficiencies in microbial fuel cells (MFCs) utilizing fermentable and non-fermentable substrates. *Water Res.* 42, 1501–1510. doi: 10.1016/j.watres.2007.10.036
- Lee, H.-S., Torres, C. I., Parameswaran, P., and Rittmann, B. E. (2009). Fate of H₂ in an upflow single-chamber microbial electrolysis cell using a metal-catalyst-free cathode. *Environ. Sci. Technol.* 43, 7971–7976. doi: 10.1021/es900204j
- Lesnik, K., and Liu, H. (2014). Establishing a core microbiome in acetate-fed microbial fuel cells. *Appl. Microbiol. Biotechnol.* 98, 4187–4196. doi: 10.1007/s00253-013-5502-9
- Liu, W., Cai, W., Guo, Z., Wang, L., Yang, C., Varrone, C., et al. (2016). Microbial electrolysis contribution to anaerobic digestion of waste activated sludge, leading to accelerated methane production. *Renew. Energy* 91, 334–339. doi: 10.1016/j.renene.2016.01.082
- Logan, B. E., Call, D., Cheng, S., Hamelers, H. V. M., Sleutels, T. H. J. A., Jeremiassie, A. W., et al. (2008). Microbial electrolysis cells for high yield hydrogen gas production from organic matter. *Environ. Sci. Technol.* 42, 8630–8640. doi: 10.1021/es801553z
- Lu, L., Xing, D., and Ren, N. (2012a). Bioreactor performance and quantitative analysis of methanogenic and bacterial community dynamics in microbial electrolysis cells during large temperature fluctuations. *Environ. Sci. Technol.* 46, 6874–6881. doi: 10.1021/es300860a
- Lu, L., Xing, D., and Ren, N. (2012b). Pyrosequencing reveals highly diverse microbial communities in microbial electrolysis cells involved in enhanced H₂ production from waste activated sludge. *Water Res.* 46, 2425–2434. doi: 10.1016/j.watres.2012.02.005
- Luo, S., Guo, W., Nealson, K. H., Feng, X., and He, Z. (2017). ¹³C pathway analysis for the role of formate in electricity generation by *Shewanella oneidensis* MR-1 using lactate in microbial fuel cells. *Sci. Rep.* 6:20941. doi: 10.1038/srep20941

- Ma, J., Carballa, M., Van De Caveye, P., and Verstraete, W. (2009). Enhanced propionic acid degradation (EPAD) system: proof of principle and feasibility. *Water Res.* 43, 3239–3248. doi: 10.1016/j.watres.2009.04.046
- Parameswaran, P., Zhang, H., Torres, C. I., Rittmann, B. E., and Krajmalnik-Brown, R. (2010). Microbial community structure in a biofilm anode fed with a fermentable substrate: the significance of hydrogen scavengers. *Biotechnol. Bioeng.* 105, 69–78. doi: 10.1002/bit.22508
- Pullammanappallil, P. C., Chynoweth, D. P., Lyberatos, G., and Svoronos, S. A. (2001). Stable performance of anaerobic digestion in the presence of a high concentration of propionic acid. *Bioresour. Technol.* 78, 165–169. doi: 10.1016/S0960-8524(00)0187-5
- Ruiz, V., Ilhan, Z. E., Kang, D.-W., Krajmalnik-Brown, R., and Buitrón, G. (2014). The source of inoculum plays a defining role in the development of MEC microbial consortia fed with acetic and propionic acid mixtures. *J. Biotechnol.* 182, 11–18. doi: 10.1016/j.biote.2014.04.016
- Santoro, C., Li, B., Cristiani, P., and Squadrito, G. (2013). Power generation of microbial fuel cells (MFCs) with low cathodic platinum loading. *Int. J. Hydrogen Energy* 38, 692–700. doi: 10.1016/j.ijhydene.2012.05.104
- Shehab, N., Li, D., Amy, G. L., Logan, B. E., and Saikaly, P. E. (2013). Characterization of bacterial and archaeal communities in air-cathode microbial fuel cells, open circuit and sealed-off reactors. *Appl. Microbiol. Biotechnol.* 97, 9885–9895. doi: 10.1007/s00253-013-5025-4
- Siegert, M., Li, X.-F., Yates, M. D., and Logan, B. E. (2014). The presence of hydrogenotrophic methanogens in the inoculum improves methane gas production in microbial electrolysis cells. *Front. Microbiol.* 5:778. doi: 10.3389/fmicb.2014.00778
- Stams, A. J., and Plugge, C. M. (2009). Electron transfer in syntrophic communities of anaerobic bacteria and archaea. *Nat. Rev. Microbiol.* 7, 568–577. doi: 10.1038/nrmicro2166
- Tandishabo, K., Iga, Y., Tamaki, H., Nakamura, K., and Takamizawa, K. (2012). Characterization of a novel *Coprototermobacter* sp. strain IT3 isolated from an anaerobic digester – hydrogen production and peptidase profiles at higher temperature. *J. Environ. Conserv. Eng.* 41, 753–761. doi: 10.5956/jriet.41.753
- Torres, C. I., Krajmalnik-Brown, R., Parameswaran, P., Marcus, A. K., Wanger, G., Gorby, Y. A., et al. (2009). Selecting anode-respiring bacteria based on anode potential: phylogenetic, electrochemical, and microscopic characterization. *Environ. Sci. Technol.* 43, 9519–9524. doi: 10.1021/es902165y
- Vanwonterghem, I., Jensen, P. D., Dennis, P. G., Hugenholtz, P., Rabaey, K., and Tyson, G. W. (2014). Deterministic processes guide long-term synchronised population dynamics in replicate anaerobic digesters. *ISME J.* 8, 2015–2028. doi: 10.1038/ismej.2014.50
- Vargas, I. T., Albert, I. U., and Regan, J. M. (2013). Spatial distribution of bacterial communities on volumetric and planar anodes in single-chamber air-cathode microbial fuel cells. *Biotechnol. Bioeng.* 110, 3059–3062. doi: 10.1002/bit.24949
- Wang, Q., Garrity, G. M., Tiedje, J. M., and Cole, J. R. (2007). Naive Bayesian classifier for rapid assignment of rRNA sequences into the new bacterial taxonomy. *Appl. Environ. Microbiol.* 73, 5261–5267. doi: 10.1128/AEM.00062-07
- Werner, C. M., Katuri, K., Logan, B. E., Amy, G. L., and Saikaly, P. E. (2016). Graphene-coated hollow fiber membrane as the cathode in anaerobic electrochemical membrane bioreactors – Effect of configuration and applied voltage on performance and membrane fouling. *Environ. Sci. Technol.* 50, 4439–4447. doi: 10.1021/acs.est.5b02833
- Yamada, T., Imachi, H., Ohashi, A., Harada, H., Hanada, S., Kamagata, Y., et al. (2007). *Bellilinea caldifistulae* gen. nov., sp. nov. and *Longilinea arvoryzae* gen. nov., sp. nov., strictly anaerobic, filamentous bacteria of the phylum *Chloroflexi* isolated from methanogenic propionate-degrading consortia. *Int. J. Syst. Evol. Microbiol.* 57, 2299–2306. doi: 10.1099/ijsm.0.65098-0
- Zhu, X., Yates, M. D., Hatzell, M. C., Ananda Rao, H., Saikaly, P. E., and Logan, B. E. (2014). Microbial community composition is unaffected by anode potential. *Environ. Sci. Technol.* 48, 1352–1358. doi: 10.1021/es404690q

Conflict of Interest Statement: The authors declare that the research was conducted in the absence of any commercial or financial relationships that could be construed as a potential conflict of interest.

Copyright © 2017 Hari, Venkidusamy, Katuri, Bagchi and Saikaly. This is an open-access article distributed under the terms of the Creative Commons Attribution License (CC BY). The use, distribution or reproduction in other forums is permitted, provided the original author(s) or licensor are credited and that the original publication in this journal is cited, in accordance with accepted academic practice. No use, distribution or reproduction is permitted which does not comply with these terms.



Electricity Generation by *Shewanella decolorationis* S12 without Cytochrome c

Yonggang Yang¹, Guannan Kong², Xingjuan Chen¹, Yingli Lian¹, Wenzong Liu^{3*} and Meiyng Xu^{1,4*}

¹ Guangdong Provincial Key Laboratory of Microbial Culture Collection and Application, Guangdong Institute of Microbiology, Guangzhou, China, ² State Key Laboratory of Applied Microbiology Southern China, Guangzhou, China, ³ Key Laboratory of Environmental Biotechnology, Chinese Academy of Sciences, Beijing, China, ⁴ Guangdong Open Laboratory of Applied Microbiology, Guangzhou, China

OPEN ACCESS

Edited by:

Yong Xiao,
Institute of Urban Environment (CAS),
China

Reviewed by:

Ashok K. Sundramoorthy,
SRM University, India
Lin Tang,
Hunan University, China

*Correspondence:

Wenzong Liu
wzliu@rcees.ac.cn
Meiyng Xu
xumy@gdim.cn

Specialty section:

This article was submitted to
Microbiotechnology, Ecotoxicology
and Bioremediation,
a section of the journal
Frontiers in Microbiology

Received: 28 November 2016

Accepted: 31 May 2017

Published: 20 June 2017

Citation:

Yang Y, Kong G, Chen X, Lian Y, Liu W and Xu M (2017) Electricity Generation by *Shewanella decolorationis* S12 without Cytochrome c. *Front. Microbiol.* 8:1115. doi: 10.3389/fmicb.2017.01115

Bacterial extracellular electron transfer (EET) plays a key role in various natural and engineering processes. Outer membrane c-type cytochromes (OMCs) are considered to be essential in bacterial EET. However, most bacteria do not have OMCs but have redox proteins other than OMCs in their extracellular polymeric substances of biofilms. We hypothesized that these extracellular non-cytochrome c proteins (ENCP) could contribute to EET, especially with the facilitation of electron mediators. This study compared the electrode respiration capacity of wild type *Shewanella decolorationis* S12 and an OMC-deficient mutant. Although the OMC-deficient mutant was incapable in direct electricity generation in normal cultivation, it regained electricity generation capacity (26% of the wild type) with the aid of extracellular electron mediator (riboflavin). Further bioelectrochemistry and X-ray photoelectron spectroscopy analysis suggested that the ENCP, such as proteins with Fe–S cluster, may participate in the falvin-mediated EET. The results highlighted an important and direct role of the ENCP, generated by either electricigens or other microbes, in natural microbial EET process with the facilitation of electron mediators.

Keywords: *Shewanella*, microbial fuel cell, extracellular electron transfer, c-type cytochrome, ccmA

INTRODUCTION

Bacterial extracellular electron transfer (EET) plays a crucial role in various natural biogeochemical cycles and engineering processes. It can deliver electrons from intracellular substrate to extracellular solid acceptors such as mineral oxides, humics. Moreover, bacterial EET to electrodes is a key process in the electricity generation and biodegradation in bioelectrochemical systems (BESs) which have promising application in wastewater treatment, bioremediation, biosensor and many other fields with simultaneous energy recovery (Lovley, 2006, 2012; Logan and Rabaey, 2012).

More and more bacteria (representatively *Shewanella* and *Geobacter* species) capable of EET have been isolated from various environments (Lovley, 2012). The reported bacterial EET strategies can be generally divided into two types, that is, (i) direct electron transfer to extracellular electron acceptors via outer membrane c-type cytochromes (OMCs) or conductively proteinaceous nanowires and (ii) indirect electron transfer via naturally occurring or biogenic electron mediators. Combined direct-indirect EET strategies can also be used by some bacteria (e.g., *Shewanella*) (Logan, 2009; Yang et al., 2012). OMCs were considered to be essential for bacterial EET as the

removal of OMCs could eliminate the electron transfer efficiency in both direct and indirect EET processes (Shi et al., 2009; Coursolle et al., 2010). However, a recent analysis of the prokaryotic proteomes suggested that most prokaryotes do not have OMCs.

In most cases, bacteria perform EET within biofilms attached on the solid electron acceptors. It has been reported that, numerous redox species and extracellular redox proteins (e.g., flavoproteins, ferredoxins) other than OMCs exist in biofilms of pure- or mixed-species (Cao et al., 2011; Yates et al., 2016). The extracellular non-cytochrome *c* proteins (ENCP) may be generated by secretion or lysis of biofilm cells and play important roles in redox processes, cell protection and other functions. For example, proteomic analysis of the extracellular polymeric substances (EPS) of *Shewanella* sp. HRCR-1 biofilms identified hundreds of proteins (including ENCP) released from the inside or outer membrane of biofilm cells (Cao et al., 2011). Recently, Yates et al. (2016) detected proteins containing Fe–S clusters in BES electrode biofilms. In contrast to the well-known role of OMCs in EET, whether bacterial ENCP participates in EET or not is yet unknown. It has been reported that many bacteria lacking of OMC and EET capacity could obtain EET capacity by providing electron mediators such as neutral red or flavins (Chung et al., 1978; Park and Zeikus, 2000). Therefore, we hypothesized that ENCP could contribute to bacterial EET processes with the facilitation of electron mediators.

To verify the hypothesis, this study investigated the EET capacities (including electrode, iron and azo dye reduction) of *Shewanella decolorationis* S12 and its mutant lacking of OMCs in the presence or absence of artificial electron mediator. The results suggested a significant role of *Shewanella* ENCP in the mediated EET process. This is the first evidence of that bacterial could use not only OMCs but also ENCP in EET process. Due to the ubiquity of ENCP and electron mediators in natural and engineering environments, bacterial ENCP may play an important but unrecognized role in many EET-dominated processes and bioreactors such as dissimilatory metal reduction and BESSs.

MATERIALS AND METHODS

Bacterial Strains

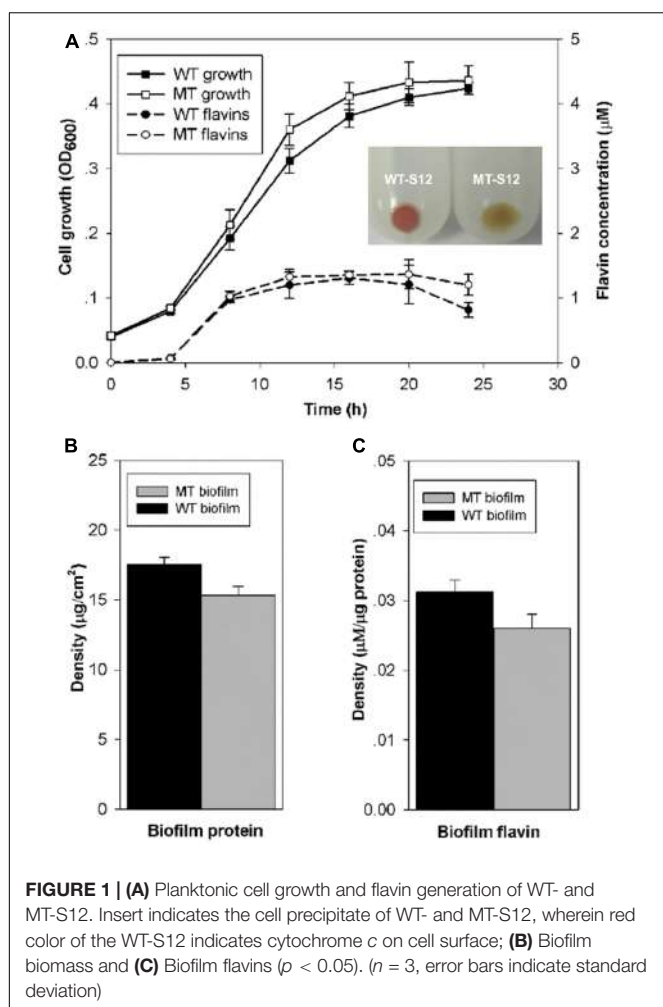
Shewanella decolorationis S12 was isolated from the activated sludge of a textile-wastewater treatment plant (Xu et al., 2005). It has been reported that the *ccmA* gene is essential for the maturation of the *c*-type cytochromes of *Shewanella* species (Ahuja and Thony-Meyer, 2003; Chen et al., 2010). To obtain a mutant strain without OMCs, the *ccmA* gene of the *S. decolorationis* S12 was deleted as previously described (Chen et al., 2010). The wild-type (WT) and mutant-type (MT) *S. decolorationis* S12 was aerobically grown in LB medium at 30°C until the late log-phase of the culture was achieved. The cultures were then centrifuged at 6000 × *g* for 2 min, and the collected cells were washed twice in sterilized phosphate buffer saline (PBS, pH7.2) for BES inoculation.

MFC Assembly and Operation

Dual-chamber glass MFCs were assembled as previously described (Yang et al., 2015). Briefly, plain graphite plates (2 cm × 3 cm × 0.2 cm) were used as anodes and cathodes. An Ag/AgCl electrode (+0.197 V vs standard hydrogen electrode, SHE) was used as a reference electrode to each anode. The anode and cathode chambers were separated with a piece of Nafion 115 membrane (7.1 cm²). After being assembled and sterilized (115°C for 20 min), the anode chamber (120 mL) was filled with 100 mL of lactate medium (12.8 g/L of Na₂HPO₄, 3 g/L of KH₂PO₄, 0.5 g/L of NaCl, 1.0 g/L of NH₄Cl, and lactate 10 mM, pH 6.8). To stimulate biofilm growth, 0.05% (w/v) yeast extract was added to the medium. Each cathode chamber was inoculated with 100 ml sterilized phosphate buffered saline solution (PBS, pH 7.2) containing 50 mM potassium ferricyanide. MFCs were inoculated with MT-S12 or WT-S12 with the same initial cell density OD₆₀₀ (optical density at the wavelength of 600 nm) = 0.04. For the first 24 h, both MFCs were operated aerobically non-electricity generating (open circuit) condition by bubbling air (0.15 L/min, filtered with a 0.2 μm membrane) in the anode culture to allow biofilm and planktonic cell growth. After that, to allow electrode reduction (electricity generation) of the MT-S12 and WT-S12, the MFCs were switched to anaerobically electricity-generating (closed circuit) condition by ceasing the air-inflow and tighten the cap of anode chambers and connecting the anode and cathode via a titanium wire with a 1000 Ω resistor. The electricity of MFCs under closed circuit condition was recorded with a multimeter (Keithley 2700, module 7702). Each MFC was operated at 30°C in triplication. To test the stimulation role of electron mediators to both WT- and MT-S12, riboflavin was added (2 μM each time) to MFC anode chambers using sterilized syringes during electricity generation.

Physiological Analyses

For the planktonic cell growth, OD₆₀₀ of the anode cultures was periodically monitored using an UV/Vis spectrophotometer (Ultraspec 6300 pro, Amersham Biosciences). Dissolved oxygen profile in the liquid culture was measured with an oxygen microelectrode (Unisense, Denmark) as reported before (Yang et al., 2015). For the biofilm growth on anodes, biofilms were sampled and the biofilm biomass was evaluated using a protein-quantification assay as previously described (Yang et al., 2015). For the flavin concentration in planktonic culture, 3 mL of the culture liquid was centrifuged at 8000 × *g* for 2 min, and the supernatant was analyzed by a fluorescence spectrometer (LS 45, PerkinElmer) with an excitation wavelength of 440 nm and an emission wavelength of 525 nm. For the flavins in biofilms, the biofilms was rinsed in PBS and scraped with a sterilized blade, followed by blending and centrifugation of 8000 × *g* for 2 min. The supernatant was analyzed with the fluorescence spectrometer. To evaluate the contribution of the biofilm ENCP in electricity generation, the biofilm were rinsed in sterilized PBS buffer (pH 7.2) containing protease K of 10 μg/ml for 5 min (Clark et al., 2007). The shorter treatment time could partially lysed the ENCP and maintain biofilm structure as verified under confocal laser scanning microscopy (CLSM).

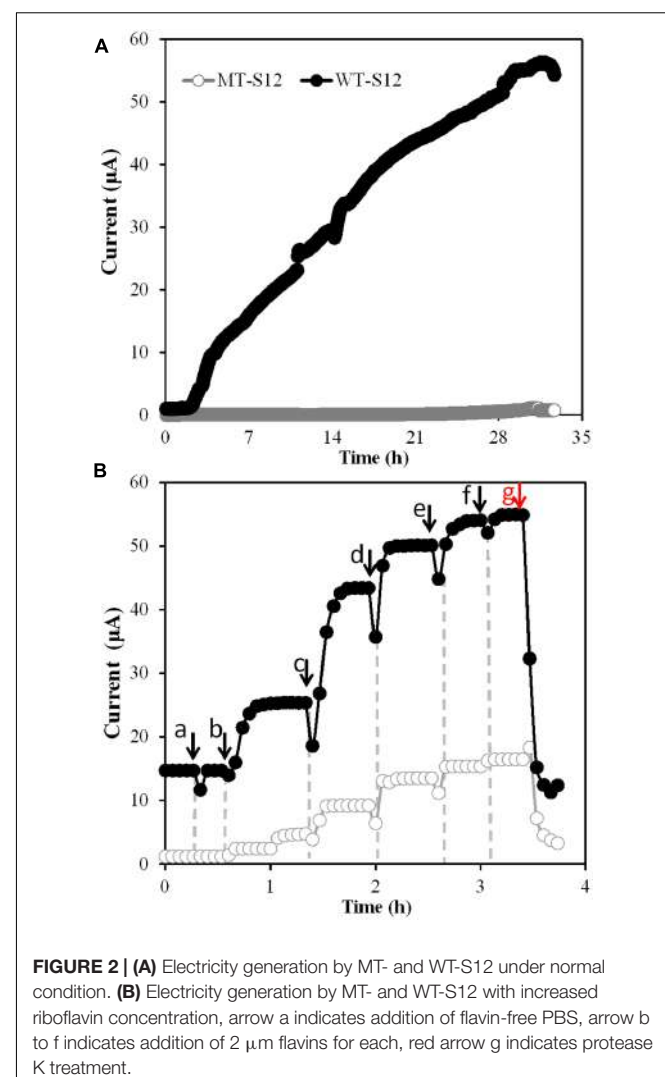


Microscope and Spectroscopy Analysis

The biofilm viability and structure were observed under a CLSM after being stained with a Live/Dead BacLight staining kit (Life Technologies, L7012) (Yang et al., 2015). The analyses of surface elements and associated chemical bonds of the biofilm and cell surface were analyzed by scanning electron microscopy-energy dispersive spectrometer (SEM-EDS, HORIBA 7962H) and X-ray photoelectron spectroscopy (XPS, Thermo K-ALPHA) with a monochromatic Al K α source, and the XPS data was fitted with the 'XPS peak' software.

Electrochemical Analyses

Before electrochemical analysis of the MFCs, the anodic culture were purged with 0.2- μm filtered purified N₂ to avoid the possible effects of soluble oxygen on flavin redox (Kumar and Chen, 2007). Cyclic voltammetry (CV) analysis of the MFC anodes was conducted as previously reported (Yang et al., 2014). Electrochemical impedance spectroscopy (EIS) of the MFC anodes was analyzed using an electrochemical workstation (Corrtest, China). Before analysis, the cell voltage of each MFC was controlled at their open-circuit voltages for 30 min as suggested by previous reports (Jung et al., 2012). A frequency

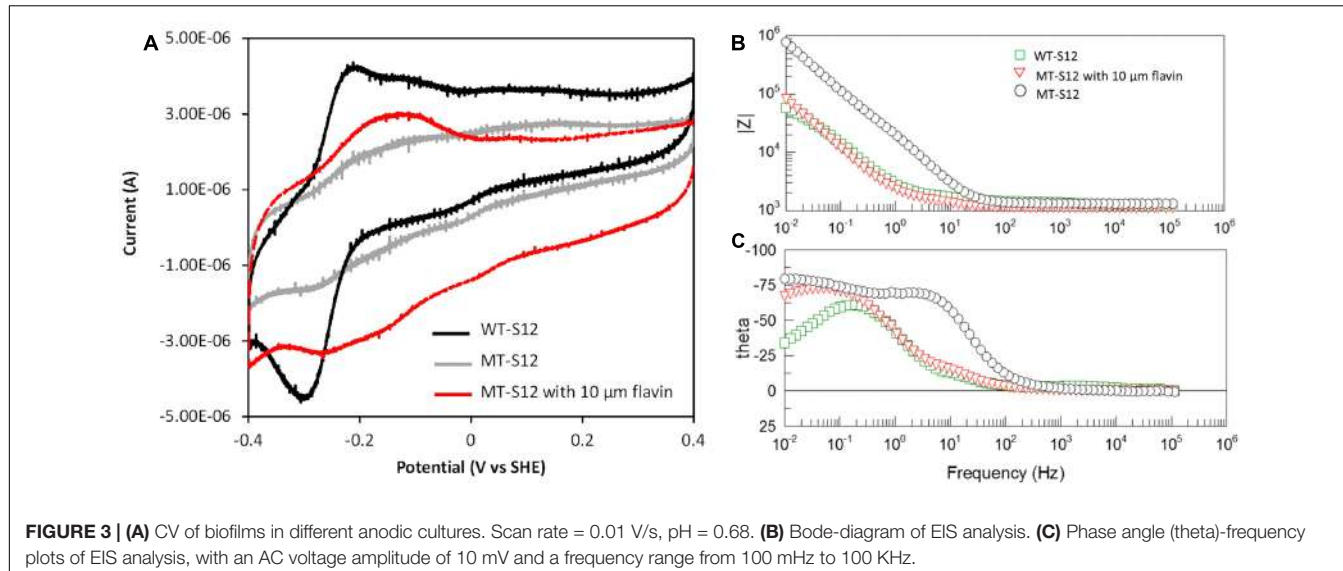


range from 10 mHz to 100 kHz with an AC signal of ± 10 mV amplitude was used. The EIS data was analyzed using Zview software and the scattered initial points were removed before data analysis as suggested by Manohar and Mansfeld (2009). The sinusoidal response was monitored which verified a stable and linear condition during the EIS measurements. According to the EIS data, an equivalent circuit ($R(R_{ct}CPE)$) consisted of an ohmic resistance(R), followed by an electrochemical charge transfer resistance (R_{ct}) in parallel with a constant phase element (CPE), was used, as suggested by reported EIS analyses for *Shewanella* anodes (Manohar and Mansfeld, 2009; Ramasamy et al., 2009; Jung et al., 2012).

RESULTS AND DISCUSSION

Planktonic and Biofilm Growth of WT- and MT-Strain

Cytochrome c is essential for the anaerobic growth of *Shewanella* species. Physiological and molecular tests in this and our previous



study demonstrated that the *ccmA*-mutant of *S. decolorationis* S12 was deficient in cytochrome *c* generation and anaerobic growth (Supplementary Figure S1) (Chen et al., 2010). To allow planktonic and biofilm cell growth of MT-S12 and WT-S12 strains, MFCs were operated aerobically for the first 24 h after inoculation which showed similar growth of the two strains (**Figure 1A**). Moreover, the flavins (including riboflavin and riboflavin-5-phosphate) generating capacity of planktonic MT-S12 and WT-S12 were comparable, indicating that cytochrome *c* had no significant effects on the aerobic growth and flavin secretion of *S. decolorationis* S12.

Regarding the biofilm growth, CLSM showed similar biofilm thickness ($17 \pm 7 \mu\text{m}$) on the electrode surface of the WT-S12 and MT-S12 MFCs (Supplementary Figure S2). Despite that, the biofilm biomass of MT-S12 was less in comparison with that of the WT-S12 ($15 \text{ vs } 17.5 \mu\text{g/cm}^2$) which is consistent with the biofilm cell density observed by CLSM (**Figure 1B**). This is reasonable as the dissolved oxygen concentration decreased dramatically from the biofilm-liquid interface to the biofilm-electrode interface (from 0.08 to 0.01 mM). It is likely that the anaerobic microenvironment within the biofilm prevented the growth of MT-S12 biofilm cells as cytochrome *c* are needed in *Shewanella* anaerobic growth. In line with the biomass content, flavin concentrations in MT-S12 biofilm are lower than that in the WT-S12 biofilms. By normalizing to biofilm biomass, it can be seen that the flavin-secretion capacity of MT-S12 biofilm cells was 12.9% lower than that of WT-S12 ($0.027 \text{ vs. } 0.031 \mu\text{M per mg protein}$, **Figure 1C**). Several previous reports have indicated that flavin secretion capacity of *Shewanella* species would decrease in unfavorable growth conditions as lower flavin generation was observed in anaerobic or single electron acceptor condition than in aerobic or multiple electron acceptor condition, respectively (von Canstein et al., 2008; Brutinel and Gralnick, 2012; Wu et al., 2012). It seemed likely that MT-S12 suffered more stress in the micro-aerobic biofilm environment relative to WT-S12. Moreover, the decreased flavin secretion of WT-S12 would save

more energy for some other essential metabolisms to survive under unfavorable conditions (Marsili et al., 2008).

Electricity Generation Capacity of MT and WT Strain

After open-circuit aerobic growth, MFCs were switched to closed-circuit anaerobic condition which allowed the WT and MT strains to use electrode as the sole electron acceptor. Electricity generation by WT-S12 started within 3 h upon switch and increased to the maximal value of $56.4 \mu\text{A}$ within 33 h (**Figure 2A**). In contrast, MT-S12 MFCs (**Figure 2A**) and abiotic controls (Supplementary Figure S3) showed no obvious electricity generation, indicating that cytochrome *c*-deficient MT-S12 lost the electrode respiration capacity. This is predictable as cytochrome *c* has been demonstrated to be essential in EET capacity of *Shewanella* and other reported microbes capable of electrode respiration (Coursolle et al., 2010; Lovley, 2012).

Electron mediators such as neutral red, flavins or AQDS are usually used to stimulate EET processes of bacteria capable or originally incapable of EET (e.g., *Escherichia coli*, *Actinobacillus succinogenes*) (Chung et al., 1978; Park and Zeikus, 2000). *Shewanella* species can secrete flavins as electron mediators or cofactors to deliver electrons from OMCs to electrode and stimulate the EET rate by up to 50-fold (Coursolle et al., 2010; Okamoto et al., 2014b). On the other hand, it was reported that over 300 proteins (including OMCs and various ENCP) existed in the EPS of *Shewanella* sp. HRGR-1 biofilm (Cao et al., 2011). The incapability in electricity generation of MT-S12 (**Figure 2A**) suggested that the ENCP has no significant interaction with the electrode, directly or indirectly via flavins, under normal cultivation condition.

However, when we increased the flavin concentration from 0 to $10 \mu\text{M}$ in both WT- and MT-S12 MFCs, the electricity generated by WT-S12 increased from $15.2 \text{ to } 55.4 \mu\text{A}$ as expected (Okamoto et al., 2014a) and intriguingly, the electricity generated by MT-S12 increased to $14.4 \mu\text{A}$ (26% of the

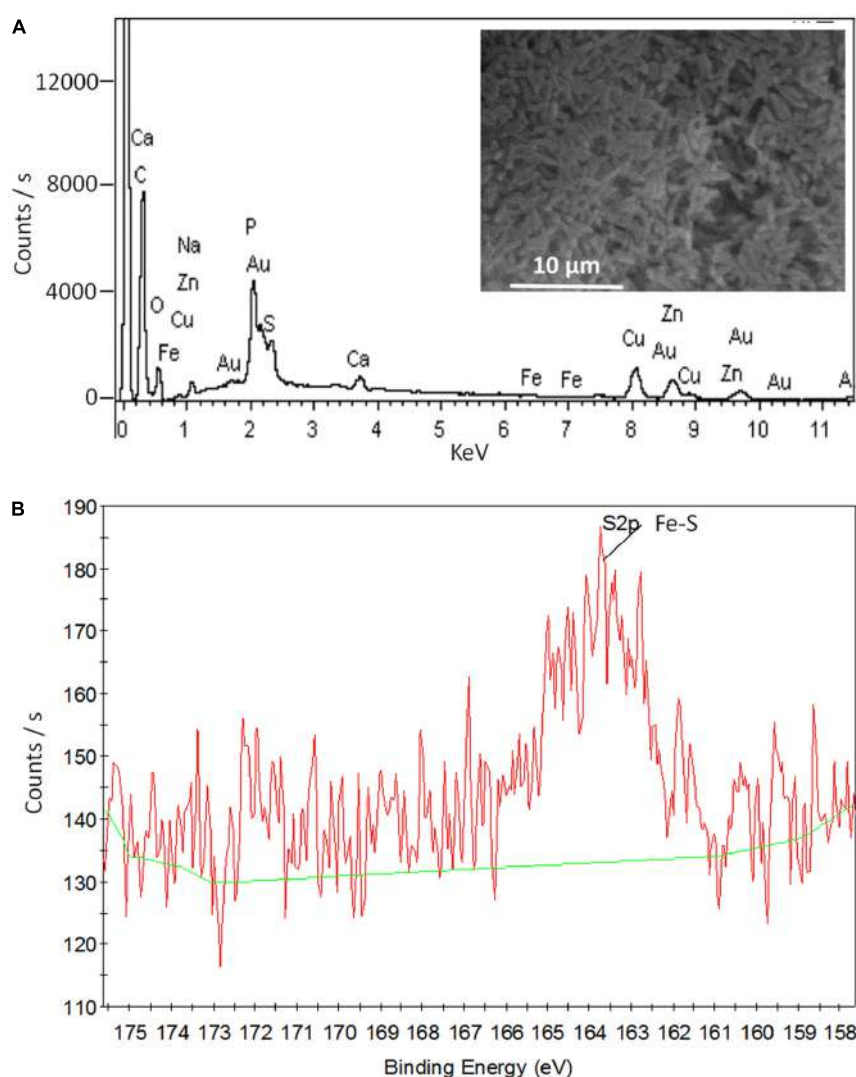


FIGURE 4 | SEM- EDS (**A**) and XPS (**B**) data of the MT-S12 cell surface. Background data was shown in Supplementary Figure S5.

WT-S12) (**Figure 2B**). In addition to electricity generation, riboflavin-stimulated EET were also founded in Fe(III) and amaranth (an cell membrane-impermeable azo dye; Hong et al., 2007) reduction of MT-S12 biofilms (Supplementary Figure S4). These results suggested that although OMCs were eliminated, the electron transfer from MT-S12 to electrode could also be stimulated by higher concentration of electron mediators. This is consistent with the fact that many OMC-free bacteria could perform EET with artificially added electron mediators. Moreover, the remained slight Fe(III) and amaranth reduction capacity of MT-S12 (Supplementary Figure S4) indicated that some extracellular redox species other than OMCs exist.

Electrochemical Interaction between Electrode and MT- and WT-S12

To further confirm and understand the interaction between electrode and MT-S12 with artificially added riboflavin, CV,

and EIS analyses were conducted. As a control, the abiotic electrode CV showed no obvious redox peak and riboflavin showed a reduction peak at -0.23 V which is consistent with previous reports (Marsili et al., 2008) (Supplementary Figure S3). WT-biofilms have a couple of reductive and oxidative peaks at -0.29 and -0.21 V (centered at -0.25 V) (**Figure 3A**), which could be attributed to flavins as cofactors of OMCs (Marsili et al., 2008; Okamoto et al., 2014b). A much wide redox area without obvious peak can be seen for MT-biofilms. After adding 10 μM of riboflavin, a wide redox couple (centered at -0.195 V) were observed. The enhanced wide-range redox peak of the MT-biofilms with added riboflavin indicated that various redox species may react with the electrode via riboflavin, which is different with the sharp CV peaks caused by the OMC-flavin of the WT-S12. It has been reported that flavins in *Shewanella* EET mainly functioned as cofactors of OMCs (one-electron reaction)

which could largely enhance the EET rate than free flavins (two-electron reaction) (Kumar et al., 2008; Okamoto et al., 2014b). For the MT-S12 biofilms, flavins could only functioned in a free state due to the deletion in OMCs. Therefore, the WT-S12 biofilms showed higher anodic peak current than that of the MT-S12 biofilms with or without artificially added riboflavin.

Electrochemical impedance spectroscopy measurements of the anodes were shown in Bode-diagram (**Figure 3B**). The phase angle (theta)-frequency plots (**Figure 3C**) suggested an one-time constant model of the anodic reactions which is consistent with the used equivalent circuit ($R(RctCPE)$). The phase angels of different anodes occurred with low frequencies (<100 Hz) indicating that the anodic reaction was dominated by flavin-mediated electron transfer processes (Ramasamy et al., 2009; Jung et al., 2012). This is consistent with the physiological analysis with several *Shewanella* mutants that flavins accounts for $\sim 75\%$ in *Shewanella* EET to solid electron acceptors (Kotloski and Gralnick, 2013). The impedance modulus (Z)-frequency plots (**Figure 3B**) showed an impedance order of the three anodes: MT-S12 > MT-S12 with flavins > WT-S12 (detailed fitting data shown in Supplementary Table S1), which is consistent with their CV profiles and electricity generation capacities. Electrochemical analyses further confirmed that riboflavin could increase the charge transfer between *S. decolorationis* S12 and electrode in the presence or absence of OMCs.

Possible Role of ENCP in MT-S12 Electricity Generation

Considering that the added flavins can only deliver extracellular electrons (Richter et al., 2010) and MT-S12 have no OMCs, it can be presumed that flavins could receive electrons from ENCP or other redox species in MT-S12 biofilm EPS and further transfer them to terminal electron acceptors.

To verify whether biofilm ENCP played a role in the flavin-enhanced electricity generation, proteinase K, a non-redox enzyme capable of destroying extracellular proteins but not intracellular proteins, was used to treat the biofilms (Clark et al., 2007). After treatment, electricity generation by MT-S12 biofilm dramatically decreased by 84% (to $2.3 \mu\text{A}$, **Figure 2B**) which suggested that ENCP played an important role in the flavin-enhanced electrode respiration by MT-S12.

Shewanella EPS contains a plenty of ENCP that might donate electrons to flavins. Among those ENCP, Fe-S cluster containing-proteins exist widely in the EPS of different bacteria species (Cao et al., 2011; Yates et al., 2016). By using EDS, we identified element Fe in the EPS of both WT-S12 and MT-S12 (0.11% and 0.07% w/w, respectively) (**Figure 4A**). Sulfur as a common element in bio-molecular was also detected. Furthermore, the XPS peak at 163.5 eV could be attributed to Fe-SH bond (Volmer-Uebing and Stratmann, 1992) (**Figure 4B**), suggesting that Fe-S cluster exists in the EPS. Fe-S cluster can donate electrons to flavins (Watanabe et al., 2016), therefore,

it is possible that Fe-S cluster-containing proteins (or other SNCP) donate electrons to the riboflavin and further to electrode. Consistently, Yates et al. (2016) recently reported that extracellular Fe-S cluster containing-proteins from *Marinobacter* spp. might play an important role in EET of an electrode attached mixed-species biofilm. To further elucidate the role of Fe-S cluster-containing proteins or other ENCP in EET, high throughput sequencing and molecular interaction analysis are needed.

Outer membrane *c*-type cytochromes-free microbes are generally considered to participate indirectly in electricity generation by providing fermentation or pre-degradation products to electricity-generating microbes rather than donating electrons to electrode (Logan, 2009; Hodgson et al., 2016). In contrast, our results indicated that the ENCP from OMC-free microbes (e.g., fermentation microbes) could also contribute to EET via electron mediators. Moreover, the contribution of OMC-free microbe in electricity generation could partially explain a repeatedly reported phenomenon that scarce or even no typical electricity generating microbes could be founded in the anode microbial communities of many well-performed BESs (Xia et al., 2015; Xiao et al., 2015).

CONCLUSION

The electricity generation capacities and bioelectrochemical properties of wild *S. decolorationis* S12 and an OMC-mutant were comparatively analyzed in this study. In comparison with the wild strain, the mutant showed similar planktonic growth but slightly decreased biofilm growth. Similarly, to the wild strain, the EET rate of the OMC-mutant could be stimulated with artificially added flavins. ENCP in the biofilm EPS, such as Fe-S cluster containing-proteins, may play an important role in the EET process of the OMC-mutant. The results indicated an unignorable role of ENCP in bacterial EET process with the facilitation of electron mediators.

AUTHOR CONTRIBUTIONS

YY, MX, WL designed the study; YY, GK operated the experiments, XC made the mutant, YL discussed the results, YY, WL wrote the paper, all authors agree to be accountable for the content of the work.

ACKNOWLEDGMENTS

This research was supported by the National Natural Science Foundation of China (31570111), the National Natural Science Foundation for Excellent Young Scholars of China (51422803), Guangdong Provincial Science and Technology Project (2016A030306021, 2014TQ01Z116, 2014TX01Z038, 2016B070701017), Guangdong Ocean and Fishery Administration Project (A201601D01), Pearl

River S&T Nova Program of Guangzhou (201610010090), Open Project of Key Laboratory of Environmental Biotechnology, CAS (kf2016003), Science and Technology Project of Guangdong Academy of Sciences (rcjj201502, 2017GDASCX-0403).

REFERENCES

- Ahuja, U., and Thony-Meyer, L. (2003). Dynamic features of a heme delivery system for cytochrome c maturation. *J. Biol. Chem.* 278, 52061–52070. doi: 10.1074/jbc.M310077200
- Brutinel, E. D., and Gralnick, J. A. (2012). Shuttling happens: soluble flavin mediators of extracellular electron transfer in *Shewanella*. *Appl. Microbiol. Biotechnol.* 93, 41–48. doi: 10.1007/s00253-011-3653-0
- Cao, B., Shi, L., Brown, R. N., Xiong, Y., Fredrickson, J. K., Romine, M. F., et al. (2011). Extracellular polymeric substances from *Shewanella* sp. HRCR-1 biofilms: characterization by infrared spectroscopy and proteomics. *Environ. Microbiol.* 13, 1018–1031. doi: 10.1111/j.1462-2920.2010.02407.x
- Chen, X., Xu, M., Wei, J., and Sun, G. (2010). Two different electron transfer pathways may involve in azoreduction in *Shewanella decolorationis* S12. *Appl. Microbiol. Biotechnol.* 86, 743–751. doi: 10.1007/s00253-009-2376-y
- Chung, K. T., Fulk, G. E., and Egan, M. (1978). Reduction of azo dyes by intestinal anaerobes. *Appl. Environ. Microbiol.* 35, 558–562.
- Clark, M. E., Edelmann, R. E., Duley, M. L., Wall, J. D., and Fields, M. W. (2007). Biofilm formation in *Desulfovibrio vulgaris* Hildenborough is dependent upon protein filaments. *Environ. Microbiol.* 9, 2844–2854. doi: 10.1111/j.1462-2920.2007.01398.x
- Coursolle, D., Baron, D. B., Bond, D. R., and Gralnick, J. A. (2010). The Mtr respiratory pathway is essential for reducing flavins and electrodes in *Shewanella oneidensis*. *J. Bacteriol.* 192, 467–474. doi: 10.1128/JB.00925-09
- Hodgson, D. M., Smith, A., Dahale, S., Stratford, J. P., Li, J., Gruning, A., et al. (2016). Segregation of the anodic microbial communities in a microbial fuel cell cascade. *Front. Microbiol.* 7:699. doi: 10.3389/fmicb.2016.00699
- Hong, Y. G., Xu, M. Y., Guo, J., Xu, Z. C., Chen, X. J., and Sun, G. P. (2007). Respiration and growth of *Shewanella decolorationis* S12 with an azo compound as the sole electron acceptor. *Appl. Environ. Microbiol.* 73, 64–72. doi: 10.1128/Aem.01415-06
- Jung, S., Ahn, Y. H., Oh, S. E., Lee, J., Cho, K. T., Kim, Y., et al. (2012). Impedance and thermodynamic analysis of bioanode, abiotic anode, and riboflavin-amended anode in microbial fuel cells. *Bull. Korean Chem. Soc.* 33, 3349–3354. doi: 10.5012/bkcs.2012.33.10.3349
- Kotloski, N. J., and Gralnick, J. A. (2013). Flavin electron shuttles dominate extracellular electron transfer by *Shewanella oneidensis*. *MBio* 4:e00553-12. doi: 10.1128/mBio.00553-12
- Kumar, S. A., and Chen, S. M. (2007). Electrochemical, microscopic, and EQCM studies of cathodic electrodeposition of ZnO/FAD and anodic polymerization of FAD films modified electrodes and their electrocatalytic properties. *J. Solid State Electrochem.* 11, 993–1006. doi: 10.1007/s10008-006-0236-6
- Kumar, S. A., Lo, P. H., and Chen, S. M. (2008). Electrochemical synthesis and characterization of TiO₂ nanoparticles and their use as a platform for flavin adenine dinucleotide immobilization and efficient electrocatalysis. *Nanotechnology* 19:255501. doi: 10.1088/0957-4484/19/25/255501
- Logan, B. E. (2009). Exoelectrogenic bacteria that power microbial fuel cells. *Nat. Rev. Microbiol.* 7, 375–381. doi: 10.1038/nrmicro2113
- Logan, B. E., and Rabaey, K. (2012). Conversion of wastes into bioelectricity and chemicals by using microbial electrochemical technologies. *Science* 337, 686–690. doi: 10.1126/science.1217412
- Lovley, D. R. (2006). Bug juice: harvesting electricity with microorganisms. *Nat. Rev. Microbiol.* 4, 497–508. doi: 10.1038/Nrmicro1442
- Lovley, D. R. (2012). Electromicrobiology. *Annu. Rev. Microbiol.* 66, 391–409. doi: 10.1146/annurev-micro-092611-150104
- Manohar, A. K., and Mansfeld, F. (2009). The internal resistance of a microbial fuel cell and its dependence on cell design and operating conditions. *Electrochim. Acta* 54, 1664–1670. doi: 10.1016/j.electacta.2008.06.047
- Marsili, E., Baron, D. B., Shikhare, I. D., Coursolle, D., Gralnick, J. A., and Bond, D. R. (2008). *Shewanella* secretes flavins that mediate extracellular electron transfer. *Proc. Natl. Acad. Sci. U.S.A.* 105, 3968–3973. doi: 10.1073/pnas.0710525105
- Okamoto, A., Hashimoto, K., and Nealson, K. H. (2014a). Flavin redox bifurcation as a mechanism for controlling the direction of electron flow during extracellular electron transfer. *Angew. Chem. Int. Ed. Engl.* 53, 10988–10991. doi: 10.1002/anie.201407004
- Okamoto, A., Saito, K., Inoue, K., Nealson, K. H., Hashimoto, K., and Nakamura, R. (2014b). Uptake of self-secreted flavins as bound cofactors for extracellular electron transfer in *Geobacter* species. *Energy Environ. Sci.* 7, 1357–1361. doi: 10.1039/C3ee43674h
- Park, D. H., and Zeikus, J. G. (2000). Electricity generation in microbial fuel cells using neutral red as an electronophore. *Appl. Environ. Microbiol.* 66, 1292–1297. doi: 10.1128/Aem.66.4.1292-1297.2000
- Ramasamy, R. P., Gadhamshetty, V., Nadeau, L. J., and Johnson, G. R. (2009). Impedance spectroscopy as a tool for non-intrusive detection of extracellular mediators in microbial fuel cells. *Biotechnol. Bioeng.* 104, 882–891. doi: 10.1002/bit.22469
- Richter, K., Bücking, C., Schicklberger, M., and Gescher, J. (2010). A simple and fast method to analyze the orientation of c-type cytochromes in the outer membrane of Gram-negative bacteria. *J. Microbiol. Methods* 82, 184–186. doi: 10.1016/j.mimet.2010.04.011
- Shi, L., Richardson, D. J., Wang, Z., Kerisit, S. N., Rosso, K. M., Zachara, J. M., et al. (2009). The roles of outer membrane cytochromes of *Shewanella* and *Geobacter* in extracellular electron transfer. *Environ. Microbiol. Rep.* 1, 220–227. doi: 10.1111/j.1758-2229.2009.00035.x
- Volmer-Uebing, M., and Stratmann, M. (1992). A surface analytical and an electrochemical study of iron surfaces modified by thiols. *Appl. Surf. Sci.* 55, 19–35. doi: 10.1016/0169-4332(92)90377-A
- von Canstein, H., Ogawa, J., Shimizu, S., and Lloyd, J. R. (2008). Secretion of flavins by *Shewanella* species and their role in extracellular electron transfer. *Appl. Environ. Microbiol.* 74, 615–623. doi: 10.1128/Aem.01387-07
- Watanabe, S., Tajima, K., Matsui, K., and Watanabe, Y. (2016). Characterization of iron-sulfur clusters in flavin-containing opine dehydrogenase. *Biosci. Biotechnol. Biochem.* 80, 2371–2375. doi: 10.1080/09168451.2016.1206812
- Wu, D., Xing, D., Lu, L., Wei, M., Liu, B., and Ren, N. (2012). Ferric iron enhances electricity generation by *Shewanella oneidensis* MR-1 in MFCs. *Bioresour. Technol.* 135, 630–634. doi: 10.1016/j.biortech.2012.09.106
- Xia, C., Xu, M., Liu, J., Guo, J., and Yang, Y. (2015). Sediment microbial fuel cell prefers to degrade organic chemicals with higher polarity. *Bioresour. Technol.* 190, 420–423. doi: 10.1016/j.biortech.2015.04.072
- Xiao, Y., Zheng, Y., Wu, S., Zhang, E.-H., Chen, Z., Liang, P., et al. (2015). Pyrosequencing reveals a core community of anodic bacterial biofilms in bioelectrochemical systems from China. *Front. Microbiol.* 6:1410. doi: 10.3389/fmicb.2015.01410
- Xu, M., Guo, J., Cen, Y., Zhong, X., Cao, W., and Sun, G. (2005). *Shewanella decolorationis* sp nov., a dye-decolorizing bacterium isolated from activated sludge of a waste-water treatment plant. *Int. J. Syst. Evol. Microbiol.* 55, 363–368. doi: 10.1099/ijts.0.63157-0
- Yang, Y., Xiang, Y., Sun, G., Wu, W., and Xu, M. (2015). Electron acceptor-dependent respiratory and physiological stratifications in biofilms. *Environ. Sci. Technol.* 49, 196–202. doi: 10.1021/es504546g

SUPPLEMENTARY MATERIAL

The Supplementary Material for this article can be found online at: <http://journal.frontiersin.org/article/10.3389/fmicb.2017.01115/full#supplementary-material>

- Yang, Y., Xiang, Y., Xia, C., Wu, W., Sun, G., and Xu, M. (2014). Physiological and electrochemical effects of different electron acceptors on bacterial anode respiration in bioelectrochemical systems. *Bioresour. Technol.* 164, 270–275. doi: 10.1016/j.biortech.2014.04.098
- Yang, Y., Xu, M., Guo, J., and Sun, G. (2012). Bacterial extracellular electron transfer in bioelectrochemical systems. *Process Biochem.* 47, 1707–1714. doi: 10.1016/j.procbio.2012.07.032
- Yates, M. D., Eddie, B. J., Kotloski, N. J., Lebedev, N., Malanoski, A. P., Lin, B., et al. (2016). Toward understanding long-distance extracellular electron transport in an electroautotrophic microbial community. *Energy Environ. Sci.* 9, 3544–3558. doi: 10.1039/c6ee02106a

Conflict of Interest Statement: The authors declare that the research was conducted in the absence of any commercial or financial relationships that could be construed as a potential conflict of interest.

Copyright © 2017 Yang, Kong, Chen, Lian, Liu and Xu. This is an open-access article distributed under the terms of the Creative Commons Attribution License (CC BY). The use, distribution or reproduction in other forums is permitted, provided the original author(s) or licensor are credited and that the original publication in this journal is cited, in accordance with accepted academic practice. No use, distribution or reproduction is permitted which does not comply with these terms.



Impact of Ferrous Iron on Microbial Community of the Biofilm in Microbial Fuel Cells

Qian Liu, Bingfeng Liu, Wei Li, Xin Zhao, Wenjing Zuo and Defeng Xing*

State Key Laboratory of Urban Water Resource and Environment, School of Municipal and Environmental Engineering, Harbin Institute of Technology, Harbin, China

The performance of microbial electrochemical cells depends upon microbial community structure and metabolic activity of the electrode biofilms. Iron as a signal affects biofilm development and enrichment of exoelectrogenic bacteria. In this study, the effect of ferrous iron on microbial communities of the electrode biofilms in microbial fuel cells (MFCs) was investigated. Voltage production showed that ferrous iron of 100 μM facilitated MFC start-up compared to 150 μM , 200 μM , and without supplement of ferrous iron. However, higher concentration of ferrous iron had an inhibitive influence on current generation after 30 days of operation. Illumina Hiseq sequencing of 16S rRNA gene amplicons indicated that ferrous iron substantially changed microbial community structures of both anode and cathode biofilms. Principal component analysis showed that the response of microbial communities of the anode biofilms to higher concentration of ferrous iron was more sensitive. The majority of predominant populations of the anode biofilms in MFCs belonged to *Geobacter*, which was different from the populations of the cathode biofilms. An obvious shift of community structures of the cathode biofilms occurred after ferrous iron addition. This study implied that ferrous iron influenced the power output and microbial community of MFCs.

OPEN ACCESS

Edited by:

Haoyi Cheng,
Research Center for
Eco-Environmental Sciences (CAS),
China

Reviewed by:

Xianhua Liu,
Tianjin University, China
Ping Li,
China University of Geosciences,
China

*Correspondence:

Defeng Xing
dxing@hit.edu.cn

Specialty section:

This article was submitted to
Microbiotechnology, Ecotoxicology
and Bioremediation,
a section of the journal
Frontiers in Microbiology

Received: 08 January 2017

Accepted: 08 May 2017

Published: 07 June 2017

Citation:

Liu Q, Liu B, Li W, Zhao X, Zuo W
and Xing D (2017) Impact of Ferrous
Iron on Microbial Community of the
Biofilm in Microbial Fuel Cells.
Front. Microbiol. 8:920.
doi: 10.3389/fmicb.2017.00920

INTRODUCTION

Microbial electrochemical cell (MEC) has been admired as a versatile device that can be used for alternative energy generation, electrosynthesis, biosensor, and waste treatment (Hou et al., 2016; Liu et al., 2016a; Huang et al., 2017). However, practical implementation of microbial fuel cells (MFCs) remains restricted by reasons of low electron transfer efficiency and high material costs (Logan et al., 2006). For the past few years, researchers studied electrode materials, exoelectrogenic bacteria, reactor configuration and operational conditions of MFCs (Watson and Logan, 2010; Yong et al., 2011; Janicek, 2015), and pointed out that microbial biofilm was the most direct and key element that affect current generation (Mohan et al., 2008). However, microbial biofilm and its community structure of MFCs can be influenced by temperature, pH, carbon source, inoculum, and metal ion (Lu et al., 2011, 2012; Patil et al., 2011; Wu et al., 2013). The diverse populations developed in the biofilms in MECs have been widely analyzed (Mei et al., 2015). *Geobacter* as a typical dissimilatory metal-reducing bacterium (DMRB) is commonly identified in MFCs (Mohan et al., 2014; Zhu et al., 2014; Kumar et al., 2016). Hence, to understand and optimize ecological conditions that facilitate exoelectrogens enrichment and electron transfer are essential for MEC application.

Iron plays a central role in the development and maintenance of biofilm of *Pseudomonas* (Hunter et al., 2013). Although ferric iron has been identified as an important parameter

affecting the biofilm formation (Banin et al., 2005), the impact of ferrous iron on the biofilm is less known. Metal ions are essential minerals to composite microorganisms and biological molecules, including metalloproteins which play key roles in most biological processes (iron for respiration; Cvetkovic et al., 2010). The reactive metal ions may have the phenomenon of redox reaction, catalysis, or precipitation, etc. and thus directly affect the performance of MECs by influencing the metabolism of microorganisms or the activity of enzymes (Lu et al., 2015). Due to its high redox activity, the Fe²⁺ is able to be oxidized at the anode in an air-cathode fuel cells which are capable of abiotic electricity generation (Cheng et al., 2007). The addition of ferrous sulfate to the anode medium has improved the power densities of MFCs during start-up period (Wei et al., 2013). However, there are less literatures concerning the response of exoelectrogenic community in the electrode biofilms to ferrous iron.

Ferrous iron used in catholyte of dual-chambered MFC enhanced power output by increasing salt concentration or improving cathode potential (Ter Heijne et al., 2007). A comparison of results with and without ferrous iron as a cathodic reactant also revealed that the addition of ferrous iron enhanced power generation in batch MFC (Wang et al., 2011). However, the knowledge related to the effects of ferrous iron on performances of MFCs and microbial communities of electrode biofilms is less known. To reveal the response of microbial community of the electrode biofilm to ferrous iron, in this study, electrochemical performances of MFCs supplemented with different concentrations of ferrous iron were investigated. Meanwhile, microbial community structures of the anodes and cathodes biofilms in MFCs were analyzed using Illumina Hiseq sequencing of 16S rRNA gene amplicons.

MATERIALS AND METHODS

MFC Configuration and Operation

Single-chamber MFCs with volume of 14 mL were constructed as previously described (Xing et al., 2008). Anodes were made of carbon paper (Toray TGP-H-090, Japan), while cathodes were stainless steel mesh by rolling activated carbon and polytetrafluoroethylene (PTFE) (Dong et al., 2012) (the area of anode and cathode were both 7 cm²). Domestic wastewater was used as inoculum in the first 5 days. Nutrient solutions were consisted of 1 g/L sodium acetate, 5 mL/L vitamins, 12.5 mL/L minerals, 100 mM phosphate buffer saline (PBS, pH of 6) and FeSO₄ with different concentrations. The final pH value of nutrient solution was 6.2 ± 0.1. The final concentrations of FeSO₄ in MFCs were 32 (control), 100, 150, and 200 μM.

Voltages across the external resistor (1000 Ω) of MFCs were measured using Keithley 2700 multimeter/data acquisition system. All MFCs were operated at 35°C and each Fe²⁺ concentration have three replicates. Cyclic voltammetry (CV) measurements of MFCs at the 15th day were performed on Autolab potentiostat (Metrohm, Netherlands) with scan rate of 0.01 V/s.

DNA Extraction and Illumina Sequencing of 16S rRNA Gene

After MFCs were operated for 2 months, the anode and cathode biofilms of MFCs (control, fed with 100 and 200 μM Fe²⁺) were sampled for genomic DNA extraction by using PowerSoil DNA Isolation Kit according the manufacturer's instructions. DNA concentration and purity were determined by NanoPhotometer P-Class (Implen, GmbH). Prior to polymerase chain reaction (PCR) amplification, DNA of anode and cathode biofilms from three duplicated bioreactors were mixed. The V4 region (length of ~373 bp) of bacterial 16S rRNA gene was amplified by using a set of bacterial primers 515F (5'-GTGCCAGCMGCCGCGTAA-3') and 806R (5'-GGACTACHVGGGTWTCTAAT-3'). After integrated with barcode, PCR amplification was implemented by using ABI GeneAmp® 9700 PCR system.

Sequencing was performed on Illumina Hiseq platforms according to the standard protocols. Raw Tags were overlapped by using the Fast Length Adjustment of SHort reads (FLASH; V1.2.7)¹ software (Magoc and Salzberg, 2011) and filtered following pipelines of Quantitative Insights Into Microbial Ecology (QIIME, V1.7.0; Caporaso et al., 2010). Effective tags were obtained by removing chimeric sequences after aligned using Gold database². Operational taxonomic units (OTUs) were determined based on the threshold of 97% similarity using UPARSE software (Uparse V7.0.1001). A representative sequence of each OTU was aligned for taxonomic identification using the GreenGene database³ and Ribosomal Database Project (RDP) classifier (version 2.2)⁴ with the threshold of 80–100% (DeSantis et al., 2006; Wang et al., 2007). The raw Illumina sequencing data were deposited in the Sequence Read Archive (SRA) of National Center for Biotechnology Information (NCBI) under the accession Nos. SRR5266191–SRR5266196.

RESULTS AND DISCUSSION

Electricity Generation and Electrochemical Activity of MFCs

Cyclic voltammetry curves showed that MFCs supplemented with 100 μM ferrous ion (Fe²⁺) obtained the highest current peak on the 15th day (Figure 1). The results suggested that low concentration of Fe²⁺ could obviously improve electrochemical activity of MFCs in the start-up period. During another 15 days of operation, MFCs with 100 μM ferrous ion showed the best electrochemical characteristics compared to MFCs with 150 and 200 μM Fe²⁺, and MFCs without additional Fe²⁺ supplement (Figure 2). The maximum voltage of 0.55 V was monitored in MFCs fed with 100 μM Fe²⁺, and then following the order control (0.54 V), 150 μM Fe²⁺ (0.52 V) and 200 μM Fe²⁺ (0.47 V). After all MFCs were operated for 30 days, MFCs of

¹<http://ccb.jhu.edu/software/FLASH/>

²http://drive5.com/uchime/uchime_download.html

³<http://greengenes.lbl.gov/cgi-bin/nph-index.cgi>

⁴<http://sourceforge.net/projects/rdp-classifier/>

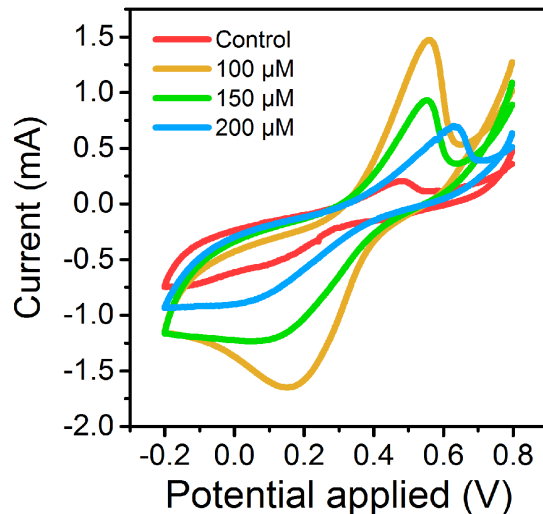


FIGURE 1 | Cyclic voltammetry curves of MFCs supplemented with different concentrations of ferrous iron on 15th day.

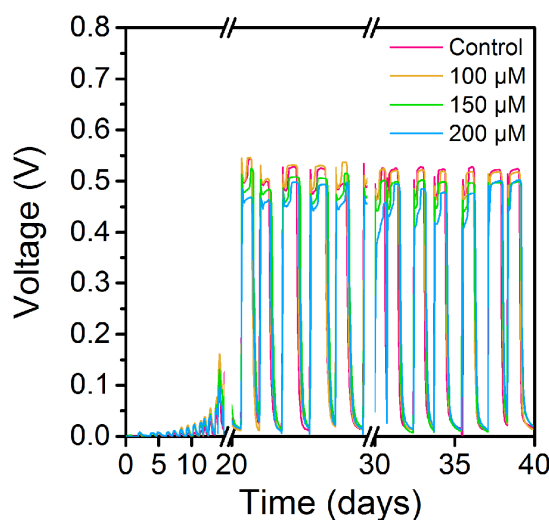


FIGURE 2 | Voltage curves of MFCs supplemented with ferrous iron of different concentrations.

control groups maintained the steady voltage output, while other MFCs with Fe²⁺ addition performed a weaken efficiency.

Community Diversity of MFCs with Different Concentrations of Fe²⁺

Since the power outputs of MFCs with 150 and 200 μM were similar, and the CV result of 200 μM adequately represented the decrease of electrochemical activity of electrode biofilms, the biofilm samples of MFCs with ferrous iron of 150 μM were not used for microbial community analysis. After quality filtering the raw tags, 50,373 to 54,932 effective tags were obtained per sample, with average length of 373 bp. Total OTUs at the 97% similarity were ranged from 630 to 824 per sample

with an average of 710 OTUs (Table 1). The anode biofilms in MFCs supplemented with ferrous iron showed slightly lower population diversity than that in control MFCs without ferrous iron supplement. Shannon indices were 3.72, 4.71, and 5.21 for the anodes biofilms with 100, 200 μM Fe²⁺, and without Fe²⁺, respectively. By contrast, Fe²⁺ increased the population diversities of the cathode biofilms, Shannon indices increased from 4.3 (control) to 5.02 (100 μM Fe²⁺) and 5.54 (200 μM Fe²⁺), suggesting that Fe²⁺ affected microbial community structure of the electrode biofilms in MFCs. Principal component analysis based on OTUs showed three clusters, the anode biofilms of MFC without Fe²⁺ was separated from the anode biofilms of MFC supplemented with Fe²⁺ of 100 and 200 μM Fe²⁺ and the cathode biofilms (control, 100, and 200 μM Fe²⁺; Figure 3).

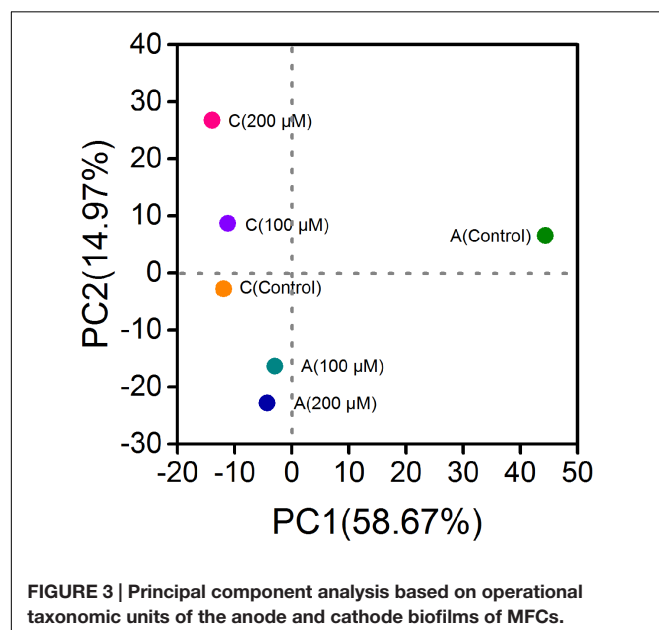
Bacterial Composition of the Anode and Cathode Biofilms

The bacterial communities of the anode biofilms were substantially shifted when additional Fe²⁺ was supplemented in MFCs. *Proteobacteria* were the most dominant phylum observed both in the anode (71–75%, relative abundance) and cathode biofilms (41–78%) (Figure 4A). *Chlorobi* (11–14%) and *Bacteroidetes* (4–8%) were also predominant phyla in the anode biofilms. The relative abundances of *Lentisphaerae* in the cathode biofilms, were much higher than that in the anode biofilms, reached to 31% (100 μM Fe²⁺), 22% (200 μM Fe²⁺), and 4% (control). *Deltaproteobacteria*, *Ignavibacteria*, and *Betaproteobacteria* were the most predominant classes in the anode biofilms and accounted for 75% more or less, of which, the abundance of *Deltaproteobacteria* in the anode of MFCs with 100 μM reached to 50%, speculating that *Deltaproteobacteria* were the dominant class since MFC start-up period (Figure 4B). By contrast, microbial community structures of cathodes were different from anodes. *Alphaproteobacteria*, *Gammaproteobacteria*, *Bacteroidia*, and *Lentisphaerae* were the predominant classes on the cathodes. Cathodes of MFCs with additional Fe²⁺ had similar communities that were much different with control group.

The predominant genera varied significantly among all anodes and cathodes biofilms (Figure 5). The majority of predominant populations in the control MFCs were affiliated with *Geobacter* spp. (30.7%) and *Legionella* spp. (50.3%). *Geobacter* was also the predominant genus in the anode of MFC supplemented with 100 and 200 μM Fe²⁺, the relative abundance of which population reached up to 49.3 and 24.4%. Another predominant genus in the anode biofilms of MFC (200 μM Fe²⁺) was affiliated to *Rhodanobacter* (19%). In the cathode biofilms of MFCs with 100 and 200 μM Fe²⁺, higher relative abundance of predominant genera belonged to *Legionella* spp. (2 and 6%), and no absolutely predominant populations were present. Hierarchical cluster analysis of microbial communities based on genus taxonomy revealed that the relative abundance of *Sphaerochaeta*, *Dechloromonas*, *Paracoccus*, *Thermomonas*, and *Rhodanobacter* increased in the anode biofilms of MFCs supplemented with 200 μM Fe²⁺ (Figure 6). Meanwhile, the

TABLE 1 | Qualities of reads identified by Illumina Hiseq sequencing and bacterial diversity estimates based on OTUs (97% similarity).

Sample name	Effective tags	OTUs	Shannon	Chao1	Simpson	ACE	Good's coverage
Anode (control)	53,807	824	5.21	908.307	0.884	900.018	0.997
Anode (100 μ M)	53,136	630	3.716	691.84	0.733	703.657	0.998
Anode (200 μ M)	54,932	679	4.706	785.135	0.886	796.327	0.997
Cathode (control)	51,054	692	4.3	755.5	0.748	773.924	0.997
Cathode (100 μ M)	54,592	697	5.021	757.026	0.879	771.527	0.998
Cathode (200 μ M)	50,373	741	5.542	810.327	0.927	813.045	0.997

**FIGURE 3 |** Principal component analysis based on operational taxonomic units of the anode and cathode biofilms of MFCs.

relative abundance of *Gordonia*, *Sphingopyxis*, *Hydrogenophaga*, and *Janthinobacterium* in the cathode biofilms of MFCs with 200 μ M Fe²⁺ were relatively higher than that in the cathodes biofilms of MFCs without Fe²⁺ and with 100 μ M Fe²⁺, but higher proportion of *Thauera*, *Dokdonella*, *Fusibacter*, *Devosia*, and *Desulfovibrio* were observed in the cathode biofilms of MFCs with 100 μ M Fe²⁺.

Effect of Fe²⁺ on Predominant Populations in the Electrode Biofilms

Ferrous iron with appropriate concentration (100 μ M) stimulated electrochemical activity of MFCs during the start-up period, but Fe²⁺ cannot enhance power output after 30 days of operation and higher concentration of Fe²⁺ had the negative effect (Wei et al., 2013), presumably the Fe²⁺ facilitated biofilm formation at the early stage. The metal ions may act as redox active sites in the enzymes which catalyze the electron transfer and redox reaction to affect the performance of bi-electrochemical systems (BESs) (Lu et al., 2015). In mature anode biofilms, pH decreased through different growth phases, showing that the pH is not always a limiting factor in a biofilm. Meanwhile, increasing redox potential at the biofilm electrode was associated only with the biofilm, demonstrating that microbial biofilms

respire in a unique internal environment (Babauta et al., 2012). Oxidation of ferrous ion by microbes is an important component of iron geochemical cycle (Croal et al., 2004). Recent studies also confirmed that Fe²⁺ oxidation provides an energetic benefit for some microbes' growth when using Fe²⁺ and acetate as the co-substrate (Muehe et al., 2009; Chakraborty et al., 2011). Illumina Hiseq sequencing of 16S rRNA gene indicated that Fe²⁺ shifted bacterial community and influenced enrichment of exoelectrogenic bacteria in the anode biofilms.

An excessive amount of metal salts may result in negative effects on the performance of BESs by inhibiting the activity of microorganisms (Jiang et al., 2011). The relative abundance of *Geobacter* increased from 30.7 to 49.3% in MFCs with 100 μ M Fe²⁺ but decreased to 24.4% in MFCs with 200 μ M Fe²⁺, implying higher Fe²⁺ concentration could not further enrich *Geobacter*. As a result, the power output of MFC with higher Fe²⁺ concentration (200 μ M) was lower than control and 100 μ M Fe²⁺ during MFC steady operation. *Rhodanobacter* accounted for a large proportion (19%) in MFCs with Fe²⁺ concentration of 200 μ M. To date, the function of *Rhodanobacter* was mostly investigated on denitrifying (Green et al., 2012) and thiosulfate-oxidizing (Lee et al., 2007), but little is reported about Fe²⁺ oxidation especially mediated by C-type cytochromes (Croal et al., 2007; Bird et al., 2011). Whether it participates in interspecies interaction with *Geobacter* should be further proved. Other exoelectrogenic bacteria also formed a certain proportion in different anode biofilms, such as *Pseudomonas* (1–6%) and *Arcobacter* (3–7%) (Fedorovich et al., 2009; Yong et al., 2011). *Pseudomonas* has a positive role to benefit other exoelectrogens in anode biofilm under a high concentration of salt addition (Liu et al., 2016b). *Arcobacter* can be selectively enriched in an acetate-fed MFC and rapidly generates a strong electronegative potential (Fedorovich et al., 2009). It indicated that additional ions, like Fe²⁺, will take part in biofilm metabolism or microbial communication, which resulted in community structure changes.

The microbial communities on the cathodes clearly differed from the anodes biofilms in all MFCs. The most predominant genera in the cathode biofilms of MFCs without additional ferrous iron came from *Legionella* spp. (50.3% of relative abundance). However, the relative abundance of *Legionella* on the cathode biofilms declined to 2–6% with Fe²⁺ addition, suggesting that *Legionella* was inhibited by high concentration of Fe²⁺. The abundance of Fe(II)-oxidizing bacteria, *Janthinobacterium* (Geissler et al., 2011), in the cathode biofilms of MFC with 200 μ M Fe²⁺ were relatively higher than other groups

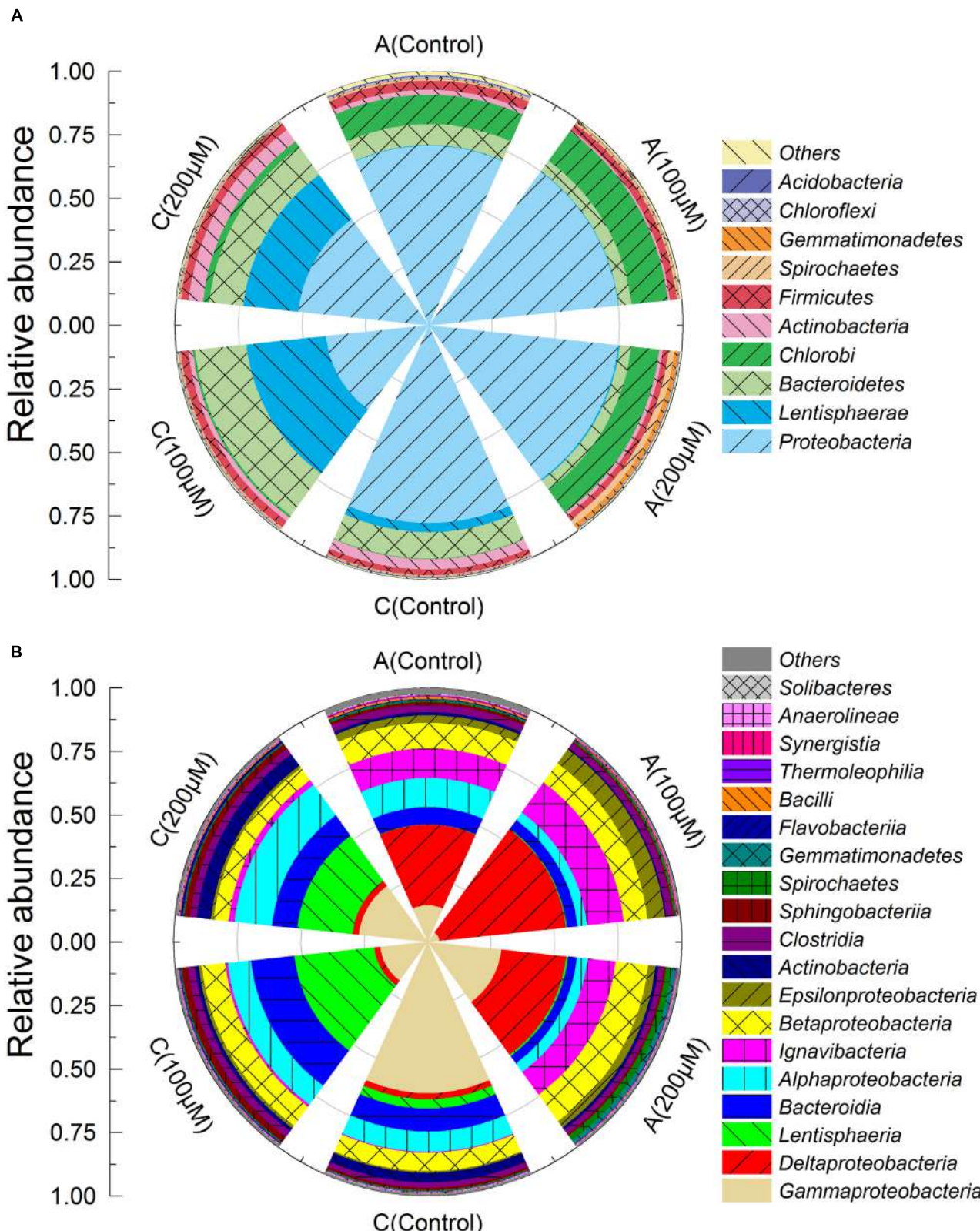


FIGURE 4 | Microbial community taxonomic wind-rose plots based on relative abundance of 16S rRNA sequences of the anode and cathode biofilms in MFCs at the phylum (A) and class levels (B).

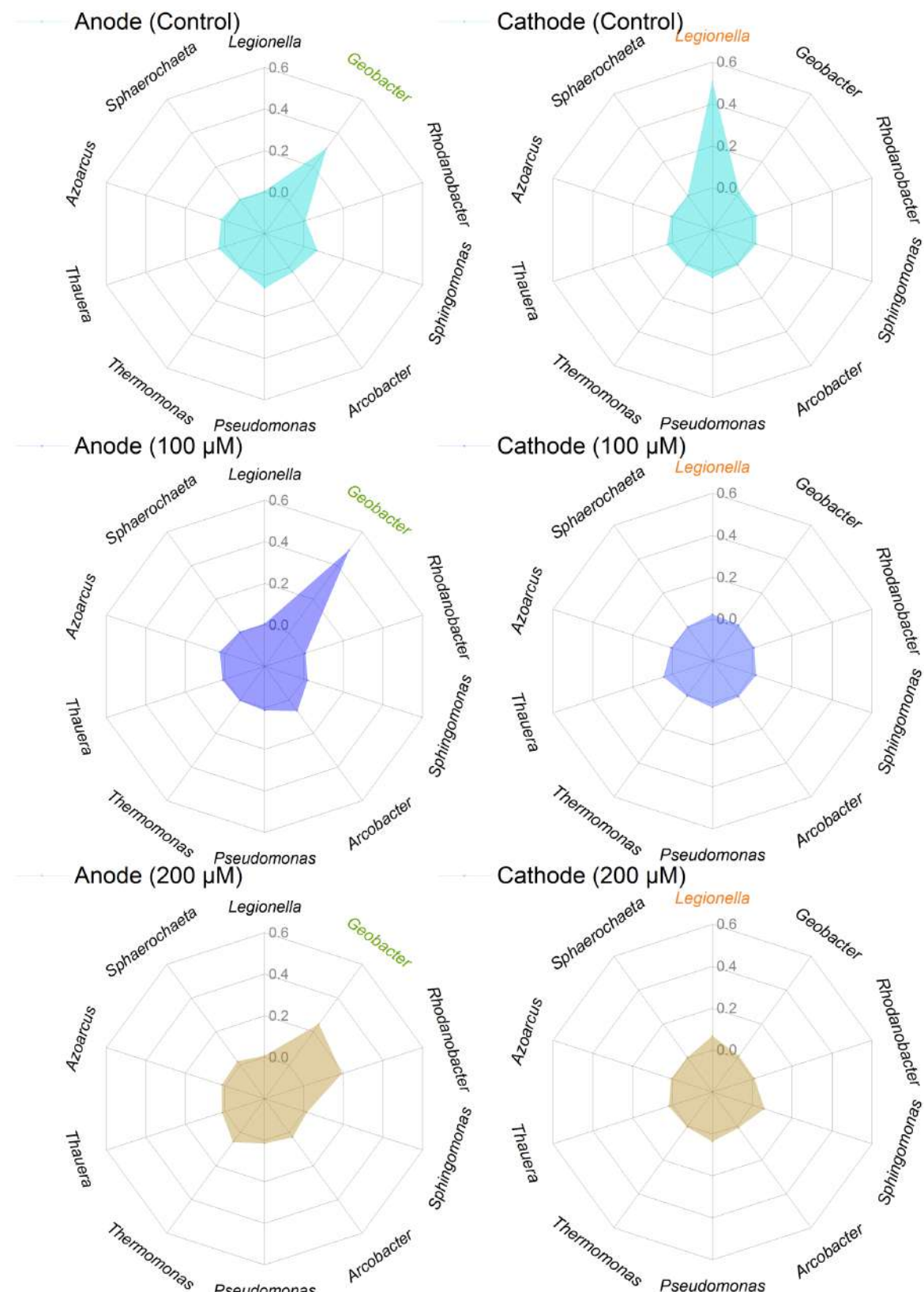
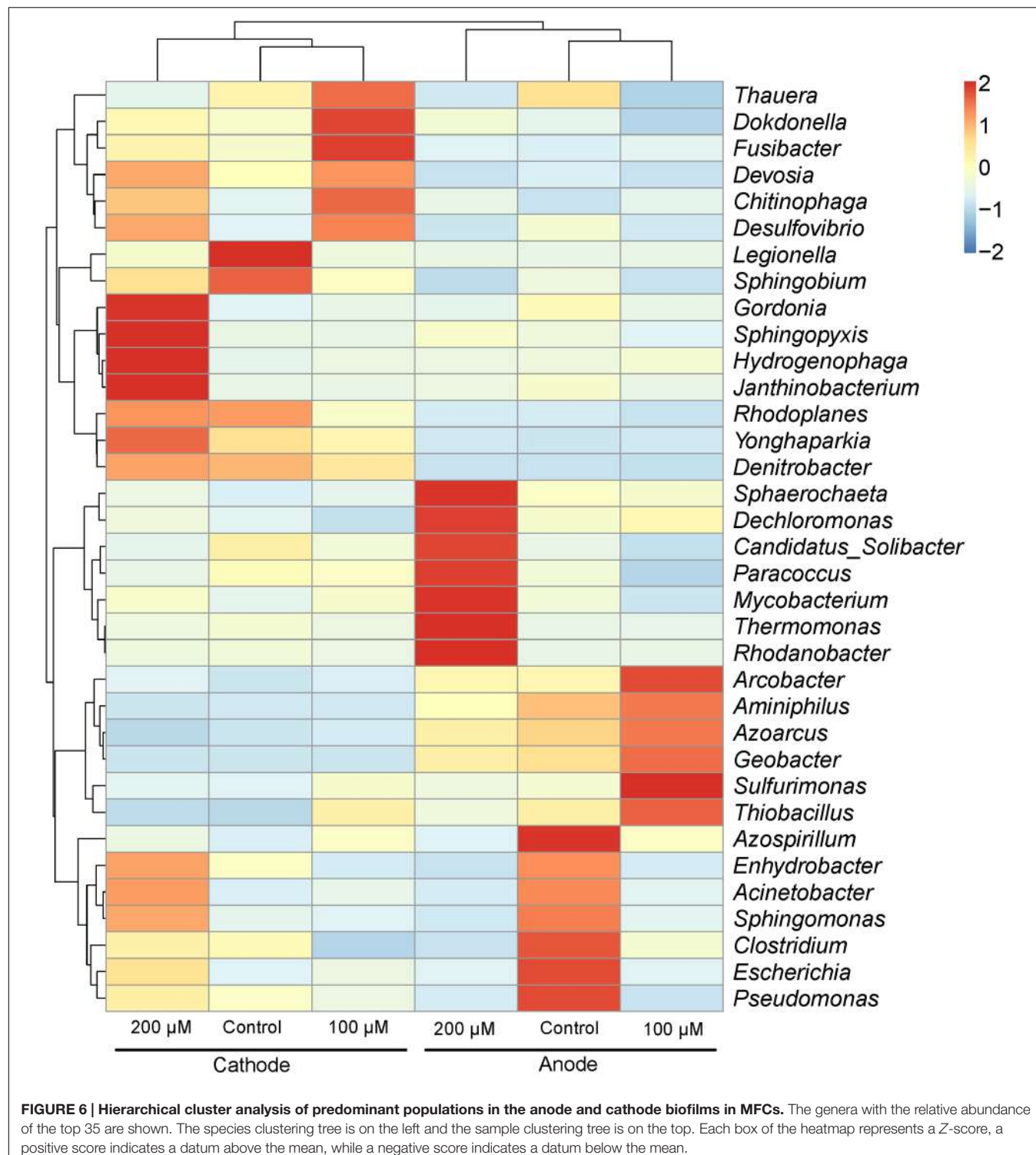


FIGURE 5 | Relative abundance of predominant genera in the anode and cathode biofilms in MFCs supplemented with different concentrations of ferrous iron.



(Figure 6). Hierarchical cluster analysis based on genus taxonomy demonstrated that the response of predominant populations in the electrode biofilms to ferrous iron occurred, indicating the effect of ferrous iron on microbial community in MFCs.

Effect of Environmental Factors on MFC Performances

Some environmental factors, such as nutrients, pH, and temperature, influence the performances of MFCs by changing microbial activity and community structure. Our study indicated

that ferrous iron changed microbial community structures of electrode biofilms of MFCs. Other metals (e.g., Ca, Mg, Pt, Au, Pd, Fe, V, Mn) and metal-nanomaterials affected current generation of MECs by changing the metabolism and enzyme activity of microorganisms (Lu et al., 2015). These studies have analyzed effect of single metal on electricity generation by MFCs, however, the effect of combined metals on microbial community structure and performance of MFCs should be further investigated.

Neutral pH is considered as the optimal condition for current generation by MFCs (Gil et al., 2003; Jadhav and Ghargrekar, 2009). However, a higher pH has been demonstrated to enhance the electrochemical activity of riboflavin which is a metabolite responsible for extracellular electron transfer in some species (Yuan et al., 2011; Yong et al., 2013). By contrast, MFCs have also been operated at pH less than 4.0 and produced high current densities by acidophilic bacterium (Malki et al., 2008; Winfield et al., 2016). Previous studies proved that temperate substantially affected the performances of MECs or MFCs by shaping microbial community (Lu et al., 2011, 2012). Synergistic effect of metals, pH and temperature on performances of MECs

and correlation analysis of these environmental factors should be further investigated in the future.

AUTHOR CONTRIBUTIONS

DX designed the experiment. QL performed specific experiments. QL, BL, and DX contributed to analyze the experiment data. QL, WL, WZ, XZ, and DX wrote the manuscript. All authors were involved in revision of the manuscript and approved its final version.

FUNDING

This study was supported by National Natural Science Foundation of China (Nos. 51422805, 31270004), the Science Fund for Distinguished Young Scholars of Heilongjiang Province (Grant No. JC201407), the State Key Laboratory of Urban Water Resource and Environment (Harbin Institute of Technology) (No. 2016DX10).

REFERENCES

- Babauta, J. T., Nguyen, H. D., Harrington, T. D., Renslow, R., and Beyenal, H. (2012). pH, redox potential and local biofilm potential microenvironments within *Geobacter sulfurreducens* biofilms and their roles in electron transfer. *Biotechnol. Bioeng.* 109, 2651–2662. doi: 10.1002/bit.24538
- Banin, E., Vasil, M. L., and Greenberg, E. P. (2005). Iron and *Pseudomonas aeruginosa* biofilm formation. *P. Natl. Acad. Sci. U.S.A.* 102, 11076–11081. doi: 10.1073/pnas.0504266102
- Bird, L. J., Bonnefoy, V., and Newman, D. K. (2011). Bioenergetic challenges of microbial iron metabolisms. *Trends Microbiol.* 19, 330–340. doi: 10.1016/j.tim.2011.05.001
- Caporaso, J. G., Kuczynski, J., Stombaugh, J., Bittinger, K., Bushman, F. D., Costello, E. K., et al. (2010). QIIME allows analysis of high-throughput community sequencing data. *Nat. Methods* 7, 335–336. doi: 10.1038/nmeth.303
- Chakraborty, A., Roden, E. E., Schieber, J., and Picardal, F. (2011). Enhanced growth of *Acidovorax* sp. strain 2AN during nitrate-dependent Fe(II) oxidation in batch and continuous-flow systems. *Appl. Environ. Microbiol.* 77, 8548–8556. doi: 10.1128/aem.06214-11
- Cheng, S., Dempsey, B. A., and Logan, B. E. (2007). Electricity generation from synthetic acid-mine drainage (AMD) water using fuel cell technologies. *Environ. Sci. Technol.* 41, 8149–8153. doi: 10.1021/es0712221
- Croal, L. R., Gralnick, J. A., Malasarn, D., and Newman, D. K. (2004). The genetics of geochemistry. *Annu. Rev. Genet.* 38, 175–202. doi: 10.1146/annurev.genet.38.072902.091138
- Croal, L. R., Jiao, Y., and Newman, D. K. (2007). The fox operon from *Rhodobacter* strain SW2 promotes phototrophic Fe(II) oxidation in *Rhodobacter capsulatus* SB1003. *J. Bacteriol.* 189, 1774–1782. doi: 10.1128/JB.01395-06
- Cvetkovic, A., Menon, A. L., Thorgersen, M. P., Scott, J. W., Poole, F. L. III, and Jenney, F. E. Jr. (2010). Microbial metalloproteomes are largely uncharacterized. *Nature* 466, 779–782. doi: 10.1038/nature09265
- DeSantis, T. Z., Hugenholtz, P., Larsen, N., Rojas, M., Brodie, E. L., Keller, K., et al. (2006). Greengenes, a chimera-checked 16S rRNA gene database and workbench compatible with ARB. *Appl. Environ. Microbiol.* 72, 5069–5072. doi: 10.1128/AEM.03006-05
- Dong, H., Yu, H., Wang, X., Zhou, Q., and Feng, J. (2012). A novel structure of scalable air-cathode without Nafion and Pt by rolling activated carbon and PTFE as catalyst layer in microbial fuel cells. *Wat. Res.* 46, 5777–5787. doi: 10.1016/j.watres.2012.08.005
- Fedorovich, V., Knighton, M. C., Pagaling, E., Ward, F. B., Free, A., and Goryaini, I. (2009). Novel electrochemically active bacterium phylogenetically related to *Arcobacter butzleri*, isolated from a microbial fuel cell. *Appl. Environ. Microbiol.* 75, 7326–7334. doi: 10.1128/AEM.01345-09
- Geissler, A., Law, G. T. W., Boothman, C., Morris, K., Burke, I. T., Livens, F. R., et al. (2011). Microbial communities associated with the oxidation of iron and technetium in bioreduced sediments. *Geomicrobiol. J.* 28, 507–518. doi: 10.1080/01490451.2010.515287
- Gil, G.-C., Chang, I.-S., Kim, B. H., Kim, M., Jang, J.-K., Park, H. S., et al. (2003). Operational parameters affecting the performance of a mediator-less microbial fuel cell. *Biosens. Bioelectron.* 18, 327–334. doi: 10.1016/s0956-5663(02)00110-0
- Green, S. J., Prakash, O., Jasrotia, P., Overholt, W. A., Cardenas, E., Hubbard, D., et al. (2012). Denitrifying bacteria from the genus *Rhodanobacter* dominate bacterial communities in the highly contaminated subsurface of a nuclear legacy waste site. *Appl. Environ. Microbiol.* 78, 1039–1047. doi: 10.1128/AEM.06435-11
- Hou, D., Lu, L., and Ren, Z. J. (2016). Microbial fuel cells and osmotic membrane bioreactors have mutual benefits for wastewater treatment and energy production. *Wat. Res.* 98, 183–189. doi: 10.1016/j.watres.2016.04.017
- Huang, Z., Lu, L., Jiang, D., Xing, D., and Ren, Z. J. (2017). Electrochemical hythane production for renewable energy storage and biogas upgrading. *Appl. Energ.* 187, 595–600. doi: 10.1016/j.apenergy.2016.11.099
- Hunter, R. C., Asfour, F., Dingemans, J., Osuna, B. L., Samad, T., Malfroot, A., et al. (2013). Ferrous iron is a significant component of bioavailable iron in cystic fibrosis airways. *mBio* 4:e00557-13. doi: 10.1128/mBio.00557-13
- Jadhav, G. S., and Ghargrekar, M. M. (2009). Performance of microbial fuel cell subjected to variation in pH, temperature, external load and substrate concentration. *Bioresour. Technol.* 100, 717–723. doi: 10.1016/j.biortech.2008.07.041
- Janicek, A. M. (2015) *Cathode Development and Reactor Design for Scaling-Up Microbial Fuel Cells*. dissertation's thesis, Oregon State University, Corvallis, OR.
- Jiang, D., Curtis, M., Troop, E., Scheible, K., McGrath, J., Hu, B., et al. (2011). A pilot-scale study on utilizing multi-anode/cathode microbial fuel cells (MAC MFCs) to enhance the power production in wastewater treatment. *Int. J. Hydrogen. Energy* 36, 876–884. doi: 10.1016/j.ijhydene.2010.08.074
- Kumar, R., Singh, L., and Zularisam, A. W. (2016). Exoelectrogens: recent advances in molecular drivers involved in extracellular electron transfer and strategies used to improve it for microbial fuel cell applications. *Renew. Sustain. Energy Rev.* 56, 1322–1336. doi: 10.1016/j.rser.2015.12.029

- Lee, C. S., Kim, K. K., Aslam, Z., and Lee, S. T. (2007). *Rhodanobacter thiooxydans* sp. nov., isolated from a biofilm on sulfur particles used in an autotrophic denitrification process. *Int. J. Syst. Evol. Microbiol.* 57, 1775–1779. doi: 10.1099/ijjs.0.65086-0
- Liu, Q., Ren, Z. J., Huang, C., Liu, B., Ren, N., and Xing, D. (2016a). Multiple syntrophic interactions drive biohythane production from waste sludge in microbial electrolysis cells. *Biotechnol. Biofuels.* 9:162. doi: 10.1186/s13068-016-0579-x
- Liu, W., He, Z., Yang, C., Zhou, A., Guo, Z., Liang, B., et al. (2016b). Microbial network for waste activated sludge cascade utilization in an integrated system of microbial electrolysis and anaerobic fermentation. *Biotechnol. Biofuels.* 9:83. doi: 10.1186/s13068-016-0493-2
- Logan, B. E., Hamelers, B., Rozendal, R., Schroder, U., Keller, J., Freguia, S., et al. (2006). Microbial fuel cells: methodology and technology. *Environ. Sci. Technol.* 40, 5181–5192. doi: 10.1021/es0605016
- Lu, L., Ren, N., Zhao, X., Wang, H., Wu, D., and Xing, D. (2011). Hydrogen production, methanogen inhibition and microbial community structures in psychrophilic single-chamber microbial electrolysis cells. *Energy Environ. Sci.* 4, 1329–1336. doi: 10.1039/C0EE00588F
- Lu, L., Xing, D., and Ren, N. (2012). Bioreactor performance and quantitative analysis of methanogenic and bacterial community dynamics in microbial electrolysis cells during large temperature fluctuations. *Environ. Sci. Technol.* 46, 6874–6881. doi: 10.1021/es300860a
- Lu, Z., Chang, D., Ma, J., Huang, G., Cai, L., and Zhang, L. (2015). Behavior of metal ions in bioelectrochemical systems: a review. *J. Power. Sour.* 275, 243–260. doi: 10.1016/j.jpowsour.2014.10.168
- Magoc, T., and Salzberg, S. L. (2011). FLASH: fast length adjustment of short reads to improve genome assemblies. *Bioinformatics* 27, 2957–2963. doi: 10.1093/bioinformatics/btr507
- Malki, M., De Lacey, A. L., Rodríguez, N., Amils, R., and Fernandez, V. M. (2008). Preferential use of an anode as an electron acceptor by an acidophilic bacterium in the presence of oxygen. *Appl. Environ. Microbiol.* 74, 4472–4476. doi: 10.1128/AEM.00209-08
- Mei, X., Guo, C., Liu, B., Tang, Y., and Xing, D. (2015). Shaping of bacterial community structure in microbial fuel cells by different inocula. *RSC Adv.* 5, 78136–78141. doi: 10.1039/C5RA16382J
- Mohan, S. V., Raghavulu, S. V., and Sarma, P. (2008). Influence of anodic biofilm growth on bioelectricity production in single chambered mediatorless microbial fuel cell using mixed anaerobic consortia. *Biosens. Bioelectron.* 24, 41–47. doi: 10.1016/j.bios.2008.03.010
- Mohan, S. V., Velvizhi, G., Modestra, J. A., and Srikanth, S. (2014). Microbial fuel cell: critical factors regulating bio-catalyzed electrochemical process and recent advancements. *Renew. Sustain. Energy Rev.* 40, 779–797. doi: 10.1016/j.rser.2014.07.109
- Muehe, E. M., Gerhardt, S., Schink, B., and Kappler, A. (2009). Ecophysiology and the energetic benefit of mixotrophic Fe(II) oxidation by various strains of nitrate-reducing bacteria. *FEMS. Microbiol. Ecol.* 70, 335–343. doi: 10.1111/j.1574-6941.2009.00755.x
- Patil, S. A., Harnisch, F., Koch, C., Hubschmann, T., Fetzer, I., Carmona-Martinez, A. A., et al. (2011). Electroactive mixed culture derived biofilms in microbial bioelectrochemical systems: the role of pH on biofilm formation, performance and composition. *Bioresour. Technol.* 102, 9683–9690. doi: 10.1016/j.biortech.2011.07.087
- Ter Heijne, A., Hamelers, H. V., and Buisman, C. J. (2007). Microbial fuel cell operation with continuous biological ferrous iron oxidation of the catholyte. *Environ. Sci. Technol.* 41, 4130–4134. doi: 10.1021/es0702824
- Wang, Q., Garrity, G. M., Tiedje, J. M., and Cole, J. R. (2007). Naive Bayesian classifier for rapid assignment of rRNA sequences into the new bacterial taxonomy. *Appl. Environ. Microbiol.* 73, 5261–5267. doi: 10.1128/AEM.00062-07
- Wang, Y., Niu, C.-G., Zeng, G.-M., Hu, W.-J., Huang, D.-W., and Ruan, M. (2011). Microbial fuel cell using ferrous ion activated persulfate as a cathodic reactant. *Int. J. Hydrogen Energy* 36, 15344–15351. doi: 10.1016/j.ijhydene.2011.08.071
- Watson, V. J., and Logan, B. E. (2010). Power production in MFCs inoculated with *Shewanella oneidensis* MR-1 or mixed cultures. *Biotechnol. Bioeng.* 105, 489–498. doi: 10.1002/bit.22556
- Wei, L., Han, H., and Shen, J. (2013). Effects of temperature and ferrous sulfate concentrations on the performance of microbial fuel cell. *Int. J. Hydrogen Energy* 38, 11110–11116. doi: 10.1016/j.ijhydene.2013.01.019
- Winfield, J., Greenman, J., Dennis, J., and Ieropoulos, I. (2016). Analysis of microbial fuel cell operation in acidic conditions using the flocculating agent ferric chloride. *J. Chem. Technol. Biotechnol.* 91, 138–143. doi: 10.1002/jctb.4552
- Wu, D., Xing, D., Lu, L., Wei, M., Liu, B., and Ren, N. (2013). Ferric iron enhances electricity generation by *Shewanella oneidensis* MR-1 in MFCs. *Bioresour. Technol.* 135, 630–634. doi: 10.1016/j.biortech.2012.09.106
- Xing, D., Zuo, Y., Cheng, S., Regan, J. M., and Logan, B. E. (2008). Electricity generation by *Rhodopseudomonas palustris* DX-1. *Environ. Sci. Technol.* 42, 4146–4151. doi: 10.1021/es800312v
- Yong, Y. C., Cai, Z., Yu, Y. Y., Chen, P., Jiang, R., Cao, B., et al. (2013). Increase of riboflavin biosynthesis underlies enhancement of extracellular electron transfer of *Shewanella* in alkaline microbial fuel cells. *Bioresour. Technol.* 130, 763–768. doi: 10.1016/j.biortech.2012.11.145
- Yong, Y. C., Yu, Y. Y., Li, C. M., Zhong, J. J., and Song, H. (2011). Bioelectricity enhancement via overexpression of quorum sensing system in *Pseudomonas aeruginosa*-inoculated microbial fuel cells. *Biosens. Bioelectron.* 30, 87–92. doi: 10.1016/j.bios.2011.08.032
- Yuan, Y., Zhao, B., Zhou, S., Zhong, S., and Zhuang, L. (2011). Electrocatalytic activity of anodic biofilm responses to pH changes in microbial fuel cells. *Bioresour. Technol.* 102, 6887–6891. doi: 10.1016/j.biortech.2011.04.008
- Zhu, X., Yates, M. D., Hatzell, M. C., Ananda Rao, H., Saikaly, P. E., and Logan, B. E. (2014). Microbial community composition is unaffected by anode potential. *Environ. Sci. Technol.* 48, 1352–1358. doi: 10.1021/es404690q

Conflict of Interest Statement: The authors declare that the research was conducted in the absence of any commercial or financial relationships that could be construed as a potential conflict of interest.

Copyright © 2017 Liu, Liu, Li, Zhao, Zuo and Xing. This is an open-access article distributed under the terms of the Creative Commons Attribution License (CC BY). The use, distribution or reproduction in other forums is permitted, provided the original author(s) or licensor are credited and that the original publication in this journal is cited, in accordance with accepted academic practice. No use, distribution or reproduction is permitted which does not comply with these terms.



Electrochemical Potential Influences Phenazine Production, Electron Transfer and Consequently Electric Current Generation by *Pseudomonas aeruginosa*

Erick M. Bosire and Miriam A. Rosenbaum*

Institute of Applied Microbiology, Aachen Biology and Biotechnology, RWTH Aachen University, Aachen, Germany

OPEN ACCESS

Edited by:

Feng Zhao,

Institute of Urban Environment (CAS),
China

Reviewed by:

Sarah Glaven,

United States Naval Research
Laboratory, United States
Deepak Pant,

Flemish Institute for Technological
Research, Belgium

***Correspondence:**

Miriam A. Rosenbaum

miriam.rosenbaum@rwth-aachen.de

Specialty section:

This article was submitted to
Microbiotechnology, Ecotoxicology
and Bioremediation,
a section of the journal
Frontiers in Microbiology

Received: 13 February 2017

Accepted: 03 May 2017

Published: 18 May 2017

Citation:

Bosire EM and Rosenbaum MA
(2017) Electrochemical Potential
Influences Phenazine Production,
Electron Transfer and Consequently
Electric Current Generation by
Pseudomonas aeruginosa.
Front. Microbiol. 8:892.
doi: 10.3389/fmicb.2017.00892

Pseudomonas aeruginosa has gained interest as a redox mediator (phenazines) producer in bioelectrochemical systems. Several biotic and abiotic factors influence the production of phenazines in synergy with the central virulence factors production regulation. It is, however, not clear how the electrochemical environment may influence the production and usage of phenazines by *P. aeruginosa*. We here determined the influence of the electrochemical potential on phenazine production and phenazine electron transfer capacity at selected applied potentials from -0.4 to +0.4 V (vs. Ag/AgCl_{sat}) using *P. aeruginosa* strain PA14. Our study reveals a profound influence of the electrochemical potential on the amount of phenazine-1-carboxylate production, whereby applied potentials that were more positive than the formal potential of this dominating phenazine ($E^{\circ'}_{PCA} = -0.24$ V vs. Ag/AgCl_{sat}) stimulated more PCA production (94, 84, 128, and 140 µg mL⁻¹ for -0.1, 0.1, 0.2, and 0.3 V, respectively) compared to more reduced potentials (38, 75, and 7 µg mL⁻¹ for -0.4, -0.3, and -0.24 V, respectively). Interestingly, *P. aeruginosa* seems to produce an additional redox mediator (with $E^{\circ'} \sim 0.052$ V) at applied potentials below 0 V, which is most likely adsorbed to the electrode or present on the cells forming the biofilm around electrodes. At fairly negative applied electrode potentials, both PCA and the unknown redox compound mediate cathodic current generation. This study provides important insights applicable in optimizing the BES conditions and cultures for effective production and utilization of *P. aeruginosa* phenazines. It further stimulates investigations into the physiological impacts of the electrochemical environment, which might be decisive in the application of phenazines for electron transfer with *P. aeruginosa* pure- or microbial mixed cultures.

Keywords: *Pseudomonas aeruginosa*, electrode potential, phenazines, bioelectrochemical system, electron transfer, phenazine-1-carboxylic acid

INTRODUCTION

Bioelectrochemical systems (BES) comprise a wide array of technologies that are based on the interaction of microorganisms with electrodes (Schröder et al., 2013). The most common technology is the microbial fuel cell (MFC) in which microbes convert organic materials in, for instance, wastewater into electrical energy. To harness the electrons liberated from oxidation of the

organic substrates at an anode, the potentials in BES are set with regard to the terminal electron acceptor at the cathode; mostly oxygen. Microbes are proposed to use different electron transfer strategies to shuttle electrons to the anode: direct electron transfer via *c*-type cytochromes and other redox proteins or cell-like extensions termed nanowires, and mediated electron transfer via endogenous or exogenous soluble redox mediators (Gorby et al., 2006; Schröder, 2007; Marsili et al., 2008; Malvankar et al., 2011; Wrighton et al., 2011). Soluble redox mediators may include phenazines, riboflavins, and quinones produced by *Pseudomonads*, *Shewanella*, and *Lactococcus*, respectively (Marsili et al., 2008; Pham et al., 2008; Freguia et al., 2009).

Phenazines are promising natural and synthetic redox mediators for enhancing current production in BES, and *Pseudomonas aeruginosa* is one of the most active producers. *P. aeruginosa* has indeed shown potential of being used as the phenazine producer in BES co-cultures, allowing partner organisms to utilize the supplied phenazines for metabolic electron discharge (Rabaey et al., 2005; Pham et al., 2008; Bosire et al., 2016). Phenazine production by *Pseudomonads* is influenced by several biotic and abiotic factors in the ecological niches (van Rij et al., 2004; Mavrodi et al., 2006). Most importantly for BES function, they play important roles in the metabolism of microorganisms in cases where the natural electron acceptor is missing or limiting. In *P. aeruginosa*, which is not able to ferment, pyocyanin (PYO) has been confirmed to contribute in maintaining the cellular redox balance by oxidizing NADH (Pierson and Pierson, 2010). Under anaerobic conditions, PYO redox cycling may enable *P. aeruginosa* to survive (Wang et al., 2010).

There are four well known *P. aeruginosa* phenazines with fairly close redox potentials vs. a Ag/AgCl reference electrode: PCA (-0.24 V), PYO (-0.116 V), 1-hydroxy-phenazine (1-HP; -0.174 V), and phenazine-1-carboxamide (PCN; -0.14 V) [given are formal potentials of standards at the conditions in our bioelectrochemical setups as determined in (Bosire et al., 2016)]. However, they have varying properties and redox reactivities to electron acceptors; suggesting that they may play different roles in, for example, biofilms. PYO reacts more readily with oxygen at neutral pH while PCA and the other phenazines are more reactive to solid electron acceptors like iron oxides and hydroxides (Wang and Newman, 2008). Hence, based on their roles, concentration gradients of the phenazine species might exist in biofilms where oxygen availability-gradients prevail. Considering that the production of phenazines is stimulated by the prevailing environmental factors including oxygen and iron (van Rij et al., 2004), it is probable that *P. aeruginosa* might produce different gradients of these phenazines depending on need or on the electron acceptor potential or properties. So far, all pure or co-culture observations of *P. aeruginosa* in BES research have been performed at one fixed electrode potential to guarantee stable electrochemical conditions (typically $+0.2$ or $+0.3$ V vs. RE) (Venkataraman et al., 2010, 2011; Bosire et al., 2016). Therefore, it is an important question whether the applied electrode potential, which determines the redox environment, might influence phenazine production or the phenazine spectrum and their

capacity in electron shuttling. For other cases, it was even shown that the applied potential might influence electron transfer strategies of the microorganism (Liu et al., 2010). Thus, for *Shewanella oneidensis*, which is able to employ different electron transfer mechanisms (i.e., direct vs. mediated or a combination), the available potential may influence the use of these mechanisms and subsequently a shift between them. This redox-stimulated switch in electron transfer mechanism is also associated with a change in the level of electric current production (Liu et al., 2010; Lian et al., 2016). Hence, there is great potential in understanding how to correctly poise or regulate the electrodes in BES in order to obtain an optimal metabolic state also for *P. aeruginosa* for most productive phenazine and current production.

Therefore, the aim of this study was to evaluate the cellular physiology, phenazine production, and subsequent electric current generation of *P. aeruginosa* strain PA14 at a broad range of applied electrode potentials ranging from potentials more negative than the phenazine formal potentials (i.e., the electrode could serve as electron donor for phenazine reduction) to common electro-positive redox potentials, which allow for electrochemical oxidation of reduced phenazines. The knowledge gained is expected to be instrumental in optimizing future (co-)cultures for efficient electron transfer in BES applications.

MATERIALS AND METHODS

Strain and Culture Conditions

In this study, *P. aeruginosa* strain PA14 (DSMZ 19882) from the German Collection of Microorganisms and Cell Culture was used. The strain was pre-cultured overnight in AB medium at 37°C and washed three times with equal volume of 0.9% NaCl before being used to inoculate the BES reactors. For BES experiments, strains were cultured in AB medium. Procedure for preparing AB was adopted from Clark and Maaløe (1967). The medium contained the following constituents (per liter): component A: 2.0 g $(\text{NH}_4)_2\text{SO}_4$, 6.0 g Na_2HPO_4 , 3.0 g KH_2PO_4 , 3.0 g NaCl , 0.011 g Na_2SO_4 , and component B: 0.2 g MgCl_2 , 0.010 g CaCl_2 and 0.5 mg $\text{FeCl}_3 \times 7 \text{ H}_2\text{O}$ (Clark and Maaløe, 1967). The two components were autoclaved separately before mixing them. Glucose was supplied as the carbon and electron donor at a concentration of 20–30 mM (see respective experiments).

BES Setup and Electrochemical Procedures

A single-chambered bioelectrochemical cell with a three-electrode configuration as described before was used (Bosire et al., 2016). The Ivium-n-Stat potentiostat (Ivium Technologies, Eindhoven, The Netherlands) was used to perform the electrochemical measurements. Chronoamperometric measurement was used to monitor electric current generation at varying potentials. A total of eight potentials ranging from -0.4 V to $+0.4$ V (vs. $\text{Ag}/\text{AgCl}_{\text{sat}}$) were tested in individual triplicate or duplicate (see individual experiments) BES setups in batch mode. Replicate reactor runs were started with the same

medium batch and inoculum culture at a starting OD of 0.1. Current generation was recorded over the entire growth period at each set potential. Chronoamperometric measurement was interrupted every 23 h to perform a cyclic voltammetry scan similar as published in Bosire et al. (2016). Cyclic voltammetry

was performed at a potential range of -0.5 to 0.5 V at a scan rate of 2 mVs $^{-1}$. Coulombic efficiency was calculated as the percentage of the collected charge compared to the charge supplied in the carbon source (glucose: 24 electrons per molecule).

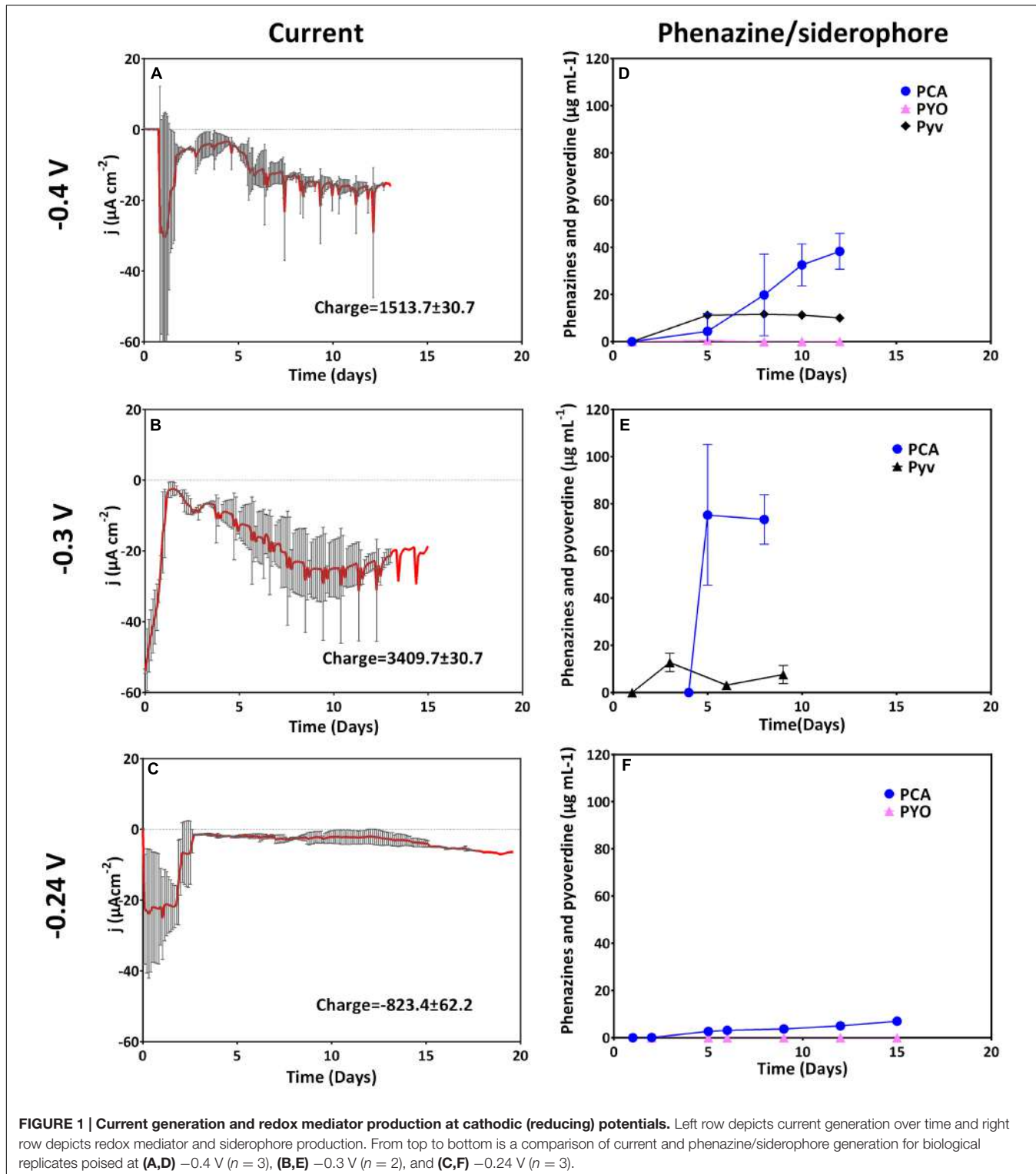


FIGURE 1 | Current generation and redox mediator production at cathodic (reducing) potentials. Left row depicts current generation over time and right row depicts redox mediator and siderophore production. From top to bottom is a comparison of current and phenazine/siderophore generation for biological replicates poised at **(A,D)** -0.4 V ($n = 3$), **(B,E)** -0.3 V ($n = 2$), and **(C,F)** -0.24 V ($n = 3$).

Biomass Measurement

Cell dry weight was measured at the end of the experiment by carefully scraping off the biofilm around the electrodes and the reactor walls into the culture medium. The whole culture medium was centrifuged at 10,000 rpm for 20 min and the

pellet was washed three times with 0.09% NaCl. The pellet was transferred into pre-weighed aluminum dishes and the containers were carefully rinsed to ensure the transfer of all the biomass. The biomass was dried overnight at 120°C and weighed in a moisture analyzer (RADWAG moisture analyzer, Hilden, Germany).

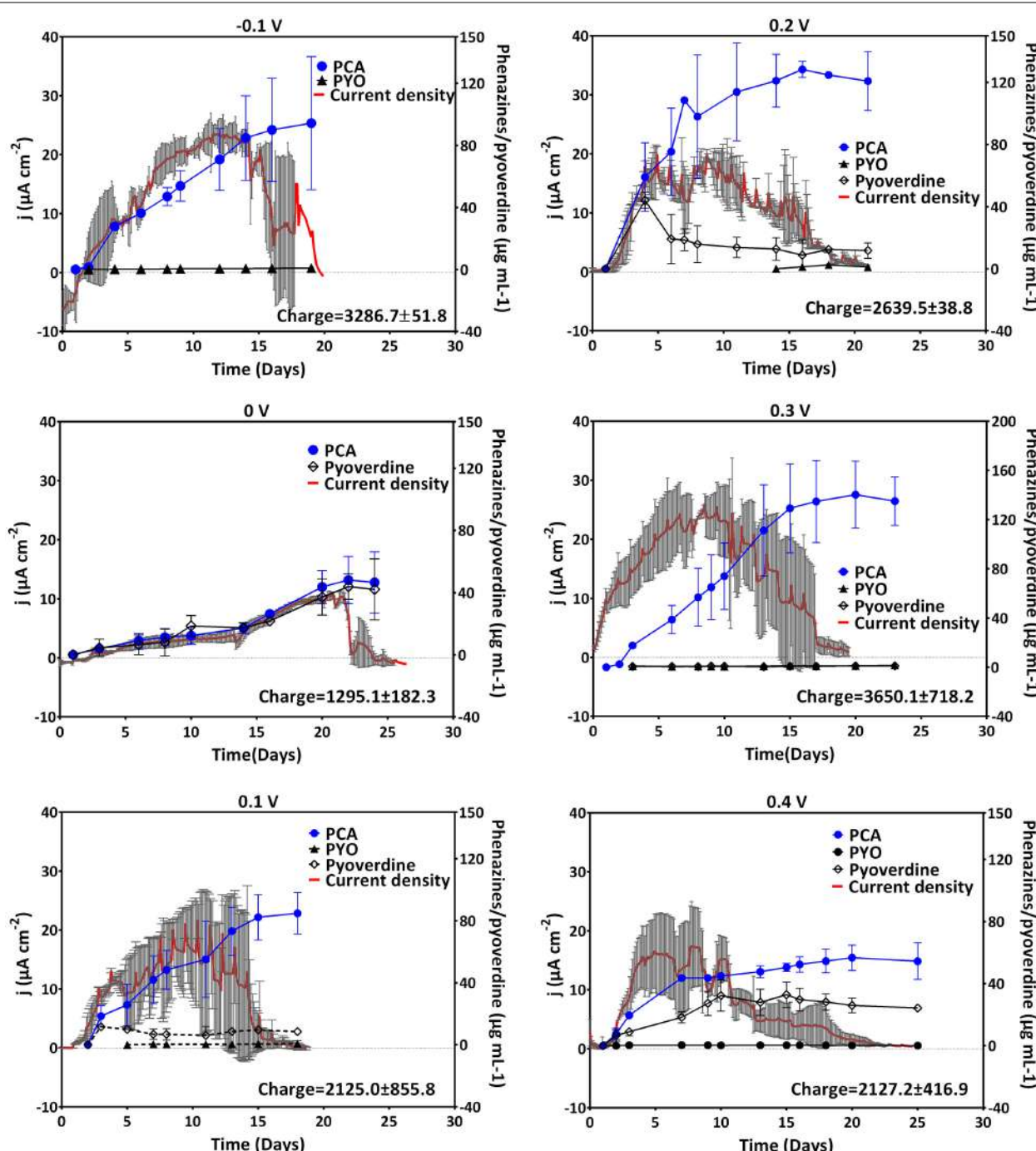


FIGURE 2 | Current generation and phenazine/pyoverdine production at anodic potentials. Data for -0.1 , 0 , 0.1 , and 0.2 V was obtained from two biological replicates whereas that of 0.3 and 0.4 V was from three replicates; the mean current density and standard deviations are shown. Pyoverdines were only detected at 0 , 0.1 , and 0.4 V. Notice the different phenazines and pyoverdine axis scale for 0.3 V.

Analytical Procedures

For phenazine detection and quantification, samples were separated in a waters symmetry column, Symmetry® 5 μm C18 4.6 mm \times 250 mm (Waters, Herts, UK) using a Beckman Gold HPLC (Beckman Coulter Inc., Brea, CA, USA) fitted with a photo diode array detector. 0.1% formic acid (pH 5) was used as solvent A and acetonitrile as solvent B at a flow rate of 0.5 mL min $^{-1}$. A linear gradient was run for 28 min as follows: 5 min 10% acetonitrile, 10 min linear gradient to 100% acetonitrile, 10 min 100% acetonitrile, 1 min linear gradient to 10% acetonitrile, and 3 min 10% acetonitrile. Phenazines were separated and detected at their characteristic wavelengths; PYO-319 nm, PCA-366 nm, 1-HP-247 nm, and PCN-366 nm. Stock solutions of PCA and PCN (Princeton Biomolecular) and 1-HP (TCA Europe), were made by dissolving 1000 $\mu\text{g mL}^{-1}$ of the phenazines in dimethyl sulfoxide (DMSO, Sigma-Aldrich). For PYO (Cayman Chemical), the stock solutions were made by dissolving 2500 $\mu\text{g mL}^{-1}$ in 100% ethanol.

For the detection and quantification of carbon sources and metabolites, an organic acid resin column (300 mm \times 8 mm polystyrol-divinylbenzol copolymer [PS-DVB], CS-Chromatography) was used to separate the culture supernatants on a Dionex Ultimate 3000 HPLC system (Sunnyvale, CA, USA) equipped with a refractive index (RI-101, Shodex) and UV detector (Ultimate 3000 UV/VIS detector, Dionex). Sulphuric acid (5 mM) was applied as the eluent at a flow rate of 0.8 mL min $^{-1}$ and a temperature of 60°C.

RESULTS

The most dominating phenazine in all previous work with *P. aeruginosa* PA14 in our group was PCA with a formal potential of -0.24 V (Bosire et al., 2016). We therefore explored applied electrode potentials more negative and more positive than this potential (eight potentials from -0.4 V to +0.4 V). Anodic (oxidative) behavior was expected at potentials above -0.24 V, where PCA can be electrochemically oxidized at the electrode

TABLE 1 | Formal potentials (E°') of the two peak systems observed at different applied electrode potentials, phenazine concentration, and pH.

Potential	E°'		Phenazines ($\mu\text{g mL}^{-1}$) ^a		
	PS 1	PS 2	PCA	PYO	pH
-0.4	-0.197	0.064	32.5	0.1	6.30
-0.3	-0.164	0.042	75.2	0	6.42
-0.24	-0.195	0.049	5.05	0	6.39
-0.1	-0.24	0.05	89.97	0.71	6.35
0	-0.21	- ^b	48.0	0	6.24
0.1	-0.22	- ^b	82.24	0.5	6.33
0.2	-0.20	- ^b	12.61	3.2	6.20
0.3	-0.217	- ^b	129.22	0.82	6.47
0.4	-0.23	- ^b	43.63	0.42	6.42

^aPhenazine concentrations correspond to the day of CV record at peak current activity. ^bNot observed.

(results grouped as anodic potentials). Below this potential, it was expected that there will be no electron discharge to the electrode using this phenazine (results grouped as cathodic potentials). To understand the influence of the applied potential on the redox mediator production, the phenazines PCA, PYO, PCN, and 1-HP were quantified. Also, the siderophore pyoverdine, which is involved in iron acquisition and might exhibit redox properties, was detected and quantified. While the phenazines PCN and 1-HP were below detection limit in all the cultures, PCA and PYO were detected in varying concentrations in cultures grown at the different potentials.

Phenazine Production and Current Generation at Cathodic Potentials

At the three most electro-negative applied potentials (-0.4, -0.3, and -0.24 V), an initial cathodic (reducing) current (days 1–2) most likely reflects abiotic oxygen reduction at the cathode. With biological oxygen consumption in the reactor, this initial current subsides around day 2. Thereafter, with culture growth, biotic cathodic currents were observed at these low potentials including the formal potential (-0.24 V) of the dominantly produced phenazine, PCA (Figure 1). At -0.4 V, an accelerating reduction current was generated at the working electrode over 12 days, at -0.3 V this reduction current increased even faster. It therefore appears that the negative current after day 2 generated can be reconciled with growth.

PCA strongly dominated at all applied potentials even though the concentration was very low when the electrode was poised right at the formal potential of PCA (-0.24 V). Concentrations of PYO were below or very close to the detection limit for all three potentials. Varying low concentrations of pyoverdine were produced at the different cathodic potentials (up to 11 $\mu\text{g mL}^{-1}$ for -0.4 V and 15.6 $\mu\text{g mL}^{-1}$ for -0.3 V, respectively (Figure 1).

Phenazine Production and Current Generation at Anodic Potentials

Anodic (oxidative) currents were observed at all potentials more positive than the formal potential of PCA (-0.1 to +0.4 V). A rapid positive increase in current reaching its maximum after 12 days was observed for cultures grown with an applied potential of -0.1 V as compared to -0.24 V (Figure 2). The elevated current production at -0.1 V coincided with very high amounts of PCA compared to the cathodic potentials described above (up to 94 $\mu\text{g mL}^{-1}$ for -0.1 V). Averagely, except for 0 V, the maximum current densities generated at anodic potentials were fairly similar. At 0.4 V, maximum current density was attained earlier in the experiment compared to all other oxidative potentials, but then the current declined faster (after 10 days). An integration of the recorded current over time delivers the collected electric charge, whereby the most charge with about 3500 C was collected at -0.1 and 0.3 V. Except for 0 V, fairly similar charges (2200–2600 C) were collected at the other anodic potentials (Figure 2).

The observed current production reflects the production of phenazine redox mediators at the anodic potentials considered (Figure 2, right axes). Except for 0 V, elevated amounts of PCA

were recorded at the anodic potentials; with cultures grown at -0.1 , 0.2 , and 0.3 V recording over $100 \mu\text{g mL}^{-1}$. In these cultures, averagely higher current densities were generated over a longer cultivation time. This was in line with the previous findings, where high concentrations of PCA were found to mediate elevated current production (Bosire et al., 2016). Consistent patterns of pyoverdine production could not be drawn.

Cyclic Voltammetric Analysis

Cyclic voltammetry allows the analysis of the redox activity in the BES system. This may provide insight into the redox species employed in electron transfer by the biocatalysts. To decipher the use of redox species and the overall redox activity

at different redox potentials, CV measurements were run by regularly (every 23 h) interrupting the potentiostatic current measurements. Redox peak systems obtained at the beginning of the experiment (blank), during rising activity and at the peak activity (in terms of electric current generation) of the culture were compared (Supplementary Figure S1). To obtain a meaningful interpretation of the redox species responsible for the peak systems, the cyclic voltammetric data was further compared to the phenazine quantification data of the time points of CV scans (Table 1).

Generally across all applied potentials, two distinct redox peak systems were observed during the peak current production activity, which differed in the current intensity and the peak separation from each other (Figure 3). The mid peak potentials of

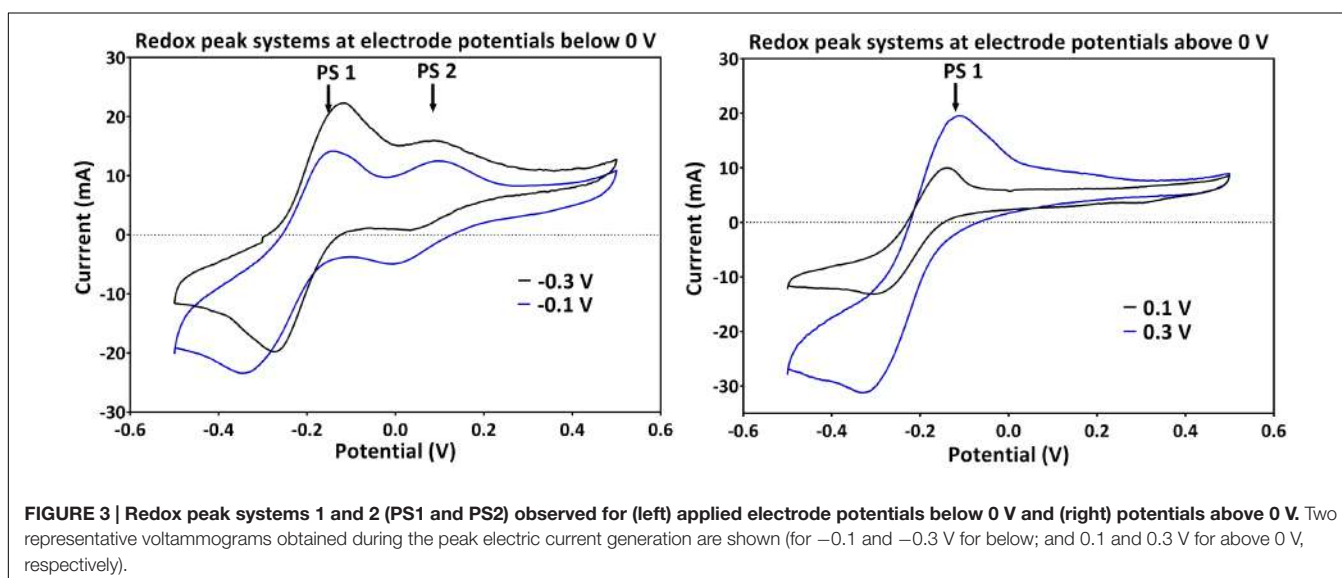


FIGURE 3 | Redox peak systems 1 and 2 (PS1 and PS2) observed for (left) applied electrode potentials below 0 V and (right) potentials above 0 V. Two representative voltammograms obtained during the peak electric current generation are shown (for -0.1 and -0.3 V for below; and 0.1 and 0.3 V for above 0 V, respectively).

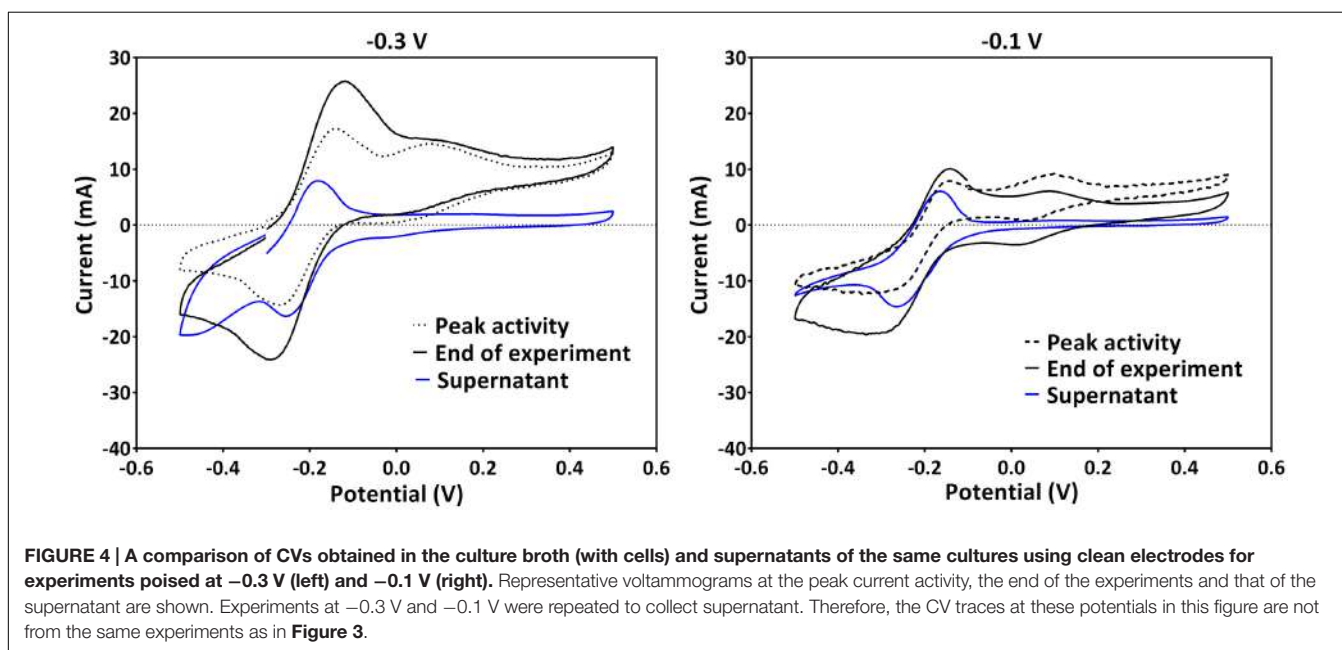


FIGURE 4 | A comparison of CVs obtained in the culture broth (with cells) and supernatants of the same cultures using clean electrodes for experiments poised at -0.3 V (left) and -0.1 V (right). Representative voltammograms at the peak current activity, the end of the experiments and that of the supernatant are shown. Experiments at -0.3 V and -0.1 V were repeated to collect supernatant. Therefore, the CV traces at these potentials in this figure are not from the same experiments as in Figure 3.

TABLE 2 |Influence of applied potential on the physiology of *Pseudomonas aeruginosa*.

Parameter	-0.4	-0.3	-0.24	-0.1	0	0.1	0.2	0.3	0.4
j_{max} ($\mu\text{A cm}^{-2}$)	-16.30 ± 1.09	-24.95 ± 6.33	-25.8 ± 0.24	22.6 ± 1.99	10.58 ± 0.51	17.8 ± 4.20	17.5 ± 1.57	23.94 ± 0.51	17.31 ± 4.83
Time of j_{max} (day)	11	9	8	12	21	10	9	8	5
Charge (Coulombs)	-1513.7 ± 30.7	-3409.7 ± 126.5	-823.4 ± 62.2	3286.6 ± 51.8	1295.1 ± 182.3	2125.0 ± 85.8	2639.5 ± 38.9	3650.1 ± 718.2	2127.2 ± 416.9
Coulombic efficiency (%) ^a	-	-	-	10.98 ± 0.27	4.30 ± 0.68	7.10 ± 2.86	7.38 ± 5.22	12.11 ± 3.36	7.08 ± 1.37
Biomass (g L^{-1} CDM) ^b	0.50 ± 0.13	0.81 ± 0.083	0.74 ± 0.08	0.55 ± 0.03	0.56 ± 0.05	0.57 ± 0.01	0.82 ± 0.31	0.72 ± 0.14	0.57 ± 0.02
Biofilm at electrode ^c	+	+++	+++	+++	+	++	+	+	+
PCA _{Max} ($\mu\text{g mL}^{-1}$)	38.3 ± 5.35	75.2 ± 7.42	7 ± 0.12	94.2 ± 30.20	48.0 ± 12.40	84.8 ± 10.90	128.4 ± 4.00	140.3 ± 22.20	56.7 ± 5.70
Pyovertine ($\mu\text{g mL}^{-1}$)	11.2	12.7 ± 2.74	0	0	43.8 ± 6.57	11.6 ± 1.60	44.1 ± 1.5	0	32.3 ± 5.77
Carbon source uptake (mM day^{-1})	0.98 ± 0.09	1.07 ± 0.11	1.91 ± 0.06	1.73 ± 0.05	0.96 ± 0.06	2.17 ± 0.06	2.302 ± 0.14	2.10 ± 0.1	1.88 ± 0.04

^aPercentage of the coulombs supplied in the substrate that were liberated as current. For cathodic currents coulombic efficiencies were not calculated (-). ^bBiomass was determined from three replicate reactors, except -0.3, -0.1, 0, 0.1, and 0.2 V...two replicates. ^cBiofilm intensity was roughly visually determined around the electrode, with the following representations: + weak biofilm formation (barely visible), ++ medium biofilm formation (clearly visible), and +++ strong biofilm formation (thick biofilm such as in Figure 6-right).

the redox peak systems slightly shifted from one potential to the other (**Table 1**). Peak system 1 (PS1) was identified for all applied electrode potentials, while peak system 2 (PS2) was only detected for applied potentials lower than 0 V (**Figure 3** and **Table 1**).

The pH of all experiments was fairly similar (**Table 1**) and thus, cannot simply explain the potential shifts, which are more prominent at low applied electrode potentials. The mean formal potential of PS1 was the same as the formal potential of PCA standards [-0.24 V; (Bosire et al., 2016)]. Indeed, PCA was detected via HPLC as the dominating phenazine species in all experiments. The activity of PS1 can therefore be associated with the activity of PCA (**Figure 3** and **Table 1**). Changes in the chemical environment due to the different redox conditions in the experiments or due to adsorption processes to the electrode might have influenced the formal potential of PCA in the individual experiments.

Since PS2 had a positive formal potential ($E^{\circ}_{1/2} \sim 0.052$ V), which is not close to the E° of any *P. aeruginosa* phenazines, it is highly probable that this is not a peak system for a phenazine redox species (**Figure 3**). The performed HPLC analysis for phenazines and other hydrophobic compounds did not highlight any new, unidentified components. In an attempt to better characterize the compound behind PS2, a CV analysis was performed in the culture supernatants of the -0.3 and -0.1 V grown cultures using clean carbon electrodes. PS2 was not found in the supernatant CVs; hence, PS2 is a redox species that is likely adsorbed to the electrodes or located on the cells that form a biofilm around the electrode (**Figure 4**).

Growth and Carbon Source Uptake

Glucose uptake and the metabolites ketogluconate, gluconate, acetate, and acetooin were quantified during the culture period. The uptake of the carbon source during growth at most of the applied electrode potentials was complete by the end of each experiment (see individual experiments), except for -0.4 V where glucose was not depleted. At applied potentials below 0.1 V (especially at 0 V), the depletion of glucose took longer compared to the other applied potentials. Glucose uptake rates, were significantly higher for more positive electrode potentials (0.1 and -0.3 V), with the exception of 0.4 V where glucose consumption was slower again (**Table 2**). Instead, at this most positive electrode potential (0.4 V), elevated amounts of ketogluconate accumulated (~8 mM). For all other potentials, ketogluconate levels – as an indicator for bottlenecks in the glucose consumption – stayed very low (<2 mM). Increased amounts of acetate (~8 mM) were produced at -0.24 V compared to all other potentials applied (**Figure 5**).

Growth during cultivation at different applied potentials was determined as total cell dry weight of the biofilm and planktonic cells at the end of the experiment (**Table 2**). Regular measurements of optical density as a measure for growth of *P. aeruginosa* is not reliable because of the strong biofilm formation tendency of this organism (especially at the air-liquid interface and around the electrodes; **Figure 6**). However, trends of total biomass generation at the different applied potentials were not clear. For instance, the most biomass was generated

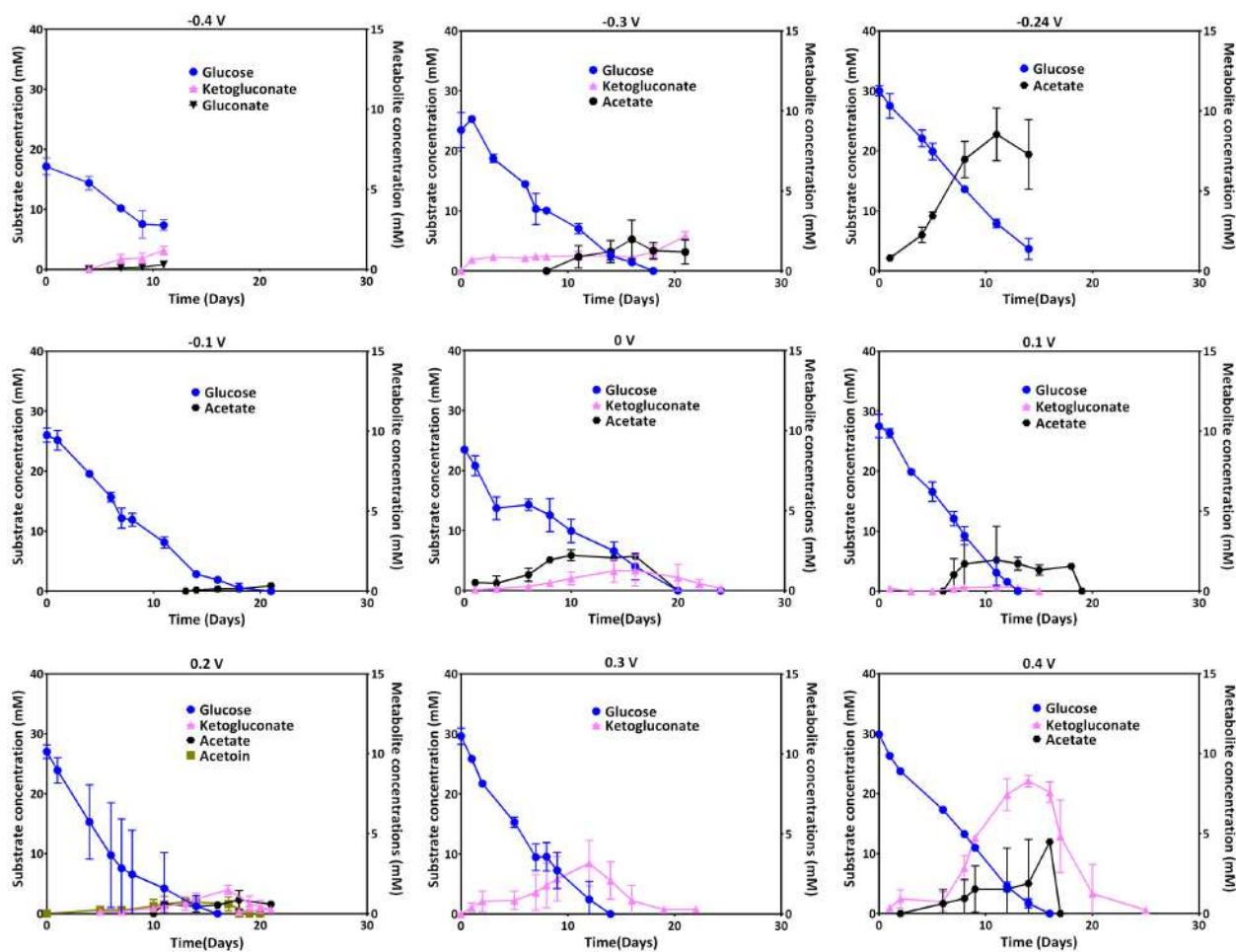


FIGURE 5 | Glucose uptake at different electrode potentials (left axis) and metabolite production (right axis; ketogluconate, gluconate, acetoin, and acetate) over time.

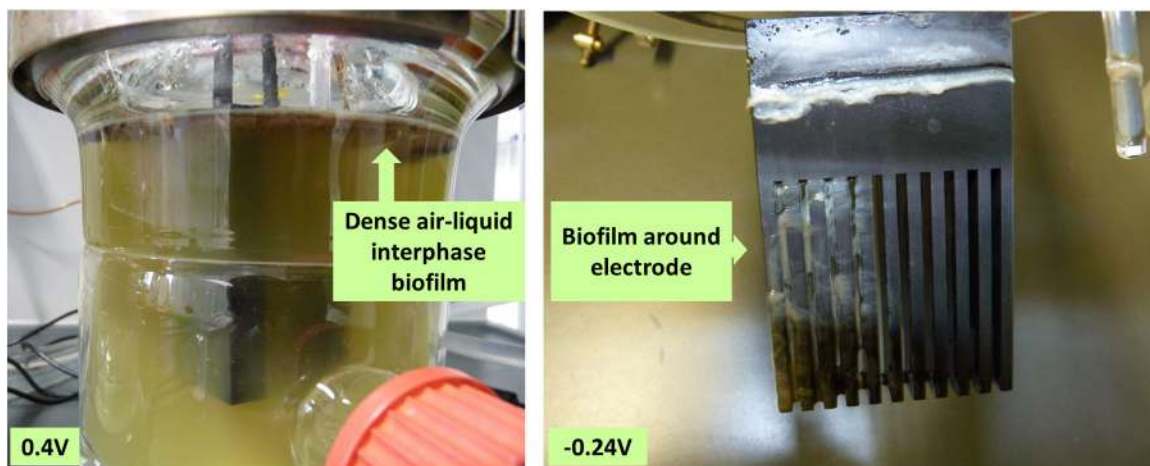


FIGURE 6 | Biofilm formation at the air-liquid interface and around the electrodes. Representative pictures of biofilm formation: left 0.4 V, where a dense biofilm forms at the air-liquid-interphase and right -0.24 V , where a biofilm additionally forms around the electrode.

at 0.2 and -0.3 V. The unclear patterns in biomass generation would be partly due to the measurement of the biomass at the end of the culture experiment (time point at which current generation stopped), when most of the cells have attained the death phase. Also, the age of cultures from which the biomass was measured varied between the experiments (10–30 days); hence, the cultures measured were at different physiological states. Oxygen availability might have also influenced biomass generation since only passive aeration through open vent filters was applied, which might lead to stronger oxygen limitation in fast growing cultures.

Biofilm formation tendency was visually determined for all the cultures. At all potentials considered, a biofilm was formed at the air-liquid interphase at a considerably similar intensity. Cultures grown at negative applied potentials formed additionally a biofilm around the electrode at the liquid interphase. High biofilm intensity around the electrode was observed at -0.3 , -0.24 , and -0.1 V (**Figure 6** and **Table 2**).

To summarize our study, the overall influence of the applied potential on the current production, the redox species, and the growth was compiled in **Table 2**.

DISCUSSION

Overall Influence of the Applied Electrode Potential on *P. aeruginosa* Physiology

The applied potential in a BES exerts an influence on the redox physiology of biocatalysts present (Busalmen et al., 2008; Wagner et al., 2010; Lian et al., 2016). *P. aeruginosa* might respond by fine tuning its electron transfer mechanism, e.g., by adjusting its spectrum or concentration of redox-active compounds. Furthermore, this might impact the central carbon metabolism and hence alter the overall respiration (Price-Whelan et al., 2007).

As stated above, there were no major differences observed in the biomass generation in cultures grown at the different potentials, except for the tendency to form a biofilm on the electrode at negative potentials (although a representative biomass determination was very difficult – see above). Theoretically, it would be possible that a beneficial use of higher electrode potentials of the extracellular electron acceptor, for instance 0.4 V for this study, would mediate higher biomass yields according to Gibbs energy (Thauer et al., 1977). However, this is only possible if different electron transfer mechanisms are available that can be employed at the different potentials for discharging electrons at these applied potentials. *P. aeruginosa*, however, uses mainly phenazines to reduce different external electron acceptors. Poisoning the electrode potential right at the formal potential of the most abundant phenazine (PCA) resulted in reduced production of this phenazine and the lack of a positive current, which is expected because current flow through this redox system is only possible if electron donor and acceptor to this system have a more negative and more positive potential, respectively, compared to its formal potential. High current densities across the potential range

clearly coincided with high PCA concentrations, indicating that the dominating redox specie does not change with the applied electrode potential. For the organism, a productive usage of the PCA redox system is only possible at more positive potentials, which is also indicated by increased carbon source uptake rates at positive potentials as compared to negative potentials. Further, the reoxidation rate of the phenazines at the electrode should be higher (e.g., through enhanced electro-migration to the electrode), the more positive the electrode potential is compared to the formal potential of the redox species. In this sense, a potential of 0.3 V seems most appropriate for efficient PCA recycling. This is also reflected by the maximum observed coulombic efficiency, i.e., the fraction of chemical energy input that could be harvested at the anode, which was $\sim 12\%$ at an applied potential of 0.3 V (**Table 2**). It appears though that increasing the potential above 0.3 V may not be beneficial for the organism, since the current production, the glucose uptake and the coulombic efficiency were all reduced at 0.4 V (**Figures 2, 5** and **Table 2**).

PCA Can Also Be Involved in Cathodic Electron Transfer

At lower electrode potentials, the electron transfer to the electrode expectedly was impaired. Considering PCA (the most abundant phenazine) as the main electron transfer route to the electrode, it was expected that at and below -0.24 V no positive (anodic) current will be generated. Indeed at -0.24 very low amounts of PCA were detected and the cultures were barely electroactive. Instead, a cathodic reduction current was recorded at -0.24 , -0.3 , and -0.4 V. In this case, the electrode might have reduced the PCA redox mediator, which donated these electrons to suitable electron acceptors. Whether this reduction current was biologically utilized, is an important question to be answered. There is an indication that the current increased over time and reduced during the death phase, which might coincide with the growth of the culture and phenazine (PCA) production. Besides the microbial cells, also oxygen or minerals in the medium likely served as electron acceptor for these electrons in our study. It is widely accepted that *Pseudomonas* phenazines mediate electron transfer to distant oxygen in oxygen limited environments (Price-Whelan et al., 2006; Pierson and Pierson, 2010; Wang et al., 2010). Overall, below 0.1 V the oxidation of glucose is somewhat impaired; depicted in the reduced uptake rates, which might point to a lack of access to a required electron acceptor under these conditions, where the phenazine redox mediators are not available to discharge metabolic electrons to the electrode. This viewpoint is generally in agreement with our data, except for the experiment performed at -0.1 V, where high levels of PCA and the second highest levels of anodic currents were found. Identifying soluble redox species that can also mediate cathodic electron uptake is also an important question for current consuming BES applications such as microbial electrosynthesis or electrofermentation. For these systems, the mode of electron transfer from the cathode to a biocatalyst is still widely uncharacterized (Nevin et al., 2010, 2011; Moscoviz et al., 2016). This work indicates that PCA indeed can

mediate cathodic electron flow, however, further work will have to show to what extend the mediated electrons flow to oxygen, minerals or into microbial processes.

Unknown Redox Specie Involved in Cathodic Electron Transfer

Another important growth aspect in BES is the biofilm formation around the electrode. For BES microorganisms that depend on direct electron transfer, it is paramount that they are attached to the electrode. Even though *P. aeruginosa* is not known to depend on direct electron transfer, observations in this study suggest that negative potentials allow the formation of a biofilm around the electrode (to a higher degree at -0.24 V, see **Figure 6** and **Table 2**). Interestingly, at these potentials, an additional redox peak system (PS2) was observed with a more positive formal potential than that of PCA (0.052 V). Since the peak system was absent in the CVs of the supernatant, it is likely that PS2 is a redox species that is located at the electrode or the biofilm that formed around the electrode (**Figure 6**). Since this observation was only made for applied electrode potentials more negative than the formal potential of PS2, this may imply that *P. aeruginosa* employs additional redox species in maybe consuming electrons from the electrode. The electrons taken up from the electrode might be used to reduce other available electron acceptors for instance oxygen and minerals in the medium or feed into the microbial metabolism. It will be very interesting to further elucidate, which redox species is responsible for this additional redox peak system in future work and if this process represents a productive interaction of the microbial biocatalyst with the cathode. Overall, the results show that the applied potential influenced the electron transfer physiology, which might also be linked to carbon metabolism physiology. This implies that, for every BES investigations, it is important to determine the appropriate potential, which will be beneficial in steering the physiology of the biocatalyst for efficient current generation. From the data presented here, it can be concluded that 0.3 V was the most appropriate potential under the conditions of the BES used. 0.3 V allows a rapid generation of maximum current density, more charge and overall higher coulombic efficiency is attained. An applied anode potential of 0.3 V (~ 0.5 V vs. SHE) is representative of the cell potential the bacteria would also encounter in a well-functioning MFC with an oxygen reduction cathode, where cell potentials are expected to reach 0.4 – 0.5 V. Thus, in such well-functioning MFCs, *P. aeruginosa* can find

optimum electrochemical conditions to participate in electron transfer.

CONCLUSION

Pseudomonas aeruginosa has demonstrated potential as a redox mediator producer for application in current generation in BES. To harness the full potential of the production of these mediators and their usage in electron shuttling, it is important to fully understand the influence of the applied electrode potential. This study reveals a profound influence of the applied potential on the levels and rate of current production for *P. aeruginosa* PA14 at different electrode potentials. Higher potentials (up to 0.3 V) increase the rate of anodic peak current generation, while potentials more negative than the formal potential of the dominating redox specie result in cathodic electron uptake. Thereby, the redox mediator PCA was identified as the dominating redox specie at all tested potentials. Further, *P. aeruginosa* activates an additional redox species at lower potentials, of which activity and specific role is yet to be identified.

AUTHOR CONTRIBUTIONS

EB designed the work, conducted the experiments, analyzed the data, and prepared the draft of the manuscript. MR conceived of the study, designed the work, analysed the data, and edited the manuscript.

FUNDING

This work was supported by a grant from the Deutsche Forschungsgemeinschaft (DFG, AG156/1-1) to MR. EB was supported by a personal stipend from the Deutscher Akademischer Austauch Dienst (DAAD).

SUPPLEMENTARY MATERIAL

The Supplementary Material for this article can be found online at: <http://journal.frontiersin.org/article/10.3389/fmicb.2017.00892/full#supplementary-material>

REFERENCES

- Bosire, E. M., Blank, L. M., and Rosenbaum, M. A. (2016). Strain- and substrate-dependent redox mediator and electricity production by *Pseudomonas aeruginosa*. *Appl. Environ. Microbiol.* 82, 5026–5038. doi: 10.1128/AEM.01342-16
- Busalmen, J. P., Esteve-Nunez, A., Berna, A., and Feliu, J. M. (2008). C-type cytochromes wire electricity-producing bacteria to electrodes. *Angew. Chem. Int. Ed. Engl.* 47, 4874–4877. doi: 10.1002/anie.200801310
- Clark, D. J., and Maaløe, O. (1967). DNA replication and the division cycle in *Escherichia coli*. *J. Mol. Biol.* 23, 99–112. doi: 10.1016/S0022-2836(67)80070-6
- Freguia, S., Masuda, M., Tsujimura, S., and Kano, K. (2009). *Lactococcus lactis* catalyses electricity generation at microbial fuel cell anodes via excretion of a soluble quinone. *Bioelectrochemistry* 76, 14–18. doi: 10.1016/j.bioelechem.2009.04.001
- Gorby, Y. A., Yanina, S., McLean, J. S., Rosso, K. M., Moyles, D., Dohnalkova, A., et al. (2006). Electrically conductive bacterial nanowires produced by *Shewanella oneidensis* strain MR-1 and other microorganisms. *Proc. Natl. Acad. Sci. U.S.A.* 103, 11358–11363. doi: 10.1073/pnas.0604517103
- Lian, Y., Yang, Y., Guo, J., Wang, Y., Li, X., Fang, Y., et al. (2016). Electron acceptor redox potential globally regulates transcriptomic profiling in *Shewanella decolorationis* S12. *Sci. Rep.* 6:31143. doi: 10.1038/srep31143
- Liu, H., Matsuda, S., Kato, S., Hashimoto, K., and Nakanishi, S. (2010). Redox-responsive switching in bacterial respiratory pathways involving extracellular electron transfer. *ChemSusChem* 3, 1253–1256. doi: 10.1002/cssc.201000213

- Malvankar, N. S., Vargas, M., Nevin, K. P., Franks, A. E., Leang, C., Kim, B.-C., et al. (2011). Tunable metallic-like conductivity in microbial nanowire networks. *Nat. Nanotechnol.* 6, 573–579. doi: 10.1038/nano.2011.119
- Marsili, E., Baron, D. B., Shikhare, I. D., Coursolle, D., Gralnick, J. A., and Bond, D. R. (2008). *Shewanella* secretes flavins that mediate extracellular electron transfer. *Proc. Natl. Acad. Sci. U.S.A.* 105, 3968–3973. doi: 10.1073/pnas.0710525105
- Mavrodi, D. V., Blankenfeldt, W., and Thomashow, L. S. (2006). Phenazine compounds in fluorescent *Pseudomonas* spp. biosynthesis and regulation. *Annu. Rev. Phytopathol.* 44, 417–445. doi: 10.1146/annurev.phyto.44.013106.145710
- Moscoviz, R., Toledo-Alarcón, J., Trably, E., and Bernet, N. (2016). Electro-fermentation: how to drive fermentation using electrochemical systems. *Trends Biotechnol.* 34, 856–865. doi: 10.1016/j.tibtech.2016.04.009
- Nevin, K. P., Hensley, S. A., Franks, A. E., Summers, Z. M., Ou, J., Woodard, T. L., et al. (2011). Electrosynthesis of organic compounds from carbon dioxide is catalyzed by a diversity of acetogenic microorganisms. *Appl. Environ. Microbiol.* 77, 2882–2886. doi: 10.1128/AEM.02642-10
- Nevin, K. P., Woodard, T. L., Franks, A. E., Summers, Z. M., and Lovley, D. R. (2010). Microbial electrosynthesis: feeding microbes electricity to convert carbon dioxide and water to multicarbon extracellular organic compounds. *MBio* 1, 1–15. doi: 10.1128/mBio.00103-10
- Pham, T. H., Boon, N., Aelterman, P., Clauwaert, P., De Schampheleire, L., Vanhaecke, L., et al. (2008). Metabolites produced by *Pseudomonas* sp. enable a Gram-positive bacterium to achieve extracellular electron transfer. *Appl. Microbiol. Biotechnol.* 77, 1119–1129. doi: 10.1007/s00253-007-1248-6
- Pierson, L. S. III, and Pierson, E. A. (2010). Metabolism and function of phenazines in bacteria: impacts on the behavior of bacteria in the environment and biotechnological processes. *Appl. Microbiol. Biotechnol.* 86, 1659–1670. doi: 10.1007/s00253-010-2509-3
- Price-Whelan, A., Dietrich, L. E., and Newman, D. K. (2006). Rethinking ‘secondary’ metabolism: physiological roles for phenazine antibiotics. *Nat. Chem. Biol.* 2, 71–78. doi: 10.1038/nchembio764
- Price-Whelan, A., Dietrich, L. E., and Newman, D. K. (2007). Pyocyanin alters redox homeostasis and carbon flux through central metabolic pathways in *Pseudomonas aeruginosa* PA14. *J. Bacteriol.* 189, 6372–6381. doi: 10.1128/JB.00505-07
- Rabaey, K., Boon, N., Höfte, M., and Verstraete, W. (2005). Microbial phenazine production enhances electron transfer in biofuel cells. *Environ. Sci. Technol.* 39, 3401–3408. doi: 10.1021/es048563o
- Schröder, U. (2007). Anodic electron transfer mechanisms in microbial fuel cells and their energy efficiency. *Phys. Chem. Chem. Phys.* 9, 2619–2629. doi: 10.1039/b703627m
- Schröder, U., Harnisch, F., and Angenent, L. (2013). Microbial electrochemistry and technology: terminology and classification. *Energy Environ. Sci.* 8, 513–519. doi: 10.1039/C4EE03359K10.1039/c4ee03359k
- Thauer, R. K., Jungermann, K., and Decker, K. (1977). Energy conservation in chemotrophic anaerobic bacteria. *Bacteriol. Rev.* 41, 100–180.
- van Rij, E. T., Wesselink, M., Chin, A. W. T. F., Bloemberg, G. V., and Lugtenberg, B. J. (2004). Influence of environmental conditions on the production of phenazine-1-carboxamide by *Pseudomonas chlororaphis* PCL1391. *Mol. Plant Microbe. Interact.* 17, 557–566. doi: 10.1094/MPMI.2004.17.5.557
- Venkataraman, A., Rosenbaum, M., Arends, J. B. A., Halitsche, R., and Angenent, L. T. (2010). Quorum sensing regulates electric current generation of *Pseudomonas aeruginosa* PA14 in bioelectrochemical systems. *Electrochim. Commun.* 12, 459–462. doi: 10.1016/j.elecom.2010.01.019
- Venkataraman, A., Rosenbaum, M. A., Perkins, S. D., Werner, J. J., and Angenent, L. T. (2011). Metabolite-based mutualism between *Pseudomonas aeruginosa* PA14 and *Enterobacter aerogenes* enhances current generation in bioelectrochemical systems. *Energy Environ. Sci.* 4, 4550–4559. doi: 10.1039/c1ee01377g
- Wagner, R. C., Call, D. F., and Logan, B. E. (2010). Optimal set anode potentials vary in bioelectrochemical systems. *Environ. Sci. Technol.* 44, 6036–6041. doi: 10.1021/es101013e
- Wang, N., and Newman, D. K. (2008). Redox reactions of phenazine antibiotics with ferric (hydr)oxides and molecular oxygen. *Environ. Sci. Technol.* 42, 2380–2386. doi: 10.1021/es702290a
- Wang, Y., Kern, S. E., and Newman, D. K. (2010). Endogenous phenazine antibiotics promote anaerobic survival of *Pseudomonas aeruginosa* via extracellular electron transfer. *J. Bacteriol.* 192, 365–369. doi: 10.1128/JB.01188-09
- Wrighton, K. C., Thrash, J. C., Melnyk, R. A., Bigi, J. P., Byrne-Bailey, K. G., Remis, J. P., et al. (2011). Evidence for direct electron transfer by a gram-positive bacterium isolated from a microbial fuel cell. *Appl. Environ. Microbiol.* 77, 7633–7639. doi: 10.1128/AEM.05365-11

Conflict of Interest Statement: The authors declare that the research was conducted in the absence of any commercial or financial relationships that could be construed as a potential conflict of interest.

Copyright © 2017 Bosire and Rosenbaum. This is an open-access article distributed under the terms of the Creative Commons Attribution License (CC BY). The use, distribution or reproduction in other forums is permitted, provided the original author(s) or licensor are credited and that the original publication in this journal is cited, in accordance with accepted academic practice. No use, distribution or reproduction is permitted which does not comply with these terms.



Energy Efficiency and Productivity Enhancement of Microbial Electrosynthesis of Acetate

Edward V. LaBelle and Harold D. May*

Hollings Marine Laboratory, Marine Biomedicine and Environmental Science Center, Department of Microbiology and Immunology, Medical University of South Carolina, Charleston, SC, USA

OPEN ACCESS

Edited by:

Feng Zhao,

Institute of Urban Environment (CAS),
China

Reviewed by:

Ahmed ElMekawy,
University of Adelaide, Australia

Seung Gu Shin,

Pohang University of Science
and Technology, South Korea

G. Velvizhi,

Indian Institute of Chemical
Technology (CSIR), India

***Correspondence:**

Harold D. May

mayh@musc.edu

Specialty section:

This article was submitted to
Microbiotechnology, Ecotoxicology
and Bioremediation,
a section of the journal
Frontiers in Microbiology

Received: 22 February 2017

Accepted: 12 April 2017

Published: 03 May 2017

Citation:

LaBelle EV and May HD (2017)
Energy Efficiency and Productivity
Enhancement of Microbial
Electrosynthesis of Acetate.
Front. Microbiol. 8:756.
doi: 10.3389/fmicb.2017.00756

It was hypothesized that a lack of acetogenic biomass (biocatalyst) at the cathode of a microbial electrosynthesis system, due to electron and nutrient limitations, has prevented further improvement in acetate productivity and efficiency. In order to increase the biomass at the cathode and thereby performance, a bioelectrochemical system with this acetogenic community was operated under galvanostatic control and continuous media flow through a reticulated vitreous carbon (RVC) foam cathode. The combination of galvanostatic control and the high surface area cathode reduced the electron limitation and the continuous flow overcame the nutrient limitation while avoiding the accumulation of products and potential inhibitors. These conditions were set with the intention of operating the biocathode through the production of H₂. Biofilm growth occurred on and within the unmodified RVC foam regardless of vigorous H₂ generation on the cathode surface. A maximum volumetric rate or space time yield for acetate production of 0.78 g/L_{catholyte}/h was achieved with 8 A/L_{catholyte} (83.3 A/m² projected surface area of cathode) supplied to the continuous flow/culture bioelectrochemical reactors. The total Coulombic efficiency in H₂ and acetate ranged from approximately 80–100%, with a maximum of 35% in acetate. The overall energy efficiency ranged from approximately 35–42% with a maximum to acetate of 12%.

Keywords: microbial electrosynthesis, acetate, hydrogen, chemicals from CO₂, biocathode, industrial biotechnology

INTRODUCTION

The desire to mitigate carbon dioxide emissions (32.1 billion tons CO₂ emitted globally in 2015) (IEA, 2016) and find sustainable energy sources for increasing global demand have stimulated research in alternative electricity generation and non-fossil fuels. In 2015, 90% of new global electricity generation capacity was renewable (IEA, 2016). With stranded and off peak power, there is a need to balance the energy in the grid and take advantage of every renewable kWh available. One technology that may help address this in the future is microbial electrosynthesis. Utilizing any electricity source, but preferably a sustainable one, different anaerobic microbes have produced several chemicals of interest by using CO₂ as the sole carbon source when operating at the cathode of an electrochemical cell (Nevin et al., 2010; Logan and Rabaey, 2012; Marshall et al., 2012, 2013; Lovley and Nevin, 2013; LaBelle et al., 2014; Blanchet et al., 2015; Jourdin et al., 2015; Schröder et al., 2015; Ammam et al., 2016; Deutzmann and Spormann, 2016).

Ultimately, products from microbial electrosynthesis would include high value chemicals and liquid fuels. However, simply producing a single C-C bond such as in acetate would be worthwhile and much of the work done thus far has focused on electroacetogenesis (Conrado et al., 2013; May et al., 2016). Closely related to this is the bioconversion of syngas (H_2 , CO, and CO_2) to fuels and chemicals (Daniell et al., 2012, 2016; Hu et al., 2013, 2016), and within this area of research is the study of $H_2:CO_2$ transformation to acetate by acetogenic bacteria. Acetate itself is of commercial importance and it can be transformed further into other products (Andersen et al., 2014; Hu et al., 2016; Pal and Nayak, 2016). For these reasons there has been a significant effort recently to improve the rates and efficiency of acetogenesis with $H_2:CO_2$ or bioelectrochemically.

Previous work in gas fermentations has illuminated reaction conditions that can limit or enhance the rates of acetogenesis. Demler and Weuster-Botz (2011) achieved a volumetric productivity or space time yield (STY) of 0.31 g/L/h with *Acetobacterium woodii* in a batch stirred tank reactor pressurized with $H_2:CO_2$. Later Kantzow et al. (2015) achieved an impressive STY of 6.16 g/L/h in continuous flow stirred tank reactors (CSTR). The investigators demonstrated that increasing the dilution rate and increasing biomass retention led to higher acetate productivity. Hu et al. (2013) showed that in bubble columns, electron transfer to *Moorella thermoacetica* was limited by the mass transfer of CO into solution at rates below 30 mM/h, which is a volumetric current density equivalent to 1.6 A/L. Hu et al. (2016), an improved design led to a STY of 1.1 g/L/h of acetate from $H_2:CO_2$ by *M. thermoacetica* first grown with CO. The investigators integrated the process with *Yarrowia lipolytica* to produce biodiesel precursors, thereby demonstrating the feasibility of linking syngas fermentation with an acetate-consuming biofuel-producing process. Overall, these investigations indicate that fuel and chemical production could be driven by H_2 gas fermentations at industrially relevant rates. Could this be accomplished with microbial electrosynthesis?

The objective of this study was to improve the productivity and efficiency of microbial electrosynthesis through reactor design and operation (galvanostatic mode, H_2 mediation, continuous flow). Data from previous studies with an acetogenic community used in bioelectrochemical systems with graphite granule cathodes (Marshall et al., 2012, 2013; LaBelle et al., 2014) generally indicated that the early reactors were of an inefficient design and that more biomass at the cathode was likely needed to improve performance. Patil et al. (2015) discussed and demonstrated the utility of delivering electrons in a MES with galvanostatic operation, and this also resulted in faster startup times and improved scalability. Instead of waiting for higher rates of H_2 evolution from the electrode as in previous MES studies operated potentiostatically, here it was hypothesized that using a high volumetric current density surpassing the 1.6 A/L elucidated from Hu et al. (2013) would result in shorter startup times, faster biomass growth rate, and faster acetate production. Biomass growth would also benefit from a continuous flow of nutrients, and a nitrogen limitation was indicated by the upregulation of nitrogen fixing enzymes in

batch-fed bioelectrochemical reactors (Marshall et al., 2016). Continuous flow of media will also alleviate product inhibition (Demler and Weuster-Botz, 2011; Kantzow et al., 2015), decrease the reactor footprint, and facilitate pH control; this acetogenic community has an acetate and H_2 product ratio that is affected by pH in potentiostatic systems (LaBelle et al., 2014). Thus, galvanostatic control and continuous flow were applied to a reactor designed for better energy efficiency and STY, which are also important to decrease capital and operating costs (Krieg et al., 2014; Papoutsakis, 2015). The goal was to develop a system that could be used to reach g/L/h productivity while maintaining a high energy efficiency. This was done with high current density normalized to surface area (projected and geometric). However, since the acetate product is soluble, the volumetric current density is important when considering the reactor productivity as well as product titer needed to devise an efficient extraction scheme (Krieg et al., 2014; Gildemyn et al., 2015; Papoutsakis, 2015; Patil et al., 2015). The approach resulted in a considerable enhancement of productivity and efficiency.

MATERIALS AND METHODS

Bioelectrochemical Reactor

The modular and scalable reactors were designed and constructed as depicted in Supplementary Figures S1A,B. The 45 pores per inch (17.7 pores per cm) reticulated vitreous carbon (RVC) foam cathode (KR Reynolds Company) was 0.6 cm × 6 cm × 8 cm (surface area to volume ratio of 26.2 cm²/cm³ per manufacturer). It was pretreated in 2N nitric acid and rinsed thoroughly with MilliQ water. It was then attached to a 6 × 6 mesh, 0.89 mm wire diameter 316L stainless steel mesh (6 cm × 8 cm) current collector that was coated with a conductive graphite and carbon black acrylic glue (Ted Pella Inc. #16050) thinned with 1:1 (v/v) acetone. Two applications were coated onto the mesh before the same glue was used to attach the RVC foam. The anode was a mixed metal oxide (IrO_2/Ta_2O_5) catalyzed titanium anode (MMO; Magneto).

Custom machined polypropylene spacers were used with customized Viton gaskets to sandwich a cation exchange membrane (CMI-7000, Membranes International Inc.) between the electrodes with a 316L stainless steel endplate and a poly(methyl methacrylate; PMMA) cathode viewing plate held together by stainless steel nuts, bolts and washers. The polypropylene spacers were 0.95 cm × 10 cm × 10 cm, with a square opening of 8 cm × 8 cm. The steel plate was 0.95 cm × 15.2 cm × 15.2 cm. The PMMA cathode viewing plate was 1.25 cm × 15.2 cm × 15.2 cm. The membrane and exposed anode surface area were each 64 cm². The projected cathode surface area was 48 cm². Polypropylene Luer fittings (McMaster Carr) were used as ports to connect tubing. Reference electrodes were constructed using a AgCl coated silver wire immersed in 3M KCl saturated with AgCl in a glass capillary tube with a Vycor frit attached via heat shrink tubing. A Luggin capillary was integrated in the reactor using 1 M KCl as supporting electrolyte, and its Vycor frit was ~2 mm from the cathode.

The anolyte was 75 mL of 50 mM sodium sulfate acidified with sulfuric acid to pH = 2. The catholyte was 50 mL of a phosphate-based medium initially prepared at pH 7 under 100% N₂ as described in LaBelle et al. (2014). It contained salts, vitamins and trace metals and minerals. 50 mM NaCl was used instead of sodium bromoethanesulfonate. No yeast extract, sulfide or cysteine was used.

Reactor Operation

An acetogenic microbiome previously enriched on graphite granule cathodes at potentials from -590 to -800 mV vs. SHE was used to inoculate the bioreactors (LaBelle et al., 2014). The cells were drawn from the cathode compartment of an active reactor and were concentrated using tangential flow filtration using a 0.2 µm polyethersulfone filter (Sartorius), spun at 5000 (RCF) for 10 min and re-suspended in fresh medium before transfer to the RVC cathode reactors. The culture, inoculum and reactor, were treated as an open, non-aseptic system.

The reactor was operated at 25°C with constant current supplied from a VMP3 Potentiostat (BioLogic) set in galvanostatic mode and the voltage monitored with EC Lab software. A galvanostatic operation of 8 A/L_{catholyte} was chosen to overcome electron limitation to a biofilm immobilized on the cathode and promote fast colonization. Humidified 100% CO₂ was passed through the catholyte headspace using Norprene tubing at an initially set rate of 25 mL/min. Filter sterilized medium was flowed into the base of the cathode compartment and exited just above the top of the RVC cathode at a rate of 250 mL/day (a dilution rate of 5 day⁻¹) using a peristaltic pump and PharMed BPT tubing. Deionized water was added to ports made from syringe housing on the anolyte compartment daily to compensate for water oxidation and evaporation.

Sampling and Analysis

The gas flow rate was monitored with an Agilent gas flow meter when sampling headspace for gas chromatographic analysis, and fatty acids were analyzed via HPLC (LaBelle et al., 2014). The pH of samples drawn from the cathode chamber was checked with a pH meter (Mettler Toledo). Optical density of the planktonic cells (OD_{600nm}) was measured at 600 nm using a Genesys UV/Vis spectrophotometer.

Space time yield was calculated as the STY = concentration times flow rate divided by catholyte volume (Krieg et al., 2014). The Coulombic efficiencies were calculated from the partial current densities of each product divided by the total applied current. Energy efficiencies were obtained by using the higher heating value (HHV) of product multiplied by the STY and then divided by the applied electrical energy to the reactor per time (Krieg et al., 2014).

RESULTS AND DISCUSSION

Biomass Growth

The initial inoculum resulted in an optical density (OD_{600nm}) of 0.34 ± 0.01 ($n = 3$) within the cathode chamber of three inoculated reactors (Figure 1A). The continuous flow of media

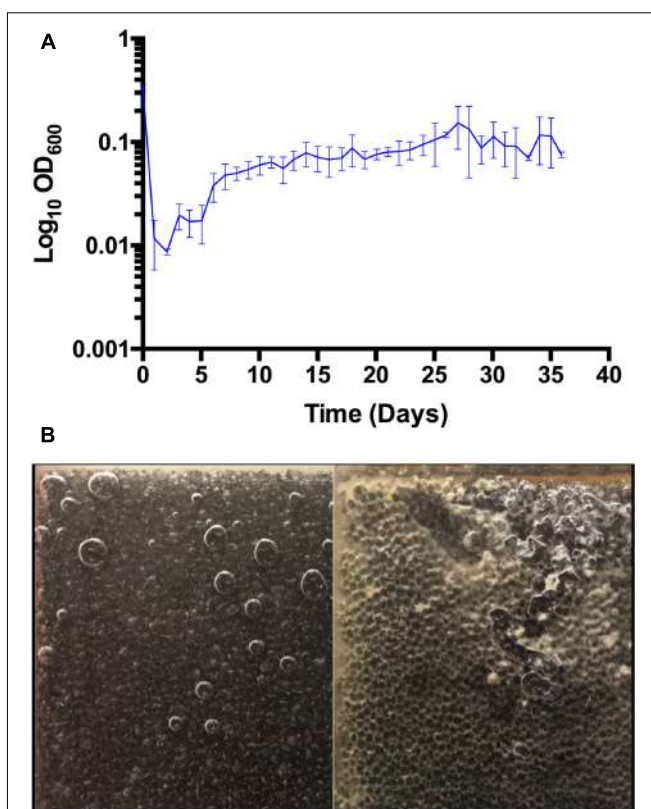


FIGURE 1 | (A) Optical density (600 nm) of planktonic cells in triplicate bioelectrochemical reactors (SD, $n = 3$). **(B)** Biofilm growth on RVC cathode. Photographs of uninoculated (left) and inoculated (right) 45 ppi RVC cathodes at 36 days.

through the reactors, and perhaps adsorption of biomass to the electrode surface, drove the OD_{600nm} down by more than an order of magnitude. Shortly thereafter the OD_{600nm} began to steadily increase and eventually remained near or above 0.1 within the reactors, indicating a constant production of bacterial cells including those that remained planktonic and were washed away with the effluent. A coating of the unmodified cathode surface with yellow and off-white material became apparent within a week of inoculation and grew heavier until the end of the experiment (Figure 1B). Microscopic examination of the material from the electrode surface and from within the interstitial space revealed that it was densely populated with bacterial cells similar to *Acetobacterium* in morphology, the genus that dominated the inoculum (LaBelle et al., 2014). Although the biomass on the electrodes was not quantified, visually it was apparent that the colonization of the electrode continued until the experiment was terminated.

While graphite granule cathodes were effective at enriching the community (Marshall et al., 2012, 2013; LaBelle et al., 2014), and are a relatively inexpensive and high surface area electrode for electroactive biofilms, their drawbacks include gas hold up, high resistance, high granular void volume, and restriction of liquid flow for continuous operation, thus warranting a different electrode geometry. RVC was chosen because of its high surface

area to volume ratio, low solid void volume due to the glassy carbon (97% air-liquid void volume), and this electrode material performs well for flow through systems (Krieg et al., 2014). Unmodified RVC has been reported to be a poor surface for bioelectrochemical systems (Flexer et al., 2013), and it did not support the electrosynthesis of any acetate with another microbial community (Jourdin et al., 2014) unless its glassy carbon surface was coated with carbon nanotubes (Jourdin et al., 2015). For the latter case a current density of 0.055 A/L (102 A/m² projected surface area) and an acetate rate of 0.015 g/L/h and electron recovery of 100% were achieved under poised potential conditions in a batch-fed reactor. In contrast, the microbial community used under the conditions described here (8 A/L, 83 A/m² projected surface area) readily colonized the unmodified RVC and generated acetate (see below) with this material serving as a biocathode. Microbubbles vigorously effervesced throughout and larger bubbles coalesced on the cathodes during the start-up. One may expect this to limit or even prevent the formation of a biofilm on the surface and within the honeycomb of the cathode (Blanchet et al., 2015; Bergel, 2016). However, biofilm became clearly visible on the cathodes following inoculation (confirmed by optical microscopy) while no visible changes were observed for more than a month with uninoculated RVC maintained under the same conditions. It is likely that biological and non-biological material was deposited on the cathode, but this was only visible when the cathodes were inoculated and the key to improved productivity was probably due to the increase in biomass on and within the RVC. Furthermore, there were no indications at the end of the experiment that the biomass/biofilm could not be increased further, which may additionally improve productivity and efficiency. How this biofilm forms and how it influences hydrogen formation and transfer, acetogenesis, and overall performance will require further inquiry.

Productivity

The STY of acetate was monitored in the three inoculated continuous flow/constant current reactors (Figure 2). Within the first 4 days of operation, the STY rapidly increased to >0.4 g/L_{catholyte}/h. From this point forward the rate steadily increased and was accelerating at the end of the experiment (day 36) when the STY reached a maximum of 0.78 g/L_{catholyte}/h, 0.74 ± 0.05 g/L_{catholyte}/h in replicates ($n = 3$). The maximum acetate produced per electrode surface area was 8.2 g/m²_{projected}/h. Hydrogen was co-produced at 0.2 g/L_{catholyte}/h at the end of the experiment. Other products included formate, propionate, and butyrate produced at <0.02 g/L_{catholyte}/h (Supplementary Figure S2). No methane was detected and biomass growth and acetate production were sustained without the addition of methanogenic inhibitors, yeast extract, or chemical reducing agents.

Shortly after inoculation, the pH of the biotic reactors rose abruptly to 8.88 ± 0.53 due to the production of base at the cathode of the electrochemical cell. However, the continuous supply of CO₂ and medium flow returned the pH to 6.75 ± 0.03 within 24 h. The pH decreased as the microbial production of acetic acid increased and the change in pH was more rapid at the end of the experiment. A single uninoculated reactor was

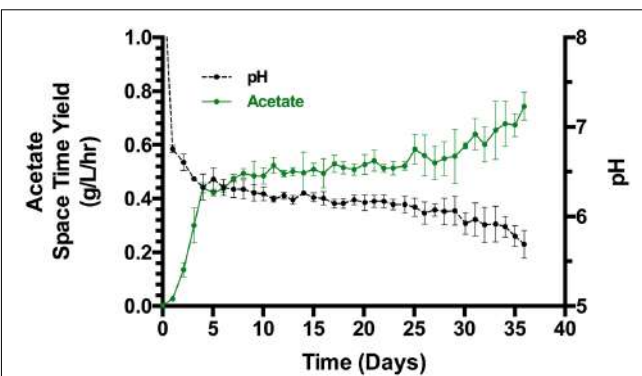


FIGURE 2 | Space time yield of acetate and pH of triplicate bioelectrochemical reactors (SD, $n = 3$).

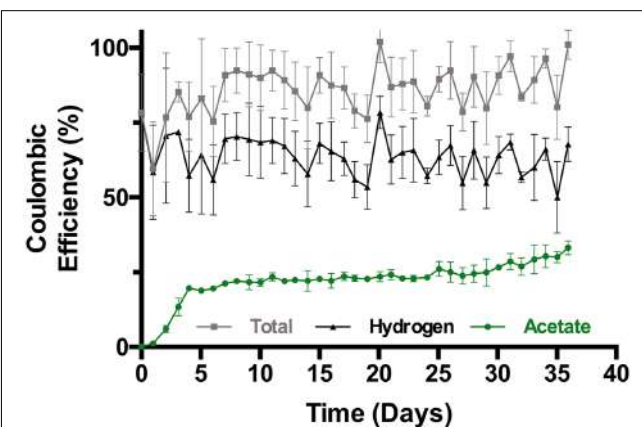


FIGURE 3 | Coulombic efficiency of triplicate bioelectrochemical reactors (SD, $n = 3$).

maintained under the same conditions as the three inoculated reactors (Supplementary Figure S3). After an initial upward spike in pH during the 1st day, the pH stabilized at 6.67 ± 0.03 for the remainder of the experiment.

Efficiency

Following the initial start-up, the overall Coulombic efficiency (CE) ranged from approximately 75–85% with about 20% in acetate (Figure 3). From then to the end of the experiment the overall CE ranged between approximately 80 and 100% with most of the variability in the measurement of H₂ (the CE for the single uninoculated control reactor was 88%). The electron recovery in acetate steadily increased to 33.2% ± 2.3% ($n = 3$) at day 36 with 35% in one reactor.

The trend in energy efficiency (Figure 4) generally followed that of the CE (Figure 3), and both efficiencies paralleled the increase in the STY of acetate (Figure 2). Following the initial increase in productivity during the first 4 days of incubation the energy efficiency fluctuated between 30 and 35% with approximately 7% invested in acetate. From then to the end of the experiment, the overall energy efficiency varied between 35 and 42% while the energetic efficiency in acetate steadily increased to

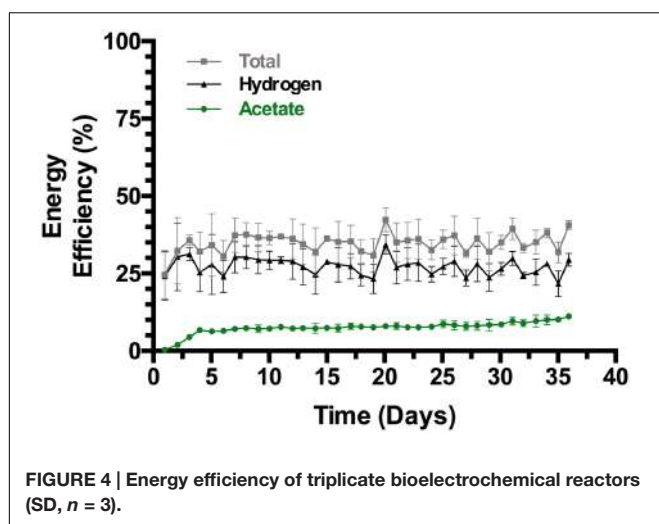


FIGURE 4 | Energy efficiency of triplicate bioelectrochemical reactors (SD, $n = 3$).

$11.2\% \pm 0.8\%$ ($n = 3$) with a 12.1% maximum in one reactor at the end of the experiment. Both the CE and energy transferred to acetate were increasing at the end of the experiment.

Voltage ranged from 3.2 to 3.6 over time with all three reactors, and potential at the cathodes was -1.1 to -1.3 V vs. SHE (Standard Hydrogen Electrode) with no clear trend up or down. The power consumption of the reactors is depicted in Supplementary Figure S4. Better electrode spacing and a more efficient anode may improve the efficiency of the reactors. What would likely most improve the efficiency to acetate for these bioelectrochemical reactors is to avoid the loss of H₂; this may be related to retaining more biomass in the reactor. Adding pH control and additional cell retention to the system may be the solution. The RVC is enabling some cell retention in the reactor in addition to efficient electron delivery, but the contribution from cells on the electrode vs. within the honeycomb of the electrode or suspended in the medium is unknown, and there is a significant fraction of planktonic biomass that is presently lost with the continuous flow (~ 0.1 OD_{600nm}). Hence further cell retention in the cathode chamber may additionally enhance productivity and efficiency and the results warrant a more detailed examination of the biofilm formation on the cathodes in relation to productivity and efficiency. For example, attaining a 100% CE to acetate under the current presently applied could result in a STY of 2.2 g/L/h and an energy efficiency $> 30\%$ to acetate.

Microbial Electrosynthesis vs. Gas Fermentations

When comparing the supply of electrons (H₂) supplied to gas-liquid contacting (GLC) bioreactors (Demler and Weuster-Botz, 2011; Hu et al., 2013, 2016; Kantzow et al., 2015), it became apparent that the electrons supplied to the bioelectrochemical reactors in the past (Marshall et al., 2012, 2013; LaBelle et al., 2014) were limited and this precluded any chance of high productivity and likely blunted the growth of biomass; hence the remedy described above. Abiotic and biotic activity may functionalize the surface of the cathode, thereby facilitating the production of H₂ or formate for the eventual generation of

acetate and other products (LaBelle et al., 2014; Yates et al., 2014; Deutzmann et al., 2015; Marshall et al., 2016; May et al., 2016), and the results presented here were dependent upon the addition of the microbial community, but the electrochemical bioreactors were intentionally operated through H₂ with the goal of improving productivity and efficiency. Therefore, it is reasonable to compare microbial electrosynthesis with H₂ gas fermentations (Blanchet et al., 2015; Tremblay et al., 2016).

Microbial electrosynthesis may be indirectly approached by the coupling of a H₂ producing electrolyzer with a GLC bioreactor such as a CSTR or a continuous flow bubble column where H₂ is delivered to a fuel or chemical producing microbe (e.g., an acetogen). Alternatively, during direct MES the microbes are incubated with the cathode of an electrochemical cell where they capture H₂ or possibly electrons directly from an electrode (Butler and Lovley, 2016; Tremblay et al., 2016). Productivity and efficiency data from these two approaches are presented in Table 1. A 70% energy efficiency for an electrolyzer (Körner et al., 2015), based on a HHV of H₂, was assumed for calculating the efficiency of an indirect MES with two reactors. Following growth with CO in a continuous flow bubble column with cell retention, the thermophile *M. thermoacetica* produced acetate at 1.1 g/L/h when supplied with H₂:CO₂, but there was a trade-off with efficiency when examining it as part of an indirect MES. The *M. thermoacetica* system was designed for use with hot syngas and the high temperature (60°) lowered the solubility of the H₂ (Hu et al., 2013, 2016), which required high sparging rates to overcome mass transfer and reduced efficiency.

When assessed as an indirect MES, a CSTR with *A. woodii* (Kantzow et al., 2015) produced acetate at nearly the same rate (0.76 g/L/h) but with substantially higher efficiency than *M. thermoacetica* in a bubble column. The highest acetate productivity (6.16 g/L/h) in combination with a high CE (55.9%) and energy efficiency (26.4%, estimated as an indirect MES including stirring energy) was achieved with *A. woodii* incubated in a CSTR with cell retention and a high rate of dilution (Kantzow et al., 2015). This energy efficiency does not match the 39–50% reported for a membraneless direct MES reactor operated in batch under constant applied voltage (Giddings et al., 2015), but due to its productivity the CSTR coupled with an electrolyzer is for now a more feasible approach. The energy efficiency of the direct MES described in the present study does exceed many of these other systems while maintaining high productivity, but its performance does not yet match that of the CSTR run with cell retention and a high dilution rate. However, as noted above the productivity and efficiency of the direct MES may be improved with more pH control and cell retention.

The results described here indicate the productivity and efficiency of a direct MES operating through H₂ in a single reactor is approaching that of an indirect MES using two reactors. Furthermore, rates of acetogenesis from H₂:CO₂ within GLC bioreactors are now on par with the productivity of ethanol fermentation and direct MES is approaching it. Starch (corn) ethanol is commercially produced at 1.25 to 3.75 g/L_{reactor volume}/h (Graves et al., 2006; Richter et al., 2013), but this rate of production ignores the time, arable land, and energy needed to grow, harvest, transport, and pretreat the

TABLE 1 | Indirect vs. direct microbial electrosynthesis of acetate.

Organism	Reactors	Temp. (C)	Dilution rate (d ⁻¹)	Yeast extract (g/L)	HFM#	pH stat*	Acetate (g/Lh)	Acetate electron recovery	Acetate energy efficiency	Reference
<i>Moorella thermoacetica</i>	70% EE electrolyzer	Bubble column	60°	2.16	10	Yes	1.1	3.7%	2.0%	Hu et al., 2016
<i>Acetobacterium woodii</i>	70% EE electrolyzer	CSTR	30°	0.84	4	No	0.76	10.3%	4.6% ^a	Kantzow et al., 2015
<i>Acetobacterium woodii</i>	70% EE electrolyzer	CSTR	30°	8.4	4	Yes	6.16	55.9%	26.4% ^a	Kantzow et al., 2015
<i>Acetobacterium sp. (mix)</i>	Bioelectrochemical constant current ^b	25°	5	0	No	No	0.78	35%	12.1%	This study
<i>Clostridiales (mix)</i>	Bioelectrochemical constant current ^c	21°	Batch	0	No	No	0.024	61%	21%	Gildemyn et al., 2015
<i>Sporomusa ovata</i>	Bioelectrochemical constant voltage ^d	25°	0.0144	0	No	No	0.0009	105%	50%	Giddings et al., 2015

Acetate electron recovery for indirect MES was based on electrons produced divided by the total electrons sparged as H₂ through the reactor from the electrolyzer. Acetate energy efficiency was calculated using the H₂/V of acetate produced divided by the energy to power an electrolyzer that has a 70% energy efficiency (EE) based on the H₂/V of H₂ produced. ^aTotal energy applied included energy required for stirring the CSTR. ^bApplied Current: 8 A/V—catholyte (83.3 A/m² projected). ^cApplied Current: 0.143 A/V—catholyte (5 A/m² projected). ^dApplied Voltage: 1.9 V. Hollow fiber membranes are used for full cell retention. ^eHollow fiber membrane.

*pH auxostat system.

substrate prior to fermentation (Fast and Papoutsakis, 2012; Conrado et al., 2013). Ethanol and acetate do not possess the same energy or commercial value and absolute comparisons of their production cannot be made. But the aforementioned comments are insightful since bioethanol from starch is the largest biorefinery process scaled to date, and if electrosynthesis of acetate or any other chemical is to ever be viable then productivity must be within the range of bioethanol production.

Cost, Titer, and Extraction

At the efficiency and rates described here for electroacetogenesis, 33.6 kWh are needed to produce 1 kg of acetate with a direct MES and 15.4 kWh with an indirect MES using a CSTR. At \$0.02 per kWh (national average levelized price of wind power purchase agreements) (Wiser and Bolinger, 2016), the electricity cost for 1 kg of acetate would range from \$0.31 to \$0.67; as with any system, the need for extraction and purification would undoubtedly add to this cost (Gildemyn et al., 2015; Papoutsakis, 2015; Xu et al., 2015). The global price of acetic acid has ranged from \$0.35 to \$0.95 per kg between 2010 and 2015 (Wakatsuki, 2015), while U.S. domestic acetic acid spot pricing was at \$0.49 per kg and U.S. spot export pricing was at \$0.60–\$0.63 per kg in September of 2016 (Raizada, 2016). Prices from \$0.90 to \$1.60 per kg were also reported in a variety of countries during 2015 and 2016 (Nayak and Pal, 2015; Nayak et al., 2015; Pal and Nayak, 2016). While these quotes indicate a range of possible commercial values for acetate, they also show that further improvements in electrosynthesis performance remain desirable. Selling the excess hydrogen and oxygen simultaneously produced could attain additional revenue, and increases in efficiency will help. For example, achieving 100% CE under the same conditions in this work would lower the energy requirement to 12 kWh per kg, with \$0.24 in electricity costs per kg acetate produced. However, titer is another factor that affects purification costs. The titer reached 3.6 g/L in the present experiment and 10.5 g/L in past batch experiments with the same microbial community (Marshall et al., 2013). Optimizing the dilution rate in relation to nutrient supply, pH control, and cell retention will increase the titer in the continuous flow/constant current reactors, but significantly higher titer still needs to be achieved.

A promising approach to increase titer has been demonstrated by Gildemyn et al. (2015), who reported on a galvanostatic microbial electrosynthesis system in batch mode that produced acetate at 0.024 g/L/h, and simultaneously extracted the acetate across an anion exchange membrane to concentrate the product in an integrated extraction compartment of equal volume to the catholyte. This method obviates the need for an external pH control system, and the 13.5 g/L titer achieved with this method is the highest reported for a direct MES. The energy efficiency to acetate, including the extraction, reached an impressive 21%.

Another possible solution is to supply the acetate to a second bioreactor that produces higher value products that may be produced at a higher titer and are more readily extracted, such as demonstrated by Hu et al. (2016) for the production of biodiesel precursors. Chemocatalytic upgrading has also been used to produce ethyl acetate by combining biphasic esterification with

an integrated electrolytic membrane extraction of acetate from fermentation of thin stillage biomass (Andersen et al., 2014). This process was also adopted to utilize acetate made from electricity and CO₂ to produce the ethyl acetate (Andersen et al., 2016).

Additional Considerations

Yeast extract has been required for the growth of acetogens in some studies (Kantzow et al., 2015; Hu et al., 2016), and at the concentrations and dilution rates used would be cost prohibitive (Lawford and Rousseau, 1997; Lau et al., 2012). A metagenomic analysis indicated that the microbial community used here possesses the full complement of genes required for the synthesis of all amino acids and vitamins needed for growth (Marshall et al., 2016), and yeast extract has never been used with this community.

The experiments reported here were done with a phosphate buffer, and to continuously supply that would also be cost prohibitive at the dilution rates in this study. Past batch-fed experiments were done with a bicarbonate buffer in place of the phosphate (LaBelle et al., 2014), which would be far more cost effective (est. 80% media cost reduction).

Both hydrogenotrophic and acetoclastic methanogens would divert electrons away from acetate synthesis. Inhibition of methanogenesis can be costly, but no inhibitor was needed for this experiment or for preparation of the inoculum. Operating a direct MES reactor through H₂ under galvanostatic control may offer a competitive advantage for the acetogens versus methanogens in that high H₂ partial pressure favors acetogenesis. Furthermore, allowing the pH to drop below 6 may also favor the acetogens since lower pH can also inhibit methanogenesis (Ni et al., 2010; Zhang et al., 2013; Spirito et al., 2014). Methanogens initially present in the community enriched for this biocathode were eliminated by repeated exposure to high H₂, low pH, and the addition of the inhibitor sodium bromoethanesulfonate (NaBES) (Marshall et al., 2012, 2013; LaBelle et al., 2014). The use of NaBES with this microbial community was ended in 2014, it was not used at any time in this study, and the inoculum used was transferred more than three times without NaBES before use in this study. The community used in this study has always been maintained in an open system (non-aseptic) in a laboratory with methanogenic cultures and sediments under investigation nearby.

The scalability and economics of MESs has been addressed in several studies and reviews (Foley et al., 2010; Desloover et al., 2012; Logan and Rabaey, 2012; Conrado et al., 2013; Brown et al., 2014; Harnisch et al., 2014; ElMekawy et al., 2016; Zhang and Angelidaki, 2016). Additionally, current legislation concerning whether the CO₂ is obtained from renewable or waste gasses can vary geographically (Daniell et al., 2016; Dürre, 2016). This can affect whether the product can qualify for credits and incentives, and thus be sold competitively. However, a life cycle analysis has

shown that ethanol produced from CO₂ recycled from a fossil fuel waste stream can still attain a net carbon emission reduction (Daniell et al., 2016; Handler et al., 2016). Further improvements in performance are still desired and product selection should go beyond acetate, but with productivity and efficiency for a direct single reactor MES approaching the best reported for an indirect MES with two reactors, successful scaling and improved performance of microbial electrosynthesis is now more feasible. Building and operating one reactor versus two may reduce capital and operating costs, and the performance of the reactor systems for acetogenesis compared in **Table 1** suggest such a consolidation warrants further consideration. What is needed is a systematic laboratory comparison of direct and indirect MES systems. Such data will help develop practical process systems and better inform life cycle assessments and technoeconomic analyses to contribute to proper implementation of MES.

CONCLUSION

This work contributes practical operating conditions for microbially producing acetic acid from electricity and carbon dioxide, with hydrogen as co-product, bringing the technology closer to real world implementation. Additionally new benchmarks in STY and efficiency are presented. Acetate was produced at a maximum STY of 0.78 g/L/h, and in replicate 0.74 ± 0.05 g/L/h (*n* = 3). The growth of this technology and its promise in complementation to other established and emerging technologies indicate the viability of microbial electrosynthesis to aid in carbon and energy management.

AUTHOR CONTRIBUTIONS

EL and HM designed and planned the research, EL conducted the experiments, and EL and HM analyzed the data and wrote the manuscript.

FUNDING

This work was funded by the Office of Naval Research grant #N00014-15-1-2219.

SUPPLEMENTARY MATERIAL

The Supplementary Material for this article can be found online at: <http://journal.frontiersin.org/article/10.3389/fmicb.2017.00756/full#supplementary-material>

REFERENCES

- Ammam, F., Tremblay, P. L., Lizak, D. M., and Zhang, T. (2016). Effect of tungstate on acetate and ethanol production by the electrosynthetic bacterium *Sporomusa ovata*. *Biotechnol. Biofuels* 9, 163. doi: 10.1186/s13068-016-0576-0

- Andersen, S. J., Berton, J. K. E. T., Naert, P., Gildemyn, S., Rabaey, K., and Stevens, C. V. (2016). Extraction and esterification of low-titer short-chain volatile fatty acids from anaerobic fermentation with ionic liquids. *ChemSusChem* 9, 2059–2063. doi: 10.1002/cssc.201600473

- Andersen, S. J., Hennebel, T., Gildemyn, S., Coma, M., Desloover, J., Berton, J., et al. (2014). Electrolytic membrane extraction enables production of fine chemicals from biorefinery sidestreams. *Environ. Sci. Technol.* 48, 7135–7142. doi: 10.1021/es500483w
- Bergel, A. (2016). How could chemical engineering help in deciphering electromicrobial mechanisms? *BIO Web Conf.* 6:02005. doi: 10.1051/bioconf/20160602005
- Blanchet, E., Duquenne, F., Raftari, Y., Etcheverry, L., Erable, B., and Bergel, A. (2015). Importance of the hydrogen route in up-scaling electrosynthesis for microbial CO₂ reduction. *Energy Environ. Sci.* 8, 3731–3744. doi: 10.1039/C5EE03088A
- Brown, R. K., Harnisch, F., Wirth, S., Wahlandt, H., Dockhorn, T., Dichtl, N., et al. (2014). Evaluating the effects of scaling up on the performance of bioelectrochemical systems using a technical scale microbial electrolysis cell. *Bioresour. Technol.* 163, 206–213. doi: 10.1016/j.biortech.2014.04.044
- Butler, C. S., and Lovley, D. R. (2016). How to sustainably feed a microbe: strategies for biological production of carbon-based commodities with renewable electricity. *Front. Microbiol.* 7:1879. doi: 10.3389/fmicb.2016.01879
- Conrado, R. J., Haynes, C. A., Haendler, B. E., and Toone, E. J. (2013). “Electrofuels: a new paradigm for renewable fuels,” in *Advanced Biofuels and Bioproducts*, ed. J. W. Lee (New York, NY: Springer Science & Business Media), 1037–1064. doi: 10.1007/978-1-4614-3348-4_38
- Daniell, J., Köpke, M., and Simpson, S. D. (2012). Commercial biomass syngas fermentation. *Energies* 5:5372. doi: 10.3390/en5125372
- Daniell, J., Nagaraju, S., Burton, F., Köpke, M., and Simpson, S. D. (2016). Low-carbon fuel and chemical production by anaerobic gas fermentation. *Adv. Biochem. Eng.* 156, 293–321.
- Demler, M., and Weuster-Botz, D. (2011). Reaction engineering analysis of hydrogenotrophic production of acetic acid by *Acetobacterium woodii*. *Biotechnol. Bioeng.* 108, 470–474. doi: 10.1002/bit.22935
- Desloover, J., Arends, J. B. A., Hennebel, T., and Rabaey, K. (2012). Operational and technical considerations for microbial electrosynthesis. *Biochim. Soc. Trans.* 40, 1233–1238. doi: 10.1042/BST20120111
- Deutzmann, J. S., Sahin, M., and Spormann, A. M. (2015). Extracellular enzymes facilitate electron uptake in biocorrosion and bioelectrosynthesis. *mBio* 6:e00496-15. doi: 10.1128/mBio.00496-15
- Deutzmann, J. S., and Spormann, A. M. (2016). Enhanced microbial electrosynthesis by using defined co-cultures. *ISME J.* 11, 704–714. doi: 10.1038/ismej.2016.149
- Dürre, P. (2016). Gas fermentation - a biotechnological solution for today's challenges. *Microb. Biotechnol.* 10, 14–16. doi: 10.1111/1751-7915.12431
- ElMekawy, A., Hegab, H. M., Mohanakrishna, G., Elbaz, A. F., Bulut, M., and Pant, D. (2016). Technological advances in CO₂ conversion electro-biorefinery: a step toward commercialization. *Bioresour. Technol.* 215, 357–370. doi: 10.1016/j.biortech.2016.03.023
- Fast, A. G., and Papoutsakis, E. T. (2012). Stoichiometric and energetic analyses of non-photosynthetic CO₂-fixation pathways to support synthetic biology strategies for production of fuels and chemicals. *Curr. Opin. Chem. Eng.* 1, 1–16. doi: 10.1016/j.coche.2012.07.005
- Flexer, V., Chen, J., Donose, B. C., Sherrell, P., Wallace, G. G., and Keller, J. (2013). The nanostructure of three-dimensional scaffolds enhances the current density of microbial bioelectrochemical systems. *Energy Environ. Sci.* 6, 1291–1298. doi: 10.1039/c3ee00052d
- Foley, J. M., Rozendal, R. A., Hertle, C. K., Lant, P. A., and Rabaey, K. (2010). Life cycle assessment of high-rate anaerobic treatment, microbial fuel cells, and microbial electrolysis cells. *Environ. Sci. Technol.* 44, 3629–3637. doi: 10.1021/es100125h
- Giddings, C. G. S., Nevin, K. P., Woodward, T., Lovley, D. R., and Butler, C. S. (2015). Simplifying microbial electrosynthesis reactor design. *Front. Microbiol.* 6:468. doi: 10.3389/fmicb.2015.00468
- Gildemyn, S., Verbeeck, K., Slabbinck, R., Andersen, S. J., Prévostea, A., and Rabaey, K. (2015). Integrated production, extraction, and concentration of acetic acid from CO₂ through microbial electrosynthesis. *Environ. Sci. Technol. Lett.* 2, 325–328. doi: 10.1021/acs.estlett.5b00212
- Graves, T., Narendranath, N. V., Dawson, K., and Power, R. (2006). Effect of pH and lactic or acetic acid on ethanol productivity by *Saccharomyces cerevisiae* in corn mash. *J. Ind. Microbiol. Biotechnol.* 33, 469–474. doi: 10.1007/s10295-006-0091-6
- Handler, R. M., Shonnard, D. R., Griffing, E. M., Lai, A., and Palou-Rivera, I. (2016). Life cycle assessments of ethanol production via gas fermentation: anticipated greenhouse gas emissions from cellulosic and waste gas feedstocks. *Ind. Eng. Chem. Res.* 55, 3253–3261. doi: 10.1021/acs.iecr.5b03215
- Harnisch, F., Rosa, L. F. M., Kracke, F., Virdis, B., and Krömer, J. O. (2014). Electrifying white biotechnology: engineering and economic potential of electricity-driven bio-production. *ChemSusChem* 8, 758–766. doi: 10.1002/cssc.201402736
- Hu, P., Chakraborty, S., Kumara, A., Woolston, B., Liu, H., Emerson, D., et al. (2016). Integrated bioprocess for conversion of gaseous substrates to liquids. *Proc. Natl. Acad. Sci. U.S.A.* 113, 3773–3778. doi: 10.1073/pnas.1516871113
- Hu, P., Rismani-Yazdi, H., and Stephanopoulos, G. (2013). Anaerobic CO₂ fixation by the acetogenic bacterium *Moorella thermoacetica*. *AICHE J.* 59, 3176–3183. doi: 10.1002/aic.14127
- IEA (2016). *Decoupling of Global Emissions and Economic growth Confirmed*. Paris: International Energy Agency.
- Jourdin, L., Freguia, S., Donose, B. C., Chen, J., Wallace, G. G., Keller, J., et al. (2014). A novel carbon nanotube modified scaffold as an efficient biocathode material for improved microbial electrosynthesis. *J. Mater. Chem. A* 2, 13093–13102. doi: 10.1039/C4TA03101F
- Jourdin, L., Griege, T., Monetti, J., Flexer, V., Freguia, S., Lu, Y., et al. (2015). High acetic acid production rate obtained by microbial electrosynthesis from carbon dioxide. *Environ. Sci. Technol.* 49, 13566–13574. doi: 10.1021/acs.est.5b03821
- Kantzow, C., Mayer, A., and Weuster-Botz, D. (2015). Continuous gas fermentation by *Acetobacterium woodii* in a submerged membrane reactor with full cell retention. *J. Biotechnol.* 212, 11–15. doi: 10.1016/j.jbiotec.2015.07.020
- Körner, A., Tam, C., Bennett, S., and Gagné, J. F. (2015). *Technology Roadmap-Hydrogen and Fuel Cells*. Paris: International Energy Agency (IEA).
- Krieg, T., Sydow, A., Schröder, U., Schrader, J., and Holtmann, D. (2014). Reactor concepts for bioelectrochemical syntheses and energy conversion. *Trends Biotechnol.* 32, 1–11. doi: 10.1016/j.tibtech.2014.10.004
- LaBelle, E. V., Marshall, C. W., Gilbert, J. A., and May, H. D. (2014). Influence of acidic pH on hydrogen and acetate production by an electrosynthetic microbiome. *PLoS ONE* 9:e109935. doi: 10.1371/journal.pone.0109935
- Lau, M. W., Bals, B. D., Chundawat, S. P. S., Jin, M., Gunawan, C., Balan, V., et al. (2012). An integrated paradigm for cellulosic biorefineries: utilization of lignocellulosic biomass as self-sufficient feedstocks for fuel, food precursors and saccharolytic enzyme production. *Energy Environ. Sci.* 5, 7100–7110. doi: 10.1039/c2ee03596k
- Lawford, H. G., and Rousseau, J. D. (1997). Corn steep liquor as a cost-effective nutrition adjunct in high-performance *Zymomonas* ethanol fermentations. *Appl. Biochem. Biotechnol.* 6, 287–304. doi: 10.1007/BF02920431
- Logan, B. E., and Rabaey, K. (2012). Conversion of wastes into bioelectricity and chemicals by using microbial electrochemical technologies. *Science* 337, 686–690. doi: 10.1126/science.1217412
- Lovley, D. R., and Nevin, K. P. (2013). Electrobiofuels: powering microbial production of fuels and commodity chemicals from carbon dioxide with electricity. *Curr. Opin. Biotechnol.* 24, 1–6. doi: 10.1016/j.copbio.2013.02.012
- Marshall, C., Ross, D., Handley, K., Weisenhorn, P., Edirisinghe, J. N., Henry, C. S., et al. (2016). Metabolic reconstruction and modeling microbial electrosynthesis. *bioRxiv* 059410. doi: 10.1101/059410
- Marshall, C. W., Ross, D. E., Fichot, E. B., Norman, R. S., and May, H. D. (2012). Electrosynthesis of commodity chemicals by an autotrophic microbial community. *Appl. Environ. Microbiol.* 78, 8412–8420. doi: 10.1128/AEM.02401-12
- Marshall, C. W., Ross, D. E., Fichot, E. B., Norman, R. S., and May, H. D. (2013). Long-term operation of microbial electrosynthesis systems improves acetate production by autotrophic microbiomes. *Environ. Sci. Technol.* 47, 6023–6029. doi: 10.1021/es400341b
- May, H. D., Evans, P. J., and LaBelle, E. V. (2016). The bioelectrosynthesis of acetate. *Curr. Opin. Biotechnol.* 42, 225–233. doi: 10.1016/j.copbio.2016.09.004

- Nayak, J., Pal, M., and Pal, P. (2015). Modeling and simulation of direct production of acetic acid from cheese whey in a multi-stage membrane-integrated bioreactor. *Biochem. Eng. J.* 93, 179–195. doi: 10.1016/j.bej.2014.10.002
- Nayak, J., and Pal, P. (2015). “A green process for acetic acid production,” in *Proceedings of the 7th International Conference on Chemical, Ecology and Environmental Sciences*, Pattaya.
- Nevin, K. P., Woodard, T. L., Franks, A. E., Summers, Z. M., and Lovley, D. R. (2010). Microbial electrosynthesis: feeding microbes electricity to convert carbon dioxide and water to multicarbon extracellular organic compounds. *mBio* 1:e00103-10. doi: 10.1128/mBio.00103-10
- Ni, B.-J., Liu, H., Nie, Y.-Q., Zeng, R. J., Du, G.-C., Chen, J., et al. (2010). Coupling glucose fermentation and homoacetogenesis for elevated acetate production: experimental and mathematical approaches. *Biotechnol. Bioeng.* 108, 345–353. doi: 10.1002/bit.22908
- Pal, P., and Nayak, J. (2016). Acetic acid production and purification: critical review towards process intensification. *Sep. Purif. Rev.* 46, 44–61. doi: 10.1080/15422119.2016.1185017
- Papoutsakis, E. T. (2015). Reassessing the progress in the production of advanced biofuels in the current competitive environment and beyond: what are the successes and where progress eludes us and why. *Ind. Eng. Chem. Res.* 54, 10170–10182. doi: 10.1021/acs.iecr.5b01695
- Patil, S. A., Arends, J., Vanwonterghem, I., van Meerbergen, J., Guo, K., Tyson, G., et al. (2015). Selective enrichment establishes a stable performing community for microbial electrosynthesis of acetate from CO₂. *Environ. Sci. Technol.* 49, 8833–8843. doi: 10.1021/es506149d
- Raizada, T. (2016). *US Acetic Acid Demand Soft in Americas*. Available at: <http://www.icis.com/resources/news/2016/09/02/10031371/us-acetic-acid-demand-soft-in-the-americas/> [accessed November 10, 2016].
- Richter, H., Martin, M., and Angenent, L. T. (2013). A two-stage continuous fermentation system for conversion of syngas into ethanol. *Energies* 6, 3987–4000. doi: 10.3390/en6083987
- Schröder, U., Harnisch, F., and Angenent, L. T. (2015). Microbial electrochemistry and technology: terminology and classification. *Energy Environ. Sci.* 8, 513–519. doi: 10.1039/C4EE03359K
- Spirito, C. M., Richter, H., Rabaey, K., Stams, A. J., and Angenent, L. T. (2014). Chain elongation in anaerobic reactor microbiomes to recover resources from waste. *Curr. Opin. Biotechnol.* 27, 115–122. doi: 10.1016/j.copbio.2014.01.003
- Tremblay, P. L., Angenent, L. T., and Zhang, T. (2016). Extracellular electron uptake: among autotrophs and mediated by surfaces. *Trends Biotechnol.* 35, 360–371. doi: 10.1016/j.tibtech.2016.10.004
- Wakatsuki, K. (2015). *Acetyls Chain - World Market Overview. Chemicals Committee Meeting at APIC 2015*. Available at: http://www.orbicem.com/userfiles/APIC%202015/APIC2015_Keiji_Wakatsuki.pdf [accessed November 10, 2016].
- Wiser, R., and Bolinger, M. (2016). *2015 Wind Technologies Market Report*. Report No: LBNL-1005951. Germantown, MD: United States Department of Energy.
- Xu, J., Guzman, J. J. L., Andersen, S. J., Rabaey, K., and Angenent, L. T. (2015). In-line and selective phase separation of medium-chain carboxylic acids using membrane electrolysis. *Chem. Commun.* 51, 6847–6850. doi: 10.1039/C5CC01897H
- Yates, M. D., Siegert, M., and Logan, B. E. (2014). Hydrogen evolution catalyzed by viable and non-viable cells on biocathodes. *Int. J. Hydrogen Energy* 39, 16841–16851. doi: 10.1016/j.ijhydene.2014.08.015
- Zhang, F., Ding, J., Zhang, Y., Chen, M., Ding, Z. W., van Loosdrecht, M. C. M., et al. (2013). Fatty acids production from hydrogen and carbon dioxide by mixed culture in the membrane biofilm reactor. *Water Res.* 47, 6122–6129. doi: 10.1016/j.watres.2013.07.033
- Zhang, Y., and Angelidaki, I. (2016). Microbial electrochemical systems and technologies: it is time to report the capital costs. *Environ. Sci. Technol.* 50, 5432–5433. doi: 10.1021/acs.est.6b01601

Conflict of Interest Statement: Patents pending in relation to this work: 1. Harold D. May, Marshall CW, and Edward V. LaBelle. Microbial Electrosynthetic Cells. PCT/US2013/060131. International filing date: 17 September 2013. 2. Harold D. May and Edward V. LaBelle. Provisional Application for United States Letters Patent for Bioelectrosynthesis of Organic Compounds.

Copyright © 2017 LaBelle and May. This is an open-access article distributed under the terms of the Creative Commons Attribution License (CC BY). The use, distribution or reproduction in other forums is permitted, provided the original author(s) or licensor are credited and that the original publication in this journal is cited, in accordance with accepted academic practice. No use, distribution or reproduction is permitted which does not comply with these terms.



An Overview of Electron Acceptors in Microbial Fuel Cells

Deniz Ucar^{1,2*}, **Yifeng Zhang**^{3*} and **Irini Angelidaki**³

¹ Department of Environmental Engineering, Harran University, Sanliurfa, Turkey, ² GAP Renewable Energy and Energy Efficiency Center, Harran University, Sanliurfa, Turkey, ³ Department of Environmental Engineering, Technical University of Denmark, Lyngby, Denmark

OPEN ACCESS

Edited by:

Yong Xiao,
Institute of Urban Environment (CAS),
China

Reviewed by:

John Stoltz,
Duquesne University, USA
Ashley Edwin Franks,
La Trobe University, Australia

*Correspondence:

Deniz Ucar
deniz@denizucar.com
Yifeng Zhang
yifz@env.dtu.dk

Specialty section:

This article was submitted to
Microbiotechnology, Ecotoxicology
and Bioremediation,
a section of the journal
Frontiers in Microbiology

Received: 14 December 2016

Accepted: 29 March 2017

Published: 19 April 2017

Citation:

Ucar D, Zhang Y and Angelidaki I (2017) An Overview of Electron Acceptors in Microbial Fuel Cells. *Front. Microbiol.* 8:643.
doi: 10.3389/fmicb.2017.00643

Microbial fuel cells (MFC) have recently received increasing attention due to their promising potential in sustainable wastewater treatment and contaminant removal. In general, contaminants can be removed either as an electron donor via microbial catalyzed oxidation at the anode or removed at the cathode as electron acceptors through reduction. Some contaminants can also function as electron mediators at the anode or cathode. While previous studies have done a thorough assessment of electron donors, cathodic electron acceptors and mediators have not been as well described. Oxygen is widely used as an electron acceptor due to its high oxidation potential and ready availability. Recent studies, however, have begun to assess the use of different electron acceptors because of the (1) diversity of redox potential, (2) needs of alternative and more efficient cathode reaction, and (3) expanding of MFC based technologies in different areas. The aim of this review was to evaluate the performance and applicability of various electron acceptors and mediators used in MFCs. This review also evaluated the corresponding performance, advantages and disadvantages, and future potential applications of select electron acceptors (e.g., nitrate, iron, copper, perchlorate) and mediators.

Keywords: microbial fuel cell, cathodic electron acceptors, cathodic reaction, electricity production, renewable energy, wastewater treatment

INTRODUCTION

A microbial fuel cell (MFC) is a bioelectrochemical device that can generate electricity by the use of electrons obtained from the anaerobic oxidation of substrates. Generally, the MFC consists of two parts, an anode and a cathode, which are separated by a proton exchange membrane (PEM). Anaerobic oxidation of organic substances such as acetate, glucose, lactate, ethanol (summarized by Pant et al., 2010) occurs in the anode compartment, during which process protons, electrons and carbon dioxide are released. In this case, the protons and electrons pass through the anode chamber to the cathode chamber via the PEM and an external circuit respectively. This electron transfer from the anode to the cathode produces an electricity current (Logan et al., 2006; Venkata Mohan et al., 2008; Kim and Lee, 2010; Mao et al., 2010; Samrot et al., 2010; Ishii et al., 2013). MFCs can be used for wastewater treatment since organic materials can be easily oxidized as fuel in the anode compartment. In recent years, MFC-based systems have also been used in a number of new applications such as hydrogen production, seawater desalination, biosensors and microbial electro synthesis (Cheng and Logan, 2007; Cao et al., 2009; Rabaey and Rozendal, 2010; Zhang and Angelidaki, 2011).

Despite promising initial results, MFCs have not been able to go further than the pilot scale due to a number of limitations (Liu and Logan, 2004; Donovan et al., 2011). The power output of the MFC depends on several factors such as type of substrate, exoelectrogenic microorganisms, circuit resistance, electrode material, reactor configuration and electron acceptors (Pant et al., 2010; Kim et al., 2011). Different electron acceptors exhibit physically and chemically different properties (e.g., oxidation potential) and therefore affect the efficiency of electricity production. Therefore, investigation of the applicability of new electron acceptors in MFCs has gained importance in recent years as they have a significant impact on electricity generation.

Oxygen is the most common electron acceptor used in the cathode compartment due to its high oxidation potential and the fact that it yields a clean product (water) after reduction. However, most studies show that the oxygen supply to the cathode compartment is energy consuming (Strik et al., 2010). Although the oxygen in the air can be used directly by using an air cathode, contact difficulties in the cathode-air surface and the need for expensive catalysts are the disadvantages of oxygen utilization (Heijne et al., 2007).

The use of alternative electron acceptors may not only increase the power generation and reduce the operating costs, but also expands the application scope of MFCs. It has been recently found that some recalcitrant compounds can be treated in the cathode as an electron acceptor (Gu et al., 2007). These findings suggest that MFCs can be used to control environmental pollutants. For example, nitrate is a well-known pollutant in wastewater streams. Since the redox potentials of nitrate and oxygen are very close to each other, nitrate can be used as

an electron acceptor in the cathode compartment (Jia et al., 2008). In this case, the nitrate is reduced to nitrogen gas by the denitrification process in the cathode compartment. Apart from nitrate, some heavy metals such as copper (Tao et al., 2011b), iron and mercury (Wang et al., 2011) can also be used as electron acceptors and thus reduced to less toxic forms. Thus, electricity generation and wastewater treatment take place simultaneously. Recently, Rahimnejad et al. reviewed the effect of anode, cathode, and membrane portions on MFC performance. In addition, the electrode materials used in the anode and cathode compartments are summarized together with some cathodic reactions such as denitrification and iron reduction (Rahimnejad et al., 2015).

Electron acceptors receive electrons from the cathode, and therefore they make a significant contribution to the performance of the MFC. Although there are many studies on different electron acceptors in the literature, no comprehensive review of this field is available. For this reason, the various electron acceptors used in MFCs have been systematically compiled in this paper and evaluated in terms of performance, advantages and application areas in wastewater treatment. Finally, this paper suggests prospects for future development.

STRUCTURE OF MFC AND OXYGEN AS TERMINAL ELECTRON ACCEPTOR

A typical MFC consists of two chambers, an anode and a cathode, separated by a PEM membrane (Figure 1). Electrons are transported from the anode compartment to the cathode compartment by external circuit, where they combine with

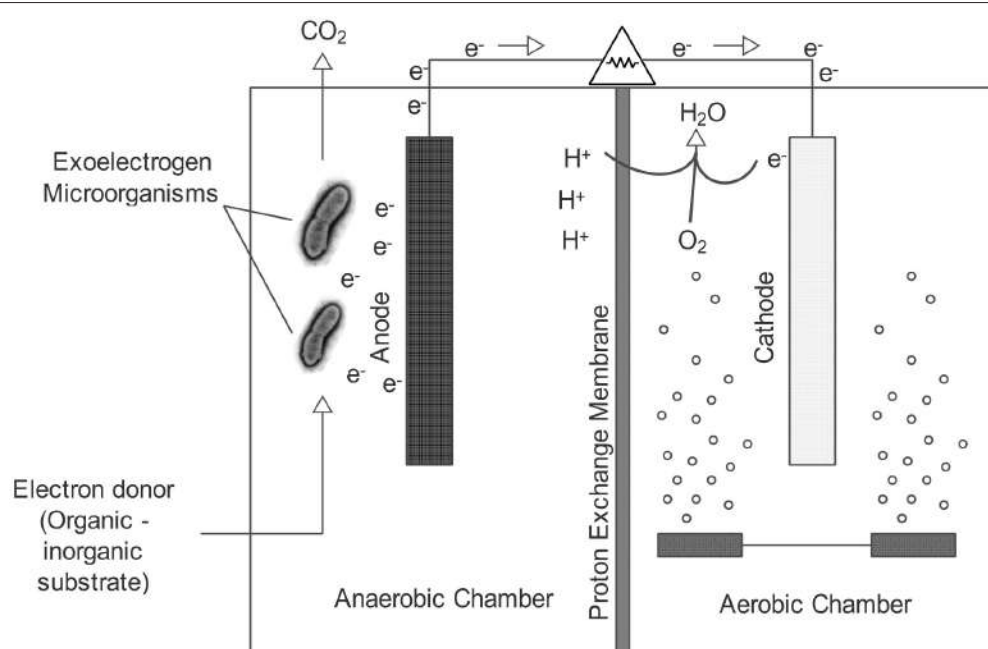


FIGURE 1 | Schematic representation of a two-chambered MFC.

protons and oxygen to form water according to the following reaction



As can be seen in Equation (1), oxygen is continuously consumed to maintain the potential for electricity generation. Oxygen can be provided in the cathode compartment by bubbling the water or by using an air cathode. Oxygen has a higher redox potential than many other electron acceptors, and therefore it is widely regarded as a good cathodic electron receiver (Oh et al., 2004). However, the poor contact of oxygen with the electrode and the slow rate of reduction of the oxygen on the normal carbon electrode are disadvantages that limit the use of oxygen in MFCs (Rhoads et al., 2005). Although the cathodic reaction can be improved by the use of catalytic-coated electrodes, catalysts are often expensive and rare metals (Zhou et al., 2011).

ALTERNATIVE ELECTRON ACCEPTORS

Ferricyanide

Besides oxygen, ferricyanide is another common electron donor used in MFC studies since its concentration is not limited to solubility like in the case of oxygen (Rhoads et al., 2005). Although the standard redox potential of ferricyanide (given in Equation 2) is not as high as that of oxygen, it has much lower overpotential, which results in not only a faster reaction rate but also much higher power output (Rabaey et al., 2003; Schröder et al., 2003; Aelterman et al., 2006). It was reported that ferricyanide with the carbon electrode produced 50–80% higher power than oxygen with Pt-carbon cathode due to increased mass transfer efficiencies and larger cathode potential (Oh et al., 2004).

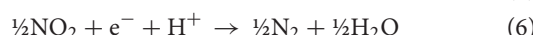
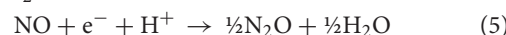


Although ferricyanide is an excellent electron acceptor in terms of power generation, it has been understood that potassium ferricyanide is not practically sustainable. It is toxic, and chemical regeneration/recycling is difficult. For this reason, the use of ferricyanide is limited to basic laboratory studies (Logan et al., 2006). However, ferricyanide is still an important cathodic electron acceptor to prove some important concepts in the laboratory due to its stability and high system performance. For example, Aelterman et al. (2006) conducted performance experiments with MFCs operated in series and in parallel to each other. They used hexacyanoferrate cathode, and six independent continuous MFC units produced the maximum hourly average power output of 258 W/m³ in the stacked configuration (Aelterman et al., 2006). Ferricyanide has also been used to compare the performance of electrode materials due to its catalytic activity. In a recent study, three different MFC processes were used to remove nitrogen and carbon from wastewater. The tested MFC types were (1) continuous operation, (2) continuous operation with ferricyanide and (3) continuous operation with oxygen, and the highest current, carbon and nitrogen removal was observed in continuously operating MFC with ferricyanide. The currents obtained are 0.833 and 0.589 V for ferricyanide and

oxygen respectively. With ferricyanide, the carbon and nitrogen removals are 36 and 9% higher than that removed with oxygen respectively (Zain et al., 2015).

Nitrogen Species

Nitrate is one of the common types of nitrogen that is widely found in waters, and causes a variety of serious environmental and health problems that threaten human and animal health (Demirel et al., 2014; Sahinkaya et al., 2015). In this respect, nitrate in drinking water is limited to 44.43 mg/L in the US and 50 mg/L in Europe (Shen et al., 2009). The application of biocathots has made nitrate usable as an electron acceptor in MFCs for denitrification and electricity generation. The feasibility of nitrate as a cathodic electron acceptor in MFCs was first demonstrated by Clauwaert et al. (2007). In this study, the denitrification by microorganisms took place in a tubular reactor without an energy input (Clauwaert et al., 2007). In the same period Lefebvre et al. (2008) investigated the same cathodic process in a two-chambered MFC. In their study, 95.7% of nitrate was removed at the cathode using acetate as an anodic substrate, and 73 ± 4% of the total nitrogen was converted to N₂ gas through electrochemical denitrification according to Equations (3–6). However, only 0.095 V was obtained as the maximum cell potential at external resistance of 1000 Ω, which was much lower than that of oxygen reported previously. This may be due to the fact that nitrate has a relatively low redox potential (0.74 V).



In order to further investigate the concept and broaden this application, Virdis et al. (2008) demonstrated a novel process which is an integration of MFC and aerobic nitrification technology for simultaneous carbon and nitrogen removal. In this process, the wastewater containing ammonium and organic matter was initially fed to the anode compartment for the oxidation of the organic material and release of the electrons. The effluent from the anode was then fed to an external aerobic nitrification vessel for oxidation of ammonium to nitrate. This nitrate-enriched stream was finally fed to the cathode compartment of the MFC for denitrification where electrons degraded nitrate. The electrons produced at the beginning were transported to nitrate, which was used as an electron acceptor at the end of the process. In this system, which is called loop configuration, a volumetric power density of 34.6 ± 1.1 W/m³ and a nitrogen removal rate of up to kg COD/(m³ NCC.d) were obtained (NCC: Net cathodic compartment; Virdis et al., 2008). However, this process has its own drawback, which is the low nitrogen removal in the effluent due to the crossover of ammonia from the anode to the cathode through the cation exchange membrane.

To further address this shortcoming, Virdis et al. (2010) integrated the nitrification stage into the cathode chamber where simultaneous nitrification and denitrification (SND) were

accomplished. In such a system, denitrification can still occur at a higher dissolved oxygen level than that of a conventional SND process. The main explanation for this finding was the formation of a micro-environment on the porous surface of graphite granule where denitrifying bacteria could grow (Virdis et al., 2010). Studies on simultaneous nitrification-denitrification in MFCs are becoming more successful and various systems are being developed. A combined use of the membrane aerated biofilm process and MFC process was proposed by Yu et al. (2011) for simultaneous nitrification, denitrification and organic carbon removal in a single two-chambered MFC system. In this system, 97 and 52% removal efficiencies for total carbon and nitrogen respectively were obtained. Xie et al. (2011), developed an oxic/anoxic biocathode system for simultaneous carbon and nitrogen removal. The idea behind the rearrangement is to remove ammonium and nitrate in the oxic and anoxic biocathode respectively, while COD is being oxidized in the anode compartment. With this system, the maximum power densities for oxic and anoxic biocathodes were 14 and 7.2 W/m³ respectively. On the other hand, the maximum COD, NH₄⁺ and TN removal rates were 98.8, 94.7, and 97.3% respectively.

Beside the denitrification of nitrate at the cathode, the electrochemical reduction of nitrate at an abiotic cathode has also been explored. Fang et al. (2011) reported that nitrate can be reduced from 49 to 25 mg N/L in the cathode compartment and a power density of up to 7.2 mW/m² can be obtained in this process at 470 Ω resistance (Fang et al., 2011). The reduction products of nitrate were mainly ammonia (51.8%) and trace amounts of nitrite (0.6%).

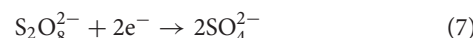
While nitrate reduction at the cathode has been extensively studied, nitrite as an important intermediate product from nitrate reduction has received little attention so far. Virdis et al. (2008) suggested that nitrite as an efficient terminal electron acceptor at the cathode of a MFC could reduce the carbon to nitrogen ratio (Virdis et al., 2008). Puig et al. (2011) demonstrated that nitrate and nitrite can be used interchangeably as an electron acceptor by exoelectrogenic bacteria for nitrogen reduction. However, nitrite is oxidized in the presence of oxygen by biological or electrochemical processes at the cathode, which affects the electricity production (Puig et al., 2011).

Up-to-date studies on MFC for nitrate removal can include field applications. Organic pollutants in river X in Romania were used for electricity generation and the nitrate in the same river was used as an electron receiver. A power density of 88 mW/m² was achieved at a current density of 310 mA/m² in a single compartment MFC. Organic pollution and nitrate removal efficiencies were 97 and 96%, respectively (Cucu et al., 2016).

Nitrous oxide is an important intermediate between the steps of the denitrification process shown in Equations (3–6). Reducing N₂O emissions is an urgent issue as it is an important greenhouse gas. According to the thermodynamic principle, N₂O has the potential to be a more suitable electron acceptor compared to the other oxidized nitrogen intermediates in the denitrification pathway. In a study conducted by Desloover et al. (2011), N₂O removal rates ranging from 0.76 to 1.83 kg N/m³ NCC were obtained at the cathode chamber.

Persulfate

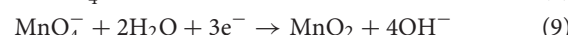
Persulfate is used in many applications such as clarifying swimming pools, hair bleaching, micro-etching of copper printed circuit boards, total organic carbon analysis and destrucing soil and groundwater contaminants. It is considered to be hazardous waste because it is an oxidizing agent (Li J. et al., 2009). Applicability of persulfate in MFCs is possible with its standard oxidation reduction potential of 2.12 V, which is higher than many electron acceptors (e.g., permanganate) used in MFCs. When persulfate is used as the electron acceptor, 1 mole S₂O₈²⁻ receives 2 electrons and forms SO₄²⁻ (Equation 7).



Because of the above properties, persulfate was used as electron acceptor. It was found that power density was doubled when K₃Fe(CN)₆ was replaced with persulfate in MFC (166.7 vs. 83.9 mW/m²). One drawback of MFC with K₂S₂O₈²⁺ could be the lower cell performance than MFC with K₃Fe(CN)₆ at medium to high current densities. This case was explained by the faster electron reduction kinetics of ferricyanide solution on the surface of the carbon electrode (Li J. et al., 2009).

Permanganate

Under both acidic and alkaline conditions, permanganate is reduced to manganese dioxide by receiving three electrons as shown in the Equations (8, 9). This property of permanganate makes it a potential electron acceptor. In acidic conditions, permanganate is expected to show higher power output since its oxidation potential is higher than it is in alkaline conditions. Therefore, studies in different pH values were done to investigate the performance of permanganate in MFCs (You et al., 2006).



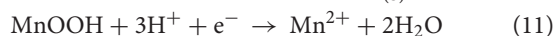
In a previous study, a power density of 115.60 mW/m² at a current density of 0.017 mA/cm² was observed by using permanganate as an electron acceptor, which was 4.5 and 11.3 fold higher than that produced from hexachnoferrate (25.62 mW/m²) and oxygen (10.2 mW/m²) respectively. Moreover, in the same study, a bushing MFC using permanganate as the electron acceptor achieved the maximum power density of 3986.72 mW/m² at 0.59 mA/cm². Therefore, it is worth pointing out that permanganate can be an efficient cathodic electron acceptor in MFCs (You et al., 2006).

However, there are also some drawbacks existing in this application. For example, like other soluble electron acceptors, depletion of permanganate during electricity generation requires continuous liquid replacements. Moreover, since the cathode potential is mainly dependent on the solution pH, pH control is required for stable power output, which may only be applied to small-scale power supplies as suggested by the authors. On the other hand, the advantage of this system is that it does not require catalysis (You et al., 2006). In a more recent study, the best permanganate concentration was studied in terms of

electricity production. The maximum power density with 400 mM of potassium permanganate and the current density at this power density were found to be 93.13 mW/m² and 0.03 mA/cm² respectively (Eliato et al., 2016).

Manganese Dioxide

Studies have reported that manganese dioxide is a good cathode material and catalysis for battery and alkaline fuel cells (Li et al., 2010). MnO₂/Mn²⁺ redox couple can be used to transfer electrons from the cathode to an electron acceptor. Rather than direct utilization of oxygen, the use of electron mediators between cathode and oxygen is more efficient because of the difficulties in the direct utilization of oxygen (i.e., low solubility). The possibility of biomineralized manganese oxides was investigated by Rhoads et al. (2005). The reaction begins with the accumulation of manganese dioxide on the cathode surface and subsequent reduction with electrons from the anode. The reaction results in the release of manganese ions which are subsequently reoxidized to manganese dioxide by manganese-oxidizing bacteria (*Leptothrix discophora* SP-6), and the cycle continues (Equations 10–12). Maximum power density of 126.7 ± 31.5 mW/m² was obtained (with 50 Ω resistor) from above redox cycle (Rhoads et al., 2005).

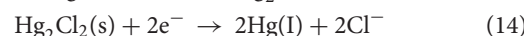


Manganese dioxide can be used not only in the electron mediator mechanism but also as an alternative cathode catalyst to platinum due to its low cost (Liew et al., 2015). Using manganese dioxide as an alternative catalyst, the maximum volumetric anode density of 3,773 ± 347 mW/m³ was obtained with a tube MFC. It could be, therefore, noted that using MnO₂ instead of Pt could serve as a suitable option for real applications due to its low cost (Zhang L. et al., 2009).

Mercury (Hg)

Since the redox potential of mercury, which is about –320 mV (Hg²⁺), is higher than that of NADH/NAD⁺, it can be accepted as an alternative electron acceptor (Wang et al., 2011). By using mercury in MFC, its removal from the aquatic environment can be achieved simultaneously with electricity

production. The possible removal mechanism is to precipitate Hg²⁺ in the presence of Cl[–] as shown in Equation (13), and subsequent reduction by the electrons at the cathode (Equation 14). Maximum power density of 433.1 mW/m² was obtained from the above process, while the end products were elemental Hg in the cathode surface and Hg₂Cl₂ as deposits on the bottom of the cathode chamber (Wang et al., 2011).



Iron (Fe)

Iron can be used as an electron mediator to enhance the performance in the cathode compartment. The most common redox couple used in MFCs is Fe⁺³/Fe²⁺. Ferric iron can be reduced to ferrous iron in the cathode chamber according to Equation (15).



This reversible electron transfer reaction provides several advantages such as fast reaction, high standard potentials, biological degradability (Heijne et al., 2006) and release of some valuable compounds such as Phosphate (Fischer et al., 2011). In a study where this redox was coupled together with a bipolar membrane and graphite electrode combination, the maximum power density of 0.86 W/m² at a current density of 4.5 A/m² was obtained (coulombic efficiency and energy recovery were 80–95 and 18–29% respectively; Heijne et al., 2006). In order to complete the Fe³⁺/Fe²⁺ redox cycle, an oxidative mechanism is needed. To achieve this, Heijne et al., used an acidophilic chemolithoautotrophic microorganism—*Acidithiobacillus ferrooxidans* to oxidize ferrous iron and investigated the performance of the MFC with continuous ferrous iron oxidation (Heijne et al., 2007). Oxidation of ferrous iron to ferric iron resulted in a 38% higher power output (1.2 W/m² and a current of 4.4 A/m²) than that which was obtained in their previous study.

Besides being an electron mediator, iron can also be used as an electron acceptor. In another study, iron in the form of FePO₄ was used (Figure 2). FePO₄ is a compound found in sewage sludge, which not only has a potential as an electron acceptor

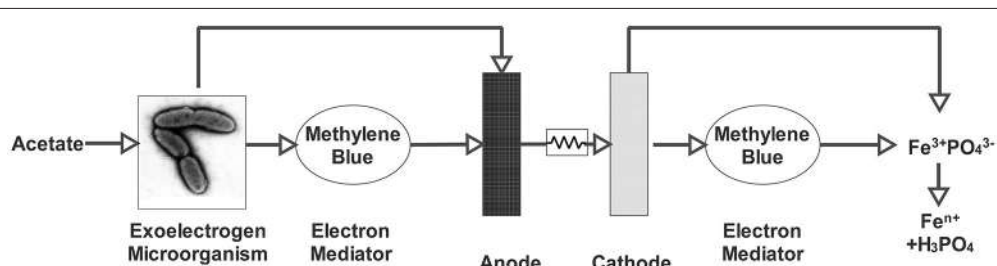


FIGURE 2 | MFC for the mobilization of orthophosphate from FePO₄ (Fischer et al., 2011).

due to its Fe^{3+} content, but also has a great importance due to its orthophosphate content (Equation 16; Fischer et al., 2011).



Phosphorus is an essential element for both agricultural and industrial production. This important element, however, is assumed to be depleted within 50–100 years (Cordell et al., 2009). Since it is also one of the primary causes of eutrophication, it is essential to consider the recovery of phosphate rather than its disposal (Usharani and Lakshmanaperumalsamy, 2010).

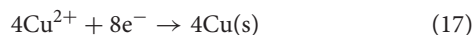
The MFC could reduce FePO_4 by delivering necessary electrons and protons. When iron cations are reduced by the electrons, iron and phosphate are separated and mobilized orthophosphate (PO_4^{3-}) is released into the solution. Released orthophosphate can be further precipitated as struvite (NH_4MgPO_4) by adding stoichiometric amounts of Mg^{2+} and NH_4^+ . By this method, 82% orthophosphate recovery was achieved with a varied current density of 0.1 and 0.7 mA (Fischer et al., 2011).

Compared to other electron acceptors and mediators, ferric iron provided relatively high power densities (Table 1). However, MFC with ferric iron requires a bipolar membrane instead of a cation exchange membrane (CEM). CEMs are not suitable for pH adjustment in the cathode chamber since they carry other cations together with protons. Therefore, either a bipolar membrane or acid addition is required when ferric iron is used (Heijne et al., 2006).

The main advantage of this process is that the phosphate is obtained in pure form. Thus, phosphate can be separated from iron and other toxic materials such as As, Pb, Cr. However, low pH is required to keep ferric iron soluble since ferric iron is tent to be precipitated as ferric iron hydroxides at pH values higher than 2.5. These precipitates are reported to be harmful to membrane use. Additionally, in order to shuttle electrons and protons to the Fe^{3+} , a cathodic mediator such as methylene blue needs to be supplied, which may hinder its wide application (Fischer et al., 2011). While iron was used as an electron acceptor, up-to-date studies show that it can also be used to prepare efficient catalysts (Nguyen et al., 2016; Santoro et al., 2016).

Copper

Copper is one of the widespread heavy metals in the soil and aquatic environment, which are mainly emitted from mining and metallurgical industries. Trace amounts of copper is an essential micronutrient to all plants and animals, but high levels of copper can become toxic to all life forms (Alaoui-Sossé et al., 2004). Therefore, the removal of copper is of great importance. Simultaneous copper recovery and energy production in a two-compartment MFC were investigated (Heijne et al., 2010; Tao et al., 2011b). The copper reduction in its basic form is shown in Equation (17).



Copper recovery in MFC was done by Heijne et al. (2010) by using a bipolar membrane as a pH separator. The maximum

power density was 0.80 W/m^2 at a current density of 3.2 A/m^2 and over 99.88% removal efficiency was achieved. Pure copper crystals were observed as the main products formed on the cathode surface and no CuO or Cu_2O was detected. As noted in the previous work of the authors, the bipolar membrane provided low pH in the cathode compartment.

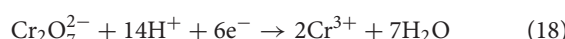
Tao et al. investigated Cu^{2+} reduction in an MFC using a PEM and cupric sulfate solution as catholyte (Tao et al., 2011b). The maximum power density at the initial copper concentration of $6412.5 \pm 26.7 \text{ mg Cu}^{2+}/\text{L}$ in glucose-fed MFC was measured as 339 mW/m^3 . High copper removal efficiency (>99%) was obtained when the initial copper concentration was $196.2 \pm 0.4 \text{ mg Cu}^{2+}/\text{L}$ and 15Ω external resistance. In order to further lower the construction cost for this process, Tao et al. (2011a) developed a lab-scale membrane free buffered MFC. At an initial copper concentration of 500 mg/L , a removal efficiency of 70% was observed over a period of 144 h (Tao et al., 2011a). Copper is an attractive electron receiver that can compete with oxygen (Tao et al., 2011b). For this reason, the cathodic copper reduction has broadened the field of MFC applications.

Copper reduction and electricity generation may vary depending on the architectural structure and operational parameters of the reactors. In an up-to-date study, electricity production was investigated by multiple batch cycle operations with different cathode materials (Wu D. et al., 2016). For the copper removal, a carbon rod, a titanium sheet, and stainless steel woven mesh materials were tested as cathode material. Stainless steel woven mesh was found as the most effective and cheap cathode material. When copper reduction is desired in MFC, the deposition of copper on the cathode has a great effect on power density and copper removal.

However, this technology is still in an early stage of development, more developments such as cost-effective reactor design and study of the catalytic behavior of copper for oxygen reduction at the cathode are required. Studies on copper removal in MFC indicate that the power density can be up to 33.6 W/m^3 depending on parameters such as reactor type, electron source, anode and cathode materials (Wu D. et al., 2016).

Chromium

The use of chromium as an electron acceptor has been demonstrated in several studies (Li et al., 2008; Li Y. et al., 2009; Sahinkaya et al., 2016). Real and synthetic wastewaters containing chromium were treated in MFCs and chromium reduction and electricity production were accomplished simultaneously. In acidic conditions Cr(IV) can be reduced to Cr(III) by the transfer of six electrons as illustrated in Equation (18).



This reduction reaction is thermodynamically feasible with a redox potential of 1.33 V. In a study, with a synthetic wastewater containing $200 \text{ mg Cr(IV)}/\text{L}$, the maximum power density of 150 mW/m^2 was obtained (0.04 mA/cm^2) and the maximum open circuit voltage was reported as 0.91 V. In this study, low pH was found to have a positive effect on Cr(VI) reduction (Wang et al., 2008). In another study, Li

TABLE 1 | Cathodic electron acceptors and the maximum power densities.

Type of substrate	Type of cathodic electron acceptor	Maximum power density	References
Acetate	Hg ²⁺	433.1 mW/m ²	Wang et al., 2011
Potassium acetate	Ferric iron	0.86 W/m ²	Heijne et al., 2006
Potassium acetate	Ferric iron	1.2 W/m ²	Heijne et al., 2007
Glucose	Biologically mineralized manganese-oxides	126.7 ± 31.5 mW/m ²	Rhoads et al., 2005
Glucose	permanganate	115.60 mW/m ²	You et al., 2006
Glucose	hexachromoferrate	25.62 mW/m ²	You et al., 2006
Glucose and sodium acetate	FePO ₄	—	Fischer et al., 2011
Acetate	Potassium persulfate	83.9 mW/m ²	Li J. et al., 2009
Acetate	Potassium ferricyanide	166.7 mW/m ²	Li J. et al., 2009
Domestic wastewater	Nitrate	9.7 mW/m ²	Lefebvre et al., 2008
Sodium acetate	Nitrate	—	Lefebvre et al., 2008
Domestic wastewater	Nitrate	117.7 mW/m ²	Fang et al., 2011
Sodium acetate	Nitrate	8.15 ± 0.02 W/m ³	Virdis et al., 2010
Glucose	Ammonium	14 W/m ³	Xie et al., 2011
Glucose	Nitrate	7.2 W/m ³	Xie et al., 2011
Acetate	Nitrate	34.6 ± 1.1 W/m ³	Virdis et al., 2008
Glucose	Cu(II) sulfate	314 mW/m ³	Tao et al., 2011a
Sodium acetate	Cr(IV)	1,600 mW/m ²	Li et al., 2008
Acetate	Cr(IV)	—	Li Y. et al., 2009
Acetate	Cr(IV)	150 mW/m ²	Wang et al., 2008
Acetic acid	Triiodide (I ₃)	484.0 mW/m ²	Li J. et al., 2010
Glucose	H ₂ O ₂	22 mW/m ²	Tartakovsky and Guiot, 2006
Fatty acids and alcohols	CO ₂	—	Villano et al., 2010
Sodium acetate	CO ₂	750 mW/m ²	Cao et al., 2009
Acetate	ClO ₄	—	Butler et al., 2010
Sulfide and glucose	Vanadium (V)	572.4 ± 18.2 mW/m ²	Zhang B. et al., 2009
Glucose	Vanadium (V)	614.1 mW/m ²	Zhang et al., 2010
Acetate	Uranium (IV)	10 mW/m ²	Williams et al., 2010
Externally supplied voltage	Chlorinated aliphatic hydrocarbons	—	Aulenta et al., 2009
Acetate/Externally supplied voltage	2-chlorophenol	—	Strycharz et al., 2010

et al., investigated the same process with real electroplating wastewater containing Cr(VI) (Li et al., 2008). In this study, Cr(VI) removal was found to be influenced by the electrode material. Graphite paper and graphite plates were used as cathode material in chrome removal and graphite paper gave better results than graphite plate (power density: 1,600 and 99.5% chromium removal rate for electroplating wastewater containing 204 mg Cr(VI)/L).

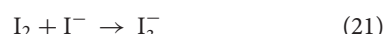
Different from conventional Cr(VI) reduction in MFCs, Li Y. et al. (2009) studied the Cr(VI) reduction in an MFC photoelectrochemical cell coupled system. Under light irradiation, 97% Cr(IV) removal was achieved within 26 h at the initial concentration of 26 mg/L (Li Y. et al., 2009). The maximum potential generated under light irradiation and dark controls were 0.80 and 0.55 V, respectively. The authors used rutile coated cathode for waste treatment and solar energy conversion in a single unit of MFC. These synergies between a biocatalyzed anode and a rutile coated cathode promoted the power output and Cr(IV) reduction (Li Y. et al., 2009).

In an up-to-date study, the microbial concentration was increased to improve chromium reduction performance in the cathode chamber. For this, the exoelectrogenic biofilm was enriched in the anode compartment and the system was subsequently established using the anode as biocathode. This new method has increased Cr(VI) reduction efficiency by 2.9 times compared to common biocathodes (Wu et al., 2015). Other recent studies on Cr(VI) reduction were focused on self-assembled graphene biocathode applications (Song et al., 2016) and on electrode material modification (Wu X. et al., 2016). Current studies are usually focused on the cathode material for chromium removal. Cr(VI) removal was studied in MFC operated with an alumina (AA)/nickel (Ni) nanoparticles (NPs)-dispersed carbon nanofiber electrode. With the developed electrode, a power density of 1,540 mW/m² was achieved together with the complete reduction of 100 mg Cr(VI)/L at a reduction rate of 2.12 g/(m³ h). The columbic efficiency was 93% (Gupta et al., 2017). In another study with abiotic cathode, a power density of 21.4 mW/m² was obtained in the treatment of alkaline Cr(VI) wastewater, while

10 mg/L chromium reduction was achieved within 45 h (Xafenias et al., 2015).

Triiodide

Similar to $\text{Fe}^{+3}/\text{Fe}^{+2}$ discussed in Section Copper, iodide/iodine redox couple is another redox couple that can serve as the electron mediator (Equation 19). There are some advantages of using this redox couple in the cathode. Since it can be regenerated in the catholyte, there is no depletion of triiodide (I_3^-). This regeneration could be done by a photo-driven reaction between I^- and oxygen (Equation 20) presented in Figure 3. After the formation of iodine, the combination of iodide anion with an iodine molecule in water forms triiodide (I_3^-) and the cycle continues (Equation 21). It also demonstrates the feasibility of using carbonaceous materials as the cathode. Triiodide is stable at both acidic and alkaline conditions. Because of all these properties, iodide/iodine redox couple could easily apply as an electron mediator in the cathode chamber for accepting and transferring electrons. The feasibility of this redox couple as the electron acceptor or mediator was first demonstrated using a two-chambered MFC (Li J. et al., 2010). Maximum power density of 484.0 mW/m² was obtained with 1.2 mM I_3^- and 0.2 M KI. (Li J. et al., 2010).

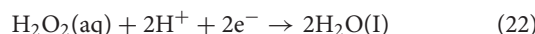


The present investigations are mainly carried out with H type MFCs, more efficient reactor design for high power generation is still required. It should be noted that I_3^- ion is toxic to electrochemically active microbes in the anodic chamber. Therefore, this negative effect should be taken into consideration

when designing a new configuration for better performance (Li J. et al., 2010).

Hydrogen Peroxide

Because of its strong oxidizing properties, H_2O_2 is used as an electron acceptor and its mechanism is presented in the following equation.



The oxygen concentration used in the cathode section can also be added to hydrogen peroxide. The use of hydrogen peroxide has been reported to provide stability in long-run operations in MFC (Tartakovsky and Guiot, 2006).

In a comparison of air with hydrogen peroxide, the power density in the air-operated MFC was 7.2 mW/m² while it increased to 22 mW/m² with hydrogen peroxide. Liquid hydrogen peroxide provides high levels of oxygen. This ensures high performance in long-run operation (Tartakovsky and Guiot, 2006).

While H_2O_2 is used to remove contaminants with hydroxyl radicals formed as a result of reaction with fenton, the remaining H_2O_2 must be removed. For this purpose, Zhang et al. have developed an innovative bioelectro-fenton system that uses an alternative switching to operate the system in microbial electrolysis cell (MEC) or MFC mode. In the MEC mode, methylene blue was removed with H_2O_2 , while the residual H_2O_2 was removed in the cathode as an electron acceptor. In this system, 50 mg/L of methylene blue was removed in the MEC system while 180 mg/L of residue H_2O_2 was used as an electron acceptor in MFC to produce a maximum current density of 0.49 A/m². With the study, H_2O_2 was effectively controlled and contaminant removal was ensured (Zhang Y. et al., 2015).

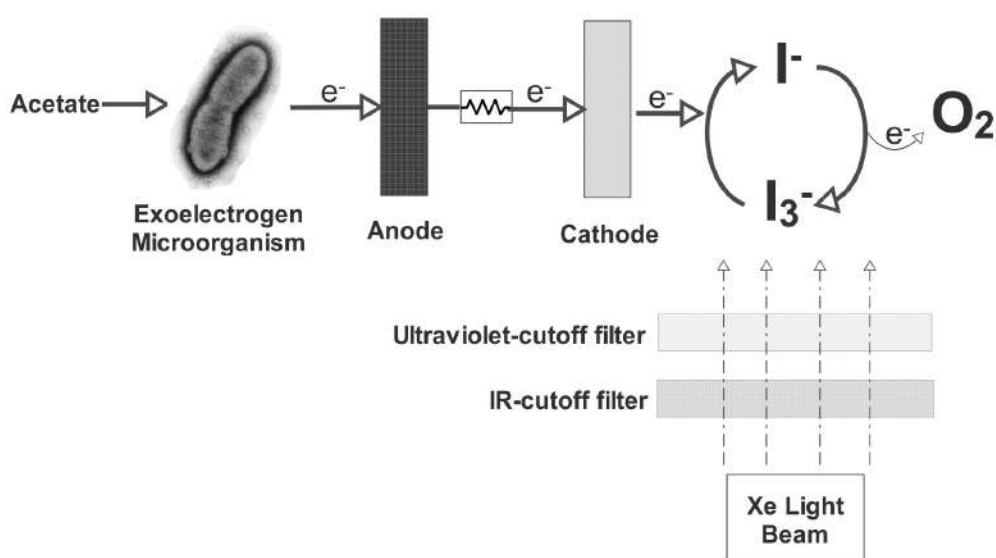


FIGURE 3 | Schematic view of the MFC using aqueous iodide ion solution as the catholyte (Li et al., 2010).

Carbon Dioxide

Thermodynamically, CO_2 reduction has a very low redox potential and its use in the cathode compartment produces a very low voltage. The CO_2 reduction potential is -0.420 V at neutral pH. However, the cathode potential must be higher than the anode potential in order to generate electricity. For this reason, external energy must be supplied in order to provide CO_2 reduction (Cao et al., 2009).

Cao et al. (2009) demonstrated the CO_2 reduction driven by sunlight with a biocathode MFC. Electrons could be received by the carbon dioxide, according to the following equation (Equation 23), where (CH_2O) represents the biomass. In this way, CO_2 reduction is provided together with biomass production. This bio-reaction allows the CO_2 sequestration.



Another application of CO_2 in the cathodic chambers is to reduce carbon dioxide to methane (Equation 24; Villano et al., 2010). Since both electrons and CO_2 are released during the oxidation of organic matter, these substances may participate in the production of methane. Villano et al. (2010) first demonstrated the feasibility of this concept using a two-chambered MFC. This process has some advantages. Firstly, the methanogens are protected from possible inhibitors present in the wastewater by separating the oxidation part of the organic matter from the methane production. Secondly, this process consumes less energy because there is no need to heat the cathode section to maintain the temperature. In addition, this process leads the operation of anaerobic digestion and methane producing steps in the series. Therefore, the system is also effective at low substrate concentrations (Villano et al., 2010).



In recent years, reduction of CO_2 to biofuels or commodity chemicals in the cathode with the help of microbes and externally supplied electricity has gained tremendous attention. Researches in this area have opened a new door for biofuel or chemical production by overcoming the limitation in natural photosynthesis processes and corresponding processes have been commonly named as microbial electrosynthesis or recently as artificial photosynthesis. Via these processes, multicarbon compounds such as acetate (Patil et al., 2015), acetic acid (Gildemyn et al., 2015), butyrate (Ganigüé et al., 2015) and ethanol (Pant et al., 2010) could be produced as a form of energy storage.

Perchlorate

Perchlorate is a drinking water contamination of interest due to its high mobility and inhibitory effect on thyroid functions (Cetin et al., 2015; Ucar et al., 2017). Among the treatment alternatives, biological reduction is a cost effective method (Ucar et al., 2015a,b, 2016). Reduction of ClO_4^- is shown as illustrated in Equation (25) (Ye et al., 2012).



Butler et al. (2010) reported the reduction of perchlorate to chloride by using highly active perchlorate reducing microbial community in the cathode chamber (Butler et al., 2010). In a MFC operated using acetate and perchlorate, 0.28 mA average current was obtained. The maximum perchlorate removal rate at this point was 24 mg/(L·d).

With this method, it is possible to purify perchlorate, which can be found in ground waters. However, in sediment waters, perchlorate is usually found in μM range, and electricity production with such low concentrations can be difficult. Nitrate is the most common pollutant found in groundwater. Thus, perchlorate and nitrate removal can be considered together in MFC.

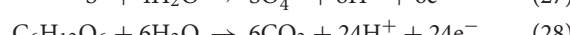
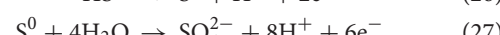
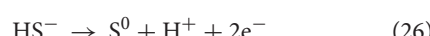
In a recent study conducted for this purpose, nitrate and perchlorate removal were investigated in the autotrophic denitrification biocathode. In acetate-fed MFC, 87.05 and 53.14% of the influent nitrate and perchlorate were removed respectively. The optimum $\text{NO}_3^-/\text{ClO}_4^-$ ratio is reported as 1:1 (Jiang et al., 2017). Acetate has been reported as the most suitable electron source for perchlorate and nitrate reductions (Lian et al., 2017). Reduction of nitrate and perchlorate with acetate can be carried out at high efficiency, but in the case of nitrates in drinking water, the use of organic electron sources such as acetate is likely to lead to unused acetate in the effluent. In such cases, the use of inorganic electron sources such as sulfur may be more appropriate. Inorganic electron donors also have their own disadvantages, for example, when sulfur is used, sulfate and acidity can occur in the effluent. However, in recent studies, the use of the advantages of both systems in the removal of nitrate and perchlorate from drinking and underground waters and the elimination of disadvantages are becoming increasingly widespread (Ucar et al., 2015b, 2017).

Vanadium

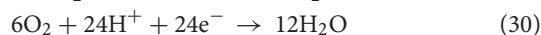
Another example of the use of MFC in pollutant removal is vanadium removal. Vanadium is usually found in wastewaters of vanadium mines and pentoxide processing activities (Carpentier et al., 2003). Vanadium has high redox potential in acidic conditions and can be successfully used in MFC (Zhang B. et al., 2009). At the vanadium reduction, both organic and inorganic compounds can be used as electron donors (Zhang et al., 2010). Zhang B. et al. (2009) used sulfide and glucose as the electron source to reduce vanadium (Equations 26–30).

The authors demonstrated the removal of sulfide and vanadium in the anode and cathode chambers of MFC respectively (Equations 26–30). Sulfur and vanadium removal rates were 84.7 ± 2.8 and $25.3 \pm 1.1\%$, respectively, with the maximum power density of 572.4 ± 18.2 mW/m².

Anode chamber



Cathode Chamber



Zhang et al. (2010) further studied the factors affecting the removal of sulfide and Vanadium (V) in MFCs respectively. It has been reported that the initial sulfur concentration has an effect on microbial activity (Zhang et al., 2010). As the initial sulfide concentration increased, microbes in the anode compartment became less effective, which resulted in a long lag time and decreased sulfide removal efficiency from 95.2% (50 mg/L) to 47.5% (200 mg/L) while average V(V) removal was $23.7 \pm 4.7\%$ in terms of V(IV) formation (with an initial V(V) concentration of 500 mg/L).

Anodic electrolyte conductivity is another factor affecting vanadium (V) removal and electricity production (Zhang et al., 2010). Increased anode electrolyte conductivity considerably raised the sulfur and vanadium reduction rates. This can be explained by the increased electron transfer rate at enhanced conductivity. Increasing anode electrolyte conductivity to 12.3 mS/cm increased V(IV) generation up to $36.0 \pm 1.6\%$. The initial concentration of Vanadium (V) is also the factor affecting the system performance. When the initial V(V) concentration is increased, the rate of V(IV) formation is also increased. The authors noted that the optimum initial V(V) concentration for 100 mg/L sulfide was 500 mg/L. Further increases in V(V) concentration resulted in a saturation in V(IV) generation. In addition, Vanadium (V) removal rate increased with the decrease of pH. Acidic conditions were necessary to compensate for the slower proton transport rate through the membrane. Under optimized conditions, average removal rates of sulfide and V(V) were 82.2 and 26.1% respectively, while the maximum power density was 614.1 mW/m^2 (Zhang et al., 2010).

Similar power densities were found in more recent studies. Hao et al. obtained a power density of 543.4 mW/m^2 at the end of 12 h of operation with a vanadium reduction of 93.6% (Hao et al., 2015). In another study, V was simultaneously reduced in both anode and cathode compartments. Power density of $419 \pm 11 \text{ mW/m}^2$ was achieved while initial vanadium concentrations in the anode and cathode were 75 and 150 mg/L respectively. The total vanadium removal rate was reported as $76.8 \pm 2.9\%$ while the final reduction product was V(IV) (Zhang B. et al., 2015).

Uranium

Leachate in uranium processing areas have low but stable uranium concentrations and can contaminate water resources, groundwater and sediment (Williams et al., 2010). To solve this problem in situ, metal reducing bacteria are usually used together with the acetate feed (Vrionis et al., 2005). While uranium removal can be done by adsorption, biological reduction or membrane filtration, cathodic U(VI) reduction seems also to be a promising method. Williams et al. (2010) set an acetate fed-MFC system which consisted of a reference electrode in a uranium contaminated aquifer sediment and another electrode at the surface. This inexpensive and minimally invasive system demonstrated 10 mW/m^2 power density during sulfate reduction

and U(IV) removal (Williams et al., 2010). The removal pathway of U(IV), however, is still uncertain. The removal mechanism of the uranium may be explained as reductive immobilization of U(IV) by non-acetate oxidizing sulfate reducers (N'Guessan et al., 2008).

Chloroethenes

Chlorinated aliphatic hydrocarbons (CAHs), which are widely used as solvents and degreasing agents, could become a huge risk due to their toxic and carcinogenic properties. These pollutants can be removed by some anaerobic bacteria which remove chlorines from CAHs by degrading them with the electrons obtained from an external electron donor or externally supplied voltage (Holliger and Schraa, 1994). An alternative version of this approach is to use insoluble electrodes to provide electrons to dechlorinating communities. Studies with two different communities (mixed culture of *dechlorinating bacteria* and pure culture of *Geobacter lovleyi*) showed that in a mixed culture, dechlorination of TCE was successfully achieved under acetate fed conditions (Aulenta et al., 2009). The formed dechlorination products were cis-DCE ($83.9 \pm 8.0\%$, on a molar basis), VC ($3.5 \pm 2.0\%$), as well as ethene and ethane ($12.6 \pm 7.0\%$). It has been proved that polarized carbon paper electrode can be used as the sole electron donor for the complete dechlorination of TCE with a mixed culture (Aulenta et al., 2009). Supplying external electron donors to the contamination zone may result in some unwanted processes and accumulate byproducts. In that case MFC with a solid electrode has a great advantage since bacterial oxidation happens in the anode and no external organic matter is added to the site (Aulenta et al., 2007).

2-Chlorophenol

As reported in the case of chloroethens, using solid electrode as the sole electron donor is more advantageous than using soluble electron donors directly (Aulenta et al., 2009). Application of electrodes to support necessary electrons for pollutant reduction, could be used for bioremediation of chlorinated contaminants and metals (Strycharz et al., 2010). *Geobacter* is one of the typical species used for this purpose. Strycharz et al. (2010) reported that *Anaeromyxobacter dehalogenans* could also transfer electrons to 2-chlorophenol and finally dechlorinate it to phenol. In their study, acetate was initially applied (10 mM) as a substrate for *Anaeromyxobacter dehalogenans* while $80 \mu\text{M}$ 2-chlorophenol was used as an electron acceptor. The most rapid rates of dechlorination were $40 \mu\text{M Cl/d}$ (in 200 mL) which shows that bioremediation of contaminants with electrodes acting as an electron donor could be useful (Strycharz et al., 2010). More recently, dechlorination of 2-chlorophenol has also been examined by Akbulut et al. (2012). One hundred fifty micro molar 2-chlorophenol was removed with a crude laccase enzyme under optimum dechlorination conditions (Akbulut et al., 2012). There are several advantages to use solid electrodes as an electron donor for chloroethens reduction (Strycharz et al., 2010). Firstly, electrons can be effectively transferred to microorganisms for reducing the pollutant. Secondly, the electrode as electron donor can be easily applied to the site. Thirdly, if contaminants are reacted directly with electrode, unwanted reaction can be

eliminated. Lastly, contaminant metals can be extracted from the electrode surface where they precipitated.

CONCLUSIONS AND FUTURE PERSPECTIVES

This review summarizes the various cathodic electron acceptors that have been used in MFCs. Some of these electron acceptors are also pollutants in aquatic systems. Therefore, a treatment process is also possible with MFC. A list of different cathodic electron acceptors used in MFC and the resulting power generation are summarized in the **Table 1**. Yet, the list is by no means exhaustive as newer electron acceptors may emerge accompanying the development of cathodic catalysts, electrode materials and solution chemistry. In the early applications of MFC, oxygen was commonly used as a terminal electron acceptor in the cathode chamber. However, in recent years, researchers are exploring more unconventional cathodic electron acceptors with an aim of improving MFC voltage potential on one hand and treating special wastewater or recovering valuable chemical on the other hand. The production of electricity with the reduction of specific electron acceptors in the cathode has promising potential in terms of bioenergy production as well as reducing the cost of special pollutant treatment (e.g., nitrogen species, persulfate, mercury, copper, chromium and perchlorate). Thus, contaminants that have high redox potential could be removed by reduction in the cathode compartment. MFC could be more efficient by using specific electron acceptors. Ferricyanide or hydrogen peroxide may be used for high power output or iron could be used to release of some valuable compounds such as phosphate from wastewaters.

REFERENCES

- Aelterman, P., Rabaey, K., Verstraete, W., Pham, H. T., and Boon, N. (2006). Continuous electricity generation at high voltages and currents using stacked microbial fuel cells. *Environ. Sci. Technol.* 40, 3388–3394. doi: 10.1021/es0525511
- Akulut, M., Aytar, P., Gedikli, S., Ünal, A., Çabuk, A., and Kolankaya, N. (2012). Dechlorination of chlorine from 2-chlorophenol with *Trametes Versicolor* crude laccase. *J. Eng. Nat. Sci.* 30:19.
- Alaoui-Sossé, B., Genet, P., Vinit-Dunand, F., Toussaint, M. L., Epron, D., and Badot, P. M. (2004). Effect of copper on growth in cucumber plants (*Cucumis sativus*) and its relationships with carbohydrate accumulation and changes in ion contents. *Plant Sci.* 166, 1213–1218. doi: 10.1016/j.plantsci.2003.12.032
- Aulenta, F., Canosa, A., Reale, P., Rossetti, S., Panero, S., and Majone, M. (2009). Microbial reductive dechlorination of trichloroethene to ethene with electrodes serving as electron donors without the external addition of redox mediators. *Biotechnol. Bioeng.* 103, 85–91. doi: 10.1002/bit.22234
- Aulenta, F., Pera, A., Rossetti, S., Petrangeli Papini, M., and Majone, M. (2007). Relevance of side reactions in anaerobic reductive dechlorination microcosms amended with different electron donors. *Water Res.* 41, 27–38. doi: 10.1016/j.watres.2006.09.019
- Butler, C. S., Clauwaert, P., Green, S. J., Verstraete, W., and Nerenberg, R. (2010). Bioelectrochemical perchlorate reduction in a microbial fuel cell. *Environ. Sci. Technol.* 44, 4685–4691. doi: 10.1021/es901758z
- Cao, X., Huang, X., Liang, P., Boon, N., Fan, M., Zhang, L., et al. (2009). A completely anoxic microbial fuel cell using a photo-biocathode for cathodic carbon dioxide reduction. *Energy Environ. Sci.* 2, 498–501. doi: 10.1039/b901069f
- Carpentier, W., Sandra, K., De Smet, I., Brigé, A., De Smet, L., and Van Beeumen, J. (2003). Microbial reduction and precipitation of vanadium by *Shewanella oneidensis*. *Appl. Environ. Microbiol.* 69, 3636–3639. doi: 10.1128/AEM.69.6.3636-3639.2003
- Cetin, U., Goncu, B., and Ucar, D. (2015). Perchlorate removal with inorganic electron donors. *Sigma J. Eng. Nat. Sci. ve Fen Bilim. Derg.* 33, 286–296.
- Cheng, S., and Logan, B. E. (2007). Sustainable and efficient biohydrogen production via electrohydrogenesis. *Proc. Natl. Acad. Sci. U. S.A.* 104, 18871–18873. doi: 10.1073/pnas.0706379104
- Clauwaert, P., Rabaey, K., Aelterman, P., de Schampheleire, L., Pham, T. H., Boeckx, P., et al. (2007). Biological denitrification in microbial fuel cells. *Environ. Sci. Technol.* 41, 3354–3360. doi: 10.1021/es062580r
- Cordell, D., Drangert, J.-O., and White, S. (2009). The story of phosphorous: global food security and food for thought. *Global Environ. Change* 19, 292–305. doi: 10.1016/j.gloenvcha.2008.10.009
- Cucu, A., Tiliakos, A., Tanase, I., Serban, C. E., Stamatin, I., Ciocanea, A., et al. (2016). Microbial fuel cell for nitrate reduction. *Energy Procedia* 85, 156–161. doi: 10.1016/j.egypro.2015.12.286
- Demirel, S., Uyanik, İ., Yurtsever, A., Çelikten, H., and Uçar, D. (2014). Simultaneous bromate and nitrate reduction in water using sulfur-utilizing autotrophic and mixotrophic denitrification processes in a fixed bed column reactor. *CLEAN Soil Air Water* 42, 1185–1189. doi: 10.1002/clen.201300475

- Desloover, J., Puig, S., Virdis, B., Boeckx, P., Verstraete, W., and Boon, N. (2011). Biocathodic nitrous oxide removal in bioelectrochemical systems. *Environ. Sci. Technol.* 45, 10557–10566. doi: 10.1021/es202047x
- Donovan, C., Dewan, A., Peng, H., Heo, D., and Beyenal, H. (2011). Power management system for a 2.5 W remote sensor powered by a sediment microbial fuel cell. *J. Power Sources* 196, 1171–1177. doi: 10.1016/j.jpowsour.2010.08.099
- Eliato, T. R., Pazuki, G., and Majidian, N. (2016). Potassium permanganate as an electron receiver in a microbial fuel cell. *Energy Sources A Recover. Util. Environ. Eff.* 38, 644–651. doi: 10.1080/15567036.2013.818079
- Fang, C., Min, B., and Angelidaki, I. (2011). Nitrate as an oxidant in the cathode chamber of a microbial fuel cell for both power generation and nutrient removal purposes. *Appl. Biochem. Biotechnol.* 164, 464–474. doi: 10.1007/s12010-010-9148-0
- Fischer, F., Bastian, C., Happe, M., Mabillard, E., and Schmidt, N. (2011). Microbial fuel cell enables phosphate recovery from digested sewage sludge as struvite. *Bioresour. Technol.* 102, 5824–5830. doi: 10.1016/j.biortech.2011.02.089
- Ganigüé, R., Puig, S., Batlle-Vilanova, P., Balaguer, M. D., and Colprim, J. (2015). Microbial electrosynthesis of butyrate from carbon dioxide. *Chem. Commun.* 51, 3235–3238. doi: 10.1039/c4cc10121a
- Gildemyn, S., Verbeeck, K., Slabbinck, R., Andersen, S. J., Prévosteau, A., and Rabaey, K. (2015). Integrated production, extraction, and concentration of acetic acid from CO₂ through microbial electrosynthesis. *Environ. Sci. Technol. Lett.* 2, 325–328. doi: 10.1021/acs.estlett.5b00212
- Gu, H., Zhang, X., Li, Z., and Lei, L. (2007). Studies on treatment of chlorophenol-containing wastewater by microbial fuel cell. *Chinese Sci. Bull.* 52, 3448–3451. doi: 10.1007/s11434-007-0503-7
- Gupta, S., Yadav, A., and Verma, N. (2017). Simultaneous Cr (VI) reduction and bioelectricity generation using microbial fuel cell based on alumina-nickel nanoparticles-dispersed carbon nanofiber electrode. *Chem. Eng. J.* 307, 729–738. doi: 10.1016/j.cej.2016.08.130
- Hao, L., Zhang, B., Tian, C., Liu, Y., Shi, C., Cheng, M., et al. (2015). Enhanced microbial reduction of vanadium (V) in groundwater with bioelectricity from microbial fuel cells. *J. Power Sources* 287, 43–49. doi: 10.1016/j.jpowsour.2015.04.045
- Heijne, A., Hamelers, H. V. M., Buisman, C. J. N., and Technology, S. W. (2007). Microbial fuel cell operation with continuous biological ferrous iron oxidation of the catholyte. *Environ. Sci. Technol.* 41, 4130–4134. doi: 10.1021/es0702824
- Heijne, A., Hamelers, H. V. M., De Wilde, V., Rozendal, R. A., and Buisman, C. J. N. (2006). A bipolar membrane combined with ferric iron reduction as an efficient cathode system in microbial fuel cells. *Environ. Sci. Technol.* 40, 5200–5205. doi: 10.1021/es0608545
- Heijne, A. T., Liu, F., van der Weijden, R., Weijma, J., Buisman, C. J. N., and Hamelers, H. V. M. (2010). Copper recovery combined with electricity production in a microbial fuel cell. *Environ. Sci. Technol.* 44, 4376–4381. doi: 10.1021/es100526g
- Holliger, C., and Schraa, G. (1994). Physiological meaning and potential for application of reductive dechlorination by anaerobic bacteria. *FEMS Microbiol. Rev.* 15, 297–305. doi: 10.1111/j.1574-6976.1994.tb00141.x
- Ishii, S., Suzuki, S., Norden-Krichmar, T. M., Wu, A., Yamanaka, Y., Nealson, K. H., et al. (2013). Identifying the microbial communities and operational conditions for optimized wastewater treatment in microbial fuel cells. *Water Res.* 47, 7120–7130. doi: 10.1016/j.watres.2013.07.048
- Jia, Y.-H., Tran, H.-T., Kim, D.-H., Oh, S.-J., Park, D.-H., Zhang, R.-H., et al. (2008). Simultaneous organics removal and bio-electrochemical denitrification in microbial fuel cells. *Bioprocess Biosyst. Eng.* 31, 315–321. doi: 10.1007/s00449-007-0164-6
- Jiang, C., Yang, Q., Wang, D., Zhong, Y., Chen, F., Li, X., et al. (2017). Simultaneous perchlorate and nitrate removal coupled with electricity generation in autotrophic denitrifying biocathode microbial fuel cell. *Chem. Eng. J.* 308, 783–790. doi: 10.1016/j.cej.2016.09.121
- Kim, M., and Lee, Y. (2010). Optimization of culture conditions and electricity generation using *Geobacter sulfurreducens* in a dual-chambered microbial fuel-cell. *Int. J. Hydrogen Energy* 35, 13028–13034. doi: 10.1016/j.ijhydene.2010.04.061
- Kim, S., Chae, K. J., Choi, M. J., and Verstraete, W. (2011). Microbial fuel cells: recent advances, bacterial communities and application beyond electricity generation. *Environ. Eng. Res.* 16, 51–65. doi: 10.4491/eer.2008.13.2.051
- Lefebvre, O., Al-Mamun, A., and Ng, H. Y. (2008). A microbial fuel cell equipped with a biocathode for organic removal and denitrification. *Water Sci. Technol.* 58, 881–885. doi: 10.2166/wst.2008.343
- Li, J., Fu, Q., Liao, Q., Zhu, X., Ye, D., ding, and Tian, X. (2009). Persulfate: a self-activated cathodic electron acceptor for microbial fuel cells. *J. Power Sources* 194, 269–274. doi: 10.1016/j.jpowsour.2009.04.055
- Li, J., Fu, Q., Zhu, X., Liao, Q., Zhang, L., and Wang, H. (2010). A solar regenerable cathodic electron acceptor for microbial fuel cells. *Electrochim. Acta* 55, 2332–2337. doi: 10.1016/j.electacta.2009.11.064
- Li, X., Hu, B., Suib, S., Lei, Y., and Li, B. (2010). Manganese dioxide as a new cathode catalyst in microbial fuel cells. *J. Power Sources* 195, 2586–2591. doi: 10.1016/j.jpowsour.2009.10.084
- Li, Y., Lu, A., Ding, H., Jin, S., Yan, Y., Wang, C., et al. (2009). Cr(VI) reduction at rutile-catalyzed cathode in microbial fuel cells. *Electrochim. Commun.* 11, 1496–1499. doi: 10.1016/j.elecom.2009.05.039
- Li, Z., Zhang, X., and Lei, L. (2008). Electricity production during the treatment of real electroplating wastewater containing Cr⁶⁺ using microbial fuel cell. *Process Biochem.* 43, 1352–1358. doi: 10.1016/j.procbio.2008.08.005
- Lian, J., Tian, X., Li, Z., Guo, J., Guo, Y., Yue, L., et al. (2017). The effects of different electron donors and electron acceptors on perchlorate reduction and bioelectricity generation in a microbial fuel cell. *Int. J. Hydrogen Energy* 42, 544–552. doi: 10.1016/j.ijhydene.2016.11.027
- Liew, K. B., Daud, W. R. W., Ghasemi, M., Loh, K. S., Ismail, M., and Lim, S. S. (2015). Manganese oxide/functionalised carbon nanotubes nanocomposite as catalyst for oxygen reduction reaction in microbial fuel cell. *Int. J. Hydrogen Energy* 40, 11625–11632. doi: 10.1016/j.ijhydene.2015.04.030
- Liu, H., and Logan, B. E. (2004). Electricity generation using an air-cathode single chamber microbial fuel cell in the presence and absence of a proton exchange membrane. *Environ. Sci. Technol.* 38, 4040–4046. doi: 10.1021/es039344
- Logan, B. E., Hamelers, B., Rozendal, R., Schröder, U., Keller, J., Freguia, S., et al. (2006). Microbial fuel cells: methodology and technology. *Environ. Sci. Technol.* 40, 5181–5192. doi: 10.1021/es0605016
- Mao, Y., Zhang, L., Li, D., Shi, H., Liu, Y., and Cai, L. (2010). Power generation from a biocathode microbial fuel cell biocatalyzed by ferro/manganese-oxidizing bacteria. *Electrochim. Acta* 55, 7804–7808. doi: 10.1016/j.electacta.2010.03.004
- N'Guessan, A. L., Vrionis, H. A., Resch, C. T., Long, P. E., and Lovley, D. R. (2008). Sustained removal of uranium from contaminated groundwater following stimulation of dissimilatory metal reduction. *Environ. Sci. Technol.* 42, 2999–3004. doi: 10.1021/es071960p
- Nguyen, M. T., Mecheri, B., Iannaci, A., D'Epifanio, A., and Licoccia, S. (2016). Iron/polyindole-based electrocatalysts to enhance oxygen reduction in microbial fuel cells. *Electrochim. Acta* 190, 388–395. doi: 10.1016/j.electacta.2015.12.105
- Oh, S., Min, B., and Logan, B. E. (2004). Cathode Performance as a factor in electricity generation in microbial fuel cells. *Environ. Sci. Technol.* 38, 4900–4904. doi: 10.1021/es049422p
- Pant, D., Van Bogaert, G., Diels, L., and Vanbroekhoven, K. (2010). A review of the substrates used in microbial fuel cells (MFCs) for sustainable energy production. *Bioresour. Technol.* 101, 1533–1543. doi: 10.1016/j.biortech.2009.10.017
- Patil, S. A., Arends, J. B. A., Vanwonterghem, I., Van Meerbergen, J., Guo, K., Tyson, G. W., et al. (2015). Selective enrichment establishes a stable performing community for microbial electrosynthesis of acetate from CO₂. *Environ. Sci. Technol.* 49, 8833–8843. doi: 10.1021/es506149d
- Puig, S., Serra, M., Vilar-Sanz, A., Cabré, M., Bañeras, L., Colprim, J., et al. (2011). Autotrophic nitrite removal in the cathode of microbial fuel cells. *Bioresour. Technol.* 102, 4462–4467. doi: 10.1016/j.biortech.2010.12.100
- Rabaey, K., Lissens, G., Siciliano, S. D., and Verstraete, W. (2003). A microbial fuel cell capable of converting glucose to electricity at high rate and efficiency. *Biotechnol. Bioeng.* 25, 1531–1535. doi: 10.1023/A:1025484009367

- Rabaey, K., and Rozendal, R. A. (2010). Microbial electrosynthesis - revisiting the electrical route for microbial production. *Nat. Rev. Microbiol.* 8, 706–716. doi: 10.1038/nrmicro2422
- Rahimnejad, M., Adhami, A., Darvari, S., Zirepour, A., and Oh, S.-E. (2015). Microbial fuel cell as new technology for bioelectricity generation: a review. *Alexandria Eng. J.* 54, 745–756. doi: 10.1016/j.aej.2015.03.031
- Rhoads, A., Beyenal, H., and Lewandowski, Z. (2005). Microbial fuel cell using anaerobic respiration as an anodic reaction and biomineralized manganese as a cathodic reactant. *Environ. Sci. Technol.* 39, 4666–4671. doi: 10.1021/es048386r
- Sahinkaya, E., Yurtsever, A., Aktaş, Ö., Ucar, D., and Wang, Z. (2015). Sulfur-based autotrophic denitrification of drinking water using a membrane bioreactor. *Chem. Eng. J.* 268, 180–186. doi: 10.1016/j.cej.2015.01.045
- Sahinkaya, E., Yurtsever, A., and Ucar, D. (2016). A novel elemental sulfur-based mixotrophic denitrifying membrane bioreactor for simultaneous Cr(VI) and nitrate reduction. *J. Hazard. Mater.* 324, 15–21. doi: 10.1016/j.jhazmat.2016.02.032
- Samrot, A. V., Senthilkumar, P., Pavankumar, K., Akilandeswari, G. C., Rajalakshmi, N., and Dhathathreyan, K. S. (2010). Electricity generation by *Enterobacter cloacae* SU-1 in mediator less microbial fuel cell. *Int. J. Hydrogen Energy* 35, 7723–7729. doi: 10.1016/j.ijhydene.2010.05.047
- Santoro, C., Serov, A., Starika, L., Kodali, M., Gordon, J., Babanova, S., et al. (2016). Iron based catalysts from novel low-cost organic precursors for enhanced oxygen reduction reaction in neutral media microbial fuel cells. *Energy Environ. Sci.* 9, 2346–2353. doi: 10.1039/C6EE01145D
- Schröder, U., Niessen, J., and Scholz, F. (2003). A generation of microbial fuel cells with current outputs boosted by more than one order of magnitude. *Angew. Chem. Int. Ed. Engl.* 42, 2880–2883. doi: 10.1002/anie.200350918
- Shen, J., He, R., Han, W., Sun, X., Li, J., and Wang, L. (2009). Biological denitrification of high-nitrate wastewater in a modified anoxic/oxic-membrane bioreactor (A/O-MBR). *J. Hazard Mater.* 172, 595–600. doi: 10.1016/j.jhazmat.2009.07.045
- Song, T., Jin, Y., Bao, J., Kang, D., and Xie, J. (2016). Graphene/biofilm composites for enhancement of hexavalent chromium reduction and electricity production in a biocathode microbial fuel cell. *J. Hazard Mater.* 317, 73–80. doi: 10.1016/j.jhazmat.2016.05.055
- Strik, D. P. B. T. B., Hamelers, H. V. M., and Buisman, C. J. N. (2010). Solar energy powered microbial fuel cell with a reversible bioelectrode. *Environ. Sci. Technol.* 44, 532–537. doi: 10.1021/es902435v
- Strycharz, S. M., Gannon, S. M., Boles, A. R., Franks, A. E., Nevin, K. P., and Lovley, D. R. (2010). Reductive dechlorination of 2-chlorophenol by *Anaeromyxobacter dehalogenans* with an electrode serving as the electron donor. *Environ. Microbiol. Rep.* 2, 289–294. doi: 10.1111/j.1758-2229.2009.00118.x
- Tao, H. C., Liang, M., Li, W., Zhang, L. J., Ni, J. R., and Wu, W. M. (2011b). Removal of copper from aqueous solution by electrodeposition in cathode chamber of microbial fuel cell. *J. Hazard Mater.* 189, 186–192. doi: 10.1016/j.jhazmat.2011.02.018
- Tao, H. C., Li, W., Liang, M., Xu, N., Ni, J. R., Wu, W. M., et al. (2011a). A membrane-free baffled microbial fuel cell for cathodic reduction of Cu(II) with electricity generation. *Bioresour. Technol.* 102, 4774–4778. doi: 10.1016/j.biortech.2011.01.057
- Tartakovsky, B., and Guiot, S. R. (2006). A comparison of air and hydrogen peroxide oxygenated microbial fuel cell reactors. *Biotechnol. Prog.* 241–246. doi: 10.1021/bp050225j
- Ucar, D., Cokgor, E. U., and Sahinkaya, E. (2015a). Evaluation of nitrate and perchlorate reduction using sulfur-based autotrophic and mixotrophic denitrifying processes. *Water Sci. Technol.* 91, 1–11. doi: 10.2166/ws.2015.129
- Ucar, D., Cokgor, E. U., and Ådahinkaya, E. (2015b). Simultaneous nitrate and perchlorate reduction using sulfur-based autotrophic and heterotrophic denitrifying processes. *J. Chem. Technol. Biotechnol.* 91, 1471–1477. doi: 10.1002/jctb.4744
- Ucar, D., Cokgor, E. U., and Sahinkaya, E. (2016). Heterotrophic-autotrophic sequential system for reductive nitrate and perchlorate removal. *Environ. Technol.* 37, 183–191. doi: 10.1080/09593330.2015.1065009
- Ucar, D., Cokgor, E. U., Sahinkaya, E., Cetin, U., Bereketoglu, C., Calimlioglu, B., et al. (2017). Simultaneous nitrate and perchlorate removal from groundwater by heterotrophic-autotrophic sequential system. *Int. Biodeterior. Biodegradation* 116, 83–90. doi: 10.1016/j.ibiod.2016.10.017
- Usharani, K., and Lakshmanaperumalsamy, P. (2010). Studies on the removal efficiency of phosphate from wastewater using *Pseudomonas* sp YLW-7 and *Enterobacter* sp KLW-2. *Glob. J. Environ. Res.* 4, 83–89.
- Venkata Mohan, S., Veer Raghavulu, S., and Sarma, P. N. (2008). Biochemical evaluation of bioelectricity production process from anaerobic wastewater treatment in a single chambered microbial fuel cell (MFC) employing glass wool membrane. *Biosens. Bioelectron.* 23, 1326–1332. doi: 10.1016/j.bios.2007.11.016
- Villano, M., Aulenta, F., Ciucci, C., Ferri, T., Giuliano, A., and Majone, M. (2010). Bioelectrochemical reduction of CO₂ to CH₄ via direct and indirect extracellular electron transfer by a hydrogenophilic methanogenic culture. *Bioresour. Technol.* 101, 3085–3090. doi: 10.1016/j.biortech.2009.12.077
- Virdis, B., Rabaey, K., Rozendal, R. A., Yuan, Z., and Keller, J. (2010). Simultaneous nitrification, denitrification and carbon removal in microbial fuel cells. *Water Res.* 44, 2970–2980. doi: 10.1016/j.watres.2010.02.022
- Virdis, B., Rabaey, K., Yuan, Z., and Keller, J. (2008). Microbial fuel cells for simultaneous carbon and nitrogen removal. *Water Res.* 42, 3013–3024. doi: 10.1016/j.watres.2008.03.017
- Vrionis, H. A., Anderson, R. T., Ortiz-Bernad, I., Neill, K. R., Resch, C. T., Peacock, A. D., et al. (2005). Microbiological and geochemical heterogeneity in an in situ uranium bioremediation field site. *Appl. Environ. Microbiol.* 71, 6308–6318. doi: 10.1128/AEM.71.10.6308-6318.2005
- Wang, G., Huang, L., and Zhang, Y. (2008). Cathodic reduction of hexavalent chromium [Cr(VI)] coupled with electricity generation in microbial fuel cells. *Biotechnol. Lett.* 30, 1959–1966. doi: 10.1007/s10529-008-9792-4
- Wang, Z., Lim, B., and Choi, C. (2011). Removal of Hg²⁺ as an electron acceptor coupled with power generation using a microbial fuel cell. *Bioresour. Technol.* 102, 6304–6307. doi: 10.1016/j.biortech.2011.02.027
- Williams, K. H., N'Guessan, A. L., Druhan, J., Long, P. E., Hubbard, S. S., Lovley, D. R., et al. (2010). Electrode voltages accompanying stimulated bioremediation of a uranium-contaminated aquifer. *J. Geophys. Res.* 115, 1–10. doi: 10.1029/2009JG001142
- Wu, D., Huang, L., Quan, X., and Li Puma, G. (2016). Electricity generation and bivalent copper reduction as a function of operation time and cathode electrode material in microbial fuel cells. *J. Power Sources* 307, 705–714. doi: 10.1016/j.jpowsour.2016.01.022
- Wu, X., Tong, F., Yong, X., Zhou, J., Zhang, L., Jia, H., et al. (2016). Effect of NaX zeolite-modified graphite felts on hexavalent chromium removal in biocathode microbial fuel cells. *J. Hazard Mater.* 308, 303–311. doi: 10.1016/j.jhazmat.2016.01.070
- Wu, X., Zhu, X., Song, T., Zhang, L., Jia, H., and Wei, P. (2015). Effect of acclimation on hexavalent chromium reduction in a biocathode microbial fuel cell. *Bioresour. Technol.* 180, 185–191. doi: 10.1016/j.biortech.2014.12.105
- Xafenias, N., Zhang, Y., and Banks, C. J. (2015). Evaluating hexavalent chromium reduction and electricity production in microbial fuel cells with alkaline cathodes. *Int. J. Environ. Sci. Technol.* 12, 2435–2446. doi: 10.1007/s13762-014-0651-7
- Xie, S., Liang, P., Chen, Y., Xia, X., and Huang, X. (2011). Simultaneous carbon and nitrogen removal using an oxic / anoxic-biocathode microbial fuel cells coupled system. *Bioresour. Technol.* 102, 348–354. doi: 10.1016/j.biortech.2010.07.046
- Ye, L., You, H., Yao, J., and Su, H. (2012). Water treatment technologies for perchlorate: a review. *Desalination* 298, 1–12. doi: 10.1016/j.desal.2012.05.006
- You, S., Zhao, Q., Zhang, J., Jiang, J., and Zhao, S. (2006). Short communication a microbial fuel cell using permanganate as the cathodic electron acceptor. *J. Power Sources* 162, 1409–1415. doi: 10.1016/j.jpowsour.2006.07.063
- Yu, C.-P., Liang, Z., Das, A., and Hu, Z. (2011). Nitrogen removal from wastewater using membrane aerated microbial fuel cell techniques. *Water Res.* 45, 1157–1164. doi: 10.1016/j.watres.2010.11.002
- Zain, S. M., Ching, N. L., Jusoh, S., and Yunus, S. Y. (2015). Different types of microbial fuel cell (MFC) systems for simultaneous electricity generation and pollutant removal. *J. Teknol.* 74, 13–19. doi: 10.11113/jt.v74.4544
- Zhang, B., Tian, C., Liu, Y., Hao, L., Liu, Y., Feng, C., et al. (2015). Simultaneous microbial and electrochemical reductions of vanadium (V) with bioelectricity generation in microbial fuel cells. *Bioresour. Technol.* 179, 91–97. doi: 10.1016/j.biortech.2014.12.010
- Zhang, B., Zhao, H., Shi, C., Zhou, S., and Ni, J. (2009). Simultaneous removal of sulfide and organics with vanadium(V) reduction in microbial fuel cells. *J. Chem. Technol. Biotechnol.* 84, 1780–1786. doi: 10.1002/jctb.2244

- Zhang, B., Zhou, S., Zhao, H., Shi, C., Kong, L., Sun, J., et al. (2010). Factors affecting the performance of microbial fuel cells for sulfide and vanadium (V) treatment. *Bioprocess Biosyst. Eng.* 33, 187–194. doi: 10.1007/s00449-009-0312-2
- Zhang, L., Liu, C., Zhuang, L., Li, W., Zhou, S., and Zhang, J. (2009). Manganese dioxide as an alternative cathodic catalyst to platinum in microbial fuel cells. *Biosens. Bioelectron.* 24, 2825–2829. doi: 10.1016/j.bios.2009.02.010
- Zhang, Y., and Angelidaki, I. (2011). Submersible microbial fuel cell sensor for monitoring microbial activity and BOD in groundwater: focusing on impact of anodic biofilm on sensor applicability. *Biotechnol. Bioeng.* 108, 2339–2347. doi: 10.1002/bit.23204
- Zhang, Y., Wang, Y., and Angelidaki, I. (2015). Alternate switching between microbial fuel cell and microbial electrolysis cell operation as a new method to control H_2O_2 level in Bioelectro-Fenton system. *J. Power Sources* 291, 108–116. doi: 10.1016/j.jpowsour.2015.05.020
- Zhou, M., Chi, M., Luo, J., He, H., and Jin, T. (2011). An overview of electrode materials in microbial fuel cells. *J. Power Sources* 196, 4427–4435. doi: 10.1016/j.jpowsour.2011.01.012

Conflict of Interest Statement: The authors declare that the research was conducted in the absence of any commercial or financial relationships that could be construed as a potential conflict of interest.

Copyright © 2017 Ucar, Zhang and Angelidaki. This is an open-access article distributed under the terms of the Creative Commons Attribution License (CC BY). The use, distribution or reproduction in other forums is permitted, provided the original author(s) or licensor are credited and that the original publication in this journal is cited, in accordance with accepted academic practice. No use, distribution or reproduction is permitted which does not comply with these terms.



The Denitrification Characteristics and Microbial Community in the Cathode of an MFC with Aerobic Denitrification at High Temperatures

Jianqiang Zhao^{1,2*}, Jinna Wu¹, Xiaoling Li³, Sha Wang¹, Bo Hu³ and Xiaoqian Ding¹

¹ School of Environmental Science and Engineering, Chang'an University, Xi'an, China, ² Key Laboratory of Subsurface Hydrology and Ecological Effect in Arid Region of Ministry of Education, Xi'an, China, ³ School of Civil Engineering, Chang'an University, Xi'an, China

OPEN ACCESS

Edited by:

Yong Xiao,
Institute of Urban Environment (CAS),
China

Reviewed by:

Xianhua Liu,
Tianjin University, China
Yifeng Zhang,
Technical University of Denmark,
Denmark

*Correspondence:

Jianqiang Zhao
626710287@qq.com

Specialty section:

This article was submitted to
Microbiotechnology, Ecotoxicology
and Bioremediation,
a section of the journal
Frontiers in Microbiology

Received: 09 September 2016

Accepted: 03 January 2017

Published: 19 January 2017

Citation:

Zhao J, Wu J, Li X, Wang S, Hu B and
Ding X (2017) The Denitrification
Characteristics and Microbial
Community in the Cathode of an MFC
with Aerobic Denitrification at High
Temperatures. *Front. Microbiol.* 8:9.
doi: 10.3389/fmicb.2017.00009

Microbial fuel cells (MFCs) have attracted much attention due to their ability to generate electricity while treating wastewater. The performance of a double-chamber MFC with simultaneous nitrification and denitrification (SND) in the cathode for treating synthetic high concentration ammonia wastewater was investigated at different dissolved oxygen (DO) concentrations and high temperatures. The results showed that electrode denitrification and traditional heterotrophic denitrification co-existed in the cathode chamber. Electrode denitrification by aerobic denitrification bacterium (ADB) is beneficial for achieving a higher voltage of the MFC at high DO concentrations (3.0–4.2 mg/L), while traditional heterotrophic denitrification is conducive to higher total nitrogen (TN) removal at low DO (0.5–1.0 mg/L) concentrations. Under high DO conditions, the nitrous oxide production and TN removal efficiency were higher with a 50 Ω external resistance than with a 100 Ω resistance, which demonstrated that electrode denitrification by ADB occurred in the cathode of the MFC. Sufficient electrons were inferred to be provided by the electrode to allow ADB survival at low carbon:nitrogen ratios (≤ 0.3). Polymerase chain reaction-denaturing gradient gel electrophoresis (PCR-DGGE) results showed that increasing the DO resulted in a change of the predominant species from thermophilic autotrophic nitrifiers and facultative heterotrophic denitrifiers at low DO concentrations to thermophilic ADB at high DO concentrations. The predominant phylum changed from *Firmicutes* to *Proteobacteria*, and the predominant class changed from *Bacilli* to *Alpha*, *Beta*, and *Gamma Proteobacteria*.

Keywords: aerobic denitrifying bacteria, dissolved oxygen, microbial fuel cell, predominant species, simultaneous nitrification and denitrification

INTRODUCTION

Microbial fuel cells (MFCs) have gained widespread attention as an innovative wastewater treatment and energy recovery technology that combines sewage purification and electricity production (Janicek et al., 2014; Li et al., 2014). Recent studies have shown that nitrate and nitrite can be removed from wastewater as electron acceptors in the cathode of an MFC through electrochemical reduction or autotrophic denitrification (Zhang and Angelidaki, 2012). Several

developments of nitrogen removal with MFCs have been achieved with various designs and configurations (He et al., 2009; Virdis et al., 2010; Zhang and Angelidaki, 2013). In the studies of Bernardino Virdis et al., the cathodic process with *in situ* nitrification through specific aeration attained simultaneous nitrification and denitrification (SND) in one half-cell (Virdis et al., 2010). Although, nitrogen recovery with MFCs through NH₃ stripping has been successfully developed to simultaneously produce energy and recover ammonium (Kuntke et al., 2012; Zhang and Angelidaki, 2015), SND in cathode of MFCs and its some new biochemical mechanisms still remain valuable to explore. Studies of simultaneous phenol removal, nitrification and denitrification using MFCs have indicated that phenol-degrading bacteria, nitrifiers, and denitrifiers in the aerobic cathode chamber are responsible for phenol oxidation, aerobic nitrification and aerobic denitrification, respectively (Feng et al., 2015). The impact of dissolved oxygen (DO) on the SND process in the cathode of an MFC has also been investigated comprehensively (Virdis et al., 2010). Because the bacteria may evolve during long-term operation, the impact of DO on the performance of cathode denitrification is different from that over shorttime periods. The SND mechanism in the aerobic cathode chamber is complex and remains unclear.

In the traditional theory of biological nitrogen removal, ammonia is first oxidized to nitrate by autotrophic nitrifiers, and the nitrate is then reduced to nitrogen by heterotrophic denitrifiers (Robertson and Kuenen, 1984). Based on the different growth conditions of nitrifiers and denitrifiers, the traditional theory of biological nitrogen removal makes a strict distinction between the nitrification and denitrification processes. The former is carried out under aerobic conditions, while the latter requires anaerobic conditions. Therefore, it is impossible for the two reactions to occur simultaneously in the same reactor. However, the discovery of heterotrophic nitrifiers and aerobic denitrifiers has made it possible for nitrification and denitrification to occur simultaneously (Huang et al., 2013; Li et al., 2015). Heterotrophic nitrifying bacteria can produce hydroxylamine, nitrite and nitrate by nitrification using organic carbon as a source for growth, and most of these bacteria can also directly convert nitrifying products to nitrogen gas through the process of aerobic denitrification (Papen and Von Berg, 1998). Aerobic denitrification bacterium (ADB) can use aerobic denitrifying enzymes for denitrification under aerobic conditions (Robertson et al., 1988; Bell and Ferguson, 1991).

In the 1980s, Robertson and Kuenen (1984) isolated the aerobic denitrifiers *Thiosphaera pantotropha*, *Pseudomonas* spp. and *Alcaligenes faecalis* for the first time and reported the existence of the aerobic denitrifying enzyme system (Robertson et al., 1988). They also confirmed that the growth rate of *Paracoccus denitrificans* will be higher in the presence of O₂ and NO₃⁻. Bell and Ferguson (1991) demonstrated that aerobic denitrifying enzymes were more active in the presence of O₂, and Meiberg et al. (Ferguson, 1994) reported that denitrification could be carried out by *Hyphomicrobium X* under aerobic conditions. Many studies have proved the existence of ADB (Chen et al., 2003; Kim et al., 2005) and found that some denitrifiers survive under high O₂ concentration conditions

(Takaya et al., 2003). Certain groups of bacteria, such as *Bacillus*, *P. putida*, *P. stutzeri*, *Hydrogenophaga*, and *Achromobacter*, have been shown to have heterotrophic nitrification and aerobic denitrification abilities and to convert ammonium to nitrogen aerobically in the cathode chamber of an MFC (Feng et al., 2015). Nevertheless, few attempts have been made to attain SND at high temperatures. Because some wastewater, similar to sludge digestion solutions and effluents of anaerobic reactors that treat landfill leachate, contains high concentrations of ammonia at high temperatures, studies of SND and the performance of ADB in the cathode of an MFC at high temperatures are important.

This study investigated the performance of a double-chamber MFC with SND in the cathode at fluctuating high temperatures (36–48°C). Synthetic wastewater that contained organics and high concentrations of ammonia was fed into the anode chamber and then turned into the cathode chamber. The denitrification characteristics were studied by comparing scenarios with two ranges of DO concentrations (0.5–1.0 and 3.0–4.2 mg/L) and scenarios with two external resistances (50 and 100 Ω) at high DO concentrations. The microbial communities at the two DO concentrations in the cathode of the MFC were identified with polymerase chain reaction-denaturing gradient gel electrophoresis (PCR-DGGE) to explore the evolution of the dominant bacteria.

MATERIALS AND METHODS

Experimental Set-up

The MFC device was constructed with cathode and anode chambers. The anode and cathode chambers were both made of organic glass tube 8 cm high and 9 cm in diameter and had an effective volume of 0.452 L (Figure 1). Each chamber used a carbon brush as the electrode. The two chambers were separated by a proton exchange membrane (Nafion 117) and placed in a water bath. The temperature was initially set to 31 ± 1°C and then changed to a dynamic temperature (36–48°C) later in the operation. The cathode and anode chambers were connected with a manual variable resistor (0–9999 Ω) to close the circuit. The cathode chamber was exposed to air, and blast aeration was used. The influent was injected into the anode chamber using a peristaltic pump (YZ1515X, Lange), and the effluent from the anode was fed into the cathode chamber.

Influent Component

The influent for the MFC reactor was an artificially simulated high strength ammonia sludge digestion solution with components of 0.38 g/L CH₃COONa, 2.708 g/L NH₄HCO₃, 0.33 g/L KH₂PO₄, 1 g/L K₂HPO₄·3H₂O, 1 g/L KCl, 1.5 g/L NaHCO₃, 0.016 g/L CaCl₂, and 1 ml/L trace nutrient solution. CH₃COONa and NH₄HCO₃ were added to maintain the chemical oxygen demand (COD) and the ammonia nitrogen concentrations in the influent at 300 and 480 mg/L, respectively.

Start-up and Operation

The anode and cathode chambers of the MFC were inoculated with aerobic sludge from the aeration tank of the Fourth Wastewater Treatment Plant in Xi'an, China. Before operating

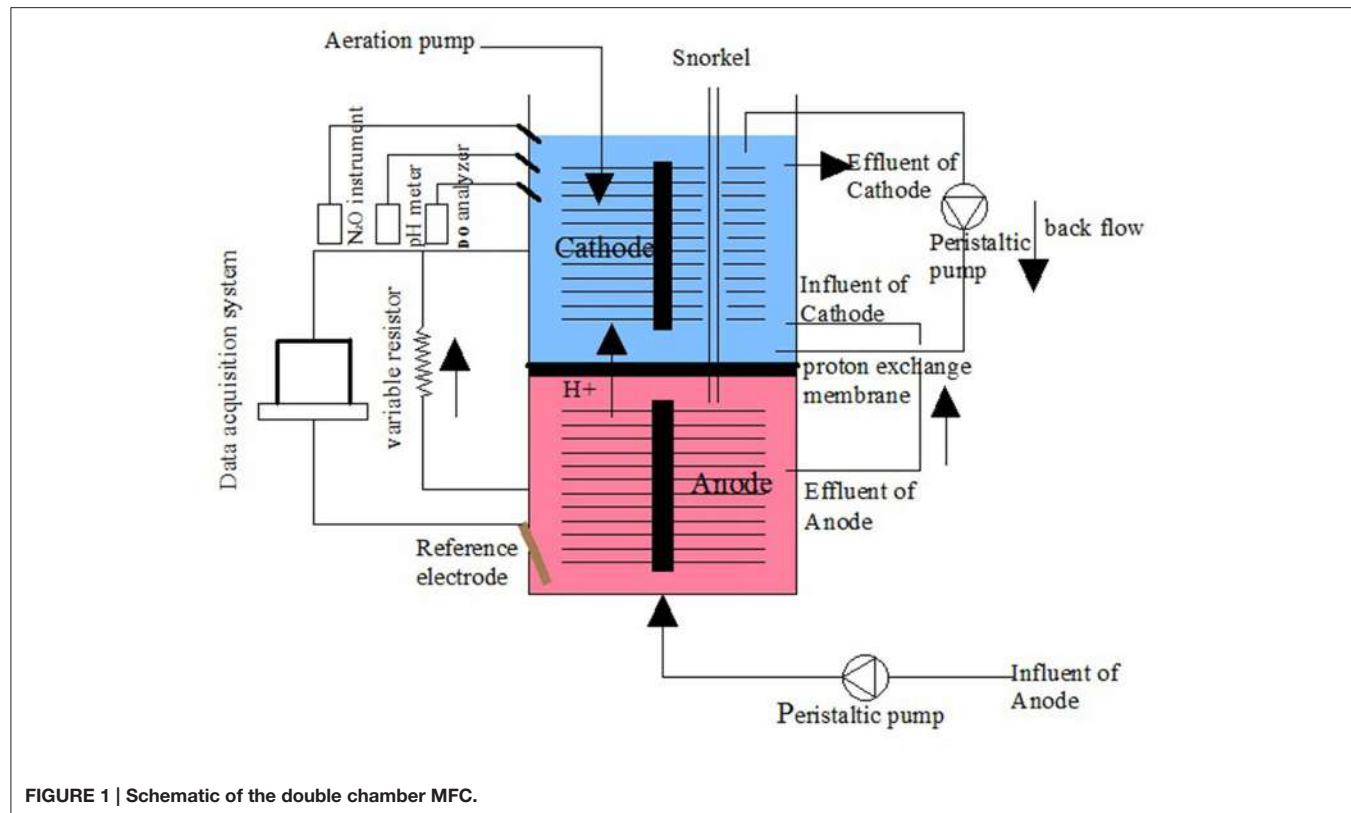


FIGURE 1 | Schematic of the double chamber MFC.

the MFC, the anode and cathode were soaked in the inoculation sludge for 24 h. Once the reactor was filled with synthetic wastewater, the MFC entered the stage of static culture without the influent while keeping the cathode aerated and the inner circuit open. The concentrations of DO, NO_3^- -N, NO_2^- -N, and NH_4^+ -N and the pH of the cathode electrolyte were measured daily. After more than half of the original NH_4^+ -N was converted to NO_2^- -N in the cathode electrolyte, the aeration mode was changed from continuous to intermittent (2 h aeration and 2 h static), and the wastewater was pumped continuously into the anode chamber with hydraulic retention times (HRTs) of 10.4 h for both the cathode and the anode chambers. After a period of continuous operation, stable partial nitrification was obtained in the cathode chamber of the MFC. An external resistance of $100\ \Omega$ was then connected, following which the operation of MFC with SND started.

Analytical Method

The anode potential was monitored with a saturated calomel electrode (SCE, +0.242 V standard hydrogen electrode; Type 232, Leici Instrument Factory, Shanghai, China). NO_3^- -N, NO_2^- -N and NH_4^+ -N were measured according to Standard Methods for the Examination of Water and Wastewater (Clesceri et al., 1998). DO was determined using a Hach-HQ30d DO analyzer (HACH, America). The voltage and anode potential were monitored and recorded using a PCI1717 voltage collector (Yanhua Company, Shenzhen, China). An N_2O microsensor (Unisense, Denmark) was used for the N_2O analysis.

Samples from the biofilm of the cathode were collected on day 27 and day 83 to investigate the microbial community with DGGE, and DNA was extracted using a fast DNA spin kit (SK8233) for soil according to the manufacturer's instructions. The bacterial 16S rRNA genes were amplified by PCR with the universal primers F357-GC (5'-CGCCCG CCGCGCCCCGCCCCGGCCGCCGCCCCCTAC GGGAGGCAGCAG-3') and R518 (5'-ATTACCGCGGCTGC TGG-3'). A polyacrylamide gel (8%) with a 30–60% denaturing gradient was used to separate the PCR products (7 mol L⁻¹ urea and 40% formamide comprising 100% denaturant), which were analyzed using DGGE technology and washed with ultrapure water to flush the gel and dye. Eight representative DGGE strips were selected by a clean scalpel and transferred to a 1.5 mL centrifuge tube. The target DNA fragments were then excised and reamplified using the primer sets F357 (5'-CCTACGGGAGGCAGCAG-3') and R518 (5'-ATTACCGCGGCTGCTGG-3'), and the obtained sequence was matched with the Seqmatch database for sequence alignment. The homology information of each strip was obtained by Sangon Biotech Co., Ltd. (Shanghai, China).

RESULTS AND DISCUSSION

Performance of the MFC

The results of the continuous operation test are shown in Figure 2.

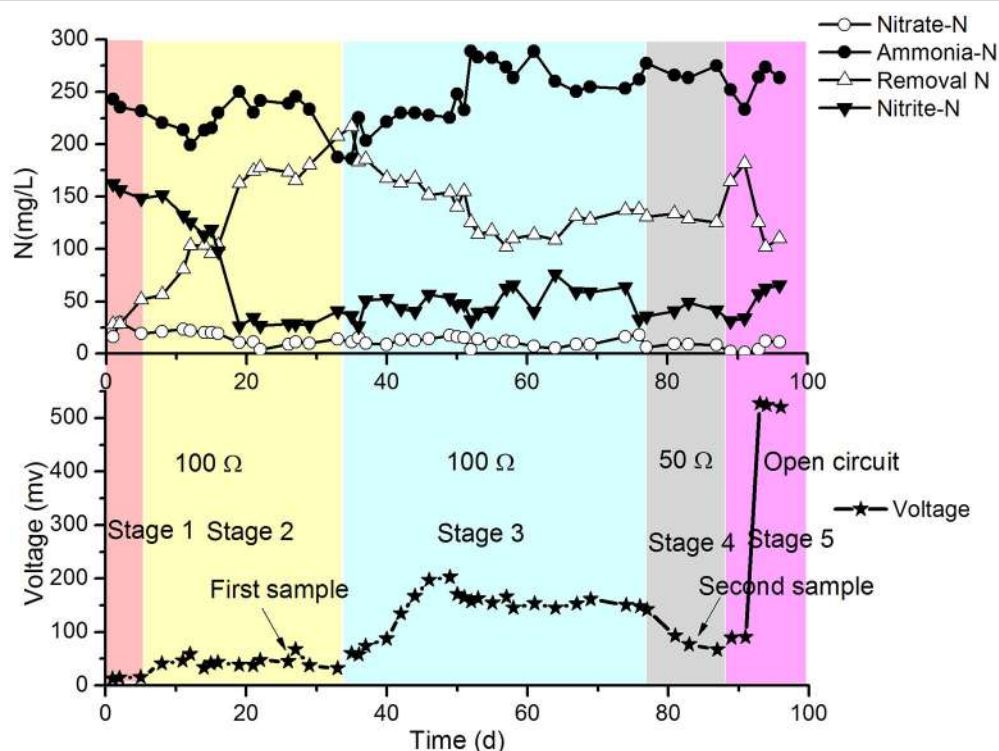


FIGURE 2 | Profiles of NH_4^+ -N, NO_2^- -N and NO_3^- -N in the effluent of the cathode chamber and voltages of the MFC.

In stage 1 (first 5 days of the test), the MFC with SND was operated at $31 \pm 1^\circ\text{C}$, 100Ω resistance and intermittent aeration (2 h aeration and 2 h static), and the DO of the catholyte was $0.5\text{--}1.0 \text{ mg/L}$. The concentrations of NH_4^+ -N and NO_2^- -N decreased with a gradual increase in the release voltage of the MFC. However, the removal of total nitrogen (TN) was much greater than that with the electrical current of the MFC. This finding implies that the traditional heterotrophic microbial denitrification with COD was more efficient at removing nitrogen than the electrode denitrification in the cathode chamber. The moderate temperature ($31 \pm 1^\circ\text{C}$) and low DO ($0.5\text{--}1.0 \text{ mg/L}$) in the cathode may be beneficial for SND with COD still present in the anode effluent.

In stage 2 (days 6–34), the temperature of the reactor increased and fluctuated over the range of $36\text{--}48^\circ\text{C}$. The removal of TN began to increase sharply, and the concentration of NO_2^- -N in the cathode effluent began to decrease correspondingly from the 6th day, while the voltage of the MFC increased slightly and then stabilized. This might have been due to the high temperature in the cathode ($36\text{--}48^\circ\text{C}$), which was harmful for the growth of normal ammonia oxidizing bacteria (AOB). Because the suitable range of temperatures for AOB metabolism is $20\text{--}30^\circ\text{C}$, the nitrification rate decreased, and the NO_2^- -N concentration decreased to approximately 30 mg/L . The increase in the TN removal was mainly caused by the volatilization of ammonium at high temperature. The TN removal from the denitrification in the electrode during stage 2 was lower and

similar to that at the end of stage 1 (not greater than $7 \text{ mg/L}\cdot\text{d}$ based on the MFC voltage). The biofilm was sampled, and the bacteria were identified with PCR-DGGE. The predominant species was found to be *Ureibacillus thermosphaericus* of the genus *Ureibacillus*, which grows at temperatures of 37° to 60°C (Fortina et al., 2001).

In stage 3 (days 35–77), the reactor was set to continuous aeration instead of intermittent aeration. As a result, the DO increased to $3 \pm 0.6 \text{ mg/L}$. The amount of TN removed per day began to decrease, but the voltage continued to increase. This might have occurred because the heterotrophic denitrification with COD as the electron donor was inhibited by the increase of DO, and the partial oxygen accepted electrons from the electrode. In stage 3, the release voltage initially increased, then dropped and finally steadied at approximately 100 mV , which was much higher than that in stage 2. The following strain sampling clearly demonstrated that the predominant species changed to aerobic denitrifiers (a detailed analysis is provided later). The curves in Figure 2 suggest that the aerobic denitrifiers might have replaced the anaerobic denitrifiers in the latter phase of stage 3. The aerobic denitrifiers appeared to be much more receptive to the electrons from the electrode than the anaerobic denitrifiers, which was determined by comparing the voltage of stage 2 with that of stage 3, in which the effects of electron acceptance by oxygen was taken into account. In contrast, TN removal by anaerobic denitrifiers was much greater than that by aerobic denitrifiers. The heterotrophic denitrification with

COD might have mainly caused TN removal, excluding the effect of volatilization in the cathode. Depending on the voltage, the TN removal by electrode denitrification was 8.5–9.0 mg/(L·d), which represented only a small part of the TN removal in stage 3.

The conditions in stage 4 (days 78–88) remained the same as those in stage 3 except for the change in the resistance of the MFC from 100 to 50 Ω . The results showed that the concentrations of NH_4^+ -N and NO_2^- -N in the cathode effluent decreased, and the amount of TN removed increased in the latter part of this stage (**Figure 2**). The voltages were greater than those in stage 3, but the TN removal by electrode denitrification was 13.5–14.6 mg/(L·d), which was greater than that in stage 3.

Electricity Production and Nitrogen Removal Performance under High DO Conditions

The electricity production performance of the MFC under high DO conditions and different external resistances was investigated as a case study (**Figures 3–5**, which correspond to days 75, 82, and 97 in **Figure 2**, respectively). The voltage was positively related to the increase in temperature under external resistances of 50 Ω and 100 Ω , while it was independent of the temperature under open circuit conditions. Regardless of whether the resistances were applied or an open circuit was used, the N_2O emissions were always positively related to the increase in temperature, while the DO was always negatively related to the increase in temperature. The characteristics of denitrification and

electricity production of the MFC can be evaluated using these factors.

The fluctuations in the concentrations of DO and N_2O caused by the temperature (**Figures 3, 5**) show that the DO fluctuation amplitude was approximately 1.2 mg/L, whereas the corresponding N_2O fluctuation was approximately 0.4 mg/L in the open circuit. With a 100 Ω resistance, the DO and N_2O fluctuation amplitudes were 1.5 mg/L and 0.3 mg/L, respectively. This demonstrated that the reduction in oxygen caused by the voltage fluctuation was approximately 0.3 mg O_2/L , and no N_2O was produced by electrode denitrification. The concentrations of N_2O were similar in both scenarios (0.7–1.1 mg/L), whereas the concentrations of DO with a 100 Ω resistance were 0.7–1.0 mg/L, which was lower than that in the open circuit (**Figures 3, 5**). This indicated that the decrease in DO was dependent on the electrode reaction, while the production of N_2O was independent of the electrode reaction. Using Coulomb's law, with a 100 Ω resistance, the electrode reduction rate of oxygen was calculated to be 1.6–2.3 mg $\text{O}_2/(\text{L} \cdot \text{d})$, whereas the rate of electrode reduction of nitrite to nitrogen gas was 8.5–9.0 mg N/(L·d) with no production of N_2O .

The fluctuations in the concentrations of DO and N_2O caused by temperature (**Figures 4, 5**) show that the decrease of DO and the increase of N_2O were both dependent on the electrode reaction. Using Coulomb's law, with a 50 Ω resistance, the electrode reduction rate of oxygen was calculated to be 2.8–4.4 mg $\text{O}_2/(\text{L} \cdot \text{d})$, whereas the rate of electrode denitrification was 13.5–14.6 mg N/(L·d), in which approximately 10% of the nitrogen removed was converted to N_2O and 90% was converted to nitrogen gas.

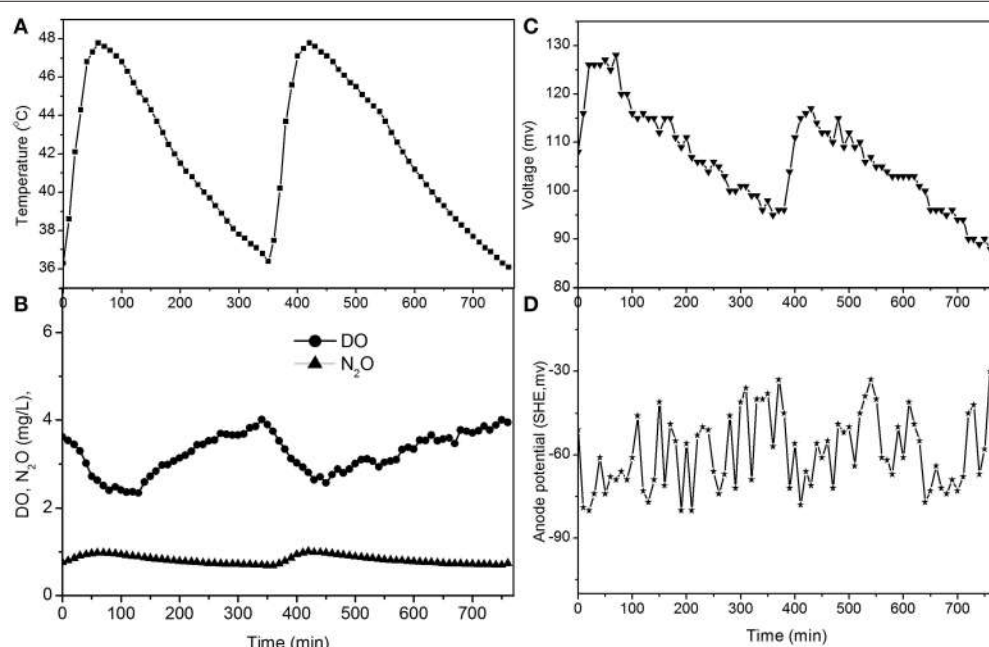


FIGURE 3 | Profiles of temperature, DO, N_2O , voltage, and anode potential of the MFC with 100 Ω external resistance at temperatures of 36–48°C (day 75 in **Figure 2**). **(A)** Temperature profile; **(B)** DO and N_2O profiles; **(C)** voltage profile; **(D)** anode potential profile.

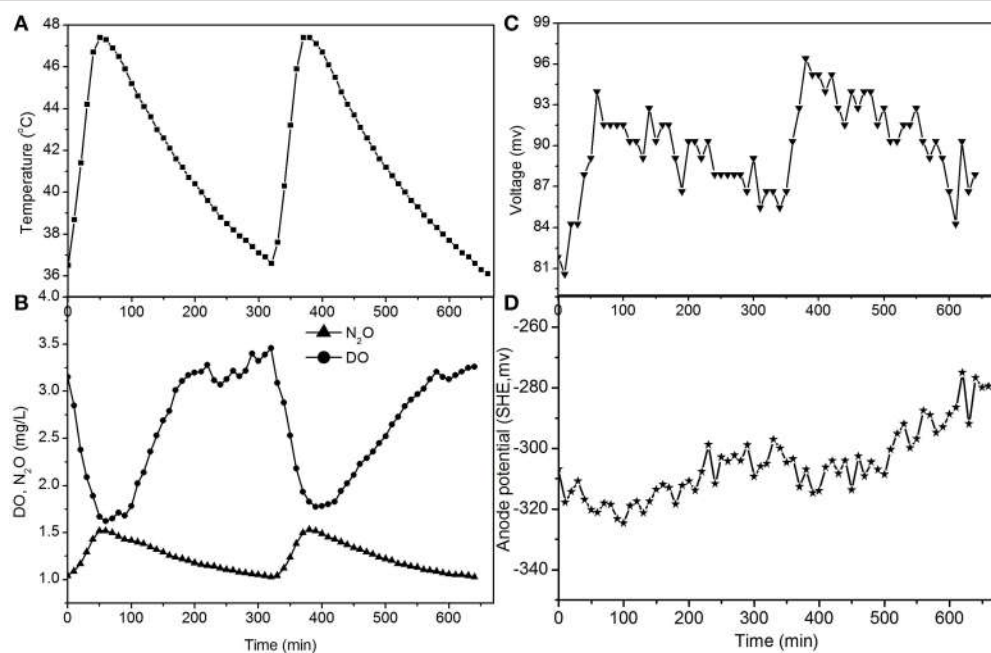


FIGURE 4 | Profiles of temperature, DO, N_2O , voltage, and anode potential of the MFC with 50Ω external resistance at temperatures of 36–48°C (day 82 in Figure 2). **(A)** Temperature profile; **(B)** DO and N_2O profiles; **(C)** voltage profile; **(D)** anode potential profile.

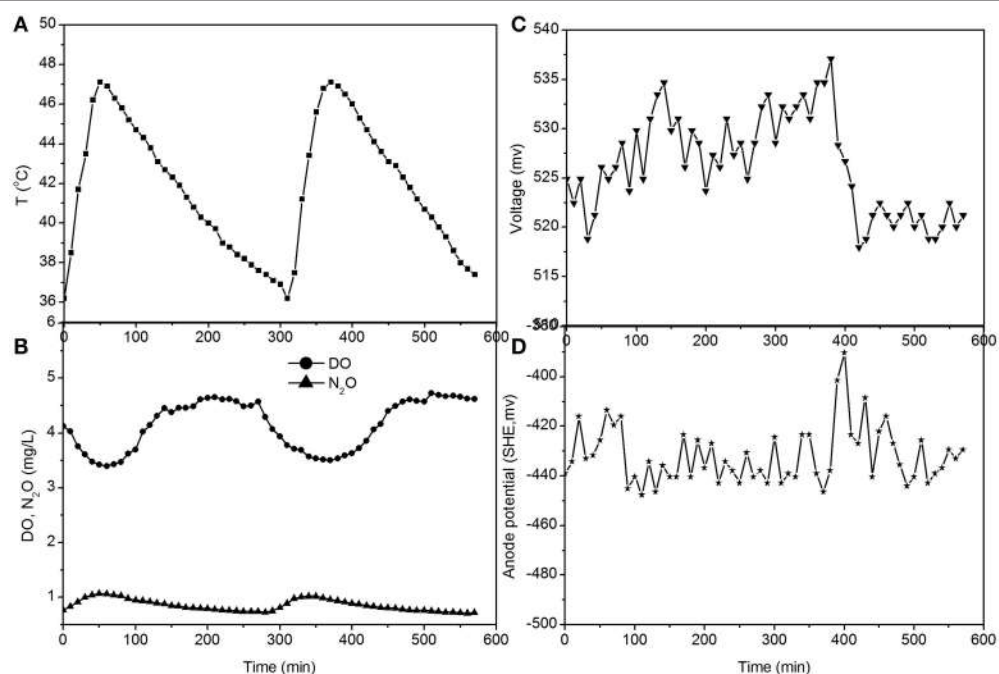


FIGURE 5 | Profiles of temperature, DO, N_2O , voltage, and anode potential of the MFC in open circuit at temperatures of 36–48°C (day 97 in Figure 2). **(A)** Temperature profile; **(B)** DO and N_2O profiles; **(C)** voltage profile; **(D)** anode potential profile.

The N_2O production and TN removal efficiencies with a 50Ω external resistance were higher than those with a 100Ω resistance, which illustrates that electrode denitrification

occurred in the cathode of the MFC. These analyses indicate that both oxygen and nitrite can obtain electrons simultaneously from the electrode in the cathode of the MFC.

Performance of the Microbial Community at Low DO and High Temperature

Biofilm samples were collected from the cathode chamber of the MFC on day 27 in stage 2 (**Figure 2**) and day 83 in stage 4 (**Figure 2**). The representative DGGE strips are shown in **Figure 6**. The closest species and classification of each representative band in the DGGE profile were deposited in the GenBank database (**Tables 1, 2**). Sequences from DGGE bands are shown in Supplementary Material.

In the first microbial identification (27th day), which corresponded to the low DO and high temperature MFC operating conditions (stage 2 in **Figure 2**), 12 bands were identified (**Table 1**). The results showed that the microbial community could be divided into 4 phyla, 4 classes and 8 genera. The phylum *Firmicutes* (bands 2, 3, 4, 5, 7, 8, 9, 10, and 13) was the predominant bacteria, while the phyla *Ignavibacteriae* (band 1), *Chloroflexi* (band 6) and *Proteobacteria* (band 14) were the subdominant groups.

Within the *Firmicutes* phylum, bands 2, 4, 5, 7, 8, and 9 belonged to the genus *Ureibacillus*, related to a species of *U. thermosphaericus* (similarity 91.2–100%), which was reported to be a thermophilic bacteria (37–60°C, optimum 50–60°C) with heterotrophic growth in aerobic environments and no ability for nitrate reduction (Fortina et al., 2001). This species was inferred to dominate the nitrification in the cathode of the MFC under low DO and high temperature conditions.

Bands 1 and 6 belonged to the genera *Ignavibacterium* and *Unclassified Anaerolineaceae*, respectively, which grow under anaerobic conditions, are heterotrophic and cannot utilize nitrate as electron acceptors (Yamada et al., 2006; Iino et al., 2010). These species were inferred to dominate the anaerobic degradation of COD.

Bands 3 (1) and 13 belonged to the genera *Geobacillus* and *Anoxybacillus*, respectively, which grow under aerobic conditions, are heterotrophic and can reduce nitrate (Poli et al., 2006; Inan et al., 2013). These species were inferred to dominate the aerobic denitrification.

Bands 3 (2) and 10 belonged to the genera *Anoxybacillus* and *Bacillus*, respectively, which grow under anaerobic conditions, are heterotrophic and can reduce nitrate (Kim et al., 1998; Cihan et al., 2014). These two species were inferred to be responsible for the anaerobic denitrification in stage 2 (**Figure 2**).

Band 14 belonged to the genus *Cucumibacter*, which grows under aerobic conditions, is heterotrophic and cannot utilize nitrate as electron acceptors (Hwang and Cho, 2008). This species was inferred to be responsible for the aerobic degradation of COD in stage 2 (**Figure 2**).

Performance of the Microbial Community at High DO and High Temperature

In the second microbial identification (83th day), which corresponded to the high DO and high temperature MFC operating conditions (stage 4 in **Figure 2**), 7 bands were identified (**Table 2**). The results showed that the microbial community could be divided into 1 phylum, 7 classes and 8 genera. The phylum *Proteobacteria* (bands 15, 18, 24, 25, 26,

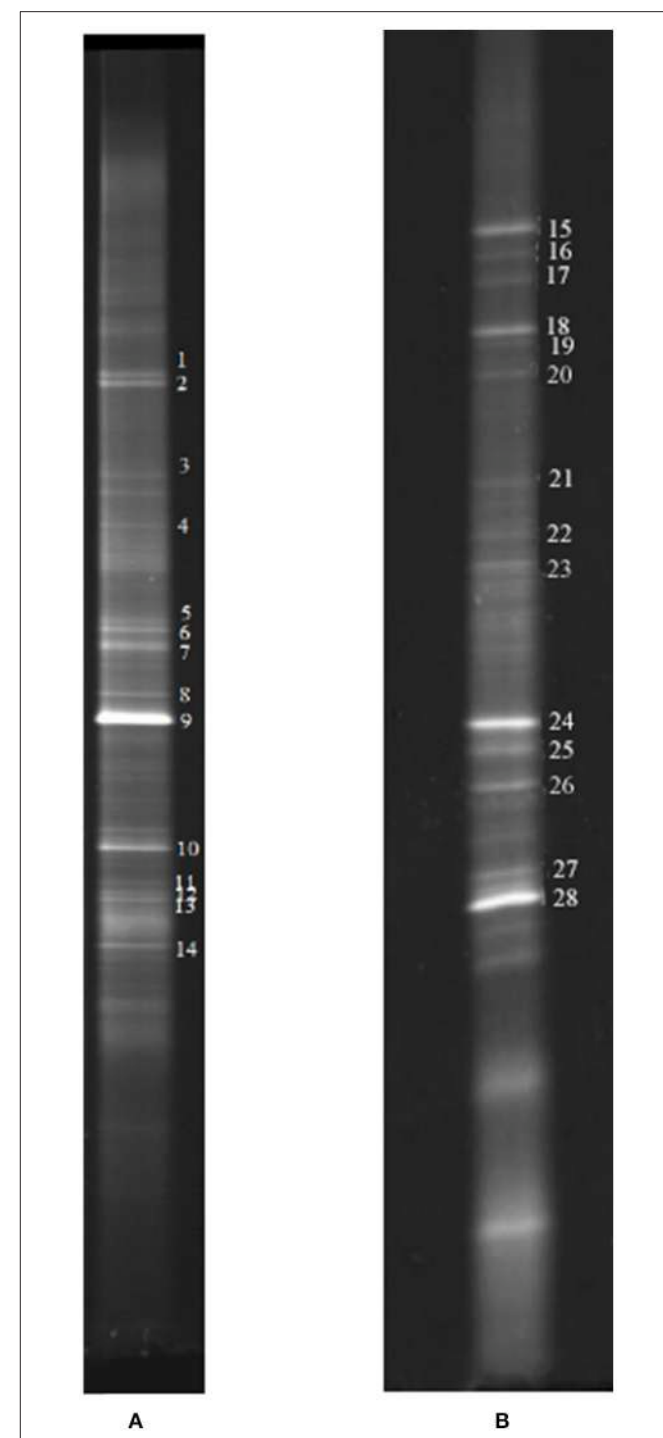


FIGURE 6 | Representative DGGE strips of samples. (A) Sampling at low DO levels (first sampling); **(B)** sampling at high DO levels (second sampling).

27, and 28) was the predominant and unique phylum. This result agrees with other studies that indicated that *Proteobacteria* dominates some cathodic denitrifying biofilms (Wrighton et al., 2010).

In the phylum *Proteobacteria*, bands 15, 24 and 27 belonged to the genera *Aquamicrobium*, *Alishewanella*, and *Brachymonas*

TABLE 1 | Identification of DGGE bands under low DO conditions (the first sampling; Figure 6A).

Band	Taxon	Similarity (%)	Accession	Phylum/Genus	Properties
2	<i>Ureibacillus thermosphaericus</i>	91.2	AF403017	<i>Firmicutes/Ureibacillus</i>	Aerobic, thermophilic, grows at 37–60°C, optimum at 50–60°C, negative for nitrate reduction, anaerobic growth, acid production from glucose (Fortina et al., 2001).
4	As above	100	As above	As above	
5	As above	94.6	As above	As above	
8	As above	92.5	As above	As above	
9	As above	97.3	As above	As above	
7	As above	95.7	As above	As above	
10	<i>Bacillus</i> sp. R-7413	100	AY422985	<i>Firmicutes/Bacillus</i>	Heterotrophic, anaerobic, nitrate reduction, optimum at 70°C (Kim et al., 1998)
13	<i>Anoxybacillus kaynarcensis</i>	97.3	EU926955	<i>Firmicutes/Anoxybacillus</i>	Heterotrophic, aerobic, can reduce nitrate to nitrite, grows from approximately 35 to 70°C, optimum at 60°C (Inan et al., 2013).
3	<i>Geobacillus toebii</i>	92.4	EU428777	<i>Firmicutes/Geobacillus</i>	Heterotrophic, aerobic, nitrate and nitrite reduction positive, grows from 55 to 75°C, optimum at 68°C (Poli et al., 2006).
	<i>Anoxybacillus calidus</i>	100	FJ430012	<i>Firmicutes/Anoxybacillus</i>	Facultatively anaerobic, heterotrophic, N ₂ gas produced from nitrate, 35–70°C, optimum at 55°C (Cihan et al., 2014).
1	Uncultured planctomycete	100	GQ35	<i>Ignavibacteriae/Ignavibacterium</i>	Refers to a strain of <i>Ignavibacterium album</i> Mat9-16T, strictly anaerobic, heterotrophic, grows at 30–55°C, optimum at 45°C (lino et al., 2010).
6	Uncultured <i>Chloroflexi</i> bacterium	83.4	JN825481	<i>Chloroflexi/Unclassified Anaerolineaceae</i>	Refers to a strain of <i>Anaerolinea thermolimosa</i> IMO-1T, strictly anaerobic, heterotrophic bacteria, cannot utilize nitrate as electron acceptors, grows at 42–55°C optimum at 50°C (Yamada et al., 2006).
14	<i>Cucumibacter marinus</i> (T)	96.8	EF211830	<i>Proteobacteria/Cucumibacter</i>	Heterotrophic aerobic bacteria, cannot reduce nitrate to nitrite, grows at 15–40°C, optimum at 30–35°C (Hwang and Cho, 2008).

TABLE 2 | Identification of DGGE bands under high DO conditions (second sampling; Figure 6B).

Band	Taxon	Similarity (%)	Accession	Phylum/Genus	Properties
15	<i>Aquamicrobiump aestuarii</i>	100	GU199003	<i>Proteobacteria/Aquamicrobiump</i>	Grows at 15–45°C, optimum at 30–35°C, can reduce nitrate to nitrite, strictly aerobic, heterotrophic bacteria (Jin et al., 2013).
25	<i>Brevundimonas diminuta</i>	98.1	X87274	<i>Proteobacteria/Brevundimonas</i>	<i>Brevundimonas</i> gen. nov. is aerobic, grows at 30–37°C, cannot reduce nitrate, 90% of the strains are autotrophic (Segers et al., 1994).
26	Uncultured bacterium	95.7	EF173342	<i>Proteobacteria/Altererythrobacter</i>	Refers to <i>Altererythrobacter epoxidivorans</i> JCS350T, cannot reduce nitrate, grows at 20–40°C, aerobic, optimum at 35°C, heterotrophic bacteria (Kwon et al., 2007).
18	<i>Pelomonas saccharophila</i> (T)	100	AB021407	<i>Proteobacteria/Pelomonas</i>	Grows at 4–40°C, optimum at 25–32°C, aerobic, able to fix nitrogen and show autotrophic growth with hydrogen but not photoautotrophic. Glucose and acetate are utilized as carbon sources for growth but negative for denitrification (Xie and Yokota, 2005).
27	<i>Brachymonas</i> sp. canine oral taxon 015	89.4	JN713175	<i>Proteobacteria/Brachymonas</i>	Refers to <i>Brachymonas denitrificans</i> , aerobic, denitrification positive, grows at 10–40°C, optimum at 30–35°C (Hiraishi et al., 1995).
	<i>Comamonas denitrificans</i>	87.8	AF233876	<i>Proteobacteria/Comamonas</i>	Grows at 20, 30, and 37°C, aerobic, heterotrophic, can reduce nitrate to nitrogen gas and contains cd1-type nitrite reductase (the only species in the genus <i>Comamonas</i> to do so) (Xing et al., 2010).
24	<i>Alishewanella</i> sp. N5	90.1	EU287929	<i>Proteobacteria/Alishewanella</i>	Refers to <i>Alishewanella aestuarii</i> , grows at 18–44°C, aerobic, optimum at 37°C, can reduce nitrate to nitrite and nitrogen gas, maltose is assimilated, heterotrophic bacteria (Roh et al., 2009).
28	<i>Acinetobacter gyllenbergii</i> (T)	100	AJ293694	<i>Proteobacteria/Acinetobacter</i>	Strictly aerobic, grows at 25–37°C, incapable of dissimilative denitrification, heterotrophic bacteria (Nemec et al., 2009).

or *Comamonas*, respectively. These three species can grow under aerobic conditions, are heterotrophic, can utilize nitrate as electron acceptors (Hiraishi et al., 1995; Roh et al., 2009; Jin et al., 2013) and were inferred to dominate the aerobic denitrification under the high DO conditions of stage 4 (Figure 2). In particular,

Comamonas denitrificans (band 27) has been reported to switch the metabolic pathway for extracellular electron transfer (Xing et al., 2010). A species in the *Comamonas* genus is known to be an aerobic denitrifier, and *C. denitrificans* is the only species in the *Comamonas* genus that can reduce nitrate to nitrogen

gas and contains cd1-type nitrite reductase (Gumaelius et al., 2001). Therefore, we propose that *C. denitrificans* be considered a species of ADB. The other two species were inferred to belong to ADB.

Bands 18, 26 and 28 belonged to the genera *Pelomonas*, *Altererythrobacter* and *Acinetobacter*, respectively. These three species can grow under aerobic conditions, are heterotrophic, cannot utilize nitrate as electron acceptors (Xie and Yokota, 2005; Kwon et al., 2007; Nemec et al., 2009) and might have dominated the aerobic degradation of COD in stage 4 (Figure 2).

Band 25 belonged to the genus *Brevundimonas*, which grows under aerobic conditions and cannot reduce nitrate, and 90% of the strains are autotrophic (Segers et al., 1994). This species was inferred to be a nitrifier.

Based on this analysis, at high temperatures, the increase in DO resulted in a change in the predominant species from thermophilic autotrophic nitrifiers and facultative heterotrophic denitrifiers at low DO concentrations to thermophilic ADB at high DO concentrations during the operation of the MFC. Three species from the genera *Aquamicrobiium*, *Brachymonas* or *Comamonas*, and *Alishewanella* were inferred to belong to ADB and dominate the aerobic denitrification at high levels of DO. Some aerobic denitrifiers were known to be heterotrophic nitrifiers, which might benefit SND under aerobic conditions. Therefore, autotrophic nitrifiers were replaced, and ADB evolved to be the predominant bacteria at high DO concentrations in stage 4 of the operation. This result is similar to the study by Feng et al., who indicated that aerobic denitrification in the cathode chamber is an

important pathway for nitrite and nitrate removal (Feng et al., 2015).

Mechanism of the Cathode Chamber

Based on the analysis of the composition of the microbial community and the experimental results, we speculated on the possible reactions in the cathode of the MFC (Figure 7).

The mechanism of aerobic denitrification was determined by studying the aerobic denitrifier *T. pantotropha*. The cooperative breathing theory, which was proposed by Robertson et al. (1988), is widely recognized as the aerobic denitrification mechanism. Cooperative breathing theory means that both NO_3^- and O_2 can be used as the final electron receptors. Therefore, the denitrifiers can transfer electrons from the reduced substance to NO_3^- or O_2 , and the denitrification can occur in an aerobic environment. According to the electron transport model proposed by Willson and Bouwer (1997), both NO_3^- and O_2 can be used as the final electron receptors, while the denitrifiers can transfer electrons from the reduced substance to O_2 or NO_3^- through nitrate reductase. Moreover, a carbon source is required for ADB. The higher the concentration of the carbon source is, the faster the aerobic denitrification rate will be (Robertson and Kuennen, 1983). Huang and Tseng (2001) indicated that the denitrification rate was highest when C/N was 5 and decreased with increasing C/N when C/N was greater than 5 and acetate was used as the carbon source. However, ADB did not appear to be required at such a high C/N ratio in our study. The influent C/N for the cathode chamber of the MFC was less than 0.3, possibly because the electrons provided by the electrode of the MFC were sufficient

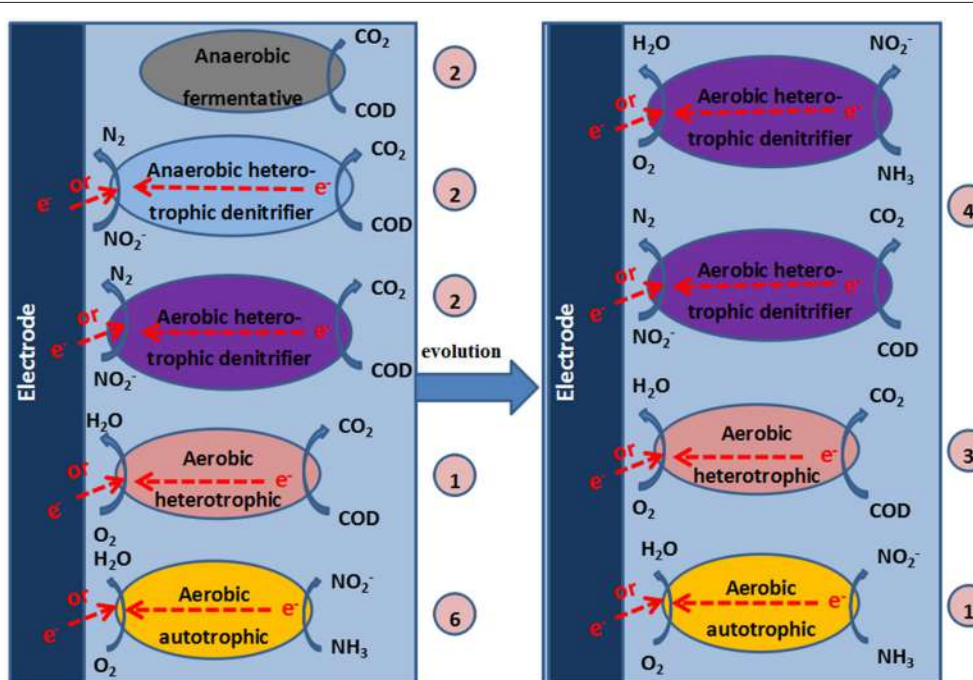


FIGURE 7 | Mechanisms in the cathode chamber of the MFC. The numbers in the circles represent the quantities of DGGE bands that correspond to the identified bacteria.

for the growth of aerobic bacteria. The aeration cathode chamber of the MFC may be beneficial for the growth of ADB.

Huang et al. indicated that DO was a key factor for aerobic denitrification (Xing et al., 2010). DO concentrations of 2–6 mg/L were beneficial for the growth of aerobic bacteria and the denitrification performance. As a result of the coexistence of aerobic respiration and the denitrifying reductase in one system, both O_2 and NO_x^- were indispensable for the growth of ADB and were used as electron acceptors. Therefore, at the high DO levels in this study (3.0–4.2 mg/L), the activity of ADB improved, and the denitrification performance of ADB was enhanced. The results that showed that the production of N_2O and the TN removal efficiency were higher with a 50 Ω external resistance than with a 100 Ω resistance at high levels of DO demonstrated that electrode denitrification with ADB occurred in the cathode of the MFC.

CONCLUSIONS

The increase of DO resulted in a change in the predominant species from thermophilic autotrophic nitrifiers and facultative heterotrophic denitrifiers at low DO levels to thermophilic ADB at high DO levels in the cathode of the MFC. The predominant phylum changed from *Firmicutes* to *Proteobacteria*, and the predominant class changed from *Bacilli* to *Alpha*, *Beta*, and *Gamma Proteobacteria*.

REFERENCES

- Bell, L. C., and Ferguson, S. J. (1991). Nitric and nitrous oxide reductases are active under aerobic conditions in cells of *Thiosphaera pantotropha*. *Biochem. J.* 273, 423–427. doi: 10.1042/bj2730423
- Chen, F., Xia, Q., and Ju, L. K. (2003). Aerobic denitrification of *Pseudomonas aeruginosa* monitored by online NAD(P)H fluorescence. *Appl. Environ. Microbiol.* 69, 6715–6722. doi: 10.1128/AEM.69.11.6715-6722.2003
- Cihan, A. C., Cokmus, C., Koc, M., and Ozcan, B. (2014). *Anoxybacillus calidus* sp. nov., a thermophilic bacterium isolated from soil near a thermal power plant. *Int. J. Syst. Evol. Microbiol.* 64(Pt 1), 211–219. doi: 10.1099/ijss.0.056549-0
- Clesceri, L., Greenberg, A. E., and Eaton, A. D. (1998). *Standard Methods for the Examination of Water and Wastewater*, 20th Edn. Washington, DC: American Public Health Association.
- Feng, C., Huang, L., Yu, H., Yi, X., and Wei, C. (2015). Simultaneous phenol removal, nitrification and denitrification using microbial fuel cell technology. *Water Res.* 76, 160–170. doi: 10.1016/j.watres.2015.03.001
- Ferguson, S. J. (1994). Denitrification and its control. *Antonie Van Leeuwenhoek*. 66, 89–110. doi: 10.1007/BF00871634
- Fortina, M. G., Pukall, R., Schumann, P., Mora, D., Parini, C., Manachini, P. L., et al. (2001). *Ureibacillus* gen. nov., a new genus to accommodate *Bacillus thermosphaericus* (Andersson et al. 1995), emendation of *Ureibacillus thermosphaericus* and description of *Ureibacillus terrenus* sp. nov. *Int. J. Syst. Evol. Microbiol.* 51, 447–455. doi: 10.1099/00207713-51-2-447
- Gumaelius, L., Magnusson, G., Pettersson, B., and Dalhammar, G. (2001). *Comamonas denitrificans* sp. nov., an efficient denitrifying bacterium isolated from activated sludge. *Int. J. Syst. Evol. Microbiol.* 51, 999–1006. doi: 10.1099/00207713-51-3-999
- He, Z., Kan, J., Wang, Y., Huang, Y., Mansfeld, F., and Nealson, K. H. (2009). Electricity production coupled to ammonium in a microbial fuel cell. *Environ. Sci. Technol.* 43, 3391–3397. doi: 10.1021/es803492c
- Hiraishi, A., Sugiyama, J., and Shin, Y. K. (1995). *Brachymonas denitrificans* gen. nov., sp. nov., an aerobic chemoorganotrophic bacterium which contains rhodoquinones, and evolutionary relationships of rhodoquinone producers to bacterial species with various quinone classes. *J. Gen. Appl. Microbiol.* 41, 99–117. doi: 10.2323/jgam.41.99
- Huang, H. K., and Tseng, S. K. (2001). Nitrate reduction by *Citrobacter diversus* under aerobic environment. *Appl. Microbiol. Biotechnol.* 55, 90–94. doi: 10.1007/s002530000363
- Huang, X., Li, W., Zhang, D., and Qin, W. (2013). Ammonium removal by a novel oligotrophic *Acinetobacter* sp. Y16 capable of heterotrophic nitrification-aerobic denitrification at low temperature. *Bioresour. Technol.* 146, 44–50. doi: 10.1016/j.biortech.2013.07.046
- Hwang, C. Y., and Cho, B. C. (2008). *Cucumibacter marinus* gen. nov., sp. nov., a marine bacterium in the family *Hyphomicrobiaceae*. *Int. J. Syst. Evol. Microbiol.* 58, 1591–1597. doi: 10.1099/ijss.0.65587-0
- Iino, T., Mori, K., Uchino, Y., Nakagawa, T., Harayama, S., and Suzuki, K. (2010). *Ignavibacterium album* gen. nov., sp. nov., a moderately thermophilic anaerobic bacterium isolated from microbial mats at a terrestrial hot spring and proposal of *Ignavibacterium* classis nov., for a novel lineage at the periphery of green sulfur bacteria. *Int. J. Syst. Evol. Microbiol.* 60, 1376–1382. doi: 10.1099/ijss.0.012484-0
- Inan, K., Belduz, A. O., and Canakci, S. (2013). *Anoxybacillus kaynarcensis* sp. nov., a moderately thermophilic, xylanase producing bacterium. *J. Basic Microbiol.* 53, 410–419. doi: 10.1002/jobm.201100638
- Janicek, A., Fan, Y., and Liu, H. (2014). Design of microbial fuel cells for practical application: a review and analysis of scale-up studies. *Biofuels* 5, 79–92. doi: 10.4155/bfs.13.69
- Jin, H. M., Kim, J. M., and Jeon, C. O. (2013). *Aquamicrombium aestuarii* sp. nov., a marine bacterium isolated from a tidal flat. *Int. J. Syst. Evol. Microbiol.* 63(Pt 11), 4012–4017. doi: 10.1099/ijss.0.048561-0
- Kim, J. K., Park, K. J., Cho, K. S., Nam, S. W., Park, T. J., and Bajpai, R. (2005). Aerobic nitrification-denitrification by heterotrophic *Bacillus* strains. *Bioresour. Technol.* 96, 1897–1906. doi: 10.1016/j.biortech.2005.01.040
- Kim, Y. O., Kim, H. K., Bae, K. S., Yu, J. H., and Oh, T. K. (1998). Purification and properties of a thermostable phytase from *Bacillus* sp. DSII. *Enzyme Microb. Technol.* 22, 2–7. doi: 10.1016/S0141-0229(97)00096-3

ADB is beneficial for achieving higher MFC voltages under high DO conditions, while traditional heterotrophic denitrification is conducive to higher TN removal under low DO conditions.

SND in the aeration cathode of the MFC may be beneficial for the growth of ADB.

AUTHOR CONTRIBUTIONS

JZ conceived and designed the experiments, and JW and SW performed the experiments. JW analyzed the data and wrote the paper, and JZ, SW, XL, BH, and XD reviewed and edited the manuscript. All of the authors approved the manuscript to be published and agreed to be accountable for all aspects of the work and for questions related to the accuracy of the results.

ACKNOWLEDGMENTS

This study was supported by the Shaanxi Province Science and Technology Development Program (2014K15-03-02).

SUPPLEMENTARY MATERIAL

The Supplementary Material for this article can be found online at: <http://journal.frontiersin.org/article/10.3389/fmicb.2017.00009/full#supplementary-material>

- Kuntke, P., Smiech, K. M., Bruning, H., Zeeman, G., Saakes, M., Sleutels, T. H., et al. (2012). Ammonium recovery and energy production from urine by a microbial fuel cell. *Water Res.* 46, 2627–2636. doi: 10.1016/j.watres.2012.02.025
- Kwon, K. K., Woo, J. H., Yang, S. H., Kang, J. H., Kang, S. G., Kim, S. J., et al. (2007). *Altererythrobacter epoxidivorans* gen. nov., sp. nov., an epoxide hydrolase-active, mesophilic marine bacterium isolated from cold-seep sediment, and reclassification of *Erythrobacter luteolus* Yoon et al. 2005 as *Altererythrobacter luteolus* comb. nov. *Int. J. Syst. Evol. Microbiol.* 57, 2207–2211. doi: 10.1099/ijjs.0.64863-0
- Li, C., Yang, J., Wang, X., Wang, E., Li, B., He, R., et al. (2015). Removal of nitrogen by heterotrophic nitrification-aerobic denitrification of a phosphate accumulating bacterium *Pseudomonas stutzeri* YG-24. *Bioresour. Technol.* 182, 18–25. doi: 10.1016/j.biortech.2015.01.100
- Li, W. W., Yu, H. Q., and He, Z. (2014). Towards sustainable wastewater treatment by using microbial fuel cells-centered technologies. *Energy Environ. Sci.* 7, 911–924. doi: 10.1039/c3ee43106a
- Nemec, A., Musilek, M., Maixnerová, M., De Baere, T., van der Reijden, T. J., Vaneechoutte, M., et al. (2009). *Acinetobacter beijerinckii* sp. nov. and *Acinetobacter gyllenbergii* sp. nov., haemolytic organisms isolated from humans. *Int. J. Syst. Evol. Microbiol.* 59, 118–124. doi: 10.1099/ijss.0.001230-0
- Papen, H., and Von Berg, R. (1998). A most probable number method (MPN) for the estimation of cell numbers of heterotrophic nitrifying bacteria in soil. *Plant Soil* 199, 123–130. doi: 10.1023/A:1004243810473
- Poli, A., Romano, I., Caliendo, G., Nicolaus, G., Orlando, P., Falco, A. D., et al. (2006). *Geobacillus toeblii* subsp. *decanicus* subsp. nov., a hydrocarbon-degrading, heavy metal resistant bacterium from hot compost. *J. Gen. Appl. Microbiol.* 52, 223–234. doi: 10.2323/jgam.52.223
- Robertson, L. A., and Kuenen, J. G. (1983). *Thiosphaera pantotropha* gen. nov. sp. nov. a facultatively anaerobic facultatively autotrophic sulphur bacterium. *J. Gen. Microbiol.* 129, 2847–2855. doi: 10.1099/00221287-129-9-2847
- Robertson, L. A., and Kuenen, J. G. (1984). Aerobic denitrification: a controversy revived. *Arch. Microbiol.* 139, 351–354. doi: 10.1007/BF00408378
- Robertson, L. A., van Niel, E. W. J., Torremans, R. A. M., and Kuenen, J. G. (1988). Simultaneous nitrification and denitrification in aerobic chemostat cultures of *Thiosphaera pantotropha*. *Appl. Environ. Microbiol.* 54, 2812–2818.
- Roh, S. W., Nam, Y. D., Chang, H. W., Kim, K. H., Kim, M. S., Oh, H. M., et al. (2009). *Alishewanella aestuarrii* sp. nov., isolated from tidal flat sediment, and emended description of the genus *Alishewanella*. *Int. J. Syst. Evol. Microbiol.* 59(Pt 2), 421–424. doi: 10.1099/ijss.0.65643-0
- Segers, P., Vancanneyt, M., Pot, B., Torck, U., Hoste, B., Dewettinck, D., et al. (1994). Classification of *Pseudomonas diminuta* Leifson and Hugh 1954 and *Pseudomonas vesicularis* Büsing, Döll, and Freytag 1953 in *Brevundimonas* gen. nov. as *Brevundimonas diminuta* comb. nov. and *Brevundimonas vesicularis* comb. nov., respectively. *Int. J. Syst. Bacteriol.* 44, 499–510. doi: 10.1099/00207713-44-3-499
- Takaya, N., Catalan-Sakai, M. A. B., Sakaguchi, Y., Kato, I., Zhou, Z., and Shoun, H. (2003). Aerobic denitrification bacteria that produce low levels of nitrous oxide. *Appl. Environ. Microbiol.* 69, 3152–3157. doi: 10.1128/AEM.69.6.3152-3157.2003
- Virdis, B., Rabaey, K., Rozendal, R. A., Yuan, Z., and Keller, J. (2010). Simultaneous nitrification, denitrification and carbon removal in microbial fuel cells. *Water Res.* 44, 2970–2980. doi: 10.1016/j.watres.2010.02.022
- Willson, L. P., and Bouwer, E. J. (1997). Biodegradation of aromatic compounds under mixed oxygen /denitrifying conditions: a review. *J. Ind. Microbiol. Biotechnol.* 18, 116–130. doi: 10.1038/sj.jim.2900288
- Wrighton, K. C., Virdis, B., Clauwaert, P., Read, S. T., Daly, R. A., Boon, N., et al. (2010). Bacterial community structure corresponds to performance during cathodic nitrate reduction. *ISME J.* 4, 1443–1455. doi: 10.1038/ismej.2010.66
- Xie, C. H., and Yokota, A. (2005). Reclassification of *Alcaligenes latus* strains IAM 12599T and IAM 12664 and *Pseudomonas saccharophila* as *Azohydromonas lata* gen. nov., comb. nov., *Azohydromonas australica* sp. nov. and *Pelomonas saccharophila* gen. nov., comb. nov., respectively. *Int. J. Syst. Evol. Microbiol.* 55, 2419–2425. doi: 10.1099/ijss.0.63733-0
- Xing, D., Cheng, S., Logan, B. E., and Regan, J. M. (2010). Isolation of the exoelectrogenic denitrifying bacterium *Comamonas denitrificans* based on dilution to extinction. *Appl. Microbiol. Biotechnol.* 85, 1575–1587. doi: 10.1007/s00253-009-2240-0
- Yamada, T., Sekiguchi, Y., Hanada, S., Imachi, H., Ohashi, A., Harada, H., et al. (2006). *Anaerolinea thermolimosa* sp. nov., *Levilinea saccharolytica* gen. nov., sp. nov. and *Leptolinea tardivitalis* gen. nov., sp. nov., novel filamentous anaerobes, and description of the new classes *Anaerolineae classis* nov. and *Caldilineae classis* nov. in the bacterial phylum Chloroflex. *Int. J. Syst. Evol. Microbiol.* 56, 1331–1340. doi: 10.1099/ijss.0.64169-0
- Zhang, Y., and Angelidaki, I. (2012). Bioelectrode-based approach for enhancing nitrate and nitrite removal and electricity generation from eutrophic lakes. *Water Res.* 46, 6445–6453. doi: 10.1016/j.watres.2012.09.022
- Zhang, Y., and Angelidaki, I. (2013). A new method for *in situ* nitrate removal from groundwater using submerged microbial desalination denitrification cell (SMDDC). *Water Res.* 47, 1827–1836. doi: 10.1016/j.watres.2013.01.005
- Zhang, Y., and Angelidaki, I. (2015). Submersible microbial desalination cell for simultaneous ammonia recovery and electricity production from anaerobic reactors containing high levels of ammonia. *Bioresour. Technol.* 177, 233–239. doi: 10.1016/j.biortech.2014.11.079

Conflict of Interest Statement: The authors declare that the research was conducted in the absence of any commercial or financial relationships that could be construed as a potential conflict of interest.

Copyright © 2017 Zhao, Wu, Li, Wang, Hu and Ding. This is an open-access article distributed under the terms of the Creative Commons Attribution License (CC BY). The use, distribution or reproduction in other forums is permitted, provided the original author(s) or licensor are credited and that the original publication in this journal is cited, in accordance with accepted academic practice. No use, distribution or reproduction is permitted which does not comply with these terms.



Identification of Electrode Respiring, Hydrocarbonoclastic Bacterial Strain *Stenotrophomonas maltophilia* MK2 Highlights the Untapped Potential for Environmental Bioremediation

OPEN ACCESS

Edited by:

Yong Xiao,

Institute of Urban Environment
(Chinese Academy of Sciences),
China

Reviewed by:

Yingying Wang,

Nankai University, China
Shaohua Chen,

Agency for Science, Technology and
Research, Singapore

*Correspondence:

Krishnaveni Venkidusamy
krishnaveni.venkidusamy@
mymail.unisa.edu.au

Specialty section:

This article was submitted to
Microbiotechnology, Ecotoxicology
and Bioremediation,
a section of the journal
Frontiers in Microbiology

Received: 09 September 2016

Accepted: 24 November 2016

Published: 09 December 2016

Citation:

Venkidusamy K and Megharaj M
(2016) Identification of Electrode
Respiring, Hydrocarbonoclastic
Bacterial Strain *Stenotrophomonas*
maltophilia MK2 Highlights the
Untapped Potential for Environmental
Bioremediation.

Front. Microbiol. 7:1965.

doi: 10.3389/fmicb.2016.01965

Krishnaveni Venkidusamy^{1,2*} and **Mallavarapu Megharaj**^{1,2,3}

¹ Centre for Environmental Risk Assessment and Remediation, University of South Australia, Mawson Lakes, SA, Australia

² Cooperative Research Centre for Contamination Assessment and Remediation of the Environment, Mawson Lakes, SA, Australia, ³ Global Centre for Environmental Remediation, The University of Newcastle, Callaghan, NSW, Australia

Electrode respiring bacteria (ERB) possess a great potential for many biotechnological applications such as microbial electrochemical remediation systems (MERS) because of their exoelectrogenic capabilities to degrade xenobiotic pollutants. Very few ERB have been isolated from MERS, those exhibited a bioremediation potential toward organic contaminants. Here we report once such bacterial strain, *Stenotrophomonas maltophilia* MK2, a facultative anaerobic bacterium isolated from a hydrocarbon fed MERS, showed a potent hydrocarbonoclastic behavior under aerobic and anaerobic environments. Distinct properties of the strain MK2 were anaerobic fermentation of the amino acids, electrode respiration, anaerobic nitrate reduction and the ability to metabolize n-alkane components (C8–C36) of petroleum hydrocarbons (PH) including the biomarkers, pristine and phytane. The characteristic of diazoic dye decolorization was used as a criterion for pre-screening the possible electrochemically active microbial candidates. Bioelectricity generation with concomitant dye decolorization in MERS showed that the strain is electrochemically active. In acetate fed microbial fuel cells (MFCs), maximum current density of $273 \pm 8 \text{ mA/m}^2$ (1000Ω) was produced (power density $113 \pm 7 \text{ mW/m}^2$) by strain MK2 with a coulombic efficiency of 34.8%. Further, the presence of possible alkane hydroxylase genes (*alkB* and *rubA*) in the strain MK2 indicated that the genes involved in hydrocarbon degradation are of diverse origin. Such observations demonstrated the potential of facultative hydrocarbon degradation in contaminated environments. Identification of such a novel petrochemical hydrocarbon degrading ERB is likely to offer a new route to the sustainable bioremedial process of source zone contamination with simultaneous energy generation through MERS.

Keywords: electrode respiring bacteria, microbial electrochemical remediation systems, *Stenotrophomonas maltophilia* MK2, facultative hydrocarbon degradation, dye decolorization, catabolic genes (*alkB*, *rubA*)

INTRODUCTION

Due to their toxicity and ubiquitous nature, petroleum hydrocarbons (PH) are of serious concern to the environmental and public health. Of these PH contaminants, diesel range organics (DRO) is constitute one of the most prevalent organic pollutants that are biodegradable in various environments. Medium chain hydrocarbons from octane to the long chain hydrocarbon dotriacontane are the constituents of DRO. They are usually assumed to be the fractional middle distillate of crude oil and are known to be highly noxious, hazardous, and carcinogenic (Chilcott, 2011). Increasing anthropogenic activities of these compounds leading to spillages, and leakages from underground storage tanks constitute the two dominant sources of penetration of DRO compounds from surface soils to subsurface. As an ultimate result, DRO became the most encountered environmental pollutants in groundwater and soils (Gallego et al., 2001). Consequently, horizons of subsoil, aquifer and groundwater systems are prone to long-term contamination of these hydrophobic contaminants. Microbial clean-up of these DRO compounds is claimed to be an efficient, economical, and versatile alternative to the established physicochemical treatments that are prone to cause recontamination by secondary contaminants (Hong et al., 2005; Megharaj et al., 2011). The biodegradation of these compounds at the surface has been well documented for a century whereas subsurface biodegradation awaits further research on deeper insights into the metabolic activities involved and the extent and rate of hydrocarbon degradation (Röling et al., 2003). Subsurface hydrocarbon contaminated reservoirs are primarily dominated by obligate and facultative anaerobic microbial communities. These microbial communities can adjust their metabolism to take account of the availability of final electron acceptors and can have more complex enzymatic systems involved in the degradation of contaminants. However, the rate of microbial utilization of these PH compounds is very slow especially under anaerobic environments where the availability of relevant electron acceptors is limited (Morris et al., 2009).

Recent research on removal of such recalcitrant contaminants using advanced microbial electrochemical systems is gaining new interest in its practical applications involved in subsurface hydrocarbon bioremediation. These microbial electrochemical remediation systems (MERS) transform the chemical energy available in organic pollutants into electrical energy by capitalizing on the biocatalytic potential of a peculiar group of microbes called “electric communities” (Logan, 2008; Morris et al., 2009). These electric microbial communities have received much attention in the field of electromicrobiology because of their exoelectrogenic capabilities to degrade substrates that range from easily degradable natural organic compounds to xenobiotic compounds such as PH contaminants (Venkidusamy and Megharaj, 2016; Venkidusamy et al., 2016; Zhou et al., 2016). Many studies have shown the predominance of many strains and species of *Geobacter* in microbial fuel cells (MFCs) fed with different types of substrates. However, the microbial community composition is divergent in MERS (Morris et al., 2009; Venkidusamy et al., 2016), and the

physiology of such populations remains to be explored in detail. The identification of such bacterial population with dual functions of electrode respiration and petrochemical degradation highlights the biotechnological potential involved in sustainable remediation of PH contaminated sites and MERS. We have therefore attempted to (i) find representative microbial candidates with such abilities of hydrocarbonoclastic electrode respiration through the anode enrichment of MERS, (ii) demonstrate the bioremediation potential of isolated bacteria to completely mineralize DRO compounds in anoxic environments and (iii) also investigate the presence of catabolic genes responsible for hydrocarbon degradation in these bacteria.

MATERIALS AND METHODS

Source of Chemicals

Refined fossil fuels such as DRO and other PH products used throughout the study were obtained from local BP outlet (Australia). Aliphatic hydrocarbon standards, solvents such as hexane and methylene chloride, redox indicators such as 2–6, dichlorophenol indophenol (DCPIP), and tetrazolium violet (2, 5-diphenyl-3-[α -naphthyl] tetrazolium chloride) and diazo dyes were purchased from Sigma Aldrich Trading Co. Ltd (Australia). All the solvents used were of HPLC grade.

Bacterial Strain, Media, and Culture Conditions

The bacterial strain MK2 was isolated from the anodic biofilm of a MERS fed with hydrocarbons operated in a fed-batch mode over a period of 12 months. Hydrocarbons contaminated groundwater (RAAF Base, Williamstown, NSW, Australia) and activated sludge (WTP, South Australia) served as inoculum for these PH fed MERS. Bacterial cells from the anodic biofilm were extracted into a sterile phosphate buffer and shaken vigorously to separate cells from the electrode. Aliquots of the extracted cell suspensions were serially diluted and plated onto mineral salt medium (MSM) agar (Grishchenkov et al., 2000) containing 1% DRO compounds and incubated for 3 weeks. Single colonies were selected and transferred to Luria Bertani (LB) agar plates. Unless otherwise stated all incubations were performed at room temperature. Media used throughout the study were Bushnell Hass (Hanson et al., 1993), mineral salts medium (Grishchenkov et al., 2000) and Luria-Bertani medium (Sambrook et al., 1989). Nitrate served as the terminal electron acceptor in anaerobic biodegradation experiments. A chemically defined medium supplemented with Wolfe's trace elements and vitamins was used in the microbial electrochemical studies as previously described (Oh et al., 2004). One liter of growth medium contains ($g\ l^{-1}$) KCl 0.13, Na₂HPO₄ 4.09, NaH₂PO₄ 2.544, NH₄Cl 0.31. The pH of the medium was adjusted to 7 ± 0.2 and further fortified with Wolfe's trace elements and vitamins. The purified strain was stored in glycerol: Bushnell Hass broth and glycerol: Luria-Bertani broth (1:20) at -80°C . Biolog-GN2 (Biolog, USA) plates were used to determine the utilization of various carbon sources according to the manufacturer's instructions.

Bacterial 16S rRNA Gene Sequencing

Genomic DNA of strain MK2 was extracted from aerobically grown cells using the UltraClean microbial DNA isolation kit (MO BIO, CA, USA) following the manufacturer's instructions. The polymerase chain reaction (PCR) mediated amplification of 16S rRNA gene fragments was performed using the combination of universal primers, E8F (5'-AGAGTTGATCCTGGCTCAG3') and 1541R (5'AAGGAGGTGATCCANCCRCA 3') (Weisburg et al., 1991). The PCR products were purified using the UltraClean PCR clean-up kit (Mo Bio, Carlsbad, CA, USA) following the manufacturer's instructions and sequenced in both directions using an automated sequencer, ABI3130 Sequencer (Applied Biosystems, USA) at the Southern Pathology Sequencing Facility, Flinders Medical Centre (South Australia). 16S rRNA sequences were analyzed using the BLAST programme against the NCBI databases. The highest hit obtained through blastn match for the strain MK2 was used for ClustalW multiple alignment and generating a phylogenetic relationship. The neighbor joining tree was constructed using the molecular evolutionary genetic analysis package version 5.0 based on 1000 bootstrap values (Tamura et al., 2011). The 16S rRNA sequence of strain MK2 was deposited in GenBank under accession number JQ316533.

Assessment of Biodegradation Potential and Electrochemical Activity

The hydrocarbonoclastic potential of strain MK2 was evaluated by measuring the reduction of metabolic indicators such as dichlorophenol indophenol and tetrazolium salts (Piröllo et al., 2008). Experiments were also conducted to pre-screen the possible candidate electroactive bacterial strains by *in vivo* biodecolourization assay using diazo dyes as stated earlier (Hou et al., 2009). Experiments were carried out in both aerobic and anaerobic environments using 20 ml of nutrient broth with different concentrations (50, 100, 150 mg l⁻¹) of an azo dye, Reactive Black5 (RB5). The dye degradation was monitored by observing the decrease in absorbance of suspension at 595 nm under a UV-visible spectroscopy system (Agilent model 8458). All decolorization studies were conducted in triplicate for each experiment, and the activity was expressed as percentage degradation as follows:

$$\text{Percentage of dye decolorization} = \frac{A_i - A_t}{A_i} \times 100$$

where A_i = initial absorbance and A_t = observed absorbance at designated intervals.

Hydrocarbon Biodegradation Experiments

To obtain 1 OD culture, overnight grown bacterial cells were centrifuged for 20 min at 4500 rpm. The cell pellet was washed three times and re-suspended in MSM until the OD₆₀₀ was equivalent to 1.00. One percent of the 1 OD culture of strain MK2 was transferred to 100 ml of MSM with a concentration of 8000 mg l⁻¹ of DRO and incubated at 25 °C for time course experiments with shaking at 150 rpm. The cell growth was determined by the comparison of optical density against

the control at designated time intervals. Hydrocarbonoclastic potential was also monitored under anaerobic nitrate reducing environments. The inoculum size was 1% of the anaerobically grown bacterial cells with nitrate (10 mM) and 8000 mg l⁻¹ of DRO as an electron acceptor and donor, respectively from an anoxic sterile stock solution. All cell cultures were maintained in triplicate for each experiment. All procedures for anoxic growth experiments, from medium preparation to manipulating the strain were performed using standard anoxic conditions. All culturing was done in sealed serum vials with nitrogen/carbon dioxide (80:20, v/v) in the headspace. The sealed vials were incubated at 25°C for time course experiments with shaking at 150 rpm. An uninoculated control was prepared for each set of biodegradation experiments. The samples from the time course experiments of aerobic and anaerobic incubations were extracted three times with 1:1 solvent mixture of acetone-methylene chloride, dewatered and concentrated by an evaporator. The evaporated hydrocarbons were taken as residual hydrocarbons and dissolved in n-hexane, filtered through 0.25 µm membrane filters and analyzed by gas chromatography.

Fuel Cell Experiments

MFC Construction and Operational Conditions

Single chamber MFC systems were constructed from laboratory bottles (320 ml capacity, Schott) as previously described (Logan et al., 2007) with a modification to increase electrode area. The anode electrodes composed of carbon fiber brushes with wire titanium cores that had an initial surface area of 6.99 m² g⁻¹. These fiber electrodes were cleaned by soaking overnight in acetone followed by pre-treatment with sulfuric acid (concentrated, 100 ml l⁻¹) and heat treatment to improve the geometric surface area of the electrodes as described by Feng et al. (2010). The cathode was fabricated using flexible carbon cloth coated with a hydrophobic PTFE layer (Cheng et al., 2006) with additional diffusional layers on the air breathing side to cut down fouling rate and evaporation of hydrocarbons. In contrast, the hydrophilic side was coated using a mixture of nafton perfluorinated ion exchange ionomer binder solution, carbon, and platinum catalyst (0.5 g of 10% loading). The electrodes were connected using copper wire with all exposed metal surfaces sealed with a non-conductive epoxy resin (Jay Car, Australia). All the reactors were sterilized before use. Strain MK2 was used for microbial electrochemical experiments with acetate (1 g l⁻¹) as the electron donor in 50 mM PBS buffer. The anodic chamber was flushed for 30 min with nitrogen gas before the operation. The anolyte was agitated using a magnetic stirrer operating at 100 rpm. Open circuit MFC studies were also carried out and then switched to the closed circuit with a selected external load (R-1000 Ω unless stated otherwise). Reactive Black 5 was used as sole source of energy in dye degradation experiments using the strain MK2 at a concentration of 50 mg l⁻¹ in MFC studies. LB medium was used in biodecolorization studies with an external load of 1000 Ω. MFCs were operated in a fed-batch mode until the voltage fell to a low level (<10 mV), and then the anolyte solution was replaced under anaerobic chamber (10% hydrogen, 10% carbon dioxide and 80% nitrogen) (Don Whitley Scientific,

MG500, Australia) conditions. All the reactors were maintained at room temperature in triplicates.

Cloning and Phylogenetic Analysis of Possible Catabolic Genes for Hydrocarbon Degradation

Genes encoding alkane hydroxylase enzyme complex including *alk* and *rub* genes were amplified by a polymerase chain reaction (PCR) method using oligonucleotides listed in Table S1. The PCR mix of 50 μ l contained the following: 10 μ l of Gotaq 5X buffer, 2.0 μ l of MgCl₂ (25 mM), 1 μ l of dNTP mix (10 mM), 2 μ l of each primer (100 mM), 10–15 ng of purified DNA and 2.5 U taq DNA polymerase (Promega, Australia). Cycling was performed with an initial denaturation for 5 min, followed by 35 cycles of 60 s at 94°C, 30 s of annealing at 40–60°C, 60 s of extension at 72°C and a final extension at 72°C for 10 min, using a Bio-Rad thermal cycler. The primers were designed based on the available draft genomes of *S. maltophilia* using Primer-BLAST tool from NCBI and assessed by Oligo 6 software. The amplification products were purified using the UltraClean PCR clean-up kit (Mo Bio, CA) and ligated into the pGEM-T-Easy vector. After transformation into *E. coli* DH5 α individual plasmid inserts were sequenced. *In silico* analysis was done by using the blast programs to search the GenBank and NCBI databases (<http://www.ncbi.nlm.nih.gov>).

Analytical Methods and Calculations

Cell voltage was monitored using a DMM (Keithly Model 2701, USA) linked to a multi-channel scanner (Module 7700, Keithly Instruments, USA). Data were recorded digitally on an Intel computer via IEEE 488 input system and Keithly cable. To measure the current under closed circuit conditions, the external resistance was connected (R-1000 Ω unless stated otherwise). Polarization curves were obtained using various external loads ranging from 10 Ω to open circuit. Current was calculated by using $I = V/R$. The power density was calculated as follows; where V was the cell voltage, I was electrical current and A denoted the electrode surface area. Power density and current density were normalized to the projected surface area of a cathode (Logan, 2008).

$$P = \frac{V \cdot I}{A} \quad (1)$$

Coulombic efficiency (CE) was calculated at the end of the cycle from COD removal as follows (Logan, 2008),

$$CE (\%) = \frac{M \int_0^t I \cdot dt}{F b q \Delta COD} \times 100 \quad (2)$$

where, M is the molecular weight of the substrate, F = Faraday's constant, b = number of electron exchanged/1 M of oxygen, Vn = volume of liquid in the anode chamber, ΔCOD = difference in the COD of initial and end batch samples from MFCs. Graphite fiber surface area was also measured using a Brunauer–Emmett–Teller (BET) isotherm (Mi micromeritics, Gemini V, Particle and Surface Science Pty Ltd.) DRO degradation experiments were conducted using data from triplicate analyses. The DRO was

extracted in acetone-methylene chloride (1:1) mixture, dewatered and concentrated by an evaporator, and then analyzed with GC-FID (Flame Ionization Detector) using an HP-5 capillary column (15 m length, 0.32 mm thickness, 0.1 μ m internal diameter) (USEPA, 1996). The estimated recovery was more than 70%. The GC programme was set up according to USEPA (USEPA, 1996). The carrier gas was helium. The operational temperature ranged from 50 to 300°C with a programmed temperature gradient of 25°C/min. The resulting chromatograms were analyzed using Agilent software (GC-FID Agilent model 6890) to identify the petroleum degradation products (Venkidusamy et al., 2016).

RESULTS

Strain Isolation and Physiology

From the anodes of enriched PH fed MERS, a pure culture of facultative, hydrocarbonoclastic bacterial strain MK2 was isolated by serial dilution and plating techniques. Cells of strain MK2 contains double membrane bilayers, produces polar flagella in tufts or as single (Figure 1A) and grow as bacillus shaped (Figure 1B). Cell growth on nutrient agar medium produces large gleaming colonies which are pale yellow in color. The bacterial strain grew at temperatures ranging from 25 to 37°C at a neutral pH (optimum temperature 30°C), while no growth was detected above 40°C. The strain was negative for oxidase and catalase is present. The bacterial strain was shown to be capable of anaerobic growth through amino acid fermentation and anaerobic nitrate reduction through quantitative biochemical analysis. However, it was unable to metabolize sugars such as glucose and lactose through the anaerobic fermentation process. Cell growth was accompanied by the strong ammonia odor with pale green discoloration in old LB plates. The strain MK2 displayed a limited nutritional spectrum as highlighted by its genus name (Table S2). The strain was unable to utilize arabinose, adonitol, fructose, xylose, rhamnose, gluconate, etc., Salient properties of the strain MK2 were direct electrode respiration and the ability to degrade n-alkane components of PH in both aerobic and anaerobic environments.

Phylogenetic Analysis and Taxonomy

An almost complete 16S rRNA gene sequence (1448 bp) was obtained for strain MK2 and analyzed phylogenetically using ClustalW alignment. Using this multiple alignment, the neighborhood phylogenetic tree was constructed (Figure 2). The taxonomic position shows that the strain MK2 was a member of the *Stenotrophomonas* subgroup in the class of γ -proteobacteria. From a BLAST analysis, the highest level of sequence similarity (98%) matched with *Stenotrophomonas maltophilia* strain ATCC 13637.

Redox Indicator Assays for the Assessment of Hydrocarbonoclastic Potential

The hydrocarbonoclastic potential of strain MK2 was assessed through a preliminary investigation of hydrocarbon consumption, a concomitant increase in biomass and reduction of redox electron acceptors such as DCPIP and tetrazolium indicators. The strain MK2 discolored the redox indicator from

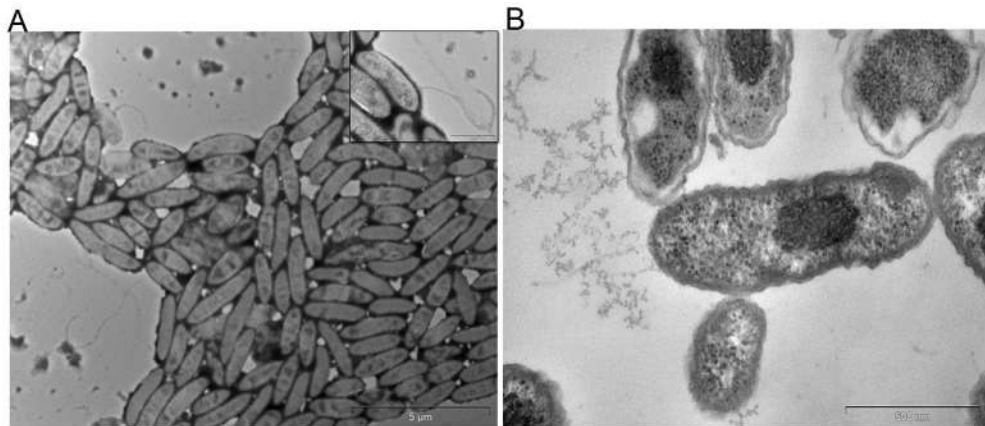


FIGURE 1 | Transmission electron micrographs of *S. maltophilia* MK2. Bar scale, 500 nm. **(A)** Cells with flagella. **(B)** Bacillus shaped cells of strain MK2.

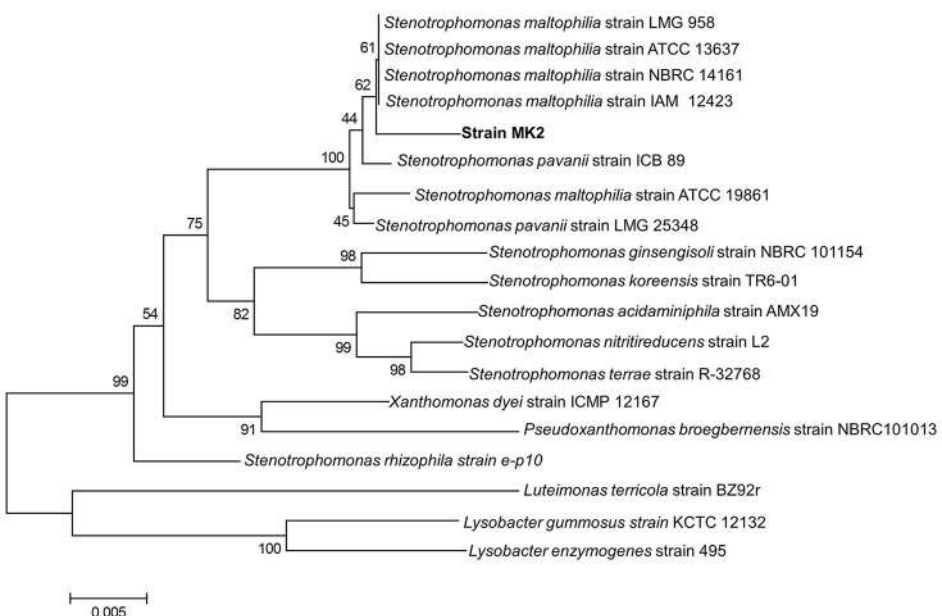


FIGURE 2 | Phylogenetic tree based on 16S rRNA sequences showing the positions of the strain MK2 and representatives of other *Stenotrophomonas* spp. The tree was constructed from 1448 aligned bases. Scale bar represents 0.005 substitution per nucleotide position.

the blue to violet during the first 24 h and complete discoloration was observed by the end of 120 h when DRO was the sole carbon and energy source. Also, the formation of a red precipitate formazan from the tetrazolium was observed while the abiotic controls remained unchanged. It is evident from the above screening assays that the strain MK2 can utilize diesel derived hydrocarbons.

Screening Assays for the Assessment of Electrochemical Activity

To pre-screen the electrochemical activity of the strain MK2, aerobic and anaerobic cultures were grown in nutrient broth

supplemented with 50 mg l⁻¹ of RB5. This concentration was found to be supportive for a higher growth rate and rapid decolorization among the various concentration of RB5 tested. The complete disappearance of the characteristic absorption peak at the region of λ_{max} (597 nm) and simultaneous decolorization were observed in aerobic and anaerobically incubated samples (Figure 3). Figure 3A shows dynamic changes of the absorption spectra observed during the decolorization process under anaerobic conditions. RB5 azoic dye was almost completely decolorized (96.23%) in 48 h by *S. maltophilia* MK2 under anaerobic environments while it took 72 h for nearly complete decolorization (97.99%) under aerobic conditions

(Figure 3B). The blue pigmented dead cell pellet from the heat-killed cells in the control showed a passive adsorption of dye, whereas colorless cell pellets obtained from the living cultures demonstrated that reduction of the RB5 indicator had occurred.

Energy Generation by *S. maltophilia* MK2 in Microbial Electrochemical Cells

Current Generation in Acetate Fed MFCs

Current was generated in all the MFCs inoculated with *S. maltophilia* MK2 within a few hours using acetate as an energy source. After 3 days, voltage started to follow a constant pattern and then stabilized. The fuel cell electrodes were connected through a resistor ($R = 1000 \Omega$) once it reached the plateau voltage generation stage. The maximum output range of voltage and current density were 414 ± 7 mV, 273 ± 8 mA/m² ($R = 1000 \Omega$) after four cycles of operation. After five refilling batches with a fresh substrate, the maximum current output of each batch became stable (270 ± 5 mA/m²). Few representative cycles (average current density from triplicates) of current density are shown in Figure 4A. The maximum CE was 34.8% which corresponded to the maximum current density of 272.96 mA/m².

Current Generation and Simultaneous Dye Decolorization in Dye Fed Microbial Electrochemical Cells

The current was rapidly generated in azo dye fed MFCs inoculated with *S. maltophilia* MK2 cells within few hours of using azoic dye as an energy source at 1000Ω . The maximum output range of voltage and current density were 145 ± 6 mV, 94 ± 6 mA/m². Constant and repeatable power cycles were obtained during five changes of the contents of the anode chamber. Using RB5 concentration of 100 mg l^{-1} in MFC, $59.3 \pm 1.25\%$ was removed during the first 12 h of operation. After 24 h, almost $97.2 \pm 1.64\%$ of RB5 was decolorized and it was below detection limits at the end of the batch operation when the voltage of the batch reached >10 mV as shown in Figure 4B.

Hydrocarbonoclastic Potential of *S. maltophilia* MK2

Aerobic Biodegradation of DRO

To evaluate the hydrocarbon degradation potential of the strain MK2, experiments were performed under two different environments *viz.*, aerobic and anaerobic. The rate and extent

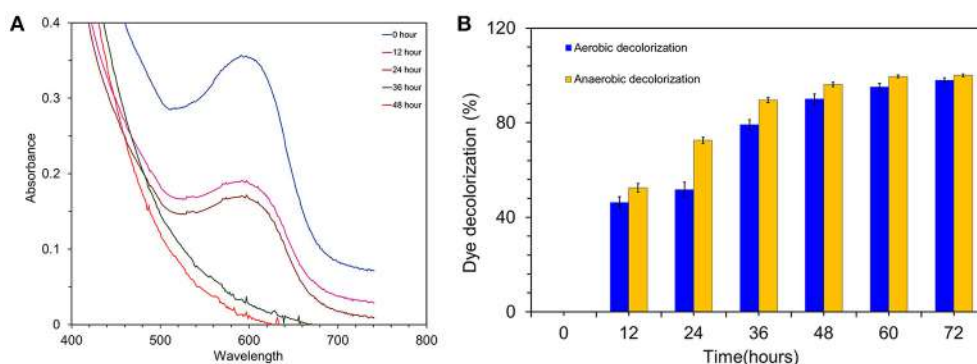


FIGURE 3 | (A) Time overlaid absorbance spectra of RB5 biodecolourization by the strain MK2. **(B)** Biodecolourization of diazoic dye RB5 by the strain *S. maltophilia* MK2 under aerobic and anaerobic environments.

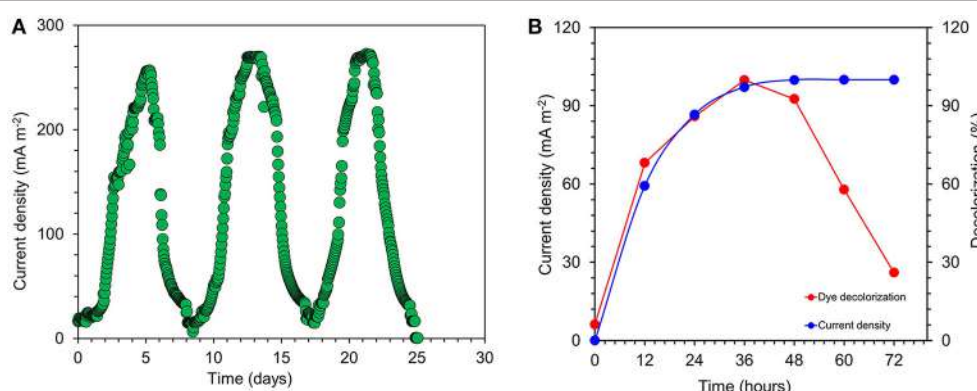


FIGURE 4 | (A) Few representative cycles of current density generated by *S. maltophilia* MK2 in acetate fed microbial fuel cells. **(B)** Current generation and simultaneous dye decolorization in dye fed MERS using *S. maltophilia* MK2.

of biodegradation were interpreted from GC chromatograms of the residual hydrocarbons. The aerobic incubation experiments indicated that the biodegradation of hydrocarbons by strain MK2 was more efficient than anaerobic incubations. **Figure 5A** shows the possible cell growth and its associated substrate degradation by strain MK2. For a substrate concentration of 8000 mg l^{-1} , cells started growing within 24 h with a rapid decrease in DRO concentration of about 53%. After 84 h, the strain reached a second peak of growth while the DRO degradation was 88%. The temporal removal of DRO reached $>90\%$ after 100 h of incubation. In general, the rate of degradation increased consistently with increasing cell biomass during the early stage of the exponential phase and then, it reached a plateau at stationary and death phase of cell growth. Abiotic loss of DRO was measured under each stage was less than 5%. The GC profile of the residual n-alkanes of DRO after the incubation was compared with that of the original as shown in Figure S1. At the end of the incubation period (150 h), the n-alkane members of C8 to C36 were almost completely metabolized in the samples inoculated with the strain MK2.

Anaerobic Biodegradation of DRO

The hydrocarbonoclastic activity of the strain MK2 was examined under anaerobic conditions with DRO as the sole source of carbon and nitrate as the final electron acceptor. The results indicated that the biodegradation of DRO (8000 mg l^{-1}) in anaerobic environments is slower in comparison to the aerobic degradation. **Figure 5B** shows the quantitative growth experiments with depletion of DRO at a time course within 14 days. The growth of strain MK2 was slow until 96 h of incubation and then reached a log phase by 100 h. The hydrocarbonoclastic potential was closely coincided with the phase of cell growth, as a result, degradation efficiency increased from the 2nd day to the 8th day of incubation, before leveling off from the 10th to the 12th day. By the 10th day, a complete degradation of the substrate had occurred. Figure S2 depicts the residual DRO concentration before and after incubation under anaerobic conditions.

Detection of Possible Catabolic Genes Involved in Hydrocarbon Degradation

The presence of specific catabolic genes (*alkB* and the related, *alkM*, *alkA*) encoding alkane hydroxylase enzyme complex was investigated by a PCR-mediated amplification with various oligonucleotide primers. Of the 15 different oligonucleotides combinations tested for PCR amplification, only the primer combination of the ALK3 set provided a positive result. Blastn searches in the GenBank database showed that the PCR product was similar to a number of known *alkB* genes, had a 96% match with the *alkB* gene encoding a putative alkane -1-monooxygenase from *Burkholderia* (**Figure 6**). In order to explore the presence of other functional genes from the strain MK2, new primers were designed to amplify the second cluster of the alkane hydroxylase complex (Table S1). A PCR product of the expected size was obtained when the primer combinations *rubF*, *rubR* used. Blastx alignments showed that this PCR product had 100% similarity to the corresponding region of the *S. maltophilia* rubredoxin type Fe(Cys)4 protein (**Figure 6**).

DISCUSSION

The enrichment of hydrocarbonoclastic Electrode respiring bacteria (ERB) able to utilize hydrocarbons as a sole source of carbon and energy in MERS led to the isolation of hydrocarbonoclastic bacterial strain identified as *S. maltophilia* MK2. *Stenotrophomonas* spp. are often considered to be ubiquitous, however, these species are frequently found in marine, soil, rhizosphere of diverse plants (Denton and Kerr, 1998) and polluted environments (Binks et al., 1995; Dungan et al., 2003; Lü et al., 2009) as their main environmental reservoirs. The representative candidate, *S. maltophilia* MK2 is a free living, facultatively anaerobic bacterium and phylogenetically placed in the phylum of Proteobacteria, Gammaproteobacteria, Xanthomonadales, Xanthomonadaceae (Palleroni and Bradbury, 1993). The environmental isolate

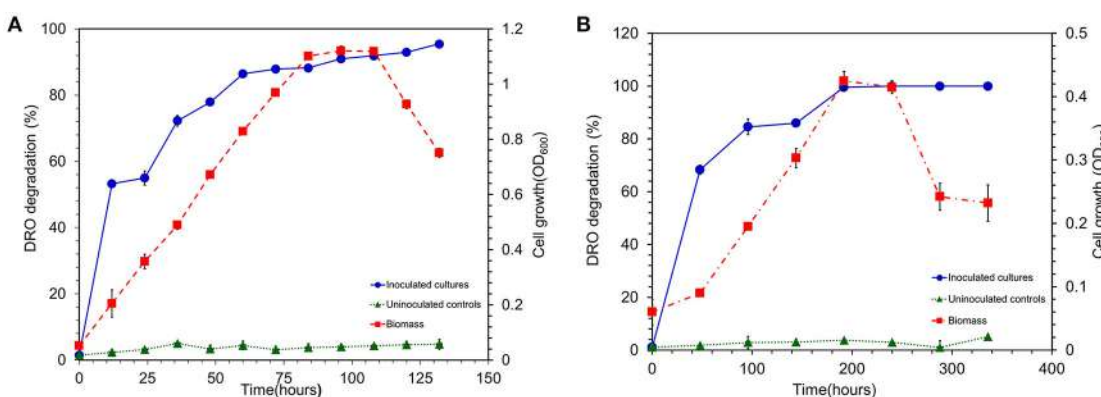


FIGURE 5 | (A) Biodegradation of DRO compounds by aerobically grown cells of *S. maltophilia* MK2 (Blue circle shows DRO degradation in MK2 inoculated samples; Red square shows the biomass density; Green triangle shows the DRO degradation in uninoculated controls). **(B)** Biodegradation of DRO compounds by anaerobically grown cells of *S. maltophilia* MK2 (Blue circle shows DRO degradation in MK2 inoculated samples; Red square shows the biomass density; Green triangle shows the DRO degradation in uninoculated controls).

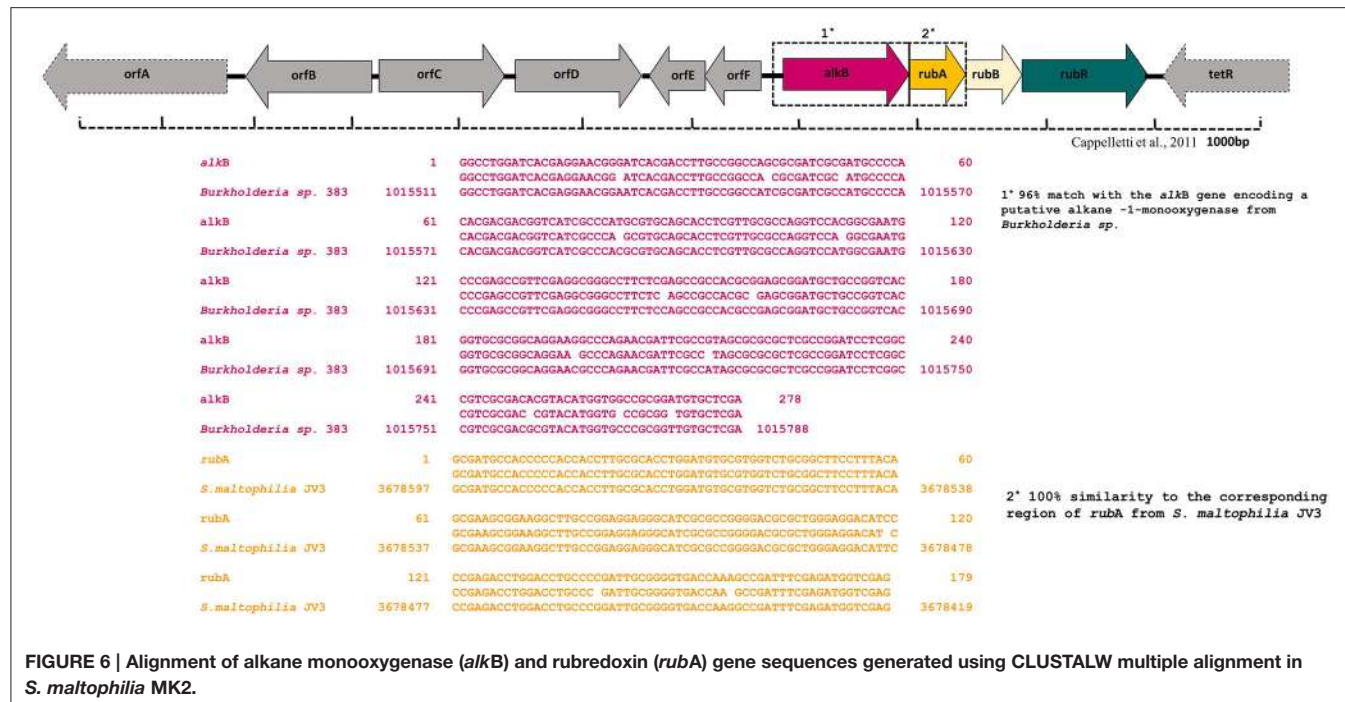


FIGURE 6 | Alignment of alkane monooxygenase (*alkB*) and rubredoxin (*rubA*) gene sequences generated using CLUSTALW multiple alignment in *S. maltophilia* MK2.

S. maltophilia MK2 reduces nitrate in anoxic environments as reported earlier in some strains of this genus (Woodard et al., 1990). However, the additional distinctive features make this strain different from the existing members of the family include (i) growth by anaerobic fermentation of the amino acids present in tryptone and peptone (ii) electrochemically active under acetotrophic environments (iii) ability to degrade n-alkane components of DRO in anaerobic conditions (iv) Biodecolorization of synthetic dyes. The regular growth mode of this bacterial strain *S. maltophilia* MK2 is aerobic heterotrophy; however, the strain MK2 can grow in anaerobic environments either through amino acid fermentation or nitrate reduction. The previous studies on strain ZZ15 belongs to *S. maltophilia* showed a microaerophilic growth under denitrifying environments (Yu et al., 2009). In contrast, the pure cultures of many *Stenotrophomonas* strains are unable to grow in oxygen lacking conditions (Assih et al., 2002; Dungan et al., 2003).

Metabolic Versatility vs. Environmental Bioremediation Potential

The genus *Stenotrophomonas* has been studied as a promising candidate for biotechnological applications involved in the detoxification of various man-made pollutants because of its broad spectrum of metabolic properties (Ryan et al., 2009). These include utilization of N-aromatic rings (Boonchan et al., 1998), alkyl benzene sulfonates of organophosphate pesticides (Dubey and Fulekar, 2012), phenyl urea herbicides (Lü et al., 2009), chlorinated compounds (Somaraja et al., 2013), heavy metals (Pages et al., 2008; Ghosh and Saha, 2013) and other groups

of xenobiotic pollutants (Tachibana et al., 2003; Li et al., 2012). Aliphatic hydrocarbons including straight and cycloalkanes, unsaturated hydrocarbons and aromatic hydrocarbons, are the building blocks of diesel oil (Air Force, 1989) and n-alkanes are the most dominant fraction. The degradation of these hydrocarbon compounds in anoxic environments by the genus *Stenotrophomonas* is previously unknown. Here, we demonstrate for the first time evidence for the occurrence of hydrocarbonoclastic behavior in the strain MK2 under anaerobic, nitrate reducing environments.

The preliminary screening assays reveal that the strain MK2 possess the hydrocarbonoclastic potential by involving redox reactions in which electrons are donated to terminal electron acceptors during the cell respiration. The reduction of a lipophilic mediator such as DCPIP (blue to colorless) coupled with the formation of oxidized products showed that the biodegradation had been carried out by metabolically active cell growth, not by adsorption to cells associated with the water-carbon interface (Kubota et al., 2008). The respiratory reduction of tetrazolium salts is another criterion employed by many researchers (Olga et al., 2008; Pirölö et al., 2008) to determine the dehydrogenase activity of hydrocarbonoclastic bacterial strains. Upon reduction of this salt, the color changed to red due to the formation of insoluble formazans by the production of superoxide radicals and electron transport in the bacterial respiratory chain (Haines et al., 1996). In order to corroborate the potential hydrocarbon degradation by the strain MK2, GC scan was performed using heterotrophically incubated samples grown under aerobic and anaerobic conditions. The highest rate of degradation of the light end hydrocarbons of DRO was observed at 24 h with aerobic incubations, whereas this tended to be slower (96 h)

under anaerobic conditions. GC resolved n-alkanes from C8 to C36 peaks (Figure S1) in inoculated samples demonstrated the occurrence of the enhanced hydrocarbon degradation when the bacterial strain grown under the aerobic conditions. It was quite possible to achieve a complete degradation of DRO under aerobic conditions by appropriately increasing the incubation time of the experiment. Such hydrocarbonoclastic behavior is in contrast to the earlier findings of Saadoun (2002) and Ueno et al. (2007) where their strain of *S. maltophilia* was unable to degrade hydrocarbons as a sole carbon source. On the other hand, members of this genus have been found along with other predominant genera of hydrocarbon degraders including *Acinetobacter*, *Pseudomonas*, *Alcaligenes*, *Sphingomonas* in oil contaminated environments as stated earlier (Van Hamme et al., 2000; Zanaroli et al., 2010). The previous studies on the microbial electrochemical remedial process of hydrocarbons have also demonstrated the ubiquity of *Stenotrophomonas* spp. and their dominance in the anodic microbial communities (Morris et al., 2009; Venkidusamy et al., 2016). The capability of hydrocarbon degradation has also been demonstrated earlier in a soil isolate of *S. maltophilia* strain DJLB only under aerobic conditions (Ganesh and Lin, 2009). It is of interest that, the present study reveals the complete mineralization of n-alkane members of DRO (C8–C36) for the first time, including the biomarkers pristine, phytane, and a short chain to long chain aliphatic hydrocarbons under anaerobic incubations by the strain MK2 during a 12 days period in the presence of nitrate.

Exoelectrogenic Potential

The characteristics of diazoic dye decolorization were used as a simple criterion for pre-screening the possible electrochemically active microbial candidates in the present study as stated earlier (Hou et al., 2009). The present study showed the simultaneous decolorization and decreased dye concentrations from batch culture studies of anaerobic and aerobic incubations with strain MK2 inoculum. The efficiency of color removal was more than 95% under anaerobic conditions as reported in another exoelectrogenic strain of *Shewanella* spp. (Pearce et al., 2006). This is in agreement with the previous studies on the assessment of electrochemically active microbial strains using MFC arrays (Hou et al., 2009). Dye decolorization occurs because of a reductive electrophilic cleavage of the chromophore, a functional group of azo linkage, by biocatalysts as reported earlier (Sun et al., 2009; Satapanajaru et al., 2011). To confirm the extracellular access to the insoluble electron acceptors, the exoelectrogenic property of the strain MK2 was also investigated in two different environments (i) acetotrophic (ii) dye decolorization, using microbial electrochemical systems. The present study exhibited a maximum power density of 113 ± 7 mW/m² with a recovery of 34.8% as an electrical current using the strain MK2 in acetotrophic conditions. In the case of the reactors fed with azoic dye demonstrated the potential of generating current (99.93 ± 6 mW/m²) with the concurrent decolorization using the strain MK2 in MFCs for the first time. The results presented in this study suggest that the strain MK2 is capable of utilizing insoluble electron acceptors such as electrodes through extracellular electron transfer mechanisms. Recent investigations

have revealed the potential of using such pure cultures of heterotrophic biofilms in microbial electrochemical remediation cells for dye detoxification (Chen et al., 2010a,b). For instance, Chen et al. (2010a), reported the possibility of using pure cultures of *Proteus hauseri* in MFC, however, decolorization efficiency and power densities generated were much lower. The performance of these microbial electrochemical cells using pure cultures of exoelectrogens are considerably affected by a number of reactor parameters and operating conditions as reported earlier (Min et al., 2005; Logan, 2008).

Genetic Potential

To gain deeper insights into the hydrocarbon degradation mechanism by the strain MK2, we carried out a gene specific PCR analysis to identify the possible catabolic genes encoding alkane degrading enzymes using different degenerate oligonucleotides. The mechanisms of these alkanes activation vary according to the lifestyle of representative candidate microorganisms and growth environments. Under aerobic environments, the biodegradation typically occurs through a sequential oxidation of n-alkanes resulting in corresponding alcohol and aldehydes groups. These aldehydes further metabolized into fatty acids and conjugated with CoA through β oxidation process which then enter into the tricarboxylic acid cycle as shown in Figure 7 (Van Hamme et al., 2003; van Beilen et al., 2004). Such a successional oxidation process is activated by a family of integral membrane proteins called alkane hydroxylase enzyme system, and this was first studied in *Pseudomonas putida* GPo1. This is of particular interest being a three component biocatalyst and composed of alkane monooxygenase (*alkB* group), dinuclear iron rubredoxins (*rubA*, *rubB*) and mononuclear rubredoxin reductase (*rubR*) (Rojo, 2009; Teimoori et al., 2011). These genes encode the alkane hydroxylase (*alk*) system in the enzyme complex which activates the terminal carbon atoms in the chain of hydrocarbons. While searching the catabolic genes that encode *alk* system in the strain *S. maltophilia* MK2, we found for the first time a conserved chromosomal region of *alkB* and *rubA* (Figure 6). In silico analysis of this gene showed that the *alkB* region was highly similar to the region observed from an *alkB* gene of *Burkholderia* spp. and this is presumably the gene providing this activity, supporting the close relationship between *S. maltophilia* and *Burkholderia* spp. (84%) at the genomic level. This result suggests that the genes involved do not correspond in terms of their sequence to the same genes as per the published *Stenotrophomonas maltophilia* genome and were instead derived from some other organism with different gene sequences (and the discovery that the *alkB* gene sequence comes from *Burkholderia* supports this). In contrast, the earlier studies on catabolic genes for alkane degradation in *Stenotrophomonas* spp. have shown negative results for the amplification of *alkB* gene (Smits et al., 1999; Vomberg and Klinner, 2000). The presence of a *rubA* gene with 100% homology to Rubredoxin-type Fe(Cys)4 protein of *S. maltophilia* R551-3, shows that the bacterial strain MK2 likely possesses an essential electron transfer components for alkane hydroxylation. Together, these results perhaps indicate the presence of the two conserved domains of *alkB-rubA* fused proteins in a contiguous open reading frame as

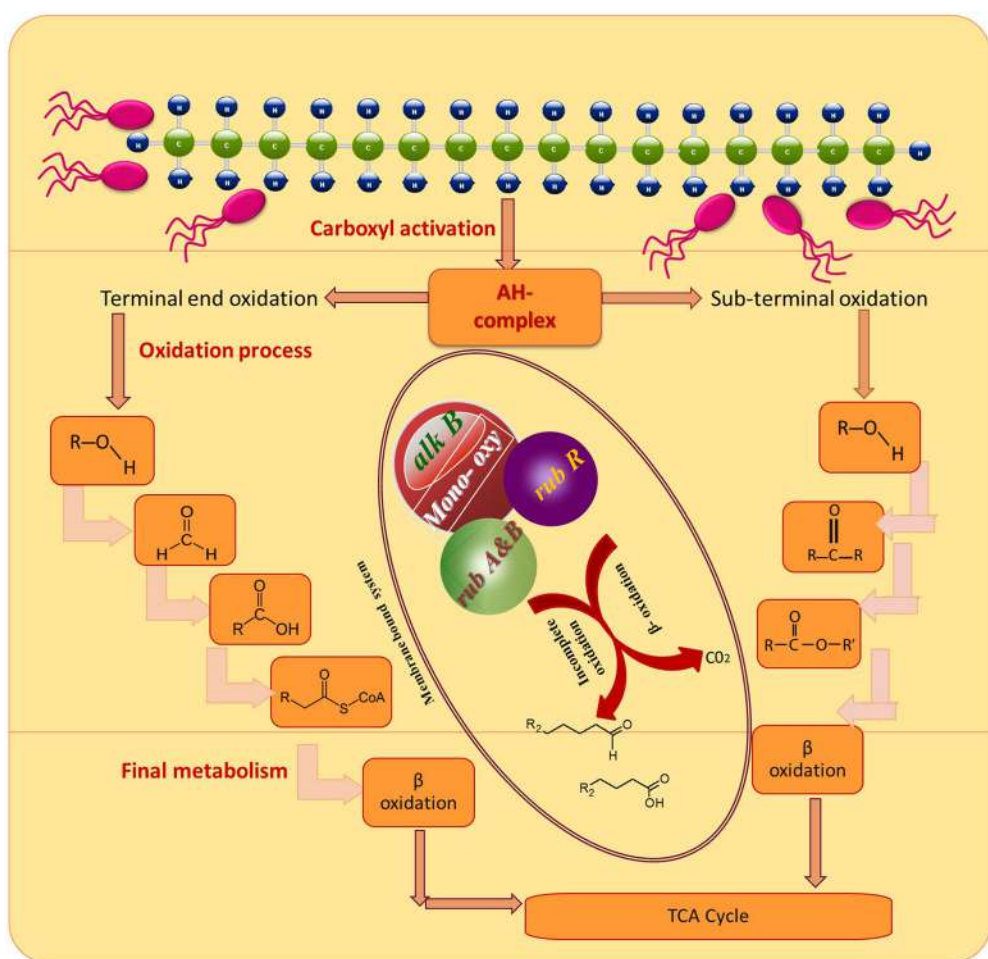


FIGURE 7 | Degradation pathways of DRO compounds in aerobic environments.

shown earlier in metagenomic analysis of *alk* genes of different microbial genomes from diverse environments (Nie et al., 2014). Such a fusion would be responsible for the extended spectrum of alkane degradation up to C36 hydrocarbons shown in the present study, as *alkB* often reported to be responsible for <C16 length (van Beilen and Funhoff, 2007). Also, the earlier studies on the disruption of the *rubA* encoding genes in bacterial strains lead to the failure of alkane degradation (Haspel et al., 1995; Ratajczak et al., 1998) which supports the aforementioned theory on fused proteins in hydrocarbon biodegradation.

Our present findings demonstrate the facultative hydrocarbonoclastic and exoelectrogenic properties in different environments (acetotrophic and dye detoxification) associated with genus *S. maltophilia* MK2. These species include both environmental non-pathogenic isolates and opportunistic clinical isolates of nosocomial origin. An increasing number of studies demonstrate the potential use of opportunistic human pathogenic bacteria in microbial electrochemical systems that include, *Ochrobactrum anothropi* (Zuo et al., 2008), *Pseudomonas aeruginosa* (Venkataraman et al., 2010), *Acrobacter butzleri* (Fedorovich et al., 2009). The production of lipopolysaccharides,

flagella or fimbriae —mediated interactions (Brooke, 2012) may involve in colonization and biofilm formation on the electrodes of microbial electrochemical systems, however their role, lifestyle and pathogenicity of the strain MK2 await further research. It will be interesting to examine the molecular mechanism of such biofilm attachment to electrodes and extracellular electron transfer potential of this strain MK2.

CONCLUSIONS

The members of *Stenotrophomonas* spp. are found to be cosmopolitan opportunists as their presence often been detected in soil and water systems. Our findings demonstrate that the hydrocarbonoclastic and exoelectrogenic potential associated with genus *Stenotrophomonas* is novel and expands the range of microbial phyla known to degrade hydrocarbon contaminants. The strain is notable in that its *alkB* gene seems to have been derived from *Burkholderia* while its *rubA* gene originated from *Stenotrophomonas*. Additionally, the decolorization of diazoic dyes also makes a supplement to

the phylogeny knowledge on bioleaching agents and showing further potential in the treatment of wastewater from textile industries using MERS. On a global scale, the strain provides many exciting opportunities for increasing our understanding on bioremediation that underpins the molecular mechanism of contaminant degradation in a relevant environmental context.

AUTHOR CONTRIBUTIONS

KV and MM proposed the study. KV conducted the experiments under the supervision of MM. KV prepared the draft with contributions from MM.

REFERENCES

- Air Force (1989). "Gasoline," in *The Installation Restoration Program Toxicology Guide*. Vol. 4. Contract no. DE-AC05840R21400. Wright-Patterson Air Force Base, OH. Document no. 65-1-65-46.
- Assih, E. A., Ouattara, A. S., Thierry, S., Cayol, J.-L., Labat, M., and Macarie, H. (2002). *Stenotrophomonas acidaminiphila* sp. nov., a strictly aerobic bacterium isolated from an upflow anaerobic sludge blanket (UASB) reactor. *Int. J. Syst. Evol. Microbiol.* 52, 559–568. doi: 10.1099/00207713-52-2-559
- Binks, P. R., Nicklin, S., and Bruce, N. C. (1995). Degradation of hexahydro-1, 3, 5-trinitro-1, 3, 5-triazine (RDX) by *Stenotrophomonas maltophilia* PB1. *Appl. Environ. Microbiol.* 61, 1318–1322.
- Boonchan, S., Britz, M. L., and Stanley, G. A. (1998). Surfactant-enhanced biodegradation of high molecular weight polycyclic aromatic hydrocarbons by *Stenotrophomonas maltophilia*. *Biotechnol. Bioeng.* 59, 482–494. doi: 10.1002/(sici)1097-0290(19980820)59:4<482::aid-bit11>3.3.co;2-t
- Brooke, J. S. (2012). *Stenotrophomonas maltophilia*: an emerging global opportunistic pathogen. *Clin. Microbiol. Rev.* 25, 2–41. doi: 10.1128/CMR.00019-11
- Chen, B.-Y., Zhang, M.-M., Chang, C.-T., Ding, Y., Lin, K.-L., Chiou, C.-S., et al. (2010a). Assessment upon azo dye decolorization and bioelectricity generation by *Proteus hauseri*. *Biores. Technol.* 101, 4737–4741. doi: 10.1016/j.biortech.2010.01.133
- Chen, B.-Y., Zhang, M.-M., Ding, Y., and Chang, C.-T. (2010b). Feasibility study of simultaneous bioelectricity generation and dye decolorization using naturally occurring decolorizers. *J. Taiwan. Inst. Chem. Eng.* 41, 682–688. doi: 10.1016/j.jtice.2010.02.005
- Cheng, S., Liu, H., and Logan, B. E. (2006). Increased performance of single-chamber microbial fuel cells using an improved cathode structure. *Electrochim. Commun.* 8, 489–494. doi: 10.1016/j.elecom.2006.01.010
- Chilcott, R. P. (2011). *Compendium of Chemical Hazards: Diesel*. Version. Available online at: cdrwww.who.int
- Denton, M., and Kerr, K. G. (1998). Microbiological and clinical aspects of infection associated with *Stenotrophomonas maltophilia*. *Clin. Microbiol. Rev.* 11, 57–80.
- Dubey, K. K., and Fulekar, M. (2012). Chlorpyrifos bioremediation in *Pennisetum* rhizosphere by a novel potential degrader *Stenotrophomonas maltophilia* MHF ENV20. *World J. Microbiol. Biotechnol.* 28, 1715–1725. doi: 10.1007/s11274-011-0982-1
- Dungan, R. S., Yates, S. R., and Frankenberger, W. T. (2003). Transformations of selenate and selenite by *Stenotrophomonas maltophilia* isolated from a seleniferous agricultural drainage pond sediment. *Environ. Microbiol.* 5, 287–295. doi: 10.1046/j.1462-2920.2003.00410.x
- Fedorovich, V., Knighton, M. C., Pagaling, E., Ward, F. B., Free, A., and Goryanin, I. (2009). Novel electrochemically active bacterium phylogenetically related to *Arcobacter butzleri*, isolated from a microbial fuel cell. *Appl. Environ. Microbiol.* 75, 7326–7334. doi: 10.1128/AEM.01345-09
- Feng, Y., Yang, Q., Wang, X., and Logan, B. E. (2010). Treatment of carbon fiber brush anodes for improving power generation in air-cathode microbial fuel cells. *J. Power Sources* 195, 1841–1844. doi: 10.1016/j.jpowsour.2009.10.030
- Gallego, J. L., Loredo, J., Llamas, J. F., Vázquez, F., and Sánchez, J. (2001). Bioremediation of diesel-contaminated soils: evaluation of potential in situ techniques by study of bacterial degradation. *Biodegradation* 12, 325–335. doi: 10.1023/A:1014397732435
- Ganesh, A., and Lin, J. (2009). Diesel degradation and biosurfactant production by Gram-positive isolates. *Afr. J. Biotechnol.* 8, 5847–5854. Available online at: <http://www.academicjournals.org/AJB>
- Ghosh, A., and Saha, P. D. (2013). Optimization of copper bioremediation by *Stenotrophomonas maltophilia* PD2. *J. Environ. Chem. Eng.* 1, 159–163. doi: 10.1016/j.jece.2013.04.012
- Grishchenkov, V., Townsend, R., McDonald, T., Autenrieth, R., Bonner, J., and Boronin, A. (2000). Degradation of petroleum hydrocarbons by facultative anaerobic bacteria under aerobic and anaerobic conditions. *Process Biochem.* 35, 889–896. doi: 10.1016/S0032-9592(99)00145-4
- Haines, J., Wrenn, B., Holder, E., Strohmeier, K., Herrington, R., and Venosa, A. (1996). Measurement of hydrocarbon-degrading microbial populations by a 96-well plate most-probable-number procedure. *J. Indus. Microbiol.* 16, 36–41. doi: 10.1007/BF01569919
- Hanson, K., Desai, J. D., and Desai, A. J. (1993). A rapid and simple screening technique for potential crude oil degrading microorganisms. *Biotechnol. Tech.* 7, 745–748. doi: 10.1007/BF00152624
- Haspel, G., Ehrt, S., and Hillen, W. (1995). Two genes encoding proteins with similarities to rubredoxin and rubredoxin reductase are required for conversion of dodecane to lauric acid in *Acinetobacter calcoaceticus* ADP1. *Microbiology* 141, 1425–1432. doi: 10.1099/13500872-141-6-1425
- Hong, J. H., Kim, J., Choi, O. K., Cho, K.-S., and Ryu, H. W. (2005). Characterization of a diesel-degrading bacterium, *Pseudomonas aeruginosa* IU5, isolated from oil-contaminated soil in Korea. *World J. Microbiol. Biotechnol.* 21, 381–384. doi: 10.1007/s11274-004-3630-1
- Hou, H., Li, L., Cho, Y., De Figueiredo, P., and Han, A. (2009). Microfabricated microbial fuel cell arrays reveal electrochemically active microbes. *PLoS ONE* 4:e6570. doi: 10.1371/journal.pone.0006570
- Kubota, K., Koma, D., Matsumiya, Y., Chung, S.-Y., and Kubo, M. (2008). Phylogenetic analysis of long-chain hydrocarbon-degrading bacteria and evaluation of their hydrocarbon-degradation by the 2, 6-DCPIP assay. *Biodegradation* 19, 749–757. doi: 10.1007/s10532-008-9179-1
- Li, Z., Nandakumar, R., Madayiputhiya, N., and Li, X. (2012). Proteomic analysis of 17 β -estradiol degradation by *Stenotrophomonas maltophilia*. *Environ. Sci. Technol.* 46, 5947–5955. doi: 10.1021/es300273k
- Logan, B., Cheng, S., Watson, V., and Estadt, G. (2007). Graphite fiber brush anodes for increased power production in air-cathode microbial fuel cells. *Environ. Sci. Technol.* 41, 3341–3346. doi: 10.1021/es062644y
- Logan, B. E. (2008). *Microbial Fuel Cells*. Hoboken, NJ: John Wiley & Sons.
- Lü, Z., Sang, L., Li, Z., and Min, H. (2009). Catalase and superoxide dismutase activities in a *Stenotrophomonas maltophilia* WZ2 resistant to herbicide pollution. *Ecotoxicol. Environ. Saf.* 72, 136–143. doi: 10.1016/j.ecoenv.2008.01.009
- Megharaj, M., Ramakrishnan, B., Venkateswarlu, K., Sethunathan, N., and Naidu, R. (2011). Bioremediation approaches for organic pollutants: a critical perspective. *Environ. Int.* 37, 1362–1375. doi: 10.1016/j.envint.2011.06.003
- Min, B., Kim, J., Oh, S., Regan, J. M., and Logan, B. E. (2005). Electricity generation from swine wastewater using microbial fuel cells. *Water Res.* 39, 4961–4968. doi: 10.1016/j.watres.2005.09.039

ACKNOWLEDGMENTS

The authors thank Dr. R. Lockington for comments and suggestions on previous versions of this manuscript. KV thanks Australian Federal Government, University of South Australia for International Postgraduate scholarship award (IPRS) and CRC CARE for the research top-up award.

SUPPLEMENTARY MATERIAL

The Supplementary Material for this article can be found online at: <http://journal.frontiersin.org/article/10.3389/fmicb.2016.01965/full#supplementary-material>

- Morris, J. M., Jin, S., Crimi, B., and Pruden, A. (2009). Microbial fuel cell in enhancing anaerobic biodegradation of diesel. *Chem. Eng. J.* 146, 161–167. doi: 10.1016/j.cej.2008.05.028
- Nie, Y., Chi, C.-Q., Fang, H., Liang, J.-L., Lu, S.-L., Lai, G.-L., et al. (2014). Diverse alkane hydroxylase genes in microorganisms and environments. *Sci. Rep.* 4:4968. doi: 10.1038/srep04968
- Oh, S., Min, B., and Logan, B. E. (2004). Cathode performance as a factor in electricity generation in microbial fuel cells. *Environ. Sci. Technol.* 38, 4900–4904. doi: 10.1021/es049422p
- Olga, P., Petar, K., Jelena, M., and Srdjan, R. (2008). Screening method for detection of hydrocarbon-oxidizing bacteria in oil-contaminated water and soil specimens. *J. Microbiol. Met.* 4, 110–113. doi: 10.1016/j.mimet.2008.03.012
- Pages, D., Rose, J., Conrod, S., Cuine, S., Carrier, P., Heulin, T., et al. (2008). Heavy metal tolerance in *Stenotrophomonas maltophilia*. *PLoS ONE* 3:e1539. doi: 10.1371/journal.pone.0001539
- Palleroni, N. J., and Bradbury, J. F. (1993). *Stenotrophomonas*, a new bacterial genus for *Xanthomonas maltophilia* (Hugh 1980) Swings et al. 1983. *Int. J. Syst. Evol. Microbiol.* 43, 606–609. doi: 10.1099/00207713-43-3-606
- Pearce, C. I., Christie, R., Boothman, C., Von Canstein, H., Guthrie, J. T., and Lloyd, J. R. (2006). Reactive azo dye reduction by *Shewanella* strain J18 143. *Biotechnol. Bioeng.* 95, 692–703. doi: 10.1002/bit.21021
- Piröollo, M., Mariano, A., Lovaglio, R., Costa, S., Walter, V., Hausmann, R., et al. (2008). Biosurfactant synthesis by *Pseudomonas aeruginosa* LBI isolated from a hydrocarbon-contaminated site. *J. App. Microbiol.* 105, 1484–1490. doi: 10.1111/j.1365-2672.2008.03893.x
- Ratajczak, A., Geissdörfer, W., and Hillen, W. (1998). Alkane Hydroxylase from *Acinetobacter* sp. Strain ADP1 Is Encoded by alkM and Belongs to a New Family of bacterial integral-membrane hydrocarbon hydroxylases. *App. Environ. Microbiol.* 64, 1175–1179.
- Rojo, F. (2009). Degradation of alkanes by bacteria. *Environ. Microbiol.* 11, 2477–2490. doi: 10.1111/j.1462-2920.2009.01948.x
- Röling, W. F., Head, I. M., and Larter, S. R. (2003). The microbiology of hydrocarbon degradation in subsurface petroleum reservoirs: perspectives and prospects. *Res. Microbiol.* 154, 321–328. doi: 10.1016/S0923-2508(03)00086-X
- Ryan, R. P., Monchy, S., Cardinale, M., Taghavi, S., Crossman, L., Avison, M. B., et al. (2009). The versatility and adaptation of bacteria from the genus *Stenotrophomonas*. *Nat. Rev. Microbiol.* 7, 514–525. doi: 10.1038/nrmicro2163
- Saadoun, I. (2002). Isolation and characterization of bacteria from crude petroleum oil contaminated soil and their potential to degrade diesel fuel. *J. Bas. Microbiol.* 42, 420–428. doi: 10.1002/1521-4028(200212)42:6<420::AID-JOBM420>3.0.CO;2-W
- Sambrook, J., Fritsch, E. F., and Maniatis, T. (1989). *Molecular Cloning*. New York, NY: Cold Spring Harbor Laboratory press.
- Satapanajaru, T., Chompuchan, C., Suntornchot, P., and Pengthamkeerati, P. (2011). Enhancing decolorization of Reactive Black 5 and Reactive Red 198 during nano zerovalent iron treatment. *Desal* 266, 218–230. doi: 10.1016/j.desal.2010.08.030
- Smits, T. H., Röthlisberger, M., Witholt, B., and Van Beilen, J. B. (1999). Molecular screening for alkane hydroxylase genes in Gram-negative and Gram-positive strains. *Environ. Microbiol.* 1, 307–317. doi: 10.1046/j.1462-2920.1999.00037.x
- Somaraja, P., Gayathri, D., and Ramaiah, N. (2013). Molecular characterization of 2-chlorobiphenyl degrading *Stenotrophomonas maltophilia* GS-103. *Bull. Environ. Contam. Toxicol.* 91, 148–153. doi: 10.1007/s00128-013-1044-1
- Sun, J., Hu, Y.-Y., Bi, Z., and Cao, Y.-Q. (2009). Simultaneous decolorization of azo dye and bioelectricity generation using a microfiltration membrane air-cathode single-chamber microbial fuel cell. *Bioresourc. Technol.* 100, 3185–3192. doi: 10.1016/j.biortech.2009.02.002
- Tachibana, S., Kuba, N., Kawai, F., Duine, J. A., and Yasuda, M. (2003). Involvement of a quinoprotein (PQQ-containing) alcohol dehydrogenase in the degradation of polypropylene glycols by the bacterium *Stenotrophomonas maltophilia*. *FEMS Microbiol. Lett.* 218, 345–349. doi: 10.1111/j.1574-6968.2003.tb11540.x
- Tamura, K., Peterson, D., Peterson, N., Stecher, G., Nei, M., and Kumar, S. (2011). MEGA5: molecular evolutionary genetics analysis using maximum likelihood, evolutionary distance, and maximum parsimony methods. *Mol. Biol. Evol.* 28, 2731–2739. doi: 10.1093/molbev/msr121
- Teimoori, A., Ahmadian, S., Madadkar-Sobhani, A., and Bambai, B. (2011). Rubredoxin reductase from *Alcanivorax borkumensis*: expression and characterization. *Biotechnol. Prog.* 27, 1383–1389. doi: 10.1002/btpr.653
- Ueno, A., Ito, Y., Yumoto, I., and Okuyama, H. (2007). Isolation and characterization of bacteria from soil contaminated with diesel oil and the possible use of these in autochthonous bioaugmentation. *World J. Microbiol. Biotechnol.* 23, 1739–1745. doi: 10.1007/s11274-007-9423-6
- USEPA (1996). *Updates, I, II, IIA and III: Test Methods for Evaluating Solid Wastes, Physical/Chemical Methods, SW-846 Method 8015B-3rd Edn.*, Superintendent of Documents, U.S. Government Printing Office, Washington, D.C.
- van Beilen, J. B., and Funhoff, E. G. (2007). Alkane hydroxylases involved in microbial alkane degradation. *Appl. Microbiol. Biotechnol.* 74, 13–21. doi: 10.1007/s00253-006-0748-0
- van Beilen, J. B., Marin, M. M., Smits, T. H., Röthlisberger, M., Franchini, A. G., Witholt, B., et al. (2004). Characterization of two alkane hydroxylase genes from the marine hydrocarbonoclastic bacterium *Alcanivorax borkumensis*. *Environ. Microbiol.* 6, 264–273. doi: 10.1111/j.1462-2920.2004.00567.x
- Van Hamme, J. D., Odumeru, J. A., and Ward, O. P. (2000). Community dynamics of a mixed-bacterial culture growing on petroleum hydrocarbons in batch culture. *Can. J. Microbiol.* 46, 441–450. doi: 10.1139/w00-013
- Van Hamme, J. D., Singh, A., and Ward, O. P. (2003). Recent advances in petroleum microbiology. *Microbiol. Mol. Biol. Rev.* 67, 503–549. doi: 10.1128/MMBR.67.4.503-549.2003
- Venkataraman, A., Rosenbaum, M., Arends, J. B., Halitschke, R., and Angenent, L. T. (2010). Quorum sensing regulates electric current generation of *Pseudomonas aeruginosa* PA14 in bioelectrochemical systems. *Electrochem. Commun.* 12, 459–462. doi: 10.1016/j.elecom.2010.01.019
- Venkidusamy, K., and Megharaj, M. (2016). A Novel Electrophototrophic Bacterium *Rhodopseudomonas palustris* Strain RP2, Exhibits Hydrocarbonoclastic Potential in Anaerobic Environments. *Front. Microbiol.* 7:1071. doi: 10.3389/fmicb.2016.01071
- Venkidusamy, K., Megharaj, M., Marzorati, M., Lockington, R., and Naidu, R. (2016). Enhanced removal of petroleum hydrocarbons using a bioelectrochemical remediation system with pre-cultured anodes. *Sci. Total Environ.* 539, 61–69. doi: 10.1016/j.scitotenv.2015.08.098
- Vomberg, A., and Klinner, U. (2000). Distribution of *alkB* genes within n-alkane-degrading bacteria. *J. App. Microbiol.* 89, 339–348. doi: 10.1046/j.1365-2672.2000.01121.x
- Weisburg, W. G., Barns, S. M., Pelletier, D. A., and Lane, D. J. (1991). 16S ribosomal DNA amplification for phylogenetic study. *J. Bacteriol.* 173, 697–703. doi: 10.1128/jb.173.2.697-703.1991
- Woodard, L. M., Bielkie, A. R., Eisses, J. F., and Ketchum, P. A. (1990). Occurrence of nitrate reductase and molybdopterin in *Xanthomonas maltophilia*. *App. Environ. Microbiol.* 6, 3766–3771.
- Yu, L., Liu, Y., and Wang, G. (2009). Identification of novel denitrifying bacteria *Stenotrophomonas* sp. ZZ15 and *Oceanimonas* sp. YC13 and application for removal of nitrate from industrial wastewater. *Biodegradation* 20, 391–400. doi: 10.1007/s10532-008-9230-2
- Zanaroli, G., Di Toro, S., Todaro, D., Varese, G. C., Bertolotto, A., and Fava, F. (2010). Characterization of two diesel fuel degrading microbial consortia enriched from a non-acclimated, complex source of microorganisms. *Microb. Cell Fact.* 9:10. doi: 10.1186/1475-2859-9-10
- Zhou, L., Deng, D., Zhang, D., Chen, Q., Kang, J., Fan, N., et al. (2016). Microbial electricity generation and isolation of exoelectrogenic bacteria based on petroleum hydrocarbon-contaminated soil. *Electroanalysis* 28, 1510–1516. doi: 10.1002/elan.201501052
- Zuo, Y., Xing, D., Regan, J. M., and Logan, B. E. (2008). Isolation of the exoelectrogenic bacterium *Ochrobactrum anthropi* YZ-1 by using a U-tube microbial fuel cell. *Appl. Environ. Microbiol.* 74, 3130–3137. doi: 10.1128/AEM.02732-07

Conflict of Interest Statement: The authors declare that the research was conducted in the absence of any commercial or financial relationships that could be construed as a potential conflict of interest.

Copyright © 2016 Venkidusamy and Megharaj. This is an open-access article distributed under the terms of the Creative Commons Attribution License (CC BY). The use, distribution or reproduction in other forums is permitted, provided the original author(s) or licensor are credited and that the original publication in this journal is cited, in accordance with accepted academic practice. No use, distribution or reproduction is permitted which does not comply with these terms.



What Is the Essence of Microbial Electroactivity?

Christin Koch * and **Falk Harnisch ***

Department of Environmental Microbiology, UFZ-Helmholtz Centre for Environmental Research, Leipzig, Germany

Keywords: extracellular electron transfer, exoelectrogenic, syntrophy, microbial electrochemical technology, *Geobacter*, microbial fuel cell

Microorganisms performing extracellular electron transfer (EET) show electroactivity and are the fundament of primary microbial electrochemical technologies (MET) (Schröder et al., 2015) as well as key players of geochemical cycles (Newman and Banfield, 2002; Melton et al., 2014). However, only a few electroactive microorganisms, like *Geobacter* or *Shewanella*, are studied in detail, e.g., for their electron transfer mechanisms (Gorby et al., 2006; Brutin and Gralnick, 2012; Lovley, 2012). Many more species are only globally assigned to be electroactive (Koch and Harnisch, 2016), but mechanistic knowledge is generally missing and the natural importance of this trait not comprehensively understood.

OPEN ACCESS

Edited by:

Feng Zhao,
Institute of Urban Environment (CAS),
China

Reviewed by:

Uri Gophna,
Tel Aviv University, Israel
Claire Dumas,
Institut National de la Recherche
Agronomique (INRA), France

*Correspondence:

Christin Koch
christin.koch@ufz.de
Falk Harnisch
falk.harnisch@ufz.de

Specialty section:

This article was submitted to
Microbiotechnology, Ecotoxicology
and Bioremediation,
a section of the journal
Frontiers in Microbiology

Received: 08 September 2016

Accepted: 11 November 2016

Published: 25 November 2016

Citation:

Koch C and Harnisch F (2016) What Is the Essence of Microbial Electroactivity? *Front. Microbiol.* 7:1890.
doi: 10.3389/fmicb.2016.01890

However, there is no common definition of electroactivity and a genetic or metabolic marker or even a gold standard does not exist. This lack together with the high diversity of electroactive microorganisms—with regard to their phylogeny but also their physiology—challenges a systematic assessment and comparison (Koch and Harnisch, 2016). This difficulty is furthermore accelerated by the diversity of experimental setups and techniques exploited (Harnisch and Rabaey, 2012). The deficit of a stringent definition of electroactivity may sound purely academic from an application or engineering perspective. However, it is not. A consensus on electroactivity combined with good craftsmanship (Egli, 2015) for studying and engineering electroactive microorganisms as well as MET has to form the fundament of future research and development. The following treatise is certainly not comprehensive, but we will show that a better understanding of the linkage between EET, microbial metabolism, and system performance is necessary to form this fundament or in other words “To distil the essence of electroactivity.”

AGONY OF CHOICE OR HOW WOULD YOU DECIDE?

Considering two electroactive microbes A and B, which one can be defined to be more electroactive? Microbe A being psychrophilic and performing (slow) EET (hence low current density¹ j) at 10°C with a coulombic efficiency² (CE) close to 100%—or—microbe B being thermophilic and performing fast EET (hence high j) at 60°C with low CE? The decision is not straightforward and would usually depend on the respective process as well as j and CE required or feasible for its application. Interestingly this example illustrates the common sense in the perception of electroactivity of microorganisms. In the outmost majority of studies system level parameters are used for characterization. These numbers related to the engineering or electrochemistry viewpoint are (i) the overall yield of electrons from a substrate (at anodes) or stored in a product (for cathodes) as expressed in CE and (ii) the “speed” of EET, i.e., electrons per time unit usually expressed

¹The current, i (usually in mA) represents the number of the transferred electrons per second to an electrode and hence can be a measure of the metabolic activity. For normalization often the current density is used by relating the current to the (geometric) surface area of an electrode, j_{geo} (in mA cm⁻²), or to the volume of the electrode chamber, j_{vol} (in mA cm⁻³).

²The coulombic efficiency, CE, is a measure of the ratio of theoretical available electrons from the substrate and the transferred electrons to the electrode at the anode; hence it can be regarded as measure of metabolic efficiency.

as current, i , or normalized to electrode surface area respectively volume as current density, j (Harnisch and Rabaey, 2012; Schröder et al., 2015). Noteworthy, these performance parameters can be, but not have to be linked to the metabolic level of microbes A and B as will be discussed in the following section and hence are not generally suitable for assessing what electroactivity is. As shown below, the answer to the introductory question will strongly depend on the individual perspective (see also Figure 1).

WHAT ARE TYPICAL CHARACTERISTICS THAT DEFINE MICROORGANISMS AS ELECTROACTIVE (OR NOT)?

Let us consider our model organism *Geobacter sulfurreducens* and its relatives: they form biofilms at anodes while oxidizing acetate and performing direct electron transfer and most express conductive nanowires. Under anodic growth conditions with the electrode as only electron acceptor the microbial metabolism is completely dependent on the EET as this is the only pathway of energy generation. This species can be clearly defined as electroactive. But how to compare it to other species differing from this model organism? Choosing an adequate measure is difficult as summarized by the different viewpoints on electroactivity in Figure 1.

FROM MICROBIAL CELLS TO ELECTROCHEMICAL CELLS AND BACK AGAIN

For microorganisms forming biofilms at electrodes like *Geobacter sulfurreducens*, the biofilm thickness³ might seem as a measure of electroactivity, as a higher cell number might go along with an increased current flow. However, differences in cell density and biofilm thickness can be specific for microbial species (and already obvious differences exist within the family of *Geobacteraceae*), thereby being dependent on its (local) environment, growth state etc. (Bonanni et al., 2013; Tan et al., 2016). From a practical perspective measuring typical parameters like, e.g., cell number, dry weight, etc. of biofilms is not simple and mostly destructive for the object of study. Hence, time resolved analyses are challenging, especially when considering what a “representative” sample is. For mixed culture biofilms it was shown that shear stress can effect the biofilm thickness and the biomass density (Pham et al., 2008). This can lead to differences regarding the substrate turnover and electron flow for an individual cell which is not necessarily reflected by the anodic current density. In this case, the coulombic efficiency might seem a good objective measure of electroactivity being independent of cell number and also considering potential electron losses within the cell. Experimentally, even harder to determine would be the electron transfer per single cell (Liu et al., 2010; Jiang et al., 2013; Gross and El-Naggar, 2015), which from our perspective could be

³Here we refer to (i) the thickness in steady-state conditions and (ii) to uniform biofilms. The definition of steady state and its experimental realization as well as biofilm stratification are worth its own treatise.

considered an excellent measure. On the technical scale, biomass respective number of cells, N_{cell} , or formed product, P , is often in focus. Here in analogy to established parameters in biotechnology (Doran, 1995) we propose that yields per electron (e.g., cell yield per electron, Y_{Ne-} , or product yield per electron, Y_{Pe-}) can be defined based on the number of transferred electrons n_{e-} . This number is derived from the transferred charge, q , and the Faraday constant, F .

$$Y_{Ne-} = \frac{(N_{cell,t} - N_{cell,0})}{(n_{e-,t} - n_{e-,0})}, \text{ with } \int_0^t idt = q \text{ and } n_{e-,t} = \frac{q}{F};$$

as $n_{e-,0} = 0$ it follows:

$$Y_{Ne-} = \frac{(N_{cell,t} - N_{cell,0})}{q} \times F$$

analogously it follows:

$$Y_{Pe-} = \frac{(P_t - P_0)}{q} \times F, \text{ when considerin } P_0 = 0,$$

it simplifies to $Y_{Pe-} = \frac{P_t}{q} \times F$.

From the electrochemical viewpoint the microbial overpotential, $\eta_{microbe}$, can be defined similar to the electrochemical overpotential (Bard et al., 2012) and can be used for a thermodynamic comparison of electroactive microorganisms. For microbial anodes it is the difference between the formal potential of the substrate, $E_{substrate}$, and the formal potential of the EET site, E_{EET} , i.e., the potential at which the electrons are released by the microbe, with $\eta_{microbe} = E_{substrate} - E_{EET}$. However, $\eta_{microbe}$ sets only the upper limit of the microbial energy gain. Yet, the true energy gain, i.e., being stored for instance in ATP or reduction equivalents and subsequently used for anabolic reactions, is decreased due to losses, like heat dissipation (Korth et al., 2016). Here species specific differences can be expected or in other words: Is a microbe more electroactive performing fast EET that strives for its living or one that harvests a lot of energy per electron but at a very slow rate?

Another potential measure of electroactivity, so far described for *G. sulfurreducens* but easily transferable to other species, is the capacity for electron storage in the cell (Esteve-Núñez et al., 2008; Malvankar et al., 2012). This capacitor principle reflects the size of the cellular redox pool to store electrons. Compared to the above described possible measures of electroactivity on the cellular level also the subcellular level can be considered, as e.g., by measuring the apparent electron transfer rate of, e.g., cytochromes (Bonanni et al., 2012), or the conductivity of, e.g., nanowires (Adhikari et al., 2016). While the presence of cellular appendices is not sufficient for claiming a microbe as being electroactive the exact determination of the specific conductivity could prove the EET capacity and also differences in transfer efficiency and transfer kinetics could potentially be explained. So far there are only a few studies on nanowire conductivity and yet no threshold value is available.

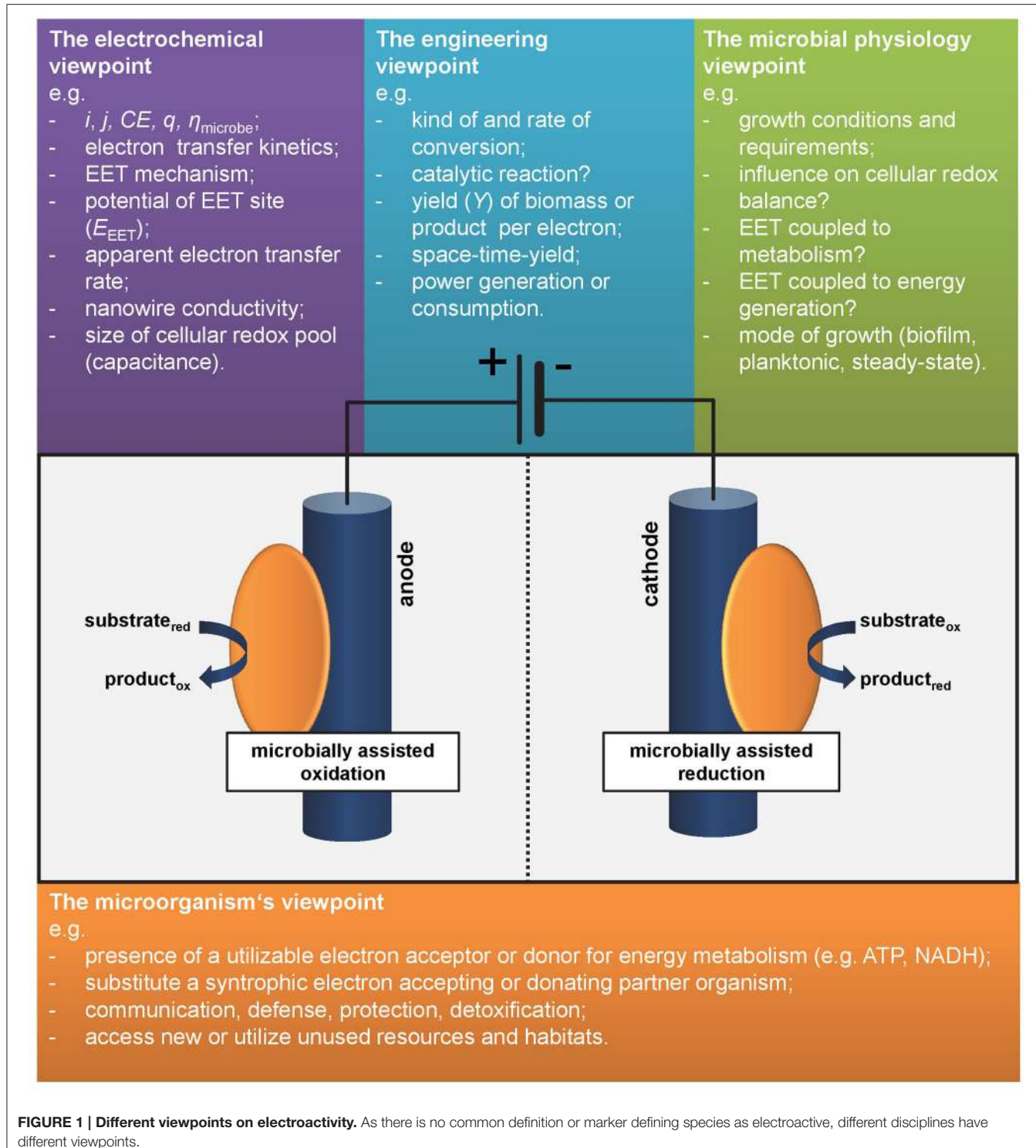


FIGURE 1 | Different viewpoints on electroactivity. As there is no common definition or marker defining species as electroactive, different disciplines have different viewpoints.

When considering full or partly planktonic living cultures, e.g., the well-studied *Shewanellaceae*, the definition of a measure of electroactivity becomes not simpler either. Here, cell density and inhomogeneities and gradients of substrates, metabolites or mediators as well as access to the electrode surface play an

additional role that makes systematic comparison even more complex (Borole et al., 2011; Harnisch and Rabaey, 2012; Patil et al., 2015).

These few considerations and surely not comprehensive treatise already shows that even for the model organisms of

Geoabacteraceae and *Shewanellaceae* there is no straightforward measure of electroactivity.

THE DIVERSITY OF ELECTROACTIVE LIVINGS

When considering less systematically studied microorganisms differing from the model organisms the definition of electroactivity becomes even more challenging. Up to now 94 microbial species are assigned to be electroactive and presumably significantly more electroactive species exist in nature (Koch and Harnisch, 2016). There is strong evidence that some electroactive microbes can only exist in microbial consortia. Therefore, the questions arises what makes the cells forming electroactive biofilms? Is it the sole presence of a potential electron acceptor or donor, as described for 54 electroactive pure cultures. In these cases, the electrode might serve as substitute to a syntrophic electron accepting or donating partner organism in a natural setting. But also in nature, microorganisms can be selective and not match with every potential partner organism. There is hardly anything known, which kind of communication, recognition or additional metabolite transfer might take place between the partners involved in consortia. These additional signals will not be provided by a sole electrode and therefore microorganisms performing EET, but not on electrodes, might accordingly not be identified as electroactive, but shouldn't they?

The comparison of electroactive microorganisms becomes even more vague when we consider electroactive microorganisms as all microorganisms that are able to lead to a Faradaic current flow at electrodes. This current flow can result from the connection of the electron flow to the microbial metabolism but also from a solely catalytic reaction performed within the cells, but being independent from their growth, maintenance or even metabolism. Interestingly, recently also ionic currents have shown to play an important role in microbial communities, especially their communication (Prindle et al., 2015). Further, even current flow resulting obviously from cell burst can be found in literature claiming species as electroactive. Here we disagree on their inclusion. Considering microbial electroactivity in a catalytic sense, i.e., based on chemical transformations taking place independently from the metabolism, seems a very artificial approach from a microbial physiology viewpoint and far away from any natural significance. At the same time these transformations can be considered as highly promising from the technical perspective, e.g., in bioelectrosynthesis. This also holds true for the concept of steering the microbial metabolism by interfering in the cellular redox balance, e.g., by redox mediators, in case the microorganisms do not interact with electrodes naturally (Park and Zeikus, 2000). This is nothing we observe in nature or that we could explain by its natural relevance, but still it results in an obvious wiring of microbial metabolism and electron flow. Is this microbial electroactivity?

There are plenty of examples in nature where microorganisms communicate, fight for resources and invade new habitats by producing redox active compounds like e.g., phenazines in *Pseudomonas* spp. (Price-Whelan et al., 2006). In this case,

the primary aim (from the viewpoint of the microbial cell) is to communicate with other cells of the own species (quorum sensing), to defend a habitat against competitors, detoxify toxic compounds or access new resources. However, the same chemicals can also serve as redox mediators for mediated electron transfer (Rabaey et al., 2005). In these cases, the EET might be no or only a minor mode of energy generation but will rather consume additional resources and provide the involved species a short time but possibly significant selection advantage. At the same time, we can utilize these microbial capacities in technical systems but do we define these species then also as electroactive? And how can one trigger these specific activities and utilize these microorganisms long term in technical systems? Is it "healthy" for a microbial cell when interfering with their metabolic pathways using electrodes?

ON THE FUTURE DISTILLING OF THE ESSENCE OF MICROBIAL ELECTROACTIVITY

Apart from maybe a dozen model organisms, the mechanism of EET in microorganisms being assigned electroactive is almost not investigated. For instance we hardly know anything about the potential electron uptake mechanism from cathodes or how gram-positive bacteria perform EET. Accordingly, it is a challenge to assess or even compare the electroactivity of different species with each other as their "motivation" for EET might be completely different as well as its connection to the cellular metabolism. Even if there is a basic understanding of the involved mechanisms it seems not applicable to compare a CE of anodic acetate oxidation to a cathodic nitrate reduction. We believe that the first steps for approaching a common sense will involve the definition of a set of basic microbial characteristics to be reported and experimental setups to characterize microbial electroactivity in pure cultures. It is not sufficient to "just" measure a current in the presence of microorganisms (even with sufficient replicates) to call this microbe electroactive. In addition to assessment of functional parameters (e.g., current density, CE) in a standardized setup the understanding of the functional connection of current flow and microbial metabolism should be aimed. As detailed above this functional characterization is not straightforward for pure cultures yet, and represents an even greater challenge when mixed cultures are considered.

Finally, a community-wide discussion leading to a (even preliminary) common sense of electroactivity is needed. Even then there seems to be not only one kind of electroactivity and assigning a microbe electroactive or not might be in the eye of the beholder or in other words "It is the distiller's personal finest selection."

AUTHOR CONTRIBUTIONS

All authors listed, have made substantial, direct and intellectual contribution to the work, and approved it for publication.

ACKNOWLEDGMENTS

FH acknowledges support by the Federal Ministry of Education and Research (Research Award “Next generation

REFERENCES

- Adhikari, R. Y., Malvankar, N. S., Tuominen, M. T., and Lovley, D. R. (2016). Conductivity of individual *Geobacter* pili. *RSC Adv.* 6, 8354–8357. doi: 10.1039/C5RA28092C
- Bard, A. J., Inzelt, G., and Scholz, F. (2012). *Electrochemical Dictionary*. Berlin; Heidelberg: Springer-Verlag. doi: 10.1007/978-3-642-29551-5
- Bonanni, P. S., Bradley, D. F., Schrott, G. D., and Busalmen, J. P. (2013). Limitations for current production in *Geobacter sulfurreducens* biofilms. *ChemSusChem* 6, 711–720. doi: 10.1002/cssc.201200671
- Bonanni, P. S., Schrott, G. D., Robuschi, L., and Busalmen, J. P. (2012). Charge accumulation and electron transfer kinetics in *Geobacter sulfurreducens* biofilms. *Energy Environ. Sci.* 5, 6188–6195. doi: 10.1039/c2ee02672d
- Borole, A. P., Reguera, G., Ringeisen, B., Wang, Z.-W., Feng, Y., and Kim, B. H. (2011). Electroactive biofilms: current status and future research needs. *Energy Environ. Sci.* 4, 4813–4834. doi: 10.1039/c1ee02511b
- Brutin, E. D., and Gralnick, J. A. (2012). Shuttling happens: soluble flavin mediators of extracellular electron transfer in *Shewanella*. *Appl. Microbiol. Biotechnol.* 93, 41–48. doi: 10.1007/s00253-011-3653-0
- Doran, P. M. (1995). *Bioprocess Engineering Principles*. London: Academic Press.
- Egli, T. (2015). Microbial growth and physiology: a call for better craftsmanship. *Front. Microbiol.* 6:287. doi: 10.3389/fmicb.2015.00287
- Esteve-Núñez, A., Sosnik, J., Visconti, P., and Lovley, D. R. (2008). Fluorescent properties of c-type cytochromes reveal their potential role as an extracytoplasmic electron sink in *Geobacter sulfurreducens*. *Environ. Microbiol.* 10, 497–505. doi: 10.1111/j.1462-2920.2007.01470.x
- Gorby, Y. A., Yanina, S., McLean, J. S., Rosso, K. M., Moyles, D., Dohnalkova, A., et al. (2006). Electrically conductive bacterial nanowires produced by *Shewanella oneidensis* strain MR-1 and other microorganisms. *Proc. Natl. Acad. Sci. U.S.A.* 103, 11358–11363. doi: 10.1073/pnas.0604517103
- Gross, B. J., and El-Naggar, M. Y. (2015). A combined electrochemical and optical trapping platform for measuring single cell respiration rates at electrode interfaces. *Rev. Sci. Instrum.* 86:064301. doi: 10.1063/1.4922853
- Harnisch, F., and Rabaey, K. (2012). The diversity of techniques to study electrochemically active biofilms highlights the need for standardization. *ChemSusChem* 5, 1027–1038. doi: 10.1002/cssc.201100817
- Jiang, X., Hu, J., Petersen, E. R., Fitzgerald, L. A., Jackan, C. S., Lieber, A. M., et al. (2013). Probing single- to multi-cell level charge transport in *Geobacter sulfurreducens* DL-1. *Nat. Commun.* 4:2751. doi: 10.1038/ncomms3751
- Koch, C., and Harnisch, F. (2016). Is there a specific ecological niche for electroactive microorganisms? *ChemElectroChem.* 3, 1282–1295. doi: 10.1002/celc.201600079
- Korth, B., Maskow, T., Picioreanu, C., and Harnisch, F. (2016). The microbial electrochemical Peltier heat: an energetic burden and engineering chance for primary microbial electrochemical technologies. *Energy Environ. Sci.* 9, 2539–2544. doi: 10.1039/C6EE01428C
- Liu, H., Newton, G. J., Nakamura, R., Hashimoto, K., and Nakanishi, S. (2010). Electrochemical characterization of a single electricity-producing bacterial cell of *Shewanella* by using optical tweezers. *Angew. Chem. Int. Ed.* 49, 6596–6599. doi: 10.1002/anie.201000315
- Lovley, D. R. (2012). Electromicrobiology. *Annu. Rev. Microbiol.* 66, 391–409. doi: 10.1146/annurev-micro-092611-150104
- Malvankar, N. S., Mester, T., Tuominen, M. T., and Lovley, D. R. (2012). Supercapacitors based on c-type cytochromes using conductive nanostructured networks of living bacteria. *Chemphyschem* 13, 463–468. doi: 10.1002/cphc.201100865
- Melton, E. D., Swanner, E. D., Behrens, S., Schmidt, C., and Kappler, A. (2014). The interplay of microbially mediated and abiotic reactions in the biogeochemical Fe cycle. *Nat. Rev. Microbiol.* 12, 797–808. doi: 10.1038/nrmicro3347
- Newman, D. K., and Banfield, J. F. (2002). Geomicrobiology: How molecular-scale interactions underpin biogeochemical systems. *Science* 296, 1071–1077. doi: 10.1126/science.1010716
- Park, D. H., and Zeikus, J. G. (2000). Electricity generation in microbial fuel cells using neutral red as an electronophore. *Appl. Environ. Microbiol.* 66, 1292–1297. doi: 10.1128/AEM.66.4.1292-1297.2000
- Patil, S. A., Gildemyn, S., Pant, D., Zengler, K., Logan, B. E., and Rabaey, K. (2015). A logical data representation framework for electricity-driven bioproduction processes. *Biotechnol. Adv.* 33, 736–744. doi: 10.1016/j.biotechadv.2015.03.002
- Pham, H. T., Boon, N., Aelterman, P., Clauwaert, P., De Schampheleire, L., van Oostveldt, P., et al. (2008). High shear enrichment improves the performance of the anodophilic microbial consortium in a microbial fuel cell. *Microb. Biotechnol.* 1, 487–496. doi: 10.1111/j.1751-7915.2008.00049.x
- Price-Welhan, A., Dietrich, L. E., and Newman, D. K. (2006). Rethinking ‘secondary’ metabolism: physiological roles for phenazine antibiotics. *Nat. Chem. Biol.* 2, 71–78. doi: 10.1038/nchembio764
- Prindle, A., Liu, J., Asally, M., Ly, S., Garcia-Ojalvo, J., and Süel, G. M. (2015). Ion channels enable electrical communication in bacterial communities. *Nature* 527, 59–63. doi: 10.1038/nature15709
- Rabaey, K., Boon, N., Höfte, M., and Verstraete, W. (2005). Microbial phenazine production enhances electron transfer in biofuel cells. *Environ. Sci. Technol.* 39, 3401–3408. doi: 10.1021/es048563o
- Schröder, U., Harnisch, F., and Angenent, L. T. (2015). Microbial electrochemistry and technology: terminology and classification. *Energy Environ. Sci.* 8, 513–519. doi: 10.1039/C4EE03359K
- Tan, Y., Adhikari, R. Y., Malvankar, N. S., Ward, J. E., Nevin, K. P., Woodard, T. L., et al. (2016). The low conductivity of *Geobacter uraniireducens* pili suggests a diversity of extracellular electron transfer mechanisms in the genus *Geobacter*. *Front. Microbiol.* 7:980. doi: 10.3389/fmicb.2016.00980

biotechnological processes—Biotechnology 2020+”) and the Helmholtz-Association (Young Investigators Group). This work was supported by the Helmholtz Association within the Research Program Renewable Energies.

Conflict of Interest Statement: The authors declare that the research was conducted in the absence of any commercial or financial relationships that could be construed as a potential conflict of interest.

Copyright © 2016 Koch and Harnisch. This is an open-access article distributed under the terms of the Creative Commons Attribution License (CC BY). The use, distribution or reproduction in other forums is permitted, provided the original author(s) or licensor are credited and that the original publication in this journal is cited, in accordance with accepted academic practice. No use, distribution or reproduction is permitted which does not comply with these terms.



Characterization of Electricity Generated by Soil in Microbial Fuel Cells and the Isolation of Soil Source Exoelectrogenic Bacteria

Yun-Bin Jiang^{1,2}, Wen-Hui Zhong^{1,2}, Cheng Han^{1,2} and Huan Deng^{1,2,3*}

¹ Jiangsu Provincial Key Laboratory of Materials Cycling and Pollution Control, School of Geography Science, Nanjing Normal University, Nanjing, China, ² Jiangsu Center for Collaborative Innovation in Geographical Information Resource Development and Application, Nanjing, China, ³ School of Environment, Nanjing Normal University, Nanjing, China

OPEN ACCESS

Edited by:

Yong Xiao,
Institute of Urban Environment (CAS),
China

Reviewed by:

Xianhua Liu,
Tianjin University, China
Weishou Shen,
The University of Tokyo, Japan

*Correspondence:

Huan Deng
hdeng@njnu.edu.cn

Specialty section:

This article was submitted to
Microbiotechnology, Ecotoxicology
and Bioremediation,
a section of the journal
Frontiers in Microbiology

Received: 15 August 2016

Accepted: 21 October 2016

Published: 08 November 2016

Citation:

Jiang Y-B, Zhong W-H, Han C and
Deng H (2016) Characterization of
Electricity Generated by Soil
in Microbial Fuel Cells
and the Isolation of Soil Source
Exoelectrogenic Bacteria.
Front. Microbiol. 7:1776.
doi: 10.3389/fmicb.2016.01776

Soil has been used to generate electrical power in microbial fuel cells (MFCs) and exhibited several potential applications. This study aimed to reveal the effect of soil properties on the generated electricity and the diversity of soil source exoelectrogenic bacteria. Seven soil samples were collected across China and packed into air-cathode MFCs to generate electricity over a 270 days period. The Fe(III)-reducing bacteria in soil were enriched and sequenced by Illumina pyrosequencing. Culturable strains of Fe(III)-reducing bacteria were isolated and identified phylogenetically. Their exoelectrogenic ability was evaluated by polarization measurement. The results showed that soils with higher organic carbon (OC) content but lower soil pH generated higher peak voltage and charge. The sequencing of Fe(III)-reducing bacteria showed that *Clostridia* were dominant in all soil samples. At the family level, *Clostridiales* Family XI incertae sedis were dominant in soils with lower OC content but higher pH (>8), while *Clostridiaceae*, *Lachnospiraceae*, and *Planococcaceae* were dominant in soils with higher OC content but lower pH. The isolated culturable strains were allied phylogenetically to 15 different species, of which 11 were *Clostridium*. The others were *Robinsoniella peoriensis*, *Hydrogenoanaerobacterium saccharovorans*, *Eubacterium contortum*, and *Oscillibacter ruminantium*. The maximum power density generated by the isolates in the MFCs ranged from 16.4 to 28.6 mW m⁻². We concluded that soil OC content had the most important effect on power generation and that the *Clostridiaceae* were the dominant exoelectrogenic bacterial group in soil. This study might lead to the discovery of more soil source exoelectrogenic bacteria species.

Keywords: Fe(III)-reducing bacteria, Illumina pyrosequencing, *Clostridiaceae*, polarization curve, soil property

INTRODUCTION

Soil can be used to generate electrical power in microbial fuel cells (MFCs), which convert chemical energy from soil organic compounds into electricity via catalysis by soil source exoelectrogenic microorganisms. The process of soil power generation has several potential applications. Firstly, the pollutant toxicity and soil microbial activity could be monitored by the generated electrical signals of the MFCs, such as peak voltage, quantity of electrons and start-up time (Deng et al., 2014, 2015;

Jiang et al., 2015). Secondly, the use of MFCs would lead to the elimination of soil pollutants including phenol, petrol and oil (Huang et al., 2011; Wang et al., 2012). Thirdly, the operation of MFCs mitigates methane emissions from paddy soil and sediment (Arends et al., 2014). MFCs do not need energy input, instead, a small amount of electrical power is generated. Therefore, MFCs are considered a sustainable technology. The performance of these MFCs is largely related to the magnitude of electrical current generated by the exoelectrogenic bacteria in soil. However, little is known about the character of power generation and the diversity of exoelectrogenic bacteria in different soils.

To date, around 50 bacteria belonging to three phyla *Proteobacteria*, *Firmicutes*, and *Acidobacteria* have been identified as exoelectrogenic (Zhi et al., 2014). Almost all the exoelectrogenic bacteria strains were isolated from wastewater, sediments of lakes and marine environments, rather than from soil. There is a lack of functional gene markers for exoelectrogenic bacteria; therefore, the main methods used to detect the composition of exoelectrogenic bacteria are isolation of pure cultured bacterial strains or sequence alignment of bacterial 16S rRNA genes with those of known exoelectrogenic bacteria (Song et al., 2012). Most of the evidence about the composition of exoelectrogenic bacteria in soil has been obtained using the “sequence alignment” method (Ishii et al., 2008; Ringelberg et al., 2011). However, novel exoelectrogenic bacteria would be excluded if their sequences were not identical to the identified strains. High throughput DNA pyrosequencing allowed the estimation that one gram of soil contains 1000s of bacterial species (Roesch et al., 2007). Therefore, it is necessary to isolate and identify more exoelectrogenic bacteria strains from soil.

Exoelectrogenic bacteria generally possess the ability to reduce Fe(III), and most Fe(III)-reducing bacteria are exoelectrogenic. However, some exoelectrogenic bacteria do not use Fe(III) as the sole acceptor. For example, *Calditerrivibrio nitroreducens* reduces nitrate rather than Fe(III) (Fu et al., 2013), *Desulfobulbus propionicus* reduces both sulfate and Fe(III) (Holmes et al., 2004), and some Fe(III)-reducing bacteria do not possess the ability to generate electrical current in MFCs, such as *Pelobacter carbinolicus* (Richter et al., 2007). As a result, the composition of Fe(III)-reducing bacteria largely represents the exoelectrogenic bacteria in soil (Lovley, 2006).

Soil physiochemical properties affect microbial diversity and activity (Kuramae et al., 2012), and could have major effects on exoelectrogenic microorganisms in soil (Dunaj et al., 2012). We hypothesized that the diversity of Fe(III)-reducing bacteria and exoelectrogenic bacteria isolates, together with the generated electrical power, would vary between different soils. To test our hypothesis, we collected seven soil samples with different physicochemical properties from Northern to Southern China and packed them into MFCs to generate power. Meanwhile, Fe(III)-reducing bacteria from the seven soil samples were sequenced using the Illumina pyrosequencing system, which can sequence millions of amplicons derived from the dominant species and rare species with high sequence quality (Degnan and Ochman, 2012). In addition culturable Fe(III)-reducing bacteria were isolated and subjected to taxonomic

analysis, and were inoculated into MFCs to determine their exoelectrogenic activities. Redundancy analysis was conducted to reveal the relationship between Fe(III)-reducing bacteria, soil physiochemical properties and power generation of soil in MFCs. We aimed to (1) understand the soil properties that had strong effects on the generated electricity and the diversity of Fe(III)-reducing bacteria; and (2) isolate exoelectrogenic bacteria from different soils.

MATERIALS AND METHODS

Soil Sampling

Soil samples were collected from seven sites, which were located in the Inner Mongolia Autonomous Region (IM), Hebei Province (HB), Henan Province (HN), Jiangsu Province (JS), Jiangxi Province (JX), Fujian Province (FJ), and Guangxi Zhuang Autonomous Region (GX), respectively. The location information of the sampling sites is shown in Supplementary Table S1. Each site was planted with one dominant vegetation type. In each site, surface soil samples (0–20 cm) from three randomly selected plots (0.5 m × 0.5 m) were collected and mixed to represent a site, after removing the surface litter. After the soil samples were sieved and passed through a 2 mm diameter mesh, they were stored at 4°C for less than 2 weeks before a series of experiments, including Fe(III)-reducing bacteria enrichment, MFCs operation and soil property measurement.

Soil Property Measurements

Each of the seven soil samples was divided into three aliquots as replicates for MFCs operation. Before the operation, soil physiochemical properties of each aliquot were analyzed using routine methods (Page et al., 1982). Briefly, soil texture was determined by the sieve and pipette method. Soil maximum water holding capacity (MWHC) was determined by the difference between dry and soaked soil weights. Soil pH was measured at 1:2.5 (soil:water) and soil electrical conductivity (EC) at 1:5 (soil:water). Soil cation exchange capacity (CEC) was analyzed by the compulsive exchange method. Soil organic carbon (OC) was determined by K₂CrO₄ oxidation; total nitrogen (TN) by Kjeldahl digestion; and total phosphorus (TP) by colorimetry following NaOH digestion. Dissolved organic carbon (DOC; extracted by 0.5 M K₂SO₄) and humic carbon (HC; extracted by 0.1 M Na₄P₂O₇ and 0.1 M NaOH) were measured using a TOC analyzer (TOC-L, Shimadzu, Kyoto, Japan). Soil total dissolved iron (DFe_T) was extracted by 0.2 M H₂C₂O₄-(NH₄)₂C₂O₄ (McKeague and Day, 1966) and measured by flame atomic absorption spectroscopy (AA240, Agilent Technologies, Santa Clara, CA, USA). Soil microbial biomass carbon (MBC) was measured by the fumigation-extraction method (Vance et al., 1987).

MFCs Setup and Operation

A picture and schematic diagram of soil MFCs are shown in Supplementary Figure S1. Twenty-one air-cathode MFC reactors were built in beakers with a 6 cm diameter and 13.5 cm height. Square carbon felt (Haoshi, Lanzhou, China) and platinized

carbon paper (Hesen, Shanghai, China) were used as the anode and cathode, respectively, with the same area of 9 cm^2 (side length 3 cm). In each reactor, the anode was embedded with 250 g soil (dry weight) and the cathode was placed on the soil surface. Deionized water was gently poured into the reactor to keep soil flooded. The two electrodes were connected to an external circuit with a resistance of $1000\ \Omega$ using titanium wire. The MFCs were operated in triplicate at a constant 30°C in an incubator. Voltage data generated by the MFCs were recorded every 10 min using a data acquisition module. Deionized water was added every 24 h to compensate for water evaporation and maintain the initial state. After 270 days of MFCs operation, flooded soil in each MFC was air dried under open circuit conditions at 30°C and sieved through a 2 mm diameter mesh to measure the soil properties using the same methods as detailed in the previous section. To confirm that the voltage originated from microbial processes rather than chemical reactions, another seven control MFCs were operated under the same conditions but with chloroform fumigation-sterilized soil (Deng et al., 2015; Jiang et al., 2015).

Enrichment of Fe(III)-Reducing Bacteria

The enrichment of Fe(III)-reducing bacteria in the soil samples was conducted under anaerobic conditions (10% CO_2 , 10% H_2 , and 80% N_2) in an anaerobic workstation (MiniMacs, Don Whitley Scientific, Shipley, UK). For each soil sample, 2.0 g soil (dry weight) was inoculated into 100 mL basal medium. One liter of basal medium (BM) contained 8 g peptone, 1 g yeast extract, 0.12 g NH_4Cl , 16 g sodium acetate, 5 g NaCl , 1.2 g K_2HPO_4 , 1 g cysteine hydrochloride, 1 mg resazurin, 5 mL mineral, and 5 mL vitamin solutions (Sigma-Aldrich, Co., St. Louis, MO, USA) (Lovley and Phillips, 1988). The electron acceptor was 25 mM ferric citrate. The medium was boiled with N_2 for 20 min and then autoclaved in sealed bottles. The pH of the autoclaved medium was 6.7. The inoculated medium was incubated at 30°C for 7 days under dark conditions. The enrichment procedure was repeated three times (Kim et al., 2005).

High-Throughput Pyrosequencing

Five-milliliters of the enrichment product were collected after the anaerobic culture and centrifuged at $14,000 \times g$ for 10 min. The genomic DNA was immediately extracted from the precipitates using a Fast DNA SPIN kit for soil (BIO101, MP Biomedicals, Carlsbad, CA, USA) following the manufacturer's instructions. The purity and the quantity of the extracted DNA were determined using a nanodrop UV-Vis spectrophotometer (ND-1000, NanoDrop, Wilmington, DE, USA) at 230, 260, and 280 nm.

The bacterial 16S rRNA genes of the seven enrichments were amplified using universal primers 515F (5'-GTG CCA GCM GCC GCG GTA A-3') and 907R (5'-CCG TCA ATT CMT TTR AGT TT-3') (Weisburg et al., 1991). The PCR reactions were quantified and the products were then purified. At least 24,000 reads were conduct for each sample using the Illumina MiSeq platform (Illumina, San Diego, CA, USA) using 2 bp \times 250 bp paired end flow cells and reagent cartridges. The Illumina sequencing data were analyzed by Mothur (Schloss et al., 2009) using the MiSeq standard operating procedure (Kozich et al., 2013). The raw data

were deposited in the NCBI Sequence Read Archive database with the accession number SRP071622.

Isolation and Taxonomic Analysis of Fe(III)-Reducing Bacteria

After the three rounds of 7 days anaerobic incubation, 0.5 ml of the enrichment products were separated by the spread plate method after 10-fold dilution for bacteria isolation using solid BM. The plates were incubated for 5 days under anaerobic condition, after which single black colonies were picked out and inoculated into liquid BM. The procedures were repeated three times to obtain pure cultures. All the experiments were conducted in the MiniMacs anaerobic workstation.

The phylogenetic analysis of the isolates was conducted based on the 16S rRNA gene sequences, which were PCR amplified using the primers 27F (5'-AGA GTT TGA TCM TGG CTC AG-3') and 1492R (5'-GGT TAC CTT TGT TAC GAC TT-3') (Suzuki and Giovannoni, 1996). The PCR products were cloned using the PeasyTM-T3 Cloning Kit (TransGen, Beijing, China) according to the manufacturer's recommendations. GeneScript (Nanjing, China) sequenced six clones for each isolate. The vector sequences were removed using DNASTAR Lasergene (version 7.1). The gene sequences of the isolates were subjected to taxonomic assignments using BlastX. The sequences of all the isolates were submitted to GenBank with the accession numbers KT889276–KT889290. One strain each of isolate 1 (CGMCC 1.5212) and isolate 2 (CGMCC 1.5211) were deposited in the China General Microbiological Culture Collection Center.

Electrochemical Tests of the Isolates

One of the strains phylogenetically related to each species was randomly selected and the exoelectrogenic activity of the strains was characterized by polarization curve measurement using H-type dual chamber MFC reactors (100-I, Fuxiao, Changshu, China). The anode and cathode were both rectangular carbon felt with the same area of 18 cm^2 ($3\text{ cm} \times 6\text{ cm}$), connected to an external resistance of $1000\ \Omega$ using titanium wire. LB medium, which is favorable for power generation by exoelectrogenic bacteria, was used in the subsequent tests of the isolates (Feng et al., 2014). The anodic chamber and cathodic chamber were filled with 120 mL LB medium and 120 mL potassium ferricyanide [100 mM $\text{K}_3\text{Fe}(\text{CN})_6$ in 50 mM, pH 7 PBS], respectively. The two chambers were separated by a cation exchange membrane (32S, Qianqiu, Hangzhou, China). The reactors and LB medium were autoclaved before use. Voltage data were recorded every 20 min using a data acquisition module.

The polarization curves of the MFC reactors with pure isolates were measured in the fed-batch mode (Lovley and Phillips, 1988). Briefly, the liquid medium containing isolated cells (200 μL) was inoculated into the anodic chamber. Eighty-milliliters of medium were replaced after the voltage of MFCs reached its peak. The reactors were then operated under open circuit conditions for 4 h and with different loads (50,000, 10,000, 5,000, 1,000, 800, 500, 300, 200, and 100 Ω) for 20 min for each load. All the MFCs were operated at a constant 30°C in an incubator.

Statistical Analysis

The charge generated from the MFCs, defined as the quantity of the generated electrons, was calculated as previously described (Deng et al., 2015). Current density was calculated from the external load and cell voltage according to Ohm's law ($I = U/R$) and normalized to the surface area (m^2) of the cathodic electrode. The power density was calculated by using P ($mW\ m^{-2}$) = $10 \times U^2/(R \times A)$, where U (mV) is the recorded voltage, A (m^2) is the surface area of the anode, and R (Ω) is the external load (Cheng et al., 2006).

Significant differences between means were determined by one-way ANOVA at a level of $P < 0.05$, using the least significance difference (LSD) test. Cluster analysis of the Fe(III)-reducing bacteria community was conducted based on the square Euclidean distance by the between-groups linkage method. Redundancy analysis (RDA) was carried out by Canoco for Windows (version 4.5) between the Fe(III)-reducing bacteria community and environmental or electrical variables, which were selected using the Monte Carlo permutations test (499 permutations). All statistical tests, except for RDA, were performed using SPSS software (version 18.0).

RESULTS

Power Generation of Soils in MFCs

The electricity generation by MFCs comprising the seven soils lasted for 270 days (Figure 1A). The voltage curves of the MFCs were characterized by a single peak. The seven soils varied in their peak voltage and also the time from the beginning to the peak. It took about 40 days for JS, 60 days for both FJ and GX, and 100 days for JX to reach to their peak voltages. IM, HB and HN reached their peaks at round 130 days. The peak voltages of JS, GX and JX were 148.1, 123.3, and 102.6 mV, respectively. They were significantly higher ($P < 0.05$) than FJ (32.9 mV), HN (8.4 mV), HB (7.4 mV), and IM (6.2 mV) (Figure 1B). After the peak data, the voltage continued to decrease until the end of MFCs operation, when the voltage data of all soils were below 30 mV. During the 270 days of MFCs operation, JX generated the highest charge (1052.4 C), followed by GX (842.2 C), JS (644.7 C), FJ (302.2 C), HN (66.4 C), HB (63.5 C), and IM (41.9 C) (Figure 1C). No voltages were detected in any MFCs containing sterilized soil samples, indicating that the electricity generation originated from microbial catalysis rather than chemical reactions.

Soil Properties before and after MFCs Operation

The soil physicochemical and microbial properties varied between soils (Table 1). Before MFCs operation, the CEC, OC, TN, and HC values in soils from JS and JX were significantly higher ($P < 0.05$) than the other soils. JS exhibited the highest MBC, followed by JX and GX. JX also had the highest DF_{ET}. Soils from IM, HB and HN exhibited higher soil pH (>8) but lower OC, DOC, HC, and MBC compared with the other soils. Compared with soil physicochemical and microbial properties

before MFCs operation, after 270 days MFCs operation, the OC and DOC of IM, HB and HN did not change significantly; however, those of JS, JX, FJ, and GX decreased significantly ($P < 0.05$). The MBC of all the seven soils decreased significantly after MFCs operation.

Diversity of Fe(III)-Reducing Bacteria in the Soils

The sequences of Fe(III)-reducing bacteria in the seven soils were assigned to the known phyla, class and family. Four phyla were observed, with *Firmicutes* being the overwhelmingly dominant phylum (Supplementary Figure S2A). Six classes were detected, including α -, β - and δ -*Proteobacteria*, *Clostridia*, *Bacilli*, and *Actinobacteria* (Supplementary Figure S2B). The most abundant class was *Clostridia*, which accounted for over 90% of the total composition in the seven soils. At the family level, the composition of Fe(III)-reducing bacteria was different between soils (Figure 2). In IM, HB and HN, *Clostridiales* Family XI. incertae sedis accounted for 30.5, 26.0, and 18.3% of total composition, respectively. However, it was a minor bacterial group in FJ (2.6%), GX (0.3%), JS (<0.1%), and JX (<0.1%). By contrast, the relative abundances of *Lachnospiraceae* in IM (7.9%), HB (3.7%), and HN (7.4%) were lower than those in JS (14.7%), JX (25.7%), and GX (29.9%). GX was dominated by *Clostridiaceae* (57.5%) and *Lachnospiraceae* (31.4%). The relative abundance of *Peptostreptococcaceae* in GX was only 0.1%, which was much lower than that of the other six soils (16.5~38.5%). *Eubacteriaceae* and *Ocillospiraceae* were detected in FJ, although their relative abundances were less than 0.1%. Cluster analysis of the Fe(III)-reducing bacterial community at the family level revealed that IM, HB, and HN were grouped in one cluster, while JS, JX, and FJ were in another cluster. GX was not grouped with either cluster (Figure 2).

Relationships between Fe(III)-Reducing Bacteria and Soil Properties

Redundancy analysis showed that the first two components (RDA1 and RDA2) together explained 65.5% of the total variation of the Fe(III)-reducing bacteria (Figure 3). Along RDA1, IM, HB, and HN were separated from FJ, JS and JX, and GX was separated from the two groups. RDA2 mainly separated the group comprising FJ, JS and JX from the other four soils. The relative abundances of the families *Clostridiales* Family XI. incertae sedis, *Ruminococcaceae*, *Bacillaceae*, *Dehalobacteriaceae*, *Symbiobacteriaceae*, and *Syntrophomonadaceae* were positively related to soil pH and were increased in IM, HB, and HN. The relative abundances of the families *Peptostreptococcaceae*, *Hyphomicrobiaceae*, *Burkholderiaceae*, and *Veillonellaceae* were positively related to soil OC and were increased in JS, JX and FJ. The families *Clostridiaceae* and *Planococcaceae* were more abundant in GX, and their relative abundances were positively correlated with soil DOC. Peak voltage and charge, which increased along with RDA1 and RDA2, were positively correlated with the families *Hyphomicrobiaceae*, *Burkholderiaceae*, *Paenibacillaceae*, *Lachnospiraceae*, *Planococcaceae*, and *Clostridiaceae*.

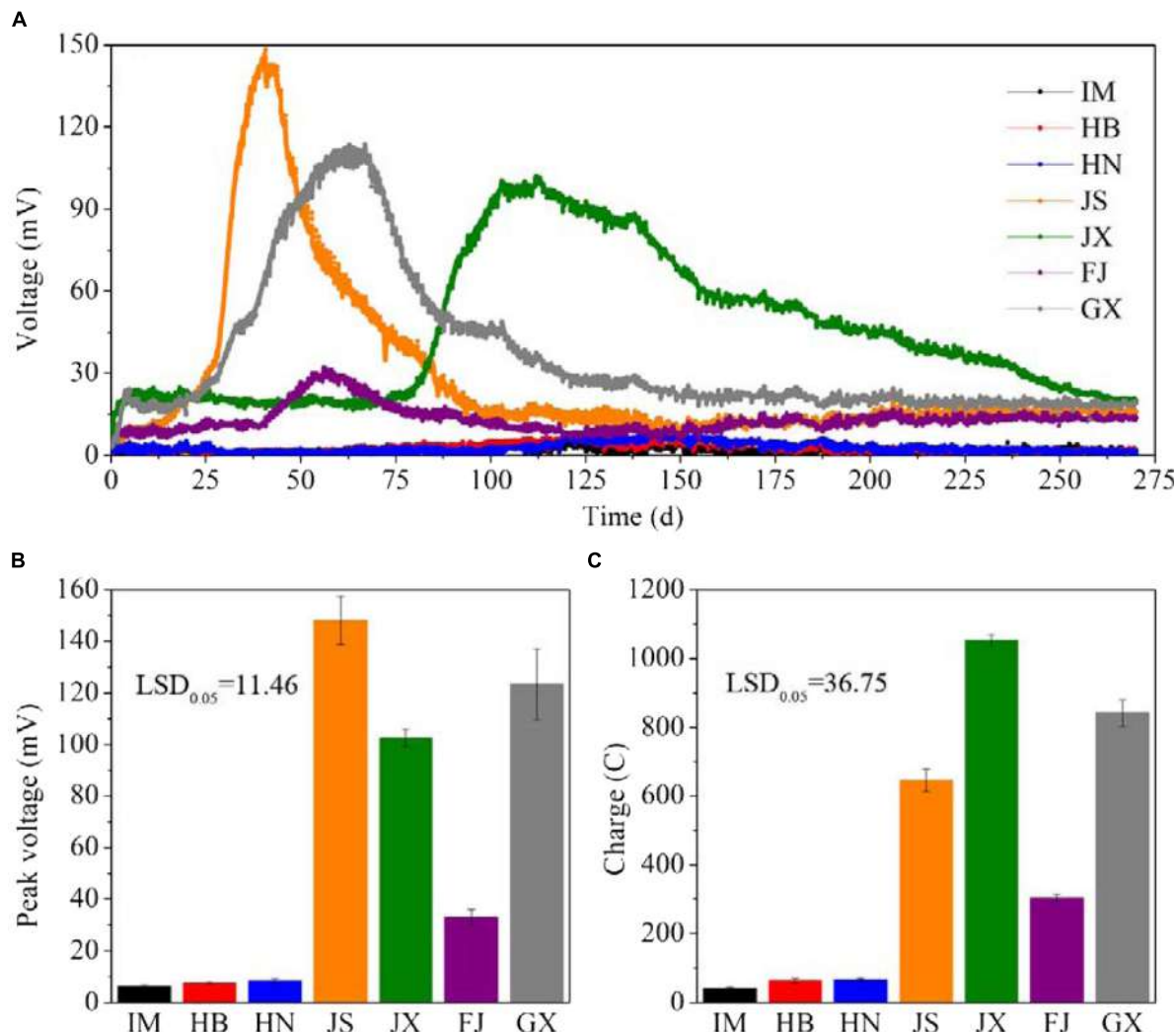


FIGURE 1 | The V-t curves (A), peak voltage (B) and charge quantity (C) of MFCs constructed using the seven soils. Data are presented as means ($n = 3$) in (A) and means with error bars as standard error ($n = 3$) in (B,C). LSD_{0.05} represents the least significant difference at level of $P < 0.05$. IM, HB, HN, JS, JX, FJ, and GX represent the seven sampling sites in Inner Mongolia, Hebei, Henan, Jiangsu, Jiangxi, Fujian, and Guangxi, respectively.

Taxonomic and Electrochemical Analysis of Fe(III)-Reducing Bacteria Isolates

Culturable strains isolated from the seven soils were phylogenetically related to 15 different species, of which 11 were *Clostridium* spp. (Table 2). Isolate 12, belonging to the *Lachnospiraceae*, was isolated from JS. Isolates 13–15, belonging to *Ruminococcaceae*, *Eubacteriaceae*, and *Oscillospiraceae*, respectively, were isolated from FJ. Polarization and power density curves of the 15 isolates are shown in Figure 4. The MFCs catalyzed by the 15 isolates showed an open circuit voltage ranging from 400 to 630 mV. The cell voltage decreased, while the electrical current increased, with decreasing external load. The voltage drops of the polarization curves showed activation losses, ohmic losses and concentration losses. The power density curves of the 15 isolates peaked at the range of 16.4~28.6 mW m⁻². Isolate 6, which was related to both *Clostridium amyloolyticum*

and *Clostridium mesophilum*, exhibited the highest P_{max} (28.6 mW m⁻²) of all the isolates.

DISCUSSION

In the present study, we investigated the characters of power generation by seven soils in MFCs over a 270 days period, and revealed that the soil OC content had the most important effect on power generation. We isolated 15 strains of exoelectrogenic bacteria from the seven soil samples, and most of them were related to *Clostridium* spp. These soil source exoelectrogenic bacteria isolates have not been reported before.

Soil from JX, GX, and JS generated higher peak voltages and charges compared with the other soils. This result might be explained by the higher OC content in JX, GX, and JS compared with the other soils. The RDA showed that the peak voltage and

TABLE 1 | Soil physicochemical and microbial properties before and after MFCs operation.

	Soil	pH	OC (g kg ⁻¹)	TN (g kg ⁻¹)	TP (g kg ⁻¹)	DOC (mg kg ⁻¹)	HC (g kg ⁻¹)	DFe _T (mg kg ⁻¹)	MBC (mg kg ⁻¹)
Before MFCs operation	IM	8.51 (0.01)	8.31 (1.71)	1.12 (0.02)	0.38 (0.06)	44.02 (6.99)	4.76 (0.05)	381.79 (15.92)	125.39 (18.62)
	HB	8.33 (0.04)	6.38 (0.70)	0.88 (0.06)	1.53 (0.26)	51.26 (2.49)	4.90 (0.33)	123.95 (7.66)	21.41 (5.62)
	HN	8.26 (0.01)	11.18 (3.28)	1.05 (0.03)	1.71 (0.30)	56.73 (7.07)	5.63 (0.19)	133.15 (11.16)	116.52 (15.93)
	JS	7.07 (0.02)	25.41 (2.87)	2.26 (0.35)	0.96 (0.11)	75.47 (6.02)	9.91 (0.16)	401.39 (1.28)	377.96 (38.98)
	JX	4.12 (0.01)	24.83 (2.71)	1.71 (0.04)	0.40 (0.10)	148.88 (11.12)	10.26 (0.34)	547.84 (14.00)	304.55 (22.85)
	FJ	7.96 (0.03)	12.60 (0.51)	1.21 (0.05)	1.85 (0.36)	123.47 (21.62)	5.29 (0.49)	150.87 (5.55)	147.34 (32.98)
	GX	4.04 (0.03)	14.96 (0.62)	1.30 (0.02)	0.27 (0.03)	228.85 (11.25)	6.86 (0.87)	347.03 (11.69)	247.76 (22.06)
After MFCs operation	IM	8.22 (0.02)	8.51 (1.28)	1.22 (0.09)	0.42 (0.16)	39.24 (4.72)	3.05 (0.08)	410.43 (10.61)	26.43 (5.41)
	HB	8.24 (0.08)	7.33 (0.49)	0.86 (0.01)	1.25 (0.22)	44.18 (4.54)	2.05 (0.16)	100.74 (4.47)	37.96 (8.92)
	HN	8.12 (0.03)	9.97 (1.46)	1.08 (0.04)	1.63 (0.04)	48.71 (1.02)	2.75 (0.32)	108.99 (8.29)	38.71 (2.87)
	JS	6.17 (0.02)	14.53 (0.77)	2.23 (0.07)	0.95 (0.18)	46.47 (4.28)	9.85 (0.43)	383.99 (17.57)	78.18 (6.75)
	JX	4.61 (0.03)	14.52 (0.60)	1.59 (0.03)	0.39 (0.03)	77.76 (4.64)	10.52 (0.68)	559.74 (6.74)	90.04 (13.83)
	FJ	8.16 (0.03)	6.03 (1.23)	1.07 (0.07)	1.32 (0.08)	67.89 (11.13)	2.69 (0.66)	128.75 (24.33)	82.78 (17.76)
	GX	4.98 (0.05)	8.06 (0.56)	1.35 (0.03)	0.54 (0.09)	49.99 (1.77)	7.25 (0.33)	351.29 (5.27)	76.07 (5.64)
LSD _{0.05}		0.05	2.72	0.55	0.29	14.62	0.72	19.87	31.44

LSD_{0.05} represents the least significant difference at level of $P < 0.05$. Data are presented as means with the standard error in parenthesis. OC, organic carbon; TN, total nitrogen; TP, total phosphorus; DOC, dissolved organic carbon; HC, total humic carbon; DFe_T, total dissolved iron; MBC, microbial biomass carbon.

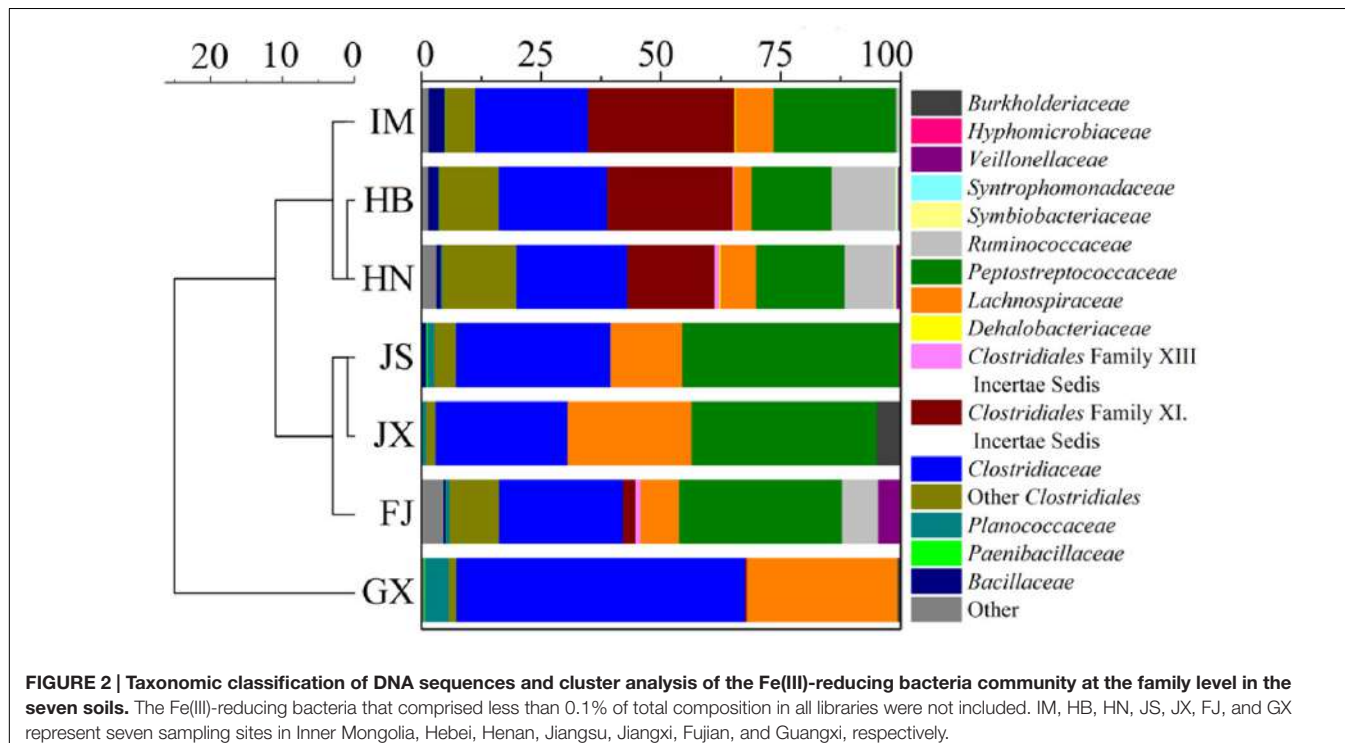
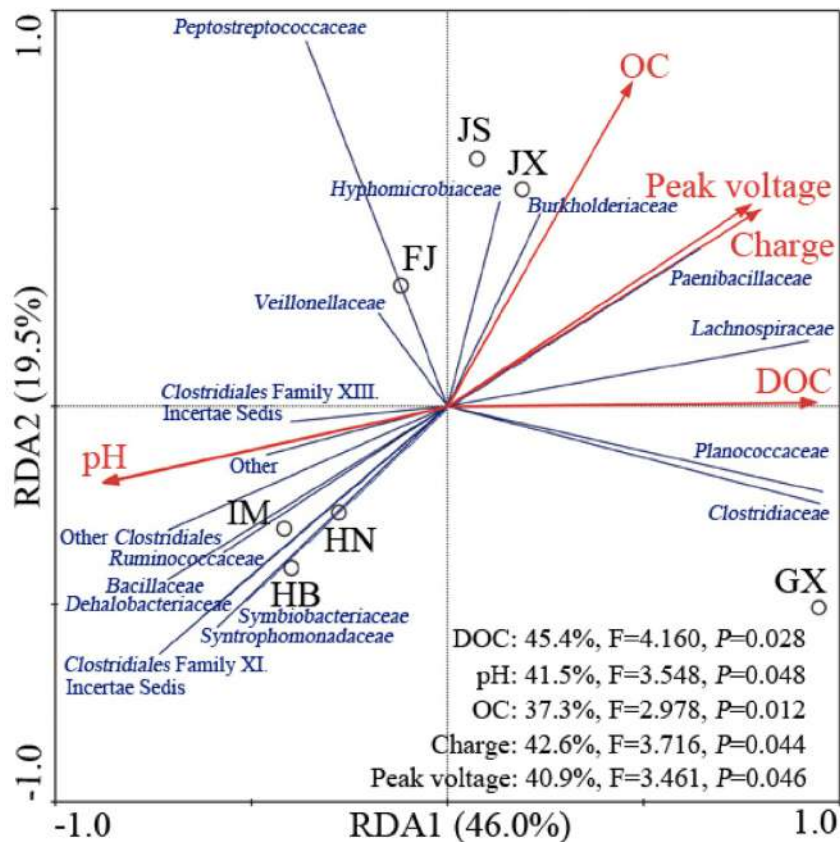


FIGURE 2 | Taxonomic classification of DNA sequences and cluster analysis of the Fe(III)-reducing bacteria community at the family level in the seven soils. The Fe(III)-reducing bacteria that comprised less than 0.1% of total composition in all libraries were not included. IM, HB, HN, JS, JX, FJ, and GX represent seven sampling sites in Inner Mongolia, Hebei, Henan, Jiangsu, Jiangxi, Fujian, and Guangxi, respectively.

charge were positively correlated with the OC and DOC content, but negatively correlated with soil pH. The OCs served as electron donors for the exoelectrogenic bacteria, whose activity increased with the input of OCs (Di Lorenzo et al., 2009). The voltage gradually decreased after the peak voltage, especially for the JX, JS, and GX samples. Soil OC and DOC content in JX, JS, and GX significantly decreased after MFCs operation, compared with before MFCs operation, suggesting that the rapid exhaustion of OCs leads to decreased power output. By contrast, studies have

shown that in air cathode MFCs, the optimal pH was between 8 and 10 for exoelectrogenic bacteria to generate power (He et al., 2008). The negative relationships between soil pH and peak voltage and charge should not indicate that acidic soil favors power generation. Therefore, we suggest that the OC and DOC contents might be more important drivers of power generation than soil pH.

Our results demonstrated that *Firmicutes* and *Clostridia* dominated the phylum and class level of Fe(III)-reducing



bacteria, respectively. A previous study also found that in paddy soil, *Firmicutes* and *Clostridia* accounted for 80 and 52% of Fe(III)-reducing bacteria, respectively (Li et al., 2011). *Clostridiales* Family XI. incertae sedis was abundant in IM, HB, and HN. However, it was a minor group in FJ and was undetected in JS, JX, and GX. Similarly, *Peptostreptococcaceae*, which was undetected in GX, was abundant in the other six soil samples. A possible reason was that the two bacterial groups were sensitive to decreased soil pH. GX had the lowest pH, which might cause stress to the bacteria, leading to the lowest diversity of Fe(III)-reducing bacteria. Nevertheless, GX generated a relatively high voltage and charge. The RDA analysis suggested that three dominant bacterial groups, *Clostridiaceae*, *Lachnospiraceae* and *Planococcaceae*, prefer low pH and high OC content in GX, and might be important for power generation. In addition, *Clostridiaceae*, *Lachnospiraceae* and *Peptostreptococcaceae*, which belong to *Clostridia*, were abundant in most tested soils and their levels were positively related to peak voltage and charge in the RDA analysis, indicating that the *Clostridia* class might play an important role in power generation in soils.

All 15 isolates of Fe(III)-reducing bacteria were confirmed to have exoelectrogenic ability by the polarization test, which is one of the most widely used techniques to determine the bioelectrochemical activity of exoelectrogenic bacteria and to test MFCs performance (Puig et al., 2010; Luo et al., 2015). Most exoelectrogenic bacteria isolates are Gram-negative and belong to the phylum *Proteobacteria* (Zhi et al., 2014). The first Gram-positive bacterium demonstrated to produce electricity in MFCs was *Clostridium butyricum* EG3 (Park et al., 2001). Our results demonstrated that *Clostridium* was the dominant exoelectrogenic bacterial group in the studied soil samples. Isolates 1 to 11 were related genetically to *Clostridium* species. It was reported that *Clostridium butyricum* had membrane-bound cytochromes which carried out the direct electron transfer (Park et al., 2001). Species of the same genus might share the same mechanism of electron transfer. *Hydrogenoanaerobacterium saccharovorans*, which was closely related to isolate 13, produces H₂ during growth (Song and Dong, 2009). H₂/H⁺ could mediate the electron transfer from exoelectrogenic bacteria to the electrode (Rosenbaum et al., 2005). *Robinsoniella peoriensis*, *Eubacterium contortum* and *Oscillibacter ruminantium*, which

TABLE 2 | Taxonomy based on 16S rRNA genes and sources of Fe(III)-reducing bacteria isolates.

Isolate	Related species	Accession number ^a	Identity	Family	Source
1	<i>Clostridium sporogenes</i>	CP009225	99%	<i>Clostridiaceae</i>	IM, HB, HN, JS, JX, FJ, GX
	<i>Clostridium botulinum</i>	CP000726	99%		
2	<i>Clostridium bifermentans</i>	JX267051	99%		IM, HB, HN, JS, JX
3	<i>Clostridium glycolicum</i>	KJ722507	99%		HB, FJ, GX
4	<i>Clostridium irregulare</i>	EU887817	99%		HN, FJ
5	<i>Clostridium</i> sp.	FJ384387	99%		HB, HN
6	<i>Clostridium amyolyticum</i> ,	NR044386	99%		HB
	<i>Clostridium mesophilum</i>	JN650296	99%		
7	<i>Clostridium beijerinckii</i>	CP006777	99%		HN
8	<i>Clostridium venationis</i>	EU089966	99%		JS
9	<i>Clostridium celerecrescens</i>	JN650298	99%		JS
10	<i>Clostridium subterminale</i> ,	NR113027	99%		FJ
	<i>Clostridium thiosulfatireducens</i>	NR042718	99%		
11	<i>Clostridium sphenoides</i> ,	LC053840	99%		JS, JX, GX
	<i>Clostridium celerecrescens</i>	JN650298	99%		
12	<i>Robinsonella peoriensis</i>	AF445283	99%	<i>Lachnospiraceae</i>	JS
13	<i>Hydrogenoanaerobacterium saccharovorans</i>	NR044425	99%	<i>Ruminococcaceae</i>	FJ
14	<i>Eubacterium contortum</i>	EU980608	99%	<i>Eubacteriaceae</i>	FJ
15	<i>Oscillibacter ruminantium</i>	NR118156	99%	<i>Ocillospiraceae</i>	FJ

^aNucleotide sequence accession number of the related species in the GenBank database.

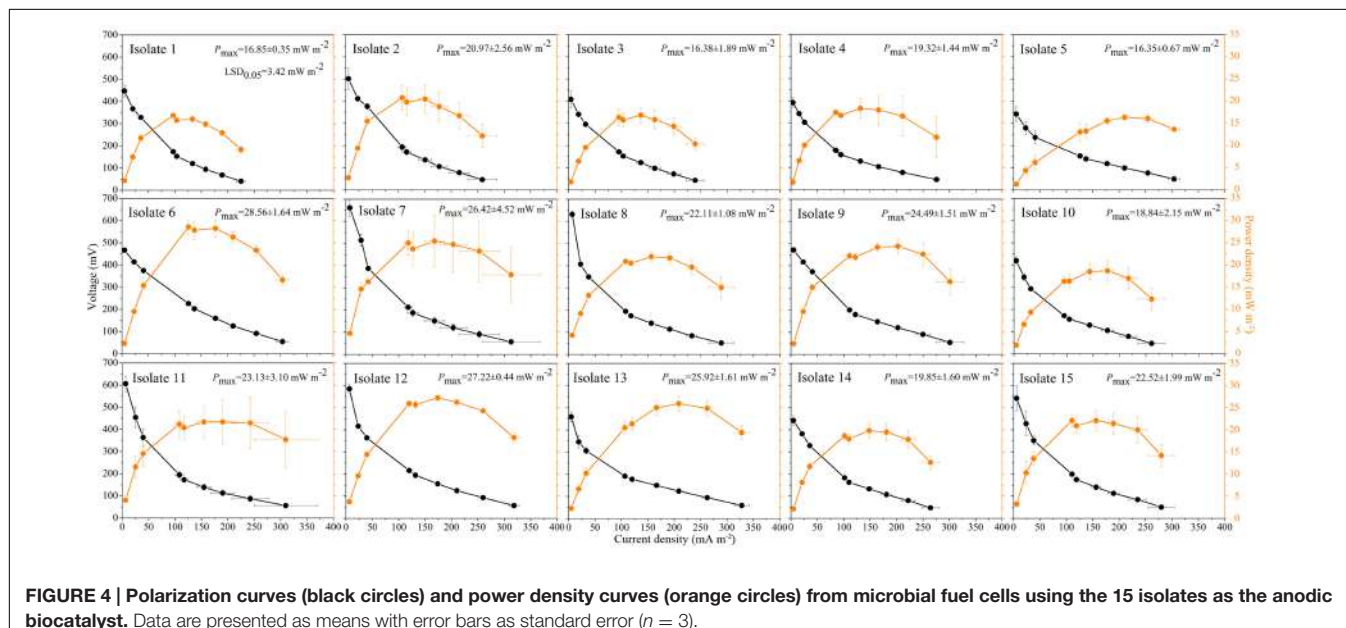


FIGURE 4 | Polarization curves (black circles) and power density curves (orange circles) from microbial fuel cells using the 15 isolates as the anodic biocatalyst. Data are presented as means with error bars as standard error ($n = 3$).

were genetically related to isolates 12, 14, and 15, respectively, have not been reported as exoelectrogenic bacteria before, and their electron transfer mechanisms remain unknown.

In our study, acetate was used as a carbon substrate in the enrichment and isolation of Fe(III)-reducing bacteria. Both acetate and glucose are the most easy-to-degrade substrates for exoelectrogenic bacteria. However, acetate exhibits higher coulombic efficiency than glucose and thus it has become the most widely applied substrate (Pham et al., 2003; Zuo et al.,

2008; Fu et al., 2013). Nevertheless, some exoelectrogenic bacteria do not utilize acetate as an optimal carbon substrate (Xu and Liu, 2011; Feng et al., 2014; Luo et al., 2015), and some cannot metabolize acetate at all. For example, *Shewanella oneidensis* oxidizes lactate rather than acetate under anaerobic conditions (Lovley et al., 1993). In addition, some exoelectrogenic bacteria are unable to reduce Fe(III) (Fu et al., 2013). We suggest that more exoelectrogenic bacterial strains should be isolated from soils using more kinds of donors and acceptors.

AUTHOR CONTRIBUTIONS

HD conceived the idea. Y-BJ and W-HZ conducted all the experiments. CH conducted the data analysis. Y-BJ wrote the first draft and HD finalized the manuscript with assistance from all co-authors.

FUNDING

This study was supported by National Natural Science Foundation of China (41301260, 41671250), National Key

Technology R&D Program (2013BAD11B01), Program of Natural Science Research of Jiangsu Higher Education Institutions of China (16KJB21007) and Outstanding Innovation Team in Colleges and Universities in Jiangsu Province.

SUPPLEMENTARY MATERIAL

The Supplementary Material for this article can be found online at: <http://journal.frontiersin.org/article/10.3389/fmib.2016.01776/full#supplementary-material>

REFERENCES

- Arends, J. B., Speckaert, J., Blondeel, E., De Vrieze, J., Boeckx, P., Verstraete, W., et al. (2014). Greenhouse gas emissions from rice microcosms amended with a plant microbial fuel cell. *Appl. Microbiol. Biotechnol.* 98, 3205–3217. doi: 10.1007/s00253-013-5328-5
- Cheng, S., Liu, H., and Logan, B. E. (2006). Power densities using different cathode catalysts (Pt and CoTMPP) and polymer binders (Nafion and PTFE) in single chamber microbial fuel cells. *Environ. Sci. Technol.* 40, 364–369. doi: 10.1021/es0512071
- Degnan, P. H., and Ochman, H. (2012). Illumina-based analysis of microbial community diversity. *ISME J.* 6, 183–194. doi: 10.1038/ismej.2011.74
- Deng, H., Jiang, Y. B., Zhou, Y. W., Shen, K., and Zhong, W. H. (2015). Using electrical signals of microbial fuel cells to detect copper stress on soil microorganisms. *Eur. J. Soil Sci.* 66, 369–377. doi: 10.1111/ejss.12215
- Deng, H., Wu, Y. C., Zhang, F., Huang, Z. C., Chen, Z., Xu, H. J., et al. (2014). Factors affecting the performance of single-chamber soil microbial fuel cells for power generation. *Pedosphere* 24, 330–338. doi: 10.1016/S1002-0160(14)60019-9
- Di Lorenzo, M., Curtis, T. P., Heada, I. M., and Scott, K. (2009). A single-chamber microbial fuel cell as a biosensor for wastewaters. *Water Res.* 43, 3145–3154. doi: 10.1016/j.watres.2009.01.005
- Dunaj, S. J., Vallino, J. J., Hines, M. E., Gay, M., Kobyljanec, C., and Rooney-Varga, J. N. (2012). Relationships between soil organic matter, nutrients, bacterial community structure, and the performance of microbial fuel cells. *Environ. Sci. Technol.* 46, 1914–1922. doi: 10.1021/es3023532
- Feng, C. J., Li, J. W., Qin, D., Chen, L. X., Zhao, F., Chen, S. H., et al. (2014). Characterization of exoelectrogenic bacteria *Enterobacter* strains isolated from a microbial fuel cell exposed to copper shock load. *PLoS ONE* 9:e113379. doi: 10.1371/journal.pone.0113379
- Fu, Q., Kobayashi, H., Kawaguchi, H., Wakayama, T., Maeda, H., and Sato, K. (2013). A thermophilic gram-negative nitrate-reducing bacterium, *Calditerrivibrio nitroreducens*, exhibiting electricity generation capability. *Environ. Sci. Technol.* 47, 12583–12590. doi: 10.1021/es402749f
- He, Z., Huang, Y. L., Manohar, A. K., and Mansfeld, F. (2008). Effect of electrolyte pH on the rate of the anodic and cathodic reactions in an air-cathode microbial fuel cell. *Bioelectrochemistry* 74, 78–82. doi: 10.1016/j.bioelechem.2008.07.007
- Holmes, D. E., Bond, D. R., and Lovley, D. R. (2004). Electron transfer by *Desulfovibulus propionicus* to Fe(III) and graphite electrodes. *Appl. Environ. Microbiol.* 70, 1234–1237. doi: 10.1128/AEM.70.2.1234-1237.2004
- Huang, D. Y., Zhou, S. G., Chen, Q., Zhao, B., Yuan, Y., and Zhuang, L. (2011). Enhanced anaerobic degradation of organic pollutants in a soil microbial fuel cell. *Chem. Eng. J.* 172, 647–653. doi: 10.1016/j.cej.2011.06.024
- Ishii, S., Shimoyama, T., Hotta, Y., and Watanabe, K. (2008). Characterization of a filamentous biofilm community established in a cellulose-fed microbial fuel cell. *BMC Microbiol.* 8:6. doi: 10.1186/1471-2180-8-6
- Jiang, Y. B., Deng, H., Sun, D. M., and Zhong, W. H. (2015). Electrical signals generated by soil microorganisms in microbial fuel cells respond linearly to soil Cd²⁺ pollution. *Geoderma* 255, 35–41. doi: 10.1016/j.geoderma.2015.04.022
- Kim, G. T., Hyun, M. S., Chang, I. S., Kim, H. J., Park, H. S., Kim, B. H., et al. (2005). Dissimilatory Fe(III) reduction by an electrochemically active lactic acid bacterium phylogenetically related to *Enterococcus gallinarum* isolated from submerged soil. *J. Appl. Microbiol.* 99, 978–987. doi: 10.1111/j.1365-2672.2004.02514.x
- Kozich, J. J., Westcott, S. L., Baxter, N. T., Highlander, S. K., and Schloss, P. D. (2013). Development of a dual-index sequencing strategy and curation pipeline for analyzing amplicon sequence data on the MiSeq Illumina sequencing platform. *Appl. Environ. Microbiol.* 79, 5112–5120. doi: 10.1128/AEM.01043-13
- Kuramae, E. E., Yergeau, E., Wong, L. C., Pijl, A. S., van Veen, J. A., and Kowalchuk, G. A. (2012). Soil characteristics more strongly influence soil bacterial communities than land-use type. *FEMS Microbiol. Ecol.* 79, 12–24. doi: 10.1111/j.1574-6941.2011.01192.x
- Li, H. J., Peng, J. J., Weber, K. A., and Zhu, Y. G. (2011). Phylogenetic diversity of Fe(III)-reducing microorganisms in rice paddy soil: enrichment cultures with different short-chain fatty acids as electron donors. *J. Soil Sediment* 11, 1234–1242. doi: 10.1007/s11368-011-0371-2
- Lovley, D. R. (2006). Bug juice: harvesting electricity with microorganisms. *Nat. Rev. Microbiol.* 4, 497–508. doi: 10.1038/nrmicro1442
- Lovley, D. R., Giovannoni, S. J., White, D. C., Champine, J. E., Phillips, E. J. P., Gorby, Y. A., et al. (1993). *Geobacter metallireducens* gen. nov. sp. nov., a microorganism capable of coupling the complete oxidation of organic compounds to the reduction of iron and other metals. *Arch. Microbiol.* 159, 336–344. doi: 10.1007/BF00290916
- Lovley, D. R., and Phillips, E. J. (1988). Novel mode of microbial energy metabolism: organic carbon oxidation coupled to dissimilatory reduction of iron or manganese. *Appl. Environ. Microbiol.* 54, 1472–1480.
- Luo, J. M., Li, M., Zhou, M. H., and Hu, Y. S. (2015). Characterization of a novel strain phylogenetically related to *Kocuria rhizophila* and its chemical modification to improve performance of microbial fuel cells. *Biosens. Bioelectron.* 69, 113–120. doi: 10.1016/j.bios.2015.02.025
- McKeague, J. A., and Day, J. H. (1966). Dithionite-and oxalate-extractable Fe and Al as aids in differentiating various classes of soils. *Can. J. Soil Sci.* 46, 13–22. doi: 10.4141/cjss66-003
- Page, A. L., Miller, R. H., and Keeney, D. R. (1982). "Chemical and microbiological properties," in *Methods of Soil Analysis*, 2nd Edn, eds A. L. Page, R. H. Miller, and D. R. Keeney (Madison, WI: American Society of Agronomy).
- Park, H. S., Kim, B. H., Kim, H. S., Kim, H. J., Kim, G. T., Kim, M., et al. (2001). A novel electrochemically active and Fe(III)-reducing bacterium phylogenetically related to *Clostridium butyricum* isolated from a microbial fuel cell. *Anaerobe* 7, 297–306. doi: 10.1006/anae.2001.0399
- Pham, C. A., Jung, S. J., Phung, N. T., Lee, J., Chang, I. S., Kim, B. H., et al. (2003). A novel electrochemically active and Fe(III)-reducing bacterium phylogenetically related to *Aeromonas hydrophila*, isolated from a microbial fuel cell. *FEMS Microbiol. Lett.* 223, 129–134. doi: 10.1016/S0378-1097(03)00354-9
- Puig, S., Serra, M., Coma, M., Cabré, M., Balaguer, M. D., and Colprim, J. (2010). Effect of pH on nutrient dynamics and electricity production using microbial fuel cells. *Bioresour. Technol.* 101, 9594–9599. doi: 10.1016/j.biortech.2010.07.082
- Richter, H., Lanthier, M., Nevin, K. P., and Lovley, D. R. (2007). Lack of electricity production by *Pelobacter carbinolicus* indicates that the capacity for Fe(III) oxide reduction does not necessarily confer electron transfer ability to fuel cell anodes. *Appl. Environ. Microbiol.* 73, 5347–5353. doi: 10.1128/AEM.00804-07
- Ringelberg, D. B., Foley, K. L., and Reynolds, C. M. (2011). Electrogenic capacity and community composition of anodic biofilms in soil-based

- bioelectrochemical systems. *Appl. Microbiol. Biotechnol.* 90, 1805–1815. doi: 10.1007/s00253-011-3264-9
- Roesch, L. F. W., Fulthorpe, R. R., Riva, A., Casella, G., Hadwin, A. K. M., Kent, A. D., et al. (2007). Pyrosequencing enumerates and contrasts soil microbial diversity. *ISME J.* 1, 283–290. doi: 10.1038/ismej.2007.53
- Rosenbaum, M., Schröder, U., and Scholz, F. (2005). Utilizing the green alga *Chlamydomonas reinhardtii* for microbial electricity generation: a living solar cell. *Appl. Microbiol. Biotechnol.* 68, 753–756. doi: 10.1007/s00253-005-1915-4
- Schloss, P. D., Westcott, S. L., Ryabin, T., Hall, J. R., Hartmann, M., Hollister, E. B., et al. (2009). Introducing mothur: open-source, platform-independent, community-supported software for describing and comparing microbial communities. *Appl. Environ. Microbiol.* 75, 7537–7541. doi: 10.1128/AEM.01541-09
- Song, L., and Dong, X. (2009). *Hydrogenoanaerobacterium saccharovorans* gen. nov., sp. nov., isolated from H₂-producing UASB granules. *Int. J. Syst. Evol. Microbiol.* 59, 295–299. doi: 10.1099/ijsl.0.000349-0
- Song, T. S., Cai, H. Y., Yan, Z. S., Zhao, Z. W., and Jiang, H. L. (2012). Various voltage productions by microbial fuel cells with sedimentary inocula taken from different sites in one freshwater lake. *Bioresour. Technol.* 108, 68–75. doi: 10.1016/j.biortech.2011.11.136
- Suzuki, M. T., and Giovannoni, S. J. (1996). Bias caused by template annealing in the amplification of mixtures of 16S rRNA genes by PCR. *Appl. Environ. Microbiol.* 62, 625–630.
- Vance, E. D., Brookes, P. C., and Jenkinson, D. S. (1987). An extraction method for measuring soil microbial biomass C. *Soil Biol. Biochem.* 19, 703–707. doi: 10.1016/0038-0717(87)90052-6
- Wang, X., Cai, Z., Zhou, Q., Zhang, Z., and Chen, C. (2012). Bioelectrochemical stimulation of petroleum hydrocarbon degradation in saline soil using U-tube microbial fuel cells. *Biotechnol. Bioeng.* 109, 426–433. doi: 10.1002/bit.23351
- Weisburg, W. G., Barns, S. M., Pelletier, D. A., and Lane, D. J. (1991). 16S ribosomal DNA amplification for phylogenetic study. *J. Bacteriol.* 173, 697–703.
- Xu, S., and Liu, H. (2011). New exoelectrogen *Citrobacter* sp. SX-1 isolated from a microbial fuel cell. *J. Appl. Microbiol.* 111, 1108–1115. doi: 10.1111/j.1365-2672.2011.05129.x
- Zhi, W., Ge, Z., He, Z., and Zhang, H. (2014). Methods for understanding microbial community structures and functions in microbial fuel cells: a review. *Bioresour. Technol.* 171, 461–468. doi: 10.1016/j.biortech.2014.08.096
- Zuo, Y., Xing, D., Regan, J. M., and Logan, B. E. (2008). Isolation of the exoelectrogenic bacterium *Ochrobactrum anthropi* YZ-1 by using a U-tube microbial fuel cell. *Appl. Environ. Microbiol.* 74, 3130–3137. doi: 10.1128/AEM.02732-07

Conflict of Interest Statement: The authors declare that the research was conducted in the absence of any commercial or financial relationships that could be construed as a potential conflict of interest.

Copyright © 2016 Jiang, Zhong, Han and Deng. This is an open-access article distributed under the terms of the Creative Commons Attribution License (CC BY). The use, distribution or reproduction in other forums is permitted, provided the original author(s) or licensor are credited and that the original publication in this journal is cited, in accordance with accepted academic practice. No use, distribution or reproduction is permitted which does not comply with these terms.



Single-Genotype Syntrophy by *Rhodopseudomonas palustris* Is Not a Strategy to Aid Redox Balance during Anaerobic Degradation of Lignin Monomers

OPEN ACCESS

Edited by:

Feng Zhao,

Institute of Urban Environment,
Chinese Academy of Sciences, China

Reviewed by:

Nicolas Toro,

Estación Experimental del
Zaidín-Consejo Superior de
Investigaciones Científica, Spain

Mohan Raj Subramanian,
Prist University, India

***Correspondence:**

Largus T. Angenent
la249@cornell.edu

†Present Address:

Devin F. R. Doud,
The DOE Joint Genome Institute,
Walnut Creek, CA, USA

Specialty section:

This article was submitted to
Microbiotechnology, Ecotoxicology
and Bioremediation,
a section of the journal
Frontiers in Microbiology

Received: 14 May 2016

Accepted: 28 June 2016

Published: 14 July 2016

Citation:

Doud DFR and Angenent LT (2016)
Single-Genotype Syntrophy by
Rhodopseudomonas palustris Is Not a
Strategy to Aid Redox Balance during
Anaerobic Degradation of Lignin
Monomers. *Front. Microbiol.* 7:1082.
doi: 10.3389/fmicb.2016.01082

Devin F. R. Doud [†] and Largus T. Angenent *

Department of Biological and Environmental Engineering, Cornell University, Ithaca, NY, USA

Rhodopseudomonas palustris has emerged as a model microbe for the anaerobic metabolism of *p*-coumarate, which is an aromatic compound and a primary component of lignin. However, under anaerobic conditions, *R. palustris* must actively eliminate excess reducing equivalents through a number of known strategies (e.g., CO₂ fixation, H₂ evolution) to avoid lethal redox imbalance. Others had hypothesized that to ease the burden of this redox imbalance, a clonal population of *R. palustris* could functionally differentiate into a pseudo-consortium. Within this pseudo-consortium, one sub-population would perform the aromatic moiety degradation into acetate, while the other sub-population would oxidize acetate, resulting in a single-genotype syntropy through acetate sharing. Here, the objective was to test this hypothesis by utilizing microbial electrochemistry as a research tool with the extracellular-electron-transferring bacterium *Geobacter sulfurreducens* as a reporter strain replacing the hypothesized acetate-oxidizing sub-population. We used a 2 × 4 experimental design with pure cultures of *R. palustris* in serum bottles and co-cultures of *R. palustris* and *G. sulfurreducens* in bioelectrochemical systems. This experimental design included growth medium with and without bicarbonate to induce non-lethal and lethal redox imbalance conditions, respectively, in *R. palustris*. Finally, the design also included a mutant strain (NifA*) of *R. palustris*, which constitutively produces H₂, to serve both as a positive control for metabolite secretion (H₂) to *G. sulfurreducens*, and as a non-lethal redox control for without bicarbonate conditions. Our results demonstrate that acetate sharing between different sub-populations of *R. palustris* does not occur while degrading *p*-coumarate under either non-lethal or lethal redox imbalance conditions. This work highlights the strength of microbial electrochemistry as a tool for studying microbial syntropy.

Keywords: single-genotype syntropy, *Rhodopseudomonas palustris*, microbial electrochemistry, lignin degradation, redox balance

IMPORTANCE

Synthrophic microbial relationships are of utmost importance in nature. They resolve important electron flow issues under anaerobic conditions and make microbial life under difficult thermodynamic conditions possible. During the anaerobic breakdown of the electron-rich aromatic ring in monomers of lignin, the photoheterotrophic bacterium *R. palustris* must strategically dispose of excess reducing equivalents. Researchers had in the past hypothesized that a syntropy may exist within a single culture—cells that convert the monomer into acetate and other cells that further oxidize acetate. However, conclusive proof is elusive. Here, we used a co-culture of *R. palustris* and *Geobacter sulfurreducens* in a bioelectrochemical system to examine if such a single-genotype syntropy exists. A 2 × 4 experimental design with several positive controls under both non-lethal and lethal conditions did not identify any evidence for a single-genotype syntropy strategy by *R. palustris*, failing to provide support for this hypothesis.

INTRODUCTION

Lignin is the most abundant source of organic aromatic compounds, and the second most abundant organic carbon source in the biosphere (Suhar et al., 2007). Due to its overwhelming supply, lignin presents itself as a prime substrate for biomass conversion to produce renewable resources and energy. Unfortunately, the abundance of lignin is rivaled only by the difficulty microbes have in metabolizing it, especially under anaerobic conditions (Beckham et al., 2016). This is because lignin is a class of structurally complex, high molecular weight molecules that contain many aromatic groups and remain largely insoluble. Previous studies on anaerobic lignin metabolism have focused primarily on the degradation of lignin monomers and the demonstration of anaerobic aromatic ring fission (Evans, 1963; Healy and Young, 1979; Colberg and Young, 1982; Porter and Young, 2013). Since this discovery, degradation of lignin oligomers and monomers have been demonstrated under strictly anaerobic conditions, though, it is still debated if complex lignin can be degraded under these conditions (Kirk and Farrell, 1987; Brown and Chang, 2014).

Rhodopseudomonas palustris is a model microbe for lignin monomer degradation and has also emerged as an attractive microbe for bioenergy production. This purple non-sulfur bacterium has been well-characterized for its anaerobic metabolism of lignin monomers (e.g., *p*-coumarate) in the presence of light (Harwood and Gibson, 1986; Pan et al., 2008; Hirakawa et al., 2012; Phattarasukol et al., 2012). However, while growing photoheterotrophically with *p*-coumarate, *R. palustris* must orchestrate a number of metabolic strategies for managing excess reducing equivalents that accumulate from this aromatic substrate. While CO₂ fixation and H₂ evolution have both been previously implicated in managing the redox balance for *R. palustris* (McKinlay and Harwood, 2010, 2011), determining whether every cell is performing these redox-balancing activities, or if it is a shared strategy between an entire community, has remained obscure.

It has been hypothesized that while degrading *p*-coumarate in pure culture, *R. palustris* forms a pseudo-consortium with division of metabolic tasks (1. *p*-coumarate to benzoate, 2. benzoate to acetate/formate/H₂, and ultimately 3. acetate/formate/H₂ oxidation) between sub-populations, resulting in a single-genotype syntropy (Karpinets et al., 2009). The observation that *R. palustris* releases acetate when growing with *n*-butyrate provides support that acetate could be a preferred metabolite to share when growing on a variety of reduced substrates (McKinlay and Harwood, 2011). By secreting acetate during *p*-coumarate degradation to be utilized by another sub-population, this strategy reduces the redox imbalance that would arise within a single cell converting *p*-coumarate completely to CO₂. We refer to this here as acetate sharing. This reduces the demand for electron acceptors within the *p*-coumarate-degrading population, and thus enables the redox balance to be shared between the members in this hypothesized pseudo-consortium. Due to the metabolic versatility of the *R. palustris* genome, acetate sharing would employ many of the same thermodynamic advantages that are present within a complex microbial consortium.

Complications in experimentally verifying acetate sharing exist since transcriptomic or proteomic analyses from bulk pure culture studies measure all sub-populations together as an average, and many limitations still exist with bacterial single-cell RNA-seq (Saliba et al., 2014). To experimentally test whether *R. palustris* utilizes acetate sharing as a redox strategy while metabolizing *p*-coumarate, we coupled *R. palustris* with the acetate-oxidizing, electrochemically active microbe *Geobacter sulfurreducens* within a bioelectrochemical system (BES). In this system, *G. sulfurreducens* functions as a surrogate for the hypothesized sub-population of *R. palustris* that is responsible for acetate oxidation, and as a reporter for the magnitude of acetate sharing.

G. sulfurreducens is a model microbe for a high efficiency conversion of both acetate and H₂ into electric current when grown at an oxidizing electrode (anode) in a BES (Bond and Lovley, 2003). Conserving energy for metabolism in the process, *G. sulfurreducens* completely oxidizes both acetate and H₂ with electrons exiting the system through an electrical circuit of a BES, resulting in an electric current. By complementing *R. palustris* growing on *p*-coumarate with *G. sulfurreducens* in a BES under conditions that present a challenge to cellular redox, an anaerobic co-culture of these two microbes could probe whether acetate sharing within a single-genotype population of *R. palustris* occurs. Therefore, the electric current (real-time output signal) from the reporter strain *G. sulfurreducens* serves as a proxy for acetate sharing by the *p*-coumarate degrading subpopulation of *R. palustris*. Because of the ability of *G. sulfurreducens* to channel electrons out of the system via the electrode, and since a buffer would neutralize excess H⁺, *G. sulfurreducens* functions as a sink for excess reducing equivalents in the form of acetate or H₂. Further, acetate oxidized by *G. sulfurreducens* can return back to *R. palustris* in the form of CO₂, even when exogenous HCO₃⁻ is omitted from the media. Therefore, if *R. palustris* engages in acetate sharing, a BES co-culture between *R. palustris* and *G. sulfurreducens* would ease the burden of redox imbalance, and

could even rescue growth of *R. palustris* from conditions that would otherwise induce a lethal redox imbalance ($-HCO_3^-$).

Our 2×4 experimental design for *p*-coumarate degradation included with and without bicarbonate in the growth medium (**Table 1**). With bicarbonate, *R. palustris* CGA009 has the exogenous electron acceptor CO_2 available to get rid of reducing equivalents by fixing CO_2 into biomass and allowing growth by avoiding lethal redox imbalance (1 in **Table 1**). Without bicarbonate, and in the presence of NH_4^+ , wild-type *R. palustris* CGA009 does not have enough electron acceptors to maintain redox balance, resulting in arrested growth (McKinlay and Harwood, 2010) (2 in **Table 1**). The study was designed based on four strain combinations and the experimental design included the mutant strain (NifA*) of *R. palustris* CGA009, which constitutively expresses nitrogenase genes in the presence of NH_4^+ to secrete H_2 . H_2 production reduces the strain of reducing equivalents in a way to ensure a non-lethal redox imbalance condition even without bicarbonate in the growth medium. It, therefore, serves as a redox-balanced positive control for without bicarbonate experiments (3 and 4 in **Table 1**).

For the co-culture experiments in BESSs with the reporter strain *G. sulfurreducens*, the wild-type *R. palustris* CGA009 cannot produce H_2 . Thus, any electric current generation with this co-culture is indicative of acetate sharing under a non-lethal redox imbalance condition with bicarbonate (5 in **Table 1**). Importantly, electric current generation for the more stringent, lethal redox imbalance condition without bicarbonate would strongly be indicative of acetate sharing because CGA009 cannot otherwise grow under these conditions (6 in **Table 1**). Finally, for the co-culture experiments with the NifA* mutant, we anticipate

electric current production even without acetate sharing because *G. sulfurreducens* can consume the H_2 secreted by NifA*, thus functioning as a positive control for *G. sulfurreducens*-produced current through consuming metabolites (H_2) shared by *R. palustris* (7 in **Table 1**). However, without bicarbonate we do not anticipate an electric current without acetate sharing. While *G. sulfurreducens* can generate current from acetate in the absence of CO_2 (Sun et al., 2014), the behavior of *G. sulfurreducens* is poorly understood in the absence of CO_2 (Soussan et al., 2013), and activity with H_2 has never been reported. Thus, any sustained electric current would be indicative of acetate sharing with NifA* in this co-culture (8 in **Table 1**).

In addition to these eight (2×4) experiments for *p*-coumarate degradation with *R. palustris* under anaerobic conditions, we performed two additional experiments with other substrates to function as positive controls for acetate sharing with the reporter strain *G. sulfurreducens*. The substrate *n*-butyrate was a positive control to show that, in principle, acetate sharing would be possible under non-lethal redox imbalance conditions for the wild-type strain CGA009 (9 in **Table 1**). In addition, acetate was fed directly to the NifA* + *G. sulfurreducens* co-culture without bicarbonate to validate the reporter strain (*G. sulfurreducens*) was active and to rule out that a negative result (no current) was indeed an indication for the absence of acetate sharing rather than a problem with the reporter strain or equipment (10 in **Table 1**). In summary, this study was designed to conclusively ascertain whether acetate sharing occurs within a single-genotype consortium of *R. palustris* while degrading *p*-coumarate for maintaining redox balance at two stringency levels: non-lethal and lethal redox imbalance conditions.

MATERIALS AND METHODS

Growth

Rhodopseudomonas palustris strains CGA009 and NifA*, which were provided by Dr. Caroline Harwood (University of Washington), and *Geobacter sulfurreducens* were routinely cultivated in filter-sterilized anaerobic fresh water (FW) medium. FW medium consisted of 2.5 g $NaHCO_3$, 0.1 g KCl, 0.25 g NH_4Cl , 0.52 NaH_2PO_4 , 10 mL FW Vitamins, and 1 mL FW Minerals per liter, which was neutralized to pH 7.0 (Li et al., 2012). Precultures of *G. sulfurreducens* were grown in FW medium with 10 mM acetate and 20 mM fumarate acting as carbon substrate and terminal electron acceptor, respectively. Precultures of *R. palustris* CGA009 and NifA* were grown in the light with 2 mM *p*-coumarate as the sole organic carbon source. $NaHCO_3$ was replaced with a 25 mM phosphate buffer at a final pH of 7.0 for precultures of NifA* intended for experiments in the absence of HCO_3^- . Toxicity screens validated that 2 mM *p*-coumarate did not inhibit any of the strains used in this study (data not shown).

R. palustris Characterization in Serum Bottles

Batch serum bottle experiments for the characterization of CGA009 and NifA* strains in pure culture with *p*-coumarate in FW media with and without bicarbonate were incubated in triplicate in an environmental growth chamber (GC8-2VH, EGC,

TABLE 1 | 2×4 experimental design for *p*-coumarate degradation with *R. palustris* and two additional positive controls with different substrates.

Substrate	Culture	<i>R. palustris</i> strain	+ HCO_3^-	- HCO_3^-
<i>p</i> -Coumarate	Pure culture	Wild-type <i>R. palustris</i> CGA009	1	2
		NifA*-mutant <i>R. palustris</i>	3	4
	Co-culture with <i>G. sulfurreducens</i>	Wild-type <i>R. palustris</i> CGA009	5	6
		NifA*-mutant <i>R. palustris</i>	7	8
<i>n</i> -Butyrate		Wild-type <i>R. palustris</i> CGA009	9	–
Acetate		NifA*-mutant <i>R. palustris</i>	–	10

Numbers in the final two columns are identified in the text. Results are shown for: 1–4 in **Figure 1**; 5 and 7 in **Figure 3**; 6, 8, and 10 in **Figure 4**; and 9 in **Figure 5**.

Non-lethal

Lethal

Non-lethal with electric current reporter

Lethal with electric current reporter

Non-lethal, electric current positive.

Chagrin Falls, OH). Conditions were maintained at 30.0°C with 80 μmol of photons/s/m² (photons between 400-700 nm) from both fluorescent and incandescent lamps.

Bioelectrochemical Reactors

Two-chamber, H-type reactors were used for all electrochemical experiments. The reactors were constructed out of autoclavable glass with water jackets for temperature control and ports for electrochemical components (TerAvest et al., 2014). The working electrode consisted of 9 × 9 cm carbon cloth (PANEX® 30 – PW06, Zoltek Corp, St Louis, MO), which was attached to a carbon rod with carbon cement (CCC Carbon Adhesive, EMS, Hatfield, PA). The working electrode was potentiostatically controlled (VSP, BioLogic USA, Knoxville, TN) at +0.300 V vs. Ag/AgCl using an Ag/AgCl/sat'd KCl reference electrode (made in-house). The counter electrode consisted of a 2 × 7 × 1 cm carbon block (Poco Graphite, Decatur, TX), which was attached to a carbon rod with carbon cement (CCC Carbon Adhesive) and was separated from the counter chamber by a cation exchange membrane (Membranes International, Ringwood, NJ). Prior to the operating period, the reactors were autoclaved and only sterile components were added. The working chamber contained 450 mL of FW medium and the counter chamber contained 450 mL of FW medium with no carbon source. The reactors were maintained at 30.0°C with water jackets and a recirculating water heater (Model 1104, VWR Scientific, Radnor, PA) and uniformly illuminated with 60-W incandescent lamps at an intensity of ~40 W/m². Lids with butyl rubber stoppers were used to maintain gastight conditions while sampling and replacing the medium. Anaerobic conditions were maintained by sparging reactors with either 80:20 N₂/CO₂ or N₂ through sterile filters for conditions with and without bicarbonate, respectively.

Electrochemical Experiments

For co-culture experiments, *G. sulfurreducens* was initially grown at the anode in FW medium with 10 mM acetate under continuous-flow conditions in biological triplicates. After a biofilm and stable current production were achieved, the working chamber was flushed at a rate of 0.75 L/h with 1.5 L of either sterile anaerobic FW medium with 2 mM *p*-coumarate and: (1) 30 mM HCO₃⁻; or (2) a 25 mM phosphate buffer and no HCO₃⁻. The reactors were then operated in batch with no sparging for the conditions with HCO₃⁻ and active N₂ sparging for the conditions without HCO₃⁻. Following media replacement, the reactors were allowed to reach an electrical baseline before inoculating them with *R. palustris*. Samples were taken throughout the operating period to monitor OD₆₀₀, pH, and relevant metabolites. All non-aromatic metabolites were detected via HPLC (600 HPLC, Waters, Milford, MA) with a refractive index detector and an Aminex HPX-87H column (Bio-Rad, Hercules, CA). The column was maintained at a temperature of 60°C, and a 5 mM sulfuric acid eluent at a flow rate of 0.6 mL/min was used as the mobile phase. Aromatic metabolites were detected via a Thermo Scientific Ion Chromatograph System (ICS-1100, Dionex, Sunnyvale, CA) with a Dionex IonPac™ AS22 column (4 × 250 mm) and a Dionex Variable Wavelength Detector set to 285 nm. AS22 eluent was used at a flow rate of 1.2 ml/min.

Metabolites were identified by retention times from high purity standards (Sigma-Aldrich, St. Louis, MO).

Microscopy

Mid-log phase cultures of *R. palustris* CGA009 and NifA* growing in batch serum bottles containing FW 2 mM *p*-coumarate with HCO₃⁻ were visualized using a KH-7700 digital microscope system (Hirox, Hackensack, NJ). Liquid samples were removed from growing cultures, 10 μL was added directly to a microscope slide with coverslip, and was directly visualized from above with a Hirox MX(G)-10C OL-140II lens. Cell aggregate geometries were measured using the integrated Hirox software and approximately 50 measurements were averaged.

RESULTS AND DISCUSSION

R. palustris Strains CGA009 and NifA* Show Similar Metabolic Profiles While Degrading *p*-Coumarate with Bicarbonate under Anaerobic Conditions

We inoculated the wild-type *R. palustris* CGA009 into serum bottles containing anaerobic FW medium with 2 mM *p*-coumarate with and without the addition of HCO₃⁻. As mentioned above and described in the literature (McKinlay and Harwood, 2010), the wild-type *R. palustris* CGA009 was only able to degrade *p*-coumarate and grow when bicarbonate was added to the anaerobic medium to avoid a lethal redox imbalance (Figure 1). The mutant *R. palustris* NifA*, on the other hand, was able to degrade *p*-coumarate and grow with and without bicarbonate due to the formation of H₂ and the resulting elimination of excess reducing equivalents (Figure 1).

The pathway for *p*-coumarate metabolism by *R. palustris* has been previously studied with identification of all intermediates and mechanisms (Pan et al., 2008). To ascertain whether any major metabolic differences between strains CGA009 and NifA* exist, we carefully compared their behavior under identical conditions in serum bottles with 2 mM *p*-coumarate under anaerobic conditions. We observed that the metabolism of *p*-coumarate by *R. palustris* occurs in distinctive phases, starting with the non-β-oxidative cleavage of the alkyl side chain, and yielding a nearly stoichiometric conversion to 4-hydroxybenzoate (Figure 1). The observation that *p*-coumarate is converted entirely to 4-hydroxybenzoate at a 1:1 ratio suggests no sub-population is degrading downstream metabolites and the only active metabolism at that time point is on the alkyl side chain. The hydroxyl group was then removed to produce benzoate (not detected), which was rapidly degraded by β-oxidation after activation and cleaving the aromatic ring (Harrison and Harwood, 2005; Pan et al., 2008). The transient production of 4-hydroxybenzoate began with the onset of *p*-coumarate metabolism and disappeared with the plateau of maximum culture OD, suggesting it is rapidly consumed once taken up by the cell (Figure 1). No other downstream metabolites, including acetate, were detected via HPLC. With bicarbonate, *R. palustris* CGA009 and NifA* both have very similar rates of metabolism of *p*-coumarate and

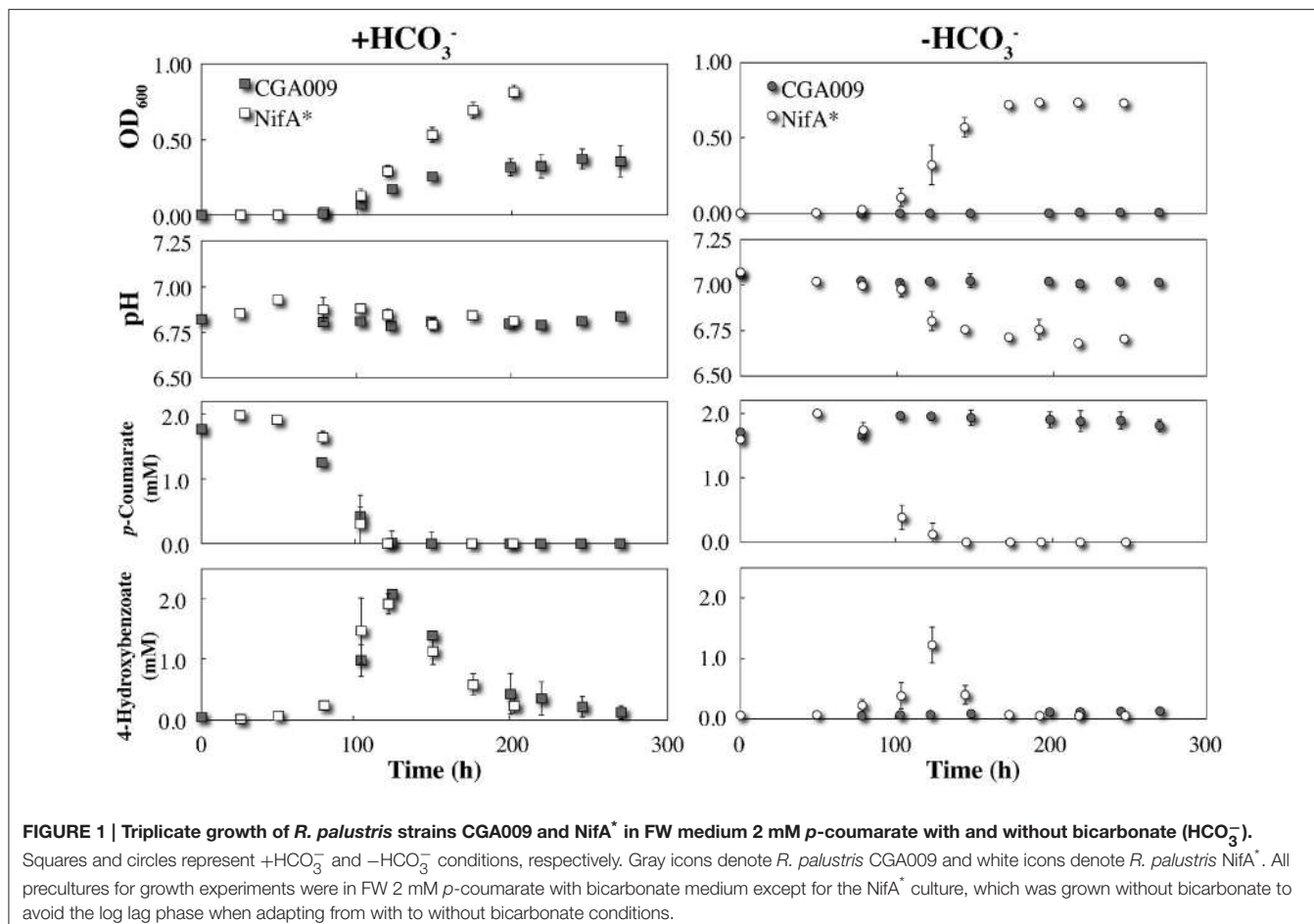


FIGURE 1 | Triplicate growth of *R. palustris* strains CGA009 and NifA* in FW medium 2 mM p-coumarate with and without bicarbonate (HCO₃⁻).

Squares and circles represent +HCO₃⁻ and -HCO₃⁻ conditions, respectively. Gray icons denote *R. palustris* CGA009 and white icons denote *R. palustris* NifA*. All precultures for growth experiments were in FW 2 mM p-coumarate with bicarbonate medium except for the NifA* culture, which was grown without bicarbonate to avoid the log lag phase when adapting from with to without bicarbonate conditions.

4-hydroxybenzoate, resulting in similar consumption profiles. This similar metabolic behavior for CGA009 and NifA* under anaerobic conditions is helpful for the rest of our comparative study.

Despite nearly identical rates of substrate consumption, the optical density between the two cultures rapidly diverged with *R. palustris* NifA* reaching a density more than double that of CGA009 (0.372 ± 0.067 vs. 0.847 ± 0.002 maximum OD₆₀₀; Figure 1). This result is counterintuitive, however, because CGA009 should produce more biomass per unit of substrate consumed compared to NifA* due to the extra reducing equivalents available to CGA009 to fix CO₂ that are not lost to H₂ evolution (McKinlay and Harwood, 2010). The observation that substrate consumption still occurred at the same rate within both environments, however, suggests that a similar level of active cells must be present within both cultures.

To investigate this, digital microscopy of the two cultures revealed that under these conditions CGA009 tended to grow primarily in granule-like aggregations ranging from 20 to 200 μm in width, while NifA* grew primarily as single cells with only infrequent small granules observed (Figure 2). The reduced optical density of CGA009 compared to NifA* is, thus, likely due to aggregation under this condition as substrate metabolism rates demonstrate that similar levels of active cells were likely

present, while optical densities varied between the two cultures. Because the only difference between strain CGA009 and NifA* is the constitutive expression of nitrogenase genes in NifA*, this phenotypic distinction can be attributed to the alternate pathways for maintaining redox balance (i.e., CO₂ fixation vs. H₂ evolution) and demonstrates the drastically different outcomes that these strategies can have on global cellular behavior. This observation further suggests that metabolite sharing could be a viable strategy undertaken by a CO₂-fixing pseudo-consortium of *R. palustris* CGA009 due to the tendency to aggregate, since this aggregating phenotype is abolished when H₂ secretion by individual cells is utilized as the primary route to redox balance.

Acetate Sharing under Non-Lethal Redox Imbalance Conditions Was Not Observed

To investigate whether acetate sharing occurs under non-lethal redox conditions, *R. palustris* CGA009 and NifA* were independently inoculated into *G. sulfurreducens*-pregrown BESSs containing 2 mM p-coumarate as the sole carbon source in FW medium with bicarbonate. Because both strains of *R. palustris* are capable of growing under these conditions, the presence of *G. sulfurreducens* on the electrode as a potential electron sink is not obligate for growth for either strain under these conditions and any current produced would be through metabolite sharing

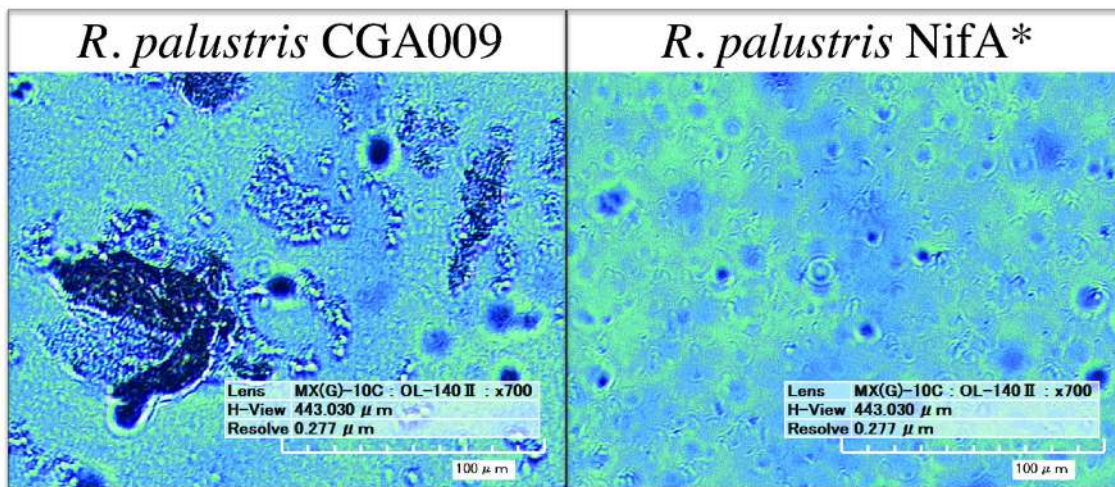


FIGURE 2 | Digital microscopy of *R. palustris* CGA009 and NifA* grown in pure culture on FW 2 mM *p*-coumarate with bicarbonate. Aggregates of cells appear as dark clumps (CGA009), single cells can be seen as ~ 4 μM long rods (NifA*).

of either acetate (CGA009 or NifA*) or H_2 (limited to NifA*). Since acetate sharing is proposed as a strategy that develops in pure cultures, the *R. palustris* precultures used to inoculate the electrochemical reactors would already be performing acetate sharing, minimizing any adaptation response upon introduction into the BES and eliminating any lag time before observable current production. In addition, because the electrode is the only terminal electron acceptor for growth of *G. sulfurreducens* under these conditions, any increase in the planktonic optical density would be attributed to *R. palustris*.

By comparing metabolite profiles with bicarbonate from the BESs (Figure 3) to those previously determined from serum bottle experiments (Figure 1), we found that conversion of *p*-coumarate to *p*-hydroxybenzoate and subsequent consumption occurred at nearly the same rate for both strains between both systems. However, the optical density for both strains was considerably lower in the BESs than when grown in serum bottles (Figures 1, 3). This was likely due to the preferential growth of *R. palustris* on the electrode and reactor surfaces compared to in the planktonic state since biofilm growth on all surfaces was observed in the BESs. Even with biofilm formation, the optical density trend with CGA009 growing at lower levels than NifA*, which we observed in serum bottles (Figure 1), was even more pronounced in the BESs (Figure 3).

While both strains appeared to perform similarly with regard to their metabolism of *p*-coumarate, NifA* was the only strain of the two to elicit an electrochemical response from *G. sulfurreducens* in the BES. The electrochemical signal produced in the *R. palustris* NifA* and *G. sulfurreducens* co-culture closely mirrored the metabolite profile, with current production beginning at the onset of *p*-coumarate consumption (Figure 3). Following the complete conversion of *p*-coumarate to 4-hydroxybenzoate, a short inflection in the current was observed while *R. palustris* transitioned to consuming 4-hydroxybenzoate (Figure 3). Finally, current production peaked at $1.43 \pm$

0.15 mA , which coincided with the decrease in measured 4-hydroxybenzoate concentrations (Figure 3). Collectively, this suggests that the observed current from the NifA* *G. sulfurreducens* co-culture closely followed the metabolic trends of NifA* growing in the electrochemical system, and was mediated by H_2 evolution from the NifA* strain rather than from acetate sharing since negligible current was produced from CGA009 under identical conditions (Figure 3). The lack of current produced from CGA009 likely demonstrates that no acetate was shared between *R. palustris* and *G. sulfurreducens* under these conditions, though, we cannot completely rule out the possibility that secreted acetate remained within the aggregations of *R. palustris* (Figure 2). On the other hand, from studies with dense anaerobic granules in bioreactors, we know that self-diffusion coefficients for granular biomass are 56–75% that of free water (Lens et al., 2003). With ample opportunities for diffusion of acetate out of the microbial aggregates and the ability of *G. sulfurreducens* to uptake acetate at μM levels (Estevez-Nunez et al., 2005), our observations strongly indicate that acetate sharing from the *p*-coumarate degrading population was not utilized as a strategy to aid redox balance under non-lethal conditions.

Acetate Sharing Was Not Initiated Even under Lethal Redox Imbalance Conditions

It is possible that acetate sharing in *R. palustris* may only be initiated under more stringent conditions, such as during a lethal redox-imbalance condition (without bicarbonate). In our BESs with *G. sulfurreducens*, we provide an efficient electron sink for acetate oxidation with an electrode. Thus, creating an ideal biological test bed in which stringent conditions can be combined with a possible solution to avoid a lethal redox imbalance—but only when acetate sharing is performed by *R. palustris*. To test this, *R. palustris* CGA009 and NifA* were separately introduced into *G. sulfurreducens* pregrown BESs with 2 mM *p*-coumarate

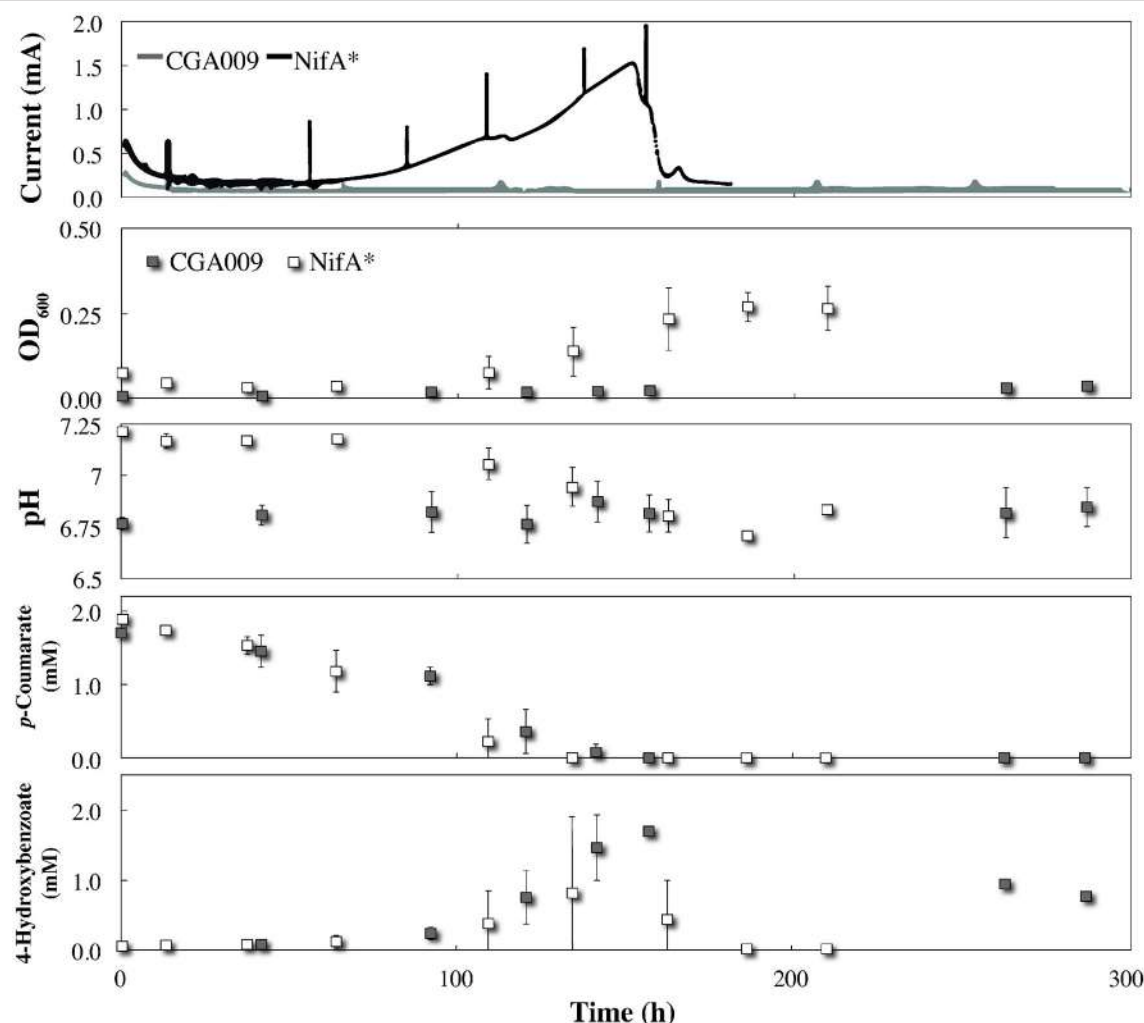


FIGURE 3 | Co-culture growth of *R. palustris* CGA009 and NifA* with *Geobacter sulfurreducens* in FW medium 2 mM *p*-coumarate with bicarbonate. Current for *R. palustris* CGA009 and NifA* denoted by gray and black lines, respectively. Growth and metabolites for *R. palustris* CGA009 and NifA* denoted by gray and white squares, respectively.

FW medium without bicarbonate. To maintain a proper pH level and to neutralize H⁺, we included a 25 mM phosphate buffer. In addition, to provide an opportunity for association between *G. sulfurreducens* and *R. palustris* at the electrode, *R. palustris* CGA009 was pre-grown together with *G. sulfurreducens* on the electrode before switching to without bicarbonate conditions.

Even though *R. palustris* CGA009 did not exhibit any planktonic growth within the BESs once conditions were switched to without bicarbonate, *p*-coumarate was rapidly taken up and metabolized to 4-hydroxybenzoate after the medium replacement was completed (Figure 4). Because the acetyl-CoA unit derived from the conversion of *p*-coumarate to 4-hydroxybenzoate can be metabolized without producing net excess reducing equivalents (McKinlay and Harwood, 2010), it is expected that this conversion can be achieved without the aid from *G. sulfurreducens* at the electrode. Indeed, no electric current was registered during this time period (Figure 4). This

conversion in the BES co-culture (Figure 4) occurred much faster than in the serum bottle cultures (Figure 1) due to the higher *R. palustris* biomass in the reactor from pre-culturing with *G. sulfurreducens*. Following the initial metabolism of *p*-coumarate to 4-hydroxybenzoate, no further metabolism was observed, resulting in a continued high concentration of this intermediate (Figure 4). This suggests that after consuming the alkyl moiety from *p*-coumarate, the excess of electrons from the aromatic group saturated the redox balance of *R. palustris* and growth was restricted. The absence of current production from *G. sulfurreducens* and inability of *R. palustris* to further catabolize the substrate demonstrates that even under restrictive growth conditions where redox imbalance becomes lethal, *R. palustris* CGA009 did not eliminate excess reducing equivalents in the form of acetate for oxidation by a syntrophic partner. Notable, however, when illumination was removed from the CGA009 culture without bicarbonate, a transient increase in

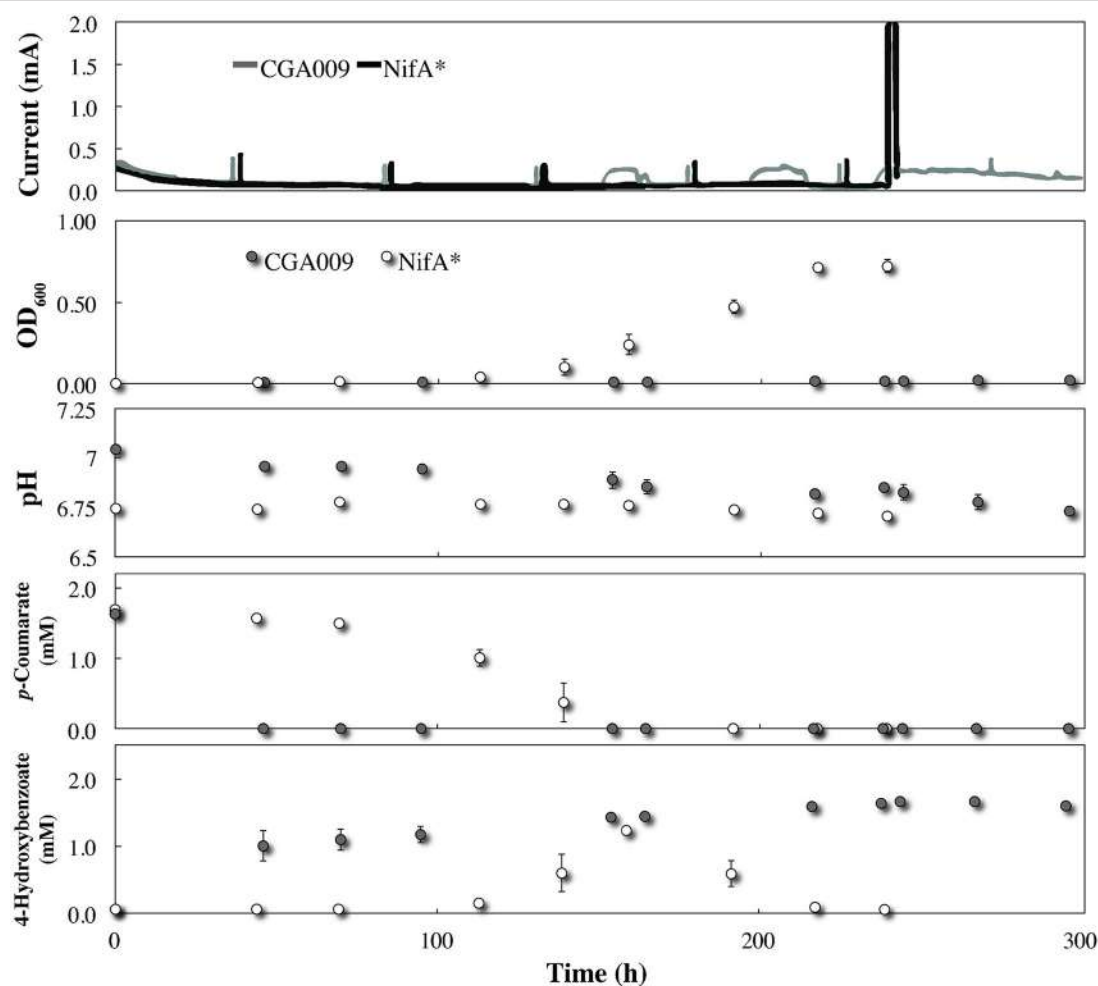


FIGURE 4 | Co-culture growth of *R. palustris* CGA009 and NifA* with *Geobacter sulfurreducens* in FW medium 2 mM *p*-coumarate without bicarbonate. *R. palustris* CGA009 and NifA* are represented by the gray line or gray circles and black line or white circles, respectively. NifA* was precultured in FW medium 2 mM *p*-coumarate without bicarbonate while CGA009 was pre-grown with *G. sulfurreducens* at the electrode.

electric current was observed without growth or further substrate metabolism (**Figure 4** time: 150, 190, and 230 h). It is unclear to us why this relatively low electric current production (and possible acetate release) occurred in the co-culture during dark conditions and would require further investigation to discern.

Growth and metabolism kinetics of NifA* in the co-culture without bicarbonate were very similar to our previous experiments including *p*-coumarate and 4-hydroxybenzoate (**Figure 4**). However, while NifA* previously elicited a current response in FW medium and 2 mM *p*-coumarate with bicarbonate due to H₂ production, no electric current was produced from growth of NifA* with *G. sulfurreducens* without bicarbonate. This negative result identifies that acetate sharing was not induced with *G. sulfurreducens*. The lack of current produced by H₂ oxidation by *G. sulfurreducens* was anticipated, since while it has been demonstrated that *G. sulfurreducens* can consume acetate and produce current in a phosphate buffer lacking bicarbonate, this has never been observed for just H₂ (Soussan et al., 2013; Sun et al., 2014). To

verify that this was a true negative result and rule out the possibility that *G. sulfurreducens* was simply inhibited following prolonged exposure to FW and 25 mM phosphate buffer without bicarbonate, sterile sodium acetate was injected into the BES at hour 240 after all *p*-coumarate had been consumed. We observed an immediate large electric current signal (current magnitude exceeded 2 mA scale) following the acetate addition, verifying that *G. sulfurreducens* was active (**Figure 4**).

During co-culture experiments we did not observe an acetate-based electric current signal from *G. sulfurreducens* as a product of the anaerobic degradation of *p*-coumarate by *R. palustris* (**Figure 4**). To validate that acetate released by *R. palustris* could in fact be utilized by *G. sulfurreducens* within this system, *R. palustris* CGA009 and *G. sulfurreducens* were co-cultured in FW with bicarbonate, and 2 mM *p*-coumarate was replaced with 11 mM *n*-butyrate. Because *G. sulfurreducens* cannot directly metabolize *n*-butyrate, and secretion of acetate had previously been measured during metabolism of *n*-butyrate by a pure culture of *R. palustris* (McKinlay and Harwood, 2011), this

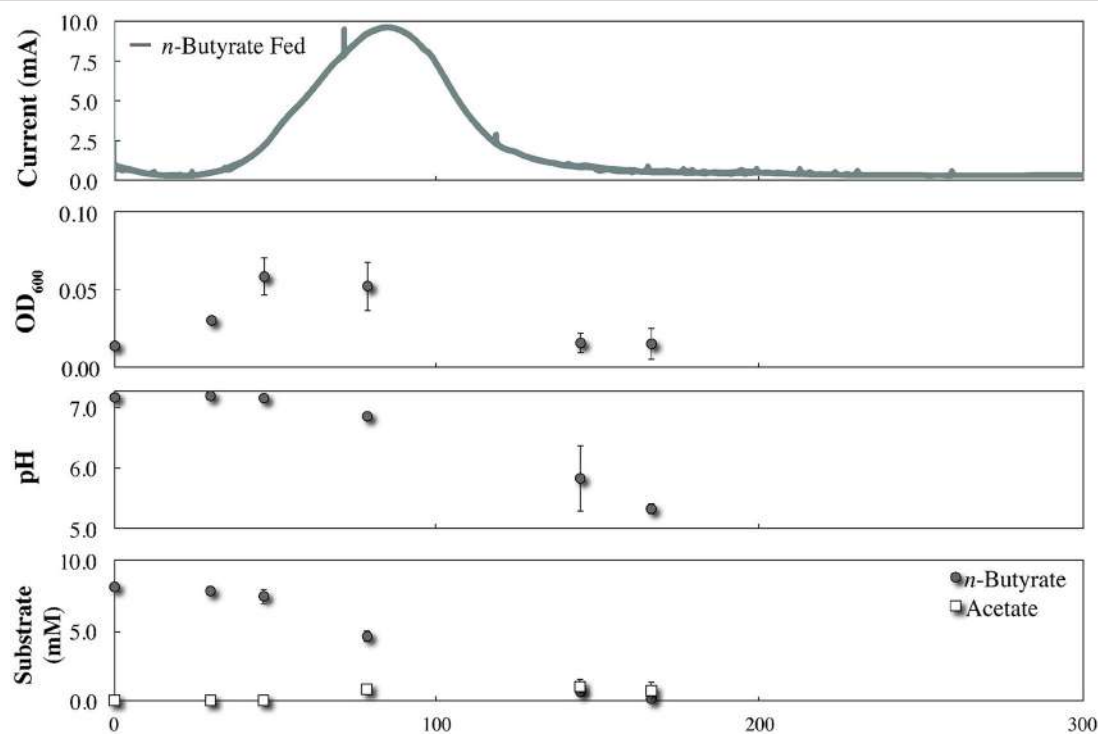


FIGURE 5 | Co-culture growth of *R. palustris* CGA009 with *Geobacter sulfurreducens* in FW medium with 11 mM *n*-butyrate and bicarbonate.

condition functions as a positive control for an acetate sharing-based electric signal (Figure 5). The production of a large current from within this system, and the emergence of a detectable concentration of acetate, coincides with butyrate consumption by *R. palustris* and validates our expectation that current would have been produced by *G. sulfurreducens* if acetate had been released by *R. palustris* during the metabolism of *p*-coumarate.

CONCLUSION

The hypothesis that *R. palustris* engages in metabolite sharing within a single-genotype consortium to avoid complications of redox imbalance that can arise within a single cell was tested by investigating metabolite sharing of acetate between *R. palustris* and *G. sulfurreducens*. Since, *R. palustris* CGA009 cannot produce H₂ when NH₄⁺ is supplied as the only N source, *R. palustris* NifA* was used as a redox balance positive control for growth and metabolite sharing (of H₂) with *G. sulfurreducens*. An aggregating phenotype was initially observed for *R. palustris* CGA009, suggesting a desire to form close cellular interactions under these conditions, whereas NifA* demonstrated no aggregating phenotype. This finding could have supported the acetate-sharing hypothesis, however, no current was produced by *G. sulfurreducens* through acetate sharing from *R. palustris* CGA009 within the BES under both non-lethal and lethal redox imbalance conditions. Although CGA009 was capable of complete metabolism of the alkyl side chain of *p*-coumarate, further metabolism of the aromatic group yielded too many reducing equivalents and quickly resulted in a

lethal redox imbalance in BES conditions without bicarbonate. Because *G. sulfurreducens* functioned as the sole electron sink for oxidizing excess reducing equivalents by conversion of acetate to CO₂ without bicarbonate, the absence of an acetate sharing-based electric current strongly indicates that *R. palustris* does not use acetate sharing to manage the excess of reducing equivalents *via* a single-genotype syntropy. It was not expected that additional incubation of the CGA009 BES without bicarbonate would eventually stimulate acetate sharing with *G. sulfurreducens*, akin to adaptation phases in similar syntropy evolution studies (Summers et al., 2010), since the acetate sharing activity would have already been present in the CGA009 preculture before the electrochemical experiment began.

AUTHOR CONTRIBUTIONS

DD and LA designed the study; DD performed the research and sample analysis; DD analyzed the data, and DD and LA wrote the manuscript.

ACKNOWLEDGMENTS

We would like to thank Dr. Hanno Richter for helpful discussions and Bahareh Guilvaeie and Prof. Tammo Steenhuis (Cornell University) for use of their digital microscope. This project was funded in part by the US DOE Advanced Research Projects Agency – Energy (ARPA-E) with project number DE-AR0000312.

REFERENCES

- Beckham, G. T., Johnson, C. W., Karp, E. M., Salvachua, D., and Vardon, D. R. (2016). Opportunities and challenges in biological lignin valorization. *Curr. Opin. Biotechnol.* 42, 40–53. doi: 10.1016/j.copbio.2016.02.030
- Bond, D. R., and Lovley, D. R. (2003). Electricity production by *Geobacter sulfurreducens* attached to electrodes. *Appl. Environ. Microbiol.* 69, 1548–1555. doi: 10.1128/AEM.69.3.1548-1555.2003
- Brown, M. E., and Chang, M. C. (2014). Exploring bacterial lignin degradation. *Curr. Opin. Chem. Biol.* 19, 1–7. doi: 10.1016/j.cbpa.2013.11.015
- Colberg, P. J., and Young, L. Y. (1982). Biodegradation of lignin-derived molecules under anaerobic conditions. *Can. J. Microbiol.* 28, 886–889.
- Esteve-Nunez, A., Rothermich, M., Sharma, M., and Lovley, D. (2005). Growth of *Geobacter sulfurreducens* under nutrient-limiting conditions in continuous culture. *Environ. Microbiol.* 7, 641–648. doi: 10.1111/j.1462-2920.2005.00731.x
- Evans, W. C. (1963). The microbiological degradation of aromatic compounds. *J. Gen. Microbiol.* 32, 177–184.
- Harrison, F. H., and Harwood, C. S. (2005). The pimFABCDE operon from *Rhodopseudomonas palustris* mediates dicarboxylic acid degradation and participates in anaerobic benzoate degradation. *Microbiology* 151, 727–736. doi: 10.1099/mic.0.27731-0
- Harwood, C. S., and Gibson, J. (1986). Uptake of benzoate by *Rhodopseudomonas palustris* grown anaerobically in light. *J. Bacteriol.* 165, 504–509.
- Healy, J. B., and Young, L. Y. (1979). Anaerobic biodegradation of eleven aromatic compounds to methane. *Appl. Environ. Microbiol.* 38, 84–89.
- Hirakawa, H., Schaefer, A. L., Greenberg, E. P., and Harwood, C. S. (2012). Anaerobic *p*-coumarate degradation by *Rhodopseudomonas palustris* and identification of CouR, a MarR repressor protein that binds *p*-coumaroyl coenzyme A. *J. Bacteriol.* 194, 1960–1967. doi: 10.1128/JB.06817-11
- Karpinets, T. V., Pelletier, D. A., Pan, C. L., Überbacher, E. C., Melnichenko, G. V., Hettich, R. L., et al. (2009). Phenotype fingerprinting suggests the involvement of single-genotype consortia in degradation of aromatic compounds by *Rhodopseudomonas palustris*. *PLoS ONE* 4:e4615. doi: 10.1371/journal.pone.0004615
- Kirk, T. K., and Farrell, R. L. (1987). Enzymatic “combustion”: the microbial degradation of lignin. *Annu. Rev. Microbiol.* 41, 465–505.
- Lens, P. N., Gastesi, R., Vergeldt, F., van Aelst, A. C., Pisabarro, A. G., and Van As, H. (2003). Diffusional properties of methanogenic granular sludge: 1H NMR characterization. *Appl. Environ. Microbiol.* 69, 6644–6649. doi: 10.1128/AEM.69.11.6644-6649.2003
- Li, Z., Venkataraman, A., Rosenbaum, M. A., and Angenent, L. T. (2012). A laminar-flow microfluidic device for quantitative analysis of microbial electrochemical activity. *ChemSusChem* 5, 1119–1123. doi: 10.1002/cssc.201100736
- McKinlay, J. B., and Harwood, C. S. (2010). Carbon dioxide fixation as a central redox cofactor recycling mechanism in bacteria. *Proc. Natl. Acad. Sci. U.S.A.* 107, 11669–11675. doi: 10.1073/pnas.1006175107
- McKinlay, J. B., and Harwood, C. S. (2011). Calvin cycle flux, pathway constraints, and substrate oxidation state together determine the H₂ biofuel yield in photoheterotrophic bacteria. *Mbio* 2:e00323-10. doi: 10.1128/mBio.00323-10
- Pan, C., Oda, Y., Lankford, P. K., Zhang, B., Samatova, N. F., Pelletier, D. A., et al. (2008). Characterization of anaerobic catabolism of *p*-coumarate in *Rhodopseudomonas palustris* by integrating transcriptomics and quantitative proteomics. *Mol. Cell. Proteomics* 7, 938–948. doi: 10.1074/mcp.M700147MCP200
- Phattarasukol, S., Radey, M. C., Lappala, C. R., Oda, Y., Hirakawa, H., Brittnacher, M. J., et al. (2012). Identification of a *p*-coumarate degradation regulon in *Rhodopseudomonas palustris* by Xpression, an integrated tool for prokaryotic RNA-seq data processing. *Appl. Environ. Microbiol.* 78, 6812–6818. doi: 10.1128/AEM.01418-12
- Porter, A. W., and Young, L. Y. (2013). The bamA gene for anaerobic ring fission is widely distributed in the environment. *Front. Microbiol.* 4:302. doi: 10.3389/fmicb.2013.00302
- Saliba, A. E., Westermann, A. J., Gorski, S. A., and Vogel, J. (2014). Single-cell RNA-seq: advances and future challenges. *Nucleic Acids Res.* 42, 8845–8860. doi: 10.1093/nar/gku555
- Soussan, L., Riess, J., Erable, B., Delia, M. L., and Bergel, A. (2013). Electrochemical reduction of CO₂ catalysed by *Geobacter sulfurreducens* grown on polarized stainless steel cathodes. *Electrochim. Commun.* 28, 27–30. doi: 10.1016/j.elecom.2012.11.033
- Suhas, Carrott, P. J., and Ribeiro Carrott, M. M. (2007). Lignin—from natural adsorbent to activated carbon: a review. *Bioresour. Technol.* 98, 2301–2312. doi: 10.1016/j.biortech.2006.08.008
- Summers, Z. M., Fogarty, H. E., Leang, C., Franks, A. E., Malvankar, N. S., and Lovley, D. R. (2010). Direct exchange of electrons within aggregates of an evolved syntrophic coculture of anaerobic bacteria. *Science* 330, 1413–1415. doi: 10.1126/science.1196526
- Sun, D., Call, D., Wang, A., Cheng, S., and Logan, B. E. (2014). *Geobacter* sp. SD-1 with enhanced electrochemical activity in high-salt concentration solutions. *Environ. Microbiol. Rep.* 6, 723–729. doi: 10.1111/1758-2229.12193
- TerAvest, M. A., Rosenbaum, M. A., Kotloski, N. J., Gralnick, J. A., and Angenent, L. T. (2014). Oxygen allows *Shewanella oneidensis* MR-1 to overcome mediator washout in a continuously fed bioelectrochemical system. *Biotechnol. Bioeng.* 111, 692–699. doi: 10.1002/bit.25128
- Conflict of Interest Statement:** The authors declare that the research was conducted in the absence of any commercial or financial relationships that could be construed as a potential conflict of interest.
- Copyright © 2016 Doud and Angenent. This is an open-access article distributed under the terms of the Creative Commons Attribution License (CC BY). The use, distribution or reproduction in other forums is permitted, provided the original author(s) or licensor are credited and that the original publication in this journal is cited, in accordance with accepted academic practice. No use, distribution or reproduction is permitted which does not comply with these terms.*



A Novel Electrophototrophic Bacterium *Rhodopseudomonas palustris* Strain RP2, Exhibits Hydrocarbonoclastic Potential in Anaerobic Environments

Krishnaveni Venkidusamy^{1,2*} and Mallavarapu Megharaj^{1,2,3}

¹ Centre for Environmental Risk Assessment and Remediation, University of South Australia, Mawson Lakes, SA, Australia

² CRC for Contamination Assessment and Remediation of the Environment, Mawson Lakes, SA, Australia, ³ Global Centre for Environmental Risk Assessment and Remediation, The University of Newcastle, Callaghan, NSW, Australia

OPEN ACCESS

Edited by:

Yong Xiao,

The Chinese Academy of Sciences,
China

Reviewed by:

Luciano Takeshi Kishi,

Universidade Estadual Paulista, Brazil
Zheng Chen,

Xi'an Jiaotong-Liverpool University,
China

*Correspondence:

Krishnaveni Venkidusamy

krishnaveni.venkidusamy@mymail.
unisa.edu.au

Specialty section:

This article was submitted to
Microbiotechnology, Ecotoxicology
and Bioremediation,
a section of the journal
Frontiers in Microbiology

Received: 19 April 2016

Accepted: 27 June 2016

Published: 12 July 2016

Citation:

Venkidusamy K and Megharaj M
(2016) A Novel Electrophototrophic
Bacterium *Rhodopseudomonas palustris* Strain RP2, Exhibits
Hydrocarbonoclastic Potential
in Anaerobic Environments.

Front. Microbiol. 7:1071.
doi: 10.3389/fmicb.2016.01071

An electrophototrophic, hydrocarbonoclastic bacterium *Rhodopseudomonas palustris* stain RP2 was isolated from the anodic biofilms of hydrocarbon fed microbial electrochemical remediation systems (MERS). Salient properties of the strain RP2 were direct electrode respiration, dissimilatory metal oxide reduction, spore formation, anaerobic nitrate reduction, free living diazotrophy and the ability to degrade n-alkane components of petroleum hydrocarbons (PH) in anoxic, photic environments. In acetate fed microbial electrochemical cells, a maximum current density of 305 ± 10 mA/m² (1000Ω) was generated (power density 131.65 ± 10 mW/m²) by strain RP2 with a coulombic efficiency of $46.7 \pm 1.3\%$. Cyclic voltammetry studies showed that anaerobically grown cells of strain RP2 is electrochemically active and likely to transfer electrons extracellularly to solid electron acceptors through membrane bound compounds, however, aerobically grown cells lacked the electrochemical activity. The ability of strain RP2 to produce current (maximum current density 21 ± 3 mA/m²; power density 720 ± 7 μ W/m², 1000Ω) using PH as a sole energy source was also examined using an initial concentration of 800 mg l⁻¹ of diesel range hydrocarbons (C9–C36) with a concomitant removal of $47.4 \pm 2.7\%$ hydrocarbons in MERS. Here, we also report the first study that shows an initial evidence for the existence of a hydrocarbonoclastic behavior in the strain RP2 when grown in different electron accepting and illuminated conditions (anaerobic and MERS degradation). Such observations reveal the importance of photoorganotrophic growth in the utilization of hydrocarbons from contaminated environments. Identification of such novel petrochemical hydrocarbon degrading electricogens, not only expands the knowledge on the range of bacteria known for the hydrocarbon bioremediation but also shows a biotechnological potential that goes well beyond its applications to MERS.

Keywords: microbial electrochemical remediation, hydrocarbonoclastic bacterium, photoorganotrophic hydrocarbon degradation, electrode respiring bacteria, *Rhodopseudomonas palustris* strain RP2

INTRODUCTION

Soil and groundwater petroleum hydrocarbon contamination has long been a serious concern to environmental and public health. Of these petroleum hydrocarbon (PH) contaminants, diesel range hydrocarbons (DRH) have been documented as one of the most abundant pollutants; they can be biodegradable in both oxic and anoxic conditions (Huang et al., 2011). Microbial remediation of these petrochemical compounds is claimed to be an efficient, economic, versatile alternative to the physicochemical methods. However, the rate of microbial utilization of these PH compounds is very slow especially in anaerobic environments where the availability of relevant electron acceptors is limited. The recent research on such recalcitrant contaminant removal using bioelectrochemical systems is leading to a new interest in its practical applications. An emerging microbial electrochemical remediation systems (MERS) shows potential as an effective approach that can exploit microorganisms for treating contaminants while generating electricity in the process. This has recently been proposed for the remediation of PH contaminants by capitalizing on the bio-catalytic potential of electrode respiring bacteria (ERB; Morris et al., 2009; Venkidusamy et al., 2016).

Electrode respiring bacteria are a group that has received much attention in the field of electromicrobiology because of their exoelectrogenic capabilities to degrade substrates that range from easily degradable natural organic compounds to xenobiotic compounds such as PH contaminants. Many studies have shown the presence of diverse, electro active-microbial communities on fuel cell electrodes including members of the *Alphaproteobacteria* (Zuo et al., 2008), *Betaproteobacteria* (Chaudhuri and Lovley, 2003), *Gammaproteobacteria* (Kim et al., 2002), *Deltaproteobacteria* (Holmes et al., 2006), and *Firmicutes* (Wrighton et al., 2008). Of these, *Gammaproteobacteria* was the dominant class found on the anodes of organic contaminants such as PH fed MERS (Morris et al., 2009; Venkidusamy et al., 2016). Several bacterial strains from this class have been isolated either from electrochemical systems fed with wastewater or defined carbons sources and their physiological roles have been studied. However, the microbial community composition is divergent in MERS (Morris et al., 2009; Venkidusamy et al., 2016), and the physiology of such populations remains to be investigated. Therefore, identification of such ERB which can be used in MERS systems for the enhanced removal of PH contaminants is of current importance.

In the present study, such a novel electrode respiring, hydrocarbonoclastic bacterial strain was isolated from the biofilms of PH fed MERS anodes and analyzed its physiology and activities in pure culture studies. This strain was found to be a Fe (III) respiring bacterium, phylogenetically related to *Rhodopseudomonas palustris* and designated as *R. palustris* strain RP2. The electrochemical activity was determined by using cyclic voltammetry and fuel cell techniques. Here, we show the existence of hydrocarbonoclastic behavior by the strain RP2, first such organism from MERS environments with several novel features.

MATERIALS AND METHODS

Bacterial Strain

The bacterium used in this study was isolated from the anodic biofilm of a MERS through serial dilution techniques. The initial source of inoculum for the PH fed MERS was a PH contaminated ground water inoculated with activated sludge. Bacterial cells of the anodic biofilm were extracted into a sterile phosphate buffer and shaken vigorously to separate cells from the electrode. The extracted cell suspensions were serially diluted and plated on modified Hungate's medium (Hungate, 1950) and incubated anaerobically in a glove box (Don Whitley Scientific, MG500, Australia) for a period of two weeks. Single colonies were randomly selected and transferred to anaerobic agar plates filled with Luria Bertani (LB) medium (Sambrook et al., 1989). Cultures were routinely cultivated using anoxic rich medium (LB) under illuminated conditions. A chemically defined medium supplemented with Wolfe's trace elements and vitamins was used in the fuel cell experiments as previously described (Oh et al., 2004).

Culture Conditions and Biodegradation Experiments

Bacterial cells were grown under anoxic photosynthetic conditions with acetate (20 mM) as an electron donor in phosphate buffer saline supplemented with Wolfe's trace elements and vitamins and sealed with aluminum crimp. For experiments with different electron acceptors 10 mM nitrate, 10 mM sulfate, 10 mM iron (III) citrate, and 10 mM iron (III) oxide were used. The cells were cultured under different physiological conditions, including phototrophic and chemotrophic, oxic and anoxic conditions. The photosynthetic pigments were analyzed by measuring the whole cell absorption spectra in the UV-visible ranges from 300 to 1100 nm as described by Mehrabi et al. (2001). Biolog-GN2 plates were used to determine the carbon source utilization using the strain RP2 (Biolog., USA) according to the manufacturer's instructions under anoxic, illuminated conditions. The cells were also tested for their growth with nitrogen-deficient solid medium lacking a carbon source according to Kranz and Haselkorn (1986). DRHs was also used as the electron donor in biodegradation experiments at a concentration of 4000 mg l⁻¹. Hydrocarbonoclastic potential of the strain RP2 was monitored under different electron accepting, growth environments (nitrate, sulfate, iron (III) as terminal electron acceptors) including phototrophic and chemotrophic conditions. All cell cultures were maintained in triplicates for each experiment. All procedures for anoxic growth experiments, from medium preparation to manipulating the strain were performed using standard anoxic conditions. All culturing was prepared in sealed serum vials with nitrogen/carbon dioxide (80:20, v/v) in the headspace.

Fe(III) Oxide Reduction

For investigating Fe(III) respiration process, cells were grown in two different environments: anoxic photoheterotrophic and chemoheterotrophic culture conditions supplemented with

crystalline Fe(III) oxide (10 mM) as the terminal electron acceptor. The cells were grown in Wolfe's medium using acetate (20 mM) supplemented with trace elements and vitamins (Lovley and Phillips, 1988a). Fe(III) reduction was determined using the ferrozine assay (Lovley and Phillips, 1988b). The bacterial suspension was added to a pre-weighed vial containing 0.5 M HCl. HCl extracted samples were added to 5 ml of ferrozine (1 g l^{-1}) in 50 mM HEPS buffer. The filtered samples were then analyzed in a UV-Vis spectrophotometer (maxima@ $\lambda = 562 \text{ nm}$) to quantify the Fe(II) formation as previously described (Lovley and Phillips, 1988b).

Microscopy

Samples for transmission electron microscopy were fixed in electron microscopy fixative (4% paraformaldehyde/1.25% glutaraldehyde in PBS, + 4% sucrose, pH-7.2) and washed with buffer. Samples were postfixated in 2% aqueous osmium tetroxide. They were dehydrated in a graded series of ethanol, and then infiltrated with procure/araldite epoxy resin. Blocks were polymerized overnight at 70°C . Sections were cut on a Leica UC6 Ultramicrotome using a diamond knife, stained with uranyl acetate and lead citrate, and examined in a FEI Tecnai G2 Spirit Transmission Electron Microscope. The electrode samples were fixed and prepared as described earlier (Venkidusamy et al., 2016). The dried brush samples were examined using a scanning electron microscope (Quanta FEG 450, FEI) at an accelerating voltage of 20 kV.

16S rRNA Gene and Phylogenetic Analysis

Genomic DNA of *R. palustris* strain RP2 was extracted from photoheterotrophically grown cells by using the UltraClean microbial DNA isolation kit (MO BIO, Carlsbad, CA, USA) following the manufacturer's instructions. The universal primers were used to amplify 16S rRNA gene according to the procedure devised by Weisburg et al. (1991). The PCR products were purified via the UltraClean PCR clean-up kit (Mo Bio, Carlsbad, CA, USA) following the manufacturer's instructions, and sequenced by the Southern Pathology Sequencing Facility at Flinders Medical Centre. The neighbor joining tree was constructed using the molecular evolutionary genetic analysis package version 5.0 based on 1000 bootstrap values (Tamura et al., 2011). The presence of the *pufM* gene was identified using published *pufM* primers (Achenbach et al., 2001). The presence of *nifH* gene was also analyzed using a gene specific primer (Cantera et al., 2004). *In silico* analysis was done by using the blast programs to search the GenBank and NCBI databases (<http://www.ncbi.nlm.nih.gov>).

Microbial Fuel Cell (MFC) construction

Single chamber and dual chamber cubic MFC reactors were used to evaluate power generation from strain RP2. Single chamber bottle MFCs were made from laboratory Schott duran bottles with a capacity of 300 ml as suggested by Logan et al. (2007). The liquid volume of the chamber was 280 ml. Dual chamber cubic MFCs were constructed using two lexan glasses separated by a

cation exchange membrane (Membrane International Inc., USA). The liquid volume of a dual chamber cubic MFC was 150 ml. Anodes were carbon paper or graphite fiber brushes of 5 cm in diameter and 7 cm in length. The graphite brushes were treated as previously described (Feng et al., 2010). Plain carbon paper was used as the anode material in dual chamber cubic MFC systems. Single chamber air cathodes contained 0.5 mg cm^{-2} of platinum catalyst on the liquid facing side with diffusional layers of PTFE applied to the air facing side (Cheng et al., 2006). All the reactors were sterilized before use.

MFC Operational Conditions

Strain RP2 was used for fuel cell experiments with acetate (1 g/L) as the electron donor in 50 mM PBS buffer. A higher concentration (200 mM) of buffer was also used in fuel cell experiments to examine the effect on power generation. A stationary phase culture was used in the anode chamber and the cells were operated under illuminated conditions. The anodic chamber was flushed with nitrogen gas and filled with anaerobic growth medium. The anolyte was agitated using a magnetic stirrer operating at 100 rpm. In the cubic MFC, the cathode chamber was provided with air through a 0.45μ pore sized membrane filter. Solutions were replaced when the voltage dropped $<10 \text{ mV}$. Open circuit MFC studies were also carried out and then switched to closed circuit with a selected external load ($R=1000 \Omega$ unless stated otherwise). DRH compounds were also used as sole source of energy in degradation experiments using the strain RP2 at a concentration of 800 mg l^{-1} in MERS studies. All the reactors were maintained in photoheterotrophic and chemoheterotrophic culture conditions at room temperature in triplicates.

Electrochemical Analysis

The electrochemical activity of strain RP2 was examined using cyclic voltammetry with a conventional three electrode electrochemical cell with a 25 ml capacity as described earlier (Kim et al., 1999). Bacterial cells grown (aerobic and anaerobic growth environments) in Fe(III) oxide liquid cultures were harvested and used for testing electrochemical activities. Cyclic voltammograms of the bacterial suspension were obtained using a potentiostat (Electrochemical analyser, BAS 100B, USA) connected to a personal computer with BAS software. A glassy carbon working electrode (3 mm, diameter, MF-2012, BAS) and silver/silver chloride reference electrode (MW-4130, BAS) and platinum counter electrode (MW-4130, BAS) were used in a conventional three electrode system. The working electrodes were polished with alumina slurry on cotton wool before each measurement. The electrochemical cells were purged with nitrogen gas for 15 minutes before each measurement. Different scan rates were used from 5 to 100 mV/sec with a potential range from -800 to 800 mV .

Analytical Methods and Calculations

Fe(III) reduction was monitored by measuring Fe(II) production by the ferrozine method (Lovley and Phillips, 1988b). The DRH was extracted in acetone-methylene chloride (1:1) mixture, dewatered and concentrated by evaporator, and then

concentrations were measured by GC-FID using a HP-5 capillary column (15 m length, 0.32 mm thickness, 0.1 μm internal diameter) following the USEPA protocol (USEPA, 1996). The resulting chromatograms were analyzed using Agilent software (GC-FID Agilent model 6890) to identify the hydrocarbon degradation products. Chemical oxygen demand was measured by COD analyser (Chemetrics, K-7365). Fuel cell power output was monitored using a DMM (Keithly Model 2701, USA) linked to a multi-channel scanner (Module 7700, Keithly Instruments, USA). Data were recorded digitally on an Intel computer via IEEE 488 input system and Keithly cable. To measure the current under closed circuit conditions, the external load was connected ($R=1000\Omega$ unless stated otherwise). Current was calculated by using $I = V/R$, and power was calculated via $P = VI$. Power density and current density were normalized to the projected surface area of a cathode. Polarization curves were plotted using various external loads with a range of 10 Ω to open circuit. Coulombic efficiency (CE) was calculated at the end of the cycle from COD removal as previously described by Logan (2008).

Nucleotide Sequence Numbers

The 16S rRNA, *pufM*, *nifH* gene sequences have been deposited in the GenBank database under the accession numbers of KJ460004, J1289478, J223658.

RESULTS

Strain Identification

In our laboratory experiments, a strain of *R. palustris* strain RP2 emerged as a dominant species was isolated from the anodic biofilm PH fed MERS. *R. palustris* strain RP2 is a cosmopolitan phototrophic bacterium, contains double membrane bilayers, lamellar thylakoid membrane system, produce chains of magnetosomes (Venkidusamy et al., 2015), and grow as long bacillus-shaped (0.5 to 1 μm wide and 2.0 to 6 μm long cells) with asymmetric cell division. Cell division occurred by budding, with dumbbell shaped daughter cells, forming rosette-like structures. Thin section transmission electron micrographs revealed the presence of a lamellar thylakoid membrane system presumably containing the photosynthetic apparatus in anoxic phototrophically grown cells (Supplementary Figure S1A) whereas cells grown in the dark lacked intra cytoplasmic (ICM) membranes (Supplementary Figure S1B).

Photosynthetic Pigments

Photosynthetically grown anoxic liquid cells were dark red (Supplementary Figure S2A) in color whereas chemosynthetically grown anoxic cells were colorless (Supplementary Figure S2B). Cultures grown under aerobic conditions were faint pink to colorless. Thin section transmission electron micrographs revealed the presence of a lamellar thylakoid membrane system presumably containing the photosynthetic apparatus in anoxic phototrophically grown cells. Absorption maxima of the homogenized photosynthetic cells showed three bacteriochlorophyll peaks at 379, 473, and 503 nm, and

peaks at 545, 594, 807, and 875 nm indicated the presence of carotenoid pigments of the spilloxanthin series. In contrast, no peaks were observed in the chemosynthetically grown cells. The presence of the photosynthetic gene (*pufM* gene) in the strain RP2 was shown using PCR with primers specific for this gene, resulting in a 230 bp product.

Physiological and Metabolic Characters

The cells of strain RP2 have exceptionally flexible growth based on environmental signals such as photoorganotrophic, photolithotrophic, dark fermentative, and aerobic heterotrophic mechanisms. Optimum bacterial growth was observed at 25 to 30°C at a neutral pH, whilst no growth was detected above 40°C. Experiments to determine the growth factor requirements for the strain RP2 clearly shows the need for *p*-aminobenzoate, pyridoxine HCl, and folic acid (Supplementary Table S1). Salient properties of the strain RP2 were direct electrode respiration, dissimilatory metal oxide reduction, anaerobic nitrate reduction, carbon dioxide fixation, free living diazotrophy, and the ability to degrade n-alkane components of PH under anoxic environments. Strain RP2 showed growth in minimal medium in the absence of both nitrogen and carbon sources under anoxic, photosynthetic conditions. Nitrogen fixation trait was confirmed by the detection of a *nifH* gene required for nitrogen fixation in the strain. The strain RP2 differed from a previously reported exoelectrogenic strain of *R. palustris* DX1 (Xing et al., 2008) with respect to its ability of photoassimilating a range of substrates including gluconate, aspartate, glycerol, and amino-ethanol. However, the strain RP2 was unable to utilize some compounds such as sebacic acid, threonine, L-ornithine, and L-proline. The ability to utilize sodium benzoate distinguishes the strain from other species of purple sulfur bacteria. The strain RP2 can assimilate acetate photosynthetically with nitrate, sulfate, and iron as terminal electron acceptors (Supplementary Figure S3). We cultured RP2 cells under two different environmental conditions: anoxic photoheterotrophic and anoxic chemoheterotrophic with crystalline Fe(III) oxide as a terminal electron acceptor to investigate the dissimilatory metal oxide reduction trait. Fe(III) oxide reduction was monitored by color change and hydroxylamine Fe(II) extraction assay. Fe(III) oxide reduction of $69.5\% \pm 0.41\%$ was observed only in anoxic photoheterotrophic environments (Venkidusamy et al., 2015) whereas chemosynthetic grown cells showed no reduction. During this process, peculiar extracellular electrically conductive nanofilamentous structures were observed in the phototrophic growth conditions as stated previously (Venkidusamy et al., 2015). When colonies are incubated for longer incubations (for a period of 4–5 weeks) under anoxic chemosynthetic conditions, they develop a complex morphology such as spore formation with a well-defined outer layer (Figure 1).

Phylogeny

ClustalW alignment was used to align 1420 bp of the 16S ribosomal RNA gene sequence of strain RP2 with the same region of several related non-sulfur alphaproteobacteria groups. Using this multiple alignment, the neighborhood phylogenetic tree was constructed (Figure 2). Phylogenetic analysis of 16S

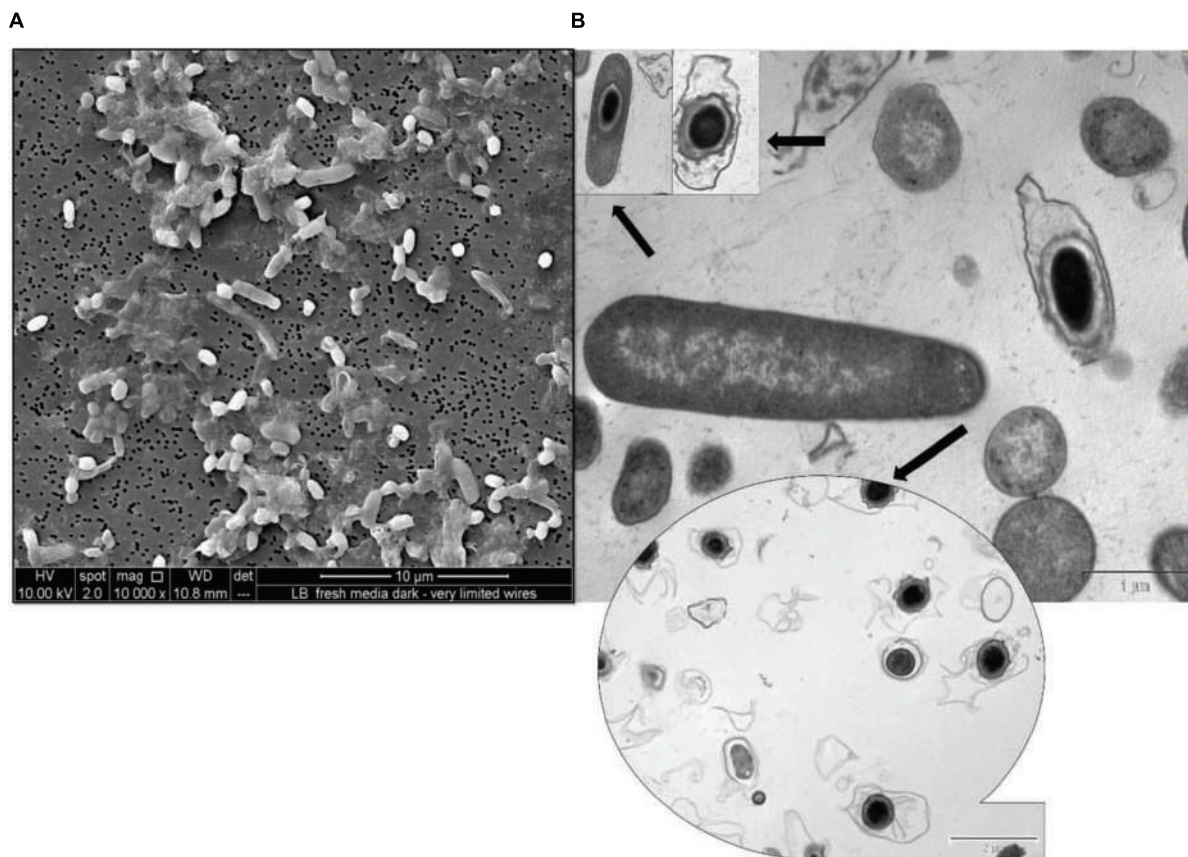


FIGURE 1 | Micrographs of spore formation in chemosynthetically grown cells of *R. palustris* strain RP2. (A) SEM micrograph. **(B)** TEM micrograph.

rRNA gene sequences of strain RP2 demonstrated that the strain was closely linked to the genera of *Rhodopseudomonas* with 98% identity to sequences from *R. palustris* ATCC (17005) and *Rhodopseudomonas* sp. DPT4 (2001).

Current Generation by *R. palustris* Strain RP2 in Acetate MFCs

Current was generated in all the MFCs inoculated with strain RP2 using acetate as an energy source. After three days, voltage started to follow a constant pattern and then stabilized. The fuel cell electrodes were discharged through a $1000\ \Omega$ external resistance once it reached the plateau voltage generation stage. The voltage fell quickly from 690 ± 10 mV to 446 ± 5 mV after a $1000\ \Omega$ fixed resistor was connected. The maximum output range of voltage and current density were 446 ± 7 mV, 305 ± 10 mA/m 2 ($R = 1000\ \Omega$) after four cycles of operation. Few representative initial cycles (average current density from triplicates) of current density are shown in (Figure 3A). After six refilling batches with a fresh substrate, the maximum current output of each batch became stable (300 ± 7 mA/m 2). The maximum open circuit voltage was 700 ± 7 mV and attainable power density was 131.65 ± 10 mW/m 2 ($R = 1000\ \Omega$) (Figure 3B). The CEs showed the increased trend with the increased current densities

as shown in the Figure 3C. The maximum CE was 46.7% which corresponded to the maximum current density of 259.90 mA/m 2 . The higher buffer (200 mM) concentration were also examined at the same resistance which produced a maximum power density of 300 ± 20 mW/m 2 .

Experiments were also conducted using dual chamber cubic MFCs (CMFC) containing carbon flat paper anodes at a fixed resistance of $1000\ \Omega$. The voltage profile of the cubic MFC revealed that the voltage produced was less than that for the air cathode MFC. A long lag time was observed with the carbon paper anode whereas a treated brush anode reduced the strain acclimation period and resulted in an increased power generation. The maximum open circuit potential and power output of CMFC were 600 ± 7 mV and 70 mW/m 2 , respectively. Constant power and voltage output indicated the formation of a stable biofilm around the electrode surface. Scanning electron micrographs revealed that the bacterial population from the graphite brush anode was homogenous in shape (Figure 4).

Electrochemical Activity of *R. palustris* Strain RP2

Cell suspensions were prepared from the bacterial cells grown under anaerobic and aerobic environments to determine

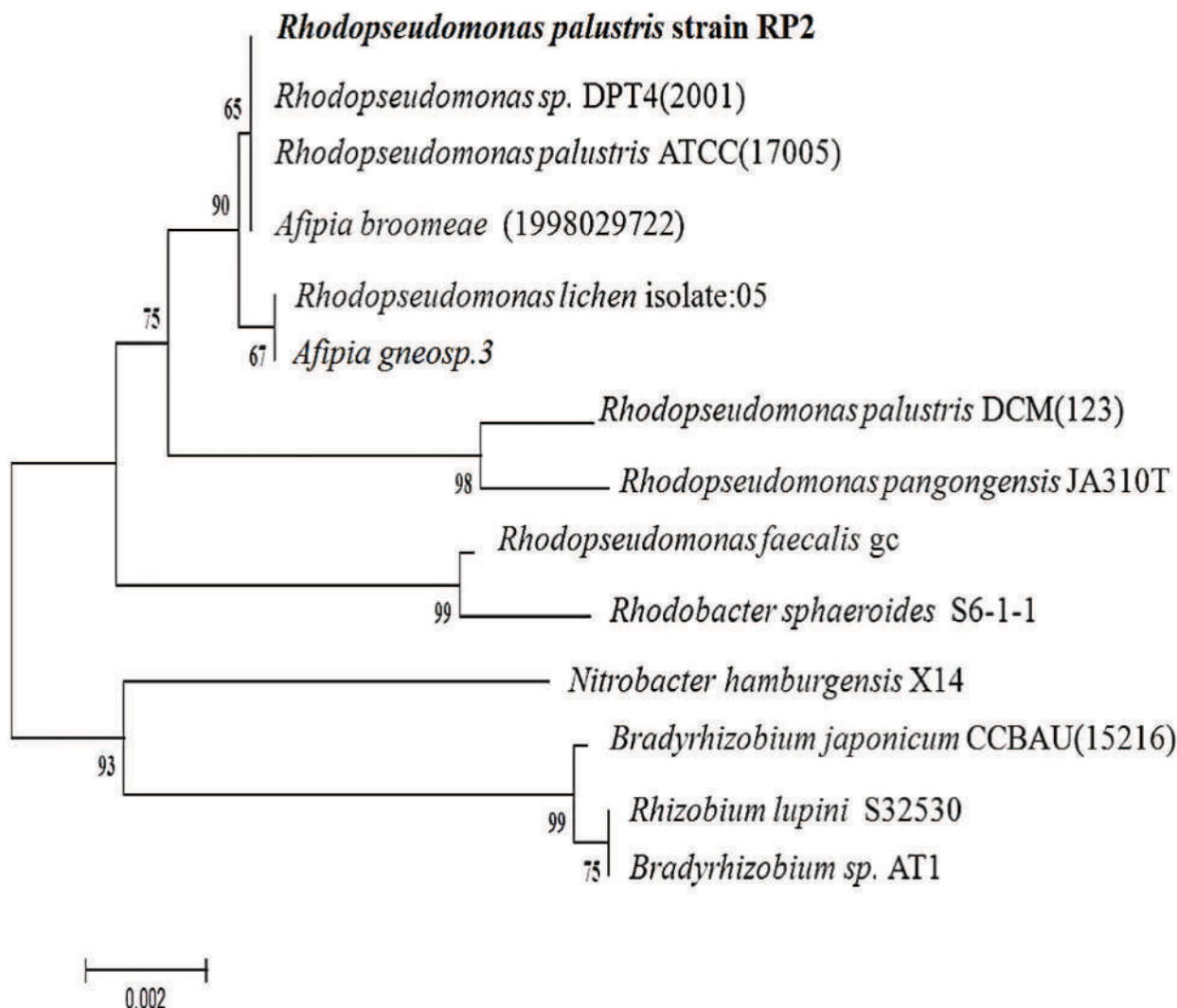


FIGURE 2 | Phylogenetic tree based on 16S rRNA sequences showing the positions of the isolate, *R. palustris* strain RP2 and representatives of other closely related species. The tree was constructed from 1,420 aligned bases; Scale bar represents 0.002 substitution per nucleotide.

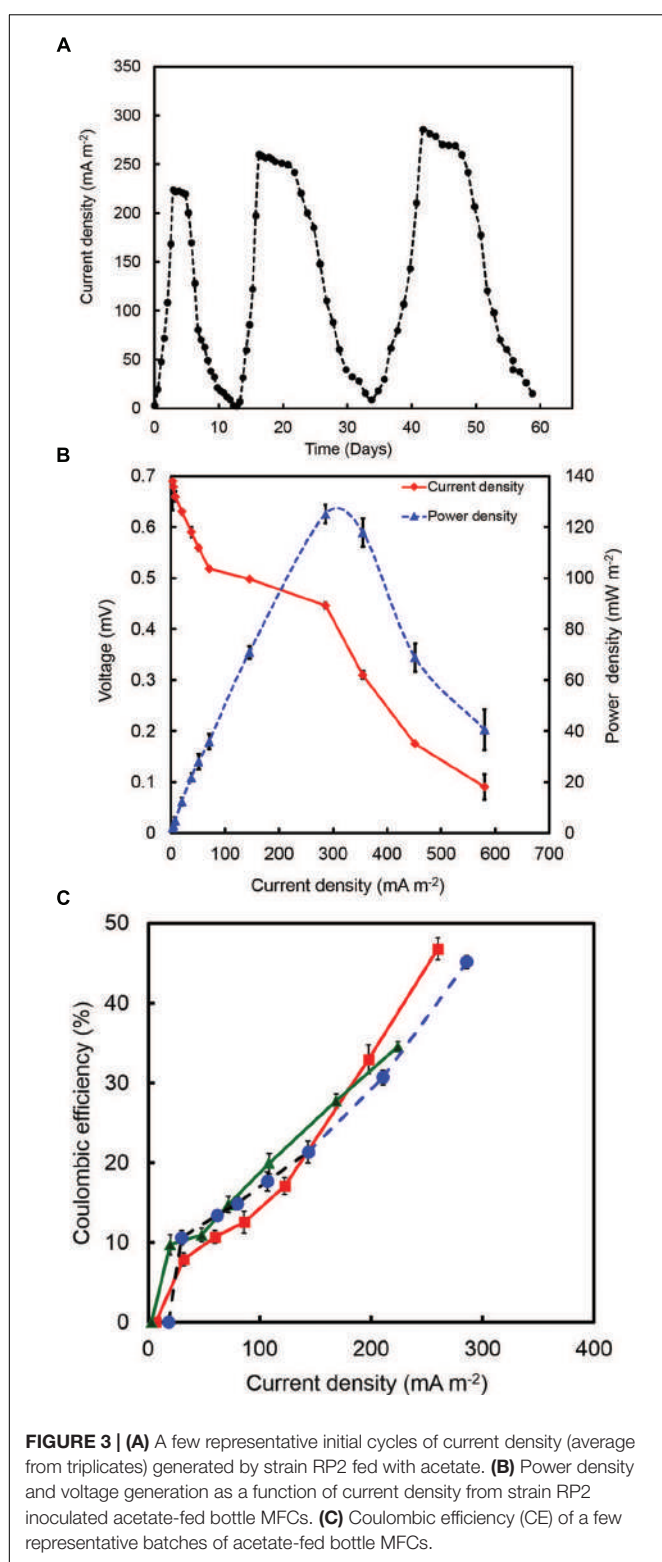
the electrochemical activities of the strain RP2 using cyclic voltammetry (CV) studies. Oxidation and reduction peaks of CV were observed in anaerobic grown bacterial cells (Figure 5A) whereas aerobically grown cells lacked the electrochemical activity (Figure 5B). Reduction peaks ranging from -394 mV to -399 mV and oxidation peaks ranging from -200 mV to $+100$ mV were observed at the electrode interface from washed cells suspensions. The calculated mid-point potential was about -278 mV. This asymmetric CV peak shows that the redox reaction is a quasi-reversible reaction. The amplitude of the peaks increased according to the growth stage of the culture in batch mode. The highest peaks were present during the exponential growth stage which indicated that the development of biofilm was the main factor for the electron transfer. One redox couple was observed from the CV peak and number of electrons transferred was calculated based on the Nernst equation (Logan, 2008). The CV peaks were not observed

from the suspension of aerobically grown cells or autoclaved controls.

Hydrocarbonoclastic Potential of *R. palustris* Strain RP2 in Anoxic Environments

Degradation of Hydrocarbons in Anoxic, Photosynthetic Incubations

To study the hydrocarbon degradation potential of the strain RP2, experiments were performed under four different environments: oxic, anoxic, photosynthetic, and chemosynthetic. Cultures were inoculated into Wolfe's media with DRHs as a sole carbon source with different electron accepting conditions. These incubation experiments indicate that photosynthetic anaerobic degradation of hydrocarbons occurred, however, no increase in biomass or hydrocarbon degradation was observed



in chemosynthetically grown anaerobic or aerobic samples. The rate and extent of biodegradation was interpreted from GC chromatograms of the residual hydrocarbons. **Figure 6A** shows the possible anoxic photoheterotrophic degradation of

DRH compounds under different electron accepting conditions [Photosynthetic only (PS); Photosynthetic + Nitrate (PS+N); Photosynthetic + Sulfate (PS+S); Photosynthetic + Iron (PS+Fe)]. For a substrate concentration of 4000 mg/l, cells showed ~10 to 30% of DRH removal by the end of the experiment. A higher percentage of DRH removal ($30.6 \pm 0.68\%$, 90th day) was noticed in the triplicates of sulfate containing anoxic, photoheterotrophic samples. Abiotic loss of DRH was measured under each condition was less than 5%.

Degradation of Hydrocarbons in MERS Environments

The ability of the strain RP2 to produce electricity using DRH as a sole carbon source was also examined using an initial concentration of 800 mg l^{-1} of DRHs for three complete cycles. A lag time of 90 h was observed in DRH fed MERS before a constant current was established. A maximum current and power density generated at this concentration were $21 \pm 3 \text{ mA/m}^2$ (**Figure 6B**), $720 \pm 7 \mu\text{W/m}^2$. An average of $47.4 \pm 2.7\%$ decrease in DRH was observed in closed circuit MERS inoculated with the strain RP2 by the end of experiment (30days). In the case of the abiotic (AC) and open circuit (OC) controls, DRH removal rates were $6.7 \pm 0.43\%$ and $10.1 \pm 1.7\%$ by the end of experiment. The current density and degradation profiles suggest that MERS could utilize the DRH as a sole source of energy generation which indicated the acclimation of strain RP2 biofilm (**Figure 6C**). However, no increase in biomass or hydrocarbon degradation or current generation was observed in chemosynthetically incubated MERS samples.

Discussion

Rhodopseudomonas species are associated with a variety of environments such as limnetic zones (Eckersley and Dow, 1980), marine environments (Larimer et al., 2004), sewage sludges (Hiraishi and Ueda, 1995), euxinic lagoons (Whittenbury and McLee, 1967), and poorly drained soils. The strain RP2 is a facultatively anaerobic, Gram negative purple non-sulfur photosynthetic rod shaped bacterium, containing lamellar ICMs as previously described (Mehrabi et al., 2001). It is a magnetotactic bacterium (Vainshtein et al., 1997), capable of nitrogen (Cantera et al., 2004), and carbon dioxide fixation (Larimer et al., 2004) as reported earlier. The detection of the *nif H* and *pufM* genes confirmed the presence of diazotrophic and photosynthetic traits as stated previously (Achenbach et al., 2001; Oda et al., 2005). With respect to this, it shares general characteristics with the *Rhodopseudomonas* genus of Rhodospirillaceae. However, a few distinctive features make this strain different from the existing members of the family, these include photoheterotrophic anoxic Fe(III) oxide reduction, electrically conductive filaments (Venkidusamy et al., 2015), spore formation, (**Figure 1**) growth factor requirements and the ability to degrade *n*-alkane components of DRHs in anoxic and MERS environments.

The normal growth mode of photosynthetic purple non-sulfur bacteria is photoheterotrophic; however, strain RP2 is able to switch to other metabolic modes such as photoorganoheterotrophic, phototoorganoautotrophic, chemorganoheterotrophic, photolithoautotrophic, and chemoautotrophic

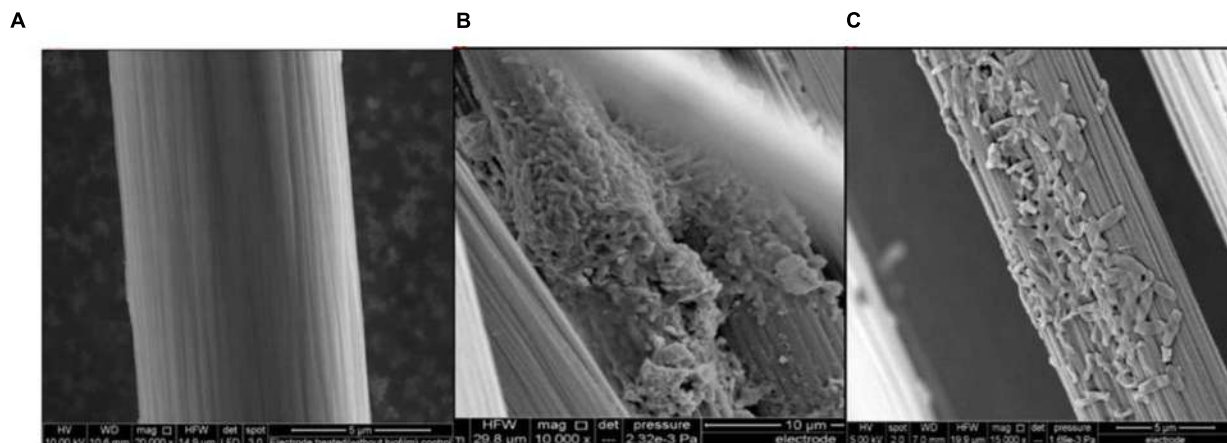
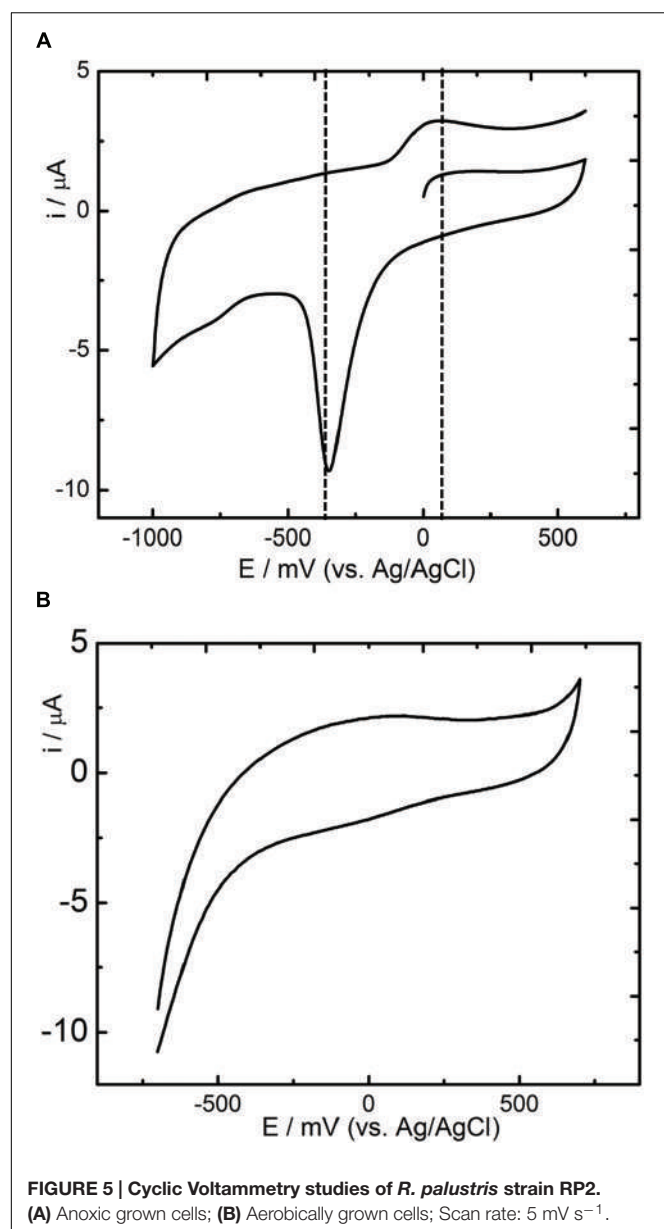


FIGURE 4 | Anode micrographs of *R. palustris* strain RP2 inoculated acetate-fed MFCs. **(A)** Treated control anode, **(B)** Strain RP2- biofilm on graphite surface and **(C)** Cells with high magnification.

growth. The strain RP2 also showed photolithotrophic growth with thiosulphate as an electron donor whereas pure cultures of *R. blastica* cannot utilize thiosulphate as an inorganic electron donor (Eckersley and Dow, 1980). Aerobic growth of the strain RP2 was also possible under both illuminated and non-illuminated conditions; however, strains of *Rhodopsedumonas* such as *R. faecalis* (Zhang et al., 2002), and *R. palustris*-17 (Dönmez et al., 1999) are unable to grow in oxygen rich, illuminated environments. The strain RP2 has a quite different pattern of carbon source utilization compared to other members of the genus *Rhodopseudomonas* (Supplementary Table S1). For example, strain RP2 was able to use gluconate and aspartate whereas *R. palustris* DX1 and *R. palustris* TIE-1 were unable to utilize those compounds (Xing et al., 2008). Under anaerobic conditions, the strain RP2 can utilize sodium benzoate as a carbon and energy source whereas the strain *Rhodopseudomonas* DCP-3 can oxidize benzoate only under aerobic conditions (Krooneman et al., 1999). The same pattern of glucose utilization under photoheterotrophic conditions has been reported (Imhoff and Bias-Imhoff, 1995), however few strains of *Rhodopseudomonas* are unable to grow when the medium is enriched with glucose as a sole substrate (Dönmez et al., 1999). Different patterns of vitamin requirements including p-amino benzoic acid, folic acid and pyridoxine HCl highlighted differences in the requirements of photosynthetic non-sulfur bacteria (Dönmez et al., 1999). The most interesting feature of the strain is photoheterotrophic ferric oxide reduction which required both light and an organic carbon source. This also provided evidence of a dissimilatory metal oxide reduction pathway (DMRB) similar to that seen in other electrochemically active bacterial strains (Lovley et al., 1993; Bretschger et al., 2007). On the other hand, photoferrotrophic growth of *R. palustris* strain TIE-1 has been demonstrated in the studies of anaerobic oxidation of Fe(II) (Bose et al., 2014; Byrne et al., 2015). Considering these features, this strain RP2 appears to be a novel member of the purple non-sulfur photosynthetic bacterial genus of *Rhodopseudomonas*.

The strain RP2 can transfer the electrons to extracellular, insoluble electron acceptors as reported earlier (Xing et al., 2008; Venkidusamy et al., 2015). Recent investigations have revealed the potential of using such phototrophic biofilms in a mediator free MFC systems (Park et al., 2014; Li et al., 2015). For instance, Xing et al. (2008), documented the highest power density of 2.72 ± 0.06 W/m² by *R. palustris* DX1 using dual chamber MFCs which is higher than that produced by mixed biofilms. *R. palustris* micro MFCs fed with renewable substrates such as blue green algae produced more power output of 10.4 mW/m³ than other chemical substrates used (Inglesby et al., 2012). The present study showed a maximum power density of 131.65 ± 10 mW/m² (acetate fed MFC, 50 mM buffer concentration) with an electron recovery of more than 40% as current using the strain RP2. However, the maximum power densities by such pure exoelectrogens are considerably influenced by a number of reactor parameters, operating conditions such as electrodes and its distance, electrode surface area to the volume ratio, pH, dissolved oxygen, resistance, electrolytes, etc. as reported earlier (Min et al., 2005; Logan, 2008). Biofilms and supernatant of the strain RP2 was used to determine the electrochemical activity through the release of redox proteins using CV analysis (Figures 5A,B). These results suggest that the presence of redox compounds in strain RP2 may be involved in extracellular electron transfer. The CV of *R. palustris* strain RP2 biofilm with Fe(III) oxide revealed the distinct redox peaks at -398 mV, +150 mV. The mid-potential of the CV peaks obtained matched the outer membrane cytochromes (OmcA) that have redox potential around -240 to -320 mV as reported in *Shewanella oneidensis* MR (Kim et al., 2002), *Geobacter*, *Desulfuromonas acetoxidans* (Lojou and Bianco, 2004). Further, CV curves from a bacterial cell suspension showed a smaller cell potential value than the theoretical electrode potential which was responsible for poor performance and operating conditions of MFCs (Kim et al., 1999). The results also suggest that oxygenated liquid cultures prevent the synthesis of the outer membrane cytochromes which



plays important role in extracellular electron transfer to insoluble metal oxides.

Metabolic Specialization and Biotechnological Potential of *R. palustris* Strain RP2

The genus *Rhodopseudomonas* has been studied as a versatile bioremediation candidate because of its exceptional growth flexibility involving the metabolism of diverse compounds. These include utilization of N-aromatic rings (Dutton and Evans, 1969), heterocyclic compounds, chlorinated compounds (McGrath and Harfoot, 1997), heavy metals and other groups of xenobiotic pollutants, for instance, phenolic compounds (Mehrabi et al., 2001), and other dihydroxylated aromatic aldehydes (Harwood

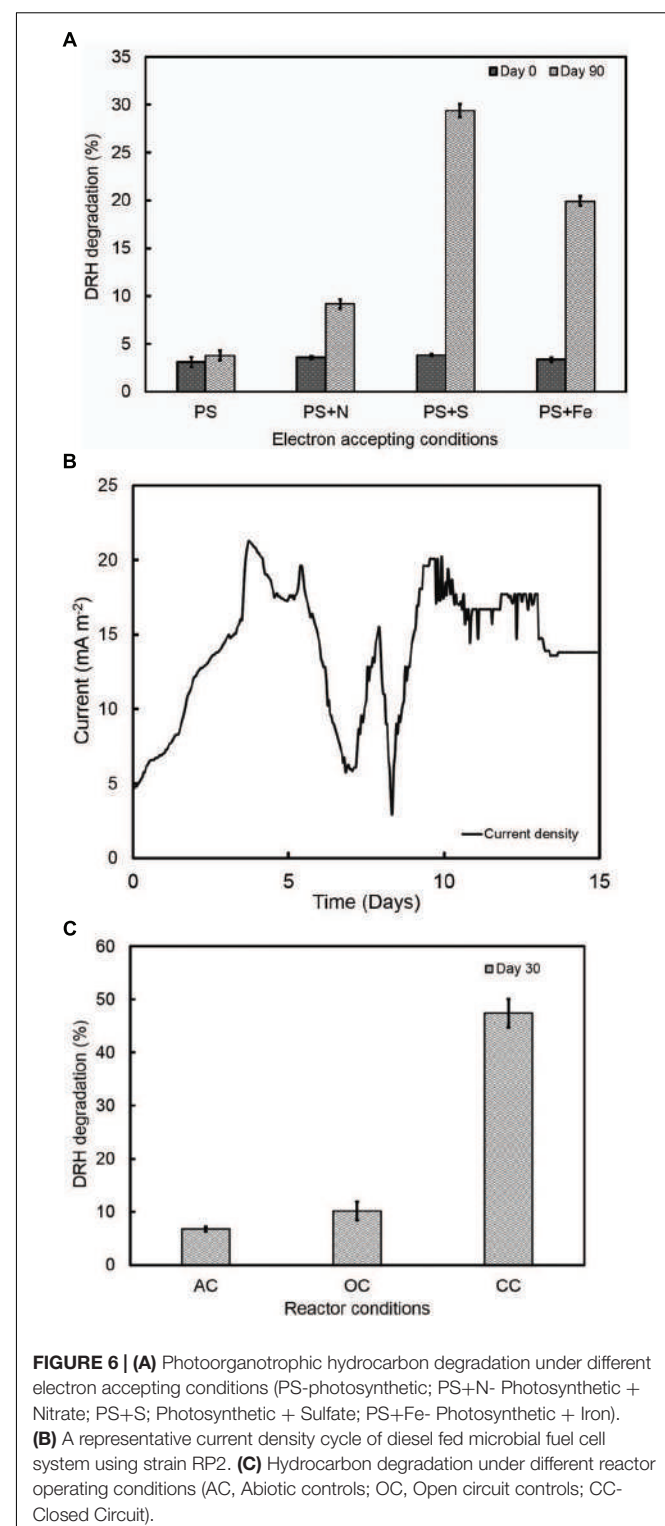


FIGURE 6 | **(A)** Photoorganotrophic hydrocarbon degradation under different electron accepting conditions (PS-photosynthetic; PS+N- Photosynthetic + Nitrate; PS+S: Photosynthetic + Sulfate; PS+Fe- Photosynthetic + Iron). **(B)** A representative current density cycle of diesel fed microbial fuel cell system using strain RP2. **(C)** Hydrocarbon degradation under different reactor operating conditions (AC, Abiotic controls; OC, Open circuit controls; CC- Closed Circuit).

and Gibson, 1986). However, the degradation of aliphatic hydrocarbons compounds by the genus *Rhodopseudomonas* is previously unknown. It was demonstrated here for the first time that the strain RP2 is capable of mineralizing DRHs in anaerobic environments.

In order to assess the hydrocarbon degradation potential of the strain RP2, GC scan was performed using the photoheterotrophically grown samples grown under different electron accepting conditions. We showed evidence for the existence of anaerobic hydrocarbon degrading capability in the strain RP2 when grown under illuminated conditions in the presence of thiosulfate. To obtain deeper insights into hydrocarbon degradation mechanism by the strain RP2, further research is required in terms of catabolic genes encoding alkane degrading enzymes such as Cytochrome 450, *alk* genes including *alkB*, *alkM*, *alkA* etc., The presence of such specific catabolic genes was investigated using the PCR mediated amplification method with various oligonucleotide primers (Supplementary Table S3). This strain, however, showed negative and non-specific results for CYP153A, *alkB* and its related, *alkM* and *alkA* genes. Efforts are being made using *R. palustris* strain RP2 genome sequence analysis to improve our understanding of anoxic photoorganotrophic hydrocarbon degradation mechanism in strain RP2. Metabolic prediction analysis using KEGG (Kyoto encyclopedia of Genes and Genome) reveals the presence of key enzymes involved in biodegradation of hydrocarbons. Supplementary Table S2 shows the comparison of metabolic genes present in the genome of *R. palustris* strain RP2 with other genomes obtained from database. Results of this study shows that the strain RP2 possesses alkane sulfonate monooxygenase and catechol 1,2-dioxygenase for hydrocarbon degradation as recently mentioned in *Pseudomonas aeruginosa* strain N0002 (Roy et al., 2013).

Previously, the remediation of hydrocarbons in MERS systems required mixed biofilms or enriched biofilms (Morris et al., 2009; Venkidusamy et al., 2016). The present study also demonstrated the potential of generating current in the presence of hydrocarbon compounds using the strain RP2 in MERS for the first time. However, the maximum current and power densities of hydrocarbons fed MERS were much lesser than the mixed culture MERS studies using freshly inoculated anodes (70.57 mA/m^2 at a concentration of 800 mg L^{-1}) (Venkidusamy et al., 2016), suggesting that the lower rate of hydrocarbons assimilation ($47.4 \pm 2.7\%$ by 30th day) limited the power generation. Whereas mixed culture MERS system showed nearly 84% of DRH removal at this concentration by the end of batch experiment (Venkidusamy et al., 2016). This perhaps indicates the presence of microbial interactions and its synergistic effects between different species in the mixed culture MERS systems. Interestingly, the strain RP2 also showed the physiological induction of electrically conductive nanofilaments

REFERENCES

- Achenbach, L. A., Carey, J., and Madigan, M. T. (2001). Photosynthetic and phylogenetic primers for detection of anoxygenic phototrophs in natural environments. *App. Environ. Microbiol.* 67, 2922–2926. doi: 10.1128/AEM.67.7.2922-2926.2001
- Bose, A., Gardel, E. J., Vidoudez, C., Parra, E., and Girguis, P. R. (2014). Electron uptake by iron-oxidizing phototrophic bacteria. *Nature commun.* 5, 3391. doi: 10.1038/ncomms4391
- Bretschger, O., Obraztsova, A., Sturm, C. A., Chang, I. S., Gorby, Y. A., Reed, S. B., et al. (2007). Current production and metal oxide reduction by *Shewanella*

oneidensis MR-1 wild type and mutants. *App. Environ. Microbiol.* 73, 7003–7012. doi: 10.1128/AEM.01087-07

- Byrne, J. M., Klueglein, N., Pearce, C., Rosso, K. M., Appel, E., and Kappler, A. (2015). Redox cycling of Fe (II) and Fe (III) in magnetite by Fe-metabolizing bacteria. *Science* 347, 1473–1476. doi: 10.1126/science.aaa4834
- Cantera, J. J. L., Kawasaki, H., and Seki, T. (2004). The nitrogen-fixing gene (nifH) of *Rhodopseudomonas palustris*: a case of lateral gene transfer? *Microbiol.* 150, 2237–2246. doi: 10.1099/mic.0.26940-0
- Chaudhuri, S. K., and Lovley, D. R. (2003). Electricity generation by direct oxidation of glucose in mediatorless microbial fuel cells. *Nat. Biotechnol.* 21, 1229–1232. doi: 10.1038/nbt867

CONCLUSION

The members of *Rhodopseudomonas* species appear to have a cosmopolitan distribution as their presence has been detected in marine environments. The present study demonstrated for the first time, the hydrocarbon bioremediation potential of *R. palustris* strain RP2 in anaerobic and MERS environments. The findings of this study not only expand our knowledge of the range of bacteria known to degrade hydrocarbon contaminants but also provide further research opportunities in the field of sustainable remediation (MERS), molecular biology of hydrocarbon biodegradative genes in EABs and their interactions in oil contaminated sites. Thus, this study will undoubtedly contribute to the biotechnological applications involved in advanced bioremediation techniques (MERS) and bioremedial process of hydrocarbons at photic, marine environments.

AUTHOR CONTRIBUTIONS

KV and MM proposed the study. KV conducted the experiments under the supervision of MM. KV prepared the draft with contributions from MM.

ACKNOWLEDGMENTS

The authors thank R. Lockington for comments and suggestions on previous versions of this manuscript. KV thanks Australian Federal Government, University of South Australia for International Postgraduate scholarship award (IPRS) and CRC CARE for the research top-up award.

SUPPLEMENTARY MATERIAL

The Supplementary Material for this article can be found online at: <http://journal.frontiersin.org/article/10.3389/fmicb.2016.01071>

- Cheng, S., Liu, H., and Logan, B. E. (2006). Increased performance of single-chamber microbial fuel cells using an improved cathode structure. *Electrochim. Commun.* 8, 489–494. doi: 10.1016/j.elecom.2006.01.010
- Dönmez, G. Ç., Öztürk, A., and Çakmakçı, L. (1999). Properties of the *Rhodopseudomonas palustris* strains isolated from an alkaline lake in Turkey. *Turkish J. Biol.* 23, 457–464.
- Dutton, P., and Evans, W. (1969). The metabolism of aromatic compounds by *Rhodopseudomonas palustris*. *Biochem. J.* 113, 525–536.
- Eckersley, K., and Dow, C. S. (1980). *Rhodopseudomonas blastica* sp. nov.: a member of the *Rhodospirillaceae*. *J. Gen. Microbiol.* 119, 465–473. doi: 10.1099/00221287-119-2-465
- Feng, Y., Yang, Q., Wang, X., and Logan, B. E. (2010). Treatment of carbon fiber brush anodes for improving power generation in air-cathode microbial fuel cells. *J. Power Sources* 195, 1841–1844. doi: 10.1016/j.jpowsour.2009.10.030
- Harwood, C. S., and Gibson, J. (1986). Uptake of benzoate by *Rhodopseudomonas palustris* grown anaerobically in light. *J. bacteriol.* 165, 504–509.
- Hiraishi, A., and Ueda, Y. (1995). Isolation and characterization of *Rhodovulum strictum* sp. nov. and some other purple nonsulfur bacteria from colored blooms in tidal and seawater pools. *Int. J. Syst. Bacteriol.* 45, 319–326.
- Holmes, D. E., Chaudhuri, S. K., Nevin, K. P., Mehta, T., Methé, B. A., Liu, A., et al. (2006). Microarray and genetic analysis of electron transfer to electrodes in *Geobacter sulfurreducens*. *Environ. Microbiol.* 8, 1805–1815. doi: 10.1111/j.1462-2920.2006.01065.x
- Huang, L., Cheng, S., and Chen, G. (2011). Bioelectrochemical systems for efficient recalcitrant wastes treatment. *J. Chem. Technol. Biotechnol.* 86, 481–491. doi: 10.1002/jctb.2551
- Hungate, R. (1950). The anaerobic mesophilic cellulolytic bacteria. *Bacteriol. Rev.* 14, 1–49.
- Imhoff, J. F., and Bias-Imhoff, U. (1995). “Lipids, quinones and fatty acids of anoxygenic phototrophic bacteria,” in *Anoxygenic Photosynthetic Bacteria*, eds R. E. Blankenship, M. T. Madigan, and C. E. Bauer (Dordrecht: Springer), 179–205.
- Ingleby, A. E., Beatty, D. A., and Fisher, A. C. (2012). *Rhodopseudomonas palustris* purple bacteria fed *Arthrosphaera maxima* cyanobacteria: demonstration of application in microbial fuel cells. *RSC. Adv.* 2, 4829–4838. doi: 10.1039/c2ra20264f
- Kim, B.-H., Kim, H.-J., Hyun, M.-S., and Park, D.-H. (1999). Direct electrode reaction of Fe (III)-reducing bacterium, *Shewanella putrefaciens*. *J. Microbiol. Biotechnol.* 9, 127–131. doi: 10.1371/journal.pone.0147899
- Kim, H. J., Park, H. S., Hyun, M. S., Chang, I. S., Kim, M., and Kim, B. H. (2002). A mediator-less microbial fuel cell using a metal reducing bacterium, *Shewanella putrefaciens*. *Enzyme Microb. Technol.* 30, 145–152. doi: 10.1016/S0141-0229(01)00478-1
- Kranz, R. G., and Haselkorn, R. (1986). Anaerobic regulation of nitrogen-fixation genes in *Rhodopseudomonas capsulata*. *Proc. Natl. Acad. Sci. U.S.A.* 83, 6805–6809. doi: 10.1073/pnas.83.18.6805
- Krooneman, J., van den Akker, S., Gomes, T. M. P., Forney, L. J., and Gottschal, J. C. (1999). Degradation of 3-chlorobenzoate under low-oxygen conditions in pure and mixed cultures of the anoxygenic photoheterotroph *Rhodopseudomonas palustris* DCP3 and an aerobic *Alcaligenes* species. *App. Environ. Microbiol.* 65, 131–137.
- Larimer, F. W., Chain, P., Hauser, L., Lamerdin, J., Malfatti, S., Do, L., et al. (2004). Complete genome sequence of the metabolically versatile photosynthetic bacterium *Rhodopseudomonas palustris*. *Nature Biotechnol.* 22, 55–61. doi: 10.1038/nbt923
- Li, X., Liu, T., Wang, K., and Waite, T. D. (2015). Light-induced extracellular electron transport by the marine Raphidophyte *Chattonella marina*. *Environ. Sci. Technol.* 49, 1392–1399. doi: 10.1021/es503511m
- Logan, B., Cheng, S., Watson, V., and Estadt, G. (2007). Graphite fiber brush anodes for increased power production in air-cathode microbial fuel cells. *Environ. Sci. Technol.* 41, 3341–3346. doi: 10.1021/es062644y
- Logan, B. E. (2008). *Microbial Fuel Cells*. Hoboken, NJ: John Wiley & Sons.
- Lojou, E., and Bianco, P. (2004). Membrane electrodes for protein and enzyme electrochemistry. *Electroanalysis* 16, 1113–1121. doi: 10.1002/elan.200403001
- Lovley, D. R., Giovannoni, S. J., White, D. C., Champine, J. E., Phillips, E., Gorby, Y. A., et al. (1993). *Geobacter metallireducens* gen. nov. sp. nov., a microorganism capable of coupling the complete oxidation of organic compounds to the reduction of iron and other metals. *Archiv. Microbiol.* 159, 336–344. doi: 10.1007/BF00290916
- Lovley, D. R., and Phillips, E. J. (1988a). Manganese inhibition of microbial iron reduction in anaerobic sediments. *Geomicrobiol. J.* 6, 145–155. doi: 10.1080/01490458809377834
- Lovley, D. R., and Phillips, E. J. (1988b). Novel mode of microbial energy metabolism: organic carbon oxidation coupled to dissimilatory reduction of iron or manganese. *App. Environ. Microbiol.* 54, 1472–1480.
- McGrath, J. E., and Harfoot, C. G. (1997). Reductive dehalogenation of halocarboxylic acids by the phototrophic genera *Rhodospirillum* and *Rhodopseudomonas*. *Appl. Environ. Microbiol.* 63, 3333–3335.
- Mehrabi, S., Ekanemesang, U. M., Aikhionbare, F. O., Kimbro, K. S., and Bender, J. (2001). Identification and characterization of *Rhodopseudomonas* spp., a purple, non-sulfur bacterium from microbial mats. *Biomol. Eng.* 18, 49–56. doi: 10.1016/S1389-0344(01)00086-7
- Min, B., Kim, J., Oh, S., Regan, J. M., and Logan, B. E. (2005). Electricity generation from swine wastewater using microbial fuel cells. *Water Res.* 39, 4961–4968. doi: 10.1016/j.watres.2005.09.039
- Morris, J. M., Jin, S., Crimi, B., and Pruden, A. (2009). Microbial fuel cell in enhancing anaerobic biodegradation of diesel. *Chem. Eng. J.* 146, 161–167. doi: 10.1016/j.cej.2008.05.028
- Oda, Y., Samanta, S. K., Rey, F. E., Wu, L., Liu, X., Yan, T., et al. (2005). Functional genomic analysis of three nitrogenase isozymes in the photosynthetic bacterium *Rhodopseudomonas palustris*. *J. Bacteriol.* 187, 7784–7794. doi: 10.1128/JB.187.22.7784-7794.2005
- Oh, S., Min, B., and Logan, B. E. (2004). Cathode performance as a factor in electricity generation in microbial fuel cells. *Environ. Sci. Technol.* 38, 4900–4904. doi: 10.1021/es049422p
- Park, T.-J., Ding, W., Cheng, S., Brar, M. S., Ma, A. P. Y., Tun, H. M., et al. (2014). Microbial community in microbial fuel cell (MFC) medium and effluent enriched with purple photosynthetic bacterium (*Rhodopseudomonas* sp.). *AMB Exp.* 4, 22. doi: 10.1186/s13568-014-0022-2
- Roy, A. S., Baruah, R., Gogoi, D., Borah, M., Singh, A. K., and Boruah, H. P. D. (2013). Draft genome sequence of *Pseudomonas aeruginosa* strain N002, isolated from crude oil-contaminated soil from Geleky, Assam, India. *Genome Announc.* 1, e00104–e00112. doi: 10.1128/genomeA.00104-12
- Sambrook, J., Fritsch, E. F., and Maniatis, T. (1989). *Molecular Cloning: A Laboratory Manual*, 2nd Edn. Plainview, NY: Cold spring harbor laboratory press.
- Tamura, K., Peterson, D., Peterson, N., Stecher, G., Nei, M., and Kumar, S. (2011). MEGA5: molecular evolutionary genetics analysis using maximum likelihood, evolutionary distance, and maximum parsimony methods. *Mol. Biol. Evol.* 28, 2731–2739. doi: 10.1093/molbev/msr121
- USEPA (1996). *SW-846 Method 8015B-3rd Edn, Updates I, II, IIA and III: Test Methods for Evaluating Solid Wastes, Physical/Chemical Methods, Superintendent of Documents*. Washington, DC: U.S.Government printing office.
- Vainshtein, M., Suzina, N., and Sorokin, V. (1997). A new type of magnet-sensitive inclusions in cells of photosynthetic purple bacteria. *Sys. Appl. Microbiol.* 20, 182–186. doi: 10.1016/S0723-2020(97)80064-1
- Venkidusamy, K., Megharaj, M., Marzorati, M., Lockington, R., and Naidu, R. (2016). Enhanced removal of petroleum hydrocarbons using a bioelectrochemical remediation system with pre-cultured anodes. *Sci. Total Environ.* 539, 61–69. doi: 10.1016/j.scitotenv.2015.08.098
- Venkidusamy, K., Megharaj, M., Schröder, U., Karouta, F., Mohan, S. V., and Naidu, R. (2015). Electron transport through electrically conductive nanofilaments in *Rhodopseudomonas palustris* strain RP2. *RSC Adv.* 5, 100790–100798. doi: 10.1039/C5RA08742B
- Weisburg, W. G., Barns, S. M., Pelletier, D. A., and Lane, D. J. (1991). 16S ribosomal DNA amplification for phylogenetic study. *J. Bacteriol.* 173, 697–703.
- Whittenbury, R., and McLee, A. (1967). *Rhodopseudomonas palustris* and Rh. viridis—photosynthetic budding bacteria. *Arch. Mikrobiol.* 59, 324–334. doi: 10.1007/BF00406346
- Wrighton, K. C., Agbo, P., Warnecke, F., Weber, K. A., Brodie, E. L., DeSantis, T. Z., et al. (2008). A novel ecological role of the Firmicutes identified in thermophilic microbial fuel cells. *ISME J.* 2, 1146–1156. doi: 10.1038/ismej.2008.48

- Xing, D., Zuo, Y., Cheng, S., Regan, J. M., and Logan, B. E. (2008). Electricity generation by *Rhodopseudomonas palustris* DX-1. *Environ. Sci. Technol.* 42, 4146–4151. doi: 10.1021/es800312v
- Zhang, D., Yang, H., Huang, Z., Zhang, W., and Liu, S.-J. (2002). *Rhodopseudomonas faecalis* sp. nov., a phototrophic bacterium isolated from an anaerobic reactor that digests chicken faeces. *Inten. J. Sys. Evol. Microbiol.* 52, 2055–2060. doi: 10.1099/0020713-52-6-2055
- Zuo, Y., Xing, D., Regan, J. M., and Logan, B. E. (2008). Isolation of the exoelectrogenic bacterium *Ochrobactrum anthropi* YZ-1 by using a U-tube microbial fuel cell. *Appl. Environ. Microbiol.* 74, 3130–3137. doi: 10.1128/AEM.02732-07

Conflict of Interest Statement: The authors declare that the research was conducted in the absence of any commercial or financial relationships that could be construed as a potential conflict of interest.

Copyright © 2016 Venkidusamy and Megharaj. This is an open-access article distributed under the terms of the Creative Commons Attribution License (CC BY). The use, distribution or reproduction in other forums is permitted, provided the original author(s) or licensor are credited and that the original publication in this journal is cited, in accordance with accepted academic practice. No use, distribution or reproduction is permitted which does not comply with these terms.



The Low Conductivity of *Geobacter uraniireducens* Pili Suggests a Diversity of Extracellular Electron Transfer Mechanisms in the Genus *Geobacter*

Yang Tan¹, Ramesh Y. Adhikari², Nikhil S. Malvankar^{1,2,3}, Joy E. Ward¹, Kelly P. Nevin¹, Trevor L. Woodard¹, Jessica A. Smith¹, Oona L. Snoeyenbos-West¹, Ashley E. Franks^{1,4}, Mark T. Tuominen² and Derek R. Lovley^{1*}

¹ Department of Microbiology, University of Massachusetts Amherst, Amherst, MA, USA, ² Department of Physics, University of Massachusetts Amherst, Amherst, MA, USA, ³ Department of Molecular Biophysics and Biochemistry, Microbial Sciences Institute, Yale University, New Haven, CT, USA, ⁴ Department of Physiology, Anatomy and Microbiology, La Trobe University, Melbourne, VIC, Australia

OPEN ACCESS

Edited by:

Yong Xiao,

Institute of Urban Environment,
Chinese Academy of Sciences, China

Reviewed by:

Tim Magnuson,

Idaho State University, USA

Yinjie Tang,

University of Washington, USA

*Correspondence:

Derek R. Lovley

dlovley@microbio.umass.edu

Specialty section:

This article was submitted to
Microbiotechnology, Ecotoxicology
and Bioremediation,
a section of the journal
Frontiers in Microbiology

Received: 07 April 2016

Accepted: 07 June 2016

Published: 28 June 2016

Citation:

Tan Y, Adhikari RY, Malvankar NS, Ward JE, Nevin KP, Woodard TL, Smith JA, Snoeyenbos-West OL, Franks AE, Tuominen MT and Lovley DR (2016) The Low Conductivity of *Geobacter uraniireducens* Pili Suggests a Diversity of Extracellular Electron Transfer Mechanisms in the Genus *Geobacter*. *Front. Microbiol.* 7:980.
doi: 10.3389/fmicb.2016.00980

Studies on the mechanisms for extracellular electron transfer in *Geobacter* species have primarily focused on *Geobacter sulfurreducens*, but the poor conservation of genes for some electron transfer components within the *Geobacter* genus suggests that there may be a diversity of extracellular electron transport strategies among *Geobacter* species. Examination of the gene sequences for PilA, the type IV pilus monomer, in *Geobacter* species revealed that the PilA sequence of *Geobacter uraniireducens* was much longer than that of *G. sulfurreducens*. This is of interest because it has been proposed that the relatively short PilA sequence of *G. sulfurreducens* is an important feature conferring conductivity to *G. sulfurreducens* pili. In order to investigate the properties of the *G. uraniireducens* pili in more detail, a strain of *G. sulfurreducens* that expressed pili comprised the PilA of *G. uraniireducens* was constructed. This strain, designated strain GUP, produced abundant pili, but generated low current densities and reduced Fe(III) very poorly. At pH 7, the conductivity of the *G. uraniireducens* pili was 3×10^{-4} S/cm, much lower than the previously reported 5×10^{-2} S/cm conductivity of *G. sulfurreducens* pili at the same pH. Consideration of the likely voltage difference across pili during Fe(III) oxide reduction suggested that *G. sulfurreducens* pili can readily accommodate maximum reported rates of respiration, but that *G. uraniireducens* pili are not sufficiently conductive to be an effective mediator of long-range electron transfer. In contrast to *G. sulfurreducens* and *G. metallireducens*, which require direct contact with Fe(III) oxides in order to reduce them, *G. uraniireducens* reduced Fe(III) oxides occluded within microporous beads, demonstrating that *G. uraniireducens* produces a soluble electron shuttle to facilitate Fe(III) oxide reduction. The results demonstrate that *Geobacter* species may differ substantially in their mechanisms for long-range electron transport and that it is important to have information beyond a phylogenetic affiliation in order to make conclusions about the mechanisms by which *Geobacter* species are transferring electrons to extracellular electron acceptors.

Keywords: electromicrobiology, microbial fuel cells, microbial nanowires, electron transfer, *Geobacter*

INTRODUCTION

The presence of *Geobacter* species is often equated with processes in which the capacity for long-range electron transfer via electrically conductive pili (e-pili) is an advantageous feature (Lovley et al., 2011). For example, molecular analyses have demonstrated that *Geobacter* species are often among the most abundant microorganisms on anodes harvesting electrons from organic wastes and sediments, as well as in soils and sediments in which Fe(III) reduction is an important process (Kiely et al., 2011; Lovley et al., 2011). Direct interspecies electron transfer (DIET) in anaerobic digesters has been attributed to an abundance and high metabolic activity of *Geobacter* species (Morita et al., 2011; Rotaru et al., 2014b; Shrestha et al., 2014). Long-range electron transport through *Geobacter* anode biofilms, as well as Fe(III) oxide reduction and syntrophy via DIET in *Geobacter* species, have all been linked to long-range electron transport through e-pili (Lovley, 2011; Malvankar and Lovley, 2014).

However, the concept that *Geobacter* species rely on e-pili for long-range electron transport is based on a rather limited dataset from studies primarily conducted with *G. sulfurreducens*. This species has been the focus of most studies because it was the first *Geobacter* species for which a genetic system (Coppi et al., 2001) and genome sequence (Methé et al., 2003) became available and because *G. sulfurreducens* produces high current densities (Nevin et al., 2008; Yi et al., 2009). More limited data are also available for *Geobacter metallireducens* which is also genetically tractable (Tremblay et al., 2012; Shrestha et al., 2013; Smith et al., 2013; Rotaru et al., 2014a,b). Efforts to genetically manipulate other *Geobacter* species have as yet been unsuccessful.

Deletion of the gene for PilA, the type IV pilus monomer in *G. sulfurreducens*, revealed the importance of the pili in Fe(III) oxide reduction (Reguera et al., 2005), current production (Reguera et al., 2006; Nevin et al., 2009), and DIET (Summers et al., 2010). A strain with a genetically modified PilA that yielded poorly conductive pili was also defective in extracellular electron transfer (Vargas et al., 2013), as was a strain of *G. sulfurreducens* that expressed non-conductive *Pseudomonas aeruginosa* pili (Liu et al., 2014). Evidence for the importance of pili in extracellular electron transfer in *G. metallireducens*, which is closely related to *G. sulfurreducens* (Lovley et al., 2011), was specific expression of the pili in *G. metallireducens* when growing on Fe(III) or Mn(IV) oxides (Childers et al., 2002) and the finding that deleting the gene for PilA in *G. metallireducens* inhibited Fe(III) oxide reduction, current production, and DIET (Tremblay et al., 2012; Shrestha et al., 2013; Rotaru et al., 2014a,b).

Consistent with the proposed role of the *G. sulfurreducens* pili in long-range electron transport, chemically fixed pili were conductive across their diameter (Reguera et al., 2005). Networks of unfixed, hydrated pili conducted electrons across a 50 μm non-conducting gap between gold electrodes, suggesting the potential for electron transport along the length of the pili (Malvankar et al., 2011). Charge injected into pili propagated along the length of the pili in a manner similar to carbon nanotubes (Malvankar et al., 2014). Although the c-type cytochrome OmcS was localized on the pili (Leang et al., 2010), the possibility of cytochrome-based electron transport along the length of the pili was ruled

out by several lines of evidence, which included the findings that (i) denaturing cytochromes had no impact on conduction of the pili networks (Malvankar et al., 2011); (ii) charge propagated along substantial lengths of the pili that lacked cytochromes (Malvankar et al., 2014); (iii) modifying the pilus structure by replacing aromatic amino acids with alanine yielded pili that were poorly conductive, even though OmcS was properly localized on the pili (Vargas et al., 2013); (iv) *P. aeruginosa* pili expressed in *G. sulfurreducens* were poorly conductive, even though OmcS was properly localized on the pili (Liu et al., 2014); and (v) the cytochromes were spaced too far apart for cytochrome-to-cytochrome electron transport to be feasible (Leang et al., 2010; Malvankar et al., 2012). The conductivity along the length of cytochrome-free sections of individual pili at pH 7 (51 mS/cm) compares favorably with the conductivity of nanowires of similar diameter produced with synthetic conducting organic polymers (Adhikari et al., 2016).

Geobacter sulfurreducens pili conductivity is attributed to a truncated PilA, which is substantially shorter than the PilA found in most bacteria (Reguera et al., 2005), and permits tighter packing of aromatic amino acids that participate in electron transport (Malvankar et al., 2015). However, not all *Geobacter* species contain a truncated PilA. The PilA of *G. uraniireducens* is much longer (193 amino acids) than the PilA of *G. sulfurreducens* (61 amino acids; Figure 1). Unlike *G. metallireducens* (Childers et al., 2002; Shrestha et al., 2013) and *G. sulfurreducens* (Nevin et al., 2009; Shrestha et al., 2013), which highly express *pilA* when growing with an extracellular electron acceptor, *G. uraniireducens* did not upregulate expression of *pilA* when grown on Fe(III) oxide (Holmes et al., 2008). Furthermore, unlike *G. sulfurreducens* and *G. metallireducens*, *G. uraniireducens* did not produce the high current densities that have been attributed to electrically conductive pili, and *G. uraniireducens* could not participate in DIET (Rotaru et al., 2015). These results suggest that *G. uraniireducens* might not rely on conductive pili for extracellular electron transfer. If so, this would significantly impact on the understanding of the mechanisms long-range electron transport in *Geobacter* species. However, the lack of tools for genetic manipulation of *G. uraniireducens* has limited experimental approaches to evaluate this hypothesis.

There are alternatives to e-pili for some forms of extracellular electron transfer in *Geobacter* species. Studies with *G. sulfurreducens* have demonstrated that cells in direct contact with electrodes do not require e-pili for extracellular electron transfer (Lovley, 2011, 2012). The electrical contact between cells and the anode appears to be made by c-type cytochromes, most notably OmcZ (Richter et al., 2009; Inoue et al., 2010, 2011). Outer surface c-type cytochromes are also important for the reduction of soluble extracellular electron acceptors (Lovley, 2011), including electron shuttles that may be found in the environment (Voordeckers et al., 2010). Although some microorganisms produce their own electron shuttles to facilitate electron transfer to electrodes or Fe(III) oxides, the *Geobacter* species that have been studied to date do not (Lovley, 2011). *G. uraniireducens* highly expresses a suite of outer-surface c-type cytochromes during growth on Fe(III) oxides, suggesting the likely importance of these cytochromes

<i>G. sulfurreducens</i>	FILIELLIVVATIIGILAAIAIPQFSAYRKAYNSAASSDLRNLTAKLESAFADDQTYPPES-----
<i>G. uraniireducens</i>	FILIELLIVVATIIGILAAIAIPQFSKYRIQQFNASGNSDLKNIRTSQESLYAEWQHGLTQQLATVAGLP-----
<i>P. aeruginosa</i>	FILIELMIVVATIIGILAAIAIPQYQNYVARSEGASALATINPLKTTVEESLSRGIAGSKIKITGTASTAT-----
<i>G. sulfurreducens</i>	GAGKVGVGALVTPTAALPVCIIITDDNNLVPRLQIPVGNNTAMATTAAAGAGDGGSYTLAAKHLQGDV-----
<i>G. uraniireducens</i>	ETYVGVEPDANKLGVIAVAIEDSGADITFTFQSGTSSPKNATKVITLNRTADGVWACKSTQDPMFPTKG-----
<i>P. aeruginosa</i>	CDN-----

FIGURE 1 | Alignment of PilA amino acid sequences of *Geobacter sulfurreducens*, *Geobacter uraniireducens*, and *Pseudomonas aeruginosa*.

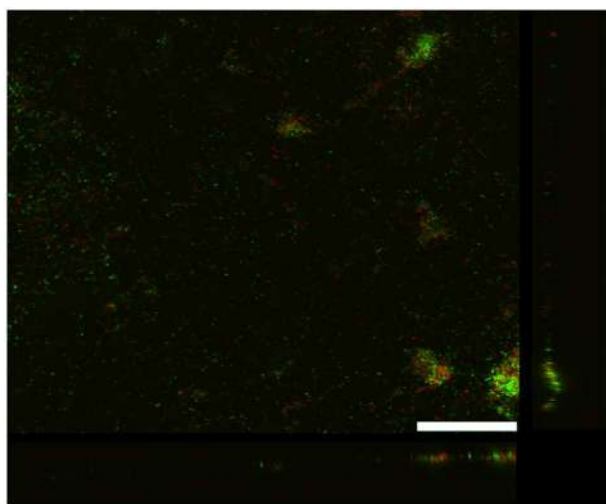


FIGURE 2 | Confocal scanning laser microscope image of an anode biofilm of *G. uraniireducens* that was producing 0.074 mA/cm² current. Top-down three-dimensional, lateral side views (right image), and horizontal side views (bottom image) of cells stained with LIVE/DEAD BacLight viability stain. The size bar is 75 microns.

in extracellular electron transfer (Holmes et al., 2008; Aklujkar et al., 2013).

The purpose of this study was to further investigate the possibility for pili-mediated long-range electron transport in *Geobacter* species by evaluating the conductivity of individual *G. uraniireducens* pili. The results demonstrate that *G. uraniireducens* pili are poorly conductive and suggest that *G. uraniireducens* relies on other strategies for extracellular electron transfer.

MATERIALS AND METHODS

Bacterial Strains, Plasmids, and Culture Conditions

All bacterial strains and plasmids used in this study are summarized in Supplementary Table S1. *Geobacter* strains were routinely cultured at 30°C under strict anaerobic conditions (80/20 N₂-CO₂) in NBAF medium containing acetate (15 mM)

as the electron donor and fumarate (40 mM) as the electron acceptor, as previously described (Coppi et al., 2001). Chemically competent *Escherichia coli* TOP10 (Invitrogen, Grand Island, NY, USA) was used routinely for cloning and cultured at 37°C in lysogeny broth medium (LB medium; Bertani, 1951) with the appropriate antibiotic added when necessary.

Construction of *G. sulfurreducens* Strain GUP

The *G. sulfurreducens* strain GUP (*G. uraniireducens* pili) was constructed using a previously described approach (Vargas et al., 2013). Primers used for construction of strain GUP are listed in Supplementary Table S2. The three DNA fragments were generated independently by PCR for the construction of the mutant. Primer pair GspilAf/GspilAr amplified the promoter region of the pilA gene using pPLT174 (Vargas et al., 2013) as the template for the generation of fragment 1. For the generation of fragment 2, primer pair GupilAf/GupilAr amplified Gura_2677 using *G. uraniireducens* RF4 genomic DNA as the template. Primer pair GupilACf/GupilACr amplified 500 bp downstream of the pilA gene using *G. sulfurreducens* genomic DNA as the template for the generation of fragment 3. Three independent fragments for strain GUP were combined via recombinant PCR with primer pair GspilAf/GspilACr as previously described (Liu et al., 2014).

The corresponding recombinant PCR products were digested with *Xba*I and *Apa*I (New England BioLabs, Ipswich, MA, USA) and ligated with the vector pPLT173 (Vargas et al., 2013) using T4 DNA ligase. The plasmid pPLT173 contains 500 bp upstream of the *Geobacter* pilA gene followed by a gentamicin resistance cassette and *Xba*I and *Apa*I restriction site. The final plasmid (pPLT173-GUP) was linearized with *Nco*I (NEB) and electroporated into *G. sulfurreducens* competent cells as previously described (Coppi et al., 2001). Transformants were selected and verified as previously described (Liu et al., 2014).

Current Production and Fe(III) Oxide Reduction

Current production was determined as previously described (Nevin et al., 2009) in flow-through, two-chambered H-cell systems with acetate (10 mM) as the electron donor and graphite stick anodes (65 cm²) poised at 300 mV versus Ag/AgCl as the electron acceptor.

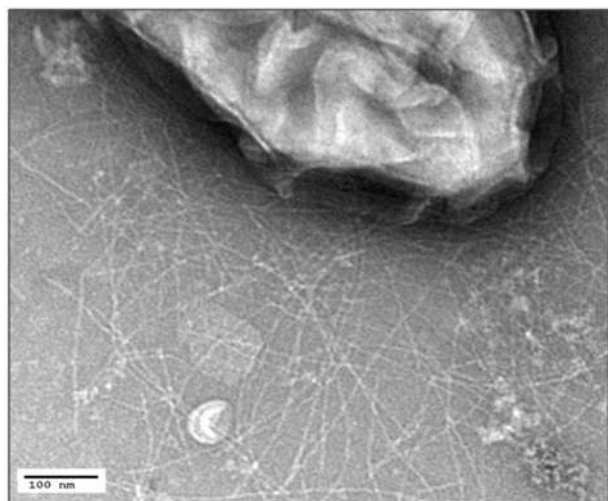


FIGURE 3 | Transmission electron micrograph of *G. sulfurreducens* strain GUP expressing abundant pili. The size bar represents 100 nm.

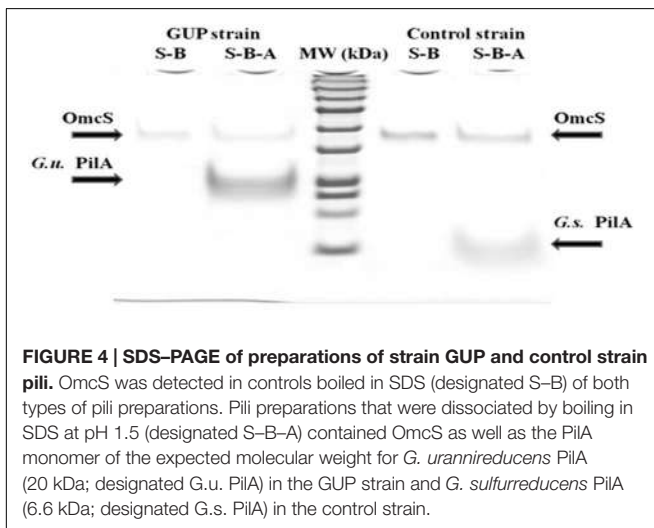


FIGURE 4 | SDS-PAGE of preparations of strain GUP and control strain pili. OmcS was detected in controls boiled in SDS (designated S-B) of both types of pili preparations. Pili preparations that were dissociated by boiling in SDS at pH 1.5 (designated S-B-A) contained OmcS as well as the PilA monomer of the expected molecular weight for *G. uraniireducens* PilA (20 kDa; designated G.u. PilA) in the GUP strain and *G. sulfurreducens* PilA (6.6 kDa; designated G.s. PilA) in the control strain.

Growth with Fe(III) oxide as the electron acceptor was evaluated as previously described (Vargas et al., 2013) in medium with acetate as the electron donor and poorly crystalline Fe(III) oxide (100 mmol l^{-1}) as the electron acceptor (Lovley and Phillips, 1988). Fe(II) production was measured with the ferrozine assay (Lovley and Phillips, 1988). For studies on the need for direct contact for Fe(III) oxide reduction, the poorly crystalline Fe(III) oxide was incorporated into microporous alginate beads (diameter, 5 mm) with a nominal molecular mass cutoff of 12 kDa, as previously described (Nevin and Lovley, 2000). Beads were added to medium to provide Fe (III) at 150 mmol l^{-1} . When noted anthraquinone-2,6-disulfonate (AQDS) was added as an electron shuttle at $50 \mu\text{M}$. The production of Fe(II) was determined with the ferrozine assay after the beads had been extracted for 12 h in 0.5 N HCl.

Pili Preparation

Geobacter sulfurreducens strain GUP biofilms grown on graphite electrodes as described above were gently scraped from the electrode surface with a plastic spatula and isotonic wash buffer (20.02 mM morpholinepropanesulfonic acid, 4.35 mM $\text{Na}_2\text{PO}_4 \cdot \text{H}_2\text{O}$, 1.34 mM KCl, 85.56 mM NaCl, 1.22 mM $\text{MgSO}_4 \cdot 7\text{H}_2\text{O}$, and 0.07 mM $\text{CaCl}_2 \cdot 2\text{H}_2\text{O}$). The cells were collected by centrifugation and re-suspended in 150 mM ethanolamine buffer (pH 10.5). Pili were sheared from the cells with a blender at low speed for 1 min. The cells were removed by centrifugation at $13,000 \times g$. The pili in the supernatant were precipitated with 10% ammonium sulfate overnight and the precipitation was collected with centrifugation at $13,000 \times g$ (Brinton et al., 1978). In order to further clean the pili, the precipitation was re-suspended in ethanolamine buffer and then additional debris were removed by centrifugation at $23,000 \times g$. The pili were again precipitated with 10% ammonium sulfate and the precipitation was again collected with centrifugation at $13,000 \times g$ (Brinton et al., 1978). The final pili preparation was re-suspended in the ethanolamine buffer and stored at 4°C .

Transmission Electron Microscopy and Confocal Scanning Laser Microscopy

For the confocal laser scanning microscopy, the anode biofilms were imaged with LIVE/DEAD BacLight viability stain kit from Molecular Probes (Eugene, OR, USA) as previously described (Franks et al., 2010; Nevin et al., 2011). Images were processed and analyzed using the Leica LAS software (Leica). For transmission electron microscopy cells from the anode biofilms were directly placed on copper grids coated with carbon and absorbed for 4 min. The cells were negatively stained with 0.2% uranyl acetate and examined with a JEOL 2000fxTEM at a 200 kV accelerating voltage.

Pili Dissociation

Pili were suspended in water and dried in a SpeedVac at room temperature. The dried preparations of pili were resuspended in the 20 μL 1% SDS (pH 1.5) and boiled for 5–10 min. The samples were neutralized with 1 N NaOH and 9 μg of protein for each sample was used for the SDS-PAGE analysis. SDS-PAGE analyses were performed using 12.5% (wt/vol) polyacrylamide gels. Proteins were stained with Coomassie brilliant blue R-250.

Pili Conductivity Measurements

The electrodes were fabricated using nano-imprint lithography (NIL) method on silicon substrate with 1000 nm thick thermally grown oxide. The substrate was cleaned with a Piranha solution ($\text{H}_2\text{SO}_4:\text{H}_2\text{O}_2 = 3:1$) and a diluted HF solution before patterning. Then 50-nm-thick poly(methyl methacrylate) (PMMA) was spin coated on the substrate followed by a 60 nm thick UV-curable resist. Circuit patterns including 50 nm electrodes separated by 50 nm spacing, microscale fanouts, and contact pads were transferred from a quartz mold to the UV resist using NIL in a homemade imprint chamber. The residual UV-resist layer and the PMMA underlayer were removed in fluorine based reactive ion etching (RIE; CHF_3/O_2) followed by oxygen-based RIE. Thin

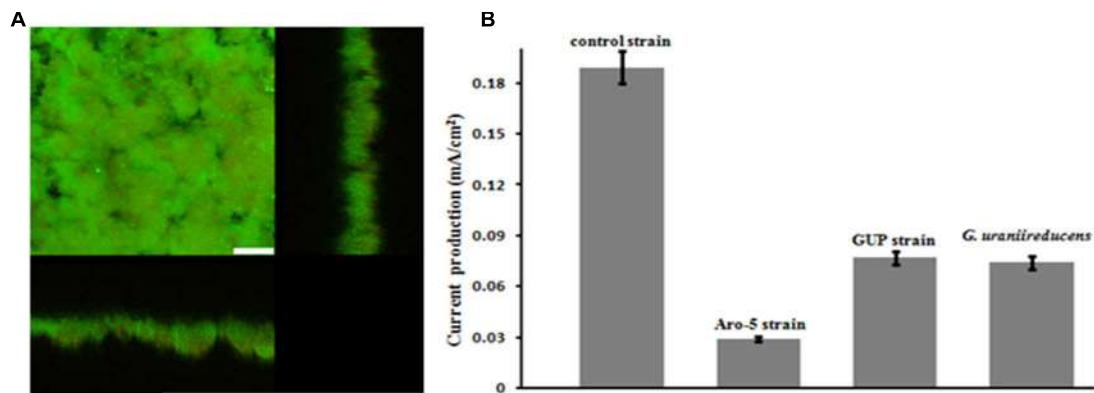


FIGURE 5 | *Geobacter sulfurreducens* strain GUP anode growth and current production. **(A)** Confocal scanning laser micrographs of graphite anode biofilms of GUP strain producing 0.077 mA/cm^2 current. Top-down three-dimensional, lateral side views (right image), and horizontal side views (bottom image) of cells stained with LIVE/DEAD BacLight viability stain. The size bar is 25 microns. **(B)** Current production of *G. sulfurreducens* strain GUP compared with previously reported current production levels for the control strain (Vargas et al., 2013), strain Aro-5 (Vargas et al., 2013), and *G. uraniireducens* (Rotaru et al., 2015).

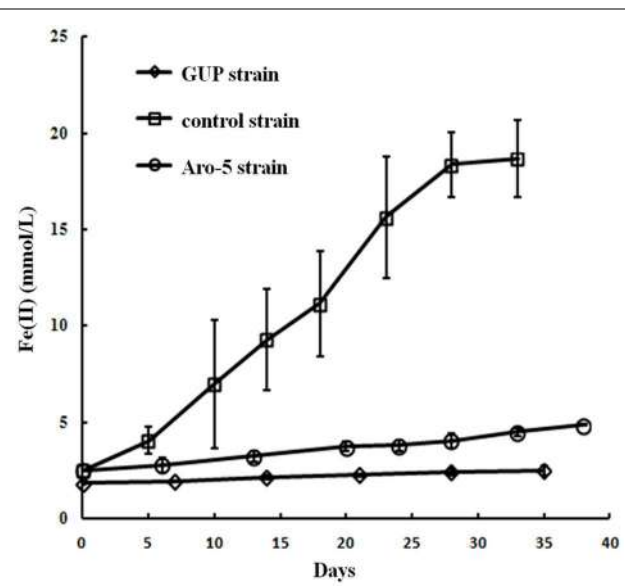


FIGURE 6 | Fe(III) oxide reduction by the GUP, and previously reported rates of Fe(III) oxide reduction (Vargas et al., 2013) for Aro-5, and control strains of *G. sulfurreducens* strain. Results are the mean and standard deviation of triplicate determinations.

films of 5-nm-thick Titanium (Ti) and 15-nm-thick gold (Au) were then deposited in an electron beam evaporator, followed by a liftoff process in acetone with ultrasonication.

As previously described (Adhikari et al., 2016), a solution (2 μl) of pili in ethanolamine buffer was dropcast on the substrate with electrodes. After letting the pili settle down for about 5 min, the sample was washed for three times with deionized water, which removed salts and left monolayer of pili on the substrate. Pili were localized with atomic force microscopy (AFM) imaging. The pili were then exposed to buffer adjusted to pH 7 with HCl and air dried.

Conductivity measurements were performed as previously described (Adhikari et al., 2016). A Keithley 4200 semiconductor characterization system (SCS) was used for the electrical measurements. The source meter for the two probe measurements was equipped with preamplifiers 4100-PA enabling the system with capacity to measure current signal of up to 100 aA. These SMUs were connected to two terminals of the double-shielded box for low noise measurement. The outer metallic box of the double shielded box acted as Faraday's cage to protect the signal from electrostatic interference while the inner box acted as guard to prevent leakage current through the circuit during the measurement. A constant potential was applied across the sample, and current response over the time was recorded. The current value for each applied potential was generated by averaging the measured steady state current over time.

Conductivity of a single pilus was calculated as

$$\sigma = \frac{G \cdot l}{A} \quad (1)$$

where, G is the conductance value of a single pili extracted from the linear fit of the current–voltage response of the sample, and l is the length of the pili between the electrodes. A ($=\pi \cdot d^2/4$) is the cross-sectional area of the pili calculated from the diameter of the pili measured from AFM images.

In order to account for the multiple pili bridging across the electrodes, we treated them to be equivalent to the multiple resistors in parallel. Assuming that all the pili have same resistance, the equivalent resistance of n number of pili across electrodes is $R_{eq} = R/n$, where R is individual resistance of the wire. This implies that the equivalent conductance would be $G_{eq} = n \cdot G$, where G is conductance of an individual pili (Supplementary Equation S1). Therefore, conductance of an individual pili can be derived from the equivalent conductance extracted from the linear fit of the CV graph and dividing the value by number of pili bridging the electrodes as observed in the AFM images.

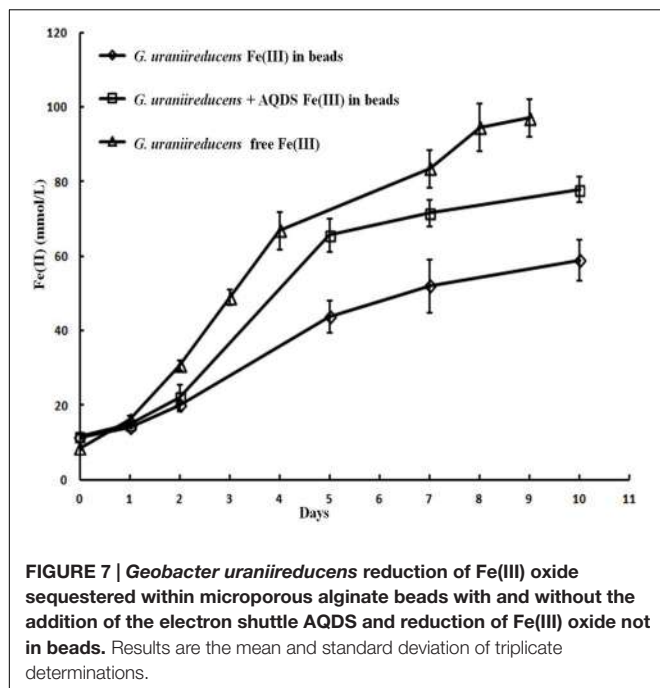


FIGURE 7 | *Geobacter uraniireducens* reduction of Fe(III) oxide sequestered within microporous alginate beads with and without the addition of the electron shuttle AQDS and reduction of Fe(III) oxide not in beads. Results are the mean and standard deviation of triplicate determinations.

RESULTS AND DISCUSSION

Geobacter uraniireducens Anode Biofilms

As previously reported (Rotaru et al., 2015), *G. uraniireducens* produces low current densities and this was associated with sparse, thin biofilms (Figure 2). Most of the cells were in close contact with the anode surface, suggesting a lack of the electron transport over multiple cell lengths that is associated with the long range electron transfer mediated by e-pili that yields high current densities in *G. sulfurreducens* biofilms.

Geobacter uraniireducens's Pili Expressed in *G. sulfurreducens*

The low biomass obtained on anodes was not sufficient to yield the dense preparations of pili required for conductivity measurements. In an attempt to develop a strain that would produce more *G. uraniireducens* pili, the gene for PilA in *G. sulfurreducens* was replaced with the *pilA* of *G. uraniireducens* with the same gene replacement method previously employed to successfully express other heterologous pili in *G. sulfurreducens* (Vargas et al., 2013; Liu et al., 2014). In medium with acetate as the electron donor and fumarate as the electron acceptor this strain, designated *G. sulfurreducens* strain GUP (*G. uraniireducens* pili), grew as well as the control strain (Supplementary Figure S1), which was constructed in the same manner but expressing the *G. sulfurreducens* *pilA* (Vargas et al., 2013). Strain GUP expressed pili at densities comparable to those previously reported (Vargas et al., 2013) for the control strain (Figure 3).

When the pili from the GUP strain were harvested and denatured they yielded a band with a molecular weight consistent with the expected molecular weight (20 kDa)

of the *G. uraniireducens* PilA, as well as a band for the Omcs c-type cytochrome (Figure 4). Omcs has previously been shown to be associated not only with wild-type *G. sulfurreducens* pili (Leang et al., 2010), but also with heterologously expressed pili (Vargas et al., 2013; Liu et al., 2014). As expected based on previous studies (Vargas et al., 2013), pili preparations from the control strain constructed in the same manner but expressing the *G. sulfurreducens* PilA gene sequence, also contained Omcs and the PilA monomer with the molecular weight (6.6 kDa) expected for the *G. sulfurreducens* PilA (Figure 4).

Impact of Heterologously Expressed *G. uraniireducens* Pili on Extracellular Electron Transfer by *G. sulfurreducens*

The GUP strain of *G. sulfurreducens* produced substantially thicker biofilms (Figure 5A) than *G. uraniireducens* (Figure 2). However, current production of the GUP strain was much lower than the *G. sulfurreducens* control strain (Figure 5B) with a maximum current density more comparable to that previously reported for *G. uraniireducens* (Rotaru et al., 2015) and strain Aro-5 (Vargas et al., 2013). The formation of thick biofilm with low current densities of the GUP strain is similar to results previously reported for the Aro-5 strain (Vargas et al., 2013).

Like the Aro-5 strain, the GUP strain poorly reduced Fe(III) oxide (Figure 6). This contrasts with the control strain expressing the *G. sulfurreducens* *pilA* which readily reduces Fe(III) oxide (Vargas et al., 2013). Although *G. sulfurreducens* GUP strain was not effective in Fe(III) oxide reduction, *G. uraniireducens* is an effective Fe(III) oxide reducer (Shelobolina et al., 2008; Rotaru et al., 2015). Intensively studied Fe(III) oxide-reducing microbes, which based on PilA sequence analysis apparently lack conductive pili, such as *S. oneidensis* and *Geothrix fermentans*, release of compounds that can serve as an electron shuttle between the outer surface of the cell and electron acceptors (Nevin and Lovley, 2002a,b; Bond and Lovley, 2005; Lanthier et al., 2008; Marsili et al., 2008; Von Canstein et al., 2008; Mehta-Kolte and Bond, 2012). Like these organisms, *G. uraniireducens* readily reduced Fe(III) oxide occluded within beads that prevented direct access to the Fe(III) oxide (Figure 7), consistent with the release of an electron shuttle that could alleviate the need for conductive pili. In contrast, *G. sulfurreducens* (Smith et al., 2014) and *G. metallireducens* (Nevin and Lovley, 2000) do not reduce Fe(III) oxide within the beads in the absence of an exogenously added shuttle, which is consistent with the proposed reliance on e-pili for long-range electron transport.

Conductivities of Heterologously Expressed *G. uraniireducens* Pili

The low current densities and poor Fe(III) oxide reduction by the GUP strain suggested that the *G. uraniireducens* pili expressed in the GUP strain were poorly conductive. In order to directly evaluate the conductivity of the *G. uraniireducens* pili, preparations of pili sheared from the GUP strain were placed on a nanoelectrode array. AFM revealed pili bridging

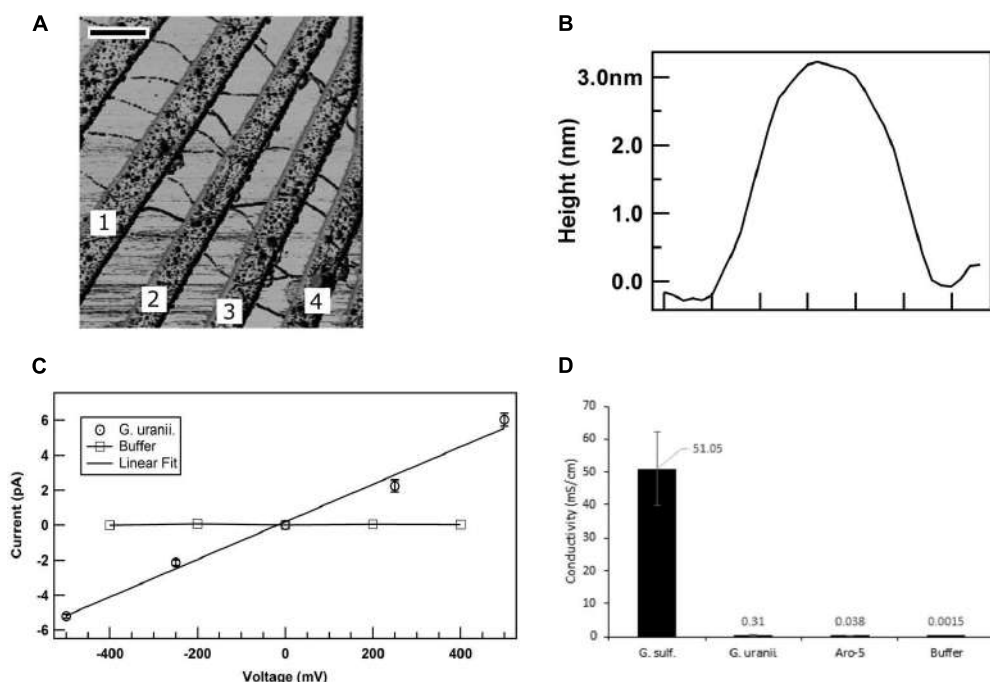


FIGURE 8 | Conductivity of *G. uraniireducens* pili. **(A)** Atomic force microscopy image of the *G. uraniireducens* pili bridging electrodes. Electrode pairs 1–2, 2–3, and 3–4 were used for the conductivity measurements. The scale bar represents 500 nm. **(B)** Diameter (height) of the *G. uraniireducens* pili. **(C)** Current–voltage response of the pili. The average value of the current from three measurements are represented as data points while the standard error is represented as the error bar. **(D)** Comparison of the conductivity of pili for *G. uraniireducens* pili and previously reported (Adhikari et al., 2016) conductivities of wild-type *G. sulfurreducens* and Aro-5 pili.

several of the electrodes (Figure 8A). The diameter of the pili was 3 nm (Figure 8B), comparable to that of the *G. sulfurreducens*. The current–voltage response of pili bridging two electrodes was linear, implying an ohmic effect (Figure 8C). The conductivity of the pili at pH 7 was 0.3 ± 0.09 mS/cm (mean \pm standard deviation; $n = 3$), which is more than two orders of magnitude lower than the previously reported (Adhikari et al., 2016) conductivity of *G. sulfurreducens* pili at pH 7 (Figure 8D).

The electron transfer rate (Γ) along the pili can be calculated as

$$\Gamma = \frac{I}{e} = \frac{\sigma \cdot A \cdot V}{e \cdot l} \quad (2)$$

where I is the current through the pili at the redox potential difference (V) over the pili length (l); σ is conductivity; A is the cross sectional area of the pili; and e is the fundamental electronic charge (1.6×10^{-19} coulombs). Thus, a 100-fold decrease in conductivity results in a 100-fold lower rate of electron transfer along the pili under comparable conditions.

Electrical potentials extending within anode biofilms are poorly defined, making it difficult to make an informed estimate of V . More information is available for Fe(III) oxide reduction. Although the electron carrier that donates electrons to the *G. sulfurreducens* pili is as yet unknown, a likely candidate is the periplasmic, multi-heme c-type cytochrome PpcA. It is one of the most abundant proteins in *G. sulfurreducens* and is considered to be an important intermediary in electron

transport from the inner membrane to outer surface electron transport components (Lloyd et al., 2003). PpcA is a conservative choice for electron transport rate estimates because its midpoint potential of -170 mV is more positive than the midpoint potentials of other potential electron carriers (Lovley et al., 2011).

The midpoint potential of poorly crystalline Fe(III) oxide, the only form of insoluble Fe(III) oxide that *G. sulfurreducens* readily reduces, is 0 mV (Thamdrup, 2000). Therefore, with PpcA as the electron donor and Fe(III) oxide as the electron acceptor V is -170 mV. The distance (l) between the cells and Fe(III) oxide associated with pili is typically less than $5\text{ }\mu\text{m}$ (Reguera et al., 2005). For wild-type cells, the conductivity of the pili is 5.1×10^{-2} S/cm (Adhikari et al., 2016) and the cross-sectional area for a 3 nm diameter pilus is ($A = \pi r^2 = \pi \times (1.5 \times 10^{-9}\text{ m})^2 = 7.07 \times 10^{-18}\text{ m}^2$). Therefore, the rate of electron flux through an individual e-pilus over $5\text{ }\mu\text{m}$ at a potential difference of -170 mV is estimated (equation 1) to be 7.6×10^6 electrons/s. The maximum potential electron transport for *G. sulfurreducens* has been estimated to be ca. 8 mA/mg protein, or ca. 1.5×10^7 electrons/s per cell (Marsili et al., 2010). Thus, a single conductive pilus could accommodate nearly half the long-range electron transport requirements of *G. sulfurreducens* for Fe(III) oxide reduction at maximum respiration rates. When it is considered that cells typically express more than twenty pili (Reguera et al., 2005; Summers et al., 2010), a single cell's full complement of pili should be more than sufficient to support electron transport

to Fe(III) oxide. However, with the 100-fold lower conductivity of the *G. uraniireducens* pili, rates of electron transport per pili under the same conditions would only be 4.5×10^4 electrons/s, requiring more than 300 pili to support maximum rates of electron transport.

Implications

The results demonstrate that the pili of *G. uraniireducens* are much less conductive than the pili of *G. sulfurreducens*, reflecting different strategies for long-range electron transport in these species. The lack of a strategy to genetically manipulate *G. uraniireducens* makes it impossible to further examine the function of the *G. uraniireducens* pili with gene deletion studies, but the poor conductivity of the pili and the finding that *G. uraniireducens* reduces Fe(III) oxide with an electron shuttle suggest that long-range electron transport along pili is not an important mechanism for Fe(III) oxide reduction in this organism. *G. uraniireducens* was unable to participate in DIET and produces low current densities (Rotaru et al., 2015), consistent with previous findings that conductive pili are required for DIET and the production of high current densities (Tremblay et al., 2012; Shrestha et al., 2013; Vargas et al., 2013; Rotaru et al., 2014a). The finding that the conductive pili model for long-range electron transport developed from studies with *G. sulfurreducens* does not apply to all *Geobacter* species is an important consideration when interpreting molecular studies of microbial communities involved in extracellular electron transfer. A phylogenetic affiliation with the genus *Geobacter* is not sufficient evidence to assume pili-based long-range electron transfer.

The unique method by which *G. uraniireducens* was isolated was probably an important factor in recovering a *Geobacter* species that does not use conductive pili for long-range electron transport. *G. uraniireducens* was recovered from subsurface sediments directly on solidified medium in which the Fe(III) in the sediment clay fraction served as the electron acceptor. It is unlikely that enough mineral Fe(III) could be incorporated into solidified medium to yield a visible colony if the cells had to be in direct contact with the Fe(III) mineral. However, producing an electron shuttle would permit cells to access Fe(III) minerals they could not directly contact. *G. uraniireducens* possess three sets of genes for cytochrome–porin outer membrane complexes that could facilitate extracellular electron transfer to an electron shuttle, or potentially directly to the surface of electrodes or Fe(III) oxides (Aklujkar et al., 2013; Shi et al., 2014). Other cytochromes that are more highly expressed during the reduction of Fe(III) oxides may also have important roles (Holmes et al., 2008; Aklujkar et al., 2013).

The results also suggest that although an electrical conductivity can be measured in pili or other filaments it is important

to determine whether the conductivity is sufficient to support physiologically relevant rates of electron transfer. For example, the 300 $\mu\text{S}/\text{cm}$ conductivity of the *G. uraniireducens* pili is probably too low to support extracellular respiration. Yet *Rhodopseudomonas palustris* filaments of unknown composition implicated in Fe(III) oxide reduction had electrical resistances that correspond to conductivities of only 35–72 $\mu\text{S}/\text{cm}$ (Supplementary Equation S2; Venkidusamy et al., 2015). However, the *R. palustris* filaments were chemically fixed and critical point dried prior to the conductivity measurements, which may have altered the filament structure and conductivity. These considerations demonstrate the need for more measurements on the conductivity of microbial filaments to assess the potential for long-range electron transport via filaments in the microbial world.

AUTHOR CONTRIBUTIONS

DL, NM, and YT designed the experiments. YT constructed the mutant and performed the experiments for the pili dissociation and Fe(III) oxidizes reduction. RA measured the conductivity of pili. JW prepared for the pili and performed the TEM. KN, OLS, and AF performed the confocal scanning laser microscopy. KN and TW measured the current production. JS conducted the alginate bead assays. YT and DL wrote the initial manuscript draft with revisions contributed from all authors.

FUNDING

This research was supported by the Office of Naval Research (grant nos. N00014-12-1-0229 and N00014-13-1-0550) and National Science Foundation (NSF) Nanoscale Science and Engineering Center (NSEC) Center for Hierarchical Manufacturing (CHM; grant no. CMMI-1025020). NM holds a Career Award at the Scientific Interface from the Burroughs Wellcome Fund.

ACKNOWLEDGMENT

The authors thank Z. Zhao for technical assistance.

SUPPLEMENTARY MATERIAL

The Supplementary Material for this article can be found online at: <http://journal.frontiersin.org/article/10.3389/fmicb.2016.00980>

REFERENCES

- Adhikari, R. Y., Malvankar, N. S., Tuominen, M. T., and Lovley, D. R. (2016). Conductivity of individual *Geobacter* pili. *RSC Adv.* 6, 8354–8357. doi: 10.1039/C5RA28092C

- Aklujkar, M., Coppi, M. V., Leang, C., Kim, B. C., Chavan, M. A., Perpetua, L. A., et al. (2013). Proteins involved in electron transfer to Fe(III) and Mn(IV) oxides by *Geobacter sulfurreducens* and *Geobacter uraniireducens*. *Microbiology* 159, 515–535. doi: 10.1099/mic.0.064089-0

- Bertani, G. (1951). Studies on lysogenesis. I. The mode of phage liberation by lysogenic *Escherichia coli*. *J. Bacteriol.* 62, 293–300.
- Bond, D. R., and Lovley, D. R. (2005). Evidence for involvement of an electron shuttle in electricity generation by *Geothrix fermentans*. *Appl. Environ. Microbiol.* 71, 2186–2189. doi: 10.1128/AEM.71.4.2186-2189.2005
- Brinton, C., Bryan, J., Dillon, J., Guerina, N., Jacobson, L., Labik, A., et al. (1978). “Uses of pili in gonorrhea control: Role of bacterial pili in disease, purification and properties of gonococcal pili, and progress in the development of a gonococcal pilus vaccine for gonorrhea,” in *Immunobiology of Neisseria gonorrhoeae*, eds G. Brooks, E. Gotschlich, K. Homes, W. Sawyer and F. Young (Washington, DC; American Society for Microbiology Press), 155–179.
- Childers, S. E., Ciufo, S., and Lovley, D. R. (2002). *Geobacter metallireducens* accesses insoluble Fe(III) oxide by chemotaxis. *Nature* 416, 767–769. doi: 10.1038/416767a
- Coppi, M. V., Leang, C., Sandler, S. J., and Lovley, D. R. (2001). Development of a genetic system for *Geobacter sulfurreducens*. *Appl. Environ. Microbiol.* 67, 3180–3187. doi: 10.1128/AEM.67.7.3180-3187.2001
- Franks, A. E., Nevin, K. P., Glaven, R. H., and Lovley, D. R. (2010). Micromining coupled to microarray analysis to evaluate the spatial metabolic status of *Geobacter sulfurreducens* biofilms. *ISME J.* 4, 509–519. doi: 10.1038/ismej.2009.137
- Holmes, D. E., O’Neil, R. A., Chavan, M. A., N’Guessan, L. A., Vrionis, H. A., Perpetua, L. A., et al. (2008). Transcriptome of *Geobacter uraniireducens* growing in uranium-contaminated subsurface sediments. *ISME J.* 3, 216–230. doi: 10.1038/ismej.2008.89
- Inoue, K., Leang, C., Franks, A. E., Woodard, T. L., Nevin, K. P., and Lovley, D. R. (2011). Specific localization of the c-type cytochrome OmcZ at the anode surface in current-producing biofilms of *Geobacter sulfurreducens*. *Environ. Microbiol. Rep.* 3, 211–217. doi: 10.1111/j.1758-2229.2010.00210.x
- Inoue, K., Qian, X., Morgado, L., Kim, B.-C., Mester, T., Izallalen, M., et al. (2010). Purification and characterization of OmcZ, an outer-surface, octaheme c-type cytochrome essential for optimal current production by *Geobacter sulfurreducens*. *Appl. Environ. Microbiol.* 76, 3999–4007. doi: 10.1128/AEM.00027-10
- Kiely, P. D., Regan, J. M., and Logan, B. E. (2011). The electric picnic: synergistic requirements for exoelectrogenic microbial communities. *Curr. Opin. Biotechnol.* 22, 378–385. doi: 10.1016/j.copbio.2011.03.003
- Lanthier, M., Gregory, K. B., and Lovley, D. R. (2008). Growth with high planktonic biomass in *Shewanella oneidensis* fuel cells. *FEMS Microbiol. Lett.* 278, 29–35. doi: 10.1111/j.1574-6968.2007.00964.x
- Leang, C., Qian, X., Mester, T., and Lovley, D. R. (2010). Alignment of the c-Type Cytochrome OmcS along pili of *Geobacter sulfurreducens*. *Appl. Environ. Microbiol.* 76, 4080–4084. doi: 10.1128/AEM.00023-10
- Liu, X., Tremblay, P. L., Malvankar, N. S., Nevin, K. P., Lovley, D. R., and Vargas, M. (2014). A *Geobacter sulfurreducens* strain expressing *Pseudomonas aeruginosa* type IV pili localizes OmcS on pili but is deficient in Fe(III) oxide reduction and current production. *Appl. Environ. Microbiol.* 80, 1219–1224. doi: 10.1128/AEM.02938-13
- Lloyd, J. R., Leang, C., Hodges-Myerson, A. L., Coppi, M. V., Ciufo, S., Methé, B., et al. (2003). Biochemical and genetic characterization of PpcA, a periplasmic c-type cytochrome in *Geobacter sulfurreducens*. *Biochem. J.* 369, 153–161. doi: 10.1042/bj20020597
- Lovley, D. R. (2011). Live wires: direct extracellular electron exchange for bioenergy and the bioremediation of energy-related contamination. *Energy Environ. Sci.* 4, 4896–4906. doi: 10.1039/C1EE02229F
- Lovley, D. R. (2012). Electromicrobiology. *Annu. Rev. Microbiol.* 66, 391–409. doi: 10.1146/annurev-micro-092611-150104
- Lovley, D. R., and Phillips, E. J. P. (1988). Novel mode of microbial energy metabolism: organic carbon oxidation coupled to dissimilatory reduction of iron or manganese. *Appl. Environ. Microbiol.* 54, 1472–1480.
- Lovley, D. R., Ueki, T., Zhang, T., Malvankar, N. S., Shrestha, P. M., Flanagan, K. A., et al. (2011) *Geobacter*: the microbe electric’s physiology, ecology, and practical applications. *Adv. Microb. Physiol.* 59, 1–100 doi: 10.1016/B978-0-12-387661-4.00004-5
- Malvankar, N. S., and Lovley, D. R. (2014). Microbial nanowires for bioenergy applications. *Curr. Opin. Biotechnol.* 27, 88–95. doi: 10.1016/j.copbio.2013.12.003
- Malvankar, N. S., Tuominen, M. T., and Lovley, D. R. (2012). Lack of cytochrome involvement in long-range electron transport through conductive biofilms and nanowires of *Geobacter sulfurreducens*. *Energy Environ. Sci.* 5, 8651–8659. doi: 10.1039/C2EE22330A
- Malvankar, N. S., Vargas, M., Nevin, K., Tremblay, P. L., Evans-Lutterodt, K., Nykypachuk, D., et al. (2015) Structural basis for metallic-like conductivity in microbial nanowires. *MBio* 6:e00084-15. doi: 10.1128/mbio.00084-15
- Malvankar, N. S., Vargas, M., Nevin, K. P., Franks, A. E., Leang, C., Kim, B. C., et al. (2011). Tunable metallic-like conductivity in microbial nanowire networks. *Nat. Nanotechnol.* 6, 573–579. doi: 10.1038/nnano.2011.119
- Malvankar, N. S., Yalcin, S. E., Tuominen, M. T., and Lovley, D. R. (2014). Visualization of charge propagation along individual pili proteins using ambient electrostatic force microscopy. *Nat. Nanotechnol.* 9, 1012–1017. doi: 10.1038/nnano.2014.236
- Marsili, E., Baron, D. B., Shikhare, I. D., Coursolle, D., Gralnick, J. A., and Bond, D. R. (2008). *Shewanella* secretes flavins that mediate extracellular electron transfer. *Proc. Natl. Acad. Sci. U.S.A.* 105, 3968–3973. doi: 10.1073/pnas.0710525105
- Marsili, E., Sun, J., and Bond, D. R. (2010). Voltammetry and growth physiology of *Geobacter sulfurreducens* biofilms as a function of growth stage and imposed electrode potential. *Electroanalysis* 22, 865–874. doi: 10.1002/elan.20080007
- Mehta-Kolte, M. G., and Bond, D. R. (2012). *Geothrix fermentans* secretes two different redox-active compounds to utilize electron acceptors across a wide range of redox potentials. *Appl. Environ. Microbiol.* 78, 6987–6995. doi: 10.1128/AEM.01460-12
- Methé, B. A., Nelson, K. E., Eisen, J. A., Paulsen, I. T., Nelson, W., Heidelberg, J. F., et al. (2003). Genome of *Geobacter sulfurreducens*: metal reduction in subsurface environments. *Science* 302, 1967–1969. doi: 10.1126/science.1088727
- Morita, M., Malvankar, N. S., Franks, A. E., Summers, Z. M., Giloteaux, L., Rotaru, A. E., et al. (2011). Potential for direct interspecies electron transfer in methanogenic wastewater digester aggregates. *MBio* 2, e00159–e00111. doi: 10.1128/mbio.00159-11
- Nevin, K. P., Hensley, S. A., Franks, A. E., Summers, Z. M., Ou, J., Woodard, T. L., et al. (2011). Electrosynthesis of organic compounds from carbon dioxide is catalyzed by a diversity of acetogenic microorganisms. *Appl. Environ. Microbiol.* 77, 2882–2886. doi: 10.1128/AEM.02642-10
- Nevin, K. P., Kim, B.-C., Glaven, R. H., Johnson, J. P., Woodard, T. L., Methé, B. A., et al. (2009). Anode biofilm transcriptomics reveals outer surface components essential for high density current production in *Geobacter sulfurreducens* fuel cells. *PLoS ONE* 4: e5628. doi: 10.1371/journal.pone.0005628
- Nevin, K. P., and Lovley, D. R. (2000). Lack of production of electron-shuttling compounds or solubilization of Fe(III) during reduction of insoluble Fe(III) oxide by *Geobacter metallireducens*. *Appl. Environ. Microbiol.* 66, 2248–2251. doi: 10.1128/AEM.66.5.2248-2251.2000
- Nevin, K. P., and Lovley, D. R. (2002a). Mechanisms for accessing insoluble Fe(III) oxide during dissimilatory Fe(III) reduction by *Geothrix fermentans*. *Appl. Environ. Microbiol.* 68, 2294–2299. doi: 10.1128/AEM.68.5.2294-2299.2002
- Nevin, K. P., and Lovley, D. R. (2002b). Mechanisms for Fe(III) oxide reduction in sedimentary environments. *Geomicrobiol. J.* 19, 141–159. doi: 10.1080/01490450252864253
- Nevin, K. P., Richter, H., Covalla, S. F., Johnson, J. P., Woodard, T. L., Orloff, A. L., et al. (2008). Power output and columbic efficiencies from biofilms of *Geobacter sulfurreducens* comparable to mixed community microbial fuel cells. *Environ. Microbiol.* 10, 2505–2514. doi: 10.1111/j.1462-2920.2008.01675.x
- Reguera, G., McCarthy, K. D., Mehta, T., Nicoll, J. S., Tuominen, M. T., and Lovley, D. R. (2005). Extracellular electron transfer via microbial nanowires. *Nature* 435, 1098–1101. doi: 10.1038/nature03661
- Reguera, G., Nevin, K. P., Nicoll, J. S., Covalla, S. F., Woodard, T. L., and Lovley, D. R. (2006). Biofilm and nanowire production leads to increased current in

- Geobacter sulfurreducens fuel cells. *Appl. Environ. Microbiol.* 72, 7345–7348. doi: 10.1128/AEM.01444–06
- Richter, H., Nevin, K. P., Jia, H., Lowy, D. A., Lovley, D. R., and Tender, L. M. (2009). Cyclic voltammetry of biofilms of wild type and mutant *Geobacter sulfurreducens* on fuel cell anodes indicates possible roles of OmcB, OmcZ, type IV pili, and protons in extracellular electron transfer. *Energy Environ. Sci.* 2, 506–516. doi: 10.1039/B816647A
- Rotaru, A. E., Shrestha, P. M., Liu, F., Markovaitė, B., Chen, S., Nevin, K. P., et al. (2014a). Direct interspecies electron transfer between Geobacter metallireducens and Methanosaeta barkeri. *Appl. Environ. Microbiol.* 80, 4599–4605. doi: 10.1128/aem.00895–14
- Rotaru, A. E., Shrestha, P. M., Liu, F., Shrestha, M., Shrestha, D., Embree, M., et al. (2014b). A new model for electron flow during anaerobic digestion: direct interspecies electron transfer to Methanosaeta for the reduction of carbon dioxide to methane. *Energy Environ. Sci.* 7, 408–415. doi: 10.1039/C3EE 42189A
- Rotaru, A.-E., Woodard, T. L., Nevin, K. P., and Lovley, D. R. (2015). Link between capacity for current production and syntrophic growth in Geobacter species. *Front. Microbiol.* 6:744. doi: 10.3389/fmicb.2015. 00744
- Shelobolina, E. S., Vrionis, H. A., Findlay, R. H., and Lovley, D. R. (2008). *Geobacter uraniireducens* sp. nov., isolated from subsurface sediment undergoing uranium bioremediation. *Int. J. Syst. Evol. Microbiol.* 58, 1075–1078. doi: 10.1099/ijss.0.65377–0
- Shi, L., Fredrickson, J. K., and Zachara, J. M. (2014). Genomic analyses of bacterial porin-cytochrome gene clusters. *Front. Microbiol.* 5:657. doi: 10.3389/fmicb.2014.00657
- Shrestha, P. M., Malvankar, N. S., Werner, J. J., Franks, A. E., Elena-Rotaru, A., Shrestha, M., et al. (2014). Correlation between microbial community and granule conductivity in anaerobic bioreactors for brewery wastewater treatment. *Bioresour. Technol.* 174, 306–310. doi: 10.1016/j.biortech.2014. 10.004
- Shrestha, P. M., Rotaru, A. E., Summers, Z. M., Shrestha, M., Liu, F., and Lovley, D. R. (2013). Transcriptomic and genetic analysis of direct interspecies electron transfer. *Appl. Environ. Microbiol.* 79, 2397–2404. doi: 10.1128/aem.03837–12
- Smith, J. A., Lovley, D. R., and Tremblay, P. L. (2013). Outer cell surface components essential for Fe(III) oxide reduction by Geobacter metallireducens. *Appl. Environ. Microbiol.* 79, 901–907. doi: 10.1128/AEM.02954–12
- Smith, J. A., Tremblay, P. L., Shrestha, P. M., Snoeyenbos-West, O. L., Franks, A. E., Nevin, K. P., et al. (2014). Going wireless: Fe(III) oxide reduction without pili by *Geobacter sulfurreducens* strain JS-1. *Appl. Environ. Microbiol.* 80, 4331–4340. doi: 10.1128/AEM.01122–14
- Summers, Z. M., Fogarty, H. E., Leang, C., Franks, A. E., Malvankar, N. S., and Lovley, D. R. (2010). Direct exchange of electrons within aggregates of an evolved syntrophic coculture of anaerobic bacteria. *Science* 330, 1413–1415. doi: 10.1126/science.1196526
- Thamdrup, B. (2000). Bacterial manganese and iron reduction in aquatic sediments. *Adv. Microb. Ecol.* 16, 41–84 doi: 10.1007/978-1-4615-4187-5_2
- Tremblay, P. L., Aklujkar, M., Leang, C., Nevin, K. P., and Lovley, D. (2012). A genetic system for *Geobacter metallireducens*: role of the flagellin and pilin in the reduction of Fe(III) oxide. *Environ. Microbiol. Rep.* 4, 82–88. doi: 10.1111/j.1758-2229.2011.00305.x
- Vargas, M., Malvankar, N. S., Tremblay, P. L., Leang, C., Smith, J. A., Patel, P., et al. (2013). Aromatic amino acids required for pili conductivity and long-range extracellular electron transport in *Geobacter sulfurreducens*. *mBio* 4, e00105–13. doi: 10.1128/mBio.00105–13
- Venkitusamy, K., Megharaj, M., Schroder, U., Karouta, F., Mohan, S. V., and Naidu, R. (2015). Electron transport through electrically conductive nanofilaments in *Rhodopseudomonas palustris* strain RP2. *RSC Adv.* 5, 100790–100798. doi: 10.1039/C5RA08742B
- Von Canstein, H., Ogawa, J., Shimizu, S., and Lloyd, J. R. (2008). Secretion of flavins by *Shewanella* species and their role in extracellular electron transfer. *Appl. Environ. Microbiol.* 74, 615–623. doi: 10.1128/aem.01387–07
- Voordekkers, J. W., Kim, B.-C., Izallalen, M., and Lovley, D. R. (2010). Role of *Geobacter sulfurreducens* outer surface c-type cytochromes in reduction of soil humic acid and anthraquinone-2, 6-disulfonate. *Appl. Environ. Microbiol.* 76, 2371–2375. doi: 10.1128/AEM.02250–09
- Yi, H., Nevin, K. P., Kim, B. -C., Franks, A. E., Klimes, A., Tender, L. M., et al. (2009). Selection of a variant of *Geobacter sulfurreducens* with enhanced capacity for current production in microbial fuel cells. *Biosens. Bioelectron.* 24, 3498–3503. doi: 10.1016/j.bios.2009.05.004.

Conflict of Interest Statement: The authors declare that the research was conducted in the absence of any commercial or financial relationships that could be construed as a potential conflict of interest.

Copyright © 2016 Tan, Adhikari, Malvankar, Ward, Nevin, Woodard, Smith, Snoeyenbos-West, Franks, Tuominen and Lovley. This is an open-access article distributed under the terms of the Creative Commons Attribution License (CC BY). The use, distribution or reproduction in other forums is permitted, provided the original author(s) or licensor are credited and that the original publication in this journal is cited, in accordance with accepted academic practice. No use, distribution or reproduction is permitted which does not comply with these terms.



Effects of Incubation Conditions on Cr(VI) Reduction by c-type Cytochromes in Intact *Shewanella oneidensis* MR-1 Cells

Rui Han^{1,2}, Fangbai Li², Tongxu Liu^{2*}, Xiaomin Li², Yundang Wu², Ying Wang² and Dandan Chen²

¹ School of Environment and Energy, South China University of Technology, Guangzhou, China, ² Guangdong Key Laboratory of Agricultural Environment Pollution Integrated Control, Guangdong Institute of Eco-Environmental and Soil Sciences, Guangzhou, China

OPEN ACCESS

Edited by:

Yong Xiao,

Institute of Urban Environment,
Chinese Academy of Sciences, China

Reviewed by:

Christiane Dahl,

Rheinische
Friedrich-Wilhelms-Universität Bonn,
Germany

Huan Deng,

Nanjing Normal University, China

*Correspondence:

Tongxu Liu

txliu@soil.gd.cn

Specialty section:

This article was submitted to
Microbiotechnology, Ecotoxicology
and Bioremediation,
a section of the journal
Frontiers in Microbiology

Received: 02 October 2015

Accepted: 03 May 2016

Published: 19 May 2016

Citation:

Han R, Li F, Liu T, Li X, Wu Y, Wang Y
and Chen D (2016) Effects
of Incubation Conditions on Cr(VI)
Reduction by c-type Cytochromes
in Intact *Shewanella oneidensis* MR-1
Cells. *Front. Microbiol.* 7:746.
doi: 10.3389/fmicb.2016.00746

It is widely recognized that the outer membrane c-type cytochromes (OM c-Cyts) of metal-reducing bacteria play a key role in microbial metal reduction processes. However, the *in situ* redox status of OM c-Cyts during microbial metal reduction processes remain poorly understood. In this study, diffuse-transmission UV/Vis spectroscopy is used to investigate the *in situ* spectral reaction of Cr(VI) reduction by c-Cyts in intact *Shewanella oneidensis* MR-1 cells under different incubation conditions. The reduced c-Cyts decreased transiently at the beginning and then recovered gradually over time. The Cr(VI) reduction rates decreased with increasing initial Cr(VI) concentrations, and Cr(III) was identified as a reduced product. The presence of Cr(III) substantially inhibited Cr(VI) reduction and the recovery of reduced c-Cyts, indicating that Cr(III) might inhibit cell growth. Cr(VI) reduction rates increased with increasing cell density. The highest Cr(VI) reduction rate and fastest recovery of c-Cyts were obtained at pH 7.0 and 30°C, with sodium lactate serving as an electron donor. The presence of O₂ strongly inhibited Cr(VI) reduction, suggesting that O₂ might compete with Cr(VI) as an electron acceptor in cells. This study provides a case of directly examining *in vivo* reaction properties of an outer-membrane enzyme during microbial metal reduction processes under non-invasive physiological conditions.

Keywords: c-type cytochromes, *Shewanella oneidensis* MR-1, Cr(VI) reduction, intact cells, incubation conditions

INTRODUCTION

The biogeochemical cycles of many major and trace elements are driven by microbial redox processes. Dissimilatory metal-reducing bacteria (DMRB) are considered the most important microorganisms for controlling metal transformations under anoxic conditions. Typical strains of DMRB, such as the *Shewanella* and *Geobacter* species, have been widely investigated in terms of genetic diversity, structural and functional characterization of highly purified proteins, and traditional reductionist approaches (Beliaev et al., 2001, 2005; Kengo et al., 2010; Tremblay et al., 2012). *In vitro* reaction kinetics between metals and outer membrane c-type cytochromes (OM c-Cyts) of DMRB were studied using highly purified OM c-Cyts extracted from *Shewanella* species (Borloo et al., 2007; Ross et al., 2009; Belchik et al., 2011), and the roles of cytochromes

(e.g., MtrC and OmcA) were characterized by examining the effects of mutant deletion. However, the purified proteins may behave differently from the protein complexes in live cells because the highly reactive enzymes may be easily changed during the purification (Nakamura et al., 2009). Hence, an *in vivo* study of the reaction between metals and *c*-Cysts in the live cells will allow a more comprehensive understanding of microbial metal reduction processes.

The electron transfer center of OM *c*-Cysts is a heme group, which has a large molar absorption coefficient. Therefore, spectroscopic methods have been applied to OM *c*-Cysts in living cells under physiological conditions (Nakamura et al., 2009; Liu et al., 2011). However, accurate measurement of heme groups in living cells is difficult due to the strong spectral interference from light scattering of cell surface. Fortunately, using a diffuse-transmission (DT) mode, this spectral interference was not observed in the absorption spectra of the multi-heme *c*-Cysts in whole cells (Nakamura et al., 2009). A number of recent studies used DT-UV/Vis spectroscopy to monitor heme groups in iron-/humic-reducing bacteria such as *Klebsiella pneumonia* L17 (Liu et al., 2014), *Shewanella putrefaciens* 200 (Zhang et al., 2014), *S. decolorationis* S12, *Aeromonas hydrophila* HS01 (Li et al., 2014), and *Leptospirillum ferrooxidans* (Blake and Griff, 2012). Recently, Wu et al. (2014) also employed DT-UV/Vis spectroscopy to analyze *in situ* spectral kinetics of electron shuttling reduction by *c*-Cysts in a living *S. putrefaciens* 200 suspension. *In situ* spectroscopy was also used to study the reaction between Fe(III) and *c*-Cysts in intact *L. ferrooxidans* under oxic conditions (Liu et al., 2014). In addition, Busalmen et al. (2008) reported an application of infrared spectroscopy in a whole-cell system in which the electron transfer between *Geobacter* and a gold electrode was monitored. It is true that there are some limitations about examining *c*-Cysts in intact cells by DT-UV/Vis spectroscopy. Using DT-UV/Vis spectroscopy, only the *c*-Cysts located on the very surface of cell outer-membrane can be measured directly by using this spectral method (Nakamura et al., 2009), but the *c*-Cysts located in periplasm and the cytoplasmic membrane were unlikely to be measured as the light was not able to penetrate the membrane. Hence, the *c*-Cysts measured in the cell suspension can only represent the outer membrane (OM) *c*-Cysts but not the total *c*-Cysts. In addition, the OM *c*-Cysts include a series of different proteins, such as MtrC and OmcA in MR-1, but it is difficult to differentiate the roles of MtrC and OmcA from those of other *c*-Cysts by just using the DT UV-Vis spectral method. Despite the aforementioned limitations of DT-UV/Vis spectroscopy, this method is promising to study the *in situ* behavior of OM *c*-Cysts in intact DMRB cells.

Chromium is toxic and is designated a priority pollutant in many countries (Middleton et al., 2003). Microbial reduction of Cr(VI) to Cr(III) can be considered as a way to remediate Cr(VI) contaminations because Cr(III) is less water-soluble, less mobile, and much less toxic than Cr(VI) (James, 1996; Barnhart, 1997). A variety of DMRB have been reported to reduce Cr(VI) to Cr(III) (Puzon et al., 2005; Cheung and Gu, 2007; He et al., 2011). Cr(VI)-reducing bacteria use electron transport systems containing cytochromes in their OM to

reduce Cr(VI) derivatives during anaerobic respiration (Myers et al., 2000; Ahemad, 2014). *S. oneidensis* MR-1 is considered a model organism for metal reduction as it is able to reduce a variety of metals. Recent studies have shown that MR-1 can reduce Cr(VI) to Cr(III) as a terminal electron acceptor under anoxic conditions with OM *c*-Cysts (e.g., OmcA and MtrC) serving as terminal reductases of Cr(VI) (Myers and Myers, 2001; Belchik et al., 2011; Wang et al., 2013). However, the molecular scale reaction mechanism of the Cr(VI) and *c*-Cysts remains poorly characterized under non-invasive physiological conditions. Direct photometric studies of intact cells and Cr(VI) will allow elucidation of these *in vivo* reaction mechanisms.

The microbial Cr(VI) reduction can be influenced by different environmental factors, such as Cr(VI) concentration, temperature, bacterial cell density, electron donor, pH, oxygen, and the presence of other metal ions (Wang and Xiao, 1995; Dey et al., 2014). Past studies (Wang and Xiao, 1995; Zakaria et al., 2007; Dey et al., 2014) mainly focused on effects of incubation factors on the apparent Cr(VI) reduction and rarely investigated the effects of incubation factors on the redox status of *c*-Cysts in the OM of DMRB, which play a key role in microbial Cr(VI) reduction. *In situ* spectral kinetics of Cr(VI) reduction by *c*-Cysts in live cells under different environmental conditions should provide a more fundamental understanding of the molecular-level mechanisms.

Actually, the previous studies on DT-UV/Vis spectroscopy just focused on qualifying the *c*-Cysts in the living cells (suspension or biofilm) but did not conduct the quantification of *c*-Cysts in the living cells. In this study, the Cr(VI) reduction was investigated in a living cell suspension of *S. oneidensis* MR-1 on DT-UV/Vis spectroscopy with the objectives: (1) to quantify the *c*-Cysts in the living MR-1 cell suspensions by DT-UV/Vis spectroscopy, (2) to directly examine *in situ* spectral kinetics of Cr(VI) and *c*-Cysts in intact cells of MR-1, and (3) to evaluate the effects of different incubation conditions, i.e., cell density, initial Cr(VI) concentration, Cr(III) concentration, pH, temperature, electron donors and oxygen on the *in vivo* reaction between Cr(VI) and *c*-Cysts.

MATERIALS AND METHODS

Materials

Shewanella oneidensis MR-1 was isolated from anoxic sediments of Lake Oneida, NY (Myers and Nealson, 1988) and purchased from MCCC (Marine Culture Collection of China, China). The strain was grown aerobically overnight as batch cultures in Luria-Bertani (LB) medium (10 g L^{-1} NaCl, 5 g L^{-1} yeast extract, 10 g L^{-1} tryptone) to exponential phase at 30°C with shaking at 180 rpm. The cells were subsequently washed and diluted before the *in situ* spectral kinetic experiments. All chemicals used in the experiments were reagent grade or better. Water for all experiments was supplied from a Milli-Q reference ultraviolet (UV)-water system. Horse heart cytochrome *c* was obtained from Sigma-Aldrich (China). Cr(VI) stock solution was prepared by dissolving potassium dichromate ($\text{K}_2\text{Cr}_2\text{O}_7$; Sigma-Aldrich) in UV-water. Chromium chloride hexahydrate ($\text{CrCl}_3 \cdot 6\text{H}_2\text{O}$;

98.45%, AR, Aladdin, China) was used as the source of Cr(III). A 30 mM solution of 4-(2-hydroxyethyl)piperazine-1-ethanesulfonic acid (HEPES, Sigma-Aldrich) adjusted to pH 7 with sodium hydroxide was used as the buffer in all experiments. Stock solutions of sodium lactate (1.0 M) were also prepared in UV-water for use in the experiments. All stock solutions were stored at 4°C before use.

Quantification of c-Cyts in a Live-Cell Suspension

The strain was aerobically inoculated in Luria-Bertani (LB) for 16 h in a shaker at 180 rpm and 30°C and harvested by centrifugation at 8,000 × g for 10 min at 4°C for three times after being washed and re-suspended using HEPES buffer when it approached the exponential phase. The cell suspension in HEPES buffer was purged with 100% N₂ for 30 min, and then the suspension with lactate (20 mM) as electron donor was added to a rectangular quartz cuvette with an optical path length of 1.0 cm for measurement before sealing in Anaerobic Chamber. The horse heart cytochrome *c* was used as a standard (Picardal et al., 1993) to quantify the *c*-Cyts in living MR-1 cell suspension. Different concentrations of horse heart cytochrome *c* were measured by a UV/Vis spectrophotometer (TU-1901 Beijing, China) equipped with an IS19-1 integrating sphere reflectance attachment, using a 10-mm optical path of dish, with 1 nm scan interval, and 1.0 nm s⁻¹ sweep speed from 300 to 600 nm. A difference of millimolar extinction coefficients ($\Delta\epsilon$) of 21.4 mM⁻¹ cm⁻¹ (Supplementary Figure S1) for reduced and oxidized forms of meso-IX pyridine hemochrome was used for quantification of heme *c* (Picardal et al., 1993). Using the spectral method, only the *c*-Cyts located on the very surface of cell outer-membrane can be measured directly, but the *c*-Cyts which located in periplasm and the cytoplasmic membranes were unlikely to be measured as the light was not able to penetrate the membrane. Hence, the *c*-Cyts measured in the cell suspension can only represent the outer membrane *c*-Cyts. In addition, we were not able to differentiate the specific roles of individual proteins from those of other *c*-Cyts by just using the DT UV-Vis spectral method, but we just examined the outer-membrane heme-containing molecules as the bulk OM *c*-Cyts in intact DMRB cells.

Procedures for Cr(VI) Reduction by MR-1

MR-1 was grown aerobically in LB at 30°C for 16 h. The suspension was subsequently centrifuged at 7000 × g for 10 min at 4°C, and the pellets were washed with sterile HEPES buffer (30 mM, pH 7.0) three times. Cells were then transferred to an Anaerobic Chamber (DG250, Don Whitley Scientific, England) with H₂:N₂ = 4:96 and resuspended in the same buffer for a final concentration of 1.07 × 10¹² cells mL⁻¹. This cell suspension was added to a rectangular quartz cuvette with an optical path length of 1.0 cm. Sodium lactate (20 mM) was added to the suspension as an electron donor. Cr(VI) was added as the sole electron acceptor at concentrations ranging from 20 to 1000 μM. The cuvette was subsequently sealed and taken out of the Anaerobic Chamber. Two control solutions that lacked cells or contained

autoclaved cells were used for each Cr(VI)-reduction assay to examine the effects of any abiotic factors or the biosorption of Cr(VI) by the cell mass on Cr(VI) reduction, respectively. The cell suspension before Cr(VI) addition was also measured. Once Cr(VI) was added, spectra were then taken using the DT-UV/Vis spectrophotometer by scanning at different intervals. The specific peaks appear at 372 nm for Cr(VI) and at 552 nm for reduced cytochrome (*c*-Cyt_{red}). A pseudo first-order model can be applied to describe the kinetics of Cr(VI) reduction by MR-1. There was no replicate in the spectral kinetic experiments for *c*-Cyts and Cr(VI). The error bars of *k*-values represent the standard error of different *k*-values calculated from linear fitting by Origin software.

Cr(VI) Reduction by MR-1 under Different Incubation Conditions

The effect of additional Cr(III) on Cr(VI) reduction by MR-1 cells was investigated using different initial concentrations of Cr(III) (50–1000 μM). To investigate the effect of MR-1 initial cell density on chromate reduction, a series of densities of MR-1 cells ranging from 2.68 × 10¹¹ cells mL⁻¹ to 2.14 × 10¹² cells mL⁻¹ were added to the system. Effects of different pH values (6.0–8.0) and temperatures (20–40°C) on the Cr(VI)-reducing capability of viable MR-1 cells were determined. The effect of pH was determined using sterile PIPES (piperazine-N, N-bis-2-ethanesulphonic) buffer (30 mM) and HEPES buffer (30 mM). In both cases, an initial concentration of 160 μM of Cr(VI) was used as the sole electron acceptor. Cr(VI) reduction by viable cells of MR-1 was studied in the presence of various electron donors, including 20 mM of D-lactose, formate, lactate and sucrose from the stock solutions (1 M). The effect of oxygen concentration on Cr(VI) reduction by MR-1 cells was investigated with different concentrations of dissolved oxygen (DO), including 1.0, 3.0, 4.0, 16, 26, 33, and 68 μM.

Cr(VI) Reduction by *c*-Cyts in Various Intact Mutant Cells

To examine the electron transport chain of MR-1, the Cr(VI) reduction was examined by using MR-1 with *c*-Cyt deletion mutants including ΔmtrC, ΔmtrF, ΔmtrA, ΔmtrD, ΔomcA, and ΔcymA (Hartshorne et al., 2009; Coursolle and Gralnick, 2010; Shi et al., 2012). The mutant strains used in this study were provided by Professor Haichun Gao in Zhejiang University, and the relevant information was provided in the reference (Gao et al., 2010). MR-1 wild type (wt) and various mutants were grown aerobically in LB at 30°C for 16 h. The suspension was subsequently centrifuged at 7000 × g for 10 min at 4°C, the pellets were washed with sterile HEPES buffer (30 mM, pH 7.0) three times and subsequently used for *in situ* spectral kinetic experiments.

Characterization of MR-1 Cells and Cr Species

After approximately 60 min of incubation, the cells were centrifuged at 7000 × g for 4 min and flash-frozen with liquid nitrogen before RNA was extracted using TRIzol reagent

(Invitrogen, USA). Reverse transcription PCR and real-time quantitative PCR were then used to measure the amount of 16S rRNA gene. The obtained bacterial RNA was reverse transcribed using a PrimeScriptTM II 1st strand cDNA Synthesis Kit (Takara, Shiga, Japan) according to the instructions of the manufacturer. Quantification of transcripts of bacterial 16S rRNA was determined by the iQTM5 Real-Time PCR Detection System (Bio-Rad, USA) and using the SYBR Green I detection method. The qPCR System using the Eub338 (ACTCCTACG GGAGGCAGCAG; Lane, 1991) and Eub518 (ATTACCGCGGCTGCTGG; Muyzer et al., 1993) primer pair. Each 20 μ L reaction solution contained the following: 1 μ L of template cDNA (1–10 ng), 10 μ L of 2 \times IQ SYBRTM Green Supermix (Bio-Rad, USA), 0.2 μ M of each primers. PCR conditions were 5 min at 95°C, followed by 40 cycles of 94°C for 20 s, 55°C for 20 s, and 72°C for 30 s (Muyzer et al., 1993). Per DNA sample and the appropriate set of standards were run in triplicates. The qPCR calibration curves were generated with serial triplicate 10-fold dilutions of plasmid DNA. The plasmid pGEM-T Easy Vector (Promega, Madison, WI, USA) contained the cloned target sequences. Plasmid DNA was extracted using an EZNA Plasmid Mini Kit I (Omega Bio-Tek, Doraville, GA, USA) and the concentration was quantified by the Qubit 2.0 Fluorometer (Invitrogen, NY, USA). Target copy numbers for each reaction were calculated from the standard curves (Pfaffl, 2001). The experiments for 16s rRNA were conducted in triplicate, and the mean values and error bars were derived from average and standard deviation values calculated from three repeats.

To identify the location and valences of the reduced product, MR-1 cells associated with the reduced product after incubation were characterized by scanning electron microscopy-energy dispersive X-ray (SEM-EDX) and X-ray photoelectron spectroscopy (XPS). For SEM-EDX analysis, the bacterial cells associated with reduced product were washed with phosphate buffer (10 mM, pH = 7.5) and fixed in 2.5% (v/v) glutaraldehyde. The sample was then dried with ethanol under ambient conditions, mounted on an aluminum stub and then coated with gold. Images and energy-dispersive X-ray spectroscopy (EDX) were taken using an FEI Quanta 400F thermal-field emission environmental SEM (FEI, Hillsboro, OR, USA) with an Oxford INCA EDX. For the XPS analysis, the cells were exposed to 1000 μ M Cr(VI) for 10 h, while the cells under the same conditions without Cr(VI) served as a control. The cells were then separated by centrifugation at 10,000 $\times g$ at 4°C for 5 min. The pellets were washed with deionized water and freeze-dried overnight at –42°C. The sample was examined by an ESCALAB 250 XPS (Thermo-VG Scientific, USA).

RESULTS

Spectral Monitoring of Cr(VI) Reduction by c-Cyts in Intact Cells

The spectra in Figure 1A clearly show changes of specific peaks at 372 nm, corresponding to Cr(VI), and at 552 nm, corresponding to Heme_{red}. The heights of these peaks were

extracted and plotted in Figure 1B. While Cr(VI) decreased substantially, the Heme_{red} transiently dropped to a low level at the very beginning (stage 1: consumption) and then gradually increased to the initial level (stage 2: recovery). It has been widely reported (Ramirez-Diaz et al., 2008; Gnanamani and Kavitha, 2010; Belchik et al., 2011) that the transformation from Cr(VI) to Cr(III) is the dominant pathway of microbial Cr(VI) reduction (Faisal and Hasnain, 2004). The redox potentials of Cr(VI)/Cr(III) and c-Cyt_{ox}/c-Cyt_{red} at pH 7 were 1.2 and 0.25 V, respectively (Morel and Hering, 1993), indicating that the reaction between c-Cyts and Cr(VI) was thermodynamically feasible. To further prove the direct redox reaction between Cr(VI) and c-Cyts, the proteins have been extracted, and similar patterns of oxidized (c-Cyt_{ox}) and reduced c-Cyts (c-Cyt_{red}) were observed in the spectra of whole cells and extracted OM proteins of MR-1 (Supplementary Figure S2A). After Cr(VI) was added to reduced OM proteins, the peak intensity at 552 nm rapidly decreased, indicating that the reaction between c-Cyt_{red} and Cr(VI) definitely occurred. Therefore, this result can provide a direct evidence for the electron transfer from c-Cyt_{red} to Cr(VI). The SEM images showed that obvious white precipitation was generated on the surfaces of the Cr(VI)-treated cells (Figure 1C). While no morphological change of the cells was observed, presumably due to the short period of experiments, a chromium signal was found in the precipitation in EDX analysis with a Cr element composition of 11.37%. The XPS results (Figure 1D) show two distinct peaks: 586.5 eV (Cr 2p1/2) and 576.8 eV (Cr 2p3/2), representing Cr(III) in the form of a Cr₂O₃-like species (Biesinger et al., 2004; Manning et al., 2007; Dong et al., 2013). A control with Cr(III) and MR-1 under anoxic conditions was also conducted (Supplementary Figure S2B), with results indicating that the Cr(III) reduction products did not influence the heme measurements. Moreover, the cells under oxic conditions showed that oxidized heme (Heme_{ox}) had no reactivity for Cr(VI) removal (Supplementary Figure S2C). Hence, it is reliable to directly measure Cr(VI) and Heme_{red} using the DT spectra.

Cr(VI) Reduction by c-Cyts in Intact Mutant Cells

Results in Figures 2A,B with various mutants showed that, compared to the results for the wild type (wt), the mutants Δ cymA and Δ mtrA exhibited distinctly low reduction rates of Cr(VI) and Heme, demonstrating their specific role in controlling the electron transport chain for Cr(VI) reduction. It was reported that CymA can oxidize the quinol in the inner membrane and then transfer the electrons to MtrA through other periplasmic proteins (Shi et al., 2012). Deletion of CymA evidently hindered the MR-1 cell to use the terminal electron acceptors (Schwalb et al., 2003). A mutant lacking MtrA also exhibited attenuated reduction of external electron acceptors, demonstrating its critical role in metal reducing processes (Beliaev et al., 2001). The MtrC and OmcA are localized on bacterial cell surfaces (Belchik et al., 2011), but the deletion of MtrC or OmcA had rarely effect on reduction rates of Cr(VI) and Heme, suggesting the existence of multiple Cr(VI) reduction

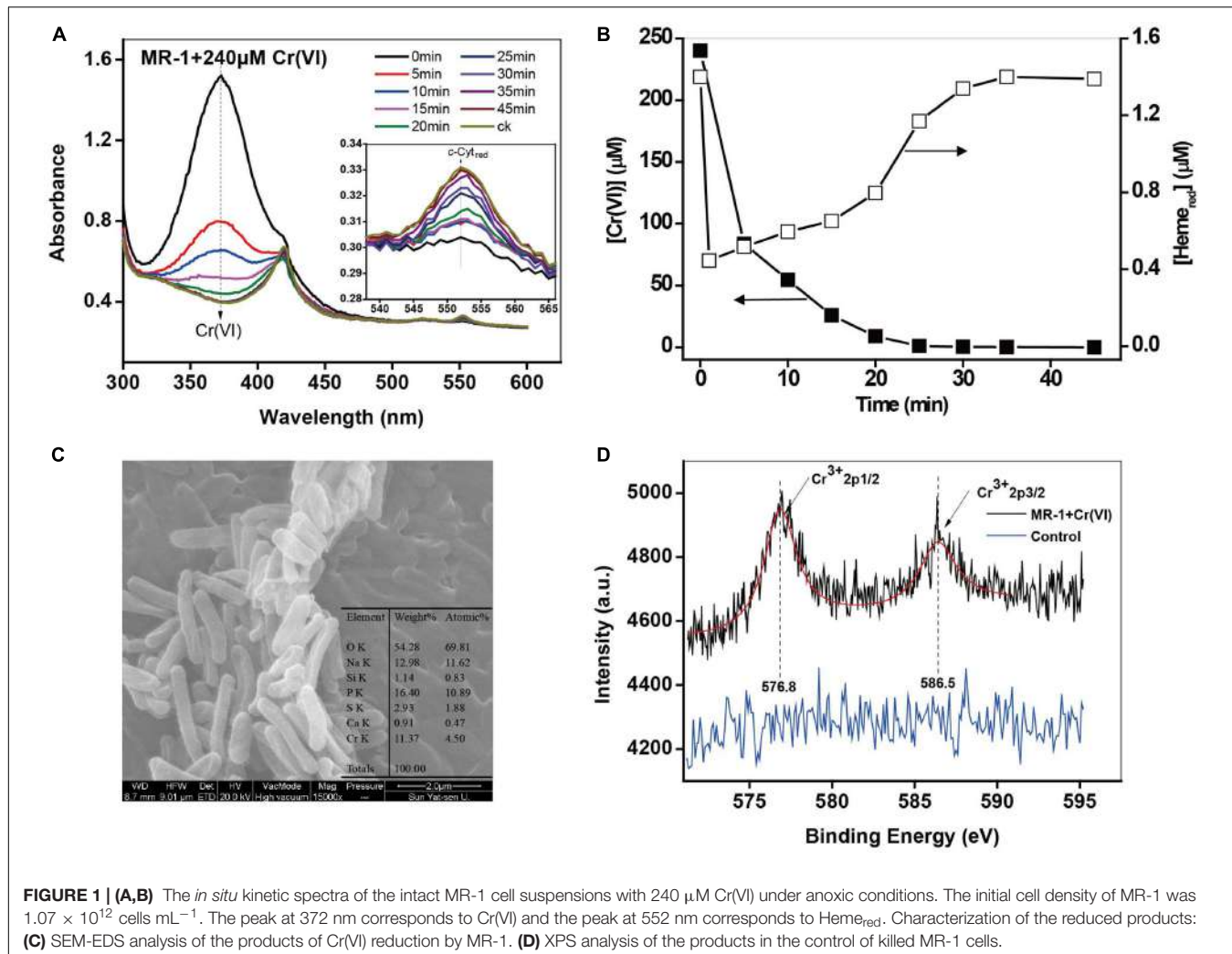


FIGURE 1 | (A,B) The *in situ* kinetic spectra of the intact MR-1 cell suspensions with 240 μM Cr(VI) under anoxic conditions. The initial cell density of MR-1 was 1.07×10^{12} cells mL⁻¹. The peak at 372 nm corresponds to Cr(VI) and the peak at 552 nm corresponds to Heme_{red}. Characterization of the reduced products: **(C)** SEM-EDS analysis of the products of Cr(VI) reduction by MR-1. **(D)** XPS analysis of the products in the control of killed MR-1 cells.

pathways, which is consistent with the existence in the MR-1 genome of numerous MtrABC paralogs (Coursolle and Gralnick, 2010).

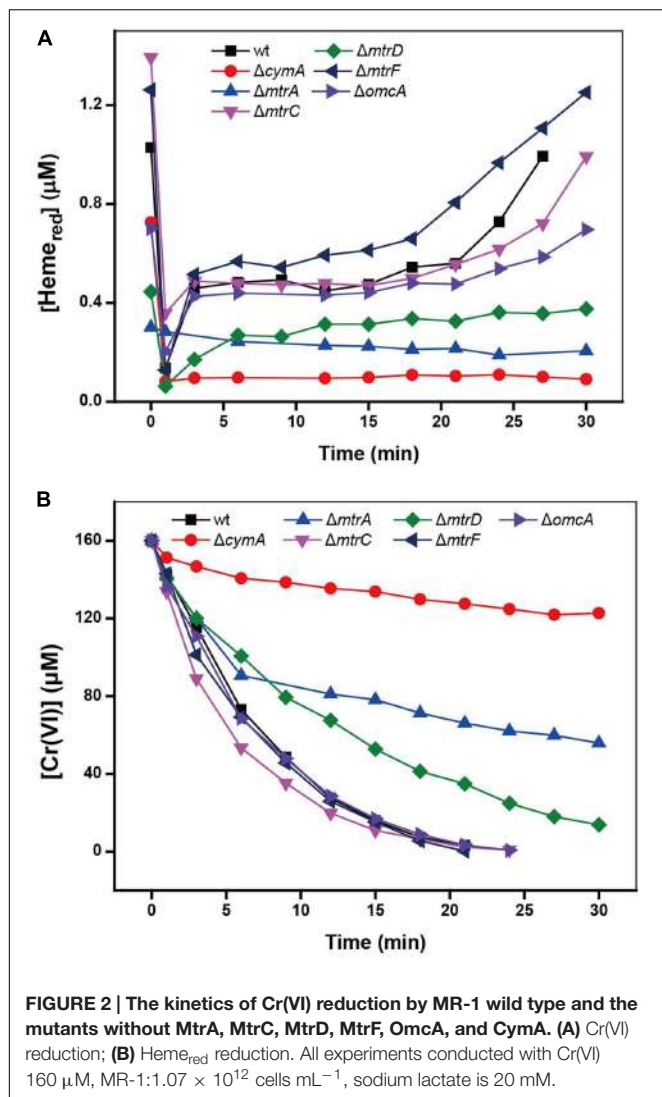
Effect of Initial Cell Densities

The heme concentration is directly dependent on the cell densities of MR-1 cell suspension, therefore, the cell densities might have a great influence on Cr(VI) reduction by MR-1. Kinetic results in Supplementary Figure S3 and **Figure 3** show that the reduction rate of Cr(VI) increased proportionally with an increase in cell densities. Similar behaviors have been reported with *Arthrobacter* sp. SUK 1201 (Dey et al., 2014), *Pseudomonas* CRB5 (McLean et al., 2000), and *Bacillus sphaericus* AND 303 (Pal and Paul, 2004). Simultaneously, the higher cell density induced faster Heme_{red} recovery. Here we provide a direct evidence of Heme_{red} recovery by measuring *in situ* kinetics of c-Cyts in intact MR-1 cells.

Effect of Initial Cr(VI) Concentrations

The kinetics of Cr(VI) and c-Cyts are examined (Supplementary Figure S4) under different initial Cr(VI) concentrations. The

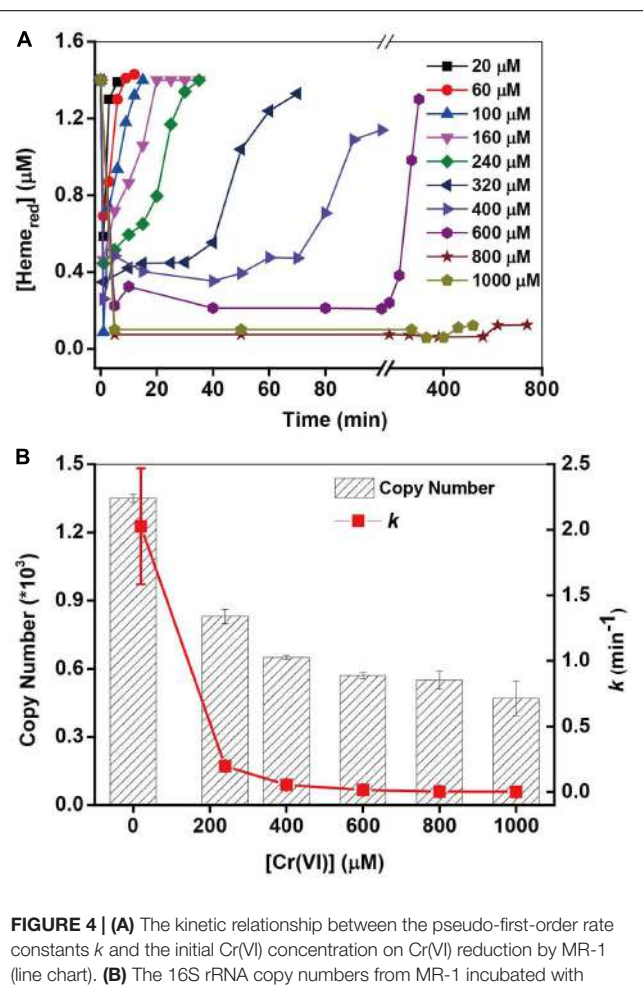
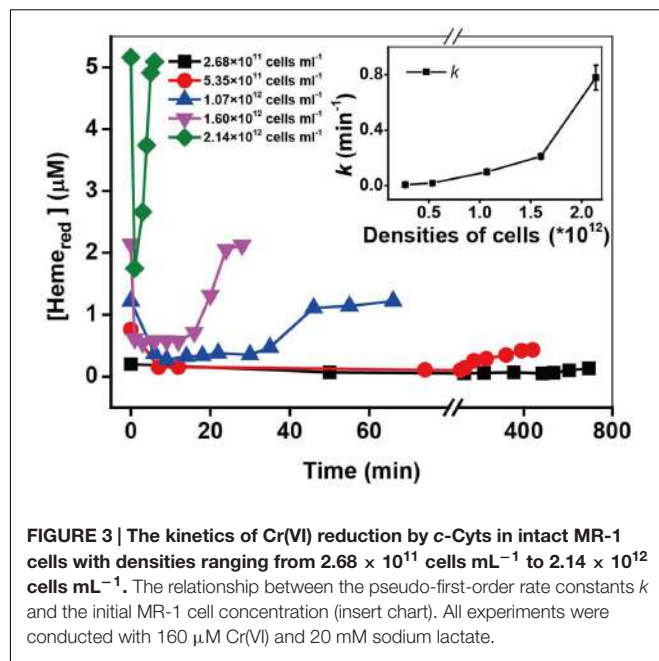
pseudo-first-order rate constant (k) of Cr(VI) reduction in **Figure 4A** decreased greatly with an increase in initial Cr(VI) concentrations. For example, the k -value of 20 μM Cr(VI) (2.027 min^{-1}) is nearly 700-fold higher than that of 1000 μM Cr(VI) (0.003 min^{-1}). Simultaneously, the Heme_{red} changed accompanying the changes of Cr(VI) (**Figure 4B**), showing that while the consumption of Heme_{red} in stage (i) of all the treatments was nearly the same, the recovery of Heme_{red} in stage (ii) became increasingly slow with an increase in initial [Cr(VI)]. The slower recovery of Heme_{red} might account for the low k -values of Cr(VI) reduction with high initial [Cr(VI)]. It has been reported that Cr(VI) is toxic to metal-reducing bacteria and has resulted in a loss of metal-reduction activity (Cervantes et al., 2001). Therefore, to examine the toxicity of Cr(VI) to MR-1 cells, 16S rRNA analysis of MR-1 was carried out after MR-1 was incubated with different Cr(VI) concentrations for 60 min. The results in **Figure 4B** show that the 16S rRNA copy numbers decreased greatly with increasing Cr(VI) concentrations, suggesting that the Cr(VI)-reducing capacity of MR-1 declined probably due to the toxicity at higher [Cr(VI)], which is consistent with other well-documented results (Sugden

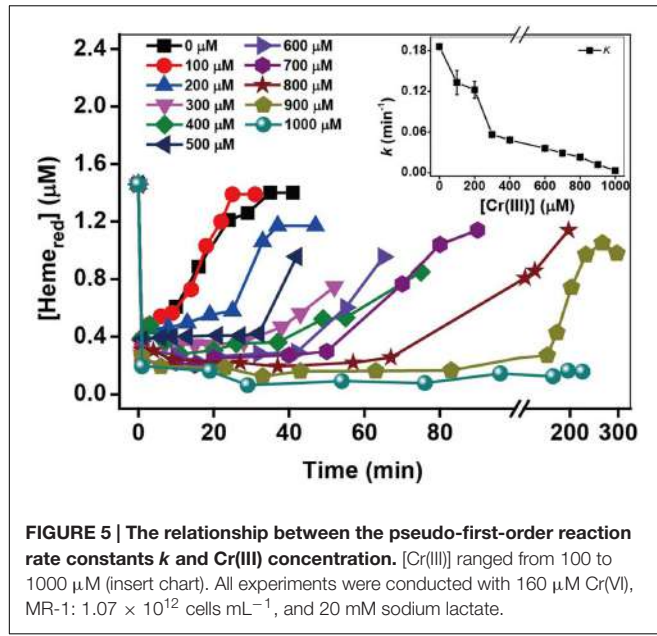


et al., 2001; Middleton et al., 2003; Viamajala et al., 2003). This studies suggested that while the high concentrations of Cr(VI) and its reduced product Cr(III) may cause toxicity to the intact cells, this might be an effective and environmental-friendly method for the bioconversion of Cr(VI) with low concentrations.

Effect of Added Cr(III) Concentrations

Kinetic results in the presence of 50–1000 μM Cr(III) in Supplementary Figure S5 and k -values in Figure 5 show that the Cr(VI) rates decreased substantially with an increase in Cr(III) concentration, indicating that the inhibitory effects of Cr(III) increased gradually with increasing [Cr(III)]. The kinetics of Heme_{red} in Figure 5 show that the recovery of Heme_{red} in the presence of 100 μM Cr(III) is almost the same as that of the control in the presence of Cr(III). However, the extent of Heme_{red} recovery decreased with increasing Cr(III) concentrations from 200 to 1000 μM , indicating that Cr(III) might be toxic to microorganisms due to its inhibition of the transformation of Heme_{ox} to Heme_{red}. The above results suggest



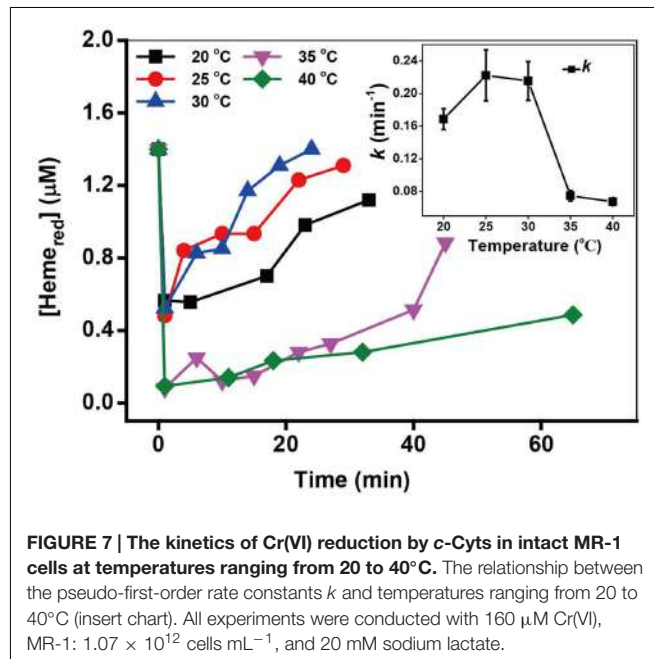
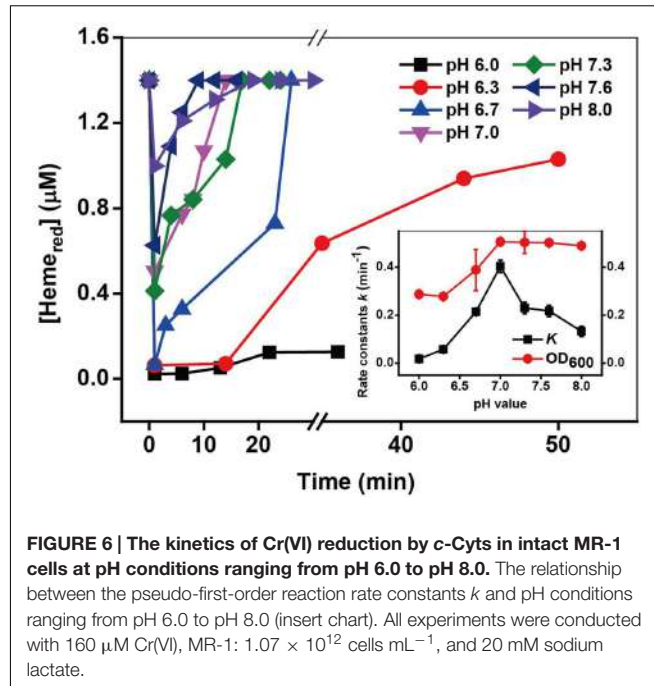


that the inhibition by added exogenous Cr(III) might result from the combination of Cr(III) and Heme_{ox} in OM of MR-1, which may prevent the reaction of Heme_{ox} to Heme_{red}, thus slowing the rate of Cr(VI) reduction. Also, the added Cr(III) as freshly dissolved CrCl₃ appeared toxicity, which be associated with extracellular interactions and caused an ultimately lethal cell morphology (Parker et al., 2011). The addition of CrCl₃ to *Shewanella* species causes an abrupt drop in cell survival (Bencheikh-Latmani et al., 2007). Hence, the results here about the effect of Cr(III) concentrations might be not only related to the combination of Cr(III) and Heme_{ox} in MR-1 OM but also related to the toxic effect of freshly dissolved CrCl₃.

The aforementioned results are mainly based on the effects of endogenous factors, added reactants [Cr(VI)] and *c*-Cysts and products [Cr(III)], and *c*-Cysts recovery. These factors can also be influenced by external incubation factors, such as suspension pH, temperature, types of electron donors, and oxygen concentrations. The *in situ* spectral kinetics of Cr(VI) reduction and *c*-Cysts recovery were further investigated in terms of these external factors.

Effect of pH

Cr(VI) reduction rates are strongly dependent on pH (Wang et al., 1989; Philip et al., 1998; Fein et al., 2010). The acidity may affect the Cr(VI) reduction through effects on the properties of the MR-1 and Cr(VI) solution, such as the growth and metabolism of cells and the speciation of Cr(VI). The kinetic results under different pH in Supplementary Figure S6 and **Figure 6** show that the optimal Cr(VI) reduction rate was obtained at pH 7; however, the achieved recovery of Heme_{red} increased with an increase in pH from 6 to 8. As the pH may influence the growth of cells, the cell density the OD₆₀₀ value was measured at the end of each reaction. The results show



that the maximum OD₆₀₀ value was also obtained at pH 7.0. This behavior is consistent with the fastest pH dependent-Cr(VI) reduction via metabolic enzymatic reactions occurring at pH 7.0 (Wang et al., 1989; Shen and Wang, 1994a; Philip et al., 1998).

Effect of Temperature

The incubating temperature is also an important factor affecting the cell growth and thus influencing the microbial Cr(VI) reduction. The kinetics of Cr(VI) reduction and the

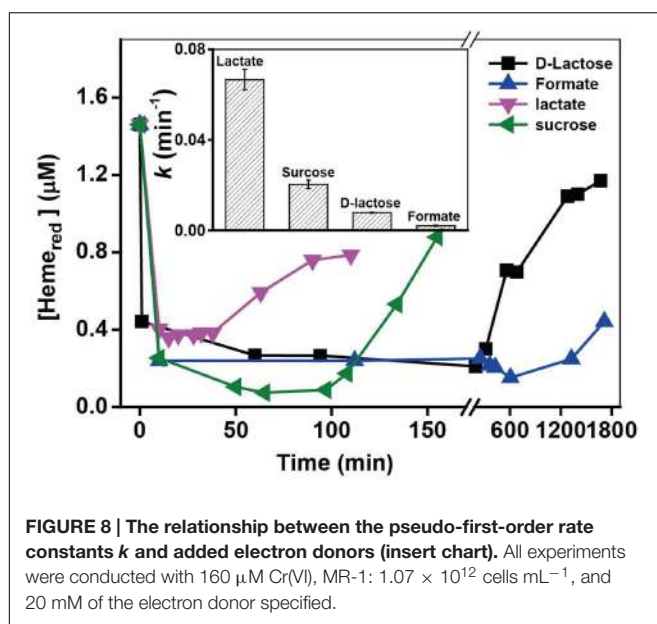


FIGURE 8 | The relationship between the pseudo-first-order rate constants k and added electron donors (insert chart). All experiments were conducted with $160 \mu\text{M}$ Cr(VI), MR-1: $1.07 \times 10^{12} \text{ cells mL}^{-1}$, and 20 mM of the electron donor specified.

transformation of Heme_{red} in (Supplementary Figure S7 and Figure 7) revealed that the optimal Cr(VI) reduction rates and Heme_{red} recovery were obtained at $25\text{--}30^\circ\text{C}$. It has previously been reported that that biological activity of MR-1 is optimal at 30°C (Burgos et al., 2008).

Effect of Different Electron Donors

MR-1 can utilize a wide range of various carbon sources as electron donors, while the utilization efficiency of those electron donors are quite different, which might further influence the metabolic processes. The heme transformation rate may be associated with the intracellular electron transfer occurring via the cell metabolism, as electron donors may control metabolic processes and ultimately affect the intracellular electron transfer to Heme_{ox}. The kinetic results with different electron donors in Supplementary Figure S8 and k -values in Figure 8 show that the added electron donors affected the reduction rates of Cr(VI) in the following order: lactate > sucrose > D-lactose > formate. The k -value with lactate (0.0666 min^{-1}) was almost 37 times higher than that in the presence of formate (0.0021 min^{-1}). Figure 8 shows that the ranking order of Heme_{red} recovery is consistent with that of Cr(VI) reduction. The fastest recovery of Heme_{red} occurred in the presence of lactate, while a barely detectable amount of Heme_{ox} was reduced in the presence of formate. The effects of electron donors on the reduction of Cr(VI) and Heme_{red} might be due to different utilization rates of electron donors by MR-1; this phenomenon was also reported in previous studies of Fe(III) reduction by MR-1 (Petrovskis et al., 1994; Park and Kim, 2001). Lactate was the most efficient carbon source for Cr(VI) reduction by MR-1. Thus, lactate is the most favorable of the tested carbon sources for facilitating the transformation from Heme_{ox} to Heme_{red} and the most efficient rate of Cr(VI) reduction.

Effect of Oxygen

The *Shewanella* strain is a facultative anaerobic bacterium; thus, oxygen not only influences the metabolic rates but also acts as an electron acceptor that competes with Cr(VI) during the Cr(VI) reduction by MR-1 (Ohtake et al., 1990; Viamajala et al., 2004). It was reported that there was immediate cessation of growth upon addition of Cr(VI) in early- and mid-log-phase cultures under anaerobic conditions, while addition of Cr(VI) to aerobically growing cultures resulted in a gradual decrease of cell growth rate (Viamajala et al., 2004). Kinetic results with different oxygen concentrations are shown in Supplementary Figure S9 and k -values are shown in the insert of Figure 9. The control, which lacked oxygen, had the highest efficiency of Cr(VI) reduction, while an obvious inhibitory effect was observed in the presence of oxygen and the inhibitory effect increased substantially with increasing oxygen. Indeed, the Cr(VI) reduction capacity even disappeared with $[O_2] \geq 26 \mu\text{M}$. Consistent with Cr(VI) reduction, the reduction of Heme_{ox} to Heme_{red} was stable for $[O_2]$ from 0 to $16 \mu\text{M}$, and then decreased with the increase of $[O_2]$ from 16 to $68 \mu\text{M}$. The above results show that although the added oxygen might enhance the metabolic processes and increase cell growth, oxygen likely plays a key role in the inhibitory effects on Cr(VI) reduction.

DISCUSSION

In the process of Cr(VI) reduction by *c*-Cysts of intact MR-1 cells, the electron transfer pathway can be concisely divided into two steps: (i) intracellular electron transport from electron donor to OM *c*-Cysts and (ii) electron transfer from *c*-Cysts to Cr(VI). The step-by-step potential losses (Wu et al., 2014) can drive

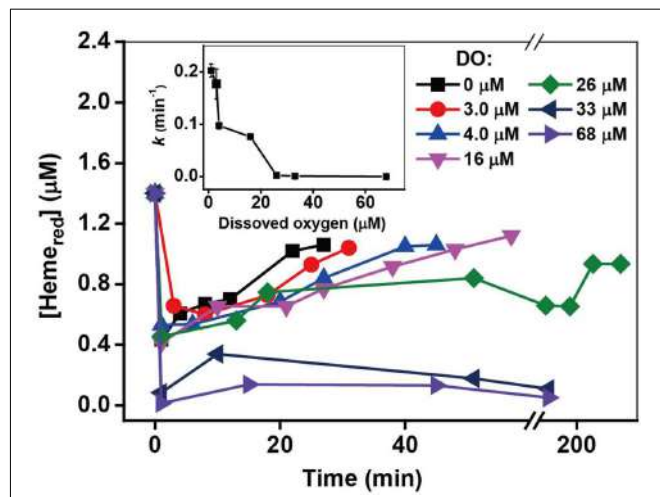
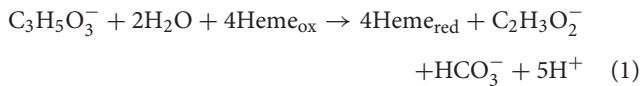


FIGURE 9 | The relationship between the pseudo-first-order rate constants k and O_2 concentration. The kinetics of Cr(VI) reduction by *c*-Cysts were measured in intact MR-1 cells at dissolved oxygen concentrations ranging from 0 to $68 \mu\text{M}$ (insert chart). All experiments were conducted with $160 \mu\text{M}$ Cr(VI), MR-1: $1.07 \times 10^{12} \text{ cells mL}^{-1}$, and 20 mM sodium lactate.

electron flow from electron donor via *c*-Cysts to Cr(VI), resulting in Cr(VI) reduction. Therefore, the current study only focuses on the Cr(VI) reduction by *c*-Cysts. In Step (i), the electron donor (lactate) can be utilized by MR-1 with concomitant intracellular electron transport from lactate to OM *c*-Cysts, resulting in the redox transformation of Heme_{ox} to Heme_{red} as shown in Eq. 1.



The Heme_{ox} and Heme_{red} represent the Fe(III)-associated and Fe(II)-associated hemes, respectively, and hence the redox transformation from Heme_{ox} to Heme_{red} can be considered as an one-electron transfer reaction. In Step (ii), Heme_{red} directly transfers electrons to Cr(VI) by generating Cr(III) when Cr(VI) is in contact with OM of MR-1.



It was reported that the reaction rate constants (Eq. 2) are $3.5 \times 10^4 \text{ M}^{-1} \text{ s}^{-1}$ for MtrC and $2.5 \times 10^5 \text{ M}^{-1} \text{ s}^{-1}$ for OmcA (Belchik et al., 2011), so the transient oxidation of the outer membrane cytochromes occurred due to the fast molecular reaction between Heme_{red} and Cr(VI), which was also supported by the SEM results with obvious Cr(III) white precipitation on the surfaces of the Cr(VI)-treated cells.

In addition, from the results of Cr(VI) reduction by MR-1 mutants, the electron transfer pathway of reaction between Cr(VI) and *c*-Cysts of MR-1 is likely to be the typical Mtr respiratory pathway which is required for the reduction of metals and electrodes (Coursolle and Gralnick, 2010), suggesting that the outer-membrane enzyme-induced extracellular electron transfer might dominate the Cr(VI) reduction by MR-1. While the roles of those mutants in **Figure 2A** did not provide new interpretation in light of previous knowledge, but we go further with using DT UV-Vis spectral approach to measure the real-time changes of the redox status of *c*-Cysts in **Figure 2B**. From this aspect, the information about the *c*-Cysts in intact cells can be a new complement to the previous interpretation about the roles of various mutants.

It was reported that many microorganisms were capable of secreting high molecular mass polymers that can either be released into the surrounding environment (extracellular polysaccharides, exopolysaccharides) or remain attached to the cell surface (capsular polysaccharides; Ozturk and Aslim, 2008), and some quinone-compounds or flavin-compounds can play a role of shuttling electrons from cells to terminal electron acceptors (Marsili et al., 2008). Hence, besides the direct electron transfer from *c*-Cysts to Cr(VI), the electron shuttle-mediated Cr(VI) reduction was also possible in Cr(VI) reduction by MR-1. Generally, these two types of polysaccharides can be separated by centrifugation, with those remaining in the supernatant being soluble EPS (Sheng et al., 2010). The strain used in this study was harvested by centrifugation at $8,000 \times g$ for 10 min at 4°C for three times after being washed and re-suspended using HEPES buffer, so the exopolysaccharides were very likely to be removed by centrifugation. *S. oneidensis* MR-1 can also produce

riboflavin combining with exopolysaccharides in the process of experiment (Harald von et al., 2008), however, our previous study (Wu et al., 2014) showed that the absorbance of self-secreted riboflavin was much lower than that of the exogenous riboflavins, and the influence of self-secreted riboflavin can be ignored. In addition, Harald von et al. (2008) showed that when MR-1 was cultured with 100 mM fumarate as the electron acceptor and 50 mM lactate as the electron donor during anaerobic growth, there was nearly no riboflavin generated at the beginning, and it took 168 h for the riboflavin increasing to a highest concentration at about 0.07 μM . Because the duration time of most kinetic experiments in this study were less than 1 h, the riboflavin self-excreted by MR-1 may have very limited influences on the overall reaction kinetics. Therefore, the contribution of riboflavin combining with exopolysaccharides to Cr(VI) reduction can be ignored in this study, and the above discussion further supported that the *c*-Cyt-mediated electron transfer played a key role in Cr(VI) reduction by MR-1.

Furthermore, as the alternation of pH can also influence the Cr speciation, the speciation of Cr(VI) and Cr(III) was analyzed using Visual Minteq 3.0, which showed that results agreed with theoretical predictions (Parker et al., 2011). Under the neutral pH range tested (Borloo et al., 2007; Ross et al., 2009; Belchik et al., 2011), the dominant species of Cr(VI) are CrO_4^{2-} and HCrO_4^- ; thus, the pH in the range of interest does not appear to significantly influence the species of Cr(VI). The dominant species of Cr(III) include not only the soluble species [Cr(OH)_2^+ , Cr(OH)_2^{2+} , and $\text{Cr(OH)}_3(\text{aq})$] but also the insoluble species [$\text{Cr(OH)}_3(\text{s})$, Cr_2O_3], and hence, the pH in the range of interest may influence the species of Cr(III). The toxicity of Cr is due to the reactivity and solubility of the chromate anion. At circumneutral pH, Cr(VI) reduction to Cr(III) leads to its precipitation as insoluble Cr(OH)_3 . The Cr(III) showed weakened toxicity as pH dropped, probably due to its increasingly limited solubility (Rai et al., 2004; Remoundaki et al., 2007). The low Cr(VI) reduction rate at low pH may be due to the low growth and metabolism of cells, which has the most suitable pH at approximately 7 (Fein et al., 2010). The results of OD₆₀₀ analysis further support the effects of pH on cell growth.

Regarding to the toxicity in increasing Cr(VI) concentration, while it has not been deeply investigated here, some proposed mechanisms have been reported previously. One possible mechanism is that Cr(VI) enters MR-1 cytoplasm through the sulfate transport mechanism to react with cellular DNA (Viamajala et al., 2004). A second possible mechanism is that the Cr(VI) reduction by MR-1 is self-inhibitory (Parker et al., 2011). Previous reports showed that MR-1 rapidly reduced Cr(VI) at the initial stage of reaction with 100–200 μM Cr(VI), but the cells gradually lost their ability to survive as the Cr(III) reduction product appeared (Benchekh-Latmani et al., 2007; Gorby et al., 2008). The Cr(III) produced inside cells during Cr(VI) reduction may cross-link the phosphate backbone of DNA with peptides and amino acids such as cysteine and histidine (Zhitkovich et al., 1996), thereby inhibiting cell function and causing toxicity.

The extracellular Cr(VI) reduction was not fast enough to prevent all Cr(VI) from entering the cell, Cr(III) precipitates were found outside and in the cytoplasm of the cells (Middleton et al., 2003). Also, higher concentration of Cr(VI) caused more intracellular precipitation of Cr(III) in MR-1 cell. The Cr(III) precipitates was only found outside MR-1 cells when 100 μM Cr(VI) was used as the sole terminal electron acceptor (Daulton et al., 2002). While Cr(III) precipitates were found both inside and outside MR-1 cells with 200 μM Cr(VI) (Belchik et al., 2011). A third possible mechanism of Cr(VI) toxicity to MR-1 is due to inhibition of anaerobic respiratory functions (Viamajala et al., 2004). It was manifested that anaerobic Cr(VI) reduction occurs in the electron transport pathway by cytochrome c or b along the respiratory chains in the inner membrane (Ahmed, 2014; Thatoi et al., 2014). The interaction of Cr(VI) with cytochromes might cause disruption of essential energy-deriving cell functions and result in inhibition of growth (Myers et al., 2000). Hence, with increasing concentration of Cr(VI), the mechanism for the toxicity might be attributed to Cr(VI) reacting with cellular DNA, the precipitation of Cr(III) inside the cells, and the inhibition of anaerobic respiratory functions by Cr(VI).

Based on the aforementioned results and discussion, it can be indicated that this study will have substantial implications for quantitatively evaluating the roles of c-Cyts in intact cells during Cr(VI) reduction processes. As c-Cyts play key roles in extracellular electron transfer processes, the direct measurement of c-Cyts reflects the real physiological and metabolic functions that take place during extracellular Cr(VI) reduction (Ross et al., 2009). In addition, despite the recent progress in describing the c-Cyt-mediated Cr(VI) reduction by various models, such as Michaelis–Menten model (Yamamoto et al., 1993; Shen and Wang, 1994b) and dual-enzyme model (Viamajala et al., 2003), the enzyme was not directly measured experimentally to further explore the enzymatic reactions. The *in situ* examination of redox status of c-Cyts will have the potential of being used to verify the outcome derived from the relevant models.

In summary, Cr(VI) and Heme_{red} were directly measured *in situ* using the DT spectra to reflect the status of Cr(VI) reduction by c-Cyts in intact cells, which provides a useful

approach to understand the behavior of outer membrane enzymes of MR-1 under non-invasive conditions. In the presence of Cr(VI), the reduced c-Cyts initially rapidly decreased and then slowly recovered under all tested incubation conditions. The reduced product, Cr(III), might cause toxicity to the cells, resulting in an inhibitory effect on the Cr(VI) reduction and Heme_{red} recovery. The highest Cr(VI) reduction rate and fastest recovery of c-Cyts were obtained at pH 7.0 and 30°C, with sodium lactate serving as an electron donor. These conditions may be optimal due to the resemblance to suitable physiological conditions, which are favorable for metabolism and Heme_{red} recovery. The presence of O₂ greatly inhibited Cr(VI) reduction by competing with Cr(VI) as an electron acceptor. Therefore, the method established for monitoring *in vivo* cytochrome activity and the optimization of incubation parameters will provide new insight into the microbial metal reduction processes under non-invasive conditions.

AUTHOR CONTRIBUTIONS

TL, RH, and FL designed the work. RH, YW, DC, and YW conducted the experiments. RH, TL, and XL wrote the manuscript.

ACKNOWLEDGMENTS

This work was funded by the National Natural Science Foundations of China (41522105, 41571130052, and 41471216), the Guangdong Natural Science Funds for Distinguished Young Scholars (2014A030306041), and an Australian Research Council DECRA grant (DE150100500).

SUPPLEMENTARY MATERIAL

The Supplementary Material for this article can be found online at: <http://journal.frontiersin.org/article/10.3389/fmicb.2016.00746>

REFERENCES

- Ahmed, M. (2014). Bacterial mechanisms for Cr(VI) resistance and reduction: an overview and recent advances. *Folia Microbiol.* 59, 321–332. doi: 10.1007/s12223-014-0304-8
- Barnhart, J. (1997). Chromium chemistry and implications for environmental fate and toxicity. *Soil Sediment Contam.* 6, 561–568. doi: 10.1080/15320389709383589
- Belchik, S. M., Kennedy, D. W., Dohnalkova, A. C., Wang, Y., Sevinc, P. C., Wu, H., et al. (2011). Extracellular reduction of hexavalent chromium by cytochromes MtrC and OmcA of *Shewanella oneidensis* MR-1. *Appl. Environ. Microbiol.* 77, 4035–4041. doi: 10.1128/AEM.02463-10
- Beliaev, A., Saffarini, D., McLaughlin, J., and Hunnicutt, D. (2001). MtrC, an outer membrane decahaem c cytochrome required for metal reduction in *Shewanella putrefaciens* MR-1. *Mol. Microbiol.* 39, 722–730. doi: 10.1046/j.1365-2958.2001.02257.x
- Beliaev, A. S., Klingeman, D. M., Klappenbach, J. A., Wu, L., Romine, M. F., Tiedje, J. M., et al. (2005). Global transcriptome analysis of *Shewanella oneidensis* MR-1 exposed to different terminal electron acceptors. *J. Bacteriol.* 187, 7138–7145. doi: 10.1128/jb.187.20.7138-7145.2005
- Bencheikh-Latmani, R., Obraztsova, A., Mackey, M. R., Ellisman, M. H., and Bm, T. (2007). Toxicity of Cr(III) to *Shewanella* sp. strain MR-4 during Cr(VI) reduction. *Environ. Sci. Technol.* 41, 214–220. doi: 10.1021/es0622655
- Biesinger, M., Brown, C., Mycroft, J., Davidson, R., and McIntyre, N. (2004). X-ray photoelectron spectroscopy studies of chromium compounds. *Surf. Interface Anal.* 36, 1550–1563. doi: 10.1002/sia.1983
- Blake, R. C., and Griff, M. N. (2012). *In situ* spectroscopy on intact *Leptospirillum ferrooxidans* reveals that reduced cytochrome 579 is an obligatory intermediate in the aerobic iron respiratory chain. *Front. Microbiol.* 3:136. doi: 10.3389/fmicb.2012.00136
- Borloo, J., Vergauwen, B., De Smet, L., Brige, A., Motte, B., Devreese, B., et al. (2007). A kinetic approach to the dependence of dissimilatory metal reduction by *Shewanella oneidensis* MR-1 on the outer membrane cytochromes c OmcA and OmcB. *FEBS J.* 274, 3728–3738. doi: 10.1111/j.1742-4658.2007.05907.x
- Burgos, W. D., Nough, J. T., Senko, J. M., Zhang, G., Dohnalkova, A. C., Kelly, S. D., et al. (2008). Characterization of uraninite nanoparticles produced by

- Shewanella oneidensis* MR1. *Geochim. Cosmochim. Acta* 72, 4901–4915. doi: 10.1016/j.gca.2008.07.016
- Busalmen, J. P., Abraham, E. N., and Feliu, J. M. (2008). Whole Cell Electrochemistry of electricity-producing microorganisms evidence an adaptation for optimal exocellular electron transport. *Environ. Sci. Technol.* 42, 2445–2450. doi: 10.1021/es702569y
- Cervantes, C., Campos-García, J., Devars, S., Gutiérrez-Corona, F., Loza-Taveras, H., Torres-Guzmán, J. C., et al. (2001). Interactions of chromium with microorganisms and plants. *FEMS Microbiol. Rev.* 25, 335–347. doi: 10.1016/s0168-6445(01)00057-2
- Cheung, K., and Gu, J.-D. (2007). Mechanism of hexavalent chromium detoxification by microorganisms and bioremediation application potential: a review. *Int. Biodeterioration Biodegr.* 59, 8–15. doi: 10.1016/j.ibiod.2006.05.002
- Coursolle, D., and Gralnick, J. A. (2010). Modularity of the Mtr respiratory pathway of *Shewanella oneidensis* strain MR-1. *Mol. Microbiol.* 77, 995–1008. doi: 10.1111/j.1365-2958.2010.07266.x
- Daulton, T. L., Little, B. J., Lowe, K., and Jones-Meehan, J. (2002). Electron energy loss spectroscopy techniques for the study of microbial chromium(VI) reduction. *J. Microbiol. Meth.* 50, 39–54. doi: 10.1016/s0167-7012(02)00013-1
- Dey, S., Pandit, B., and Paul, A. (2014). Reduction of hexavalent chromium by viable cells of chromium resistant bacteria isolated from chromite mining environment. *J. Min.* 2014, 1–8. doi: 10.1155/2014/941341
- Dong, G., Wang, Y., Gong, L., Wang, M., Wang, H., He, N., et al. (2013). Formation of soluble Cr(III) end-products and nanoparticles during Cr(VI) reduction by *Bacillus cereus* strain XMCr-6. *Biochem. Eng. J.* 70, 166–172. doi: 10.1016/j.bej.2012.11.002
- Faisal, M., and Hasnain, S. (2004). Microbial conversion of Cr (VI) in to Cr (III) in industrial effluent. *Afr. J. Biotechnol.* 3, 610–617.
- Fein, J. B., Fowle, D. A., Cahill, J., Kemner, K., Boyanov, M., and Bunker, B. (2010). Nonmetabolic reduction of Cr(VI) by bacterial surfaces under nutrient-absent conditions. *Geomicrobiol. J.* 19, 369–382. doi: 10.1080/014904502900 98423
- Gao, H., Barua, S., Liang, Y., Dong, Y., Reed, S., Chen, J., et al. (2010). Impacts of *Shewanella oneidensis* c-type cytochromes on aerobic and anaerobic respiration. *Microb. Biotechnol.* 3, 455–466. doi: 10.1111/j.1751-7915.2010.00181.x
- Gnanamani, A., and Kavitha, V. (2010). Microbial products (biosurfactant and extracellular chromate reductase) of marine microorganism are the potential agents reduce the oxidative stress induced by toxic heavy metals. *Colloids Surf. B Biointerfaces* 79, 334–339. doi: 10.1016/j.colsurfb.2010.04.007
- Gorby, Y., Mclean, J., Korenevsky, A., Rosso, K., El-Naggar, M. Y., and Beveridge, T. J. (2008). Redox-reactive membrane vesicles produced by *Shewanella*. *Geobiology* 6, 232–241. doi: 10.1111/j.1472-4669.2008.00158.x
- Harald von, C., Jun, O., Sakayu, S., and Jonathan, R. L. (2008). Secretion of flavins by *Shewanella* species and their role in extracellular electron transfer. *Appl. Environ. Microbiol.* 74, 615–623. doi: 10.1128/aem.01387-07
- Hartshorne, R. S., Reardon, C. L., Daniel, R., Jochen, N., Clarke, T. A., Gates, A. J., et al. (2009). Characterization of an electron conduit between bacteria and the extracellular environment. *Proc. Natl. Acad. Sci. U.S.A.* 106, 22169–22174. doi: 10.1073/pnas.0900086106
- He, M., Li, X., Liu, H., Miller, S. J., Wang, G., and Rensing, C. (2011). Characterization and genomic analysis of a highly chromate resistant and reducing bacterial strain *Lysinibacillus fusiformis* ZC1. *J. Hazard. Mater.* 185, 682–688. doi: 10.1016/j.jhazmat.2010.09.072
- James, B. R. (1996). Peer reviewed: the challenge of remediating chromium-contaminated soil. *Environ. Sci. Technol.* 30, 248A–251A. doi: 10.1021/es962269h
- Kengo, I., Xinlei, Q., Leonor, M., Byoung-Chan, K., Tünde, M., Mounir, I., et al. (2010). Purification and characterization of OmcZ, an outer-surface, octaheme c-type cytochrome essential for optimal current production by Geobacter sulfurreducens. *App. Environ. Microbiol.* 76, 3999–4007. doi: 10.1128/aem.00027-10
- Lane, D. (1991). “16S/23S rRNA sequencing,” in *Nucleic Acid Techniques in Bacterial Systematics*, eds E. Stackebrandt and M. Goodfellow (West Sussex: John Wiley & Sons), 115–175.
- Li, X., Liu, T., Liu, L., and Li, F. (2014). Dependence of the electron transfer capacity on the kinetics of quinone-mediated Fe (iii) reduction by two iron/humic reducing bacteria. *RSC Adv.* 4, 2284–2290. doi: 10.1039/c3ra45458d
- Liu, T., Li, X., Zhang, W., Hu, M., and Li, F. (2014). Fe(III) oxides accelerate microbial nitrate reduction and electricity generation by *Klebsiella pneumoniae* L17. *J. Colloid Interface Sci.* 423, 25–32. doi: 10.1016/j.jcis.2014.02.026
- Liu, Y., Kim, H., Franklin, R. R., and Bond, D. R. (2011). Linking spectral and electrochemical analysis to monitor c-type cytochrome redox status in living *geobacter sulfurreducens* biofilms. *ChemPhysChem* 12, 2235–2241. doi: 10.1002/cphc.201100246
- Manning, B. A., Kiser, J. R., Kwon, H., and Kanel, S. R. (2007). Spectroscopic investigation of Cr (III)-and Cr (VI)-treated nanoscale zerovalent iron. *Environ. Sci. Technol.* 41, 586–592. doi: 10.1021/es061721m
- Marsili, E., Baron, D. B., Shikhare, I. D., Coursolle, D., Gralnick, J. A., and Bond, D. R. (2008). *Shewanella* secretes flavins that mediate extracellular electron transfer. *Proc. Natl. Acad. Sci. U.S.A.* 105, 3968–3973. doi: 10.1073/pnas.0710525105
- McLean, J. S., Beveridge, T. J., and Phipps, D. (2000). Isolation and characterization of a chromium-reducing bacterium from a chromated copper arsenate-contaminated site. *Environ. Microbiol.* 2, 611–619. doi: 10.1046/j.1462-2920.2000.00143.x
- Middleton, S. S., Latmani, R. B., Mackey, M. R., Ellisman, M. H., Tebo, B. M., and Criddle, C. S. (2003). Cometabolism of Cr(VI) by *Shewanella oneidensis* MR-1 produces cell-associated reduced chromium and inhibits growth. *Biotechnol. Bioeng.* 83, 627–637. doi: 10.1002/bit.10725
- Morel, F. M. M., and Hering, J. G. (1993). *Principles and Applications of Aquatic Chemistry*. New York, NY: John Wiley & Sons.
- Muyzer, G., de Waal, E. C., and Uitterlinden, A. G. (1993). Profiling of complex microbial populations by denaturing gradient gel electrophoresis analysis of polymerase chain reaction-amplified genes coding for 16S rRNA. *Appl. Environ. Microbiol.* 59, 695–700.
- Myers, C. R., Carstens, B. P., Antholine, W. E., and Myers, J. M. (2000). Chromium(VI) reductase activity is associated with the cytoplasmic membrane of anaerobically grown *Shewanella putrefaciens* MR-1. *J. Appl. Microbiol.* 88, 98–106. doi: 10.1046/j.1365-2672.2000.00910.x
- Myers, C. R., and Nealson, K. H. (1988). Bacterial manganese reduction and growth with manganese oxide as the sole electron acceptor. *Science* 240, 1319–1321. doi: 10.1126/science.240.4857.1319
- Myers, J. M., and Myers, C. R. (2001). Role for outer membrane cytochromes OmcA and OmcB of *Shewanella putrefaciens* MR-1 in reduction of manganese dioxide. *Appl. Environ. Microbiol.* 67, 260–269. doi: 10.1128/aem.67.1.260-269.2001
- Nakamura, R., Ishii, K., and Hashimoto, K. (2009). Electronic absorption spectra and redox properties of C type cytochromes in living microbes. *Angew. Chem. Int. Edit.* 48, 1606–1608. doi: 10.1002/anie.200804917
- Ohtake, H., Komori, K., Cervantes, C., and Toda, K. (1990). Chromate-resistance in a chromate-reducing strain of *Enterobacter cloacae*. *FEMS Microbiol. Lett.* 67, 85–88. doi: 10.1111/j.1574-6968.1990.tb13841.x
- Ozturk, S., and Aslim, B. (2008). Relationship between chromium(VI) resistance and extracellular polymeric substances (EPS) concentration by some cyanobacterial isolates. *Environ. Sci. Pollut. Res. Int.* 15, 478–480. doi: 10.1007/s11356-008-0027-y
- Pal, A., and Paul, A. (2004). Aerobic chromate reduction by chromium-resistant bacteria isolated from serpentine soil. *Microbiol. Res.* 159, 347–354. doi: 10.1016/j.micres.2004.08.001
- Park, D. H., and Kim, B. H. (2001). Growth properties of the iron-reducing bacteria, *Shewanella putrefaciens* IR-1 and MR-1 coupling to reduction of Fe(III) to Fe(II). *J. Microbiol.* 39, 273–278.
- Parker, D. L., Borer, P., and Bernier, R. (2011). The response of *Shewanella oneidensis* MR-1 to Cr(III) toxicity differs from that to Cr(VI). *Front. Microbiol.* 2:223. doi: 10.3389/fmicb.2011.00223
- Petrovskis, E. A., Vogel, T. M., and Adriaens, P. (1994). Effects of electron acceptors and donors on transformation of tetrachloromethane by *Shewanella putrefaciens* MR-1. *FEMS Microbiol. Lett.* 121, 357–363. doi: 10.1016/0378-1097(94)90317-4
- Pfaffl, M. (2001). A new mathematical model for relative quantification in real-time RT-PCR. *Nucleic Acids Res.* 29, 2002–2007. doi: 10.1093/nar/29.9.e45
- Philip, L., Iyengar, L., and Venkobachar, C. (1998). Cr (VI) reduction by *Bacillus coagulans* isolated from contaminated soils. *J. Environ. Eng.* 124, 1165–1170. doi: 10.1061/(ASCE)0733-9372(1998)124:12(1165)

- Picardal, F. W., Arnold, R., Couch, H., Little, A., and Smith, M. (1993). Involvement of cytochromes in the anaerobic biotransformation of tetrachloromethane by *Shewanella putrefaciens* 200. *Appl. Environ. Microbiol.* 59, 3763–3770.
- Puzon, G. J., Roberts, A. G., Kramer, D. M., and Xun, L. (2005). Formation of soluble organo-chromium (III) complexes after chromate reduction in the presence of cellular organics. *Environ. Sci. Technol.* 39, 2811–2817. doi: 10.1021/es048967g
- Rai, D., Moore, D. A., Hess, N. J., Rao, L., and Clark, S. B. (2004). Chromium(III) hydroxide solubility in the aqueous $\text{Na}^+ - \text{OH}^- - \text{H}_2\text{PO}_4^- - \text{HPO}_4^{2-} - \text{PO}_4^{3-}$ system: a thermodynamic model. *J. Solution Chem.* 33, 1213–1242. doi: 10.1007/s10953-004-7137-z
- Ramirez-Diaz, M. I., Diaz-Perez, C., Vargas, E., Riveros-Rosas, H., Campos-Garcia, J., and Cervantes, C. (2008). Mechanisms of bacterial resistance to chromium compounds. *Biometals* 21, 321–332. doi: 10.1007/s10534-007-9121-8
- Remoundaki, E., Hatzikoseyian, A., and Tsezos, M. (2007). A systematic study of chromium solubility in the presence of organic matter: consequences for the treatment of chromium-containing wastewater. *J. Chem. Technol. Biotechnol.* 82, 802–808. doi: 10.1002/jctb.1742
- Ross, D. E., Brantley, S. L., and Tien, M. (2009). Kinetic characterization of OmcA and MtrC, terminal reductases involved in respiratory electron transfer for dissimilatory iron reduction in *Shewanella oneidensis* MR-1. *Appl. Environ. Microbiol.* 75, 5218–5226. doi: 10.1128/aem.00544-09
- Schwalb, C., Chapman, S. K., and Reid, G. A. (2003). The tetraheme cytochrome CymA is required for anaerobic respiration with dimethyl sulfoxide and nitrite in *Shewanella oneidensis*. *Biochemistry* 42, 9491–9497. doi: 10.1021/bi034456f
- Shen, H., and Wang, Y.-T. (1994a). Biological reduction of chromium by *E. coli*. *J. Environ. Eng.* 120, 560–572. doi: 10.1061/(ASCE)0733-9372
- Shen, H., and Wang, Y.-T. (1994b). Modeling hexavalent chromium reduction in *Escherichia coli* 33456. *Biotechnol. Bioeng.* 43, 293–300. doi: 10.1002/bit.260430405
- Sheng, G. P., Yu, H. Q., and Li, X. Y. (2010). Extracellular polymeric substances (EPS) of microbial aggregates in biological wastewater treatment systems: a review. *Biotechnol. Adv.* 28, 882–894. doi: 10.1016/j.biotechadv.2010.08.001
- Shi, L., Rosso, K. M., Clarke, T. A., Richardson, D. J., Zachara, J. M., and Fredrickson, J. K. (2012). Molecular underpinnings of Fe(III) oxide reduction by *Shewanella oneidensis* MR-1. *Front. Microbiol.* 3:50. doi: 10.3389/fmicb.2012.00050
- Sugden, K. D., Campo, C. K., and Martin, B. D. (2001). Direct oxidation of guanine and 7,8-dihydro-8-oxoguanine in DNA by a high-valent chromium complex: A possible mechanism for chromate genotoxicity. *Chem. Res. Toxicol.* 14, 1315–1322. doi: 10.1021/tx010088
- Thatoi, H., Das, S., Mishra, J., Rath, B. P., and Das, N. (2014). Bacterial chromate reductase, a potential enzyme for bioremediation of hexavalent chromium: a review. *J. Environ. Manage.* 146, 383–399. doi: 10.1016/j.jenvman.2014.07.014
- Tremblay, P. L., Aklujkar, M., Leang, C., Nevin, K. P., and Lovley, D. (2012). A genetic system for *Geobacter metallireducens*: role of the flagellin and pilin in the reduction of Fe(III) oxide. *Environ. Microbiol. Rep.* 4, 82–88. doi: 10.1111/j.1758-2229.2011.00305.x
- Viamajala, S., Peyton, B. M., and Petersen, J. N. (2003). Modeling chromate reduction in *Shewanella oneidensis* MR-1: development of a novel dual-enzyme kinetic model. *Biotechnol. Bioeng.* 83, 790–797. doi: 10.1002/bit.10724
- Viamajala, S., Peyton, B. M., Sani, R. K., Apel, W. A., and Petersen, J. N. (2004). Toxic effects of Chromium(VI) on anaerobic and aerobic growth of *Shewanella oneidensis* MR-1. *Biotechnol. Prog.* 20, 87–95. doi: 10.1021/bp034131q
- Wang, P.-C., Mori, T., Komori, K., Sasatsu, M., Toda, K., and Ohtake, H. (1989). Isolation and characterization of an *Enterobacter cloacae* strain that reduces hexavalent chromium under anaerobic conditions. *Appl. Environ. Microbiol.* 55, 1665–1669.
- Wang, Y., Sevinc, P. C., Belchik, S. M., Fredrickson, J., Shi, L., and Lu, H. P. (2013). Single-cell imaging and spectroscopic analyses of Cr(VI) reduction on the surface of bacterial cells. *Langmuir* 29, 950–956. doi: 10.1021/la303779y
- Wang, Y.-T., and Xiao, C. (1995). Factors affecting hexavalent chromium reduction in pure cultures of bacteria. *Water Res.* 29, 2467–2474. doi: 10.1016/0043-1354(95)00093-z
- Wu, Y., Liu, T., Li, X., and Li, F. (2014). Exogenous electron shuttle-mediated extracellular electron transfer of *Shewanella putrefaciens* 200: electrochemical parameters and thermodynamics. *Environ. Sci. Technol.* 48, 9306–9314. doi: 10.1021/es5017312
- Yamamoto, K., Kato, J., Yano, T., and Ohtake, H. (1993). Kinetics and modeling of hexavalent chromium reduction in *Enterobacter cloacae*. *Biotechnol. Bioeng.* 41, 129–133. doi: 10.1002/bit.260410117
- Zakaria, Z. A., Zakaria, Z., Surif, S., and Wan, A. A. (2007). Hexavalent chromium reduction by *Acinetobacter haemolyticus* isolated from heavy-metal contaminated wastewater. *J. Hazard. Mater.* 146, 30–38. doi: 10.1016/j.jhazmat.2006.11.052
- Zhang, W., Li, X., Liu, T., Li, F., and Shen, W. (2014). Competitive reduction of nitrate and iron oxides by *Shewanella putrefaciens* 200 under anoxic conditions. *Colloids Surf. A Physicochem. Eng. Asp.* 445, 97–104. doi: 10.1016/j.colsurfa.2014.01.023
- Zhitkovich, A., Voitkun, V., and Costa, M. (1996). Formation of the amino acid-DNA complexes by hexavalent and trivalent chromium *in vitro*: importance of trivalent chromium and the phosphate group. *Biochemistry* 35, 7275–7282. doi: 10.1021/bi960147w

Conflict of Interest Statement: The authors declare that the research was conducted in the absence of any commercial or financial relationships that could be construed as a potential conflict of interest.

Copyright © 2016 Han, Li, Liu, Li, Wu, Wang and Chen. This is an open-access article distributed under the terms of the Creative Commons Attribution License (CC BY). The use, distribution or reproduction in other forums is permitted, provided the original author(s) or licensor are credited and that the original publication in this journal is cited, in accordance with accepted academic practice. No use, distribution or reproduction is permitted which does not comply with these terms.



Segregation of the Anodic Microbial Communities in a Microbial Fuel Cell Cascade

Douglas M. Hodgson¹, Ann Smith², Sonal Dahale¹, James P. Stratford³, Jia V. Li^{4,5}, André Grünig⁶, Michael E. Bushell¹, Julian R. Marchesi^{2,4} and C. Avignone Rossa^{1*}

¹ Department of Microbial and Cellular Sciences, University of Surrey, Guildford, UK, ² Cardiff School of Biosciences, Cardiff University, Cardiff, UK, ³ Warwick Integrative Synthetic Biology Centre, University of Warwick, Coventry, UK, ⁴ Centre for Digestive and Gut Health, Department of Surgery and Cancer, Imperial College London, London, UK, ⁵ Division of Computational and Systems Medicine, Department of Surgery and Cancer, Imperial College London, London, UK, ⁶ Department of Computer Science, University of Surrey, Guildford, UK

OPEN ACCESS

Edited by:

Haoyi Cheng,
Chinese Academy of Sciences, China

Reviewed by:

Christopher L. Hemme,
University of Rhode Island, USA
Chu-Ching Lin,
National Central University, Taiwan
Yonggang Yang,
Guangdong Institute of Microbiology,
China

*Correspondence:

C. Avignone Rossa
c.avignone-rossa@surrey.ac.uk

Specialty section:

This article was submitted to
Microbiotechnology, Ecotoxicology
and Bioremediation,
a section of the journal
Frontiers in Microbiology

Received: 31 January 2016

Accepted: 26 April 2016

Published: 11 May 2016

Citation:

Hodgson DM, Smith A, Dahale S, Stratford JP, Li JV, Grünig A, Bushell ME, Marchesi JR and Avignone Rossa C (2016) Segregation of the Anodic Microbial Communities in a Microbial Fuel Cell Cascade. *Front. Microbiol.* 7:699.
doi: 10.3389/fmicb.2016.00699

Metabolic interactions within microbial communities are essential for the efficient degradation of complex organic compounds, and underpin natural phenomena driven by microorganisms, such as the recycling of carbon-, nitrogen-, and sulfur-containing molecules. These metabolic interactions ultimately determine the function, activity and stability of the community, and therefore their understanding would be essential to steer processes where microbial communities are involved. This is exploited in the design of microbial fuel cells (MFCs), bioelectrochemical devices that convert the chemical energy present in substrates into electrical energy through the metabolic activity of microorganisms, either single species or communities. In this work, we analyzed the evolution of the microbial community structure in a cascade of MFCs inoculated with an anaerobic microbial community and continuously fed with a complex medium. The analysis of the composition of the anodic communities revealed the establishment of different communities in the anodes of the hydraulically connected MFCs, with a decrease in the abundance of fermentative taxa and a concurrent increase in respiratory taxa along the cascade. The analysis of the metabolites in the anodic suspension showed a metabolic shift between the first and last MFC, confirming the segregation of the anodic communities. Those results suggest a metabolic interaction mechanism between the predominant fermentative bacteria at the first stages of the cascade and the anaerobic respiratory electrogenic population in the latter stages, which is reflected in the observed increase in power output. We show that our experimental system represents an ideal platform for optimization of processes where the degradation of complex substrates is involved, as well as a potential tool for the study of metabolic interactions in complex microbial communities.

Keywords: microbial fuel cells, microbial communities, electroactive bacteria, metagenomic analysis, metabolite profiling, anodic biofilms

INTRODUCTION

The diverse microbial species present in natural environments interact with each other through metabolic and functional relationships that ensure the activity and stability of the community. Growth and survival of the species in the community depend on the exchange of metabolic products, especially in processes such as the degradation of complex natural polymers, such as

polysaccharides, proteins, nucleic acids, and lipids (Sieber et al., 2012; Morris et al., 2013). Those synergistic interactions are the basis of natural processes such as the degradation of plant or animal residues, or the biogeochemical cycling of carbon, nitrogen or sulfur, but can also be essential in managed or artificial processes for agriculture, the food industry, wastewater treatment, or industrial bioprocesses (Brenner et al., 2008; Fuhrman, 2009; Chiu et al., 2014; Jacobsen and Hjelmsø, 2014).

The interactions among the species in a microbial consortium affect the function, activity, and stability of the community, providing improved metabolic capabilities. This is exploited in microbial fuel cells (MFCs), bioelectrochemical devices that convert organic or inorganic substrate chemical energy into electrical energy, by the metabolic activity of microorganisms. The power output of an MFC will depend on how efficiently the anodic biofilm catalyzes the decomposition of the fuel source and transfers electrons to the anode (Wrighton et al., 2010). While single microbial species are very efficient for the conversion of simple molecules into electricity, MFCs inoculated with microbial communities are used to catalyze the degradation of substrate mixtures (Feng et al., 2008; Greenman et al., 2009). Efficient degradation of complex feedstocks requires the complete breakdown of different macromolecules, achievable only through the combination of diverse microbial metabolic activities and long residence times in the anode chamber.

In an MFC inoculated with a natural microbial community, acclimatization to a given substrate drives the assembly of anode-associated mixed species biofilms toward definable consortia (Chae et al., 2009; Yates et al., 2012). The anaerobic environment in the MFC anode chamber results in a microbial community composed predominantly of fermentative bacteria and electrogenic anodophilic species. Our recent studies have demonstrated that increased power output is associated with both elevated microbial diversity (Stratford et al., 2014) and abundance of anaerobic respirors (Grüning et al., 2015). Fermentative species are unable to fully oxidize carbohydrates and instead undergo fermentative metabolism (Pfeiffer et al., 2001), while electrogenic bacteria oxidize non-fermentable substrates (e.g., acetate), and transfer the resulting electrons to an electron acceptor (EA; Kiely et al., 2011; Sun et al., 2015). Previous reports in single MFCs have suggested a syntrophic link between fermentation and electogenesis (Freguia et al., 2008; Kimura and Okabe, 2013), but no assignment of specific taxa participating in the relationship has been provided. Syntrophic interactions have been studied using single substrates in MFCs (Lu et al., 2012) or in microbial electrolysis cells (MECs), a different bioelectrochemical system (Sun et al., 2012), while metabolic interactions and the mechanisms of electron transfer have been analyzed in binary systems, confirming syntrophy in co-cultures of two species (Butler et al., 2009; Rotaru et al., 2012).

Although almost all of the studies reported make use of individual MFCs, systems where a series of smaller MFCs units is connected in a hydraulic cascade (“stack”) have resulted in improved power output and increased efficiency (Gálvez et al., 2009; Gurung and Oh, 2012; Winfield et al., 2012; Zhuang et al., 2012; Ledezma et al., 2013). Therefore understanding the microbial ecology of such cascading systems is key to improving

their yield and stability. In this work, we studied the anodic microbial communities and their associated metabolism in a cascade of MFCs fed with dried distiller’s grain with solubles (DDGS), a downstream product of the bioethanol industry (Eskicioglu et al., 2011) which has not been previously reported as a feed substrate in MFCs. We analyzed the changes in the taxonomic, metabolic, and electrochemical characteristics of each MFC within the cascade, with the objective of understanding the functional and structural modifications of the microbial community involved in the process. We show that communities with different metabolic characteristics can be identified along the cascade, as a result of the metabolic interactions between species. We suggest that the experimental approach presented would be applicable to other processes involving microbial communities.

MATERIALS AND METHODS

Preparation of DDGS Medium

The medium used throughout this study was 10% w/v DDGS, prepared by autoclaving a 10% (w/v) suspension of wheat DDGS in distilled water for 1 h at 121°C. The DDGS slurry obtained was then sieved through a 0.3 mm mesh (Endecotts Ltd., UK) and centrifuged at 6370×*g* for 30 min to remove insoluble particles. The medium was adjusted to pH 7 and autoclaved at 121°C for 15 min. The composition of the 10% DDGS medium was (g.l⁻¹): total carbohydrates (as glucose equivalents), 16.80; free glucose, 0.14; glycerol, 6.60; pentosans, 2.98; L-lactate, 1.61; total phosphates, 0.67.

Preparation of MFC Inoculum

A microbial community derived from lignocellulose compost was used as the inoculum for the MFC cascade. The community was obtained by vigorously mixing 10% w/v lignocellulosic compost with PBS and inoculating the liquid fraction into a bioreactor (working volume 1 l), which was continuously fed with 10% DDGS medium (flow rate = 50 ml.h⁻¹) for 840 h. The enrichment process was performed under aerobic and anaerobic conditions, and both enriched communities were tested for their electrogenic activity in single MFCs. The aerobically enriched community generated a higher peak power at 120 h, and was therefore chosen as the inoculum for the MFCs used in this study (Supplementary Figure S1).

MFCs Design and Operation

The single-chamber MFCs used in this study were designed to allow anode biofilm samples to be removed without the need to disassemble the MFC. Each cell consisted of a 140 cm³ Perspex anode chamber with Perspex plates on either side. Air was able to access the cathode through four 0.5 cm × 4 cm slots cut into the cathode-side plate. Insulated Ni/Cr wire (Advent Research Materials, UK) was threaded through the cathode and protruded between the plate and chamber. The anode consisted of an 8 cm by 22 cm carbon fiber cloth wrapped around a Perspex rod, with insulated Ni/Cr wire threaded through and around the carbon fiber cloth and rod; held in place with a rubber bung. The exposed anode surface area was 96.5 cm².

The air-breathing cathode consisted of 410 μm thick carbon cloth, coated with 4 mg cm^{-2} of Pt black catalyst with polytetrafluoroethylene binder (FuelCellsEtc, USA) and was hot-pressed onto Nafion[®] 115 proton-exchange membrane (DuPont, USA) as previously described (Beecroft et al., 2012).

The working volume of each MFC was 127 cm^3 . A magnetic bar placed in each anode compartment was used to ensure sufficient mixing of the anolyte suspension.

MFC Cascade

Four MFCs were connected hydraulically, with the effluent of one MFC feeding into the next downstream (Figure 1). The medium was continuously purged with oxygen-free nitrogen gas (OFN) and supplied to the MFC cascade at a flow rate of 6.35 $\text{ml}\cdot\text{h}^{-1}$, resulting in a hydraulic retention time (HRT) of 20 h for each MFC in the cascade (80 h for the whole cascade). Each MFC was inoculated with 1 ml of enriched lignocellulosic culture and operated in batch mode for the first 24 h. The MFCs were operated at 30°C and samples taken for microbial and chemical analysis every 120 h (six anode chamber volume changes) thereafter. All the results were obtained from three independent biological replicates.

Electrochemical Measurements

Microbial fuel cell voltage was monitored using an Arbin BT2143 battery tester controlled with MITS Pro software (Arbin Instruments, USA) across a fixed external resistance of 1000 Ω . The electrical current was calculated using Ohm's law, $I = V/R$, where V is the measured voltage and R is the external resistance. Electrical power production was determined using the derivation of Joule's law, where power $P = V \times I$. Volumetric power and current density were calculated by dividing the output by the total anode chamber volume. Polarization curves were carried out for the single MFC units in the cascade every 120 h by connecting the MFC to external load values ranging from 700 000 to 250 Ω for 5 min intervals at each resistance, to ensure the MFC reached a stable output.

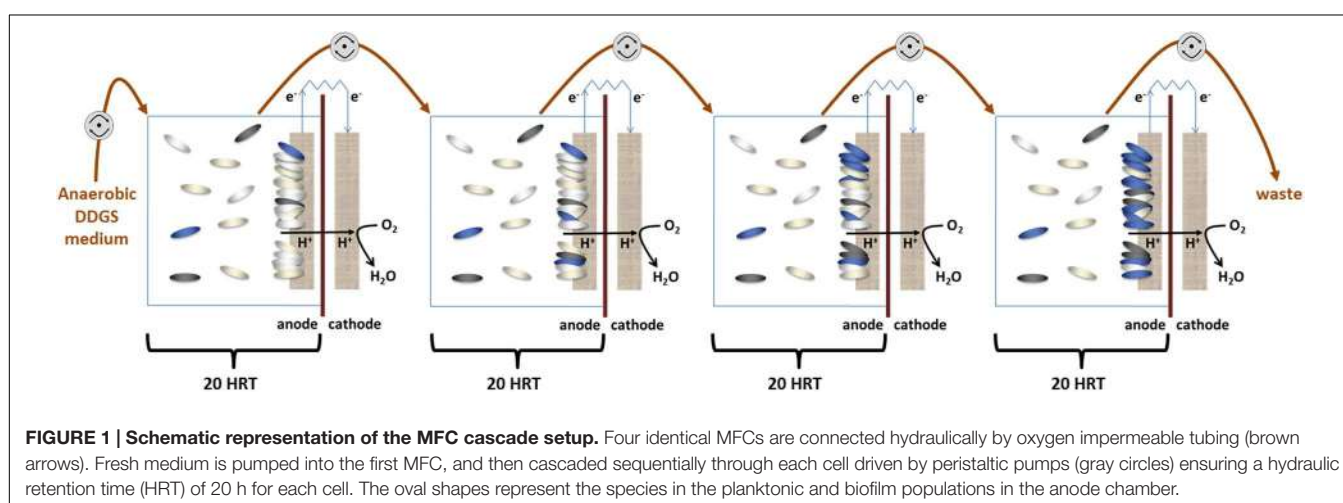
Microbial Community Analysis

Total DNA was extracted from either the anode biofilm or the anolyte suspension using FastDNA Spin Kit for Soil (MP Biomedicals, UK). To sample the anodic biofilm, the anode, wrapped around a central Perspex rod, was removed briefly from the MFC set up in an aseptic environment. Biofilm samples were taken from the anode using a sterile scalpel and suspended in 1 ml of PBS containing 20% (w/v) glycerol and stored at -20°C. The anolyte suspension was sampled by taking 500 μl of the suspension under aseptic conditions and added to 500 μl of 40% (w/v) glycerol – PBS and stored at -20°C. Prior to DNA extraction, the samples were centrifuged (10 000 $\times g$, 5 min), washed three times with 1 mL PBS and resuspended in 100 μl of nuclease free water (Promega, UK).

PCR and subsequent sequencing are described in the literature (Dowd et al., 2008) and were performed at the Research and Testing Laboratory (Lubbock, USA). The V1–V3 hypervariable regions of 16S rRNA genes were amplified for sequencing using the following forward and reverse fusion primers: 28F-GAGTTTGATCNGGCTCAG and 519R-GTNTTACNGCGCKGCTG. Trace data was deposited at the EMBL-EBI European Nucleotide Archive with the project accession PRJEB9971. Analysis of the 16S rRNA sequencing data was performed using Mothur v1.32.1 to v1.34.1 as previously described (MacIntyre et al., 2015). All OTUs were defined using a cut off value of 97%. Taxonomic relative abundances are available in the Supplementary Information.

Chemical Analyses

All liquid samples (anolyte suspension or fresh medium) were filtered through 0.22 μm membranes (Millex, Merck Millipore Ltd., Ireland). Total carbohydrate analysis was performed using a colorimetric phenol/sulphuric acid method (Dubois et al., 1956). Total phosphate concentration was determined using a phosphate assay kit (Merck, Germany). L-lactate and glycerol were determined using EnzyChrom enzymatic assay kits ECLC-100 and EGLY-100, respectively (BioAssay Systems, USA). The concentrations of glucose and iron were determined



using Sigma assay kits GAGO20 and MAK025 (Sigma-Aldrich, USA). The pentosan content in the medium was quantified using a colorimetric method (Finnie et al., 2006) and xylose concentration was measured using an enzymatic assay kit (Megazyme, Ireland). Acetate, succinate, and propionate in the suspension were determined using ^1H NMR spectroscopy as previously described Li et al. (2011). Measurement of pH was performed on 10 ml of anolyte suspension using a pH-meter (Mettler Toledo MP220, Switzerland).

Statistical Analysis

Linear mixed effect models were built wherein biological replicate (cascade run: 1,2,3) was included as a random factor, while fixed effects included time, fermenter abundance, and fermentation products. The significance associated with including a variable was determined by stepwise addition followed by likelihood ratio testing to compare the new model with the previous (null) model lacking the additional variable. Each model was assembled and tested in the order: intercept, time, abundance of fermenters, or metabolite concentration. For each model, standardized coefficients (β) and significances were calculated for effects associated with each independent variable.

Three models were constructed. Model (1) tested the hypothesis that time and hydraulic series order had distinct effects on MFC power output. This model also included an interaction between hydraulic series position and time. The interaction term was included to determine if the passage of time significantly altered the order of the hydraulic series. Models (2) and (3) were subsequently assembled to test the hypothesis that the concentration of acetate and fermenter abundance, respectively, predict power output. All statistical analysis was carried out using the LME4 package in R version 2.15.2

RESULTS

Electrogenic Activity and Power Output of the MFC Cascade

The microbial community in the anode of an MFC converts the chemical energy of substrates into electricity through the metabolic activity of the species present. A direct evaluation of the electrogenic activity of the system can be obtained by measuring the power output. In our experimental system (Schematically represented in Figure 1), four individual MFCs were connected hydraulically and the voltage and power output were monitored during the experiment.

The mean maximum voltage observed in the first, second, third, and fourth MFCs were 0.51, 0.54, 0.55, and 0.64 V, respectively, while the mean peak powers attained were 0.37, 0.43, 0.50, and 0.73 W.m^{-3} . The polarization curves (Figure 2) demonstrate that the medium fed at the selected flow rate facilitated power production in the four MFCs, with the performance of each MFC consistently increasing along the cascade.

In order to confirm that the increase of power along the MFC cascade is significant, a linear effects model was constructed

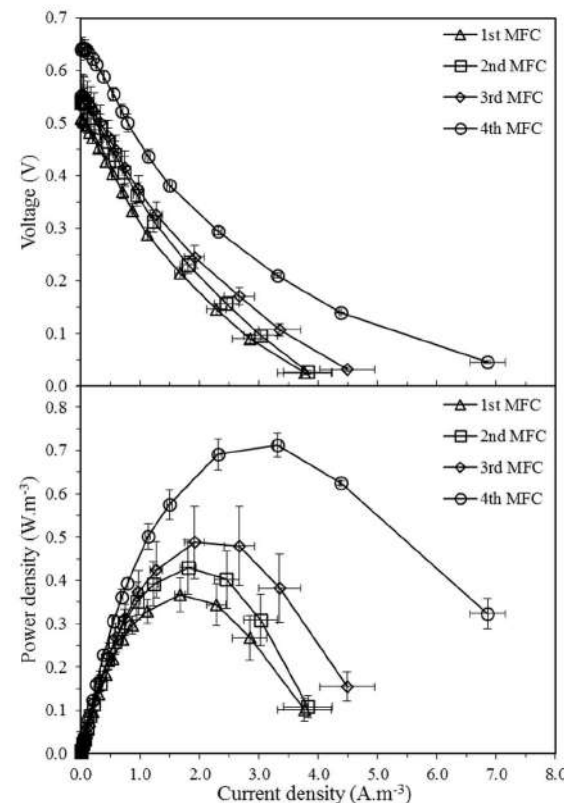


FIGURE 2 | Voltage output and volumetric power density curves as a function of volumetric current density of four MFCs connected hydraulically in cascade. Results are mean values of three cascade biological replicates at 120, 240, 360, and 480 h. Error bars represent standard error of the biological replicates.

to correlate power output with the time at which peak power was measured and with the position of the MFC in the cascade (Table 1, Model 1). The position of the MFC in the cascade showed a statistically significant positive correlation with peak power ($\beta = 0.73, p \leq 0.0001$), confirming that the power output does indeed increase along the cascade. On the other hand, time had no significant effect on the relationship between the position of the MFC in the cascade and the peak power output ($\beta = -0.21, p = 0.45$), thus confirming that the power output of the MFCs in the cascade remained at steady state over the course of the experiment.

Metabolic Product Analysis

The concentrations of carbon sources and metabolic end products in the anolyte suspension were measured in each MFC during the experiment to obtain an indication of the activity of the different metabolic pathways in the species present in the communities. Identification of those pathways is essential to understand the metabolic mechanisms prevailing in each stage of the cascade.

Dried distiller's grain with solubles contains a variety of carbohydrates and other organic compounds, including glycerol,

TABLE 1 | Mixed effect models, testing the effect of cascade MFC position, time, fermentative population abundance and fermentation on peak power, assessed by β weight.

Independent variables		β	SE	χ^2	p
Model 1	Hydraulic series position	0.73	0.21	21	<0.0001*
	Time	-0.36	0.21	26	0.0001*
	Time*series position	-0.21	0.29	0.6	0.45
Model 2	Acetate	0.67	0.15	16	<0.0001*
	Time	-0.73	0.11	14	0.0001*
Model 3	Total fermentative population	0.50	0.11	18	<0.0001*
	Time	-0.44	0.10	15	0.0001*

*Statistical significance value <0.05 .

pentosans and glucose, that can be fermented by several of the species present in the community to generate short chain fatty acids (SCFAs) such as propionate, succinate, or acetate. In general, SCFAs are ideal carbon sources for anodophilic bacteria (Jang et al., 2010), with acetate being the preferred substrate for electron donation to the anode by various species (Choi et al., 2011; Sun et al., 2015). In the first MFC, glycerol (present in the feed at 6.60 g l^{-1}) was almost completely consumed (**Figure 3A**). Almost no lactate was consumed in that MFC (lactate concentration remained close to 1.6 g l^{-1} , the concentration in DDGS), but it was undetectable in the second MFC. Acetate concentration increased consistently across the cascade (**Figure 3C**), reaching a maximum concentration of 2.57 g l^{-1} . The concentration of acetate significantly correlates with peak power ($\beta = 0.67, p \leq 0.0001$), as shown from the results of a linear effects model correlating power output with substrate concentration across the cascade (**Table 1**, Model 2).

Another significant source of organic carbon in the medium is the pentosan fraction, present at a concentration of $\sim 3 \text{ g l}^{-1}$. Although no free xylose was detected in DDGS, this sugar is most likely released by microbial hydrolysis of the pentosan fraction. It is present in the MFC cascade at the relatively low concentration of 0.20 g l^{-1} (Supplementary Information). It has been reported that xylose in MFCs can be fermented into acetate (Huang and Logan, 2008; Mäkinen et al., 2013), which is used as a substrate for electricity production.

Principal component analysis (PCA) of the ^1H NMR spectral data of the MFC cascade anolyte suspension (**Figure 4**) shows a clear metabolic shift between the first and last MFC in the cascade along the second principal component, which is further supported by a supervised orthogonal partial least squares discriminant analysis (O-PLS-DA) between the two groups (**Figure 5**). These results strongly suggest a segregation of the anodic communities across the cascade.

Microbial Community Analysis

The observed changes in the power output and in the metabolite profile of the MFC cascade are suggestive of changes in the metabolic activity of the anodic microbial community. The composition, dynamics, and taxonomy of the bacterial communities in the anodic biofilm and in the anolyte suspended culture were analyzed by next-generation sequencing of the amplified 16S rRNA genes of the entire microbial community in each sample. To avoid PCR-induced artifacts and bias (Youssef et al., 2009; Engelbrektson et al., 2010), the same DNA extraction, amplification, and sequencing methods were applied to all samples to allow fair comparison of taxonomic data sets (Dowd et al., 2008; MacIntyre et al., 2015).

Four genera made up on average 74.3% of the microbial communities observed in each MFC anodic biofilm and anolyte suspension. In order of mean % relative abundance, these

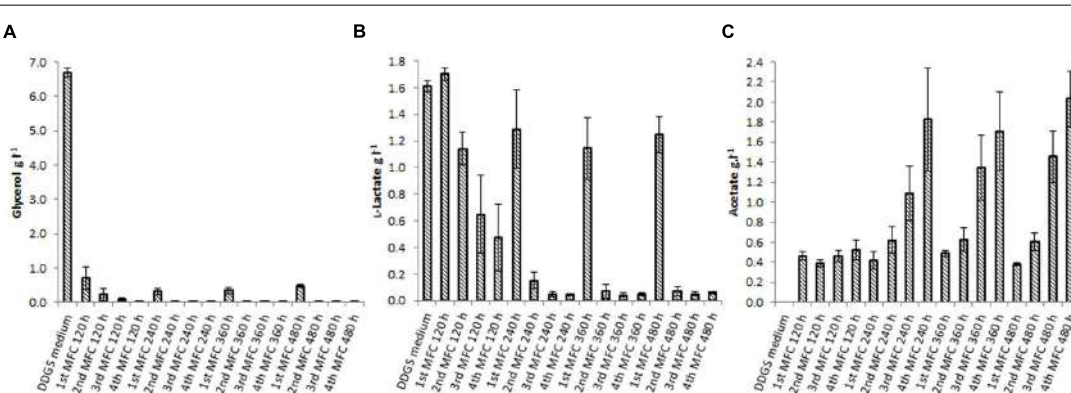


FIGURE 3 | Concentration of the fermentable carbohydrates glycerol (A) and lactate (B), and the fermentation end product acetate (C) measured in the DDGS medium and the anolyte suspension across the MFC cascade. Error bars are standard error of three cascade biological replicates, apart from the DDGS medium which are standard error of three technical replicates.

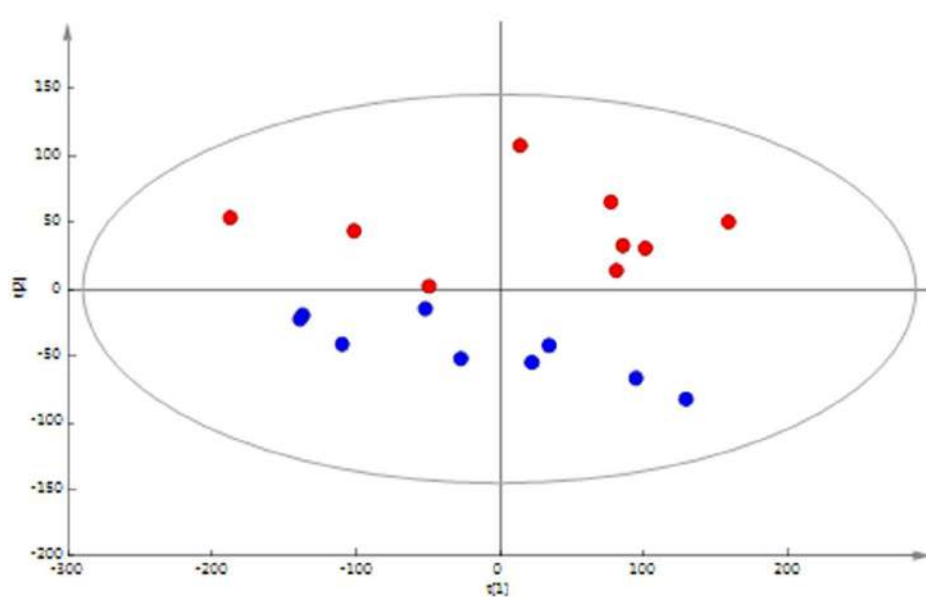


FIGURE 4 | PCA scores plot of ^1H NMR spectral data of anolyte from MFC1 (blue) and MFC4 (red). A clear separation between the initial and final MFCs in the cascade along the second principal component (PC2) is observed [R^2X (PC1) = 57.2%; R^2X (PC2) = 14.5%; Q^2 = 0.53].

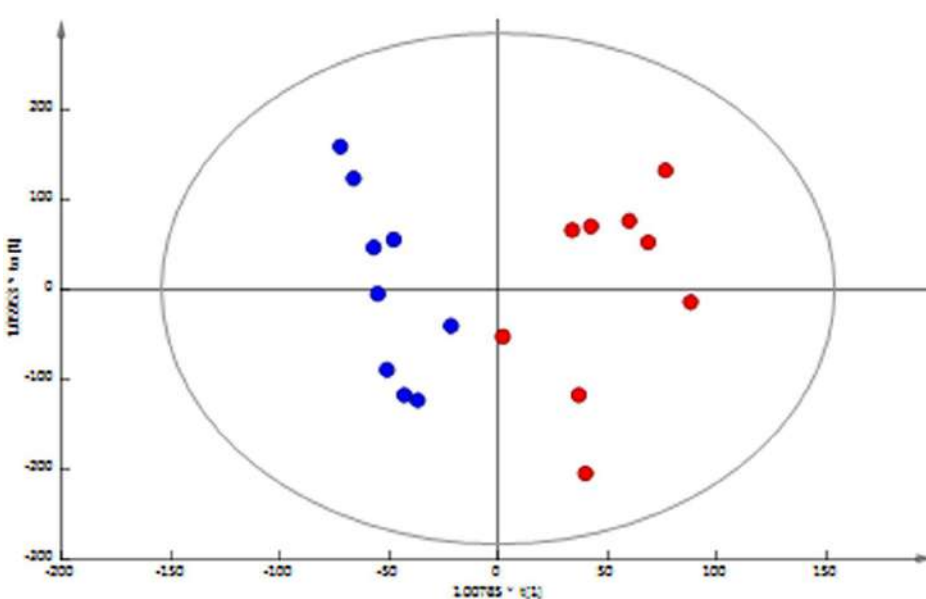


FIGURE 5 | OPLS-DA scores plot of ^1H NMR spectral data of anolyte from MFC1 (blue) and MFC4 (red) shows a significant difference between the initial and final MFCs in the cascade (R^2X = 71.5%; Q^2Y = 0.78; cross-validated ANOVA p = 0.0003).

were: *Clostridium* ($35.7 \pm 14.1\%$), *Rummeliibacillus* ($19.0 \pm 5.9\%$), *Lactococcus* ($11.4 \pm 3.5\%$), and *Bacteroides* ($8.2 \pm 3.6\%$). Ten other genera with lower abundances were *Streptococcus* ($4.1 \pm 1.8\%$), *Enterococcus* ($3.9 \pm 1.3\%$), *Proteinilasticum* ($3.3 \pm 2.7\%$), *Dysgonomonas* ($1.1 \pm 0.3\%$), and *Leuconostoc* ($1.1 \pm 0.3\%$), *Ethanoligenes* ($0.8 \pm 0.4\%$), *Comamonas* ($0.7 \pm 0.2\%$), *Sporobacterium* ($0.7 \pm 0.5\%$), *Anaerotruncus* ($0.6 \pm 0.4\%$), and *Stenotrophomonas* ($0.5 \pm 0.2\%$). Those 14 strains made up to 96.1% of the identified

genera in the population. The complete list of identified genera and their relative abundances are available in the Supplementary Information.

Each genus was assigned a metabolic class with respect to terminal EAs according to their typical metabolism according to the literature (Table 2). These were either fermenters, which use intracellular metabolites as EAs, or anaerobic respirators, which are able to fully oxidize fermentation products using a

terminal EA other than oxygen, such as sulfate, nitrate or an external anode with the appropriate redox potential. However, some species are capable of performing either metabolic function, depending on the prevalent environmental and/or physiological conditions. As it is impossible to identify the precise metabolic function of individual species in a complex microbial community, we have made the classification according to the predominant (or more likely) metabolic type at the level of genus, informed by the literature and by the type of metabolic products detected in the medium. We have used this approach before in the analysis of the microbial communities in single MFCs (Stratford et al., 2014; Grüning et al., 2015).

The shifting dynamics of these 14 genera in the anodic biofilm and the anolyte suspension across the MFC cascade is shown in **Figure 6**. The heatmap shows the temporal changes of the most abundant genera in the individual MFCs, and the changes in abundances according to the position of the relevant MFC in the cascade. While the overall temporal trend along the cascade shows a clear increase of the respirators and a decrease of the fermenters, the time-course of the first two MFCs shows a slight increase of the fermenters, and an even slighter increase of respirators in the anolyte. At 120 h, the system has probably not reached the definitive composition, as it is suggested by the lower power output and the metabolite profile. Previous work has differentiated between electrical steady state and biological steady state (Ren et al., 2011), and our observation could be explained using this concept: even though the system might have reached steady electrical output, the biofilms were still maturing at 120 h, reaching the biological steady state at 240 h. Our results show that the system is fully mature at longer times: The segregation of the communities in the MFC cascade occurs as the biofilm reaches biological steady state.

The % relative abundance of genera with fermentative metabolism in each MFC decreased from an average of 75.6%

($\pm 10.1\%$) of the anodic biofilm in the first MFC in the cascade to just 36.7% ($\pm 8.3\%$) in the final MFC (**Figure 6A**). The largest changes were observed for *Proteiniclasticum* (7.4-fold decrease), *Clostridium* (2.5-fold decrease), and *Anaerotruncus* (1.5-fold decrease). Conversely, the % relative abundance of anaerobic respiring genera in each MFC increased from an average of just 24.4% ($\pm 10.1\%$) of the anodic biofilm in the first MFC in the cascade to 63.3% ($\pm 8.3\%$) in the final MFC (**Figure 6A**). The largest increases were observed for *Comamonas* (7.7-fold), *Rummeliibacillus* (2.4-fold), and *Stenotrophomonas* (twofold).

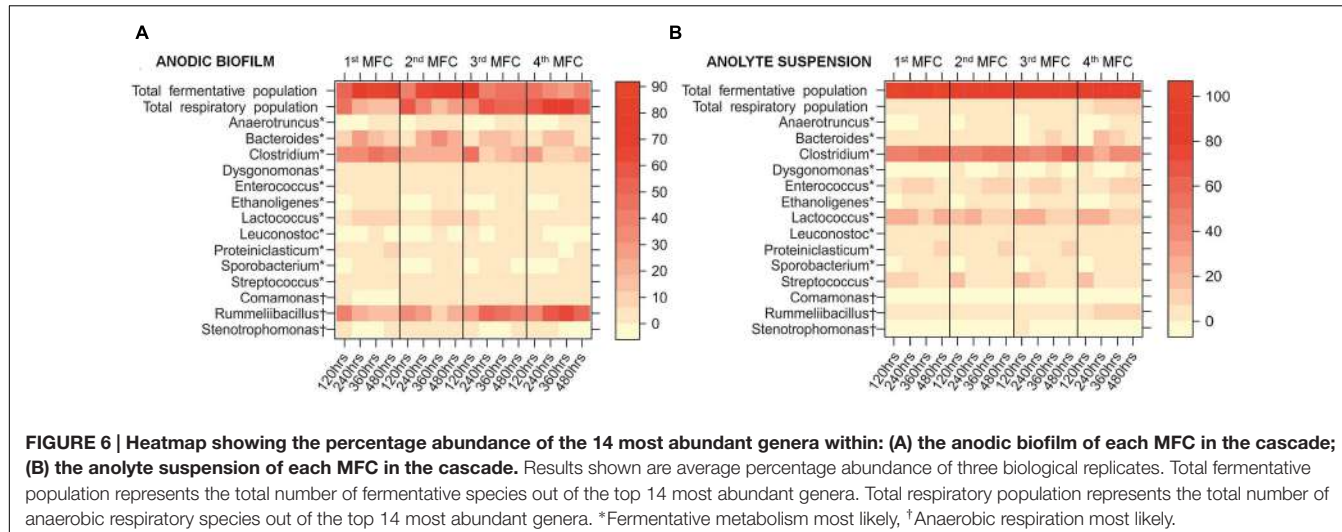
The composition of the suspended community in the anodic chamber (**Figure 6B**) was very different to that of the biofilm, and remained constant across the cascade. On average, 57.0% ($\pm 5.6\%$) of the anodic biofilm community is composed of a fermentative population, whereas in the anolyte suspension, the fermentative population makes up on average 96.1% ($\pm 1.4\%$) of the community. Fermentative metabolism does not require the use of external EAs (the anode, in an MFC), and metabolic energy is obtained by the conversion of substrates into fermentation products, which are normally excreted. On the other hand, the anaerobic respiratory population cannot fully oxidize those fermentation products without an external EA, and so are in high abundance in the anodic biofilm community.

The most abundant genus found in the MFC cascade is *Clostridium*, a member of the phylum *Firmicutes*. *Firmicutes* have been found to dominate anodic communities of acetate-fed MFCs (Aelterman et al., 2006; Wrighton et al., 2008; Beecroft et al., 2012) and cellulose-fed MFCs (Rismani-Yazdi et al., 2007). In our study, the abundance of *Clostridium* species in the anodic biofilm community (average relative abundance of $24.6 \pm 13\%$, **Figure 6A**) was nearly half of that in the anolyte suspension ($46.8 \pm 11\%$, **Figure 6B**). *Clostridium* species are able to ferment glycerol (Yazdani and Gonzalez, 2007), xylose (Balasubramanian

TABLE 2 | The 14 most abundant genera found in the anodic biofilm and anolyte suspension of triplicate MFC cascades, classified according to their most likely metabolic function.

Genus	Metabolism	Anode biofilm main	Suspension main	Biofilm cascade ↗	Biofilm cascade ↘	Reference
<i>Anaerotruncus</i>	F		X		X	Lawson et al., 2004
<i>Bacteroides</i>	F	X			X	Nishiyama et al., 2009
<i>Clostridium</i>	F		X		X	Holt, 1994
<i>Comamonas</i>	R	X		X		Gumaelius et al., 2001
<i>Dysgonomonas</i>	F	X				Lawson et al., 2002
<i>Enterococcus</i>	F		X			Cai, 1999
<i>Ethanoligenes</i>	F		X		X	Xu et al., 2010
<i>Lactococcus</i>	F		X		X	Tanaka et al., 2002
<i>Leuconostoc</i>	F		X			Giglio and McCleskey, 1953
<i>Proteiniclasticum</i>	F		X		X	Zhang et al., 2010
<i>Rummeliibacillus</i>	R	X		X		Her and Kim, 2013
<i>Sporobacterium</i>	F		X		X	Mechichi et al., 1999
<i>Stenotrophomonas</i>	R	X		X		Yu et al., 2009
<i>Streptococcus</i>	F		X		X	Thomas and Turner, 1981

F, fermentative metabolism; R, anaerobic respiration; Anode Biofilm Main: more abundant in anodic biofilm than anolyte suspension; Suspension Main: more abundant in anolyte suspension than in anodic biofilm; Biofilm Cascade ↗: increase in abundance in anodic biofilm across MFC cascade; Biofilm Cascade ↘: decrease in abundance in anodic biofilm across cascade.



et al., 2001), and various pentosans (Rogers and Baecker, 1991; Broda et al., 2000) into acetate.

Similarly to *Clostridium*, species of the fermentative *Lactococcus* genus were abundant in the anolyte suspension (average relative abundance of $18.2 \pm 1.8\%$, Figure 6B), but were much less abundant in the anodic community (average relative abundance of $4.7 \pm 1.4\%$, Figure 6A). While *Lactococcus* species are able to ferment xylose into lactic acid and acetic acid (Tanaka et al., 2002), *Lactococcus lactis* can transfer electrons to an anode using mediators such as quinones (Freguia et al., 2009) or flavins (Masuda et al., 2010).

The third most abundant fermentative genus in the anodic community was *Bacteroides* (average relative abundance of $13.3 \pm 4.6\%$, Figure 6A), which has been previously reported to be abundant in anodic communities (Beecroft et al., 2012; Jia et al., 2013). *Bacteroides* species are able to ferment a range of plant polysaccharides and xylans (Salyers et al., 1977; Cooper et al., 1985) as well as some of the sugars present in DDGS, such as xylose (Turner and Roberton, 1979).

This is the first time a *Rummeliibacillus* species has been shown to be dominant in anodic communities (Figure 6A). *Rummeliibacillus*, previously classified as *Bacillus*, are generally unable to ferment common hexoses, pentoses, hexitols, disaccharides, and trisaccharides (Nakamura et al., 2002). *Rummeliibacillus* produces the menaquinones MK-7 and MK-8 (Her and Kim, 2013), which mediate anaerobic respiration by shuttling electrons from an oxidized fermentation product to an EA. Despite playing a dominant role in the anodic biofilm (average relative abundance of $34.5 \pm 3.8\%$), the abundance of *Rummeliibacillus* species is low in the anolyte suspension, with an average relative abundance of $3.6 \pm 1.2\%$ (Figure 6B).

The effect of the abundance of fermenters in the biofilm across the cascade on the power output was tested by a linear effects model (Table 1, Model 3), which showed that the fermenters responsible for converting DDGS components into acetate have a statistically negative correlation with peak power ($\beta = -0.50, p \leq 0.0001$). This confirms that along the cascade,

the fermentative population in the suspension generates the substrates for the electrogenic population in the biofilm.

DISCUSSION

Relationships between metabolite pools, microbial functional types and power output were characterized in a hydraulic cascade of MFCs inoculated with a complex microbial community. The results obtained indicate that the microbial community in the anode self-organizes in accordance to the substrate availability. Considered individually, the MFCs showed changes in the composition of the community and in the metabolic profile, attributable to the acclimation and maturation of the community to the available substrates. When considering the whole cascade, the abundance of fermentative genera is highest in the first MFC, and decreases across the cascade. This can be explained by the decrease in fermentable substrates, which prevents the formation of a stable fermentative community in the biofilm. The anaerobic respirors, on the other hand, become more abundant in the anodic community further along the cascade due to the highest availability of SCFAs. Respirator species can oxidize those compounds and utilize the anode as the EA, resulting in the observed trends in power output.

The microbial communities in the anode could also be separated into two groups, one associated to the biofilm and another associated to the anolyte suspension. Those populations were composed by fermentative and anaerobic respiratory genera, as determined by both taxonomic and extracellular metabolite analyses. Mean genera abundances were very different, with the vast majority (>90%) of the anolyte suspension being composed of fermentative microorganisms, whereas in the anodic biofilm community the fermentative population abundance was only 50%. These differences suggest that the anode is selecting for anaerobic respirors with redox systems best suited for utilizing the anode as an EA.

Our experimental data provide evidence that fermentative pathways are active in the MFCs, converting the components

of DDGS (carbohydrates and pentosans) to yield free sugars (e.g., glucose, xylose) that can be metabolized to yield the SCFAs commonly used by electrogenic species. This is in agreement with the presence of fermentative metabolism products which accumulated across the MFC cascade, notably acetate (**Figure 3C**), propionate and succinate (Supplementary Information). The increased concentration of acetate in the fourth MFC indicates that the fermentative population in the early stages has converted all fermentable substrates into SCFAs for respiration. These might have been accumulated due to the external resistance of the MFC being too high to drain all acetate electrons through the anode.

The fermentative population themselves contribute little to power production but produce acetate, which can only be completely oxidized by the anaerobic respiratory population if electrons are donated to the anode (Grüning et al., 2015; Sun et al., 2015). Therefore for complex substrates, fermentative species play a crucial role in the ability of microbial communities to fully oxidize carbohydrates in MFCs. Although a pre-fermentation step prior to feeding MFCs could be used to provide substrates for the respiratory population (Sharma and Li, 2010; Goud and Mohan, 2011), our cascade system naturally generates a selective environment for the evolution of communities with the right composition and activities for the given substrate and HRT. Considerably longer residence times would be required in single MFCs, to achieve the same bioconversion of complex substrates to power production and the HRT would need to be fine-tuned to achieve the optimal proportions of fermentative and respiratory communities. From a scalability perspective, studies focusing on improving single MFC performance have demonstrated that increasing anodic chamber size results in an increase in internal resistance (Ieropoulos et al., 2008); connecting a series of smaller, more efficient MFCs in hydraulic cascade overcomes this limitation (Walter et al., 2015). Understanding how MFCs will perform depending on their position in the cascade is an important step toward application of this technology.

To the best of our knowledge, this is the first exhaustive analysis of microbial communities in MFC cascades, showing the link between the composition of the community, the metabolic profile and the power output, and demonstrating how the relationship between the fermentative and anodophilic populations underpin the observed increase in power yields across the cascade. Previous reports have mentioned the existence of syntrophic relationships in single MFCs fed with simple carbon sources (Freguia et al., 2008; Yamamuro et al., 2014), or simplified systems involving only two species (Kimura and Okabe, 2013).

We show here that a cascade of multiple MFCs is an ideal platform for the study of those relationships, as it provides a high-resolution map of the interactions between species. The presence of different anodic communities in the MFCs in the cascade, as demonstrated by the taxonomic analysis and illustrated in the heatmap (**Figure 6**), together with the different metabonomic profiles discussed above (**Figures 3–5**) clearly indicate that the effect of a cascade set up is the segregation of different communities according to the metabolic functions prevailing in each MFC unit. The native initial community is therefore

“stretched” along the different MFCs in the cascade, ensuring that the generated sub-communities act optimally. Changes in the structure of the cascade (e.g., changing the number of MFCs and/or the HRT) will promote changes in the structure of the sub-communities, allowing not only for a more efficient performance but also to disentangle the taxonomic structure of functional consortia (Dolfing, 2014). This approach could be extended to the study of other equally complex processes where the concerted activity of microbial communities is required.

AUTHOR CONTRIBUTIONS

DH designed and performed the experiments, and contributed in the analysis of the data, discussion and preparation of the manuscript. AS performed the genotypic analysis and contributed to the discussion. SD contributed with the bioinformatic analysis. JVL performed the metabolic analysis and discussion of the data. JS performed the statistical analysis and contributed to the discussion. AG contributed in the interpretation and discussion of the electrochemical results. MB contributed to the design of the experiments, the analysis of the metabolic data and the discussion. JM contributed in the design of the genotypic and metagenomic experimental details, and contributed in the analysis of the results. CAR supervised the design of the experiments, the overall analysis and discussion of the results, and prepared the manuscript.

FUNDING

This work was supported by grants BB/J01916X/1 and BB/J019143/1 from the UK's Biotechnology and Biological Sciences Research Council (BBSRC), under the Integrated Biorefining Research and Technology Club (IBTI) initiative.

ACKNOWLEDGMENTS

The authors would like to thank Dr. Ondrej Kosik (Centre for Crop Genetic Improvement, Rothamsted Research, UK) for assaying the pentosan content. The comments and suggestions provided by Dr. M Victoria Flores are gratefully acknowledged.

SUPPLEMENTARY MATERIAL

The Supplementary Material for this article can be found online at: <http://journal.frontiersin.org/article/10.3389/fmicb.2016.00699>

FIGURE S1 | Performance at 120 h of MFCs inoculated with aerobic and anaerobic enriched microbial community derived from lignocellulose compost. Lignocellulosic compost was used to inoculate chemostats continuously fed with 10% DDGS medium. The process was performed under aerobic and anaerobic conditions, and both enriched communities were tested for their electrogenic activity in single MFCs. The aerobically enriched community produced higher peak power at 120 h, and was therefore chosen as the inoculum for the MFC cascade.

REFERENCES

- Aelterman, P., Rabaey, K., Pham, H. T., Boon, N., and Verstraete, W. (2006). Continuous electricity generation at high voltages and currents using stacked microbial fuel cells. *Environ. Sci. Technol.* 40, 3388–3394. doi: 10.1021/es0525511
- Balasubramanian, N., Kim, J. S., and Lee, Y. Y. (2001). Fermentation of xylose into acetic acid by *Clostridium thermoaceticum*. *Appl. Biochem. Biotechnol.* 91–93, 367–376. doi: 10.1385/ABAB:91-93:1-9:367
- Beecroft, N. J., Zhao, F., Varcoe, J. R., Slade, R. C. T., Thumser, A. E., and Avignone-Rossa, C. (2012). Dynamic changes in the microbial community composition in microbial fuel cells fed with sucrose. *Appl. Microbiol. Biotechnol.* 93, 423–437. doi: 10.1007/s00253-011-3590-y
- Brenner, K., You, L., and Arnold, F. H. (2008). Engineering microbial consortia: a new frontier in synthetic biology. *Trends Biotechnol.* 26, 483–489. doi: 10.1016/j.tibtech.2008.05.004
- Broda, D. M., Saul, D. J., Bell, R. G., and Musgrave, D. R. (2000). *Clostridium algidixylanolyticum* sp. nov., a psychrotolerant, xylan-degrading, spore-forming bacterium. *Int. J. Syst. Evol. Microbiol.* 50, 623–631. doi: 10.1099/00207713-50-2-623
- Butler, J. E., Young, N. D., and Lovley, D. R. (2009). Evolution from a respiratory ancestor to fill syntrophic and fermentative niches: comparative genomics of six Geobacteraceae species. *BMC Genomics* 10:103. doi: 10.1186/1471-2164-10-103
- Cai, Y. (1999). Identification and characterization of Enterococcus species isolated from forage crops and their influence on silage fermentation. *J. Dairy Sci.* 82, 2466–2471. doi: 10.3168/jds.S0022-0302(99)75498-6
- Chae, K.-J., Choi, M.-J., Lee, J.-W., Kim, K.-Y., and Kim, I. S. (2009). Effect of different substrates on the performance, bacterial diversity, and bacterial viability in microbial fuel cells. *Bioresour. Technol.* 100, 3518–3525. doi: 10.1016/j.biortech.2009.02.065
- Chiu, H.-C., Levy, R., and Borenstein, E. (2014). Emergent biosynthetic capacity in simple microbial communities. *PLoS Comput. Biol.* 10:e03695. doi: 10.1371/journal.pcbi.1003695
- Choi, J., Chang, H. N., and Han, J. I. (2011). Performance of microbial fuel cell with volatile fatty acids from food wastes. *Biotechnol. Lett.* 33, 705–714. doi: 10.1007/s10529-010-0507-2
- Cooper, S. W., Pfeiffer, D. G., and Tally, F. P. (1985). Evaluation of xylan fermentation for the identification of *Bacteroides ovatus* and *Bacteroides thetaiotaomicron*. *J. Clin. Microbiol.* 22, 125–126.
- Dolfing, J. (2014). Syntropy in microbial fuel cells. *ISME J.* 8, 4–5. doi: 10.1038/ismej.2013.198
- Dowd, S. E., Callaway, T. R., Wolcott, R. D., Sun, Y., McKeehan, T., Hagevoort, R. G., et al. (2008). Evaluation of the bacterial diversity in the feces of cattle using 16S rDNA bacterial tag-encoded FLX amplicon pyrosequencing (bTEFAP). *BMC Microbiol.* 8:125. doi: 10.1186/1471-2180-8-125
- Dubois, M., Gilles, K. A., Hamilton, J. K., Rebers, P. A., and Smith, S. (1956). Colorimetric method for the determination of sugars and related substances. *Analyt. Chem.* 28, 350–356. doi: 10.1021/ac60111a017
- Engelbrektson, A., Kunin, V., Wrighton, K. C., Zvenigorodsky, N., Chen, F., Ochman, H., et al. (2010). Experimental factors affecting PCR-based estimates of microbial species richness and evenness. *ISME J.* 4, 642–647. doi: 10.1038/ismej.2009.153
- Eskicioglu, C., Kennedy, K. J., Marin, J., and Strehler, B. (2011). Anaerobic digestion of whole stillage from dry-corn ethanol plant under mesophilic and thermophilic conditions. *Bioresour. Technol.* 102, 1076–1086. doi: 10.1016/j.biortech.2010.08.061
- Feng, Y., Wang, X., Logan, B. E., and Lee, H. (2008). Brewery wastewater treatment using air-cathode microbial fuel cells. *Appl. Microbiol. Biotechnol.* 78, 873–880. doi: 10.1007/s00253-008-1360-2
- Finnie, S. M., Bettge, A. D., and Morris, C. F. (2006). Influence of cultivar and environment on water-soluble and water-insoluble arabinoxylans in soft wheat. *Cereal Chem.* 83, 617–623. doi: 10.1094/CC-83-0617
- Freguia, S., Masuda, M., Tsujimura, S., and Kano, K. (2009). *Lactococcus lactis* catalyses electricity generation at microbial fuel cell anodes via excretion of a soluble quinone. *Bioelectrochemistry* 76, 14–18. doi: 10.1016/j.bioelechem.2009.04.001
- Freguia, S., Rabaey, K., Yuan, Z., and Keller, J. (2008). Syntrophic processes drive the conversion of glucose in microbial fuel cell anodes. *Environ. Sci. Technol.* 42, 7937–7943. doi: 10.1021/es00482e
- Fuhrman, J. A. (2009). Microbial community structure and its functional implications. *Nature* 459, 193–199. doi: 10.1038/nature08058
- Gálvez, A., Greenman, J., and Ieropoulos, I. (2009). Landfill leachate treatment with microbial fuel cells; scale up through plurality. *Bioresour. Technol.* 100, 5085–5091. doi: 10.1016/j.biortech.2009.05.061
- Giglio, D. M., and McCleskey, C. S. (1953). The fermentation of sucrose by *Leuconostoc mesenteroides*. *J. Bacteriol.* 65, 75–78.
- Goud, R. K., and Mohan, S. V. (2011). Pre-fermentation of waste as a strategy to enhance the performance of single chambered microbial fuel cell (MFC). *Int. J. Hydrog. Ener.* 36, 13753–13762. doi: 10.1016/j.ijhydene.2011.07.128
- Greenman, J., Gálvez, A., Giusti, L., and Ieropoulos, I. (2009). Electricity from landfill leachate using microbial fuel cells: comparison with a biological aerated filter. *Enzyme Microb. Technol.* 44, 112–119. doi: 10.1016/j.enzmictec.2008.09.012
- Grüning, A., Beecroft, N. J., and Avignone-Rossa, C. (2015). Low-potential respirators support electricity production in microbial fuel cells. *Microb. Ecol.* 70, 266–273. doi: 10.1007/s00248-014-0518-y
- Gumaelius, L., Magnusson, G., Pettersson, B., and Dalhammar, G. (2001). Comamonas denitrificans sp. nov., an efficient denitrifying bacterium isolated from activated sludge. *Int. J. Syst. Evol. Microbiol.* 51, 999–1006. doi: 10.1099/00207713-51-3-999
- Gurung, A., and Oh, S.-E. (2012). The improvement of power output from stacked microbial fuel cells (MFCs). *Energy Source Part A* 34, 1569–1576. doi: 10.1080/15567036.2012.660561
- Her, J., and Kim, J. (2013). *Rummeliibacillus suwonensis* sp. nov., isolated from soil collected in a mountain area of South Korea. *J. Microbiol.* 51, 268–272. doi: 10.1007/s12275-013-3126-5
- Holt, J. (1994). *Bergey's Manual of Determinative Bacteriology*, 9th Edn. Baltimore: Williams and Wilkins.
- Huang, L., and Logan, B. E. (2008). Electricity production from xylose in fed-batch and continuous-flow microbial fuel cells. *Appl. Microbiol. Biotechnol.* 80, 655–664. doi: 10.1007/s00253-008-1588-x
- Ieropoulos, I., Greenman, J., and Melhuish, C. (2008). Microbial fuel cells based on carbon veil electrodes: stack configuration and scalability. *Int. J. Hydrogen Res.* 32, 1228–1240.
- Jacobsen, C. S., and Hjelmsø, M. H. (2014). Agricultural soils, pesticides and microbial diversity. *Curr. Opin. Biotechnol.* 27, 15–20. doi: 10.1016/j.copbio.2013.09.003
- Jang, J. K., Chang, I. S., Hwang, H. Y., Choo, Y. F., Lee, J. Y., Cho, K. S., et al. (2010). Electricity generation coupled to oxidation of propionate in a microbial fuel cell. *Biotechnol. Lett.* 32, 79–85. doi: 10.1007/s10529-009-0118-y
- Jia, J., Tang, Y., Liu, B., Wu, D., Ren, N., and Xing, D. (2013). Electricity generation from food wastes and microbial community structure in microbial fuel cells. *Bioresour. Technol.* 144, 94–99. doi: 10.1016/j.biortech.2013.06.072
- Kiely, P. D., Regan, J. M., and Logan, B. E. (2011). The electric picnic: synergistic requirements for exoelectrogenic microbial communities. *Curr. Opin. Biotechnol.* 22, 378–385. doi: 10.1016/j.copbio.2011.03.003
- Kimura, Z. I., and Okabe, S. (2013). Acetate oxidation by syntrophic association between *Geobacter sulfurreducens* and a hydrogen-utilizing exoelectrogen. *ISME J.* 7, 1472–1482. doi: 10.1038/ismej.2013.40
- Lawson, P., Falsen, E., Inganäs, E., Weyant, R., and Collins, M. (2002). *Dysgonomonas mossii* sp. nov., from human sources. *Syst. Appl. Microbiol.* 25, 194–197. doi: 10.1078/0723-2020-00107
- Lawson, P. A., Song, Y., Liu, C., Molitoris, D. R., Vaisanen, M.-L., Collins, M. D., et al. (2004). *Anaerotruncus colihominis* gen. nov., sp. nov., from human faeces. *Int. J. Syst. Evol. Microbiol.* 54, 413–417. doi: 10.1099/ijs.0.02653-0
- Ledezma, P., Greenman, J., and Ieropoulos, I. (2013). MFC-cascade stacks maximise COD reduction and avoid voltage reversal under adverse conditions. *Bioresour. Technol.* 134, 158–165. doi: 10.1016/j.biortech.2013.01.119
- Li, J. V., Ashrafi, H., Bueter, M., Kinross, J., Sands, C., le Roux, C. W., et al. (2011). Metabolic surgery profoundly influences gut microbial-host metabolic cross-talk. *Gut* 60, 1214–1223. doi: 10.1136/gut.2010.234708

- Lu, L., Xing, D., Ren, N., and Logan, B. E. (2012). Syntrophic interactions drive the hydrogen production from glucose at low temperature in microbial electrolysis cells. *Bioresour. Technol.* 124, 68–76. doi: 10.1016/j.biortech.2012.08.040
- MacIntyre, D. A., Chandiramani, M., Lee, Y. S., Kindinger, L., Smith, A., Angelopoulos, N., et al. (2015). The vaginal microbiome during pregnancy and the postpartum period in a European population. *Sci. Rep.* 5:8988. doi: 10.1038/srep08988
- Mäkinen, A. E., Lay, C.-H., Nissilä, M. E., and Puhakka, J. A. (2013). Bioelectricity production on xylose with a compost enrichment culture. *Int. J. Hydro. Ener.* 38, 15606–15612. doi: 10.1016/j.ijhydene.2013.04.137
- Masuda, M., Freguia, S., Wang, Y.-F., Tsujimura, S., and Kano, K. (2010). Flavins contained in yeast extract are exploited for anodic electron transfer by *Lactococcus lactis*. *Bioelectrochemistry* 78, 173–175. doi: 10.1016/j.bioelechem.2009.08.004
- Mechichi, T., Labat, M., Garcia, J.-L., Thomas, P., and Patel, B. K. C. (1999). *Sporobacterium olearium* gen. nov., sp. nov., a new methanethiol-producing bacterium that degrades aromatic compounds, isolated from an olive mill wastewater treatment digester. *Int. J. Syst. Bacteriol.* 49, 1741–1748. doi: 10.1099/00207713-49-3-1201
- Morris, B. E., Henneberger, R., Huber, H., and Moissl-Eichinger, C. (2013). Microbial syntrophy: interaction for the common good. *FEMS Microbiol. Rev.* 37, 384–406. doi: 10.1111/1574-6976.12019
- Nakamura, L. K., Shida, O., Takagi, H., and Komagata, K. (2002). *Bacillus pycnus* sp. nov. and *Bacillus neidei* sp. nov., round-spored bacteria from soil. *Int. J. Syst. Evol. Microbiol.* 52, 501–505. doi: 10.1099/00207713-52-2-501
- Nishiyama, T., Ueki, A., Kaku, N., Watanabe, K., and Ueki, K. (2009). *Bacteroides graminisolvans* sp. nov., a xylanolytic anaerobe isolated from a methanogenic reactor treating cattle waste. *Int. J. Syst. Evol. Microbiol.* 59, 1901–1907. doi: 10.1099/ijss.0.008268-0
- Pfeiffer, T., Schuster, S., and Bonhoeffer, S. (2001). Cooperation and competition in the evolution of ATP-producing pathways. *Science* 292, 504–507. doi: 10.1126/science.1058079
- Ren, Z., Yan, H., Wang, W., Mench, M. M., and Regan, J. M. (2011). Characterization of Microbial Fuel Cells at microbially and electrochemically meaningful time scales. *Environ. Sci. Technol.* 45, 2435–2441. doi: 10.1021/es103115a
- Rismani-Yazdi, H., Christy, A. D., Dehority, B. A., Morrison, M., Yu, Z., and Tuovinen, O. H. (2007). Electricity generation from cellulose by rumen microorganisms in microbial fuel cells. *Biotechnol. Bioeng.* 97, 1398–1407. doi: 10.1002/bit.21366
- Rogers, G. M., and Baecker, A. A. W. (1991). *Clostridium xyloolyticum* sp. nov., an anaerobic xylanolytic bacterium from decayed *Pinus patula* wood. *Int. J. Syst. Evol. Microbiol.* 41, 140–143.
- Rotaru, A. E., Shrestha, P. M., Liu, F., Ueki, T., Nevin, K., Summers, Z. M., et al. (2012). Interspecies electron transfer via hydrogen and formate rather than direct electrical connections in cocultures of *Pelobacter carbinolicus* and *Geobacter sulfurreducens*. *Appl. Environ. Microbiol.* 78, 7645–7651. doi: 10.1128/AEM.01946-12
- Salyers, A. A., Vercellotti, J. R., West, S. E. H., and Wilkins, T. D. (1977). Fermentation of mucin and plant polysaccharides by strains of *Bacteroides* from the human colon. *Appl. Environ. Microbiol.* 33, 319–322.
- Sharma, Y., and Li, B. (2010). Optimizing energy harvest in wastewater treatment by combining anaerobic hydrogen producing biofermentor (HPB) and microbial fuel cell (MFC). *Int. J. Hydro. Ener.* 35, 3789–3797. doi: 10.1016/j.ijhydene.2010.01.042
- Sieber, J. R., McInerney, M. J., and Gunsalus, R. P. (2012). Genomic insights into syntropy: the paradigm for anaerobic metabolic cooperation. *Annu. Rev. Microbiol.* 66, 429–452. doi: 10.1146/annurev-micro-090110-102844
- Stratford, J. P., Beecroft, N. J., Slade, R. C. T., Grünig, A., and Avignone-Rossa, C. (2014). Anodic microbial community diversity as a predictor of the power output of microbial fuel cells. *Bioresour. Technol.* 156, 84–91. doi: 10.1016/j.biortech.2014.01.041
- Sun, D., Call, D. F., Kiely, P. D., Wang, A., and Logan, B. E. (2012). Syntrophic interactions improve power production in formic acid fed MFCs operated with set anode potentials or fixed resistances. *Biotechnol. Bioeng.* 109, 405–414. doi: 10.1002/bit.23348
- Sun, G., Thygesen, A., and Meyer, A. S. (2015). Acetate is a superior substrate for microbial fuel cell initiation preceding bioethanol effluent utilization. *Appl. Microbiol. Biotechnol.* 99, 4905–4915. doi: 10.1007/s00253-015-6513-5
- Tanaka, K., Komiyama, A., Sonomoto, K., Ishizaki, A., Hall, S. J., and Satisbury, P. F. (2002). Two different pathways for D-xylose metabolism and the effect of xylose concentration on the yield coefficient of L-lactate in mixed-acid fermentation by the lactic acid bacterium *Lactococcus lactis* 10-1. *Appl. Microbiol. Biotechnol.* 60, 160–167. doi: 10.1007/s00253-002-1078-5
- Thomas, T. D., and Turner, K. W. (1981). Carbohydrate fermentation by *Streptococcus cremoris* and *Streptococcus lactis* growing in agar gels. *Appl. Environ. Microbiol.* 41, 1289–1294.
- Turner, K. W., and Robertson, A. M. (1979). Xylose, arabinose, and rhamnose fermentation by *Bacteroides ruminicola*. *Appl. Environ. Microbiol.* 38, 7–12.
- Walter, X. A., Greenman, J., Taylor, B., and Ieropoulos, I. A. (2015). Microbial fuel cells continuously fuelled by untreated fresh algal biomass. *Algal Res.* 11, 103–107. doi: 10.1016/j.algal.2015.06.003
- Winfield, J., Ieropoulos, I., and Greenman, J. (2012). Investigating a cascade of seven hydraulically connected microbial fuel cells. *Bioresour. Technol.* 110, 245–250. doi: 10.1016/j.biortech.2012.01.095
- Wrighton, K. C., Agbo, P., Warnecke, F., Weber, K. A., Brodie, E. L., DeSantis, T. Z., et al. (2008). A novel ecological role of the Firmicutes identified in thermophilic microbial fuel cells. *ISME J.* 2, 1146–1156. doi: 10.1038/ismej.2008.48
- Wrighton, K. C., Virdis, B., Clauwaert, P., Read, S. T., Daly, R. A., Boon, N., et al. (2010). Bacterial community structure corresponds to performance during cathodic nitrate reduction. *ISME J.* 4, 1443–1455. doi: 10.1038/ismej.2010.66
- Xu, J.-F., Ren, N.-Q., Su, D.-X., and Qiu, J. (2010). Bio-hydrogen production from acetic acid steam-exploded corn straws by simultaneous saccharification and fermentation with *Ethanoligenes harbinense* B49. *Int. J. Energy Res.* 34, 381–386. doi: 10.1002/er.1659
- Yamamoto, A., Kouzuma, A., Abe, T., and Watanabe, K. (2014). Metagenomic analyse reveal the involvement of syntrophic consortia in methanol/electricity conversion in microbial fuel cells. *PLoS ONE* 9:e98425. doi: 10.1371/journal.pone.0098425
- Yates, M. D., Kiely, P. D., Call, D. F., Rismani-Yazdi, H., Bibby, K., Peccia, J., et al. (2012). Convergent development of anodic bacterial communities in microbial fuel cells. *ISME J.* 6, 2002–2013. doi: 10.1038/ismej.2012.42
- Yazdani, S. S., and Gonzalez, R. (2007). Anaerobic fermentation of glycerol: a path to economic viability for the biofuels industry. *Curr. Opin. Biotechnol.* 18, 213–219. doi: 10.1016/j.copbio.2007.05.002
- Youssef, N., Sheik, C. S., Krumholz, L. R., Najar, F. Z., Roe, B. A., and Elshahed, M. S. (2009). Comparison of species richness estimates obtained using nearly complete fragments and simulated pyrosequencing-generated fragments in 16S rRNA gene-based environmental surveys. *Appl. Environ. Microbiol.* 75, 5227–5236. doi: 10.1128/AEM.00592-09
- Yu, L., Liu, Y., and Wang, G. (2009). Identification of novel denitrifying bacteria *Stenotrophomonas* sp. ZZ15 and *Oceanimonas* sp. YC13 and application for removal of nitrate from industrial wastewater. *Biodegradation* 20, 391–400. doi: 10.1007/s10532-008-9230-2
- Zhang, K., Song, L., and Dong, X. (2010). *Proteinilasticum ruminis* gen. nov., sp. nov., a strictly anaerobic proteolytic bacterium isolated from yak rumen. *Int. J. Syst. Evol. Microbiol.* 60, 2221–2225. doi: 10.1099/ijss.0.011759-0
- Zhuang, L., Zheng, Y., Zhou, S., Yuan, Y., Yuan, H., and Chen, Y. (2012). Scalable microbial fuel cell (MFC) stack for continuous real wastewater treatment. *Bioresour. Technol.* 106, 82–88. doi: 10.1016/j.biortech.2011.11.019
- Conflict of Interest Statement:** The authors declare that the research was conducted in the absence of any commercial or financial relationships that could be construed as a potential conflict of interest.
- Copyright © 2016 Hodgson, Smith, Dahale, Stratford, Li, Grünig, Bushell, Marchesi and Avignone Rossa. This is an open-access article distributed under the terms of the Creative Commons Attribution License (CC BY). The use, distribution or reproduction in other forums is permitted, provided the original author(s) or licensor are credited and that the original publication in this journal is cited, in accordance with accepted academic practice. No use, distribution or reproduction is permitted which does not comply with these terms.



K-shell Analysis Reveals Distinct Functional Parts in an Electron Transfer Network and Its Implications for Extracellular Electron Transfer

Dewu Ding^{1,2}, Ling Li¹, Chuanjun Shu¹ and Xiao Sun^{1*}

¹ State Key Laboratory of Bioelectronics, School of Biological Science and Medical Engineering, Southeast University, Nanjing, China, ² Department of Mathematics and Computer Science, Chizhou College, Chizhou, China

OPEN ACCESS

Edited by:

Yong Xiao,

The Institute of Urban Environment,
Chinese Academy of Sciences, China

Reviewed by:

Seung Gu Shin,

Pohang University of Science
and Technology, South Korea

Yue Zheng,

The Institute of Urban Environment,
Chinese Academy of Sciences, China

*Correspondence:

Xiao Sun

xsun@seu.edu.cn

Specialty section:

This article was submitted to
Microbiotechnology, Ecotoxicology
and Bioremediation,
a section of the journal
Frontiers in Microbiology

Received: 05 January 2016

Accepted: 31 March 2016

Published: 20 April 2016

Citation:

Ding D, Li L, Shu C and Sun X (2016)
K-shell Analysis Reveals Distinct
Functional Parts in an Electron
Transfer Network and Its Implications
for Extracellular Electron Transfer.
Front. Microbiol. 7:530.
doi: 10.3389/fmicb.2016.00530

Shewanella oneidensis MR-1 is capable of extracellular electron transfer (EET) and hence has attracted considerable attention. The EET pathways mainly consist of c-type cytochromes, along with some other proteins involved in electron transfer processes. By whole genome study and protein interactions inquisition, we constructed a large-scale electron transfer network containing 2276 interactions among 454 electron transfer related proteins in *S. oneidensis* MR-1. Using the k-shell decomposition method, we identified and analyzed distinct parts of the electron transfer network. We found that there was a negative correlation between the k_s (k-shell values) and the average DR_100 (disordered regions per 100 amino acids) in every shell, which suggested that disordered regions of proteins played an important role during the formation and extension of the electron transfer network. Furthermore, proteins in the top three shells of the network are mainly located in the cytoplasm and inner membrane; these proteins can be responsible for transfer of electrons into the quinone pool in a wide variety of environmental conditions. In most of the other shells, proteins are broadly located throughout the five cellular compartments (cytoplasm, inner membrane, periplasm, outer membrane, and extracellular), which ensures the important EET ability of *S. oneidensis* MR-1. Specifically, the fourth shell was responsible for EET and the c-type cytochromes in the remaining shells of the electron transfer network were involved in aiding EET. Taken together, these results show that there are distinct functional parts in the electron transfer network of *S. oneidensis* MR-1, and the EET processes could achieve high efficiency through cooperation through such an electron transfer network.

Keywords: c-type cytochrome, extracellular electron transfer, k-shell decomposition, protein disordered region, protein–protein interaction network

INTRODUCTION

The transmission of electrons to extracellular solid acceptors (extracellular electron transfer, EET) is an important reaction in some microorganisms, such as *Geobacter sulfurreducens* and *Shewanella oneidensis* (Shi et al., 2007). C-type cytochromes play important roles in the EET processes (Shi et al., 2012; Tremblay and Zhang, 2015), for example, four c-type

cytochromes, CymA, MtrA, MtrC, and OmcA, can form an electron transfer chain with a trans-outer membrane protein MtrB in *S. oneidensis* MR-1 (the classical MtrCAB pathway). Some other EET pathways (such as MtrDEF and the dimethyl sulfoxide (DMSO) pathway) have also been proposed in recent years (Gralnick et al., 2006; Coursolle and Gralnick, 2010, 2012; Breuer et al., 2012, 2014). However, because of the diversity of *c*-type cytochromes, *Shewanella* can express different *c*-type cytochrome genes in different environments. Thus it remains challenging to accurately characterize the EET processes in such species.

Previous studies have revealed the high efficiency of the prediction of biological pathways from biological networks (Planas-Iglesias et al., 2012; Huang et al., 2013; Mukhopadhyay and Maulik, 2014). Following initial work on a small-scale *c*-type cytochrome network (Zhang et al., 2008), a recent study constructed a network for all of 41 *c*-type cytochromes in *S. oneidensis* MR-1 and the classical EET pathways (e.g., MtrCAB, MtrDEF) can be identified from the *c*-type cytochrome network (Ding et al., 2014). Furthermore, from the view of steric properties of individual proteins, Volkov and van Nuland (2012) performed extensive conformational sampling, mapped out functional epitopes in *c*-type cytochrome complexes (involving cytochrome *c* and other redox-active proteins such as peroxidase and cytochrome *b*₅) and then assessed the electron transfer properties of such interactions.

To take advantage of the extracellular solid electron acceptors which widely exist in cellular living environment, *Shewanella* species develop effective EET strategies based upon *c*-type cytochromes and other redox-active proteins. Here, we explored such processes by constructing an electron transfer network and analyzing its formation and extension, as well as the functional parts in the network. Proteins in the core of a genome-scale protein–protein interaction (PPI) network have a high probability of being essential (Wuchty and Almaas, 2005), and network peripheral proteins tend to be preferentially involved in recent or ongoing adaptive events (Kim et al., 2007), therefore such a core-periphery structure can be helpful to understand PPI networks. Furthermore, k-shell analysis has been widely used to explain both network formation and current structure (Kitsak et al., 2010; Pei et al., 2014), we thus engaged it in this study.

After whole genome study and identification of interactions of proteins that are potentially involved in electron transfer processes in *S. oneidensis* MR-1, a large-scale electron transfer network was constructed (see Construction of the Electron Transfer Network). Then, by integrating protein disordered regions and subcellular localization data, we found that the k-shell structure can be helpful for understanding the formation and extension of the electron transfer network (see K-shell Structure of the Electron Transfer Network). Finally, the functional significance of the various shells in the network is discussed in this paper (see The Top Three Shells Take Charge of Electron Generation, The Fourth Shell Is Responsible for Extracellular Electron Transfer, The *c*-type Cytochromes in the Remaining Shells Are Involved in Aiding Extracellular Electron Transfer).

MATERIALS AND METHODS

Protein Selection

C-type cytochromes, which play the most important roles in the EET processes, were identified from genome annotation data (Meyer et al., 2004), and then were verified according to the literature. Other proteins that are potentially involved in electron transfer processes (such as pilin proteins, flavoproteins, and various redox-active proteins) were manually selected from the complete genome of *S. oneidensis* MR-1 (Heidelberg et al., 2002) via the KEGG genome database¹.

Network Construction

Interaction information for these manually selected proteins was obtained from the famous protein interaction database STRING² (Franceschini et al., 2013). Furthermore, experimentally identified and verified interactions from the literature were also considered. Then, the PPI network was built based on these interaction data. GO biological process and KEGG pathway enrichment analyses were carried out using STRING online tools.

K-shell Analysis

As described elsewhere (Kitsak et al., 2010; Pei et al., 2014), the k-shell decomposition method assigns a k_s value to each node in a network. Such values can be obtained by successive pruning of nodes level by level. That is, removing all nodes with degree $k = 1$ and repeatedly making such procedure, until there are no remaining nodes with degree $k = 1$; all such removed nodes are then assigned a k_s value with $k_s = 1$. Then, via a similar procedure, one can iteratively obtain the next k_s value ($k_s = 2$), and so on until all nodes are removed.

Disordered Regions

Protein disordered regions are functionally versatile and can mediate new interactions of proteins (Buljan et al., 2013; Uhart and Bustos, 2014); they thus play an important role in the formation and extension of PPI networks. The disordered regions of proteins were identified with the tool IsUnstruct (v2.02³) (Lobanov and Galzitskaya, 2011). All disordered segments with two or more continuous amino acid residues were considered as disordered regions.

Subcellular Localization

The subcellular localization of proteins contributes to understand EET processes and the role of different proteins in EET; in this study, it was performed by the following procedures: (1) using PSORTb⁴ (Yu et al., 2010), which is one of the best tools for current subcellular localization analysis; then, (2) using CELLO⁵ (Yu et al., 2006) for proteins that were not resolved by PSORTb; and at last, (3) referring to specific-protein-related literature

¹http://www.genome.jp/dbget-bin/get_linkdb?-t+genes+genome:T00099

²<http://string.embl.de>

³<http://bioinfo.protres.ru/IsUnstruct/>

⁴<http://www.psorth.org/psorth>

⁵<http://cello.life.nctu.edu.tw/>

or known molecular function for checking or revising of the subcellular localization.

Protein Domains and Their Interactions

Protein (families) domains were mainly determined from Pfam (release 27.0⁶) (Finn et al., 2014), and proteins without domain information in Pfam were analyzed by the prediction tool FFAS⁷ [note that if the predicted templates had overlap area, only the template with the best score was chosen (Jaroszewski et al., 2005)]. Protein domain-domain interactions (DDIs) were mainly resolved from 3did⁸ (Mosca et al., 2014).

RESULTS AND DISCUSSION

Construction of the Electron Transfer Network

C-type cytochromes play important roles in the transmission of electrons from intracellular space to extracellular acceptors (Shi et al., 2012; Tremblay and Zhang, 2015). These highly water soluble proteins covalently bind heme via two cysteine residues. Using pattern matching (the heme-binding CXXCH motif), Meyer et al. (2004) identified 42 genes encoding c-type cytochromes in the *S. oneidensis* MR-1 genome. However, according to published literatures, we found that SO_4570 is a pseudo gene and SO_3623 is a degenerate gene; these two genes were thus eliminated. SO_1748 was identified as a periplasmic monoheme c-type cytochrome following several recent reports (Romine et al., 2008; Gao et al., 2010; Jin et al., 2013). Furthermore, other proteins that play roles in electron transfer were identified by analyzing genome-wide annotation data. The main types of these proteins are: pilin proteins, flavoproteins, quinone/ubiquinone oxidoreductases, and other various redox-active proteins (e.g., flavodoxins, ferredoxins, and metalloproteases). Overall, 481 proteins were identified (**Supplementary Data Sheet S1**).

Next, we needed to obtain all interaction information on these 481 proteins. Because large-scale experimental data are not presently available, we performed protein interaction inquisition in STRING. The most important parameter for protein interaction inquisition in STRING is the confidence score, which is defined as the approximate probability that a predicted interaction exists between two proteins in the same metabolic map in the KEGG database. To obtain more comprehensive information, medium confidence (0.4) was set. The interaction information was then obtained (**Supplementary Data Sheet S2**, December 2014) and a large-scale electron transfer network was constructed accordingly. After removing isolated nodes (23 proteins) and separated links (two interactions), we obtained a network with 2266 interactions among 454 proteins (**Supplementary Methods**). Furthermore, experimentally identified and verified interactions were also considered. We found that most of the experimentally

verified interactions were included in STRING's predictions. Nevertheless, 10 further interactions were discovered by literature retrieval (Borloo et al., 2011; Schutz et al., 2011; Fonseca et al., 2013) (**Supplementary Methods**). Overall, 2276 interactions among 454 proteins were determined in the final electron transfer network.

The electron transfer network was then modeled as an undirected graph, in which nodes represent the proteins and the links represent protein interactions. It is clear that network structure strongly correlates with its function, for example, several classical EET pathways have been identified by modular analysis of a c-type cytochrome network (Ding et al., 2014). As k-shell analysis has been widely used to explain both the formation and current structure of networks (Kitsak et al., 2010; Pei et al., 2014), we thus engaged this method to study the formation and extension of *Shewanella* electron transfer network and its functional parts, as well as their potential implications for EET processes.

K-shell Structure of the Electron Transfer Network

We first performed k-shell decomposition for the *S. oneidensis* MR-1 electron transfer network (**Figure 1A, Supplementary Methods, Supplementary Data Sheet S3**). From the network formation and extension view, it is clear that the nodes with high k-shell values (k_s) were those connected initially (Kitsak et al., 2010; Pei et al., 2014). These nodes form a core network that was reconstructed and expanded as new nodes were constantly connected. Since PPIs are strongly influenced by their local environment, the protein interaction system is constantly reconstructed (e.g., by rewiring interactions among existing proteins [Kim et al., 2012]) and expanded (e.g., by recruiting new proteins into the network for highly specific and/or more efficient functions [Nam et al., 2012]) according to changes in the environment. As a result, the structure of the PPI network evolves. Therefore, such a k-shell network structure reflects the formation and extension of the PPI network.

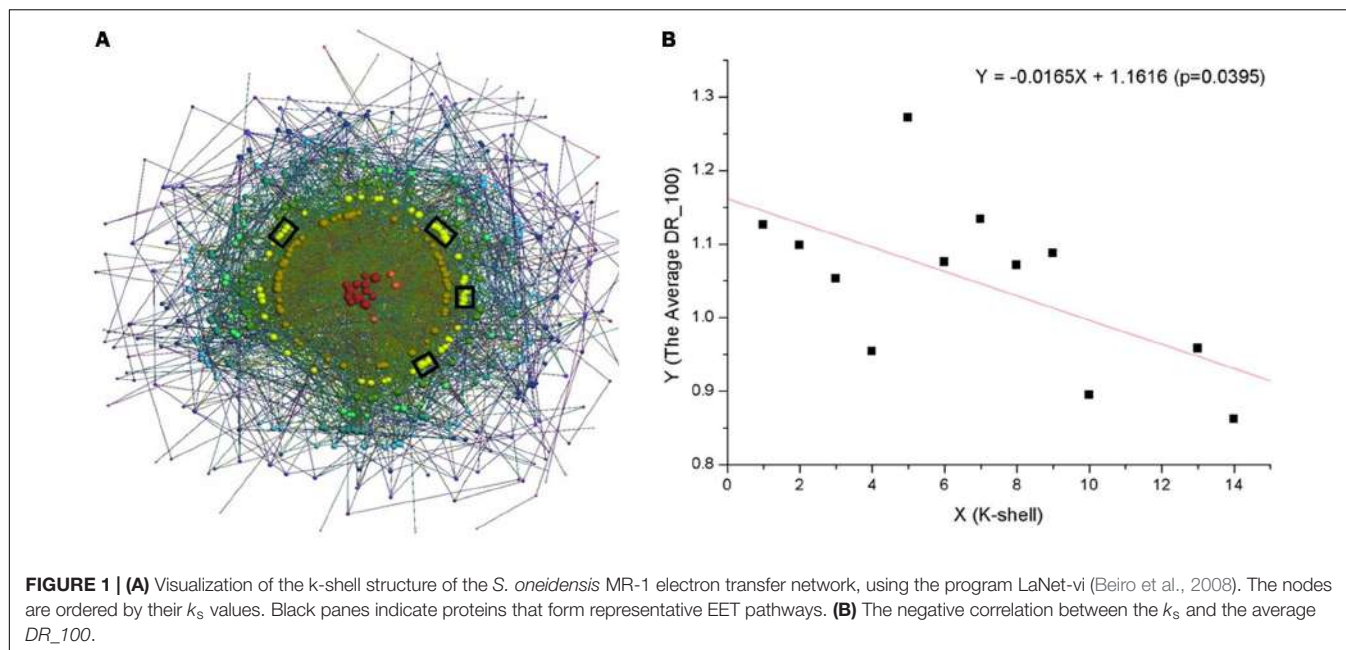
To further explore the formation and extension of the electron transfer network, we considered an important feature of proteins, namely disordered regions. Such disordered regions cannot fold into stable three dimensional structures but increase the functional versatility of proteins; they can also mediate new protein interactions (Buljan et al., 2013; Uhart and Bustos, 2014) and thus play an important role in the formation and extension of PPI networks. For each protein, we first obtained its disordered regions (**Supplementary Data Sheet S4**) and computed the disordered regions per 100 amino acids (DR_{100}). Since many disordered regions locate at the termini of proteins, small proteins will significantly perturb the statistical results. Therefore, the proteins that are less than 100 amino acids were excluded (19 proteins). Then, we analyzed the average DR_{100} for the proteins in every shell of the electron transfer network, and found that there was a negative correlation between the k_s and the average DR_{100} ($DR_{100Ave} = -0.0165 \times k_s + 1.1616$, $p = 0.0395$) (**Figure 1B**).

The results demonstrated that there has been a selection preference for proteins during the formation and extension of the

⁶<http://pfam.xfam.org/>

⁷<http://ffas.sanfordburnham.org>

⁸<http://3did.irbbarcelona.org/>



electron transfer network. Proteins with fewer disordered regions seem to have been preferably selected in the core of the electron transfer network. Because the intrinsically disordered regions in proteins do not fold into stable structures under physiological conditions, the proteins in the core of the electron transfer network, with less disordered regions, have a high probability of being stable. The stability of these proteins could favor formation of the macromolecular complexes required to carry out essential cellular processes. For example, metabolic proteins have been shown to possess the lowest disordered content (Pavlovic-Lazetic et al., 2011). In contrast, with the more disordered regions in network peripheral proteins suggests there are frequent dynamic interactions, since protein disordered regions are functionally versatile, and allow the same polypeptide to undertake different interactions with different consequences (Wright and Dyson, 2015). Protein disordered regions can interact with numerous different partners by using molecular recognition features (or linear motifs), participate in the assembly of protein complexes, and provide accessible sites for post-translational modification (van der Lee et al., 2014; Wright and Dyson, 2015), which enables that proteins in the network periphery can aid essential cellular processes and/or function in a wide variety of environmental conditions.

As previous studies have indicated that nodes with similar k_s values in a network have equal importance (Kitsak et al., 2010; Pei et al., 2014), and proteins with similar interactions (or topology) in PPI networks have been widely recognized to carry out similar functions (Vazquez et al., 2003; Radivojac et al., 2013; Davis et al., 2015). We thus speculated that various shells in the network might take different biological functions. To address this point, we first analyzed proteins with different k_s values and their subcellular localization (Figure 2, Supplementary Data Sheet S5). We discuss the biological significance of the different shells in the following sections.

The Top Three Shells Take Charge of Electron Generation

As Figure 2 shows, the proteins in the top three shells (with k_s 14, 13, and 10, respectively) are mainly located in the cytoplasm and inner membrane, with a small number in the periplasm, without outer membrane and extracellular space. Because there are dense interactions among network core proteins; by taking a larger fraction of their surface involved in many interactions, these proteins tend to be constrained, without further need of adaptive evolution that preferentially occurs in outer membrane and extracellular space (Kim et al., 2007). The Gene Ontology (GO) biological processes were exploited to obtain biological insights into these proteins; we found that the most representative category is metabolic processes (Figure 3). The results indicate that these proteins are mostly capable of cellular metabolism.

Then, KEGG enrichment analysis was used to probe into the details (Table 1). The enrichments results were highly consistent with the metabolism of *Shewanella* species. Metabolic pathways and carbon metabolism were the most common enrichments. The enrichment of oxidative phosphorylation reflected that it is the primary ATP synthesis pathway in *Shewanellae* (Venkateswaran et al., 1999). Enrichments of glyoxylate and dicarboxylate metabolism (a variation of the TCA cycle) and the citrate cycle (TCA cycle) correspond to *Shewanella* species having a complete TCA cycle under aerobic conditions (Pinchuk et al., 2010), and pyruvate fermentation in *S. oneidensis* MR-1 can provide essential energy for cell survival (Pinchuk et al., 2011).

Methane metabolism was also identified as an important enriched pathway. This was because anaerobic methane oxidation can be carried out for interspecies electron transfer (Stams and Plugge, 2009). The processes are thought to

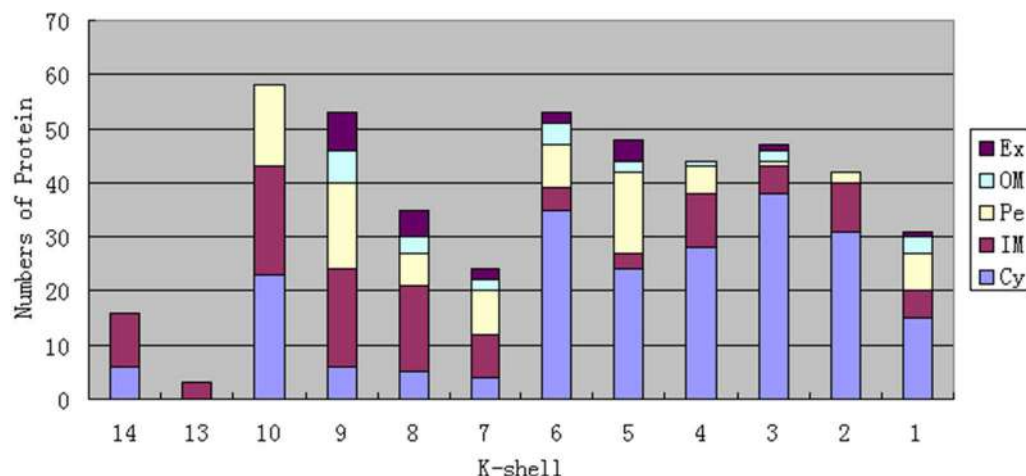


FIGURE 2 | Numbers of proteins and their subcellular localization in every shell in the *S. oneidensis* MR-1 electron transfer network. Ex, Extracellular; OM, Outer Membrane; Pe, Periplasm; IM, Inner Membrane; Cy, Cytoplasm.

help bacteria sustain growth in syntrophic communities, which differ markedly from pure cultures and occur where diverse microbes exist in natural environments (Rotaru et al., 2015; Smith et al., 2015). Furthermore, there were 24 proteins identified to associate with microbial metabolism in diverse environments, such as FccA (fumarate reductase), Mdh (malate dehydrogenase), and SdhABC (succinate dehydrogenase). These diverse metabolic capabilities imply that *S. oneidensis* MR-1 has evolved flexible metabolic mechanisms to survive in a wide variety of environmental

conditions, which agrees with the observation that a wide variety of type and concentration of substrates (e.g., fumarate, malate, and succinate) can be utilized by *S. oneidensis* MR-1 (Pinchuk et al., 2010). More importantly, with such a variety of metabolic capabilities, *S. oneidensis* MR-1 can oxidize many different substrates in different environments. Then, the generated electrons can be delivered into the quinone pool by NADH-quinone reductase (Nqr) and NADH-ubiquinone oxidoreductase (Nuo), which are found in the top three shells.

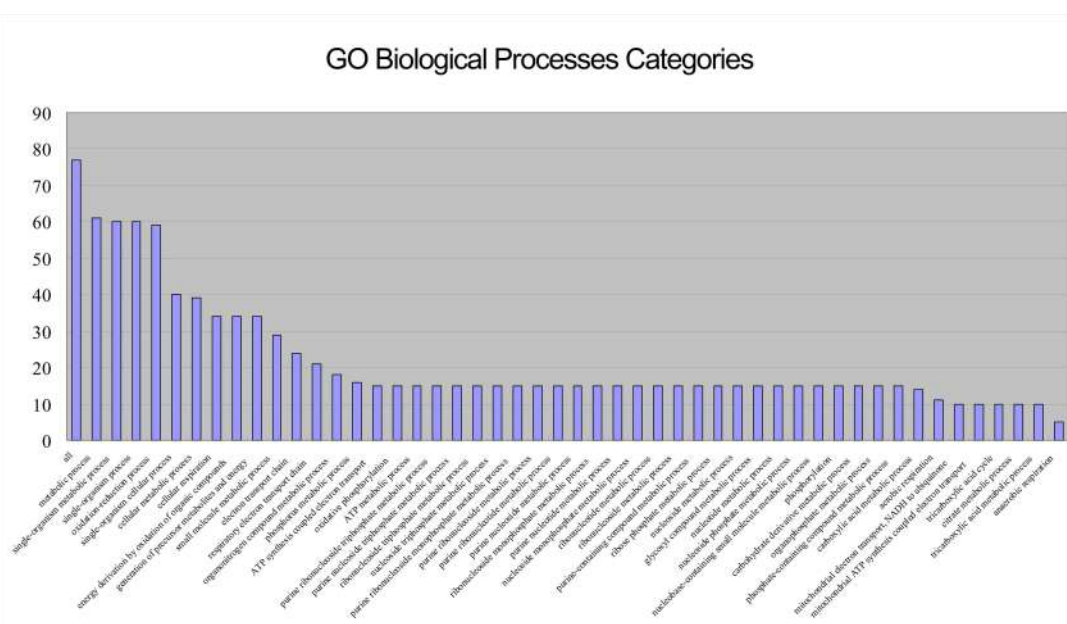


FIGURE 3 | Bar chart showing the GO biological process categories for the 77 proteins (or their encoding genes) in the top three shells of the *S. oneidensis* MR-1 electron transfer network ($p < 0.0001$). The most representative category is “metabolic processes”.

The Fourth Shell Is Responsible for Extracellular Electron Transfer

Unlike the top three shells, which contain no outer membrane or extracellular proteins, the fourth shell ($k_s = 9$) contains such proteins (Figure 2). We considered detailed subcellular localization information for all proteins in this shell (Table 2). The outer membrane proteins (DmsF, MtrB, MtrE, SO_1659, SO_4359) and extracellular proteins (DmsA, DmsB, MtrC, MtrF, OmcA, SO_4357, SO_4358) in this shell are mostly functionally important for EET, as indicated by previous studies (Coursolle and Gralnick, 2010, 2012). Furthermore, proteins in this shell are broadly located in all five compartments of *S. oneidensis* MR-1 (i.e., the cytoplasm, inner membrane, periplasm, outer membrane and extracellular). Such diversified subcellular localization of proteins endows *S. oneidensis* MR-1 with the important EET ability, since electrons must be transferred from cytoplasm, via inner membrane, periplasm and outer membrane, to extracellular electron acceptors.

We found that the proteins in this shell can be categorized into several modules according to their roles in EET (Figure 4):

Module 1 – Reduction of Extracellular Insoluble Electron Acceptors

With these outer membrane and extracellular proteins previously mentioned in this section, *S. oneidensis* MR-1 is capable of

transferring electrons generated in the cytoplasm and gathered in the quinone pool (see The Top Three Shells Take Charge of Electron Generation) to extracellular insoluble acceptors. According to reported literatures (Coursolle and Gralnick, 2010, 2012), four EET pathways are formed from these proteins and their functional partners. These pathways include: (1) the MtrCAB pathway: CymA → MtrA → MtrB → MtrC → OmcA (Shi et al., 2012), and (2) the MtrDEF pathway: CymA → MtrD → MtrE → MtrF → OmcA (Breuer et al., 2012, 2014). In these two pathways, inner membrane CymA obtains electrons from the quinone pool, then transfers them via periplasmic MtrA/MtrD, outer membrane MtrB/MtrE, and extracellular MtrC-OmcA/MtrF-OmcA complexes, respectively, and finally to extracellular electron acceptors. These two pathways are considered to be metal reduction pathways. (3) The DMSO pathway: CymA → DmsE → DmsF → DmsAB complex; it was found that DmsE and DmsF play important roles in DMSO reduction, and the DMSO pathway was thus proposed (Gralnick et al., 2006). (4) The SO_4360-57 pathway: CymA → SO_4360 → SO_4359 → SO_4358/4357; analysis of homologs and subcellular localization has revealed that SO_4360/4359 are similar to MtrAB/MtrDE/DmsEF (Ding et al., 2014). That is, this pathway might be functionally redundant to the other three EET pathways. These results are consistent with Coursolle and Gralnick (2010, 2012) work, in which they deduced that the pathway shared overlapping functionality with the DMSO and MtrDEF pathways.

Module 2 – Reduction of Extracellular Soluble Electron Acceptors

This module deals with extracellular soluble electron acceptors that can be respiration inside the cell. The *napDAGHB* gene cluster encodes nitrate reductase (NapA) and accessory proteins, the *nrfA* gene encodes the nitrite reductase (NrfA); they reduce nitrate to ammonium in a two-step manner in *S. oneidensis* MR-1, that is, reduction of nitrate to nitrite by NapA and followed by reduction of nitrite to ammonium by NrfA (Gao et al., 2009). The *torCAD* genes are three conserved structural components of the trimethylamine *N*-oxide (TMAO) respiratory system, which encode the Tor pathway that endows *Shewanella* species to use TMAO as a terminal electron acceptor for extracellular anaerobic respiration (Gon et al., 2002). PhsA is also functionally important for reduction of extracellular soluble electron acceptors, since Burns and DiChristina have shown that the anaerobic respiration of elemental sulfur and thiosulfate by *S. oneidensis* MR-1 requires PsrA, which is a homolog of PhsA (Burns and DiChristina, 2009).

Module 3 – Cytochrome c Maturation System

It has been shown that multiple post-translational modifications are required to synthesize the components of the EET pathways (such as the MtrCAB pathway). With reference to *c*-type cytochromes, this process is assured by the inner membrane proteins CcmABC₂EFGHI in this shell. These proteins are the components of the cytochrome *c* maturation (Ccm) system, which loads heme into the apocytochromes *c* to form mature cytochromes, such as MtrA and MtrC (Goldbeck et al., 2013). Be similar with the Ccm family proteins, the heme synthetases SirE

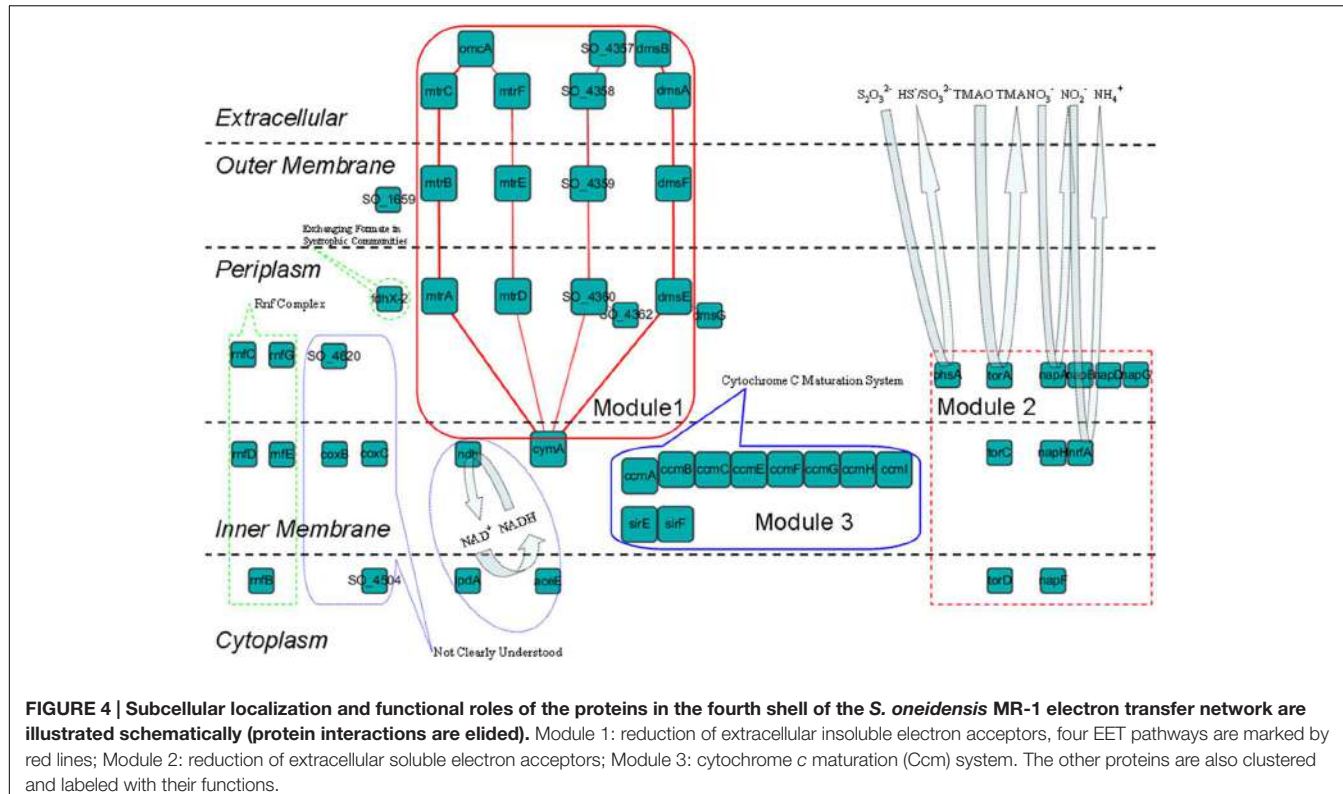
TABLE 1 | KEGG enrichment analysis for the 77 proteins (or genes) in the top three shells of the *S. oneidensis* MR-1 electron transfer network ($p < 0.0001$).

KEGG Pathway	Number	P-value
Metabolic pathways	44	1.74E-20
Oxidative phosphorylation	28	5.69E-39
Carbon metabolism	24	1.30E-22
Microbial metabolism in diverse environments	24	1.11E-16
Methane metabolism	12	2.86E-14
Glyoxylate and dicarboxylate metabolism	12	1.12E-13
Two-component system	12	8.90E-07
Pyruvate metabolism	8	5.27E-08
Citrate cycle (TCA cycle)	6	5.96E-07

TABLE 2 | Subcellular localization of proteins in the fourth shell of the *S. oneidensis* MR-1 electron transfer network.

Subcellular	Numbers	Proteins
Cy	6	AceE, LpdA, NapF, RnfB, SO_4504, TorD
IM	19	CcmA, CcmB, CcmC, CcmE, CcmF, CcmG, CcmH, CcmI, CoxB, CoxC, CymA, NapH, Ndh, NrfA, RnfD, RnfE, SirE, SirF, TorC
Pe	16	DmsE, DmsG, FdhX-2, MtrA, MtrD, NapA, NapB, NapD, NapG, PhsA, RnfC, RnfG, SO_4620, SO_4360, SO_4362, TorA
OM	5	DmsF, MtrB, MtrE, SO_1659, SO_4359
Ex	7	DmsA, DmsB, MtrC, MtrF, OmcA, SO_4357, SO_4358

Ex, extracellular; OM, outer membrane; Pe, periplasm; IM, inner membrane; Cy, cytoplasm.



and SirF in this shell also play an important role in the maturation of *c*-type cytochromes (Brockman, 2014).

Other Proteins Related to Extracellular Electron Transfer

The other proteins in the fourth shell have also been investigated. FdhX-2 is a formate dehydrogenase, gene expression of the *fdh* family genes has been shown to be significantly increased in syntrophic communities between *S. oneidensis* and *Escherichia coli* (Wang et al., 2015). The results of Wang et al. strongly suggest that the exchange of formate is favored in such a mutualistic condition, which might be because that formate serves as an electron carrier for direct interspecies EET between these two species (Shrestha and Rotaru, 2014). Despite no report in *Shewanella* species, the membrane-bound Rnf complex encoded by *rnfBCDEG* can combine carbon dioxide fixation with the generation and use of a sodium ion gradient for ATP synthesis in many bacteria, and this complex has been shown to be a major electron transport mechanism linked to energy conservation (Tremblay et al., 2012; Kracke et al., 2015).

Our results indicate that important *c*-type cytochromes were in the fourth shell of the network, including those that form the well-known EET pathways for reduction of extracellular insoluble electron acceptors and several respiratory systems for reduction of extracellular soluble electron acceptors. The accessory Ccm system and some other proteins linked to EET were also in this shell. From the network formation and extension view, that might be because many extracellular electron acceptors (such as various iron ores) exist in the environment of

S. oneidensis MR-1, but the proteins in the top three shells cannot transfer electrons to the outside of cells. Thus, in order to take advantage of these extracellular electron acceptors, these EET-related *c*-type cytochromes were connected into the network. Then, other *c*-type cytochromes were continuously connected into the network to aid more efficient EET or accommodate other environmental conditions. In the long-term formation and extension of the network, these early *c*-type cytochromes that can transfer electrons outside of the cell gradually became part of a relative inner-shell of the network (here, the fourth).

The C-type Cytochromes in the Remaining Shells Are Involved in Aiding Extracellular Electron Transfer

There is a huge periplasmic space between the inner membrane and outer membrane in *S. oneidensis* MR-1, and a 23.5 ± 3.7 nm distance has been determined by cryo-TEM measurements (Dohnalkova et al., 2011). To facilitate electrons crossing the periplasmic space of *S. oneidensis* MR-1, some periplasmic *c*-type cytochromes are needed.

Periplasmic tetraheme cytochrome *c* CctA can interact with its redox partners (CymA and MtrA) through a single heme. Therefore, it can serve as periplasmic electron relay to facilitate electrons transfer through the periplasmic space, that is, CymA → CctA → MtrA (Fonseca et al., 2013); CctA was found in shell 6 of the electron transfer network. As one of the most abundant periplasmic *c*-type cytochromes, ScyA in shell 7 has been shown to function as a mediator of electron transfer between

CymA and CcpA (*c*-type cytochrome peroxidase) (Schutz et al., 2011; Fonseca et al., 2013). Furthermore, the cytochrome *bc*₁ complex (encoded by the *pet* gene cluster) has been predicted to be the dominant electron donor to the *ccb*₃-HCO-type oxidase (encoded by the *cco* gene cluster), and it has been shown that ScyA increases the electron flow from the *bc*₁ complex to cytochrome *ccb*₃-HCO oxidase (Yin et al., 2015). The expression level of the monoheme cytochrome *c* SorB and the decaheme cytochrome *c* SO_4360 were found to be upregulated with soluble iron(III) and oxygen as electron acceptors (Rosenbaum et al., 2012), and these two *c*-type cytochromes directly interact with each other, which raised a speculation that SorB can be used to help electrons reach SO_4360 and assist the SO_4360-57 pathway. It should be noted that fumarate reductase (FccA) also plays such an assistant role, just be similar with CctA (Fonseca et al., 2013). However, to support cellular metabolism as previous determined, this *c*-type cytochrome was found in the top three shells (see The Top Three Shells Take Charge of Electron Generation), rather than in a peripheral shell here.

Furthermore, although the physiological role remains to be examined *in vivo*, the octaheme tetrathionate reductase Otr displays nitrite, hydroxylamine, and tetrathionate reduction activities *in vitro* (Atkinson et al., 2007), which enhanced periplasmic electron transfer. It was also found that periplasmic *c*-type cytochromes can interact with several non *c*-type cytochrome proteins (Supplementary Data Sheet S2), which suggested that they also cooperated with non *c*-type cytochromes to facilitate periplasmic electron transfer in various environmental conditions. This mechanism offers one of the ways that ensure electricigens thrive in extreme environments. For example, Embree et al. (2014) recently reported that the expression of almost all *c*-type cytochromes of *G. sulfurreducens* sharply decreased when the iron ion concentration decreased, but the expression of *c*-type cytochrome

GSU3274 increased gradually in these conditions, which can be reasonably interpreted to mean that GSU3274 is used in electron transfer by interacting with other non *c*-type cytochrome proteins, when the iron concentration becomes extreme limited.

Therefore, overall, functioning as multiple electron mediators or enhancing periplasmic electron transfer, the *c*-type cytochromes in the peripheral shells of the *S. oneidensis* MR-1 electron transfer network can help electrons cross the periplasmic space and hence they are involved in aiding EET processes. Furthermore, it is also interested that most (18 in 24) of the *c*-type cytochromes in the shells with *k*_s values less than 9 are located in the periplasm (Table 3). We speculated that they will form some short-range channels with other proteins by transient protein interactions, such as those formed by CctA/FccA (CymA → CctA/FccA → MtrA) (Fonseca et al., 2013).

To assess this, we analyzed the protein disordered regions in these 18 periplasmic *c*-type cytochromes and computed their DR_100. All of the 18 *c*-type cytochromes had a high level of disordered content compared with the average DR_100 of the other proteins in the corresponding shells (Figure 5). Although protein disordered regions can fluctuate rapidly through a range of conformations, such conformational flexibility of disordered protein regions are quickly lost upon binding, which will reduce the overall free energy of binding and lead to weaker and more transient interactions (van der Lee et al., 2014).

We then analyzed the PPIs of these 18 periplasmic *c*-type cytochromes with all of their direct protein partners (interactions among these partners were not considered). As Figure 6 shows, these *c*-type cytochromes (green nodes) were highly interconnected. Indeed, the density of this sub-network was 2.12-times higher than that of the whole electron transfer network, even though many interactions were not considered here. Their interaction partners included both other *c*-type cytochromes (red

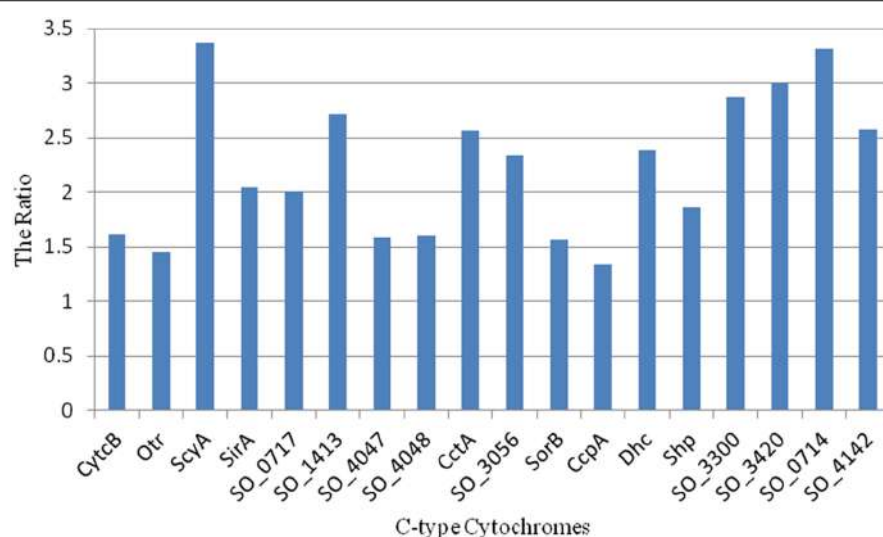
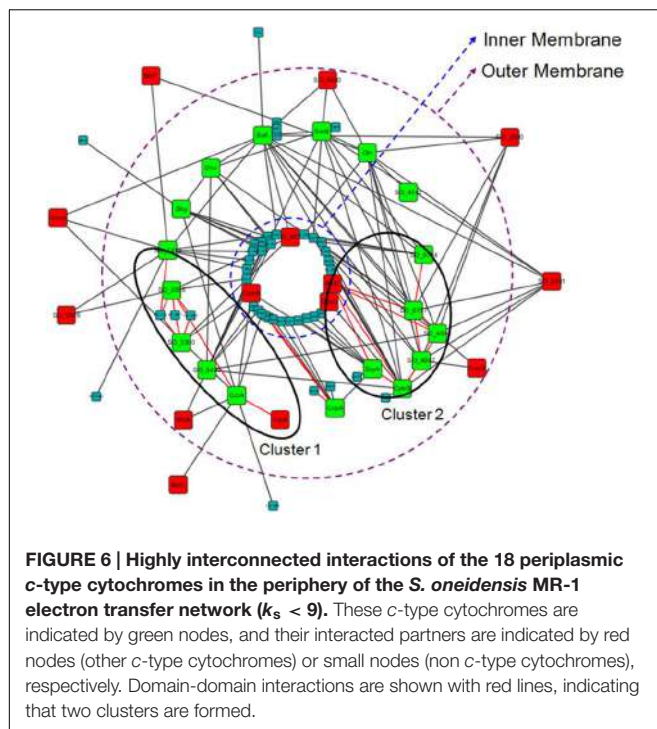


FIGURE 5 | Ratio of DR_100 of the 18 periplasmic *c*-type cytochromes in the periphery of the *S. oneidensis* MR-1 electron transfer network (*k*_s < 9) to the average DR_100 of the other proteins in the corresponding shells.



nodes in **Figure 6**) and non c-type cytochromes (**Figure 6**, small nodes). To further investigate whether weaker interactions could be formed, we performed domain-domain interaction (DDI, which correspond to strong interaction) analysis for this sub-network (see **Supplementary Data Sheet S6** for protein domain). We found that there are only a few DDIs in the sub-network (**Figure 6**, red lines), and therefore, most of these periplasmic c-type cytochromes make weak, transient interactions with other proteins, rather than permanent interactions. Then, a dynamic electron transfer network forms in periplasm via the high frequency of transient protein interactions, as discussed elsewhere (Sturm et al., 2015). Since periplasmic electron transfer processes involve in assigning specific c-type cytochromes for particular electron acceptors and triggering of different pathways

TABLE 3 | Subcellular localization of c-type cytochromes in the periphery of the *S. oneidensis* MR-1 electron transfer network ($k_s < 9$).

K-shell	Cy//IM	Pe	OM//Ex
8	CcoO, CcoP		
7		CytB, Otr, ScyA, SirA, SO_0717, SO_1413, SO_4047, SO_4048	SO_0939, SO_2930, SO_2931
6		CctA, SO_3056, SorB	
5		CcpA, Dhc, Shp, SO_3300, SO_3420	
4		SO_0714	
3	SO_4572		
1	SO_4142		

Ex, extracellular; OM, outer membrane; Pe, periplasm; IM, inner membrane; Cy, cytoplasm.

to achieve electron transfer (Sturm et al., 2015), thus the assignment of these periplasmic c-type cytochromes to different parts of the network (different shells here, see **Table 3**) is an effective strategy to achieve fast and efficient periplasmic electron transfer.

Furthermore, although there were only a few DDIs in this sub-network, two clusters were clearly formed from these DDIs (**Figure 6**). Previous studies have concluded that DDIs correspond to strong interactions that form functional modules in PPI networks (Kim et al., 2014). We therefore suggest that two functional clusters exist in periplasmic electron transfer (**Figure 6**, clusters 1 and 2). These clusters could be used to assist electrons to reach MtrA and DmsE, respectively, completing the most representative EET pathways: the MtrCAB pathway and the DMSO pathway. In addition to these EET pathways, they can also aid other proteins located at outer membrane or extracellularly (**Figure 6**).

CONCLUSION

Shewanella oneidensis MR-1 is able to utilize a wide variety of extracellular solid electron acceptors such as iron or manganese oxides, which implies that it has evolved effective EET strategies (Kasai et al., 2015). Typically, this species uses numerous diverse biological pathways to efficiently perform such processes, which means that there is an interconnected network existent. As networks have been shown to strongly correlate with their function, and previous studies have shown high efficiency in the prediction of biological relevancy using network topology (Planas-Iglesias et al., 2012; Huang et al., 2013; Mukhopadhyay and Maulik, 2014), we thus explored such EET processes through an electron transfer network in *S. oneidensis* MR-1. We identified that protein disordered regions played an important role during the formation and extension of the electron transfer network, by analyzing the average disordered regions of proteins in every shell of the network. We also found that there are distinct functional parts in the network, and the functional significance of the various shells was discussed. Such a network-based study can be helpful for understanding potential EET processes in *S. oneidensis* MR-1.

AUTHOR CONTRIBUTIONS

DD designed the study, carried out the study and drafted the manuscript; LL helped construct the network and write the manuscript; CS helped write the manuscript; XS conceived of the study and was the lead writer of the manuscript. All authors read and approved the final manuscript.

FUNDING

The work was supported by the National Natural Science Foundation of China (No. 61472078), the Open Research Fund of State Key Laboratory of Bioelectronics from Southeast

University, and the Natural Science Foundation of Anhui Education Department (KJ2015A264, KJ2015A290).

ACKNOWLEDGMENT

We would like to thank Prof. Hernan A. Makse and Dr. Sen Pei (City College of New York) for the discussion about the k-shell method.

SUPPLEMENTARY MATERIAL

The Supplementary Material for this article can be found online at: <http://journal.frontiersin.org/article/10.3389/fmicb.2016.00530>

REFERENCES

- Atkinson, S. J., Mowat, C. G., Reid, G. A., and Chapman, S. K. (2007). An octaheme c-type cytochrome from *Shewanella oneidensis* can reduce nitrite and hydroxylamine. *FEBS Lett.* 581, 3805–3808. doi: 10.1016/j.febslet.2007.07.005
- Beiro, M. G., Alvarez-Hamelin, J. I., and Busch, J. R. (2008). A low complexity visualization tool that helps to perform complex systems analysis. *New J. Phys.* 10, 125003. doi: 10.1088/1367-2630/10/12/125003
- Borloo, J., Desmet, L., Beeumen, J. V., and Devreese, B. (2011). Bacterial two-hybrid analysis of the *Shewanella oneidensis* MR-1 multi-component electron transfer pathway. *J. Integr. OMICS* 1, 68. doi: 10.5584/jomics.v1i2.68
- Breuer, M., Rosso, K. M., and Blumberger, J. (2014). Electron flow in multiheme bacterial cytochromes is a balancing act between heme electronic interaction and redox potentials. *Proc. Natl. Acad. Sci. U.S.A.* 111, 611–616. doi: 10.1073/pnas.1316156111
- Breuer, M., Zarzycki, P., Blumberger, J., and Rosso, K. M. (2012). Thermodynamics of electron flow in the bacterial deca-heme cytochrome mtrF. *J. Am. Chem. Soc.* 134, 9868–9871. doi: 10.1021/ja3027696
- Brockman, K. L. (2014). *Enzyme Activity, Maturation and Regulation of Anaerobic Reductases in Shewanella oneidensis MR-1*. Ph.D. theses and dissertations Paper 669. Available at: <http://dc.uwm.edu/etd/669>
- Buljan, M., Chalancon, G., Dunker, A. K., Bateman, A., Balaji, S., Fuxreiter, M., et al. (2013). Alternative splicing of intrinsically disordered regions and rewiring of protein interactions. *Curr. Opin. Struct. Biol.* 23, 443–450. doi: 10.1016/j.sbi.2013.03.006
- Burns, J. L., and DiChristina, T. J. (2009). Anaerobic respiration of elemental sulfur and thiosulfate by *Shewanella oneidensis* MR-1 requires psrA, a homolog of the phsA gene of *Salmonella enterica* serovar typhimurium LT2. *Appl. Environ. Microbiol.* 75, 5209–5217. doi: 10.1128/AEM.00888-09
- Coursolle, D., and Gralnick, J. A. (2010). Modularity of the Mtr respiratory pathway of *Shewanella oneidensis* strain MR-1. *Mol. Microbiol.* 77, 995–1008. doi: 10.1111/j.1365-2958.2010.07266.x
- Coursolle, D., and Gralnick, J. A. (2012). Reconstruction of extracellular respiratory pathways for iron(III) reduction in *Shewanella oneidensis* strain MR-1. *Front. Microbiol.* 3:56. doi: 10.3389/fmicb.2012.00056
- Davis, D., Yaveroglu, O. N., Malod-Dognin, N., Stojmirovic, A., and Przulj, N. (2015). Topology-function conservation in protein-protein interaction networks. *Bioinformatics* 31, 1632–1639. doi: 10.1093/bioinformatics/btv026
- Ding, D. W., Xu, J., Li, L., Xie, J. M., and Sun, X. (2014). Identifying the potential extracellular electron transfer pathways from a c-type cytochrome network. *Mol. Biosyst.* 10, 3138–3146. doi: 10.1039/c4mb00386a
- Dohnalkova, A. C., Marshall, M. J., Arey, B. W., Williams, K. H., Buck, E. C., and Fredrickson, J. K. (2011). Imaging hydrated microbial extracellular polymers: comparative analysis by electron microscopy. *Appl. Environ. Microbiol.* 77, 1254–1262. doi: 10.1128/AEM.02001-10
- DATA SHEET S1 | Four hundred and eighty-one electron transfer proteins which were identified to be potentially involved in the EET processes.
- DATA SHEET S2 | Electron transfer network which was obtained from STRING (December 2014).
- DATA SHEET S3 | K-shell values for the proteins in the final electron transfer network.
- DATA SHEET S4 | The numbers of disordered regions for the proteins (aa length \geq 100) in the final electron transfer network.
- DATA SHEET S5 | Subcellular localization for the proteins in the final electron transfer network.
- DATA SHEET S6 | Protein domains for the proteins in the final electron transfer network.
- METHODS | Detailed information on the methods used.**
- Embree, M., Qiu, Y., Shieh, W., Nagarajan, H., O’Neil, R., Lovley, D., et al. (2014). The iron stimulon and fur regulon of *Geobacter sulfurreducens* and their role in energy metabolism. *Appl. Environ. Microbiol.* 80, 2918–2927. doi: 10.1128/AEM.03916-13
- Finn, R. D., Bateman, A., Clements, J., Coggill, P., Eberhardt, R. Y., Eddy, S. R., et al. (2014). Pfam: the protein families database. *Nucleic Acids Res.* 42, D222–D230. doi: 10.1093/nar/gkt1223
- Fonseca, B. M., Paquete, C. M., Neto, S. E., Pacheco, I., Soares, C. M., and Louro, R. O. (2013). Mind the gap: cytochrome interactions reveal electron pathways across the periplasm of *Shewanella oneidensis* MR-1. *Biochem. J.* 449, 101–108. doi: 10.1042/BJ20121467
- Franceschini, A., Szklarczyk, D., Frankild, S., Kuhn, M., Simonovic, M., Roth, A., et al. (2013). STRING v9.1: protein-protein interaction networks, with increased coverage and integration. *Nucleic Acids Res.* 41, D808–D815. doi: 10.1093/nar/gks1094
- Gao, H., Barua, S., Liang, Y., Wu, L., Dong, Y., Reed, S., et al. (2010). Impacts of *Shewanella oneidensis* c-type cytochromes on aerobic and anaerobic respiration. *Microb. Biotechnol.* 3, 455–466. doi: 10.1111/j.1751-7915.2010.00181.x
- Gao, H., Yang, Z. K., Barua, S., Reed, S. B., Romine, M. F., Nealson, K. H., et al. (2009). Reduction of nitrate in *Shewanella oneidensis* depends on atypical NAP and NRF systems with NapB as a preferred electron transport protein from CymA to NapA. *ISME J.* 3, 966–976. doi: 10.1038/ismej.2009.40
- Goldbeck, C. P., Jensen, H. M., TerAvest, M. A., Beedle, N., Appling, Y., Hepler, M., et al. (2013). Tuning promoter strengths for improved synthesis and function of electron conduits in *Escherichia coli*. *ACS Synth. Biol.* 2, 150–159. doi: 10.1021/sb300119v
- Gon, S., Patte, J. C., Dos Santos, J. P., and Mejean, V. (2002). Reconstitution of the trimethylamine oxide reductase regulatory elements of *Shewanella oneidensis* in *Escherichia coli*. *J. Bacteriol.* 184, 1262–1269. doi: 10.1128/JB.184.5.1262-1269.2002
- Gralnick, J. A., Vali, H., Lies, D. P., and Newman, D. K. (2006). Extracellular respiration of dimethyl sulfoxide by *Shewanella oneidensis* strain MR-1. *Proc. Natl. Acad. Sci. U.S.A.* 103, 4669–4674. doi: 10.1073/pnas.0505959103
- Heidelberg, J. F., Paulsen, I. T., Nelson, K. E., Gaidos, E. J., Nelson, W. C., Read, T. D., et al. (2002). Genome sequence of the dissimilatory metal ion-reducing bacterium *Shewanella oneidensis*. *Nat. Biotechnol.* 20, 1118–1123. doi: 10.1038/nbt749
- Huang, C., Ba, Q., Yue, Q., Li, J., Li, J., Chu, R., et al. (2013). Artemisinin rewrites the protein interaction network in cancer cells: network analysis, pathway identification, and target prediction. *Mol. Biosyst.* 9, 3091–3100. doi: 10.1039/c3mb70342h
- Jaroszewski, L., Rychlewski, L., Li, Z., Li, W., and Godzik, A. (2005). FFAS03: a server for profile-profile sequence alignments. *Nucleic Acids Res.* 33, W284–W288. doi: 10.1093/nar/gki418
- Jin, M., Jiang, Y., Sun, L., Yin, J., Fu, H., Wu, G., et al. (2013). Unique organizational and functional features of the cytochrome c maturation system

- in *Shewanella oneidensis*. *PLoS ONE* 8:e75610. doi: 10.1371/journal.pone.0075610
- Kasai, T., Kouzuma, A., Nojiri, H., and Watanabe, K. (2015). Transcriptional mechanisms for differential expression of outer membrane cytochrome genes omcA and mtrC in *Shewanella oneidensis* MR-1. *BMC Microbiol.* 15:68. doi: 10.1186/s12866-015-0406-8
- Kim, I., Lee, H., Han, S. K., and Kim, S. (2014). Linear motif-mediated interactions have contributed to the evolution of modularity in complex protein interaction networks. *PLoS Comput. Biol.* 10:e1003881. doi: 10.1371/journal.pcbi.1003881
- Kim, J., Kim, I., Yang, J. S., Shin, Y. E., Hwang, J., Park, S., et al. (2012). Rewiring of PDZ domain-ligand interaction network contributed to eukaryotic evolution. *PLoS Genet.* 8:e1002510. doi: 10.1371/journal.pgen.1002510
- Kim, P. M., Korbel, J. O., and Gerstein, M. B. (2007). Positive selection at the protein network periphery: evaluation in terms of structural constraints and cellular context. *Proc. Natl. Acad. Sci. U.S.A.* 104, 20274–20279. doi: 10.1073/pnas.0710183104
- Kitsak, M., Gallos, L. K., Havlin, S., Liljeros, F., Muchnik, L., Stanley, H. E., et al. (2010). Identification of influential spreaders in complex networks. *Nat. Phys.* 6, 888–893. doi: 10.1038/nphys1746
- Kracke, F., Vassilev, I., and Kromer, J. O. (2015). Microbial electron transport and energy conservation – the foundation for optimizing bioelectrochemical systems. *Front. Microbiol.* 6:575. doi: 10.3389/fmicb.2015.00575
- Lobanov, M. Y., and Galzitskaya, O. V. (2011). The Ising model for prediction of disordered residues from protein sequence alone. *Phys. Biol.* 8:035004. doi: 10.1088/1478-3975/8/3/035004
- Meyer, T. E., Tsapin, A. I., Vandenberghe, I., de Smet, L., Frishman, D., Nealson, K. H., et al. (2004). Identification of 42 possible cytochrome c genes in the *Shewanella oneidensis* genome and characterization of six soluble cytochromes. *OMICS* 8, 57–77. doi: 10.1089/153623104773547499
- Mosca, R., Ceol, A., Stein, A., Olivella, R., and Aloy, P. (2014). 3did: a catalogue of domain-based interactions of known three-dimensional structure. *Nucleic Acids Res.* 42, D374–D379. doi: 10.1093/nar/gkt887
- Mukhopadhyay, A., and Maulik, U. (2014). Network-based study reveals potential infection pathways of hepatitis-c leading to various diseases. *PLoS ONE* 9:e94029. doi: 10.1371/journal.pone.0094029
- Nam, H., Lewis, N. E., Lerman, J. A., Lee, D. H., Chang, R. L., Kim, D., et al. (2012). Network context and selection in the evolution to enzyme specificity. *Science* 337, 1101–1104. doi: 10.1126/science.1216861
- Pavlovic-Lazetic, G. M., Mitic, N. S., Kovacevic, J. J., Obradovic, Z., Malkov, S. N., and Beljanski, M. V. (2011). Bioinformatics analysis of disordered proteins in prokaryotes. *BMC Bioinformatics* 12:66. doi: 10.1186/1471-2105-12-66
- Pei, S., Muchnik, L., Andrade, J. S. Jr., Zheng, Z., and Makse, H. A. (2014). Searching for superspreaders of information in real-world social media. *Sci. Rep.* 4, 5547. doi: 10.1038/srep05547
- Pinchuk, G. E., Geydebrekht, O. V., Hill, E. A., Reed, J. L., Konopka, A., Beliaev, A. S., et al. (2011). Pyruvate and lactate metabolism by *Shewanella oneidensis* MR-1 under fermentation, oxygen limitation, and fumarate respiration conditions. *Appl. Environ. Microbiol.* 77, 8234–8240. doi: 10.1128/AEM.05382-11
- Pinchuk, G. E., Hill, E. A., Geydebrekht, O. V., De Ingeniis, J., Zhang, X., Osterman, A., et al. (2010). Constraint-based model of *Shewanella oneidensis* MR-1 metabolism: a tool for data analysis and hypothesis generation. *PLoS Comput. Biol.* 6:e1000822. doi: 10.1371/journal.pcbi.1000822
- Planas-Iglesias, J., Guney, E., Garcia-Garcia, J., Robertson, K. A., Raza, S., Freeman, T. C., et al. (2012). Extending signaling pathways with protein-interaction networks. Application to apoptosis. *OMICS* 16, 245–256. doi: 10.1089/omi.2011.0130
- Radivojac, P., Clark, W. T., Oron, T. R., Schnoes, A. M., Wittkop, T., Sokolov, A., et al. (2013). A large-scale evaluation of computational protein function prediction. *Nat. Methods* 10, 221–227. doi: 10.1038/nmeth.2340
- Romine, M. F., Carlson, T. S., Norbeck, A. D., McCue, L. A., and Lipton, M. S. (2008). Identification of mobile elements and pseudogenes in the *Shewanella oneidensis* MR-1 genome. *Appl. Environ. Microbiol.* 74, 3257–3265. doi: 10.1128/AEM.02720-07
- Rosenbaum, M. A., Bar, H. Y., Beg, Q. K., Segre, D., Booth, J., Cotta, M. A., et al. (2012). Transcriptional analysis of *Shewanella oneidensis* MR-1 with an electrode compared to Fe(III) citrate or oxygen as terminal electron acceptor. *PLoS ONE* 7:e30827. doi: 10.1371/journal.pone.0030827
- Rotaru, A. E., Woodard, T. L., Nevin, K. P., and Lovley, D. R. (2015). Link between capacity for current production and syntrophic growth in *Geobacter* species. *Front. Microbiol.* 6:744. doi: 10.3389/fmicb.2015.00744
- Schutz, B., Seidel, J., Sturm, G., Einsle, O., and Gescher, J. (2011). Investigation of the electron transport chain to and the catalytic activity of the diheme cytochrome c peroxidase CcpA of *Shewanella oneidensis*. *Appl. Environ. Microbiol.* 77, 6172–6180. doi: 10.1128/AEM.00606-11
- Shi, L., Rosso, K. M., Clarke, T. A., Richardson, D. J., Zachara, J. M., and Fredrickson, J. K. (2012). Molecular underpinnings of Fe(III) oxide reduction by *Shewanella oneidensis* MR-1. *Front. Microbiol.* 3:50. doi: 10.3389/fmicb.2012.00050
- Shi, L., Squier, T. C., Zachara, J. M., and Fredrickson, J. K. (2007). Respiration of metal (hydr)oxides by *Shewanella* and *Geobacter*: a key role for multihaem c-type cytochromes. *Mol. Microbiol.* 65, 12–20. doi: 10.1111/j.1365-2958.2007.05783.x
- Shrestha, P. M., and Rotaru, A. E. (2014). Plugging in or going wireless: strategies for interspecies electron transfer. *Front. Microbiol.* 5:237. doi: 10.3389/fmicb.2014.00237
- Smith, J. A., Nevin, K. P., and Lovley, D. R. (2015). Syntrophic growth via quinone-mediated interspecies electron transfer. *Front. Microbiol.* 6:121. doi: 10.3389/fmicb.2015.00121
- Stams, A. J., and Plugge, C. M. (2009). Electron transfer in syntrophic communities of anaerobic bacteria and archaea. *Nat. Rev. Microbiol.* 7, 568–577. doi: 10.1038/nrmicro2166
- Sturm, G., Richter, K., Doetsch, A., Heide, H., Louro, R. O., and Gescher, J. (2015). A dynamic periplasmic electron transfer network enables respiratory flexibility beyond a thermodynamic regulatory regime. *ISME J.* 9, 1802–1811. doi: 10.1038/ismej.2014.264
- Tremblay, P. L., and Zhang, T. (2015). Electrifying microbes for the production of chemicals. *Front. Microbiol.* 6:201. doi: 10.3389/fmicb.2015.00201
- Tremblay, P. L., Zhang, T., Dar, S. A., Leang, C., and Lovley, D. R. (2012). The Rnf complex of *Clostridium ljungdahlii* is a proton-translocating ferredoxin:NAD+ oxidoreductase essential for autotrophic growth. *MBio* 4, e406–e412. doi: 10.1128/mBio.00406-12
- Uhart, M., and Bustos, D. M. (2014). Protein intrinsic disorder and network connectivity, the case of 14-3-3 proteins. *Front. Genet.* 5:10. doi: 10.3389/fgene.2014.00010
- van der Lee, R., Buljan, M., Lang, B., Weatheritt, R. J., Daughdrill, G. W., Dunker, A. K., et al. (2014). Classification of intrinsically disordered regions and proteins. *Chem. Rev.* 114, 6589–6631. doi: 10.1021/cr40525m
- Vazquez, A., Flammini, A., Maritan, A., and Vespignani, A. (2003). Global protein function prediction from protein-protein interaction networks. *Nat. Biotechnol.* 21, 697–700. doi: 10.1038/nbt825
- Venkateswaran, K., Moser, D. P., Dollhopf, M. E., Lies, D. P., Saffarini, D. A., MacGregor, B. J., et al. (1999). Polyphasic taxonomy of the genus *Shewanella* and description of *Shewanella oneidensis* sp. nov. *Int. J. Syst. Bacteriol.* 49, 705–724. doi: 10.1099/00207713-49-2-705
- Volkov, A. N., and van Nuland, N. A. J. (2012). Electron transfer interactome of cytochrome c. *PLoS Comput. Biol.* 8:e1002807. doi: 10.1371/journal.pcbi.1002807
- Wang, V. B., Sivakumar, K., Yang, L., Zhang, Q., Kjelleberg, S., Loo, S. C. J., et al. (2015). Metabolite-enabled mutualistic interaction between *Shewanella oneidensis* and *Escherichia coli* in a co-culture using an electrode as electron acceptor. *Sci. Rep.* 5, 11222. doi: 10.1038/srep11222
- Wright, P. E., and Dyson, H. J. (2015). Intrinsically disordered proteins in cellular signalling and regulation. *Nat. Rev. Mol. Cell Biol.* 16, 18–29. doi: 10.1038/nrm3920
- Wuchty, S., and Almaas, E. (2005). Peeling the yeast protein network. *Proteomics* 5, 444–449. doi: 10.1002/pmic.200400962

- Yin, J., Jin, M., Zhang, H., Ju, L., Zhang, L., and Gao, H. (2015). Regulation of nitrite resistance of the cytochrome *cbb3* oxidase by cytochrome *c* ScyA in *Shewanella oneidensis*. *Microbiol. Open* 4, 84–99. doi: 10.1002/mbo3.224
- Yu, C. S., Chen, Y. C., Lu, C. H., and Hwang, J. K. (2006). Prediction of protein subcellular localization. *Proteins* 64, 643–651. doi: 10.1002/prot.21018
- Yu, N. Y., Wagner, J. R., Laird, M. R., Melli, G., Rey, S., Lo, R., et al. (2010). PSORTb 3.0: improved protein subcellular localization prediction with refined localization subcategories and predictive capabilities for all prokaryotes. *Bioinformatics* 26, 1608–1615. doi: 10.1093/bioinformatics/btq249
- Zhang, H., Tang, X., Munske, G. R., Zakharova, N., Yang, L., Zheng, C., et al. (2008). In vivo identification of the outer membrane protein OmcA-MtrC interaction network in *Shewanella oneidensis* MR-1 cells using novel hydrophobic chemical cross-linkers. *J. Proteome Res.* 7, 1712–1720. doi: 10.1021/pr7007658

Conflict of Interest Statement: The authors declare that the research was conducted in the absence of any commercial or financial relationships that could be construed as a potential conflict of interest.

Copyright © 2016 Ding, Li, Shu and Sun. This is an open-access article distributed under the terms of the Creative Commons Attribution License (CC BY). The use, distribution or reproduction in other forums is permitted, provided the original author(s) or licensor are credited and that the original publication in this journal is cited, in accordance with accepted academic practice. No use, distribution or reproduction is permitted which does not comply with these terms.



Performance of Denitrifying Microbial Fuel Cell with Biocathode over Nitrite

Huimin Zhao^{1,2}, Jianqiang Zhao^{1*}, Fenghai Li² and Xiaoling Li¹

¹ Department of Environmental Engineering, School of Environmental Science and Engineering, Chang'an University, Xi'an, China, ² Department of Chemistry and Chemical Engineering, Heze University, Heze, China

Microbial fuel cell (MFC) with nitrite as an electron acceptor in cathode provided a new technology for nitrogen removal and electricity production simultaneously. The influences of influent nitrite concentration and external resistance on the performance of denitrifying MFC were investigated. The optimal effectiveness were obtained with the maximum total nitrogen (TN) removal rate of $54.80 \pm 0.01 \text{ g m}^{-3} \text{ d}^{-1}$. It would be rather desirable for the TN removal than electricity generation at lower external resistance. Denaturing gradient gel electrophoresis suggested that *Proteobacteria* was the predominant phylum, accounting for 35.72%. *Thiobacillus* and *Afipia* might benefit to nitrite removal. The presence of nitrifying *Devosia* indicated that nitrite was oxidized to nitrate via a biochemical mechanism in the cathode. *Ignavibacterium* and *Anaerolineaceae* was found in the cathode as a heterotrophic bacterium with sodium acetate as substrate, which illustrated that sodium acetate in anode was likely permeated through proton exchange membrane to the cathode.

OPEN ACCESS

Edited by:

Yong Xiao,

Chinese Academy of Sciences, China

Reviewed by:

S. Venkata Mohan,
CSIR-Indian Institute of Chemical

Technology, India

Jie Wang,

Tianjin Polytechnic University, China

*Correspondence:

Jianqiang Zhao

626710287@qq.com

Specialty section:

This article was submitted to
*Microbiotechnology, Ecotoxicology
and Bioremediation*,
a section of the journal
Frontiers in Microbiology

Received: 17 September 2015

Accepted: 03 March 2016

Published: 22 March 2016

Citation:

Zhao H, Zhao J, Li F and Li X (2016)
Performance of Denitrifying Microbial
Fuel Cell with Biocathode over Nitrite.
Front. Microbiol. 7:344.
doi: 10.3389/fmicb.2016.00344

INTRODUCTION

Microbial fuel cell (MFC) possesses great potential in the application of wastewater treatment because of its unique capability of converting the chemical energy of organic waste into electrical energy (Logan et al., 2006). It has been proved that both nitrate and nitrite can be removed from wastewater as electron acceptors in the cathode of MFCs through electrochemical reduction or autotrophic denitrification (Wang et al., 2009; Desloover et al., 2011; Zhao et al., 2011). In MFC, the organic substrates are oxidized by exoelectrogenic microbes in the anode chamber to produce electrons and protons. Electrons produced are transferred through the external circuit to the cathode while protons move through the proton exchange membrane to the cathode, where they combine to an electron acceptor (e.g., nitrate or nitrite) to complete the circuit (Van Doan et al., 2013). Virdis et al. (2008) discovered that nitrite could serve as an efficient terminal electron acceptor at the cathode of MFC, which further reduced the carbon-nitrogen ratio demand. The similar results were also demonstrated by Puig et al. (2011) and Desloover et al. (2011). The biotic cathode using nitrite as an electron acceptor showed a TN removal percentage of 48% and a removal rate of $7.6 \text{ g } (\text{NO}_2^- - \text{N}) \text{ m}^{-3} \text{ d}^{-1}$ during the 4 h continuing mode of operation (Puig et al., 2011). Although the TN removal rate via cathodic (autotrophic) denitrification in MFC is generally lower than that via heterotrophic denitrification, it is very important to notice that autotrophic microbes need few carbon source and their slow growth results in small sludge production (Wang et al., 2009; Zhao et al., 2011). Consequently, autotrophic denitrifying MFCs are promising technologies to treat low organic carbon wastewater, which greatly reduced the dependence on carbon in denitrifying process.

However, nitrite is oxidized easily by biological or electrochemical processes which significantly degraded the TN removal and electricity generation efficiency. Puig et al. (2011) found that about 52% nitrite oxidized to nitrate in the MFC cathode at an external resistance of $100\ \Omega$. And he speculated that disappeared nitrite was oxidized by nitrite oxidizing bacteria (NOBs) or by other electrochemical processes. Li et al. (2014) also found that about 80% nitrite oxidized to nitrate. To inhibit the nitrification, one way was to add sodium azide in the cathode (Guisasola et al., 2005; Puig et al., 2011), the other way was to change the operating conditions of a cathode chamber (e.g. external resistance and HRT and temperature; Li et al., 2014). In order to further clarify these influencing factors of denitrifying MFC and the mechanism of nitrite conversion to nitrate in the cathode of MFC without the addition of chemical inhibitors, this study aimed to investigate the performance of the denitrification of MFC, which based on electricity generation and nitrite removal with different nitrite concentrations and external resistances in the denitrifying MFC at the long duration of the operation. PCR-DGGE was used to assess the cathode microbial community to speculate for possible reactions in the cathode.

MATERIALS AND METHODS

Structure of MFC and Operation

The MFC consisting of an anode chamber and a cathode chamber placed on opposite sides of a single methacrylate rectangular chamber with dimensions of 15 cm high, 5 cm long, and 2.5 cm wide. A proton exchange membrane (nafion117, DuPont, USA) was used as a separator between anode and cathode chambers. Each chamber was filled with rectangular graphite felts (140 mm long, 11.7 mm wide, and 5 mm thick) as electrode and inserted with a graphite rod, which led to the eventual volume of 160 cm^3 for cathodic and anodic chamber, respectively. The electrodes were sequentially washed in 1 M HCl and 1 M NaOH to remove possible metal and biomass contamination (Bond and Lovley, 2003). The cathodic and the anodic electrodes were connected to the external resistor to close the electric circuit. A Hg/Hg Cl electrode ($+0.242\text{ V}$ vs. SHE) was used as a reference electrode placing in the cathode solution. Three peristaltic pumps (Lan Ge YZ1515X, Baoding, China) were used to continuously supply influents to anode and cathode chambers, and reflux the cathode solution. All experiments were performed at $32 \pm 1^\circ\text{C}$. **Figure 1** showed the schematic diagram of the MFC in this study.

The electrode material was immersed in corresponding seeding sludge (anaerobic sludge from Xi'an Hans Brewery Wastewater Treatment, China) for 48 h to absorb bacteria and then loaded in corresponding chambers. The starting procedure of the MFC was followed as reported by Virdis et al. (2008). The flow rate of influent was maintained at 3 mL h^{-1} . The initial resistance was set at $1000\ \Omega$ for 15 days and then turned to $100\ \Omega$ for about a month. When the output voltage of the MFC was stable and reached 200 mV with external resistance of $100\ \Omega$, the start-up of the MFC was considered to be successful. Then, the resistance was kept constant at $10\ \Omega$, and maintained for 240

days. A series of experiments were performed, the performance of MFC was studied in terms of changing the nitrite nitrogen concentrations of ($60, 90$, and 180 mg L^{-1}) at external resistance of $10\ \Omega$. Afterward, the effect of external resistance was studied by varying external resistances in the range from 5 to 10, 25, 50, 100, and $200\ \Omega$.

The anode solution was composed of CH_3COONa (3.84 g L^{-1}), KCl (0.13 g L^{-1}), $\text{MgSO}_4 \cdot 7\text{H}_2\text{O}$ (0.1 g L^{-1}), CaCl_2 (0.015 g L^{-1}), $\text{K}_2\text{HPO}_4 \cdot 3\text{H}_2\text{O}$ (8.57 g L^{-1}), KH_2PO_4 (2.88 g L^{-1}), and trace elements 1 mL L^{-1} .

The cathode solution was composed of NaNO_2 (0.15 g L^{-1}), NaHCO_3 (1 g L^{-1}), $\text{MgSO}_4 \cdot 7\text{H}_2\text{O}$ (0.1 g L^{-1}), CaCl_2 (0.015 g L^{-1}), $\text{K}_2\text{HPO}_4 \cdot 3\text{H}_2\text{O}$ (8.57 g L^{-1}), KH_2PO_4 (2.88 g L^{-1}), and trace elements 1 mL L^{-1} .

Data Calculation and Analysis

The voltage (V) and cathode potentials of the MFC were monitored at 1 min intervals and 10 min averaged with a data acquisition system (Yanhua PCI1713, China). Current (I) and power ($P = I \cdot V$) were determined according to Ohm's law. Power and current densities were calculated by dividing power or current by the net cathodic volume. The cathodic Coulombic efficiencies was calculated according to Logan et al. (2006). DO was determined using Hach-HQ30d (HACH, USA). The concentrations of NO_2^- -N and NO_3^- -N were measured according to standard methods (APHA, 1998). During the experimental, all analyses under the same operations were carried out more than triplicate.

DNA Analysis

After being operated stably for 9 months at the external resistance of $10\ \Omega$ and the flow rate of 3 mL h^{-1} and the nitrite nitrogen concentrations of 188 mg L^{-1} , biofilm sample from the suspension liquid of the cathode was taken to be investigated with denaturing gradient gel electrophoresis (DGGE), and DNA was extracted using a fast DNA spin kit (SK8233) for soil according to the manufacturer's instructions. The bacterial 16S rRNA genes were amplified by polymerase chain reaction (PCR) techniques with the universal primers F357-GC (5'-CGCCCGCCGCCGCCGC CGCCGGCCGCCGCC CGCCCCCTACGGGAGGCAGCAG-3') and R518 (5'-ATT ACCGCG GCTGCTGG-3'). Polyacrylamide gel (8%) with a 30–60% denaturing gradient was used to separate the PCR products (7 mol L^{-1} urea and 40% formamide comprising 100% denaturant), and the PCR product was analyzed by the DGGE technology and washed with ultrapure water for flushing the gel and dye. The eight representative DGGE strips were selected by a clean scalpel to select and transfer in a 1.5 mL centrifuge tube. Then, the target DNA fragments were excised and reamplified by using the primer sets F357 (5'-CCTACGGGAGGCAGCAG-3') and R518 (5'-ATTACCGCGGCTGCTGG-3'), and the obtained sequence was matched with the Seqmatch database for sequence alignment. The homology information of each strip was obtained by Shanghai Sangon Biological Engineering Co., Ltd. China. This process was similar to that reported by Deng et al. (2016).

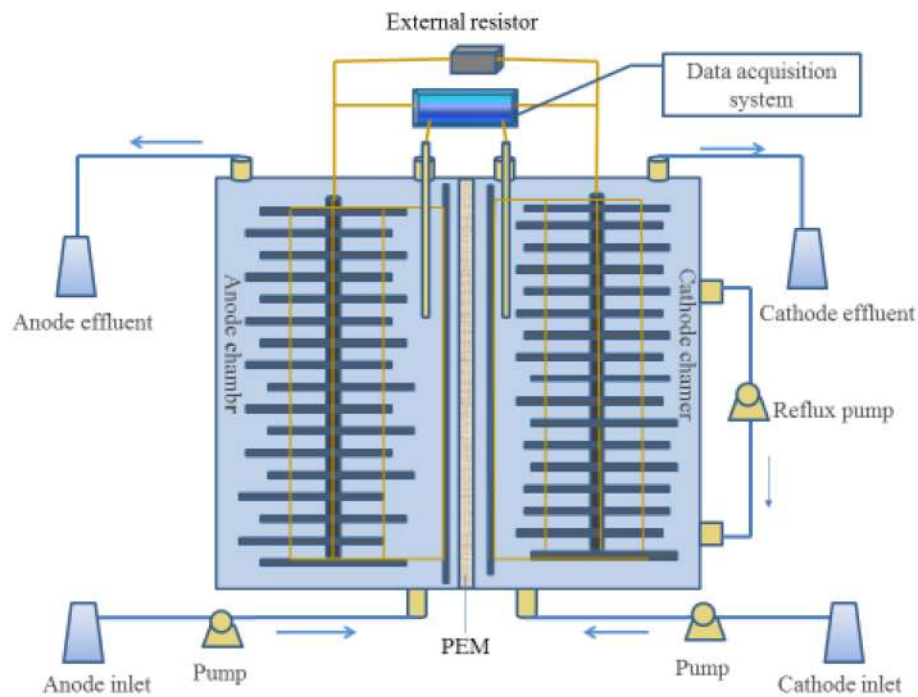


FIGURE 1 | Schematic of the double chamber MFC.

TABLE 1 | Electrical characteristics of the MFC with different nitrite concentrations.

Inflow rate (mL h ⁻¹)	Influent NO ₂ ⁻ -N (mg L ⁻¹)	Cathode potential (mV)	Current density (A m ⁻³)	Power density (W m ⁻³)	Coulombic efficiency (%)
3	60.11 ± 0.34	-35.2 ± 3.2	18.02 ± 0.81	0.518 ± 0.035	279.5 ± 32.15
3	86.65 ± 0.61	-47.22 ± 5.3	19.25 ± 1.07	0.594 ± 0.071	231.53 ± 28.53
3	188.12 ± 2.3	-38.36 ± 2.5	18.40 ± 0.36	0.541 ± 0.004	140.12 ± 0.71

TABLE 2 | Characteristics of denitrification with different nitrite concentrations.

Inflow rate (mL h ⁻¹)	Influent NO ₂ ⁻ -N (mg L ⁻¹)	Effluent NO ₂ ⁻ -N (mg L ⁻¹)	Δ NO ₃ ⁻ -N (mg L ⁻¹)	Nitrification Percentage (%)	TN removal (g m ⁻³ d ⁻¹)	Δ pH Effluent
3	60.11 ± 0.34	0	0.2 ± 0.1	0.33	26.91 ± 1.72	0.85
3	86.65 ± 0.61	4.03 ± 2.17	5.03 ± 3.35	5.81	34.92 ± 2.2	1.03
3	188.12 ± 2.3	16.72 ± 0.59	49.5 ± 0.5	26.33	54.80 ± 0.01	1.18

Δ NO₃⁻-N = incremental nitrate.

RESULTS AND DISCUSSION

Performance of Denitrification MFC with Different Nitrite Concentrations

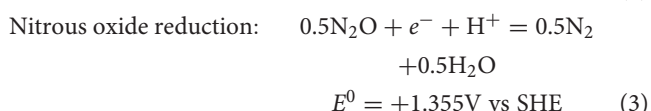
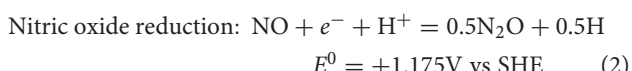
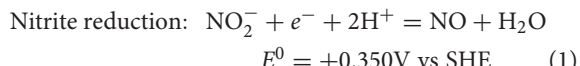
The results of different influent nitrite concentration at the inflow rate of 3 mL h⁻¹ and the external resistance of 10 Ω and temperature of 32°C were listed in Tables 1, 2.

As shown in Table 1, when the flow rate was 3 mL·h⁻¹, the increase of influent nitrite concentration had little benefit on current density and power density. The cathode potential decreased with the increase of current density. The cathode

coulombic efficiency was higher than 100% due to other oxidizing substances (e.g., oxygen) in the cathode functioning as a terminal electron acceptor especially when the nitrite concentration of the effluent was about zero (Table 2; Xie et al., 2011). Cha et al. (2010) found that microorganism using with oxygen as electron acceptor for oxygen utilization efficiency was very high, which might compete with denitrifying microorganism and affect the cathode denitrification.

The autotrophic denitrification of nitrite to nitrogen gas in the bio-cathode can be described by the following equations (reaction 1-3; Clauwaert et al., 2007). Table 2 showed that when

the flow rate was maintained at 3 mL h^{-1} , with increasing concentration of the influent nitrite, the TN removal rate increased significantly from $26.91 \pm 1.72\text{ g m}^{-3}\text{ d}^{-1}$ to the maximum of $54.80 \pm 0.01\text{ g m}^{-3}\text{ d}^{-1}$; but the nitrification percentage increased from 0.33 to 26.33% meanwhile. Therefore, considering two factors of nitrification and the TN removal, we operated the MFC at the high influent nitrite of 188 mg L^{-1} which would be favorable.



Under the condition of strict measures to maintain the anoxic condition in the cathode, but the cathode still showed obvious nitrite nitrification. The small part of nitrite to nitrate transformation might be caused by biological nitrification in this study (reaction 4) because of trace oxygen in the cathode. While the other part of the nitrite transformation also might be oxidized by other electrochemical processes (Puig et al., 2011).

Performance of Denitrification MFC at Different External Resistances

When the influent nitrogen concentration and influent flow rate were $188 \pm 2.3\text{ mg L}^{-1}$, 3 mL h^{-1} , respectively. The results of denitrification at different external resistances were shown in Figures 2, 3, respectively.

Different external resistances cause different electron transfer rates and variations in microbial metabolic activities and kinetic differences in substrate utilization (Zhang et al., 2011). Usually, the pollutant removal of MFC is faster at the smaller external

resistance which can reduce the extracellular electron transfer resistance and increase the electron transfer rate (Katuri et al., 2011). As external resistance was increased from 5 to 200Ω , the concentrations of nitrite in effluent and the TN removal rate decreased significantly from 26.55 ± 0.85 to $1.26 \pm 0.09\text{ mg L}^{-1}$ and 51.51 ± 0.17 to $42.25 \pm 0.24\text{ g m}^{-3}\text{ d}^{-1}$, whereas the nitrate concentration in effluent increased from 52.84 ± 0.48 to $92.62 \pm 1.47\text{ mg L}^{-1}$ (Figure 2), the increase of effluent pH changed with the increase of the TN removal rate, which showed that a large external resistance was not help to denitrification. Zhang and He (2012) found that the TN removal rate increased from 51.9 to 68% with decreasing external resistance from 712 to 10Ω in a dual chamber MFC. At the same time, the potential of cathode increased (excepting at 5Ω) -35.49 to 31.11 mV, while the current density and the cathode coulombic efficiency decreased 15.66–6.7 Am^{-3} and 133.91 to 65.05%. The low coulombic efficiency (65.05%) indicated possible intermediate accumulation such as N_2O and NO. Because the reduction of nitrite to N_2 requires 3 mol electrons, whereas the reduction of nitrite to NO and N_2O need 1 mol and 2 mol electron, respectively, which causing low current density and coulombic efficiency (Wrage et al., 2001). These results were in accordance with Virdis et al. (2010) who observed 29.2% total nitrogen conversion to N_2O , Puig et al. (2011) also showed that the cathode coulombic efficiency was ~48%, confirming the existence of the intermediate product NxO in the process of denitrification, causing the cathode coulombic efficiency to be below 100%.

It was found that the highest power density (1.71 W m^{-3}) was obtained at 50Ω while the highest TN removal rate ($54.80 \pm 0.01\text{ g m}^{-3}\text{ d}^{-1}$) was at 10Ω (Figures 2, 3). The result implied that operation of denitrifying MFC at a lower external resistance would be desirable for the TN removal but not electricity generation (Li et al., 2013). The performance of the MFC became poor when the external resistance was turned to 5Ω , which indicated the MFC reaching the limit current. Therefore, if the aim of the MFC was the TN removal over electricity generation for a denitrifying MFC, operation would be desirable at lower external resistance (except generating limit current).

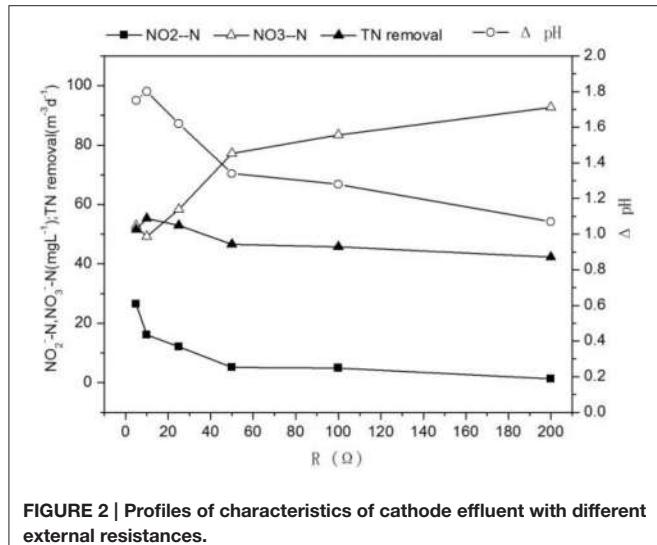


FIGURE 2 | Profiles of characteristics of cathode effluent with different external resistances.

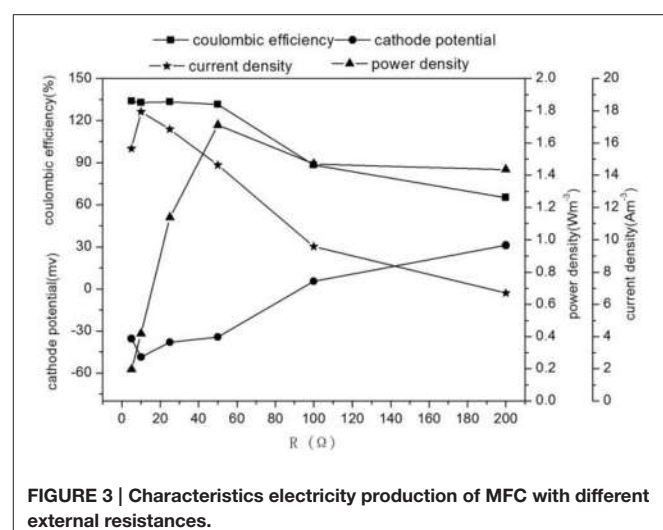
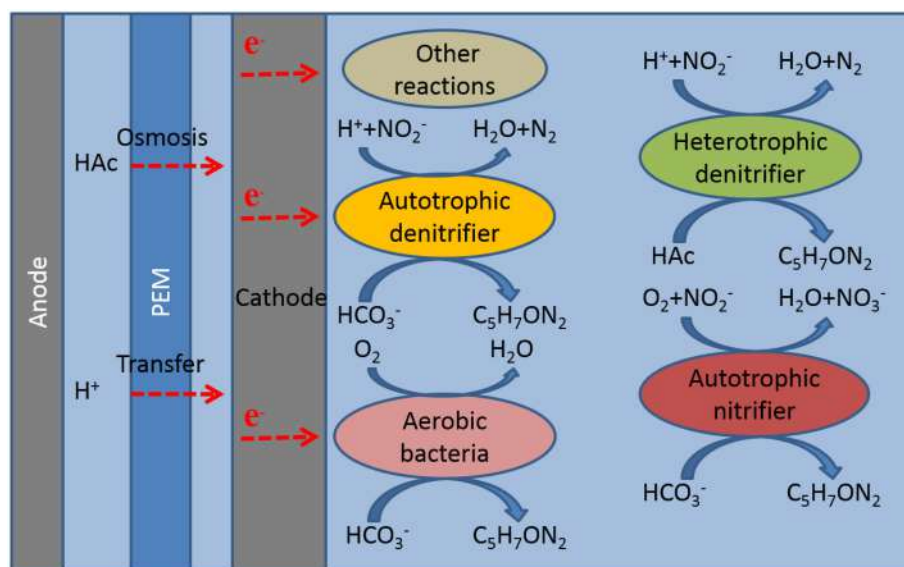


FIGURE 3 | Characteristics electricity production of MFC with different external resistances.

TABLE 3 | The identifications of DGGE bands.

Band	Proportion (%)	Taxon	Similarity (%)	Accession	Phylum/Genus
5	8.19	Uncultured bacterium	100	AY548931	<i>Ignavibacteriae/Ignavibacterium</i>
22	8.95	uncultured bacterium	93	EU283596	<i>Ignavibacteriae/Ignavibacterium</i>
6	4.69	<i>Candidatus Devosia euplotis</i>	81	AJ548823	<i>Proteobacteria/Devosia</i>
19	8.86	uncultured bacterium	88	AB487482	<i>Proteobacteria/Pelomonas</i>
20	8.19	uncultured bacterium	83	FJ516975	<i>Proteobacteria/Thiobacillus</i>
29	13.98	<i>Afipia massiliensis</i>	100	AB272322	<i>Proteobacteria/Afipia</i>
9	7.96	Uncultured bacterium	100	EU083501	<i>Deinococcus-Thermus /Truepera</i>
18	23.02	Uncultured bacterium	93	FN436167	<i>Deinococcus-Thermus/Truepera</i>
16	7.06	<i>Bellilinea caldifistulae</i>	87	AB355078	<i>Chloroflexi/Bellilinea</i>
31	9.09	uncultured bacterium	88	JQ408049	<i>Chloroflexi/Anaerolineaceae</i>

**FIGURE 4 |** Mechanism of the cathode chamber.

Identification of Cathode Microbial Species

The microbial communities of the nitrite bio-cathodes were analyzed by DGGE. As shown in **Table 3**. The microbial community structure was diversity in the cathode of MFC. In addition to these bands, the bio-cathode samples contained clones that were mostly assigned to known sequences. The bacterial communities were *Devosia*(bands 6), *Pelomonas*(bands 19), *Thiobacillus*(bands 20), and *Afipia*(bands 29) in Phylum *Proteobacteria* (35.72%), *Proteobacteria* was found to be dominative in the denitrification of MFC cathode (Karanasios et al., 2010). Kondaveeti et al. (2014) also identified several members of *Proteobacteria* and *Firmicutes* in cathodic nitrate and nitrite reduction. *Truepera*(bands 9 and 18) related to Phylum *Deinococcus-Thermus* (30.98%), *Ignavibacterium*(bands 5 and 22) similar to Phylum *Ignavibacteriae* (17.14%), and *Bellilinea*(bands 16) and *Anaerolineaceae* (bands 31) corresponding to Phylum *Chloroflexi* (16.15%).

Analysis of the microbial communities newly developed on the bio-cathodes revealed that most of them have previously

been demonstrated to be capable of communicating with the electrode. For example, *Afipia* and *Thiobacillus* were dominant species responsible for autotrophic denitrifying in the cathode of MFC (Kelly and Wood, 2000; La Scola et al., 2002). *Devosia* had nitrification ability contributing to the nitration phenomenon in the experiment (Vanparnis et al., 2005). *Ignavibacterium* (Okamoto et al., 2013) was distinctively detected on the bio-cathode and involved in heterotrophic denitrifying bacteria. *Anaerolineaceae* was the anaerobic methanogenesis for sodium acetate as the substrate (Yamada et al., 2006). The proportion of aerobic *Truepera* and *Pelomonas* was 39.64%, which exhibited the ability of respiration with oxygen (Albuquerque et al., 2005; Chandra et al., 2011).

Mechanism of the Cathode Chamber

From the analysis of the microbial community composition and the experimental results, we speculated for possible reactions in the cathode of MFC (**Figure 4**).

- (1) Autotrophic denitrification: Known as autotrophic electrotrophs with an electrode as the electron donor in the cathode of MFC (Virdis et al., 2008; Puig et al., 2011). *Afipia* and *Thiobacillus* directly contributed to autotrophic denitrification. Several researchers also demonstrated the autotrophic bacterium dominated in the cathode microbial community (Wrighton et al., 2010).
- (2) Heterotrophic denitrification: Organic matter was not added in the cathode, however, about 25 mg L⁻¹ of COD was detected, so the existence of heterotrophic denitrifying bacteria *Ignavibacterium* might be caused by sodium acetate in the anode permeate through proton membrane to the cathode (Kim et al., 2007; Chae et al., 2008; Okamoto et al., 2013). Xiao et al. indicated the heterotrophic bacterium survival in the autotrophic denitrifying cathode of MFC (Xiao et al., 2015).
- (3) Autotrophic nitrification: The high convert of nitrite to nitrate in this experiment and autotrophic nitrifying bacteria *Devosia* indicated nitrification happened in the cathode (Vanparry et al., 2005).
- (4) Oxygen reduction: The cathode coulombic efficiency over 100% in most of the experiments and aerobic *Truepera* and *Pelomonas* indicated oxygen as the electron acceptor in the cathode (Albuquerque et al., 2005; Chandra et al., 2011; Xie et al., 2011).
- (5) Other electrochemical reactions: Although oxygen was not detected in cathode through the whole experiment, the high cathode coulombic efficiency and nitrification rate showed the presence of other oxidant. We speculated that the oxidant might be produced from the other electrochemical reactions.

REFERENCES

- Albuquerque, L., Simoes, C., Nobre, M. F., Pino, N. M., Battista, J. R., Silva, M. T., et al. (2005). *Truepera radiovictrix* gen. nov., sp. nov., a new radiation resistant species and the proposal of *Trueperaceae* fam. nov. *FEMS Microbiol. Lett.* 247, 161–169. doi: 10.1016/j.femsle.2005.05.002
- APHA (1998). *Standard Methods for the Examination of Water and Wastewater, 20th Edn.* Washington, DC: United Book Press.
- Bond, D. R., and Lovley, D. R. (2003). Electricity production by *Geobacter sulfurreducens* attached to electrodes. *Appl. Environ. Microbiol.* 69, 1548–1555. doi: 10.1128/AEM.69.3.1548-1555.2003
- Cha, J., Choi, S., Yu, H. N., Kim, H., and Kim, C. (2010). Directly applicable microbial fuel cells in aeration tank for wastewater treatment. *Bioelectrochemistry* 78, 72–79. doi: 10.1016/j.bioelechem.2009.07.009
- Chae, K. J., Choi, M., Ajayi, F. F., Park, W., Chang, I. S., and Kim, I. S. (2008). Mass transport through a proton exchange membrane (Nafion) in microbial fuel cells. *Energy Fuels* 22, 169–176. doi: 10.1021/ef700308u
- Chandra, R., Bharagava, R. N., Kapley, A., and Purohit, H. J. (2011). Bacterial diversity, organic pollutants and their metabolites in two aeration lagoons of common effluent treatment plant (CETP) during the degradation and detoxification of tannery wastewater. *Bioresour. Technol.* 102, 2333–2341. doi: 10.1016/j.biortech.2010.10.087
- Clauwaert, P., Rabaey, K., Aelterman, P., de Schampheleire, L., Pham, T. H., Boeckx, P., et al. (2007). Biological denitrification in microbial fuel cells. *Environ. Sci. Technol.* 41, 3354–3360. doi: 10.1021/es062580r
- Deng, Y., Zhang, X., Miao, Y., and Hu, B. (2016). Exploration of rapid start-up of the CANON process from activated sludge inoculum in a sequencing biofilm batch reactor (SBBR). *Water Sci. Technol.* 73, 535–542. doi: 10.2166/wst.2015.518
- Desloover, J., Puig, S., Virdis, B., Clauwaert, P., Boeckx, P., Verstraete, W., et al. (2011). Biocathodic nitrous oxide removal in bioelectrochemical systems. *Environ. Sci. Technol.* 45, 10557–10566. doi: 10.1021/es202047x
- Guisasola, A., Jubany, I., Baeza, J. A., Carrera, J., and Lafuente, L. (2005). Respirometric estimation of the oxygen affinity constants for biological ammonium and nitrite oxidation. *J. Chem. Technol. Biotechnol.* 80, 388–396. doi: 10.1002/jctb.1202
- Karanasios, K. A., Vasiliadou, I. A., Pavlou, S., and Vayenas, D. V. (2010). Hydrogenotrophic denitrification of potable water: a review. *J. Hazard. Mater.* 180, 20–37. doi: 10.1016/j.jhazmat.2010.04.090
- Katuri, K. P., Scott, K., Head, I. M., Picioreanu, C., and Curtis, T. P. (2011). Microbial fuel cells meet with external resistance. *Bioresour. Technol.* 102, 2758–2766. doi: 10.1016/j.biortech.2010.10.147
- Kelly, D. P., and Wood, A. P. (2000). Reclassification of some species of *Thiobacillus* to the newly designated genera *Acidithiobacillus* gen. nov., *Halothiobacillus* gen. nov. and *Thermithiobacillus* gen. nov. *Int. J. Syst. Evol. Microbiol.* 50, 511–516. doi: 10.1099/00207713-50-2-511
- Kim, J. R., Cheng, S., Oh, S. E., and Logan, B. E. (2007). Power generation using different cation, anion and ultrafiltration membranes in microbial fuel cells. *Environ. Sci. Technol.* 41, 1004–1009. doi: 10.1021/es062202m
- Kondaveeti, S., Lee, S. H., Park, H. D., and Min, B. (2014). Bacterial communities in a bioelectrochemical denitrification system: the effects of supplemental electron acceptors. *Water Res.* 51, 25–36. doi: 10.1016/j.watres.2013.12.023
- La Scola, B., Mallet, M. N., Grimont, P. A., and Raoult, D. (2002). Description of *Afipia birgiae* sp. nov. and *Afipia massiliensis* sp. nov. and recognition of *Afipia felis* genospecies A. *Int. J. Syst. Evol. Microbiol.* 52, 1773–1782. doi: 10.1099/00207713-52-5-1773

CONCLUSIONS

Nitrite reduction has been shown to be a bio-catalytic process in denitrifying MFCs that could produce bioelectricity. Nitrite could be oxidized in the cathode via biological or electrochemical processes; the maximum TN removal rate of $54.80 \pm 0.01 \text{ g m}^{-3} \text{ d}^{-1}$ was obtained. It would be desirable for the TN removal but not electricity generation at a lower external resistance in MFC. An analysis of bio-cathode biofilms indicated *Proteobacteria* was the dominant species, accounting for 35.72%. *Afipia* and *Thiobacillus* mainly benefit to autotrophic denitrification in MFC. *Truepera*, *Devsia*, and *Pelomonas* might contribute to electricity generation. We speculated for possible reactions in the cathode according to the microbial community analysis and the experimental results.

AUTHOR CONTRIBUTIONS

HZ and JZ designed the experiment, and supervised conduct of the experiment. HZ supervised the data collection. HZ and JZ drafted the manuscript, FL and XL contributed substantially to the revision.

ACKNOWLEDGMENTS

This study was supported by the Fundamental Research Funds for the Central Universities (No. 2013G3292017) and the Fundamental Research Funds for Shanxi province department (2014K15-03-02).

- Li, J. T., Zhang, S. H., and Hua, Y. M. (2013). Performance of denitrifying microbial fuel cell subjected to variation in pH, COD concentration and external resistance. *Water Sci. Technol.* 68, 251–256. doi: 10.2166/wst.2013.250
- Li, W. Q., Zhang, S. H., Chen, G., and Hua, Y. M. (2014). Simultaneous electricity generation and pollutant removal in microbial fuel cell with denitrifying biocathode over nitrite. *Appl. Energy* 126, 136–141. doi: 10.1016/j.apenergy.2014.04.015
- Logan, B. E., Aelterman, P., Hamelers, B., Rozendal, R., Schröder, U., Keller, J., et al. (2006). Microbial fuel cells: methodology and technology. *Environ. Sci. Technol.* 40, 5181–5192. doi: 10.1021/es0605016
- Okamoto, H., Kawamura, K., Nishiyama, T., Fujii, T., and Furukawa, K. (2013). Development of a fixed-bed anammox reactor with high treatment potential. *Biodegradation* 24, 99–110. doi: 10.1007/s10532-012-9561-x
- Puig, S., Marc, S., Vilar-Sanz, A., Cabré, M., Bañeras, L. L., Colprim, J., et al. (2011). Autotrophic nitrite removal in the cathode of microbial fuel cells. *Bioresour. Technol.* 102, 4462–4467. doi: 10.1016/j.biortech.2010.12.100
- Van Doan, T., Lee, T. K., Shukla, S. K., Tiedje, J. M., and Park, J. (2013). Increased nitrous oxide accumulation by bioelectrochemical denitrification under autotrophic conditions: kinetics and expression of denitrification pathway genes. *Water Res.* 47, 7087–7097. doi: 10.1016/j.watres.2013.08.041
- Vanparrys, B., Heylen, K., Lebbe, L., and Vos, P. D. (2005). *Devosia limi* sp. nov., isolated from a nitrifying inoculum. *Int. J. Syst. Evol. Microbiol.* 55, 1997–2000. doi: 10.1099/ijsl.0.63714-0
- Virdis, B., Rabaey, K., Rozendal, R. A., Yuan, Z., and Keller, J. (2010). Simultaneous nitrification, denitrification and carbon removal in microbial fuel cells. *Water Res.* 44, 2970–2980. doi: 10.1016/j.watres.2010.02.022
- Virdis, B., Rabaey, K., Yuan, Z., and Keller, J. (2008). Microbial fuel cells for simultaneous carbon and nitrogen removal. *Water Res.* 42, 3013–3024. doi: 10.1016/j.watres.2008.03.017
- Wang, Q., Feng, C., Zhao, Y., and Hao, C. (2009). Denitrification of nitrate contaminated groundwater with a fiber-based biofilm reactor. *Bioresour. Technol.* 100, 2223–2227. doi: 10.1016/j.biortech.2008.07.057
- Wrage, N., Velthof, G. L., Van Beusichem, M. L., and Oenema, O. (2001). Role of nitrifier denitrification in the production of nitrous oxide. *Soil Biol. Biochem.* 33, 1723–1732. doi: 10.1016/S0038-0717(01)00096-7
- Wrighton, K. C., Virdis, B., Clauwaert, P., Read, S. T., Daly, R. A., Boon, N., et al. (2010). Bacterial community structure corresponds to performance during cathodic nitrate reduction. *ISME J.* 4, 1443–1455. doi: 10.1038/ismej.2010.66
- Xiao, Y., Zheng, Y., Wu, S., Yang, Z. H., and Zhao, F. (2015). Bacterial community structure of autotrophic denitrification biocathode by 454 pyrosequencing of the 16S rRNA Gene. *Environ. Microbiol.* 69, 492–499. doi: 10.1007/s00248-014-0492-4
- Xie, S., Liang, P., Chen, Y., Xia, X., and Huang, X. (2011). Simultaneous carbon and nitrogen removal using an oxic/anoxic-biocathode microbial fuel cells coupled system. *Bioresour. Technol.* 102, 348–354. doi: 10.1016/j.biortech.2010.07.046
- Yamada, T., Sekiguchi, Y. S., Imachi, H., Ohashi, A., Harada, H., and Kamagata, Y. (2006). *Anaerolinea thermolimosa* sp. nov., *Levilinea saccharolytica* gen. nov., sp. nov. and *Leptolinea tardivitalis* gen. nov., sp. nov., novel filamentous anaerobes, and description of the new classes *Anaerolineae classis* nov. and *Caldilineae classis* nov. in the bacterial phylum Chloroflex. *Int. J. Syst. Evol. Microbiol.* 56, 1331–1340. doi: 10.1099/ijsl.0.64169-0
- Zhang, F., and He, Z. (2012). Simultaneous nitrification and denitrification with electricity generation in dual-cathode microbial fuel cells. *Chem. Technol. Biotechnol.* 87, 153–159. doi: 10.1002/jctb.2700
- Zhang, L., Zhu, X., Li, J., Liao, Q., and Ye, D. D. (2011). Biofilm formation and electricity generation of a microbial fuel cell started up under different external resistances. *Power Sources* 196, 6029–6035. doi: 10.1016/j.jpowsour.2011.04.013
- Zhao, Y., Feng, C., Wang, Q., Yang, Y., Zhang, Z., and Sugiura, N. (2011). Nitrate removal from groundwater by cooperating heterotrophic with autotrophic denitrification in a biofilm-electrode reactor. *J. Hazard. Mater.* 192, 1033–1039. doi: 10.1016/j.jhazmat.2011.06.008

Conflict of Interest Statement: The authors declare that the research was conducted in the absence of any commercial or financial relationships that could be construed as a potential conflict of interest.

Copyright © 2016 Zhao, Zhao, Li and Li. This is an open-access article distributed under the terms of the Creative Commons Attribution License (CC BY). The use, distribution or reproduction in other forums is permitted, provided the original author(s) or licensor are credited and that the original publication in this journal is cited, in accordance with accepted academic practice. No use, distribution or reproduction is permitted which does not comply with these terms.



Carbon Material Optimized Biocathode for Improving Microbial Fuel Cell Performance

Hairti Tursun¹, Rui Liu¹, Jing Li¹, Rashid Abro², Xiaohui Wang^{1*}, Yanmei Gao¹ and Yuan Li¹

¹ Beijing Engineering Research Center of Environmental Material for Water Purification, Beijing University of Chemical Technology, Beijing, China, ² Beijing Key Laboratory of Membrane Science and Technology, College of Chemical Engineering, Beijing University of Chemical Technology, Beijing, China

OPEN ACCESS

Edited by:

Haoyi Cheng,
Research Center for
Eco-Environmental Sciences, China

Reviewed by:

Deepak Pant,
Flemish Institute for Technological
Research, Belgium
Jinyou Shen,
Nanjing University of Science
and Technology, China

*Correspondence:

Xiaohui Wang
37997997@qq.com

Specialty section:

This article was submitted to
Microbiotechnology, Ecotoxicology
and Bioremediation,
a section of the journal
Frontiers in Microbiology

Received: 01 September 2015

Accepted: 05 January 2016

Published: 26 January 2016

Citation:

Tursun H, Liu R, Li J, Abro R, Wang X, Gao Y and Li Y (2016) Carbon Material Optimized Biocathode for Improving Microbial Fuel Cell Performance. *Front. Microbiol.* 7:6. doi: 10.3389/fmicb.2016.00006

To improve the performance of microbial fuel cells (MFCs), the biocathode electrode material of double-chamber was optimized. Alongside the basic carbon fiber brush, three carbon materials namely graphite granules, activated carbon granules (ACG) and activated carbon powder, were added to the cathode-chambers to improve power generation. The result shows that the addition of carbon materials increased the amount of available electroactive microbes on the electrode surface and thus promote oxygen reduction rate, which improved the generation performance of the MFCs. The Output current (external resistance = 1000 Ω) greatly increased after addition of the three carbon materials and maximum power densities in current stable phase increased by 47.4, 166.1, and 33.5%, respectively. Additionally, coulombic efficiencies of the MFC increased by 16.3, 64.3, and 20.1%, respectively. These results show that MFC when optimized with ACG show better power generation, higher chemical oxygen demands removal rate and coulombic efficiency.

Keywords: microbial fuel cells, biocathode, carbon materials, power generation, coulombic efficiency

INTRODUCTION

Microbial fuel cell (MFC) is an emerging and rapidly developing interdisciplinary technology that combines biotechnology, environmental engineering, and electrochemistry (ElMekawy et al., 2014; Sharma et al., 2014). MFCs use electrochemically active microorganisms as catalysts to convert chemical energy directly into electrical energy and are expected to realize the production of clean energy during sewage treatment (Mohan et al., 2014). Based on thermodynamic theory, taking acetic acid as the electron donor and oxygen as the electron acceptor, the maximum theoretical voltage of a MFC system is 1.105 V (Logan, 2008). Currently, the open circuit voltage achieved by MFCs is almost equal to that of traditional fuel cells. However, the achievable output power is still at a low level. Thus, most studies of MFCs are still stuck in the laboratory stage owing to their inefficiency in large-scale applications. The main factors influencing the electricity generation performance of MFCs include exoelectrogens (Sun et al., 2012; Debuy et al., 2015; Rimboud et al., 2015), reactor structure (Izadi et al., 2015; Tian et al., 2015), electrode material (Guerrini et al., 2015), and substrate type (Zhang et al., 2013; Tang et al., 2014; Zhang et al., 2015a). It is generally believed that the electrode material is one of the most critical factors determining MFC performance.

An excellent electrode material should have qualities such as high conductivity, low corrodibility, high specific surface area and porosity, suitability for microorganism growth, and low cost (Wei et al., 2011b). Because many carbon-based materials such as carbon paper (Zhang et al., 2012), activated carbon (Zhang et al., 2014b; Pasupuleti et al., 2015), carbon cloth (Wang et al., 2013), graphite granules (GG; Ye et al., 2015), and carbon fiber brushes (Lanas and Logan, 2013; Liao et al., 2015) have all of these qualities, nowadays they are widely used as MFC electrodes. There has been a number of works carried out on anode material modification and optimization to obtain maximum output power and to improve MFC electricity generation performance (Liang et al., 2011; Li et al., 2014; Liu et al., 2014; Ge et al., 2015). The results of these studies have shown that such approaches can efficiently shorten the MFC startup time, increase the anode biofilm activity, reduce the resistance and increase the output voltage of the system.

Microbial fuel cell cathodes can be divided into chemical and biological cathodes. To improve their performance, chemical cathodes often require precious metals (Quan et al., 2015), metal complex catalysts (Zhang et al., 2015b), or an electrolytic medium (Wetser et al., 2015) to be involved in the reaction. The high cost of suitable catalysts and the easily caused secondary pollution limits the development of chemical cathodes. In contrast, using functional microorganisms as the catalyst, biocathodes have the advantages of low cost, sustainable operation, and wide application. Zhang et al. (2012) found that the use of graphite felt in biocathodes improved catalytic activity toward the oxygen reduction reaction beyond that achieved with carbon paper and stainless steel mesh. Carbon nanotube (Jourdin et al., 2014) and polyaniline/tourmaline (Zhang et al., 2014a) modified electrode were also found to improve biocathode performance by enhancing bacteria-electrode interaction and microbial extracellular electron transfer. Zhang et al. (2011) compared the performance of three types of electrode materials: graphite brushes, GG, and graphite brushes + GG. They found that the MFC startup time was shorter with the graphite brushes + GG cathode than with graphite brushes alone, and a maximum power density of $38.2 \pm 12.6\%$ could achieve a correspondingly higher coulombic efficiency.

All previous studies focus on pre-MFC startup, using different electrode materials, applying processing or modifications to the test materials to observe the resulting impacts on MFC startup time and MFC performance (at its stationary phase). However, the electricity generation performance of an MFC is determined by exoelectrogenic growth, which is sensitive to the external environment. Even if two MFCs started up under exactly the same external environment, their electricity generation performance may still vary. In this study, four MFCs were started up with the same electrode material (carbon fiber brushes). GG, activated carbon granules (ACG) and activated carbon powder (ACP) were added to the cathodes after the MFC output voltage reached the stationary phase. After eliminating the errors caused by different microbial growth situations in different

treatment phases, through vertical self-comparison we observed the impact of cathode material optimization on the MFC electricity generation performance and the corresponding effect on the contaminant removal from an entirely new point of view.

MATERIALS AND METHODS

Sludge Inoculation

The inoculation sludge used in this experiment was collected from the mixed sludge of the Beijing Qinghe Wastewater Treatment Plant, China. Part of the sludge was held under anaerobic conditions for 7 days, while the other was held under aerated conditions. 10 mL of each sample ($\text{MLSS} \approx 4000 \text{ mg/L}$) were injected into the anode chamber and the cathode chamber of the MFCs.

Electrode Materials

During the cell start-up phase, both the anode and cathode electrode materials were carbon fiber brushes, which were twisted from carbon fibers and titanium wires (brush head of 3 cm length and 3 cm diameter, titanium wire of 3 cm length). The brushes were soaked in acetone overnight and then heated at 450°C for 30 min in a muffle furnace (Feng et al., 2010). After being soaked in HCl and NaOH solution for 18 h in each turn (Kim et al., 2007), the GG (1–5 mm in diameter) and ACG (1–2 mm in diameter) were washed and soaked in deionized water, and then dried for further use. Part of the processed ACG were passed through a 100-mesh sieve to obtain ACP.

Experimental Apparatus

The MFC reactor in this experiment was constructed of two chambers, the main parts of which were made of plexiglass. The two chambers were both cylindrical, separated by a cation exchange membrane (CMI-7000, Membranes International Inc., USA). Each chamber was 3 cm in length and 4 cm in diameter (net volume of 28 cm^3), and contained two small holes (1 cm in diameter) on the top usually closed with rubber plugs. The chamber solutions used in the experiments provided nutrients for the electricogens. The anode solution contained 3.4 g/L K_2HPO_4 , 4.4 g/L KH_2PO_4 , 1.5 g/L NH_4Cl , 0.1 g/L MgCl_2 , and 0.1 g/L CaCl_2 , while 1.625 g/L CH_3COONa was used as a carbon source. The cathode solution contained the same components except for the use of 0.94 g/L NaHCO_3 ($\text{pH} = 7$, while the phosphate buffer maintained the pH in the range of 7–8 during each batch, to avoid the pH affect the ability to establish an active biofilm on the cathode) as an inorganic carbon source. The anode and cathode solutions were circulated at a rate of 1 mL/min and 5 mL/min using separate peristaltic pumps (BT00-1L, Lange, China) to create an external cycle inside 250 mL circulating containers. An aquarium micro aeration pump was placed inside the circulating container of the cathode chamber to ensure an adequate level of dissolved oxygen. The circulating container was thermostatically heated to 30°C in a water bath to provide a comfortable growth temperature for the microorganisms.

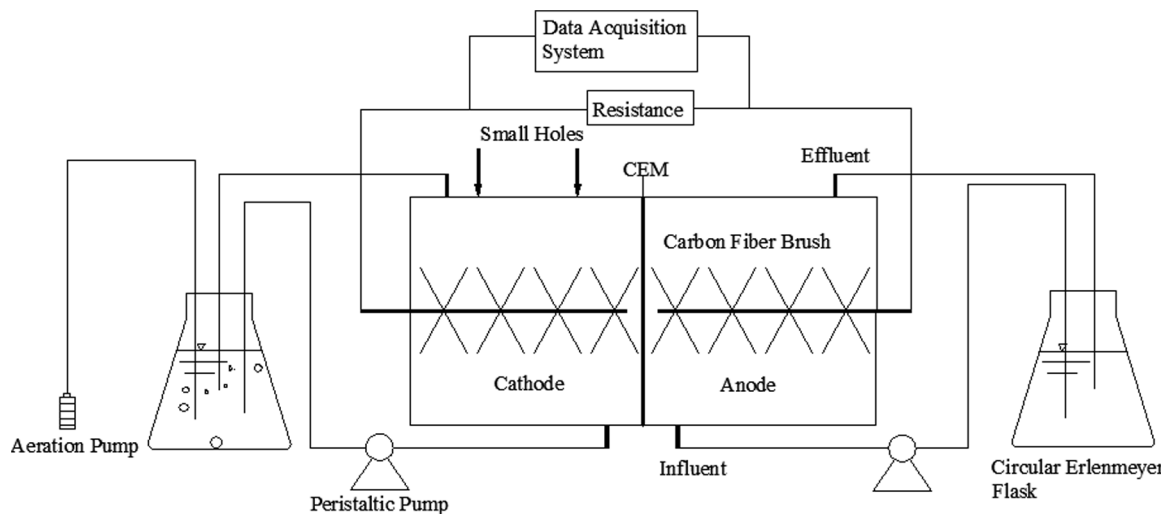


FIGURE 1 | Schematic diagram of the reactor.

A schematic diagram of the experimental apparatus is shown in **Figure 1**.

Data Acquisition and Analysis

The output voltage data were recorded every minute with a data acquisition card (7660B, ZTIC, China), and its hourly average was archived. The apparent cell internal resistance was measured using the static discharge method (Liang et al., 2007). The voltage values corresponding to the change in external resistance from high to low were recorded, and the corresponding current values were calculated using the following equation

$$I = U/R \quad (1)$$

Where, I is the output current (A), U is the output voltage (V) and R is the external resistance (Ω)

Plotting the voltage values versus the current values yielded the polarization curve. The fitted ohmic polarization region of the polarization curve typically showed a linear relationship, the slope of which was the apparent internal resistance. Meanwhile, a saturated calomel electrode was inserted into the cathode chamber as a reference electrode to measure cathode potential. The anode potential was calculated as the cell voltage minus the measured cathode potential. The output power of the cell was calculated using Eq. (2)

$$P = U^2/R \quad (2)$$

Where, P is the output power (W).

The power density of the cell was calculated based on the area of the cation exchange membrane. Plotting the power density values versus the current values yielded the power-density curve. Generally, the highest point of such a curve is the maximum power density of the cell.

The soluble chemical oxygen demands (COD) of the MFCs were measured according to the standard method. Coulombic

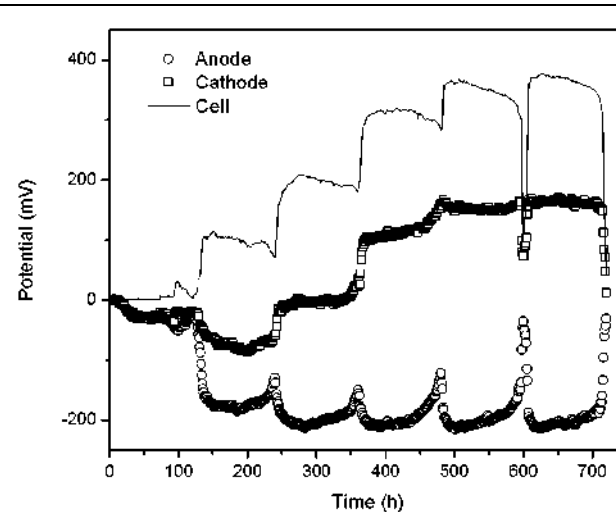


FIGURE 2 | Electrode potential changes during the start-up period.

efficiency is the ratio between the number of output electrons and the number of electrons that the consumed organic compounds can provide. It describes the energy transfer efficiency of an MFC, and is an important indicator of MFC electricity generation performance. For the present experiments, the coulombic efficiency was calculated as follows:

$$C_E = \frac{8Q}{FV\Delta COD} \quad (3)$$

Where, C_E is the coulombic efficiency (%), Q is the total output of the MFC during a cycle (C), F is the Faraday constant (96485 C/mol), V is the volume of anode solution (mL), ΔCOD is the change in the COD concentration during a cycle (mg/L) and “8” is the constant when using oxygen as the electron acceptor.

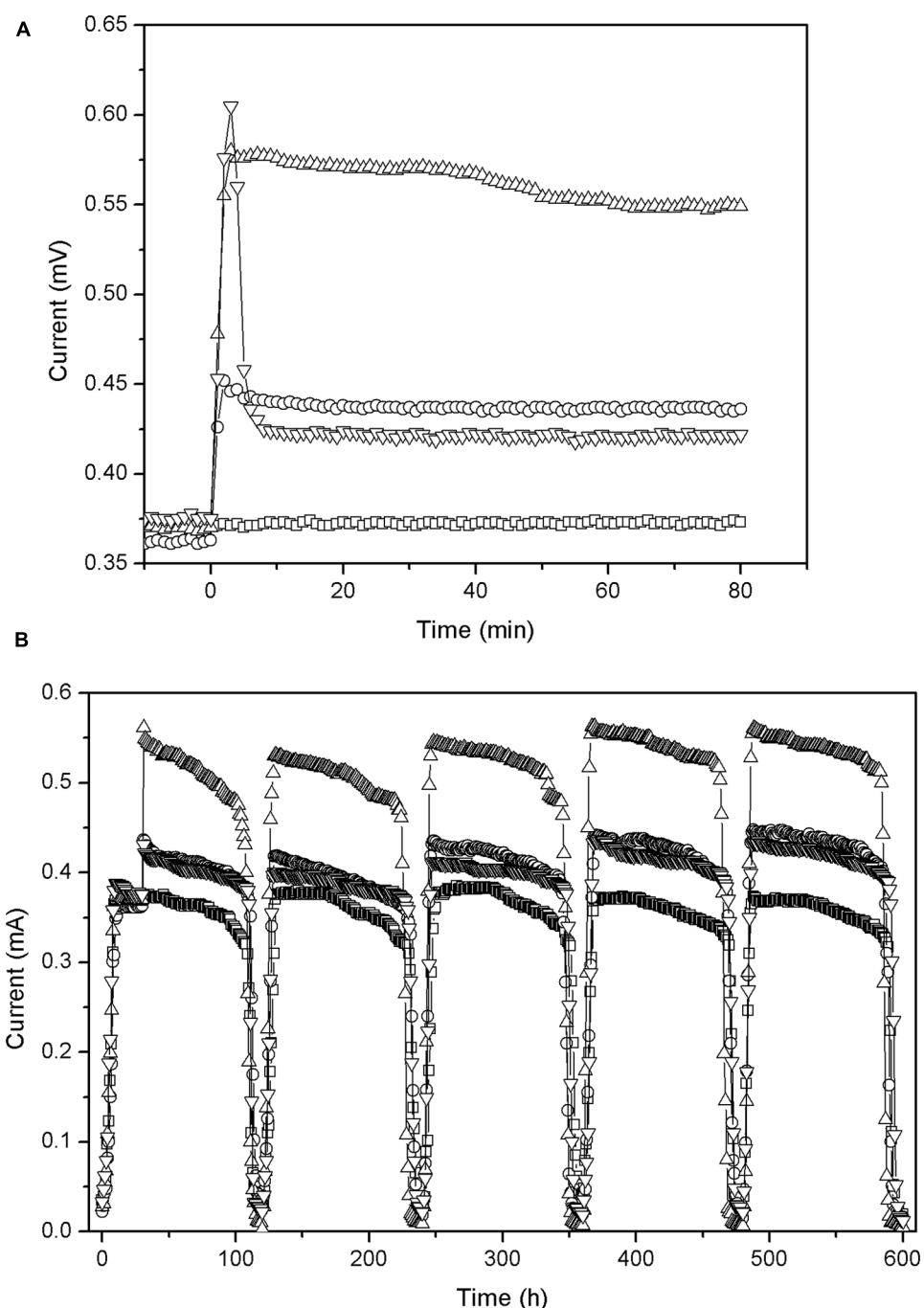


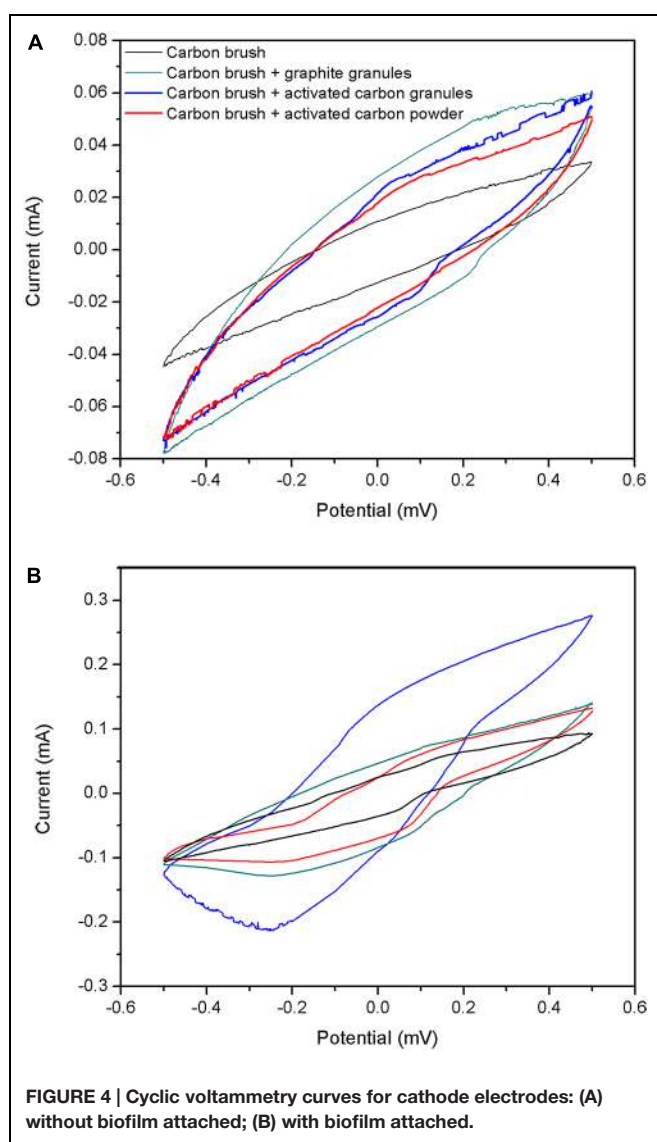
FIGURE 3 | Change in output current (external resistance = 1000 Ω) before and after addition of carbon material: (A) first 2 h; (B) during five cycles.
-□- CFB, -○- graphite granules (GG), -△- activated carbon granules (ACG), -▽-activated carbon powder (ACP).

Cyclic voltammetry curve was implemented by electrochemical workstation (CHI-604E, CH Instruments, China) through conventional three electrode system. The morphology of the biofilms on the electrode materials was examined by scanning electron microscopy (SEM; S-3400N, Hitachi, Japan). The samples were processed for imaging according to the method described in Zhang et al.'s (2012) report.

RESULTS AND DISCUSSION

MFC Start-Up and Stationary Phase

Four reactors were used in this experiment labeled: CFB (control reference), GG (adding graphite granules), ACG (adding activated carbon granules), and ACP (adding activated carbon powder). All four reactors were identical in structure and



operating conditions. The cycling time of the solutions was 5 days. During the start-up phase, the generation capacity was low and unstable owing to the lack of biofilm on the electrode material. In the second cycle, anode potential began to drop significantly (see **Figure 2**) due to the rapidly growing of electricigens in the anode chamber. Meanwhile dissolved oxygen without catalyst hardly accepted the electrons from organic matter degradation leading to electron enrichment on the surface of carbon fiber, which caused cathode potential going downward. However, when the biofilm grew-up, cathode potential started to ascend. After 30 days, when the maximum output voltage no longer increased during three consecutive cycles, the MFCs were considered to have successfully started and reached the stationary phase.

The output voltages of the four fully started MFCs ranged between 350 and 385 mV. The corresponding current densities (external resistance = 1000 Ω) were all in the range of 0.50–0.55 mA/cm². These results show that the differences

among the four MFCs are unremarkable, and indicate that the microbial growth and distribution of each MFC is relatively consistent and that their electricity generation performance is comparable. As such, these results allowed us to move to the next phase.

MFC Generation Performance

Thirty hours after the solutions were replaced at stable output voltage; 1 g GG, 1 g ACG and 1 g ACP were added into the corresponding cathode chambers through the small holes at the top of each reactor (**Figure 1**). The earlier results of preliminary experiment suggested that the best dosage of carbon material is 1 g. Therefore, the output voltages were monitored by data acquisition card and the currents of each MFC was calculated accordingly to assess the MFC performances.

As shown in **Figure 3A**, the output currents of all the MFCs (after addition of carbon material) display a significant increase, and their maximum values are achieved within 3 min. This might be due to the following reasons: (1) the electrical conductivity of carbon materials reduced the internal activation resistance of the MFC in a short time. (2) The dry carbon materials that contain oxygen may increase oxygen content of the cathode solutions, thus speeding up oxygen reduction rate and leading to the greatly enhanced cathode performance. (3) Graphite and activated carbon have been reported as effective catalysts for oxygen reduction in cathodes of MFCs (Freguia et al., 2007; Zhang et al., 2014b).

However, after 3 min different MFCs show substantial differences in performance (**Figure 3A**). (1) The current of GG stabilized at around 0.436 mA. (2) The current of ACG continued to increase and reached a maximum 0.575 mA after 10 min while after about 40 min, it started to decline and finally remained at about 0.549 mA. (3) The current of ACP began to drop rapidly, from about 0.605 mA to about 0.422 mA, and then remained stable. At the end of the experiment, when we washed the apparatus, we found that the filaments of the carbon brush blocked the ACG owing to granule's large diameter. This increased the specific surface area of the electrode to some extent, which may have attracted more aerobic microbes and increased the productivity of ACG accordingly. In contrast, the powder was too small to be blocked by or attached to the brushes effectively, thus passed through the brush filaments into the reactor bottom (the non-conductive dead zone), and part of them passed out of the reactor with the effluent. This resulted in a lower conductivity and underutilized biocompatibility for ACP. Accordingly, after adding the ACP the output voltage and current of ACP increased rapidly and then declined significantly as the powder started to deposit.

To investigate the catalytic behaviors caused by chemical catalysis or biological catalysis, four types of electrodes (carbon fiber brush, carbon fiber brush + GG, carbon fiber brush + ACG and carbon fiber brush + ACP) without and with biofilm attached were characterized by cyclic voltammetry. The measurement was performed in air-saturated cathode solution as reported in Section "Experimental Apparatus." As

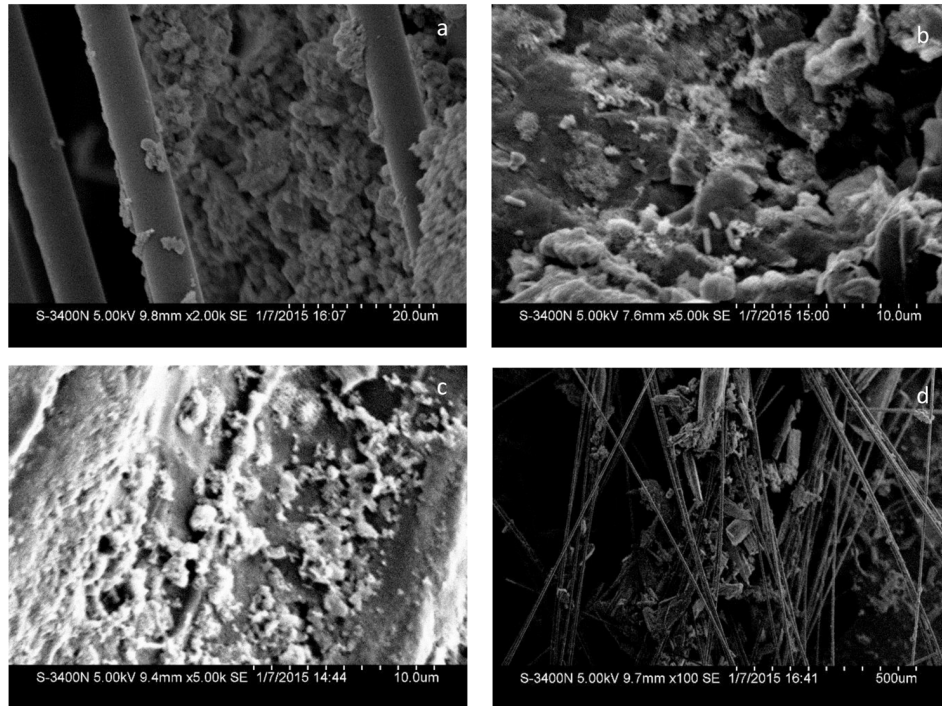


FIGURE 5 | SEM images of biofilms attached to the cathodes: (a) CFB; (b) GG; (c) ACG; (d) ACP.

shown in **Figure 4**, there was no remarkable redox peak in four types of electrodes without biofilm, suggesting that the raw electrodes had no chemical catalysis in this experiment. On the contrary, electrodes with biofilm had remarkable reductive peaks. Moreover, the peak current of carbon fiber brush + ACG electrode with biofilm was higher than that of the others. This result further indicates that electrochemical active microorganisms in the cathodes catalyze oxygen reduction reaction.

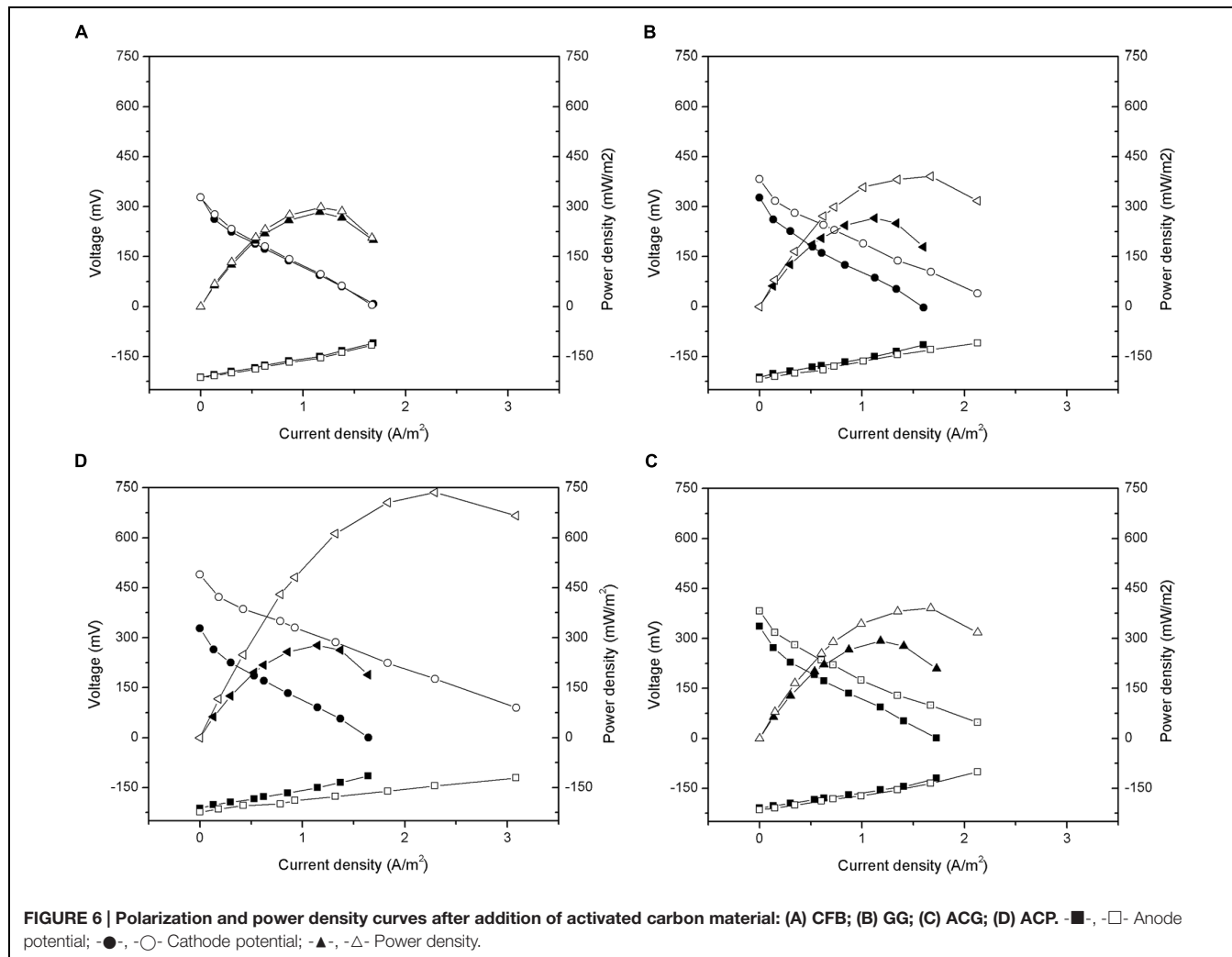
All the MFC reactors remained stable and functional for several cycles after the carbon materials were added (**Figure 3B**). The output current of CFB almost did not change, indicating that the external environment did not influence the power generation of the MFCs during the test period. The output current of the other reactors did not obviously increase beyond the maximum current which was observed just after the addition of the carbon materials. Moreover, the surface morphology of the carbon material observed by SEM (**Figure 5**) showed the biofilm attached on carbon fiber, GG, and activated carbon. Because the carbon fiber surface was smooth, only a small amount of microbes could adhere and most of the microbes clumped together away from the filaments (**Figure 5A**). As a result, the power generation performances of the MFCs were low before the addition of carbon materials. This phenomenon is similar to the observation by Karra et al. (2013) and Sonawane et al. (2014).

The added graphite and activated carbon had large porosity and adsorptive capacity that could spread the clumped microbes adsorbed on the electrode surface and increased the surface area

of the electrode. Previous studies suggested that the amount of bacteria on the biocathode should be one of the limiting factors to determine the charge transfer resistance and power generation (Rabaey, 2010; Zhang et al., 2012). Since the area of biofilm in direct contact with dissolved oxygen was increased, the oxygen reduction rate was promoted and the electricity generation performance of the MFC was improved.

In addition, it has been reported that the specific area of activated carbon was approximately 2.4 times higher than the specific area of GG (Wei et al., 2011a). This higher specific area enabled the more effective collection of electrochemical active microorganisms and the performance of ACG increased accordingly.

As shown in **Figure 6**, the anode potential measured after the addition of carbon material did not have obvious change. Thus, the improvement in the performance of the MFCs occurred mainly because of cathode polarization. After the addition of carbon material, the open circuit voltages of GG, ACG, and ACP were increased by 11.3, 31.7, and 9.5% to approximately 601, 713, and 597 mV, respectively. After linear fitting of the polarization curves, the internal resistances of GG, ACG, and ACP were calculated to be 269, 204, and 299 Ω , respectively, all lower than their initial values. Early research indicated that the total internal resistance of an MFC consists of three components: ohmic resistance, activation resistance, and diffusion resistance (Logan et al., 2006). Ohmic resistance depends on the type of electrolyte and membrane; activation resistance is determined by the activation rate of the electrode surface; diffusion resistance (aka.



concentration resistance) is dependent on the diffusion rate of the reaction products transferring toward the electrode surface and solution.

The cathode resistance is generated from the electrochemical oxygen reduction reaction on the cathode surface. Thus, taking the same experimental conditions into account, apparatus, and ohmic resistance, a reduction in cathode activation resistance may have been the main cause of the observed drop in the total internal resistance of all three reactors. This result was similar to Zhang et al. (2011) and Zhang et al. (2014a). Furthermore, the diffusion resistance also decreased owing to the increase in the specific surface area of the electrodes after addition. The in-depth study on the composition and mechanism of change in the MFC internal resistance are still required.

According to equation (2), the output power density of the MFC was proportional to the square of the open circuit voltage, and inversely proportional to its internal resistance. Under the condition that the open circuit voltage increased while the internal resistance decreased, the maximum power densities of GG, ACG, and ACP reached approximately 391,

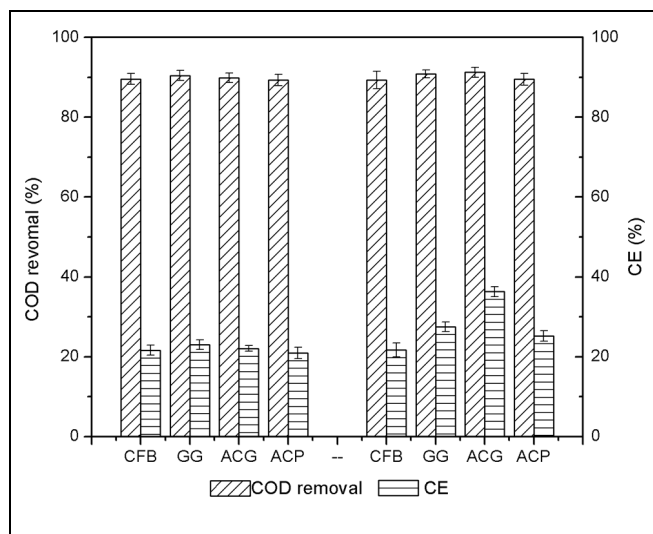


FIGURE 7 | Changes in chemical oxygen demands (COD) removal and coulombic efficiency before and after addition of activated carbon materials.

736, and 391 mW/m², increased by 47.4, 166.1, and 33.5%, respectively, after the addition of carbon materials. This further indicated the significant improvement in the electricity generation performance of the MFCs after the addition of carbon materials (ACG especially) to the cathode. This improvement was caused by the reduction of the internal resistance due to higher specific surface area of the graphite and activated carbon than the carbon fiber brushes. A higher specific surface area could increase the growth of electrochemically active microorganisms, which catalyze the oxygen reduction reaction, and could reduce the activation internal resistance of the cell, thereby increasing the electricity generation performance.

COD Removal and Coulombic Efficiency

The changes in COD removal and coulombic efficiency before and after the addition of the carbon materials were measured. The COD removal and coulombic efficiency data were collected and averaged from the three cycles before and after the addition of carbon material. The results are illustrated in **Figure 7**.

As shown in **Figure 7**, before the addition of carbon materials to the MFCs, the COD removal rates of the four reactors were between 89.3 and 90.5%. This demonstrated that the microbial growth and the performance of the four anodes were similar. The coulombic efficiency of each reactor was low, only between 20 and 23%. The majority of the energy was lost during the process of converting COD removal to electricity generation. After the addition of ACG, the COD removal increased to 91.2%, indicating that the optimization of the cathode could also have an indirect effect on anode COD removal. Accordingly, after the addition of GG and ACP, the COD removals were almost unchanged but the output power increased a little. This result confirmed that the increased electricity generation performance

was mainly determined by the improvement of the cathode. With similar initial COD removals, the coulombic efficiency of GG, ACG, and ACP increased by 16.3, 64.3, and 20.1%, respectively. This further verified that the MFC coulombic efficiency varied directly with the output power density.

CONCLUSION

The experimental results of this study showed that the current of an MFC (double-chambers, carbon brush as start-up electrode material) in stationary phase rapidly increased by the addition of carbon materials due to the physical property of the materials. The addition of carbon material increased the specific surface area of electrode material and improved the activity of the catalytic microorganisms toward the oxygen reduction reaction, and thus maintained the high performance of the MFCs in following cycles. As a result, the internal resistance of the MFCs reduced effectively and electricity generation performance improved. Using ACG, the maximum power density increased significantly by 166.1%. The ACG optimized anode also showed higher COD removal rate than those with GG or carbon powder. However, all three-carbon materials improve the coulombic efficiency rate of the MFCs.

FUNDING

This study was financially supported by the International Science-Technology Cooperation Program of China (No. 2013DFR60250), the Natural Science Foundation of China (No. 51408020), and Beijing Municipal Science and Technology Project (Z15111000210000).

REFERENCES

- Debuy, S., Pecastaings, S., Bergel, A., and Erable, B. (2015). Oxygen-reducing biocathodes designed with pure cultures of microbial strains isolated from seawater biofilms. *Int. Biodeterior. Biodegradation* 103, 16–22. doi: 10.1016/j.ibiod.2015.03.028
- ElMekawy, A., Hegab, H. M., Vanbroekhoven, K., and Pant, D. (2014). Techno-productive potential of photosynthetic microbial fuel cells through different configurations. *Renew. Sustain. Energy Rev.* 39, 617–627. doi: 10.1016/j.rser.2014.07.116
- Feng, Y., Yang, Q., Wang, X., and Logan, B. E. (2010). Treatment of carbon fiber brush anodes for improving power generation in air-cathode microbial fuel cells. *J. Power Sources* 195, 1841–1844. doi: 10.1016/j.jpowsour.2009.10.030
- Freguia, S., Rabaey, K., Yuan, Z., and Keller, J. (2007). Non-catalyzed cathodic oxygen reduction at graphite granules in microbial fuel cells. *Electrochim. Acta* 53, 598–603. doi: 10.2166/wst.2010.140
- Ge, B., Li, K., Fu, Z., Pu, L., and Zhang, X. (2015). The addition of orthohexagon nano spinel Co₃O₄ to improve the performance of activated carbon air cathode microbial fuel cell. *Bioresour. Technol.* 195, 180–187. doi: 10.1016/j.biortech.2015.06.054
- Guerrini, E., Grattieri, M., Faggianelli, A., Cristiani, P., and Trasatti, S. (2015). PTFE effect on the electrocatalysis of the oxygen reduction reaction in membranous microbial fuel cells. *Bioelectrochemistry* 106(Pt A), 240–247. doi: 10.1016/j.bioelechem.2015.05.008
- Izadi, P., Rahimnejad, M., and Ghoreyshi, A. (2015). Power production and wastewater treatment simultaneously by dual-chamber microbial fuel cell technique. *Biotechnol. Appl. Biochem.* 62, 483–488. doi: 10.1002/bab.1345
- Jourdin, L., Freguia, S., Donose, B. C., Chen, J., Wallace, G. G., Keller, J., et al. (2014). A novel carbon nanotube modified scaffold as an efficient biocathode material for improved microbial electrosynthesis. *J. Mater. Chem. A* 2, 13093–13102. doi: 10.1039/C4TA03101F
- Karra, U., Manickam, S. S., McCutcheon, J. R., Patel, N., and Li, B. (2013). Power generation and organics removal from wastewater using activated carbon nanofiber (ACNF) microbial fuel cells (MFCs). *Int. J. Hydrog. Energy* 38, 1588–1597. doi: 10.1016/j.ijhydene.2012.11.005
- Kim, J. R., Cheng, S., Oh, S.-E., and Logan, B. E. (2007). Power generation using different cation, anion, and ultrafiltration membranes in microbial fuel cells. *Environ. Sci. Technol.* 41, 1004–1009. doi: 10.1021/es062202m
- Lanas, V., and Logan, B. E. (2013). Evaluation of multi-brush anode systems in microbial fuel cells. *Bioresour. Technol.* 148, 379–385. doi: 10.1016/j.biortech.2013.08.154
- Li, B., Zhou, J., Zhou, X., Wang, X., Li, B., Santoro, C., et al. (2014). Surface modification of microbial fuel cells anodes: approaches to practical design. *Electrochim. Acta* 134, 116–126. doi: 10.1016/j.electacta.2014.04.136
- Liang, P., Huang, X., Fan, M.-Z., Cao, X.-X., and Wang, C. (2007). Composition and distribution of internal resistance in three types of microbial fuel cells. *Appl. Microbiol. Biotechnol.* 77, 551–558. doi: 10.1007/s00253-007-1193-4

- Liang, P., Wang, H., Xia, X., Huang, X., Mo, Y., Cao, X., et al. (2011). Carbon nanotube powders as electrode modifier to enhance the activity of anodic biofilm in microbial fuel cells. *Biosens. Bioelectron.* 26, 3000–3004. doi: 10.1016/j.bios.2010.12.002
- Liao, Q., Zhang, J., Li, J., Ye, D., Zhu, X., and Zhang, B. (2015). Increased performance of a tubular microbial fuel cell with a rotating carbon-brush anode. *Biosens. Bioelectron.* 63, 558–561. doi: 10.1016/j.bios.2014.08.014
- Liu, J., Liu, J., He, W., Qu, Y., Ren, N., and Feng, Y. (2014). Enhanced electricity generation for microbial fuel cell by using electrochemical oxidation to modify carbon cloth anode. *J. Power Sour.* 265, 391–396. doi: 10.1016/j.jpowsour.2014.04.005
- Logan, B. E. (2008). *Microbial Fuel Cells*. Hoboken, NJ: John Wiley & Sons.
- Logan, B. E., Hamelers, B., Rozendal, R., Schröder, U., Keller, J., Freguia, S., et al. (2006). Microbial fuel cells: methodology and technology. *Environ. Sci. Technol.* 40, 5181–5192. doi: 10.1021/es0605016
- Mohan, S. V., Velvizhi, G., Modestra, J. A., and Srikanth, S. (2014). Microbial fuel cell: critical factors regulating bio-catalyzed electrochemical process and recent advancements. *Renew. Sustain. Energy Rev.* 40, 779–797. doi: 10.1016/j.rser.2014.07.109
- Pasupuleti, S. B., Srikanth, S., Mohan, S. V., and Pant, D. (2015). Continuous mode operation of microbial fuel cell (MFC) stack with dual gas diffusion cathode design for the treatment of dark fermentation effluent. *Int. J. Hydrol. Energy* 40, 12424–12435. doi: 10.1016/j.ijhydene.2015.07.049
- Quan, X., Mei, Y., Xu, H., Sun, B., and Zhang, X. (2015). Optimization of Pt-Pd alloy catalyst and supporting materials for oxygen reduction in air-cathode Microbial Fuel Cells. *Electrochim. Acta* 165, 72–77. doi: 10.1016/j.electacta.2015.02.235
- Rabaey, K. (2010). *Bioelectrochemical Systems: from Extracellular Electron Transfer to Biotechnological Application*. London: IWA publishing.
- Rimboud, M., Desmond-Le Quemener, E., Erable, B., Bouchez, T., and Bergel, A. (2015). The current provided by oxygen-reducing microbial cathodes is related to the composition of their bacterial community. *Bioelectrochemistry* 102, 42–49. doi: 10.1016/j.bioelechem.2014.11.006
- Sharma, M., Bajracharya, S., Gildemyn, S., Patil, S. A., Alvarez-Gallego, Y., Pant, D., et al. (2014). A critical revisit of the key parameters used to describe microbial electrochemical systems. *Electrochim. Acta* 140, 191–208. doi: 10.1016/j.electacta.2014.02.111
- Sonawane, J. M., Marsili, E., and Ghosh, P. C. (2014). Treatment of domestic and distillery wastewater in high surface microbial fuel cells. *Int. J. Hydrol. Energy* 39, 21819–21827. doi: 10.1016/j.ijhydene.2014.07.085
- Sun, Y., Wei, J., Liang, P., and Huang, X. (2012). Microbial community analysis in biocathode microbial fuel cells packed with different materials. *AMB Express* 2:21. doi: 10.1186/2191-0855-2-21
- Tang, X., Li, H., Du, Z., and Ng, H. Y. (2014). A phosphorus-free anolyte to enhance coulombic efficiency of microbial fuel cells. *J. Power Sour.* 268, 14–18. doi: 10.1016/j.jpowsour.2014.06.009
- Tian, Y., Li, H., Li, L., Su, X., Lu, Y., Zuo, W., et al. (2015). In-situ integration of microbial fuel cell with hollow-fiber membrane bioreactor for wastewater treatment and membrane fouling mitigation. *Biosensors Bioelectron.* 64, 189–195. doi: 10.1016/j.bios.2014.08.070
- Wang, Z., Zheng, Y., Xiao, Y., Wu, S., Wu, Y., Yang, Z., et al. (2013). Analysis of oxygen reduction and microbial community of air-diffusion biocathode in microbial fuel cells. *Bioresour. Technol.* 144, 74–79. doi: 10.1016/j.biortech.2013.06.093
- Wei, J., Liang, P., Cao, X., and Huang, X. (2011a). Use of inexpensive semicoke and activated carbon as biocathode in microbial fuel cells. *Bioresour. Technol.* 102, 10431–10435. doi: 10.1016/j.biortech.2011.08.088
- Wei, J., Liang, P., and Huang, X. (2011b). Recent progress in electrodes for microbial fuel cells. *Bioresour. Technol.* 102, 9335–9344. doi: 10.1016/j.biortech.2011.07.019
- Wetser, K., Sudirjo, E., Buisman, C. J., and Strik, D. P. (2015). Electricity generation by a plant microbial fuel cell with an integrated oxygen reducing biocathode. *Appl. Energy* 137, 151–157. doi: 10.1016/j.apenergy.2014.10.006
- Ye, Z. F., Zhang, B. G., Liu, Y., Wang, Z. Y., and Tian, C. X. (2015). Continuous electricity generation with piggyback wastewater treatment using an anaerobic baffled stacking microbial fuel cell. *Desalin. Water Treat.* 55, 2079–2087. doi: 10.1080/19443994.2014.930702
- Zhang, F., Ge, Z., Grimaud, J., Hurst, J., and He, Z. (2013). Long-term performance of liter-scale microbial fuel cells treating primary effluent installed in a municipal wastewater treatment facility. *Environ. Sci. Technol.* 47, 4941–4948. doi: 10.1021/es400631r
- Zhang, G., Zhao, Q., Jiao, Y., and Lee, D.-J. (2015a). Long-term operation of manure-microbial fuel cell. *Bioresour. Technol.* 180, 365–369. doi: 10.1016/j.biortech.2015.01.002
- Zhang, X., Li, K., Yan, P., Liu, Z., and Pu, L. (2015b). N-type Cu₂O doped activated carbon as catalyst for improving power generation of air cathode microbial fuel cells. *Bioresour. Technol.* 187, 299–304. doi: 10.1016/j.biortech.2015.03.131
- Zhang, G.-D., Zhao, Q.-L., Jiao, Y., Zhang, J.-N., Jiang, J.-Q., Ren, N., et al. (2011). Improved performance of microbial fuel cell using combination biocathode of graphite fiber brush and graphite granules. *J. Power Sour.* 196, 6036–6041. doi: 10.1016/j.jpowsour.2011.03.096
- Zhang, H., Zhang, R., Zhang, G., Yang, F., and Gao, F. (2014a). Modified graphite electrode by polyaniline/tourmaline improves the performance of bio-cathode microbial fuel cell. *Int. J. Hydrol. Energy* 39, 11250–11257. doi: 10.1016/j.ijhydene.2014.05.057
- Zhang, X., Pant, D., Zhang, F., Liu, J., He, W., and Logan, B. E. (2014b). Long-term performance of chemically and physically modified activated carbons in air cathodes of microbial fuel cells. *ChemElectroChem* 1, 1859–1866. doi: 10.1002/celc.201402123
- Zhang, Y., Sun, J., Hu, Y., Li, S., and Xu, Q. (2012). Bio-cathode materials evaluation in microbial fuel cells: a comparison of graphite felt, carbon paper and stainless steel mesh materials. *Int. J. Hydrol. Energy* 37, 16935–16942. doi: 10.1016/j.ijhydene.2012.08.064

Conflict of Interest Statement: The authors declare that the research was conducted in the absence of any commercial or financial relationships that could be construed as a potential conflict of interest.

Copyright © 2016 Tursun, Liu, Li, Abro, Wang, Gao and Li. This is an open-access article distributed under the terms of the Creative Commons Attribution License (CC BY). The use, distribution or reproduction in other forums is permitted, provided the original author(s) or licensor are credited and that the original publication in this journal is cited, in accordance with accepted academic practice. No use, distribution or reproduction is permitted which does not comply with these terms.



Pyrosequencing Reveals a Core Community of Anodic Bacterial Biofilms in Bioelectrochemical Systems from China

OPEN ACCESS

Edited by:

Qiaoyun Huang,
Huazhong Agricultural University,
China

Reviewed by:
Jiangxin Wang,
Shenzhen University, China

Bharath Prithiviraj,
The Samuel Roberts Noble
Foundation Inc., USA

***Correspondence:**
Yong Xiao
yxiao@iue.ac.cn;
Feng Zhao
fzhao@iue.ac.cn

Specialty section:

This article was submitted to
Microbiotechnology, Ecotoxicology
and Bioremediation,
a section of the journal
Frontiers in Microbiology

Received: 25 September 2015

Accepted: 27 November 2015

Published: 16 December 2015

Citation:

Xiao Y, Zheng Y, Wu S, Zhang E-H, Chen Z, Liang P, Huang X, Yang Z-H, Ng I-S, Chen B-Y and Zhao F (2015) Pyrosequencing Reveals a Core Community of Anodic Bacterial Biofilms in Bioelectrochemical Systems from China.

Front. Microbiol. 6:1410.
doi: 10.3389/fmicb.2015.01410

Yong Xiao^{1*}, Yue Zheng^{1,2}, Song Wu^{1,2}, En-Hua Zhang^{1,2}, Zheng Chen³, Peng Liang⁴, Xia Huang⁴, Zhao-Hui Yang², I-Son Ng⁵, Bor-Yann Chen⁶ and Feng Zhao^{1*}

¹ Key Laboratory of Urban Pollutant Conversion, Institute of Urban Environment, Chinese Academy of Sciences, Xiamen, China, ² College of Environmental Science and Engineering, Hunan University, Changsha, China, ³ Research Center for Eco-Environmental Sciences, Chinese Academy of Sciences, Beijing, China, ⁴ School of Environment, Tsinghua University, Beijing, China, ⁵ Department of Chemical Engineering, National Cheng Kung University, Tainan, Taiwan, ⁶ Department of Chemical and Materials Engineering, National I-Lan University, I-Lan, Taiwan

Bioelectrochemical systems (BESs) are promising technologies for energy and product recovery coupled with wastewater treatment, and the core microbial community in electrochemically active biofilm in BESs remains controversy. In the present study, 7 anodic communities from 6 bioelectrochemical systems in 4 labs in southeast, north and south-central of China are explored by 454 pyrosequencing. A total of 251,225 effective sequences are obtained for 7 electrochemically active biofilm samples at 3% cutoff level. While Alpha-, Beta-, and Gamma-proteobacteria are the most abundant classes (averaging 16.0–17.7%), Bacteroidia and Clostridia are the two sub-dominant and commonly shared classes. Six commonly shared genera i.e., *Azospira*, *Azospirillum*, *Acinetobacter*, *Bacteroides*, *Geobacter*, *Pseudomonas*, and *Rhodopseudomonas* dominate the electrochemically active communities and are defined as core genera. A total of 25 OTUs with average relative abundance >0.5% were selected and designated as core OTUs, and some species relating to these OTUs have been reported electrochemically active. Furthermore, cyclic voltammetry and chronoamperometry tests show that two strains from *Acinetobacter guillouiae* and *Stappia indica*, bacteria relate to two core OTUs, are electrochemically active. Using randomly selected bioelectrochemical systems, the study has presented extremely diverse bacterial communities in anodic biofilms, though, we still can suggest some potentially microbes for investigating the electrochemical mechanisms in bioelectrochemical systems.

Keywords: high-throughput sequencing, microbial community, electrochemically active microorganisms, microbial fuel cells, bioelectrochemical systems, electron transfer

INTRODUCTION

Bioelectrochemical systems (BESs) are promising technologies for energy and products recovery coupled with wastewater treatment and have attracted increasing attention (Liu and Logan, 2004; Lovley, 2006a; Zhao et al., 2009b; Liu et al., 2013). Many studies have been conducted to expand the application of BESs and increase the efficiency of electricity production (Zhao et al., 2009a; Zhou et al., 2011; Xiao et al., 2013a). Microorganisms are believed to play key roles in electricity production (Logan and Regan, 2006; Lovley, 2006b), and extracellular electron transfer, the basis of electricity production, is the most frequent concern in BESs research. However, most studies on extracellular electron transfer are focusing on the two model species of *Shewanella oneidensis* (Marsili et al., 2008; Jiang et al., 2010) and *Geobacter sulfurreducens* (Reguera et al., 2005; Shrestha et al., 2013).

Electrochemically active microorganisms (EAMs) are a group of microorganisms which can transfer electrons from cells to an electron acceptor or accept electrons from an electron donor. Up to date, several EAMs have been identified (Xiao et al., 2013b). However, the understanding of performance of electrochemically active biofilm (EAB), which consists of EAMs and other microorganisms, is still poor due to limited knowledge on the microbial community in EAB.

Similar to soil and activated sludge, EAB is a very complex system consisting of viruses, bacteria, archaea, and fungi. However, the microbial community in EAB remains largely unstudied. This should be partly ascribed to the lack of robust techniques required to explore the highly complex community. In previous studies on the microbial community in EAB, denaturing gradient gel electrophoresis (DGGE) and cloning library are two commonly used techniques (Jung and Regan, 2007; Sun et al., 2011; Beecroft et al., 2012; Liang et al., 2013), and these traditional molecular approaches provide relative low sequencing depth while compared with the vast microbial diversity in EAB. The current investigations merely represent a snapshot of some dominant species in EAB community without providing information on species with medium to low abundances.

High-throughput sequencing, which can provide enough sequencing depth to cover a complex microbial community (Shendure and Ji, 2008), is a promising technology to explore the microbial communities in EAB. Up to now, the method has been widely used to analyze environmental microbial communities in marine water (Stoeck et al., 2010), activated sludge (Zhang et al., 2012), soil (Rousk et al., 2010), and also in BESs (Lee et al., 2010; Miceli et al., 2012; Xiao et al., 2015), these studies gained limited sequences. Therefore, people have not yet pictured full profiles of the microbial communities in EAB.

Six anodic EAB samples were randomly collected from four laboratories in Beijing, Changsha, and Xiamen in China. The 454 pyrosequencing targeting 16S rRNA genes was used (1) to profile the abundance, diversity, and composition of different anodic communities, (2) to investigate whether there are commonly shared species in randomly selected anodic EAB, (3) to compare the variability in anodic EAB during substrate

replacing, and (4) to confirm whether dominant species in EAB are electrochemically active.

EXPERIMENTAL

Samples

The samples of anodic biofilm were collected from six BESs at steady operation in Changsha (CS-LXM) (Liu et al., 2009), Beijing (BJ-CZ, BJ-HX) and Xiamen (XM1, XM2, and XM3). As the object of the study was to profile the bacterial communities and summarize the core members in anodic biofilm, we only showed some common information of the stably operated BESs (Table 1). To test the reproducibility of pyrosequencing, sample BJ-HX was divided into two samples (designated as BJ-HX1 and BJ-HX2) and subjected to sequential DNA extraction, PCR and pyrosequencing.

DNA Extraction

For each sample, the genomic DNA was extracted by a previously reported protocol using CTAB and proteinase K (Yang et al., 2007), which can successfully extracted genomic DNA from microbes in various environments e.g., compost and sludge (Xiao et al., 2009; Xiao et al., 2011a,b). The extracted genomic DNA was purified with a kit (DP1501, BioTeke, China). DNA quality was assessed by agarose gel electrophoresis and the 260/280- and 260/230-nm absorption ratios on an ND-2000 spectrophotometer (Nanodrop, USA).

PCR and 454 Pyrosequencing

Before pyrosequencing, the purified DNA was amplified with a set of primers targeting the V1-V3 hypervariable regions of bacterial 16S rRNA genes. The forward primer was 5'-AGAGTTGATCCTGGCTCAG-3' (27F) with the Roche 454 "B" adapter, and the reverse primer was 5'-TTACCGCGGCTGCTGGCAC -3' (533R) which containing the Roche 454 "A" adapter and specific 10 bp barcode. The Roche 454 "A"/"B" adapter located on the 5'-end of each primer, respectively. Each 20 μ L of PCR reaction system contained 4 μ L of 5 \times FastPfu buffer, 2 μ L of dNTPs (2.5 mM), 0.8 μ L of forward primer (5 μ M), 0.8 μ L of reverse primer (5 μ M), 0.4 μ L of FastPfu polymerase and 10 ng of template DNA (the rest of bulk was Milli-Q water). The PCR amplification followed the conditions: one cycle of initial denaturation at 95°C for 2 min; 25 cycles of denaturation at 95°C for 30 s, annealing at 55°C for 30 s and extension at 72°C for 30 s; a final extension at 72°C for 5 min.

The PCR products were quantitated by QuantiFluorTM -ST (Scientific Products, USA) and then mixed for pyrosequencing. The high-throughput pyrosequencing was processed on Roche GS FLX+ System (Roche, USA).

Post-run Analysis

The pyrosequencing data were processed using Quantitative Insights Into Microbial Ecology (QIIME) pipeline (Caporaso et al., 2010b). Before the statistical analysis of data, QIIME were used to (1) check the completeness of the barcodes and the

TABLE 1 | Characteristics of the anodic electrochemically active biofilm samples.

Code	Source (name, city, and location)	Substrate	Inoculant	Electrode material	Output power density/W m ⁻³
CS-LXM	Prof. Xiao-Ming Li, Changsha, central south China	Excess sludge	Activated sludge	Carbon cloth	0.31 (Liu et al., 2009)
BJ-CZ	Dr. Zheng Chen, Beijing, north China	Sodium acetate	Paddy soil	Carbon cloth	12.5
BJ-HX1 and 2	Prof. Xia Huang, Beijing, north China	Sodium acetate	Activated sludge	Carbon granule	38.2
XM1 ^a	Dr. Yong Xiao, Xiamen, southeast China	Sodium acetate	Activated sludge	Carbon felt	10.1
XM2 ^a		Organic kitchen waste	—	Carbon felt	9.5
XM3 ^a		Sodium acetate	—	Carbon felt	9.7

^aThe three samples were collected from the same BES which was sequentially fed with sodium acetate, organic kitchen waste, and sodium acetate. Each material was used as substrate for 60 days.

primer sequencing, (2) remove reads shorter than 200 bp, and (3) remove reads comprising chimera and quality score below 25. Secondly, the sequences belonging to different samples were exactly assigned using the unique 10 bp barcodes from raw data, and then the barcodes sequences were removed. Only the 97% identity of the effective sequences were divided into OTUs for further analysis, and the most abundant sequence from each OTU was selected as the representative sequence by PyNAST (Caporaso et al., 2010a). Then, these representative sequences were used for the classification of taxonomic according the Greengenes database. The sequences were used to explore the Alpha-diversity in each sample, and the UniFrac metric was employed to compare the beta-diversity between samples. To study the diversity in every sample, the number of OTUs, Chao1 index and phylogenetic richness index diversity were calculated from each sample. In the light of OTUs table, we performed principal component analysis by R v.2.15.0. OTU abundance is relative abundance determined by dividing the sequence number of any given OTU by the total sequence number of that sample.

Electrochemical Test

The strain of *Acinetobacter guillouiae* Ax-9 was screened from Yi-lan in Taiwan (Ng et al., 2014) and cultured in LB broth at 37°C. The strain of *Stappia indica* MCCC 1A01226 was bought from Marine Culture Collection of China (Lai et al., 2010) and cultured with Difco™ Marine Broth 2216 (BD, USA) at 25°C. The cyclic voltammetry (CV) test was anaerobically conducted on glassy carbon electrode using strains at the late-log growth phase after washed twice with PBS buffer (pH 7.0) (Wu et al., 2014). Chronoamperometry (CA) measurements were conducted in three-electrode systems where carbon felts (9 cm; Liu et al., 2013), stainless steel mesh (9 cm²) and saturated Ag/AgCl were used as working electrode, counter electrode and reference electrode, respectively. LB broth and Difco™ Marine Broth 2216 were added as culturing medium, respectively, and the reactor was sealed by rubber seal to maintain anaerobic condition in the chamber. During the test, 1% of bacteria suspension was inoculated into the reactors and a potential of +0.30 V (vs. Ag/AgCl) was applied onto the working electrodes by an electrochemistry workstation. In the abiotic control experiment, only LB broth or Difco™ Marine Broth 2216 was added into the reactor.

Nucleotide Sequence Accession Numbers

Twenty-five OTU sequences with high average abundance in the 7 samples have been deposited in the GenBank database under accession numbers KJ009261-KJ009285.

RESULTS AND DISCUSSION

Overall Pyrosequencing Information

After filtering the low quality reads (length <200 bp and quality score <25) and trimming adapters and barcodes, a total of 266,791 high quality reads were obtained for the 7 EAB samples using QIIME (Table S1). Then, the high quality reads were denoised, and chimeras were filtered out. There were 30,269–43,868 effective reads (a total of 251,225 sequences) for the 7 EAB samples. Since the smallest library among the 7 samples consisted of 30,269 sequences, the library size of each EAB sample was normalized to 30,269 sequences, and the downstream analyses for different samples were conducted at the same sequencing depth of 30,269 sequences. For the selected 211,883 sequences (7 samples), the average length of sequences is 485.8 bp. According to the Pearson correlation coefficient for the relation between samples BJ-HX1 and BJ-HX2 ($R^2 = 0.903$; Figure S1), the pyrosequencing showed high repeatability and reliability.

Diversity of Bacterial Communities

The numbers of operational taxonomic units (OTUs), Chao 1, Phylogenetic Diversity index and Good's coverage at the cutoff level of 3% are summarized in Table S1. Good's coverage shows the sampling completeness and the probability i.e., the possibility of a randomly selected sequence from the sequence data of a sample has already been sequenced. Though, 30,269 sequences for each sample were obtained from pyrosequencing, the Good's coverage ranged between 78.4 and 98.2%. The Good's coverage result together with the plots of OTU number, Chao 1 and Phylogenetic Diversity Index vs. sequence number (Figure S2) demonstrated that enough sequence depth was necessary for profiling complex EAB samples.

Based on the 251,225 effective sequences, a total of 31,502 OTUs were detected in 7 EAB samples. While each OTU could be assigned to a different microbial species, the diversity in EAB community is considerably rich, even higher than that

in activated sludge (Zhang et al., 2012). There were only 1129 OTUs in sample BJ-CZ, while the OTU numbers in the other 6 samples varied from 3695 to 9468 and were 3.5–8.5 times of that in this sample. According to the three indices of OTUs, Chao 1 and Phylogenetic Diversity index, the lowest diversity of community was found in sample BJ-CZ which was inoculated with paddy soil. The other 6 BESs were inoculated with activated sludge. Some studies, at the same sequencing depth, show that the bacterial diversity in soil is as rich as or even richer than that in activated sludge (Zhang et al., 2012). However, the results in this study seemed to demonstrate that BESs inoculated with activated sludge had considerably richer community diversity than that inoculated with soil. Some studies, at the same sequencing depth, show that the bacterial diversity in soil is as rich as or even richer than that in activated sludge (Zhang et al., 2012). However, the results in this study seemed to demonstrate that BESs inoculated with activated sludge had considerably richer community diversity than that inoculated with soil. The microbial diversity in CS-LXM and XM3 was considerably richer than that in the other samples, which might be attributable to the complex organic substrates of excess sludge and organic kitchen waste in these BESs.

In most of samples (6 in 7), Proteobacteria was the most dominant phylum (**Figure 1**), accounting for 37.5–92.8% of the 211,883 sequences (30,269 sequences for each sample). The results were similar to previous reports on anodic communities (Lee et al., 2010; Yates et al., 2012) or isolated EAMs (Xiao et al., 2013b). In these 6 samples, Bacteroidetes (3.4–19.2%, averaging at 9.7%), Firmicutes (0.9–13.8%, averaging at 4.7%), and Chloroflexi (0.02–11.2%, averaging at 4.4%) were the other sub-dominant phyla. Unlike that in the other 6 samples and previous reports (Lee et al., 2010; Miceli et al., 2012; Yates et al., 2012), Firmicutes was the most (39.6%) abundant phylum in sample XM2, while Bacteroidetes,

and Proteobacteria were the second (25.0%) and the third (22.5%) abundant phylum, respectively. Firmicutes usually is the dominant phylum in cellulose degradation system (Kröber et al., 2009; Eichorst et al., 2013). Therefore, that Firmicutes dominated sample XM3 might be ascribed to the feeding substrate of kitchen waste which is rich in cellulose.

Within Proteobacteria, Alpha-, Beta-, and Gamma-proteobacteria showed similar abundance (averaging 17.7, 17.1, and 16.0%, respectively) in the 7 EAB samples. Though, showing similar average abundance in all samples, Alpha- and Gamma-proteobacteria had extremely high abundance (>60%) in XM1 and BJ-CZ, respectively. Deltaproteobacteria was usually reported as the most dominant class in anodic EAB. However, the class occurred at relative low levels (0.1–10.7, averaging 4.5%) in this study, which was considerably different from previous studies with very low pyrosequencing depth (Lee et al., 2010; Yates et al., 2012).

It is interesting that Epsilonproteobacteria showed very low abundance in 6 samples (0–0.5%) except for CS-LXM (8.2%) which was fed with excess sludge. Previous studies showed that Epsilonproteobacteria occurred at very low level (<1%) in activated sludge (Zhang et al., 2012), anodic biofilm (Lee et al., 2010; Miceli et al., 2012; Yates et al., 2012), and excess sludge anaerobic digester (Zhang et al., 2009). The result in this study seemed to show the ability of BES to enrich some strains in Epsilonproteobacteria for excess sludge degradation.

Besides Alpha-, Beta-, Delta-, and Gamma-proteobacteria, two classes of Bacteroidia and Clostridia were dominant and commonly shared class (relative abundance >1.0%, occurring in at least 5 of 7 samples; Figure S3). Clostridia, typical cellulose degradators in mesophilic environment, was the most dominant (39.3%) class in sample XM2, which could be attributable to the cellulose rich substrate used in this BES.

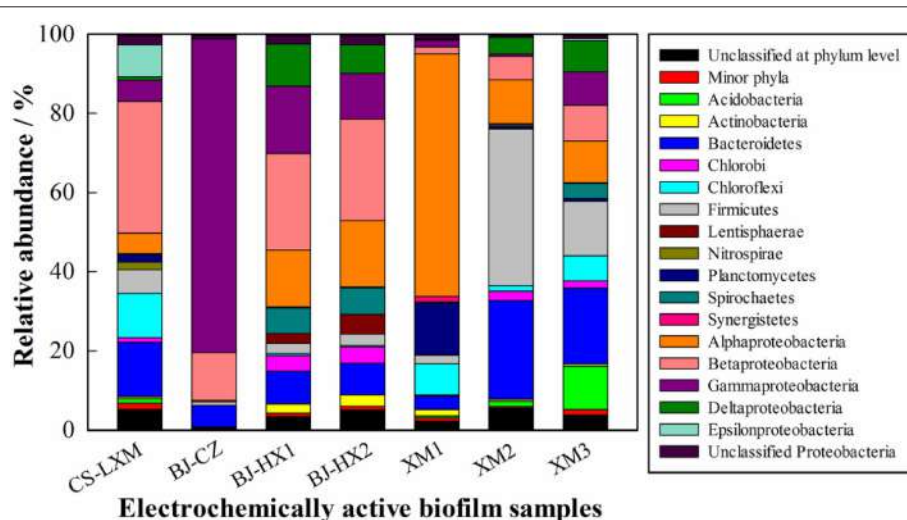


FIGURE 1 | Relative abundances of major phyla (>1% in at least one sample) and classes in Proteobacteria in the 7 EAB samples. The relative abundance is presented as the percentage in 30269 effective sequences in each sample. Minor phyla refer to taxa with a maximum relative abundance <1% in any sample.

Similarity Analysis of the EAB Samples

Using OTUs abundance, principal coordinate analysis (PCoA) using weighted UniFrac approach was conducted to compare the similarities between the 7 EAB samples (**Figure 2**). Though being fed with sodium acetate, the three samples from Beijing were different from XM1 and XM3. Some research indicates significant differences between the microbial communities in sewage treatment plants from different geographical areas (Zhang et al., 2012). Since most of the EAB was inoculated with activated sludge, the PCoA analysis demonstrates that the geographical areas other than the substrates significantly influenced the microbial communities in EAB. The close relationship of samples BJ-HX1 and BJ-HX2 also indicated high repeatability and reliability of the pyrosequencing. Results from OTU based cluster analysis (Figure S4) well agreed with the PCoA analysis.

Core Genera

There were 275 OTUs that could be assigned at genera level (Table S2). OTU number was significantly less than that reported in activated sludge (Zhang et al., 2012), indicating that there are many unknown bacteria in EAB. Among these genera, only 20 genera (accounting for 3.6–76.0% of total sequences) could be found in all the 7 samples, and a total of 81 genera (accounting for 7.9–83.4% of total sequences) could be classified as commonly shared genera which were shared by at least 5 samples (Table S3).

There were 60 abundant genera of 275 assigned genera, whose average relative abundance in 7 EAB samples was higher than 0.1% (a total of >0.71%; **Figure 3**), and 33 genera belong to Proteobacteria. Though, there were 81 commonly shared genera, only 47 genera showed high abundance (a total of >0.71%) in these samples. Among the 60 abundant genera, genera *Azospirillum* (0–4.3%, averaging 1.8%) and *Geobacter* (0–7.5%, averaging 2.4%) showed higher abundance (>1%) in five and four samples, respectively.

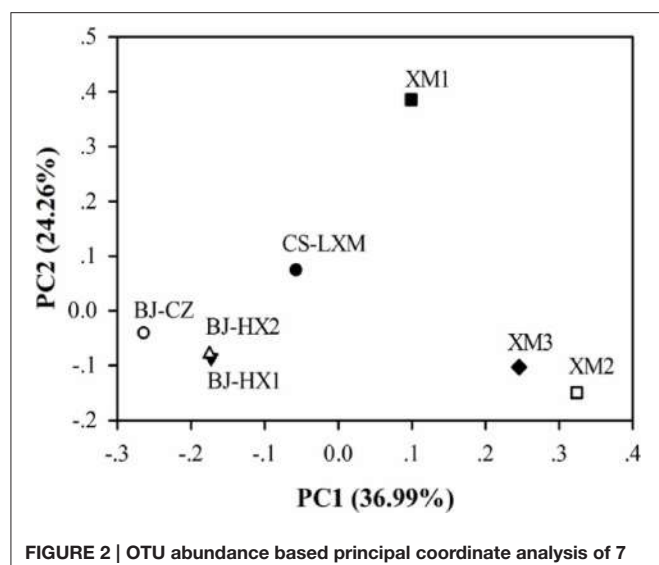
Genus *Azospirillum* is reported to be able to fix molecular nitrogen under microaerophilic conditions (Tarrand et al., 1978)

and have been rarely detected in bioelectrochemical systems (Hou et al., 2011; Pisciotta et al., 2012). However, a recent study reports (42) that a novel species of *Azospirillum humicireducens* can reduce extracellular anthraquinone-2,6-disulfonate, which is an analog of humic substances and known to function as electron shuttle for the bioreduction of U(VI) (Jeon et al., 2004). Though no study has directly reported *Azospirillum* as EAMs, the results seemed to predict their important roles in anodic communities by using electron shuttles e.g., humic substances to perform extracellular electron transfer.

As a model of extracellular electron transfer, genus *Geobacter* is one of the most widely reported EAMs (Lovley, 2012). In some previous studies, *Geobacter* was detected as the most dominant microorganisms in anodic community by low depth pyrosequencing (Lee et al., 2010; Miceli et al., 2012; Yates et al., 2012). With a much deeper sequencing depth in this study, genus *Geobacter* was detected in 6 but not all anodic samples, and only in 4 samples its abundance was >1%. The results indicated that *Geobacter* was not always the dominant microorganisms in anodic communities of BESs, and low sequencing depth would have introduced inaccurate conclusions in analyzing complex microbial communities.

There were four genera i.e., *Acinetobacter*, *Bacteroides*, *Pseudomonas*, and *Rhodopseudomonas* which dominate one or two samples with very high abundance (>10%). (i) Genus *Acinetobacter*, reported as nosocomial pathogens (Bergogne-Bérénin and Towner, 1996), was detected as dominant bacteria in samples BJ-CZ and BJ-HX1 (abundance >7% in BJ-HX2). Based on clone libraries, previous studies have detected the genus as abundant bacteria in anodic (Sun et al., 2010) or cathodic communities (Rabaey et al., 2008). Together with all these results, *Acinetobacter* was suggested to be an important composition in EAB community and further electrochemical test might be helpful to understand their roles in EAB. (ii) A previous study has once isolated a Fe(III)-reducing fermentative bacterium *Bacteroides* sp. W7 from the anode suspension of a BES (Wang et al., 2010). A Fe(III)-reducing usually suggests the potential of extracellular electron transfer. This genus was the most dominant genus in sample XM2 which was fed with kitchen waste and the abundance of this genus decreased as sodium acetate was used as substrate again. Therefore, it's speculated that *Bacteroides* might be very important for BESs' current generation with complex substrate. (iii) It's very interesting that genus *Pseudomonas* accounts for 56.4% of total sequences in sample BJ-CZ. Though some studies have reported *Pseudomonas aeruginosa* as an EAM by secreting electron shuttle of pyocyanin (Rabaey et al., 2005), no research have ever reported such a dominance of *Pseudomonas* in BESs. The results might also suggest mediated extracellular electron transfer mainly contributing to current generation in BJ-CZ. (iv) Genus *Rhodopseudomonas* consists of a group of photosynthetic bacteria, and a strain of *Rhodopseudomonas palustris* can directly produce current coupling with acetate respiration (Xing et al., 2008).

Besides the six genera mentioned above, genus of *Azospira* (formally *Dechlorosoma*) which was detected in all the 7 samples seemed to be another core genus in anodic EAB. Though, the



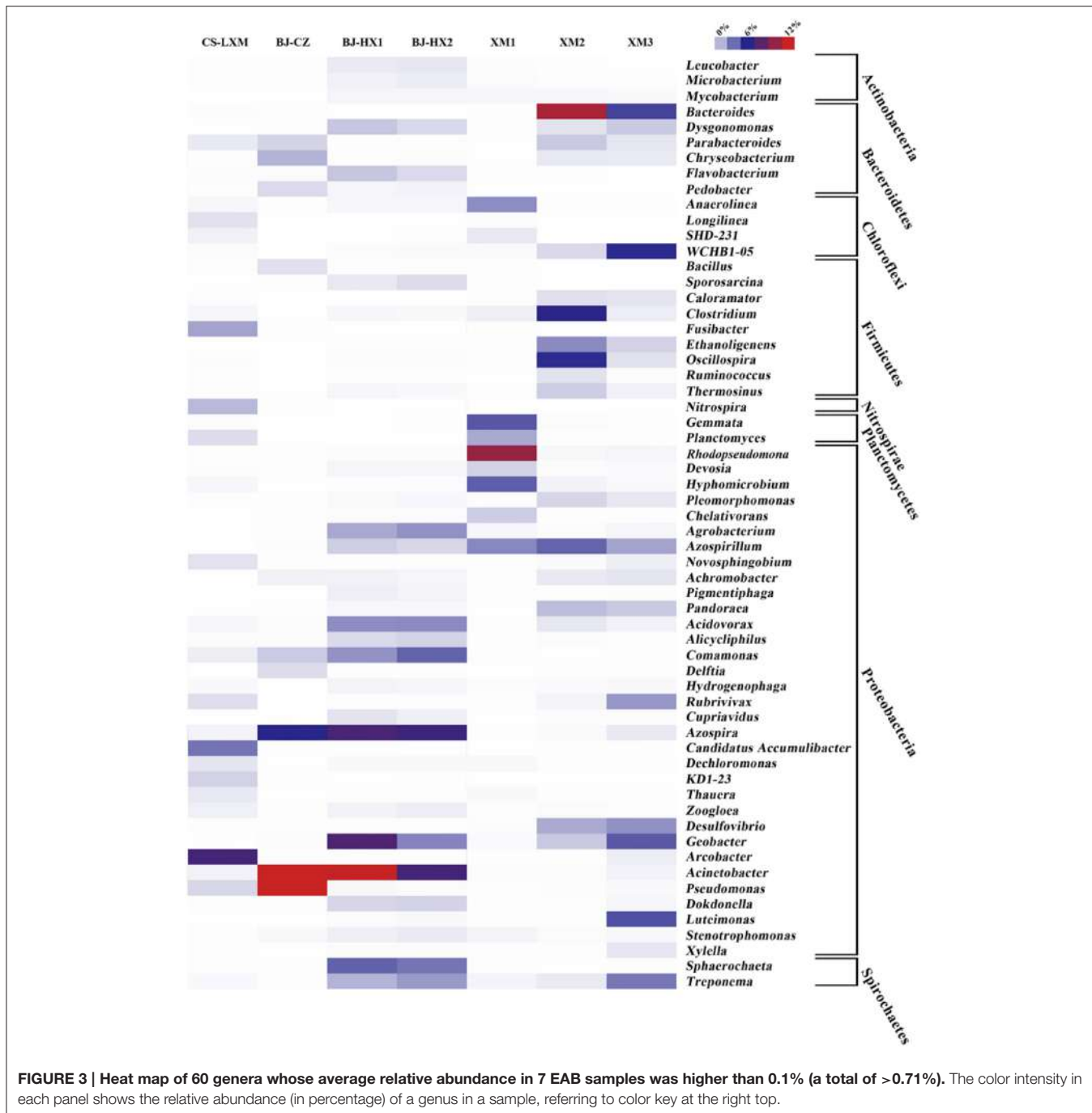


FIGURE 3 | Heat map of 60 genera whose average relative abundance in 7 EAB samples was higher than 0.1% (a total of >0.71%). The color intensity in each panel shows the relative abundance (in percentage) of a genus in a sample, referring to color key at the right top.

genus was not the most abundant genus in any sample, it showed high abundance (>5%) in BJ-CZ, BJ-HX1, and BJ-HX2. The genus was previously detected as dominant residents in anodic EAB (Sun et al., 2011). Therefore, further investigation on the electrochemical activity of *Azospira* spp. is an urgent need for understanding their roles in EAB due to the absent research on this aspect.

The genus *Shewanella* contains several species of EAMs (especially *Shewanella oneidensis*) and therefore has been widely investigated (Borole et al., 2011). However, the pyrosequencing

detected no sequence related to this genus, which suggested that *Shewanella* was not a widely spread EAM. The results from the pyrosequencing showed that some commonly shared genera i.e., *Azospira*, *Azospirillum*, *Acinetobacter*, *Bacteroides*, *Geobacter*, *Pseudomonas*, and *Rhodopseudomonas* dominate the bacteria community and therefore were defined as core genera in EAB. Though, the electron transfer of *Geobacter* has been widely studied, very limited attention has been paid to the other genera. The results suggest that, to better understand the electrochemical activity of EAB, the research community should conduct some

extra studies to investigate the electron transfer of the bacteria in the other 6 genera.

Core OTUs

A total of 31502 OTUs (3% distance) were detected in the present study. Among these genera, only 9 OTUs were found in all the 7 samples, and a total of 115 OTUs (accounting for 1.3–38.4% of total sequences) could be classified as commonly shared OTUs which were shared by at least 5 samples (Table S4).

The pyrosequencing detected 108 OTUs with an average relative abundance higher than 0.1%, which accounted for 18.1–81.7% of total sequences (Table S5). While 17, 21, 6, and 15 of 108 OTUs belong to classes Alpha-, Beta-, Delta-, and Gamma-proteobacteria, respectively, only 1 OTU belongs to Epsilonproteobacteria. Besides, 12 and 13 of 108 OTUs belong to classes Bacteroidia and Clostridia, respectively.

Though six genera have been proposed as core genera in EAB, specific species was still unknown. Therefore, a total of 25 OTUs, average relative abundance >0.5%, were selected and designated as core OTUs for further analysis (Figure 4).

Fifteen of 25 OTUs belong to phylum Proteobacteria, and 6 OTUs belong to Alphaproteobacteria. OTU 36744 was the most abundant OTU (abundance of about 20%) in sample XM1. The OTU was 99% identical to strains of *Stappia indica* (GenBank accession number of EU726271.1), which has never been reported as an EAM. OTU 28339 was 99% identical to

strain *Rhodopseudomonas palustris* DX-1 which was reported as an EAM (Xing et al., 2008). The OTU was shared by all 7 samples, suggesting that the photosynthetic strain is a widely spread EAM in anodic EAB. Though, OTU 6374 showed high abundance (abundance of 4–5%) in samples BJ-HX1 and BJ-HX2, it could be classified to any specific genus. OTU 14215 was highly identical to strains of *Rhizobium* sp. (99%) or *Agrobacterium tumefaciens* (98%) which both were detected in anodic biofilm of microbial fuel cell (Ishii et al., 2008; Sun et al., 2010). OTUs 16867 and 32034 were highly identical to *Azospirillum lipoferum* (96%) and *Azospirillum zae* (99%), respectively. As previously discussed, these strains may be able to use electron shuttles for extracellular electron transfer, which still needs further confirmation.

Three OTUs belong to Betaproteobacteria, and OTUs 14184, 15613, and 19577 were highly identical to *Acidovorax caeni* (99%), *Azospira oryzae* (100%), and *Rhodocyclosp* sp. (99%), respectively. Though, all the three known genera/species were detected in anodic EAB (Borole et al., 2009; Song et al., 2012), no extracellular electron transfer in these species has been reported (Xiao et al., 2013b). Two OTUs within Deltaproteobacteria i.e., 960 and 14436 shared high similarity to *Geobacter sulfurreducens* strain PCA (97%) and *Geobacter* sp. (99%), respectively. *Geobacter sulfurreducens* strain PCA is known as the model strain for studying bioelectricity generation (Bond and Lovley, 2003), and genus *Geobacter* is one of the most widely reported EAMs (Lovley, 2012). While OTU 960 was a dominant OTU

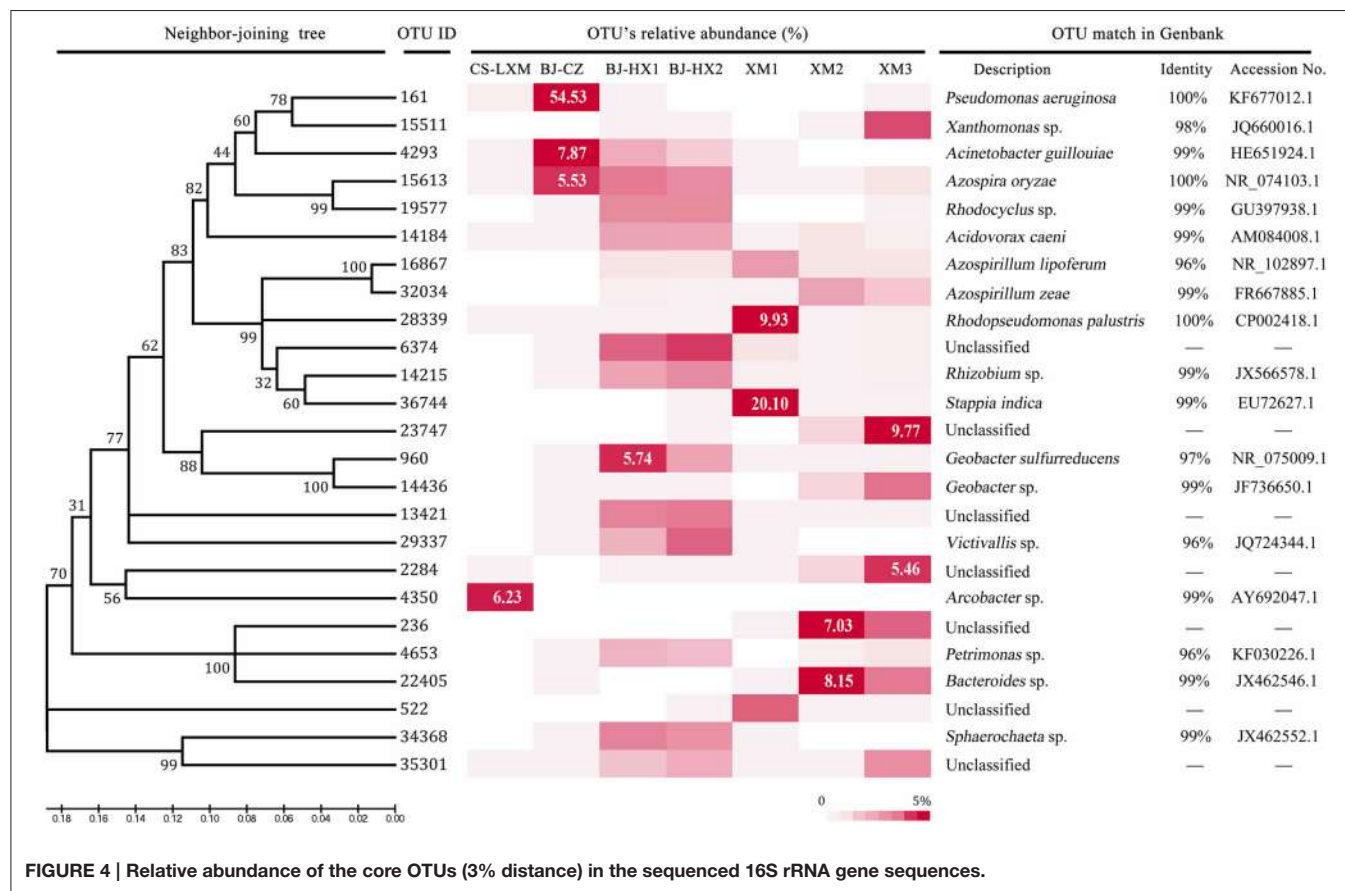


FIGURE 4 | Relative abundance of the core OTUs (3% distance) in the sequenced 16S rRNA gene sequences.

(2.3–5.7%) in BJ-HX1 and BJ-HX2, OTU 14436 was abundant in samples XM2 (0.9%) and XM3 (3.7%). The results seemed to show a geography discrepancy in *Geobacter* species. OTU 4350 belong to Epsilonproteobacteria and shared 99% similarity to uncultured *Arcobacter* sp.. Though, this OTU was the most dominant one (abundance of 6.2%) in sample CS-LXM, it was not detected in the other six samples, which might be attributable to the substrate of excess sludge used in this BES. Three OTUs i.e., 161, 4293, and 15511 belong to Gammaproteobacteria. OTU 161 was 100% identical to *Pseudomonas aeruginosa* which was reported as a producer of electron shuttle of pyocyanin (Rabaey et al., 2005). The OTU accounted for more than 54.5% of total sequences in sample BJ-CZ, which confirmed our previous speculation that mediated extracellular electron transfer mainly contributed to current generation in this BES. OTU 4293, sharing 98% similarity to *Acinetobacter guillouiae*, was the second abundant OTU (abundance of 7.9%) in BJ-CZ and also shared high abundance in BJ-HX1 (abundance of 2.0%) and BJ-HX2 (abundance of 1.1%), which indicated that the OTU might be important to the current generation. A strain Ax-9 of *Acinetobacter guillouiae* could degrade synthetic dye (Ng et al., 2014), indicating that the species of bacterium may be electrochemically active.

OTUs 236, 4653, and 22405 belong to class Bacteroidia. OTUs 4653 and 22405 were 96 and 99% identical to *Petrimonas* sp. and *Bacteroides* sp., but OTU 236 did not share high similarity to any specific genus. Previous studies have classified some strains in *Bacteroides* sp. as EAMs (Xiao et al., 2013b), indicating that OTU 22405 relating strain might be important to the current generation of EAB as it accounted for 3.5 and 8.1% of total sequences in XM3 and XM2, respectively. OTUs 29337 and 34368 were 96 and 99% identical to *Victivallis* sp. and *Sphaerochaeta* sp., respectively. Though, strains close to these genera have been detected in microbial fuel cells, no EAM has been reported yet. The left 5 OTUs did not share >95% similarity to known genus, though their abundance was higher than 2% in one or two samples. The results indicated that a great number of dominant strains in EAB are still not isolated and identified.

Electrochemical Tests

The redox peaks in the CVs of the two bacteria (**Figure 5A**) provide the first indications that both *Acinetobacter guillouiae* Ax-9 and *Stappia indica* MCCC 1A01226 may be electrochemically active. While four redox peaks (at -0.41 , -0.38 , -0.14 , and $+0.95$ V vs. Ag/AgCl, respectively) could be counted in the CV of *Acinetobacter guillouiae*, only one oxidation peak at $+0.12$ V vs. Ag/AgCl could be observed in the CV of *Stappia indica*.

Since redox peaks in a CV don't guarantee bio-electricity production, we employed CA to test the current yield by the bacteria (**Figure 5B**). The background current of LB and Marine broth were about 4 and 15 μ A, respectively. While *Acinetobacter guillouiae* could produce a current higher than 400 μ A, a relative low current of about 50 μ A was produced by *Stappia indica*. To summarize, CA measurement and CV tests notably indicated that the both bacteria are electrochemically active and can produce electricity, and the results also implied that core OTUs of 36744

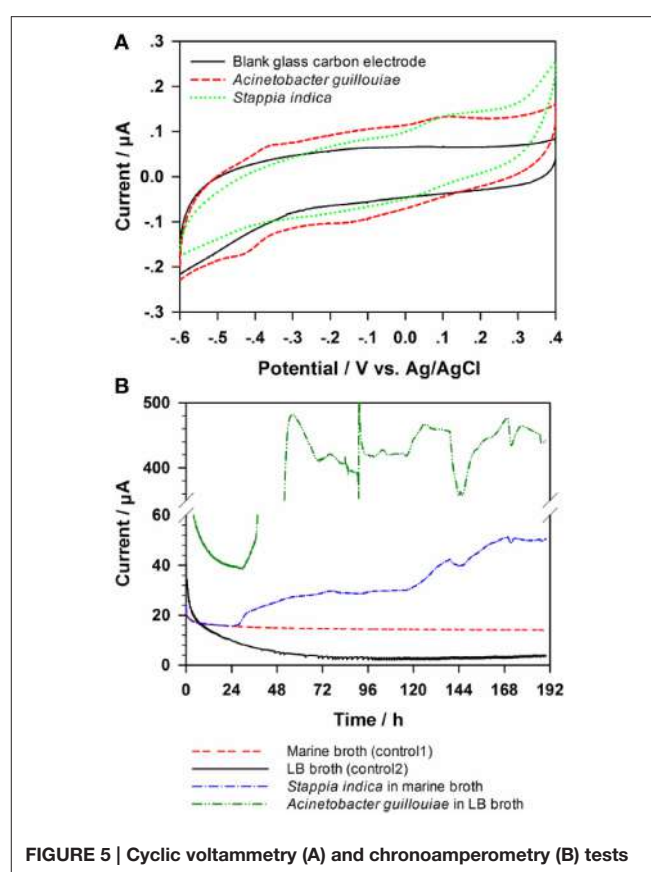


FIGURE 5 | Cyclic voltammetry (A) and chronoamperometry (B) tests for *Stappia indica* and *Acinetobacter guillouiae*.

and 4293 were electrochemically active and played important roles in current production in anode.

Community Dynamics Following Substrate Change

Sample XM1 was collected after the BES was fed with sodium acetate for 8 months. Samples of XM2 and XM3 were collected from the same BES after it was sequentially fed with organic kitchen wastes and sodium acetate for 60 days. The performance of the BES was illustrated in Supporting Material (Figure S5). The relative abundance fold change of OTUs for the substrate of BESs was evaluated as a microbial community dynamics using scatter plots (**Figures 6A,B**). The scatter plots distinctly showed that 84.20% of OTUs was over 10-fold change or under 1/10-fold change in the first substrate alternation (from acetate to organic kitchen wastes), and 26.80% of OTUs was over 10-fold change or under 1/10-fold change in the second substrate alternation (from organic kitchen wastes back to acetate). The distribution of OTUs was more centralized after the first alternation than that after the second alternation, suggesting microbial community was more impacted by the first substrate alternation. We could infer that the start-up substrate of BESs exerts further influence on substrate changes in the process of operation.

To address the prominent OTUs related to substrate change in the microbial community, we classified those OTUs that upregulated in the first alternation or downregulation in the

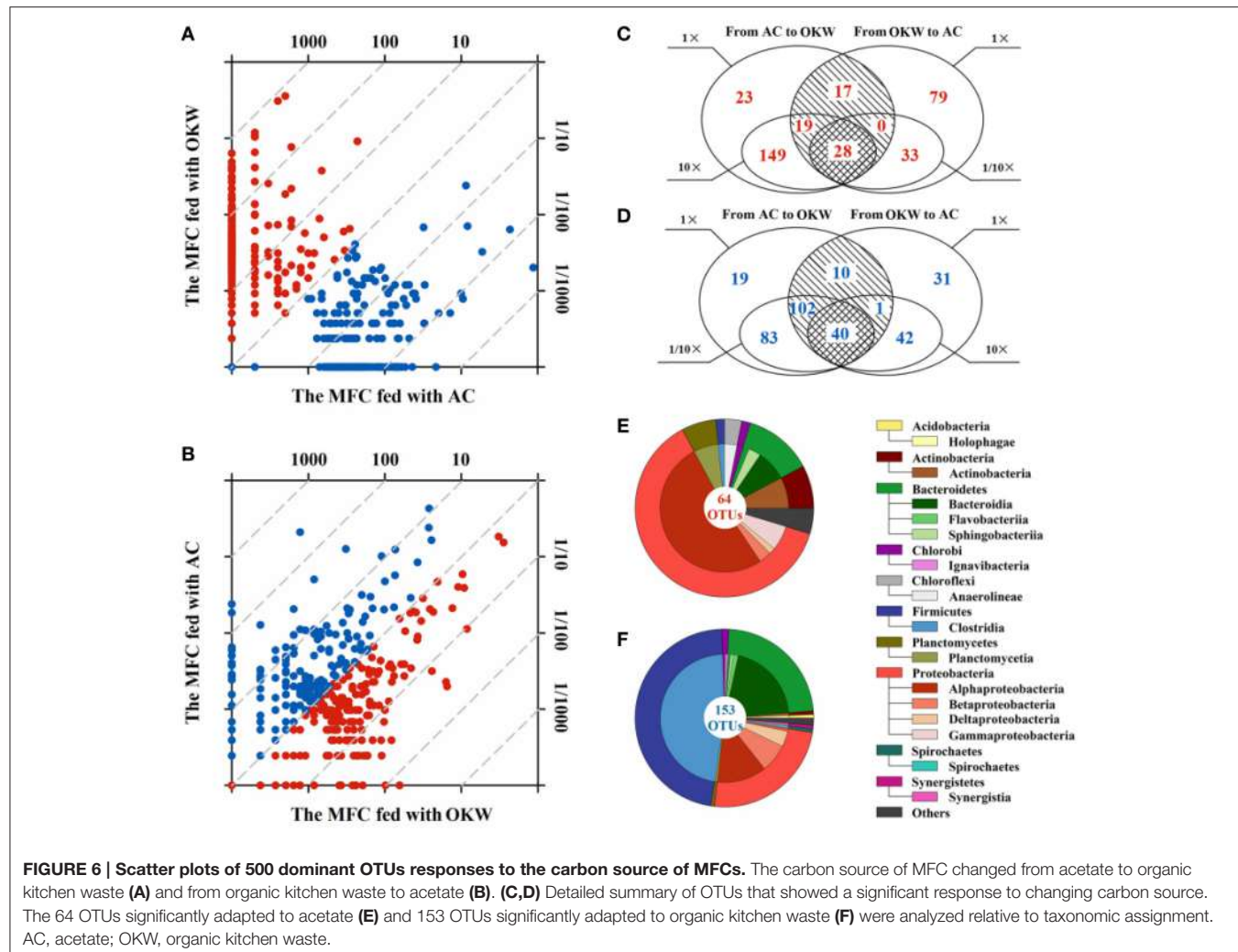


FIGURE 6 | Scatter plots of 500 dominant OTUs responses to the carbon source of MFCs. The carbon source of MFC changed from acetate to organic kitchen waste (**A**) and from organic kitchen waste to acetate (**B**). (**C,D**) Detailed summary of OTUs that showed a significant response to changing carbon source. The 64 OTUs significantly adapted to acetate (**E**) and 153 OTUs significantly adapted to organic kitchen waste (**F**) were analyzed relative to taxonomic assignment. AC, acetate; OKW, organic kitchen waste.

second alternation as objects which were apt to acetate. Another part of OTUs which adapted to organic kitchen wastes were selected following the similar way which downregulated in the first alternation or upregulation in the second alternation. Above two kinds of OTUs (>1-fold, ≥ 10 -fold change) were figured using Venn diagram between carbon source conditions (**Figures 6C,D**). 64 OTUs significantly adapted to acetate and 153 OTUs significantly adapted to organic kitchen wastes, suggesting microbial community better adapted to multicomponent organic kitchen wastes. Among 64 OTUs, 20 OTUs were not detected by pyrosequencing after the first alternation and were came back after retrieving acetate, which suggesting that OTUs had a certain degree of preference on the substrate.

Based on taxonomic assignment, 7 and 9 dominant phyla were detected in the 64 OTUs and 153 OTUs (**Figures 6E,F**, respectively. Three dominant phyla (relative abundances over 1%), that was Bacteroidetes (22.22%), Firmicutes (47.06%), Proteobacteria (23.53%), were detected in apt-organic kitchen wastes OTUs. Among apt-acetate OTUs, a wider range of phyla was identified as dominant, i.e., Actinobacteria (7.81%), Bacteroidetes (10.94%), Chloroflexi (3.13%), Firmicutes

(1.56%), Planctomycetes (6.25%), and Proteobacteria (62.50%). The dominant portion was changed from Proteobacteria to Firmicutes between apt-acetate OTUs and apt-kitchen garbage OTUs, suggesting the substrate of BESs could drive the change of microbial community. Such as those described genera, *Bacteroides* was abound in XM2 which fed with multicomponent substrate, and *Rhodopseudomonas* was a dominant genus in XM1.

Compare with previous Studies on EAB

Most previous studies on microbial community in anodic EAB have been heavily relied on 16S rRNA gene fragments based DGGE and clone library analysis (Jung and Regan, 2007; Sun et al., 2011; Beecroft et al., 2012; Liang et al., 2013). Though, some researchers have applied 454 pyrosequencing to investigate the anodic communities in microbial fuel cells (Lee et al., 2010; Yates et al., 2012), their results are sometimes insufficient to fully profile the microbial communities due to limited sequences obtained in those studies. It should be noted that most pyrosequencing studies on EAB try to understand the complex microbial community under control conditions (i.e., primary inoculum,

and substrates etc.; Lee et al., 2010; Yates et al., 2012; Wang et al., 2013). There is no doubt that the experiment using controlled conditions is conducive to explore the function under this specific condition. However, a control experiment is limited for studying EAB in specific BEss. It is necessary from an overall point, to develop the heterogenous BEss for fully understanding EAB.

The study is the first systematic work on the microbial communities of multiple anodic EAB samples by investigating >30,269 and 16S rRNA gene fragments per sample. By employing PCR-based 454 pyrosequencing technique, the deep sequencing showed a high diverse microbial community in anodic EAB and proposed some core genera and OTUs in the 7 geographically separated EAB samples from China.

Some of our findings agree with part of previous research. For example, Proteobacteria were the dominant members in most anodic EAB samples, and Epsilonproteobacteria were the rarely existed bacteria (Lee et al., 2010; Yates et al., 2012). However, our study showed below novel findings: (1) extremely diverse bacterial communities were found in anodic EAB samples, and Deltaproteobacteria was not the dominant class in all samples, the results should be attributable to the deeper sequencing depth used in this study. (2) Several genera of *Azospira*, *Azospirillum*, *Acinetobacter*, *Bacteroides*, *Geobacter*, *Pseudomonas*, and *Rhodopseudomonas* played roles as core members in randomly selected anodic EAB samples, and studies on their EET, rather than confined to *Geobacter*, will help us understand the electron transfer within mixed bacterial EAB. The genus of *Shewanella*, one of the model strains for electron transfer studies, was not detected in all EAB samples. (3) The study showed that some pathogens i.e., *Acinetobacter* spp. and *Pseudomonas aeruginosa* were highly dominant members in some samples, which reminds the research community to be very careful in conducting research.

REFERENCES

- Beecroft, N. J., Zhao, F., Varcoe, J. R., Slade, R. C., Thumser, A. E., and Avignone-Rossa, C. (2012). Dynamic changes in the microbial community composition in microbial fuel cells fed with sucrose. *Appl. Microbiol. Biot.* 93, 423–437. doi: 10.1007/s00253-011-3590-y
- Bergogne-Bérénin, E., and Towner, K. (1996). *Acinetobacter* spp. as nosocomial pathogens: microbiological, clinical, and epidemiological features. *Clin. Microbiol. Rev.* 9, 148–155.
- Bond, D. R., and Lovley, D. R. (2003). Electricity production by *Geobacter sulfurreducens* attached to electrodes. *Appl. Environ. Microb.* 69, 1548–1555. doi: 10.1128/AEM.69.3.1548-1555.2003
- Borole, A. P., Mielenz, J. R., Vishnivetskaya, T. A., and Hamilton, C. Y. (2009). Controlling accumulation of fermentation inhibitors in biorefinery recycle water using microbial fuel cells. *Biotechnol. Biofuels* 2, 1–14. doi: 10.1186/1754-6834-2-7
- Borole, A. P., Reguera, G., Ringeisen, B., Wang, Z.-W., Feng, Y., and Kim, B. H. (2011). Electroactive biofilms: current status and future research needs. *Energy Environ. Sci.* 4, 4813–4834. doi: 10.1039/c1ee02511b
- Caporaso, J. G., Bittinger, K., Bushman, F. D., DeSantis, T. Z., Andersen, G. L., and Knight, R. (2010a). PyNAST: a flexible tool for aligning sequences to a template alignment. *Bioinformatics* 26, 266–267. doi: 10.1093/bioinformatics/btp636
- Caporaso, J. G., Kuczynski, J., Stombaugh, J., Bittinger, K., Bushman, F. D., Costello, E. K., et al. (2010b). QIIME allows analysis of high-throughput community sequencing data. *Nat. Methods* 7, 335–336. doi: 10.1038/nmeth.f.303
- Eichorst, S. A., Varanasi, P., Stavila, V., Zemla, M., Auer, M., Singh, S., et al. (2013). Community dynamics of cellulose-adapted thermophilic bacterial consortia. *Environ. Microbiol.* 15, 2573–2587. doi: 10.1111/1462-2920.12159
- Hou, B., Sun, J., and Hu, Y. (2011). Effect of enrichment procedures on performance and microbial diversity of microbial fuel cell for Congo red decolorization and electricity generation. *Appl. Microbiol. Biot.* 90, 1563–1572. doi: 10.1007/s00253-011-3226-2
- Ishii, S., Hotta, Y., and Watanabe, K. (2008). Methanogenesis versus electrogenesis: morphological and phylogenetic comparisons of microbial communities. *Biosci. Biotech. Bioch.* 72, 286–294. doi: 10.1271/bbb.70179
- Jeon, O.-H., Kelly, S. D., Kemner, K. M., Barnett, M. O., Burgos, W. D., Dempsey, B. A., et al. (2004). Microbial reduction of U (VI) at the solid-water interface. *Environ. Sci. Technol.* 38, 5649–5655. doi: 10.1021/es0496120
- Jiang, X. C., Hu, J., Fitzgerald, L. A., Biffinger, J. C., Xie, P., Ringeisen, B. R., et al. (2010). Probing electron transfer mechanisms in *Shewanella oneidensis* MR-1 using a nanoelectrode platform. *Proc. Natl. Acad. Sci. U.S.A.* 107, 16806–16810. doi: 10.1073/pnas.1011699107

CONCLUSIONS

Using randomly selected EAB samples and pyrosequencing technology, we have profiled a diverse bacterial community in anodic biofilm of BES. Six commonly shared and abundant genera i.e., *Azospira*, *Azospirillum*, *Acinetobacter*, *Bacteroides*, *Geobacter*, *Pseudomonas*, and *Rhodopseudomonas* were defined as core genera in electrochemically active communities. Twenty-five OTUs were selected as core OTUs in EABs, and two core OTUs related strains from *Stappia indica* and *Acinetobacter guillouiae* were proven to be electrochemically active. Most dominant bacteria in EAB may be electrochemically active, and high-throughput sequencing such as pyrosequencing is helpful to suggest potential EAMs.

AUTHOR CONTRIBUTIONS

Idea: YX; data analysis: YX, YZ, SW, and FZ; data collection: YX, YZ, SW, EZ, ZC, PL, XH, and FZ; writing and reviewing the manuscript: all authors.

ACKNOWLEDGMENTS

This study was sponsored by the Knowledge Innovation Program of the Chinese Academy of Sciences (IUEQN201306), the Ministry of Science and Technology (2011AA060907), and National Natural Science Foundation of China (51208490, 51478451). We would like to thank Prof. Xiaoming Li (Hunan University) for providing the sample CS-LXM.

SUPPLEMENTARY MATERIAL

The Supplementary Material for this article can be found online at: <http://journal.frontiersin.org/article/10.3389/fmicb.2015.01410>

- Jung, S., and Regan, J. M. (2007). Comparison of anode bacterial communities and performance in microbial fuel cells with different electron donors. *Appl. Microbiol. Biot.* 77, 393–402. doi: 10.1007/s00253-007-1162-y
- Kröber, M., Bekel, T., Diaz, N. N., Goesmann, A., Jaenicke, S., Krause, L., et al. (2009). Phylogenetic characterization of a biogas plant microbial community integrating clone library 16S-rDNA sequences and metagenome sequence data obtained by 454-pyrosequencing. *J. Biotechnol.* 142, 38–49. doi: 10.1016/j.biote.2009.02.010
- Lai, Q., Qiao, N., Wu, C., Sun, F., Yuan, J., and Shao, Z. (2010). *Stappia indica* sp. nov., isolated from deep seawater of the Indian Ocean. *Int. J. Syst. Evol. Micr.* 60, 733–736. doi: 10.1099/ijss.0.013417-0
- Lee, T., Van Doan, T., Yoo, K., Choi, S., Kim, C., and Park, J. (2010). Discovery of commonly existing anode biofilm microbes in two different wastewater treatment MFCs using FLX Titanium pyrosequencing. *Appl. Microbiol. Biot.* 87, 2335–2343. doi: 10.1007/s00253-010-2680-6
- Liang, F., Xiao, Y., and Zhao, F. (2013). Effect of pH on sulfate removal from wastewater using a bioelectrochemical system. *Chem. Eng. J.* 218, 147–153. doi: 10.1016/j.cej.2012.12.021
- Liu, H., and Logan, B. E. (2004). Electricity generation using an air-cathode single chamber microbial fuel cell in the presence and absence of a proton exchange membrane. *Environ. Sci. Technol.* 38, 4040–4046. doi: 10.1021/es0499344
- Liu, S., Ying, G.-G., Liu, Y.-S., Peng, F.-Q., and He, L.-Y. (2013). Degradation of norgestrel by bacteria from activated sludge: comparison to progesterone. *Environ. Sci. Technol.* 47, 10266–10276. doi: 10.1021/es304688g
- Liu, Z., Li, X., Jia, B., Zheng, Y., Fang, L., Yang, Q., et al. (2009). Production of electricity from surplus sludge using a single chamber floating-cathode microbial fuel cell. *Water Sci. Technol.* 60, 2099–2404. doi: 10.2166/wst.2009.313
- Logan, B. E., and Regan, J. M. (2006). Electricity-producing bacterial communities in microbial fuel cells. *Trends Microbiol.* 14, 512–518. doi: 10.1016/j.tim.2006.10.003
- Lovley, D. (2006a). Microbial fuel cells: novel microbial physiologies and engineering approaches. *Curr. Opin. Biotechnol.* 17, 327–332. doi: 10.1016/j.copbio.2006.04.006
- Lovley, D. R. (2006b). Bug juice: harvesting electricity with microorganisms. *Nat. Rev. Microbiol.* 4, 497–508. doi: 10.1038/nrmicro1442
- Lovley, D. R. (2012). Electromicrobiology. *Annu. Rev. Microbiol.* 66, 391–409. doi: 10.1146/annurev-micro-092611-150104
- Marsili, E., Baron, D. B., Shikhare, I. D., Coursolle, D., Gralnick, J. A., and Bond, D. R. (2008). *Shewanella* secretes flavins that mediate extracellular electron transfer. *Proc. Natl. Acad. Sci. U.S.A.* 105, 3968–3973. doi: 10.1073/pnas.0710525105
- Miceli, J. F. III, Parameswaran, P., Kang, D.-W., Krajmalnik-Brown, R., and Torres, C. S. I. (2012). Enrichment and analysis of anode-respiring bacteria from diverse anaerobic inocula. *Environ. Sci. Technol.* 46, 10349–10355. doi: 10.1021/es301902h
- Ng, I. S., Xu, F., Ye, C., Chen, B.-Y., and Lu, Y. (2014). Exploring metal effects and synergistic interactions of ferric stimulation on azo-dye decolorization by new indigenous *Acinetobacter guillouiae* Ax-9 and *Rahnella aquatilis* DX2b. *Bioprocess Biosyst. Eng.* 37, 217–224. doi: 10.1007/s00449-013-0988-1
- Pisciotta, J. M., Zaybak, Z., Call, D. F., Nam, J.-Y., and Logan, B. E. (2012). Enrichment of microbial electrolysis cell biocathodes from sediment microbial fuel cell bioanodes. *Appl. Environ. Microb.* 78, 5212–5219. doi: 10.1128/AEM.00480-12
- Rabaey, K., Boon, N., Hofte, M., and Verstraete, W. (2005). Microbial phenazine production enhances electron transfer in biofuel cells. *Environ. Sci. Technol.* 39, 3401–3408. doi: 10.1021/es0485630
- Rabaey, K., Read, S. T., Clauwaert, P., Freguia, S., Bond, P. L., Blackall, L. L., et al. (2008). Cathodic oxygen reduction catalyzed by bacteria in microbial fuel cells. *ISME J.* 2, 519–527. doi: 10.1038/ismej.2008.1
- Reguera, G., McCarthy, K. D., Mehta, T., Nicoll, J. S., Tuominen, M. T., and Lovley, D. R. (2005). Extracellular electron transfer via microbial nanowires. *Nature* 435, 1098–1101. doi: 10.1038/nature03661
- Rousk, J., Bååth, E., Brookes, P. C., Lauber, C. L., Lozupone, C., Caporaso, J. G., et al. (2010). Soil bacterial and fungal communities across a pH gradient in an arable soil. *ISME J.* 4, 1340–1351. doi: 10.1038/ismej.2010.58
- Shendure, J., and Ji, H. (2008). Next-generation DNA sequencing. *Nat. Biotechnol.* 26, 1135–1145. doi: 10.1038/nbt1486
- Shrestha, P. M., Rotaru, A.-E., Summers, Z. M., Shrestha, M., Liu, F., and Lovley, D. R. (2013). Transcriptomic and genetic analysis of direct interspecies electron transfer. *Appl. Environ. Microb.* 79, 2397–2404. doi: 10.1128/AEM.03837-12
- Song, T.-S., Cai, H.-Y., Yan, Z.-S., Zhao, Z.-W., and Jiang, H.-L. (2012). Various voltage productions by microbial fuel cells with sedimentary inocula taken from different sites in one freshwater lake. *Bioresour. Technol.* 108, 68–75. doi: 10.1016/j.biortech.2011.11.136
- Stoeck, T., Bass, D., Nebel, M., Christen, R., Jones, M. D., Breiner, H. W., et al. (2010). Multiple marker parallel tag environmental DNA sequencing reveals a highly complex eukaryotic community in marine anoxic water. *Mol. Ecol.* 19, 21–31. doi: 10.1111/j.1365-294X.2009.04480.x
- Sun, M., Tong, Z.-H., Sheng, G.-P., Chen, Y.-Z., Zhang, F., Mu, Z.-X., et al. (2010). Microbial communities involved in electricity generation from sulfide oxidation in a microbial fuel cell. *Biosens. Bioelectron.* 26, 470–476. doi: 10.1016/j.bios.2010.07.074
- Sun, Y., Wei, J., Liang, P., and Huang, X. (2011). Electricity generation and microbial community changes in microbial fuel cells packed with different anodic materials. *Bioresour. Technol.* 102, 10886–10891. doi: 10.1016/j.biortech.2011.09.038
- Tarrand, J. J., Krieg, N. R., and Döbereiner, J. (1978). A taxonomic study of the *Spirillum lipoferum* group, with descriptions of a new genus, *Azospirillum* gen. nov. and two species, *Azospirillum lipoferum* (Beijerinck) comb. nov. and *Azospirillum brasiliense* sp. nov. *Can. J. Microbiol.* 24, 967–980. doi: 10.1139/m78-160
- Wang, A., Liu, L., Sun, D., Ren, N., and Lee, D. J. (2010). Isolation of Fe (III)-reducing fermentative bacterium *Bacteroides* sp. W7 in the anode suspension of a microbial electrolysis cell (MEC). *Int. J. Hydrogen Energ.* 35, 3178–3182. doi: 10.1016/j.ijhydene.2009.12.154
- Wang, Z., Zheng, Y., Xiao, Y., Wu, S., Wu, Y., Yang, Z., et al. (2013). Analysis of oxygen reduction and microbial community of air-diffusion biocathode in microbial fuel cells. *Bioresour. Technol.* 144, 74–79. doi: 10.1016/j.biortech.2013.06.093
- Wu, S., Xiao, Y., Wang, L., Zheng, Y., Chang, K., Zheng, Z., et al. (2014). Extracellular electron transfer mediated by flavins in gram-positive *Bacillus* sp. WS-XY1 and Yeast *Pichia stipitis*. *Electrochim. Acta* 146, 564–567. doi: 10.1016/j.electacta.2014.09.096
- Xiao, Y., Wu, S., Yang, Z., Zheng, Y., and Zhao, F. (2013b). Isolation and identification of electrochemically active microorganisms. *Prog. Chem.* 25, 1771–1780. doi: 10.7536/PC130125
- Xiao, Y., Wu, S., Zhang, F., Wu, Y.-C., Yang, Z.-H., and Zhao, F. (2013a). Promoting electrogenic ability of microbes with negative pressure. *J. Power Sour.* 229, 79–83. doi: 10.1016/j.jpowsour.2012.11.139
- Xiao, Y., Zeng, G. M., Yang, Z. H., Liu, Y. Sh., Ma, Y. H., Yang, L., et al. (2009). Coexistence of nitrifiers, denitrifiers and Anammox bacteria in a sequencing batch biofilm reactor as revealed by PCR-DGGE. *J. Appl. Microbiol.* 106, 496–505. doi: 10.1111/j.1365-2672.2008.04017.x
- Xiao, Y., Zeng, G. M., Yang, Z. H., Ma, Y. H., Huang, C., Shi, W. J., et al. (2011b). Effects of continuous thermophilic composting (CTC) on bacterial community in the active composting process. *Microbial. Ecol.* 62, 599–608. doi: 10.1007/s00248-011-9882-z
- Xiao, Y., Zeng, G. M., Yang, Z. H., Ma, Y. H., Huang, C., Shi, W. J., et al. (2011a). Changes in the actinomycetal communities during continuous thermophilic composting as revealed by denaturing gradient gel electrophoresis and quantitative PCR. *Bioresour. Technol.* 102, 1383–1388. doi: 10.1016/j.biortech.2010.09.034
- Xiao, Y., Zheng, Y., Wu, S., Yang, Z.-H., and Zhao, F. (2015). Bacterial community structure of autotrophic denitrification biocathode by 454 Pyrosequencing of the 16S rRNA Gene. *Microbial. Ecol.* 69, 492–499. doi: 10.1007/s00248-014-0492-4
- Xing, D., Zuo, Y., Cheng, S., Regan, J. M., and Logan, B. E. (2008). Electricity generation by *rhodopseudomonas palustris* DX-1. *Environ. Sci. Technol.* 42, 4146–4151. doi: 10.1021/es800312v
- Yang, Z. H., Xiao, Y., Zeng, G., Xu, Z. Y., and Liu, Y. S. (2007). Comparison of methods for total community DNA extraction and purification from compost. *Appl. Microbiol. Biot.* 74, 918–925. doi: 10.1007/s00253-006-0704-z
- Yates, M. D., Kiely, P. D., Call, D. F., Rismani-Yazdi, H., Bibby, K., Peccia, J., et al. (2012). Convergent development of anodic bacterial communities in microbial fuel cells. *ISME J.* 6, 2002–2013. doi: 10.1038/ismej.2012.42

- Zhang, H., Banaszak, J. E., Parameswaran, P., Alder, J., Krajmalnik-Brown, R., and Rittmann, B. E. (2009). Focused-Pulsed sludge pre-treatment increases the bacterial diversity and relative abundance of acetoclastic methanogens in a full-scale anaerobic digester. *Water Res.* 43, 4517–4526. doi: 10.1016/j.watres.2009.07.034
- Zhang, T., Shao, M.-F., and Ye, L. (2012). 454 Pyrosequencing reveals bacterial diversity of activated sludge from 14 sewage treatment plants. *ISME J.* 6, 1137–1147. doi: 10.1038/ismej.2011.188
- Zhao, F., Rahunen, N., Varcoe, J. R., Roberts, A. J., Avignone-Rossa, C., Thumser, A. E., et al. (2009a). Factors affecting the performance of microbial fuel cells for sulfur pollutants removal. *Biosens. Bioelectron.* 24, 1931–1936. doi: 10.1016/j.bios.2008.09.030
- Zhao, F., Slade, R. C. T., and Varcoe, J. R. (2009b). Techniques for the study and development of microbial fuel cells: an electrochemical perspective. *Chem. Soc. Rev.* 38, 1926–1939. doi: 10.1039/b819866g
- Zhou, M., Chi, M., Luo, J., He, H., and Jin, T. (2011). An overview of electrode materials in microbial fuel cells. *J. Power Sour.* 196, 4427–4435. doi: 10.1016/j.jpowsour.2011.01.012

Conflict of Interest Statement: The authors declare that the research was conducted in the absence of any commercial or financial relationships that could be construed as a potential conflict of interest.

Copyright © 2015 Xiao, Zheng, Wu, Zhang, Chen, Liang, Huang, Yang, Ng, Chen and Zhao. This is an open-access article distributed under the terms of the Creative Commons Attribution License (CC BY). The use, distribution or reproduction in other forums is permitted, provided the original author(s) or licensor are credited and that the original publication in this journal is cited, in accordance with accepted academic practice. No use, distribution or reproduction is permitted which does not comply with these terms.

Advantages of publishing in Frontiers



OPEN ACCESS

Articles are free to read for greatest visibility and readership



FAST PUBLICATION

Around 90 days from submission to decision



HIGH QUALITY PEER-REVIEW

Rigorous, collaborative, and constructive peer-review



TRANSPARENT PEER-REVIEW

Editors and reviewers acknowledged by name on published articles



REPRODUCIBILITY OF RESEARCH

Support open data and methods to enhance research reproducibility



DIGITAL PUBLISHING

Articles designed for optimal readership across devices



FOLLOW US
@frontiersin



IMPACT METRICS

Advanced article metrics track visibility across digital media



EXTENSIVE PROMOTION

Marketing and promotion of impactful research



LOOP RESEARCH NETWORK

Our network increases your article's readership